

Universiteit
Leiden
The Netherlands

Incremental value of advanced cardiac imaging modalities for diagnosis and patient management : focus on real-time three-dimensional echocardiography and magnetic resonance imaging

Marsan, N.A.

Citation
Marsan, N. A. (2011, November 7). *Incremental value of advanced cardiac imaging modalities for diagnosis and patient management : focus on real-time three-dimensional echocardiography and magnetic resonance imaging*. Retrieved from https://hdl.handle.net/1887/18020

Version:	Corrected Publisher's Version
License:	Licence agreement concerning inclusion of doctoral thesis in the Institutional Repository of the University of Leiden
Downloaded from:	https://hdl.handle.net/1887/18020

Note: To cite this publication please use the final published version (if applicable).

INCREMENTAL VALUE OF ADVANCED CARDIAC IMAGING MODALITIES FOR DIAGNOSIS AND PATIENT MANAGEMENT

Focus on real-time three-dimensional echocardiography and magnetic resonance imaging

Nina Ajmone Marsan

The research described in this thesis was performed at the Department of Cardiology of the Leiden University Medical Center, Leiden, The Netherlands

Cover: Nina Ajmone Marsan

Lay-out and printing: Optima Grafische Communicatie, Rotterdam, The Netherlands

ISBN: 978-94-6169-133-0

Copyright© Nina Ajmone Marsan, Leiden, the Netherlands. All rights reserved. No part of this book may be reproduced or transmitted, in any form or by any means, without permission of the author.

Financial support to the costs associated with the publication of this thesis from Philips Healthcare is gratefully acknowledged. Additional gratitude goes to Meda Pharma, Boehringer Ingelheim, Biotronik and Boston Scientific Nederland BV.

Incremental value of advanced cardiac imaging modalities for diagnosis and patient management

Focus on real-time three-dimensional echocardiography and magnetic resonance imaging

Proefschrift

ter verkrijging van
de graad van Doctor aan de Universiteit Leiden,
op gezag van Rector Magnificus prof. mr. P.F. van der Heijden,
volgens besluit van het College voor Promoties
te verdedigen op donderdag 3 november 2011
klokke 16:15 uur

door

Nina Ajmone Marsan

geboren te Rome, Italië in 1976

PROMOTIECOMMISSIE

Promotores:	Prof. dr. J.J. Bax
	Prof. dr. M.J. Schalij
Overige leden:	Dr. V. Delgado
	Dr. E.R. Holman
	Prof. dr. P. Nihoyannopoulos (Imperial London Hammersmith Hospital)
	Prof. dr. A. de Roos
	Dr. H.F. Verwey
	Prof. dr. E.E. van der Wall

To my parents and to Rutger

TABLE OF CONTENTS

	General introduction and outline of the thesis	13
PART I	**REAL-TIME THREE-DIMENSIONAL ECHOCARDIOGRAPHY**	
Chapter 1	Real-time three dimensional echocardiography: current and future clinical applications. *Heart 2009*	27
Part IA	**Real-time three-dimensional echocardiography as a novel approach to assess left ventricular size, function and dyssynchrony.**	
Chapter 2	Predicting response to CRT. The value of two- and three-dimensional echocardiography. *Europace 2008*	53
Chapter 3	Real-time three-dimensional echocardiography permits quantification of left ventricular mechanical dyssynchrony and predicts acute response to cardiac resynchronization therapy. *J Cardiovasc Electrophysiol 2008*	67
Chapter 4	Real-time three-dimensional echocardiography as a novel approach to quantify left ventricular dyssynchrony: a comparison study with phase analysis of gated myocardial perfusion SPECT. *J Am Soc Echocardiogr 2008*	85
Chapter 5	Usefulness of multimodality imaging for detecting differences in temporal occurrence of left ventricular systolic mechanical events in healthy young adults. *Am J Cardiol 2009*	101
Chapter 6	Tri-plane tissue Doppler imaging: a novel 3-dimensional imaging modality that predicts reverse left ventricular remodeling after cardiac resynchronization therapy. *Heart 2008*	117
Chapter 7	Left ventricular dyssynchrony assessed by two 3-dimensional imaging modalities: phase analysis of gated myocardial perfusion SPECT and tri-plane tissue Doppler imaging. *Eur J Nucl Med Mol Imaging 2008*	133

Chapter 8 Noninvasive imaging of cardiac venous anatomy with 64-slice multi-slice computed tomography and noninvasive assessment of left ventricular dyssynchrony by 3-dimensional tissue synchronization imaging in patients with heart failure scheduled for cardiac resynchronization therapy. 151

Am J Cardiol 2008

Part IB **Real-time three-dimensional echocardiography for the assessment of left atrium volumes and function.**

Chapter 9 Real-time three-dimensional echocardiography as a novel approach to assess left ventricular and left atrium reverse remodeling and to predict response to cardiac resynchronization therapy. 169

Heart Rhythm 2008

Chapter 10 Comparison of left atrial volumes and function by real-time three-dimensional echocardiography in patients having catheter ablation for atrial fibrillation with persistence of sinus rhythm versus recurrent atrial fibrillation three months later. 187

Am J Cardiol 2008

PART II **CONTRAST-ENHANCED ECHOCARDIOGRAPHY**

Chapter 11 Safety of contrast-enhanced echocardiography within 24 h after acute myocardial infarction. 203

Eur J Echocardiogr 2008

Chapter 12 Real-time 3-dimensional echocardiography early after acute myocardial infarction: incremental value of echo-contrast for assessment of left ventricular function. 213

Am Heart J 2009

Chapter 13 Impact of left ventricular dyssynchrony early on left ventricular function after first acute myocardial infarction. 231

Am J Cardiol 2010

Chapter 14 Reduced left ventricular torsion early after myocardial infarction is related to left ventricular remodeling. 245

Circ Cardiovasc Imaging 2010

PART III MAGNETIC RESONANCE IMAGING

Part IIIA Magnetic resonance imaging for the assessment of left ventricular dyssynchrony and myocardial viability.

Chapter 15 Comparison between tissue Doppler imaging and velocity-encoded magnetic resonance imaging for measurement of myocardial velocities, assessment of left ventricular dyssynchrony, and estimation of left ventricular filling pressures in patients with ischemic cardiomyopathy. 269

Am J Cardiol 2008

Chapter 16 Magnetic resonance imaging and response to cardiac resynchronization therapy: relative merits of left ventricular dyssynchrony and scar tissue. 283

Eur Heart J 2009

Chapter 17 Agreement and disagreement between contrast-enhanced magnetic resonance imaging and nuclear imaging for assessment of myocardial viability. 301

Eur J Nucl Med Mol Imaging 2009

Chapter 18 Three-dimensional echocardiography for the preoperative assessment of patients with left ventricular aneurysm. 317

Ann Thoracic Surg 2011

Part IIIB Magnetic resonance imaging for the assessment of valvular heart disease.

Chapter 19 Mitral valve and tricuspid valve blood flow: accurate quantification with 3D velocity-encoded MR imaging with retrospective valve tracking. 337

Radiology 2008

Chapter 20 Quantification of functional mitral regurgitation by real-time 3D echocardiography: comparison with 3D velocity-encoded cardiac magnetic resonance. 355

JACC Cardiovasc Imaging 2009

PART IV **INCREMENTAL VALUE OF ADVANCED IMAGING MODALITIES IN CARDIAC RESYNCHRONIZATION THERAPY**

Chapter 21 Left ventricular rotational mechanics in acute myocardial infarction and in chronic (ischemic and nonischemic) heart failure patients. 373

Am J Cardiol 2009

Chapter 22 Effects of cardiac resynchronization therapy on left ventricular twist. 387

J Am Coll Cardiol 2009

Chapter 23 Cardiac resynchronization therapy as a therapeutic option in patients with moderate-severe functional mitral regurgitation and high operative risk. 407

Circulation 2011

Chapter 24 Effect of cardiac resynchronization therapy on cerebral blood flow. 425

Am J Cardiol 2010

Chapter 25 Cardiac resynchronization therapy in patients with ischemic versus non-ischemic heart failure: Differential effect of optimizing interventricular pacing interval. 437

Am Heart J 2009

Chapter 26 Comparison of time course of response to cardiac resynchronization therapy in patients with ischemic versus nonischemic cardiomyopathy. 453

Am J Cardiol 2009

Summary and Conclusions 467

Samenvatting en Conclusies 477

List of publications 487

Acknowledgements 497

Curriculum Vitae 501

General introduction and outline of the thesis

GENERAL INTRODUCTION AND OUTLINE OF THE THESIS

Conventional echocardiography is the most commonly used imaging technique in clinical cardiology, due to its non-invasive approach and wide-availability. Diagnosis, therapeutic management and monitoring of patients with cardiovascular diseases are mostly based on echocardiographic assessments [1, 2], including left ventricular (LV) volumes and ejection fraction (EF), LV thickness and wall motion abnormalities, LV diastolic function measurements, and valvular stenosis or regurgitation severity. However, conventional echocardiography is characterized by several important limitations: 1) for the quantification of LV volumes and EF, 2-dimensional (2D) echocardiography relies on significant geometric assumptions, it might be affected by oblique or "foreshortened" views and showed modest reproducibility [3]; 2) LVEF and the conventional assessment of LV diastolic function have been shown to be not sensitive enough to detect subtle myocardial systolic and diastolic dysfunction that may occur in several cardiac conditions and should be the target for an early therapeutic approach [4]; furthermore, these conventional measurements are not sophisticated enough to describe thoroughly the complex LV mechanics [4]; 3) 2D echocardiography permits only limited cross-sectional views, which make in some cases the interpretation and diagnosis of cardiac pathologies, and in particular of valvular disease, extremely complex and achievable only by experienced operators; 4) image quality is often an important issue that may significantly affect the accuracy of this imaging modality.

Advances in echocardiography have more recently provided novel approaches, which may overcome the abovementioned limitations. Real-time 3D echocardiography (RT3DE), tissue Doppler imaging (TDI), 2D speckle tracking imaging and contrast-enhanced echocardiography have demonstrated their incremental value over conventional echocardiography for the assessment of global and regional LV function and for a better understanding of cardiac mechanics[4–7].

In addition, non-echocardiographic imaging modalities, such as multi-detector row computed tomography and magnetic resonance imaging (CMR) provide high-resolution images of the cardiac structures and therefore important additional information. In particular, CMR has emerged as the gold standard technique for the assessment of LV volumes and function and for the identification and quantification of myocardial scar/fibrotic tissue [8, 9].

Therefore, advanced cardiac imaging modalities may play a crucial role to improve the diagnosis process and the clinical management of patients with different cardiac diseases, including heart failure, valvular heart disease, myocardial infarction and atrial fibrillation.

Real-time three-dimensional echocardiography

Thanks to significant technological developments, RT3DE is now readily available as a clinically applicable imaging technique and allows for the assessment of the whole heart in 3 dimensions, including all LV segments and unlimited image plane orientations. Therefore using this novel modality, quantification of LV size and function (but also of left atrium and of right ventricle) does not rely anymore on geometric assumptions and has been shown to be more accurate as compared to conventional echocardiographic measurements [6]. Furthermore, regional LV function can be fully assessed based on the 3D endocardial motion of volumetric segments, giving the opportunity of having complete dynamic information on LV chamber contraction (Chapter 1, Figure 3). Therefore, accurate evaluation of LV regional motion can be performed in patients with ischemic cardiomyopathy. Furthermore, temporal sequence of regional myocardial contraction can be studied and measures of LV dyssynchrony can be derived and applied in patients with advanced heart failure referred for cardiac resynchronization therapy (CRT) [10].

Finally, the 3D approach permits a direct visualization of the complex anatomy and the sophisticated functional mechanisms of the cardiac valves (in particular of the mitral valve), allowing for a unique evaluation of valve morphology and for an accurate assessment of valvular disease severity [11, 12].

Assessment of myocardial velocity and deformation

Tissue Doppler imaging and more recently 2D speckle tracking imaging have been introduced for the quantification of myocardial velocity and deformation (strain). These techniques have been largely validated against sonomicrometry and are proposed as novel approaches for a more sensitive and accurate assessments of global and regional LV function[4, 13–15].

In particular, TDI is an echocardiographic modality characterized by high frame rate (until 200 fps) and which is able to record myocardial velocities thanks to specific filter settings that exclude the blood flow high velocities [16]. This modality can also be applied to a 3D dataset, displaying simultaneously 3 apical views (tri-plane modality) and therefore including all myocardial segments into account and avoiding potential problems of heart rate variability (Chapter 2, Figure 3). In clinical practice, TDI has been validated for the estimate of LV filling pressures [17, 18], measuring the early diastolic relaxation (E') of the mitral annulus segments, and for the assessment of LV dyssynchrony, identifying the delay between myocardial peak systolic velocities of different LV segments [19, 20]. However, the measure of myocardial velocities does not reflect only the active contraction of the myocardium but is also strongly influenced by the tethering of the adjacent segments or translation motion. Therefore, in certain cases (especially of ischemic cardiomyopathy), it might not be an accurate measure

of myocardial contractility. Conversely, myocardial deformation (strain) can be obtained as spatial derivative, integrated over time of myocardial velocity and reflects more closely the active component of myocardial contraction (Chapter 2, Figure 1). Therefore, it has been applied, together with strain rate (deformation velocity), as a promising direct measure of myocardial contractility [21]. Being TDI a Doppler-based technique, however, makes these measures dependent on the insonation angle of the ultrasound beam and therefore limited in case of suboptimal alignment, such as in the evaluation of apical segments and of radial and circumferential deformation.

Two-dimensional speckle tracking imaging in turn, permits and angle-independent assessment of myocardial strain (and strain rate) in multiple directions (longitudinal, radial and circumferential), tracking over time in standard grey-scale 2D images the presence of natural acoustic markers (so-called *speckles*), equally distributed within the myocardial wall. Using this technique, regional and global LV contractility can be therefore accurately quantified and LV dyssynchrony can be assessed looking at the time sequence of LV segmental deformation [14, 22]. In addition, more complex cardiac mechanics can be studied. The human heart for example has a specific helical arrangement of the myofibers with a right-hand orientation from the base towards the apex in the endocardial layers and a left-hand orientation in the epicardial layers. This spiral architecture of the myofibers leads to the typical LV systolic wringing motion as a result of an opposite rotation of LV apex and base. The gradient between apex and base in the rotation angle along LV longitudinal axis is called twist and contributes significantly to LV systolic function, in addition to myocardial shortening and thickening [23]. Speckle tracking imaging allows the quantification of LV twist as the net difference between apical (counterclockwise) and basal (clockwise) rotations and as a novel parameter of global LV performance (Chapter 22, Figure1) [24].

Contrast-enhanced echocardiography

In patients with suboptimal acoustic windows, intravenous echocardiographic contrast is normally administered to improve endocardial border delineation, to increase accuracy and reproducibility of regional and global LV function assessment and to detect intracavitary thrombus [5, 7]. RT3DE image quality is highly dependent on the acoustic window, due to a lower spatial and temporal resolution as compared to 2D echocardiography. Accordingly, adequate endocardial border delineation may be difficult with this imaging modality, even in the presence of relatively good 2D image quality. Few studies explored the feasibility of RT3DE, in relation to the image quality, for the assessment of LV systolic function and reported a relative high prevalence of uninterpretable or poor quality RT3DE images [25]. However, data regarding the use of contrast agents during RT3DE are scarce and only few studies evaluated the feasibility and accuracy of contrast-enhanced RT3DE [26].

Contrast-enhanced echocardiography may be particularly important in the management of patients presenting with acute myocardial infarction, in which urgent and repeated echocardiographic examinations are indeed crucial in order to evaluate LV global and regional function and to exclude infarction complications. Furthermore, this approach enables evaluation of myocardial perfusion and microvascular integrity, providing valuable information about myocardial viability, which is an important prognostic factor after infarction [27]. Alternative diagnostic imaging techniques (i.e. transesophageal echocardiography, radionuclide ventriculography and cardiac magnetic resonance) are conversely more invasive or expensive.

Substantial safety data already exist for the use of echocardiographic contrast in stable patients with known or suspected cardiac disease [28]. However, safety data on contrast-echocardiography in critically ill patients and particularly in patients within 24 hours of acute myocardial infarction are lacking. As a consequence, the use of this echocardiographic approach in these patients is limited, although of potential great importance. Contrast-echocardiography could in fact provide information on the extent of infarction, which is crucial, together with other parameters such as LV dyssynchrony and novel measurement of LV mechanics, to predict LV functional recovery or development of LV remodeling, and long-term morbidity and mortality [27].

Magnetic resonance imaging

CMR is currently considered the gold standard for the assessment of several cardiac measurements, providing highly accurate and reproducible data.

In particular, it was proven to be far superior to other techniques for quantification of LV volumes and EF, and for the assessment of LV regional wall motion and segmental thickness. Therefore, it has been used as a reference technique for the quantification of LV size and function in validation studies of different imaging modalities, including RT3DE [6].

In addition, CMR with delayed-gadolinium enhancement is considered the gold standard for the assessment of myocardial infarction extent. This technique in fact offers a direct visualization of scar/fibrotic tissue with high spatial resolution, enabling distinction between subendocardial and transmural myocardial involvement (Chapter 16, Figure 1)[8]. Therefore, it is widely applied for the assessment of myocardial viability and for treatment optimization and risk stratification of patients with ischemic LV dysfunction.

Velocity encoded CMR is also particularly suitable for determining trans-valvular blood flow, providing quantitative information on moving spins, and has been recently proposed as a reference method for the assessment of valvular heart disease [29, 30]. However, conventional single-slice one-directional velocity encoded CMR showed some limitations, mainly due to the fact that the acquisition plane can not be adapted to the systolic-diastolic motion of the valves. A more accurate approach is offered by the 3D 3-directional velocity encoded

CMR with retrospective valve tracking. This technique is able to cover the complete velocity vector field of the blood flow and to correct for the through-plane myocardial motion in the apical-basal direction (Chapter 20, Figure 1). This approach can be therefore applied for the assessment of all 4 cardiac valves in one acquisition and to accurately evaluate potential flow abnormalities (valve stenosis or regurgitation) [8, 31].

When applied for myocardial wall motion measurement, velocity encoded CMR may obtain similar data to that provided by TDI, without the limitations of the acoustical window, and can be used for the assessment of myocardial velocities. As above-mentioned, potential clinical applications might be therefore in the assessment of LV diastolic function and for the measures of LV dyssynchrony [32, 33]. More recently, CMR has also been proposed for the assessment of LV dyssynchrony looking at the changes in radial wall motion over time [34]. With this approach, which includes the identification of the endocardial and epicardial border of a series of short axis slices, the temporal sequence of LV segments contraction can be studied and measures of LV dyssynchrony can be derived.

CMR therefore provides unique detailed information about cardiac morphology and function, as well as assessment of myocardial viability, LV dyssynchrony and quantification of trans-valvular flows. This comprehensive approach is particularly useful in heart failure patients, especially as potential candidates to CRT.

OBJECTIVES AND OUTLINE OF THE THESIS

The objectives of this thesis were to investigate the incremental value of advanced cardiac imaging modalities for diagnosis and patient management in different cardiac disease. In **Part I,** current and future applications of RT3DE will be introduced. The use of this technique for the quantification of LV volumes and function and for the assessment of LV dyssynchrony is explored in heart failure patients before and after CRT implantation (Part IA). In particular, different 3D measures of LV dyssynchrony, based on the full volume approach (Chapter 2, 3 and 4) or on the tri-plane approach (Chapter 5, 6 and 7), are applied to improve candidate selection for CRT and to predict favorable response after implantation. In Part IB, RT3DE is applied in patients with atrial fibrillation or heart failure for the quantification of left atrium volume and for the assessment of different left atrial functions (conduit function, active contraction, reservoir function).

Part II will discuss the additional diagnostic and prognostic value of contrast-enhanced echocardiography, particularly in patients within 24 hours after acute myocardial infarction. Safety and accuracy (in combination with RT3DE) of this modality in this specific group are evaluated. In addition, the incremental value of myocardial infarction extension, as assessed with myocardial perfusion analysis, to predict LV remodeling after infarction is explored together with novel measures of LV performance (LV twist).

The use of CMR for a comprehensive assessment of patients with different cardiac disease will be the focus of **Part III**. Novel CMR approaches for an accurate and reproducible measure of LV dyssynchrony are proposed and applied in heart failure patients in order to predict significant LV reverse remodeling after CRT implantation (Part IIIA). In addition, the value of CMR for the assessment of myocardial viability is discussed in different groups of patients (heart failure, LV aneurysm, ischemic cardiomyopathy, Part IIIA). Part IIIB explores the values of CMR in valvular heart disease, and particularly as a reference technique for the assessment of mitral regurgitation severity.

Finally in **Part IV**, novel physiopathological aspects in CRT patients will be studied using advanced echocardiographic imaging modalities. In particular, this part of the thesis evaluates the effect of CRT on: 1) LV rotational mechanics, as assessed by speckle tracking strain analysis; 2) severity of mitral regurgitation, especially in patients with high operative risk; 3) cerebral blood flow, as measured by transcranial Doppler. Furthermore, whether the etiology of heart failure and biventricular pacemaker settings (when optimized) have a significant influence on response to CRT is further explored.

REFERENCES

1. Dickstein K, Cohen-Solal A, Filippatos G et al. ESC Guidelines for the diagnosis and treatment of acute and chronic heart failure 2008: the Task Force for the Diagnosis and Treatment of Acute and Chronic Heart Failure 2008 of the European Society of Cardiology. Developed in collaboration with the Heart Failure Association of the ESC (HFA) and endorsed by the European Society of Intensive Care Medicine (ESICM). *Eur Heart J* 2008;29:2388-2442.
2. Vahanian A, Baumgartner H, Bax J et al. Guidelines on the management of valvular heart disease: The Task Force on the Management of Valvular Heart Disease of the European Society of Cardiology. *Eur Heart J* 2007;28:230-268.
3. Gordon EP, Schnittger I, Fitzgerald PJ, Williams P, Popp RL. Reproducibility of left ventricular volumes by two-dimensional echocardiography. *J Am Coll Cardiol* 1983;2:506-513.
4. Mor-Avi V, Lang RM, Badano LP et al. Current and evolving echocardiographic techniques for the quantitative evaluation of cardiac mechanics: ASE/EAE consensus statement on methodology and indications endorsed by the Japanese Society of Echocardiography. *J Am Soc Echocardiogr* 2011;24:277-313.
5. Hoffmann R, von BS, Kasprzak JD et al. Analysis of regional left ventricular function by cineventriculography, cardiac magnetic resonance imaging, and unenhanced and contrast-enhanced echocardiography: a multicenter comparison of methods. *J Am Coll Cardiol* 2006;47:121-128.
6. Mor-Avi V, Jenkins C, Kuhl HP et al. Real-time 3-dimensional echocardiographic quantification of left ventricular volumes: multicenter study for validation with magnetic resonance imaging and investigation of sources of error. *JACC Cardiovasc Img* 2008,1:413-423
7. Thomson HL, Basmadjian AJ, Rainbird AJ et al. Contrast echocardiography improves the accuracy and reproducibility of left ventricular remodeling measurements: a prospective, randomly assigned, blinded study. *J Am Coll Cardiol* 2001;38:867-875.
8. Kim RJ, Fieno DS, Parrish TB et al. Relationship of MRI delayed contrast enhancement to irreversible injury, infarct age, and contractile function. *Circulation* 1999;100:1992-2002.
9. Kwon DH, Halley CM, Carrigan TP et al. Extent of left ventricular scar predicts outcomes in ischemic cardiomyopathy patients with significantly reduced systolic function: a delayed hyperenhancement cardiac magnetic resonance study. *JACC Cardiovasc Imaging* 2009;2:34-44.
10. Kapetanakis S, Kearney MT, Siva A, Gall N, Cooklin M, Monaghan MJ. Real-time three-dimensional echocardiography: a novel technique to quantify global left ventricular mechanical dyssynchrony. *Circulation* 2005;112:992-1000.
11. Poh KK, Levine RA, Solis J et al. Assessing aortic valve area in aortic stenosis by continuity equation: a novel approach using real-time three-dimensional echocardiography. *Eur Heart J* 2008;29:2526-2535.
12. Pepi M, Tamborini G, Maltagliati A et al. Head-to-head comparison of two- and three-dimensional transthoracic and transesophageal echocardiography in the localization of mitral valve prolapse. *J Am Coll Cardiol* 2006;48:2524-2530.
13. Amundsen BH, Helle-Valle T, Edvardsen T et al. Noninvasive myocardial strain measurement by speckle tracking echocardiography: validation against sonomicrometry and tagged magnetic resonance imaging. *J Am Coll Cardiol* 2006;47:789-793.
14. Brown J, Jenkins C, Marwick TH. Use of myocardial strain to assess global left ventricular function: a comparison with cardiac magnetic resonance and 3-dimensional echocardiography. *Am Heart J* 2009;57:102-105.

15. Reisner SA, Lysyansky P, Agmon Y, Mutlak D, Lessick J, Friedman Z. Global longitudinal strain: a novel index of left ventricular systolic function. *J Am Soc Echocardiogr* 2004;17:630-633.
16. Sutherland GR, Stewart MJ, Groundstroem KW et al. Color Doppler myocardial imaging: a new technique for the assessment of myocardial function. *J Am Soc Echocardiogr* 1994;7:441-458.
17. Nagueh SF, Middleton KJ, Kopelen HA, Zoghbi WA, Quinones MA. Doppler tissue imaging: a non-invasive technique for evaluation of left ventricular relaxation and estimation of filling pressures. *J Am Coll Cardiol* 1997;30:1527-1533.
18. Paulus WJ, Tschope C, Sanderson JE et al. How to diagnose diastolic heart failure: a consensus statement on the diagnosis of heart failure with normal left ventricular ejection fraction by the Heart Failure and Echocardiography Associations of the European Society of Cardiology. *Eur Heart J* 2007;28:2539-2550.
19. Bax JJ, Bleeker GB, Marwick TH et al. Left ventricular dyssynchrony predicts response and prognosis after cardiac resynchronization therapy. *J Am Coll Cardiol* 2004;44:1834-1840.
20. Bax JJ, Abraham T, Barold SS et al. Cardiac resynchronization therapy: Part 1--issues before device implantation. *J Am Coll Cardiol* 2005;46:2153-2167.
21. Urheim S, Edvardsen T, Torp H, Angelsen B, Smiseth OA. Myocardial strain by Doppler echocardiography. Validation of a new method to quantify regional myocardial function. *Circulation* 2000;102:1158-1164.
22. Delgado V, Ypenburg C, van Bommel RJ et al. Assessment of left ventricular dyssynchrony by speckle tracking strain imaging comparison between longitudinal, circumferential, and radial strain in cardiac resynchronization therapy. *J Am Coll Cardiol* 2008;51:1944-1952.
23. Sengupta PP, Korinek J, Belohlavek M et al. Left ventricular structure and function: basic science for cardiac imaging. *J Am Coll Cardiol* 2006;48:1988-2001.
24. Notomi Y, Lysyansky P, Setser RM et al. Measurement of ventricular torsion by two-dimensional ultrasound speckle tracking imaging. *J Am Coll Cardiol* 2005;45:2034-2041.
25. Tighe DA, Rosetti M, Vinch CS et al. Influence of image quality on the accuracy of real time three-dimensional echocardiography to measure left ventricular volumes in unselected patients: a comparison with gated-SPECT imaging. *Echocardiography* 2007;24:1073-1080.
26. Krenning BJ, Kirschbaum SW, Soliman OI et al. Comparison of contrast agent-enhanced versus non-contrast agent-enhanced real-time three-dimensional echocardiography for analysis of left ventricular systolic function. *Am J Cardiol* 2007;100:1485-1489.
27. Dwivedi G, Janardhanan R, Hayat SA, Swinburn JM, Senior R. Prognostic value of myocardial viability detected by myocardial contrast echocardiography early after acute myocardial infarction. *J Am Coll Cardiol* 2007;50:327-334.
28. Dolan MS, Gala SS, Dodla S et al. Safety and efficacy of commercially available ultrasound contrast agents for rest and stress echocardiography a multicenter experience. *J Am Coll Cardiol* 2009;53:32-38.
29. Buck T, Plicht B, Kahlert P, Schenk IM, Hunold P, Erbel R. Effect of dynamic flow rate and orifice area on mitral regurgitant stroke volume quantification using the proximal isovelocity surface area method. *J Am Coll Cardiol* 2008;52:767-778.
30. Stewart RA, Raffel OC, Kerr AJ et al. Pilot study to assess the influence of beta-blockade on mitral regurgitant volume and left ventricular work in degenerative mitral valve disease. *Circulation* 2008;118:1041-1046.
31. Westenberg JJ, Danilouchkine MG, Doornbos J et al. Accurate and reproducible mitral valvular blood flow measurement with three-directional velocity-encoded magnetic resonance imaging. *J Cardiovasc Magn Reson* 2004;6:767-776.

32. Delfino JG, Bhasin M, Cole R et al. Comparison of myocardial velocities obtained with magnetic resonance phase velocity mapping and tissue Doppler imaging in normal subjects and patients with left ventricular dyssynchrony. *J Magn Reson Imaging* 2006;24:304-311.
33. Westenberg JJ, Lamb HJ, van der Geest RJ et al. Assessment of left ventricular dyssynchrony in patients with conduction delay and idiopathic dilated cardiomyopathy: head-to-head comparison between tissue doppler imaging and velocity-encoded magnetic resonance imaging. *J Am Coll Cardiol* 2006;47:2042-2048.
34. Chalil S, Stegemann B, Muhyaldeen S et al. Intraventricular dyssynchrony predicts mortality and morbidity after cardiac resynchronization therapy: a study using cardiovascular magnetic resonance tissue synchronization imaging. *J Am Coll Cardiol* 2007;50:243-252.

PART I

Real-time three-dimensional echocardiography

CHAPTER 1

Real-time three dimensional echocardiography: current and future clinical applications

N Ajmone Marsan, L F Tops, P Nihoyannopoulos, E R Holman, J J Bax

Heart 2009;95:1881–90.

INTRODUCTION

Conventional echocardiography is the most commonly used imaging technique in clinical cardiology. However, the complex cardiac anatomy and the sophisticated functional mechanisms of the cardiac structures require a transition from a 2-dimensional (2D) to a 3-dimensional (3D) approach. In fact, conventional 2D echocardiography makes significant geometric assumptions for the quantification of cardiac size, and only permits cross-sectional views for interpretation of cardiac pathologies. Real-time 3D echocardiography (RT3DE) may overcome most of these limitations and is now readily available as a clinically applicable imaging technique [1].

Early approaches to 3D echocardiography were based on off-line and time-consuming reconstructions of a series of 2D images obtained by either a freehand scanning or a mechanically driven rotating transducer [2]. Current generation 3D echo-transducers consist of a fully sampled matrix array of more than 3000 simultaneously active ultrasound elements that provide a real-time volumetric scanning with rapid post-processing. Recently, this novel technology has also been applied to a new generation transesophageal probes, broadening the possibility of clinical applications [3,4]. The main advantages of a 3D echocardiographic

Table 1. Current clinical applications of real-time 3-dimensional echocardiography (RT3DE) and its advantages over conventional 2-dimensional (2D) echocardiography.

Clinical application	Advantages of RT3DE vs. 2D echocardiography
Assessment of LV volumes, mass and ejection fraction Assessment of LA size and function	No need for geometric assumptions and no errors caused by foreshortened views: - more accurate - more reproducible - semi-automated procedure
Assessment of LV wall motion abnormalities	The 3D dataset contains the complete dynamic information on LV contraction: - faster acquisition (important during stress-echo) - more accurate identification of wall motion abnormalities
Assessment of LV dyssynchrony	- analysis of 16 segments in 1 single acquisition - semi-automated procedure----more reproducible - angle-independent measurement of the composite effect of longitudinal, radial and circumferential contraction - combination with quantification of LV volumes and function
Assessment of RV volumes and function	Advantage over 2D not yet established, accuracy of RT3DE needs further validation
Evaluation of valve function and diseases	Unlimited image plane orientation for better understanding of the complex geometry of valves and subvalvular apparatus: - MV and AV stenosis: "en face" view with more accurate valve area measurement - MV prolapse: accurate identification of the scallop involved - MV and AV regurgitation: identification of the precise mechanism and assessment of the exact size of vena contracta area with color Doppler Guide for surgical or percutaneous procedures
Evaluation of congenital heart diseases	Ability to display complex spatial relationship between cardiac structures Guide for surgical or percutaneous procedures

AV: aortic valve; LA: left atrium; LV: left ventricle; MV: mitral valve; RV: right ventricle

approach are summarized in Table 1. In this article, the role of RT3DE for the assessment of cardiac chambers size and function and for the evaluation of valvular and congenital heart diseases will be reviewed. In addition, the potential future applications of RT3DE will be discussed.

ASSESSMENT OF LEFT VENTRICULAR SIZE AND FUNCTION

The most common indication for performing an echocardiogram in adult patients is the assessment of left ventricular (LV) size and function. Diagnostic clues, prognostic implications and important therapeutic decisions rest upon the results of this evaluation that consequently needs to be as accurate and reproducible as possible.

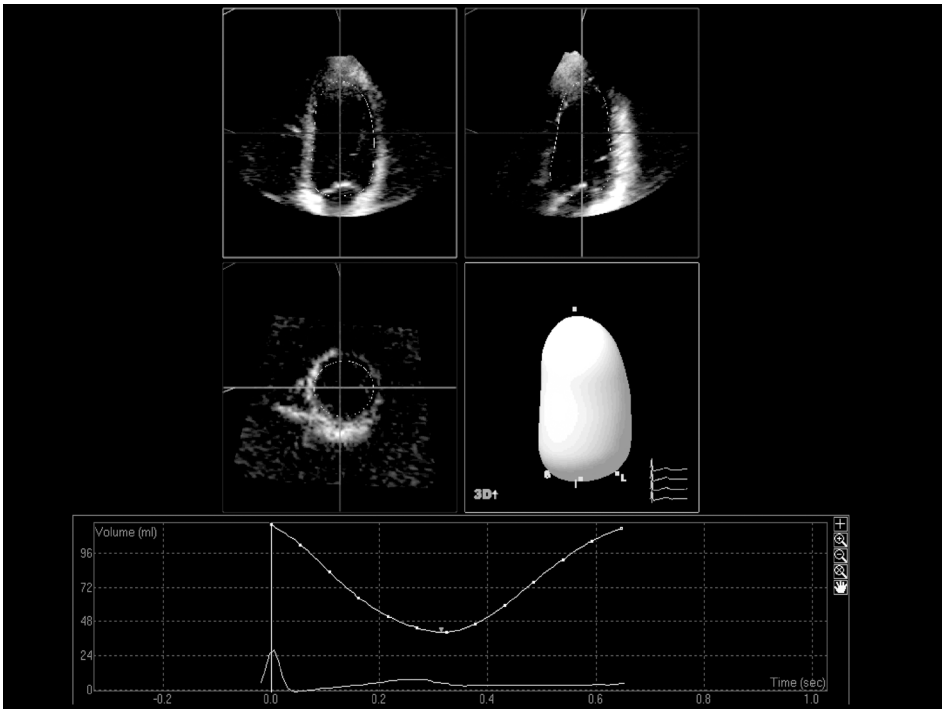


Figure 1. Example of 3D left ventricular model obtained by post-processing of a full-volume 3D dataset, acquired in a normal subject. In the upper panel, the 3D dataset is automatically cropped (according to the interface of the software Q-Lab, Philips Medical Systems) to visualize the 4-chamber view (top left), the 2-chamber view (top right) and the short-axis view (bottom left). After first identifying the apex and mitral annulus on the end-diastolic and end-systolic frames (using 5 reference points), an automated endocardial tracing is generated for each frame and may be manually adjusted as required. From this, the 3D cast (bottom right) of the LV is created and LV volumes and ejection fraction are obtained. In the lower panel, LV volume is plotted over time throughout the cardiac cycle.

Quantification of LV volumes

The conventional 2D quantification of LV volumes is based on the biplane method of discs (Simpson's rule) [5]. This method assumes that the LV can be represented by a series of stacked discs with different diameters. However, this assumption may fail in the presence of an irregular LV shape (in case of an LV aneurysm), wall motion abnormalities and oblique or "foreshortened" views of the ventricle. All these issues have important impact on the accuracy of this approach. In addition, it has been demonstrated that conventional 2D echocardiography has a relatively modest inter- and intra-observer agreement and cut-plane reproducibility in sequential studies [6]. In contrast, RT3DE enables a largely automated analysis of LV volumes, based on direct endocardial surface detection (Figure 1), and therefore avoids the need for geometric assumptions and is not hampered by foreshortened views. Several single-center studies have compared RT3DE with magnetic resonance imaging (MRI) that is currently considered the gold standard for the assessment of LV volumes [7–11]. These studies showed that conventional 2D echocardiography consistently underestimates LV volumes (mean bias with MRI for LV end-diastolic volume: 70±39 ml) and demonstrated the superiority of RT3DE in both accuracy and reproducibility (mean bias with MRI: 15±28 ml). Recently, RT3DE was also validated with a standardized protocol in a multi-centre setting with variable levels of experience [12]. In this study, RT3DE demonstrated to be an accurate tool, with only a minimal bias compared to MRI. Furthermore, this bias could be optimized easily by tracing the endocardial border to include the trabeculae in the LV cavity.

Evaluation of LV mass and shape

Several studies have demonstrated that an increased LV mass is an independent predictor of adverse cardiovascular outcomes, particularly in hypertensive patients [13]. Calculation of LV mass by either M-mode or 2D echocardiography suffers from the same limitations previously described for LV volume quantification. A new method derived from the full-volume 3D dataset is based on the identification of the LV epicardial and endocardial boundaries, providing the volume of LV myocardium. Next, LV mass is calculated multiplying myocardial volume for the specific weight of the myocardium. This method is rapid and reproducible and has a better agreement with MRI as compared to conventional methods [14–16]. In addition, RT3DE may be of great value for the analysis of LV shape. This technique can be applied with a qualitative approach to detect more accurately the presence of aneurysmatic, hypertrofic or non-compacted regions. In addition, RTDE can provide a quantitative approach with a 3D derived sphericity index that showed to accurately reflect LV shape and to be an early and independent predictor of LV remodeling after acute myocardial infarction [17].

Assessment of LV global and regional function

Assessment of global LV function is frequently performed using visual interpretation or "eye-balling", providing an estimate of LV ejection fraction (LVEF). This subjective interpretation may be comparable to the existing quantification methods derived from 2D LV volumes, and has limited reproducibility. In turn, RT3DE, based on 3D LV volumes, provides more accurate and reproducible quantification of LVEF with significant impact upon clinical decision-making [18,19].

Similarly, evaluation of regional LV function with conventional 2D echocardiography is routinely performed by visually integrating endocardial motion and wall thickness. However, endocardial segments that are poorly visualized may be incorrectly interpreted, and discrete areas of hypokinesis can be missed because these are areas are not included in the standard 2D views. Furthermore, transducer positioning errors may result in inadequate imaging planes. Therefore, the interpretation of wall motion abnormalities is extremely dependent on the experience of the reader and has a poor reproducibility. Since any possible 2D view is included in the 3D dataset and can be obtained by "cropping" the LV full-volume, RT3DE offers the opportunity of having the complete dynamic information on LV chamber contraction and to consistently reproduce the same imaging plane in sequential exams. Besides the conventional 2-, 4- and 3-chambers views, multiple parallel short axis slices can be used for systematic analysis of wall motion abnormalities. In addition, RT3DE has the potential of quantitative evaluation of regional LV function based on segmental analysis of 3D endocardial motion [8,20]. However, no studies have validated RT3DE for this specific analysis.

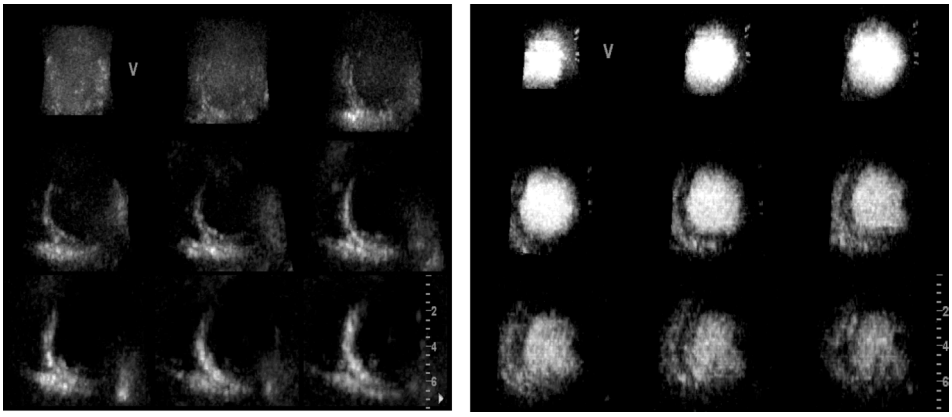


Figure 2. On the left panel, an example of moderate-to-poor quality RT3DE. In particular, the LV anterior and lateral walls are not visible. On the right panel, the improvement of endocardial border delineation with optimal LV chamber opacification in the same patient during contrast-enhanced RT3DE. The 3D dataset is cropped to extract multiple short-axis views at different levels of the LV.

In the subset of patients with inadequate RT3DE images, echo contrast agents could be of incremental value, as previously demonstrated for 2D echocardiography. Initial studies have shown that intravenous administration of echo contrast during RT3DE improves LV endocardial border visualization, increasing the feasibility, accuracy and reproducibility of both LV volumes quantification and LV global and regional function assessment [21,22] (Figure 2).

RT3DE during stress echocardiography

Considering the superiority over 2D echocardiography for the evaluation of LV global and regional function, RT3DE can be also applied in stress testing. This technique, in fact, has several potential advantages in this setting: 1) shorter scanning time, due to the simultaneous acquisition of 3 imaging planes (tri-plane imaging) or of a complete full-volume dataset, instead of the serially acquired 3 apical views; 2) no need to change the transducer position, avoiding a false-positive or negative stress echo due to imaging plane errors; 3) inclusion of the whole LV in one acquisition, with the potential of analyzing the standard long axis views but also multiple parallel short axis slices [23]. Initial studies showed similar sensitivity and specificity for 2D and 3D stress echo, but with a dramatically shorter scanning time [24]. Limitations of the clinical application may be related to the image quality, which is still lower than 2D echocardiography (but may be improved with the use of eco contrast) [25], and to the temporal resolution, which may be unsatisfactory especially during peak stress.

Assessment of LV dyssynchrony

In the last years, several studies emphasized the importance of LV dyssynchrony assessment to improve the selection of candidates to cardiac resynchronization therapy (CRT) [25,26], beyond the application of the current guidelines. However, data from the recent PROSPECT study revealed that standard echocardiography and tissue Doppler imaging (TDI) had modest reproducibility for the assessment of LV dyssynchrony and yielded modest sensitivity/specificity for prediction of response to CRT [27]. More recently, 3D echocardiographic approaches have been proposed for assessment of LV dyssynchrony. Color-coded TDI has been used in combination with tri-plane imaging, which allows for simultaneous visualization of the 3 apical views and may be able to improve the reproducibility of TDI measures [28]. Furthermore, RT3DE has been proposed as a promising technique for assessment of LV dyssynchrony based on analysis of LV regional volumetric changes. The LV 3D model is divided in 17 standard sub-volumes. For each volumetric segment, it is possible to derive time-volume data during the cardiac cycle and assess the time taken to reach the minimum systolic volume (Tmsv) (Figure 3). When all segments reach the minimum systolic volume at the same time, the LV

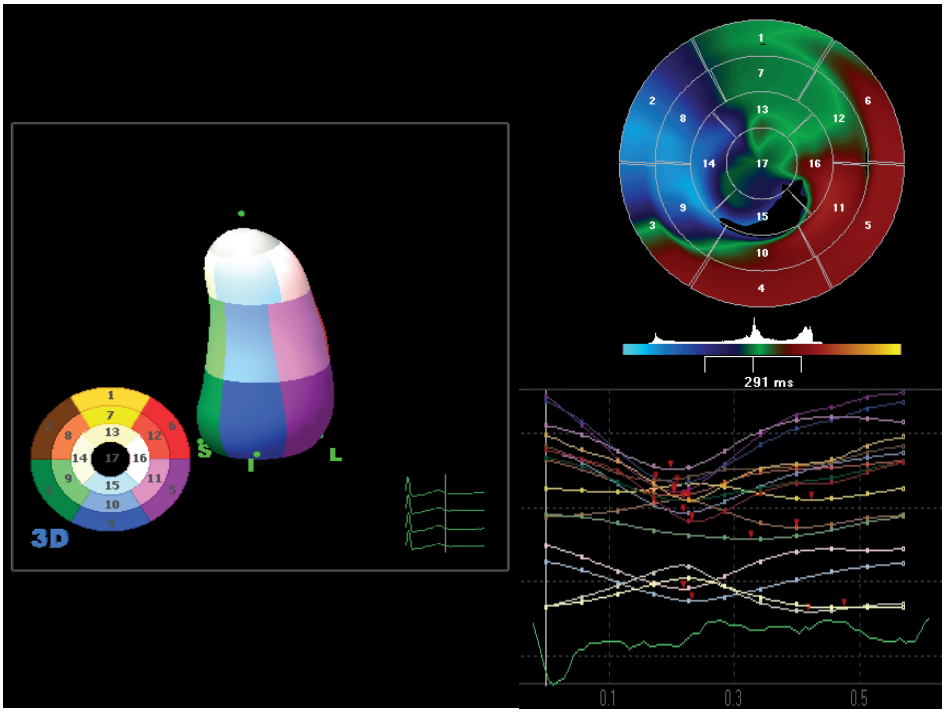


Figure 3. Example of the 3D LV model generated by post-processing of a RT3DE dataset and subdivided by the software in 17 sub-volumes (left panel). Right lower panel: for each volumetric segment, it is possible to derive time-volume curves over the cardiac cycle and assess the time needed to reach the minimum systolic volume (Tmsv, red dots). In this example, LV contraction is dyssynchronous and the standard deviation of 16 segment Tmsv, expressed in percentage of the cardiac cycle (SDI) is 11.7%.
Right upper panel: example of parametric image, which employs color-coding (blue indicating early mechanical activation and orange-red is late activation) to represent Tmsv. In this heart failure patient, the infero-postero-lateral wall (segments 4, 5, 6, 10 and 11) is clearly the latest activated region.

has synchronous contraction. Conversely, in a dyssynchronous ventricle a dispersion of the Tmsv is evident. The standard deviation of Tmsv for 16 segments (excluding the true apex) can be used as a marker of global LV dyssynchrony and can be expressed as a percentage of cardiac cycle rather than in ms to avoid the confounding effect of the heart rate. In this way, the 'systolic dyssynchrony index' (SDI) can be obtained. Therefore, in one acquisition RT3DE includes all myocardial segments and, measuring the regional volumetric changes, it evaluates the composite effect of longitudinal, radial and circumferential contraction. Kapetanakis et al[29] demonstrated the feasibility of SDI assessment in a large group of patients and normal subjects. The authors found an average SDI of 3.5% in normal individuals. In the patient population, the SDI showed an inverse correlation with LVEF and mean values ranged from 4.5% to 15.6% according to the degree of LV systolic dysfunction. Recently, the value of the SDI index for the prediction of CRT response was studied, both acutely and late after device

implantation. Marsan et al [30,31] demonstrated that a cut-off value of SDI of 6.4% has high sensitivity and specificity (88% and 85% respectively in a long-term follow-up study) and good reproducibility. The currently available software can also provide parametric images with a visual color-coded summary (in polar plot format) of LV regional contraction timings and a rapid identification of the latest activated LV wall (Figure 3).

In summary, RT3DE has several potential advantages over other echocardiographic techniques for the assessment of LV dyssynchrony: 1) LV dyssynchrony analysis is combined with highly accurate quantification of LV size and function which enables simultaneous evaluation of therapy success, 2) RT3DE includes all LV segments in the dyssynchrony analysis, using an angle-independent measurement, 3) RT3DE uses a semi-automated procedure potentially resulting in more reproducible measurements, and it allows for a rapid assessment of the area of latest mechanical activation.

ASSESSMENT OF LEFT ATRIUM SIZE AND FUNCTION

Left atrium (LA) enlargement is associated with several cardiovascular diseases and is a well known predictor of adverse cardiovascular outcomes, including atrial fibrillation, heart failure, stroke and death [32,33]. Accurate assessment of LA size is therefore crucial and, as recommended, should be based on LA volume measurement [5]. For this purpose, 2D echocardiography is the most commonly used imaging technique, although it relies on significant geometric assumptions and has poor test-retest reproducibility. Recently, RT3DE has been validated against MRI and showed to be more accurate and reproducible than 2D echocardiography for LA volume assessment [34,35], applying the same algorithm previously described for the LV (Figure 4). This technique can be used to quantify LA maximum volume (LAmax, just before mitral valve opening), but also minimum volume (LAmin, just before mitral valve closure) and the volume before atrial active contraction (LA_{preA}, obtained from the last frame before mitral valve reopening). All LA volumes should be indexed to the body surface area [5].

By providing a detailed analysis of the phasic changes of LA volumes throughout the cardiac cycle, RT3DE enables the assessment of different LA functions [36–38]. In fact, during LV systole and isovolumic relaxation, LA operates as a "reservoir" that receives blood from pulmonary veins and stores energy in form of pressure; during early diastole, it operates as a "conduit" for transfer blood into the LV; during late diastole, the LA "active" contraction contributes to LV stroke volume by 20–30% [39]. Using RT3DE, several studies suggested to explore these different functions assessing the following indices[36–38]:

1) Atrial expansion index = [(LAmax – Lamin)/LAmin] x100, which is considered an index of LA reservoir function and is influenced by LA wall stiffness and systolic displacement of the mitral annulus.

2) Passive atrial emptying fraction (LApassive) = [(LAmax – LApreA)/LAmax] x100, as an index of LA conduit function, which is mainly related to LV diastolic function.

3) Active atrial emptying fraction = [(LApreA – LAmin)/LApreA] x100, as an index of LA active function. The major determinants of this function are the heart rhythm, the intrinsic contractility of the atrial myocardium and LA_{preA} (according to the Frank-Starling effect).

Recent studies have used RT3DE to assess LA volume and function in different cardiac diseases, such as mitral valve diseases, atrial fibrillation, heart failure. Furthermore, the effect of specific therapies, such as cardiac resychronization therapy, atrial fibrillation ablation and mitral valve repair [31,40] on LA volume and functions has been evaluated. Using RT3DE, reverse remodeling of the LA and improvement in LA function has been demonstrated.

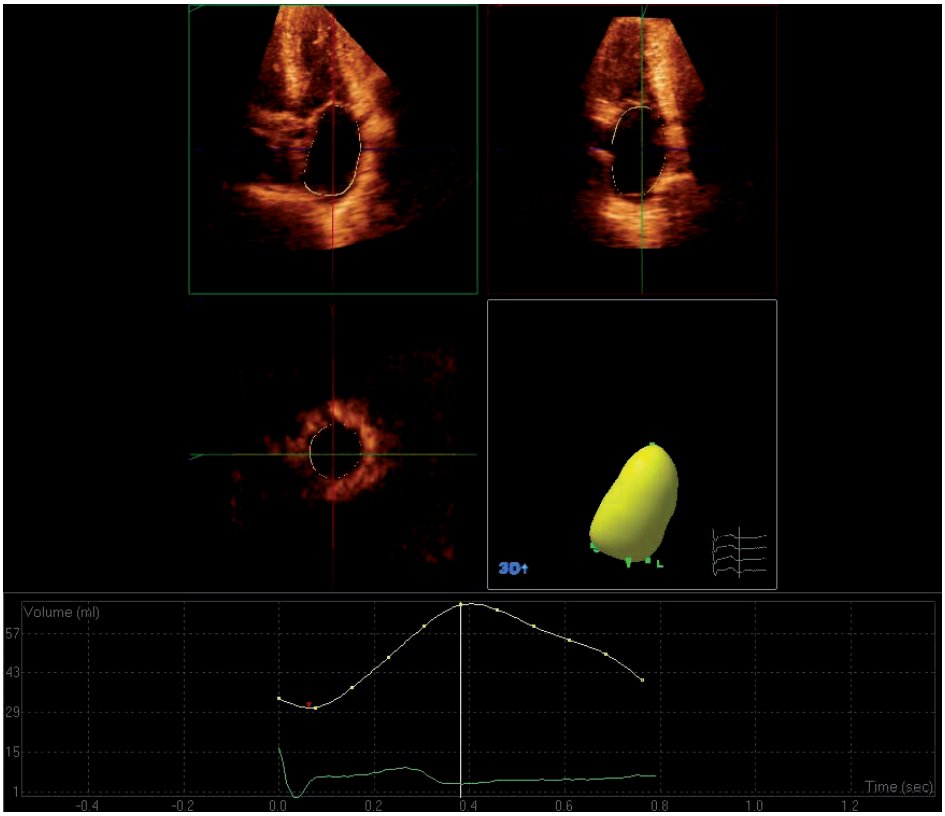


Figure 4. Assessment of LA volumes using RT3DE. Automatic border detection (yellow line) is obtained marking 5 reference points in the apical 2- and 4-chamber views (upper panel) and manual corrections can be made to exclude the LA appendage and the pulmonary vein ostia. The LA 3D model is automatically provided by the software (right lower panel) and can be evaluated also using the short-axis view (left lower panel). The changes in LA volumes during the heart cycle are plotted as a curve.

ASSESSMENT OF RIGHT VENTRICULAR SIZE AND FUNCTION

Because of its complex geometry, the assessment of right ventricular (RV) volumes and function is extremely challenging. Conventional 2D echocardiography may be therefore inadequate, because it relies on significant geometrical assumptions. However, an accurate assessment of RV size and function is of great importance because of the diagnostic and prognostic implications in several cardiac diseases. Without the need for geometrical modelling, RT3DE showed to be able to improve the accuracy and reproducibility of RV volumes quantification, as compared to 2D echocardiography [41,42]. Furthermore, a new software for the 3D dataset post-processing, specifically adapted for RV morphology, has recently been

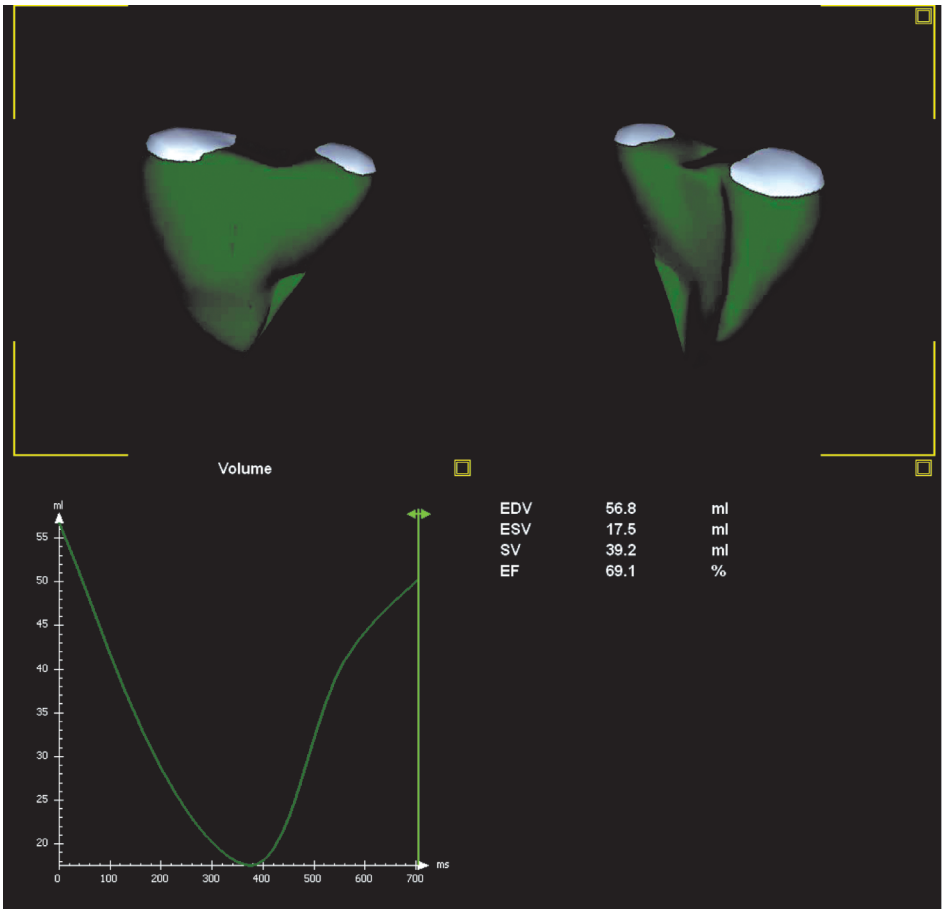


Figure 5. Example of a 3D right ventricular (RV) reconstruction in a normal subject, using a dedicated software (TomTec Imaging Systems, Munich, Germany). The RV 3D model (upper panel) is obtained applying a semiautomated border detection algorithm over a complete cardiac cycle and RV end-diastolic (EDV) and end-systolic (ESV) volumes are automatically displayed, together with RV stroke volume (SV) and RV ejection fraction (RVEF).

introduced (Figure 5). Tamborini et al applied this software in a large population for the assessment of RV volume and ejection fraction and found this analysis feasible and not time-consuming [43].

VALVULAR HEART DISEASES

The study of valvular heart diseases is one of the most important application of RT3DE. This technique is in fact ideally suited for a comprehensive assessment of the geometry of valves and subvalvular apparatus, given the non-planar anatomy and the complex function of these structures. By cropping the 3D dataset, unique "en face" views from both sides of the valve can be generated in real-time. Furthermore, any other possible oblique cut-plane or so-called multiplanar reconstructions (MPRs) can be easily obtained. Consequently, this approach certainly provides a more complete picture of valve diseases and may also lead to a better communication of the echocardiographic findings to the surgeon and to a more appropriate choice of treatment.

Mitral valve

RT3DE has provided important insights into mitral valve (MV) physiopathology and significantly contributed to the understanding of its anatomy and function. This technique was able to demonstrate the saddle shape of the annulus and the important interrelationship between mitral leaflets, chordae, papillary muscles and the LV [44]. Dedicated software, such as 4D MV-Assessment (TomTec Imaging systems, Unterschleissheim, Germany) and MV-Quantification (Philips Medical System, Bothell, Washington, USA), are now available to derive 3D quantification of the MV annulus dimension, leaflet surface, tenting volume, aorto-mitral angle and papillary muscles geometry (Figure 6).

In patients with mitral stenosis, RT3DE can provide accurate planimetry of the valve orifice area, identifying the correct plane of the valve opening and obtaining, by cropping the image, the real smallest orifice area (Figure 7). Compared with 2D traditional planimetry and Doppler-derived methods (pressure half-time, proximal isovelocity surface area), RT3DE showed the best agreement ($r = 0.9$) with the invasive measurement (mitral orifice area obtained using the Gorlin formula) and lower intra- and inter-observer variability [45,46]. Furthermore, this approach is less influenced by cardiac rhythm and hemodynamic conditions. In addition, RT3DE provides an accurate visualization of the degree of leaflet thickness, commissural fusion and calcification and can be applied after percutaneous mitral valvuloplasty to assess the commissural splitting.

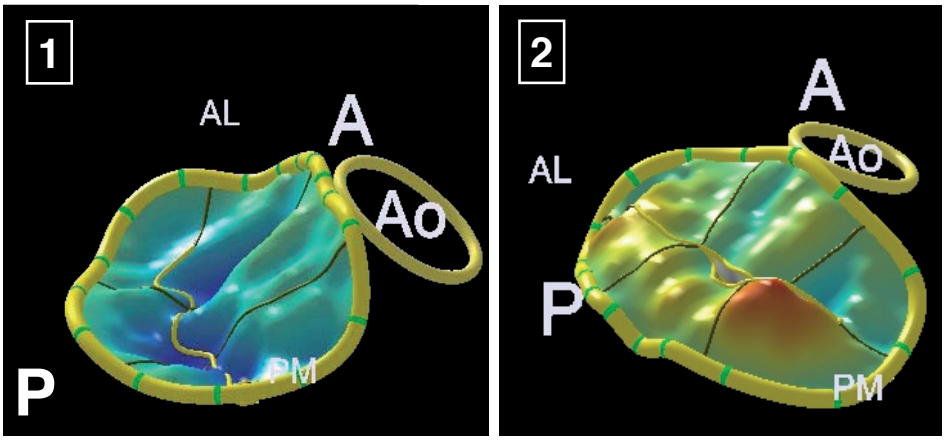


Figure 6. 3D reconstruction of mitral valve (MV) anatomy using MV-Quantification software (Philips Medical System, Bothell, Washington, USA) from transesophageal 3D images. In the first panel an example of normal MV anatomy. In the second panel an example of a prolapsed (P3) MV. From these models, several measurements of MV annulus, leaflets and subvalvular apparatus can be derived. Furthermore, the aorto-mitral relationship can be studied. A = anterior leaflet; AL = antero-lateral commisure; Ao = aortic valve; P = posterior leaflet; P = postero-medial commisure.

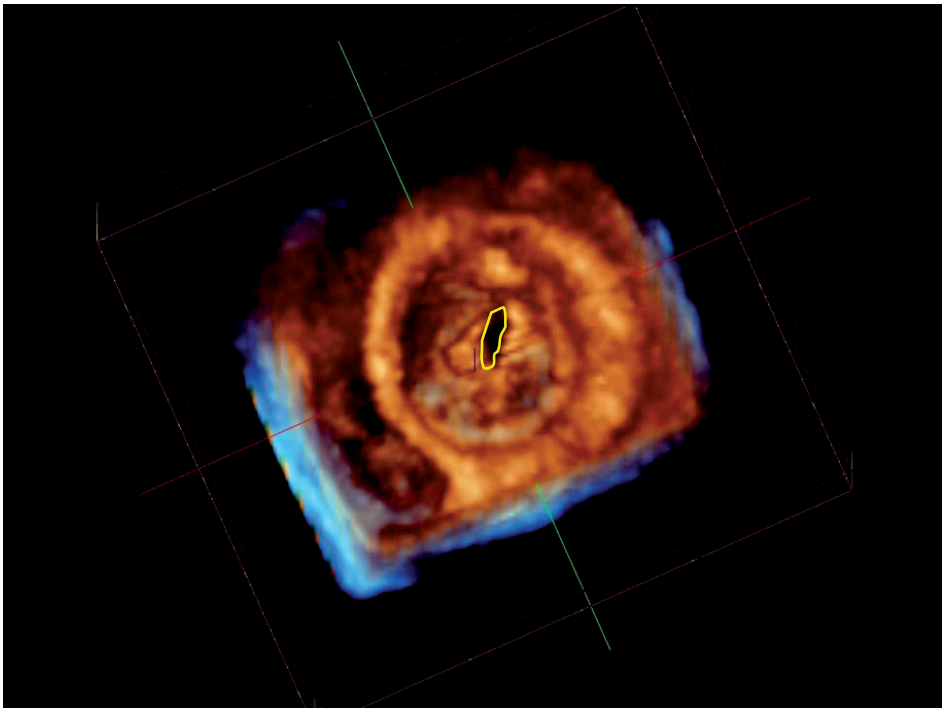


Figure 7. Mitral valve stenosis: 3D transversal section viewed from the apex of the left ventricle. The commissural fusion is clearly visible and the residual smallest mitral valve orifice can be measured directly (yellow line) identifying the correct plane.

The presence of MV prolapse is often over- or under-estimated using conventional 2D echocardiography, due to its non-planar leaflet-annulus relationship. In turn, RT3DE permits detailed visualization of the scallops involved, the chordal anatomy and the annulus enlargement that is often coexisting (Figure 6). Recently in more than 100 patients undergoing MV repair, Pepi et al demonstrated the accuracy of transthoracic and transesophageal RT3DE, as compared to 2D echocardiography, for the localization of MV prolapse [47]. Transthoracic RT3DE (90%) and 2D transesophageal (85%) approaches showed similar accuracy, slightly lower than transesophageal RT3DE (96%) but significantly higher than 2D transthoracic echocardiography. In particular, RT3DE was highly accurate also in patients with complex MV prolapse (commissural lesions, bileaflet lesions, P1 and P3 prolapse), helping the surgeon to plan an appropriate procedure and improving the likelihood of MV repair.

With the advent of a fully-sampled matrix array transducer, the application of Color Doppler RT3DE has become feasible, although still with a low temporal resolution. This modality

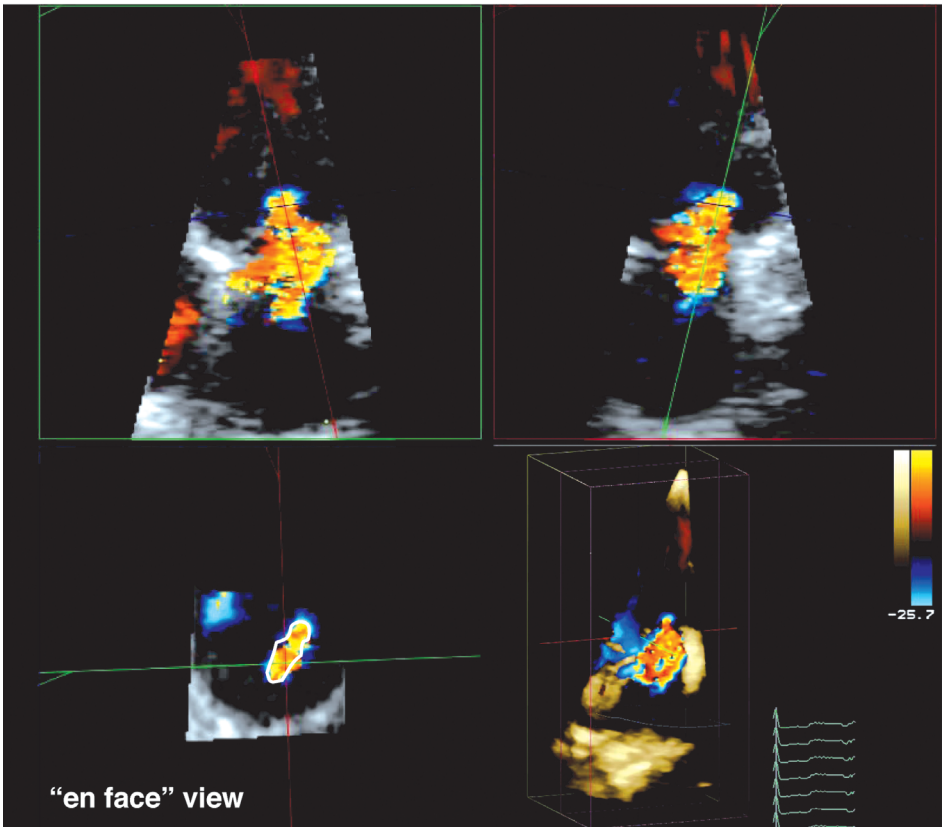


Figure 8. Direct assessment of size and shape of mitral valve effective regurgitant orifice area (EROA). The 3D dataset is manually cropped by an image plane perpendicularly oriented to the jet direction until the narrowest cross-sectional area of the jet. EROA is measured by manual planimetry (white line) of the color Doppler signal tilting the image in an 'en face' view.

provides important information to grade the severity of mitral regurgitation, crucial for appropriate patient management and timing of surgical intervention. In fact, Color Doppler RT3DE, allowing for an unlimited plan orientation and in particular for an "en face" view of the MV, provides a direct assessment of size and shape of the effective regurgitant orifice area (EROA), obviating the geometric assumptions applied by 2D echocardiography (Figure 8). Initial studies showed the incremental value of RT3DE measurements of EROA over 2D proximal isovelocity surface area and vena contracta width methods. The studies by Iwakura et al [48] and Kahlert et al [49] emphasized the importance of a 3D approach in patients with functional MR, in whom 2D echocardiography significantly underestimated the size of the regurgitant orifice.



Figure 9. Example of percutaneous aortic valve replacement in a patient with severe aortic stenosis (aortic valve area = 0.72 cm^2). In the upper panel, a 3D short-axis view of the aortic valve with extensive calcifications of the 3 cusps. The moment when the catheter goes through LV outflow tract and the aortic valve is depicted in the left lower panel. Of note, no echo-markers for the identification of the exact position of the balloon are available so far. In the lower right panel, a 3D image of the aortic valve prosthesis, with a clear visualization of the leaflets inside the stent.

Other valves

Compared with MV, experience visualizing aortic valve with RT3DE is limited, because of the low accessibility (in the far field) and the thin cusps. Most of the studies on aortic valve diseases have been performed using a real-time 3D transesophageal approach with a feasibility in over 80% of patients (more in native than in prosthetic valves) [50]. In patients with aortic stenosis, preliminary studies showed that the direct planimetry of the valve orifice is more accurate using RT3DE as compared to conventional 2D echocardiography [51]. In addition, the evaluation of the stenosis severity by the continuity equation was more accurate using a 3D approach for LV outflow tract measurement [52]. Recently, 3D transesophageal echocardiography has also been proposed as a new tool to guide and monitor percutaneous aortic valve replacement (Figure 9) [53].

The utility of RT3DE for the study of RV valves (tricuspid and pulmonary) has not been comprehensively explored. However, this technique has the unique capability of obtaining the short-axis plane of the tricuspid valve (TV) with a simultaneous visualization of the three leaflets that is not possible to achieve with conventional 2D echocardiography. This characteristic opens new opportunities for the evaluation of TV stenosis, regurgitation and congenital diseases. So far, initial observations, mostly in the pediatric population, showed promising results using RT3DE for the study of TV anatomy (annulus and leaflets) [54,55].

CONGENITAL HEART DISEASES

Three-dimensional echocardiography, using both reconstructions methods and real-time analysis, has been applied to detect several forms of congenital heart diseases. This technique permits a complete visualization of the complex spatial relationships of the cardiac lesions without extending the examination time. Furthermore, it provides a realistic and almost specimen-like preview of the surgical anatomy that facilitates planning of the surgical treatment. In patients with atrial or ventricular septal defects for example, RT3DE allows accurate evaluation of type, size, location and motion of the defect as well as the spatial relationships with the adjacent structures (Figures 10 and 11). Furthermore, measurement of the magnitude of shunting and information about adequacy of rims for device closure can be also obtained [53,56,57]. RT3DE also showed to reliably define anatomic details of bicuspid aortic valves, Tetralogy of Fallot, patent ductus arteriosus, sinus of Valsalva aneurysm, Ebstein's anomaly, subvalvular membranes and several other complex congenital diseases [58].

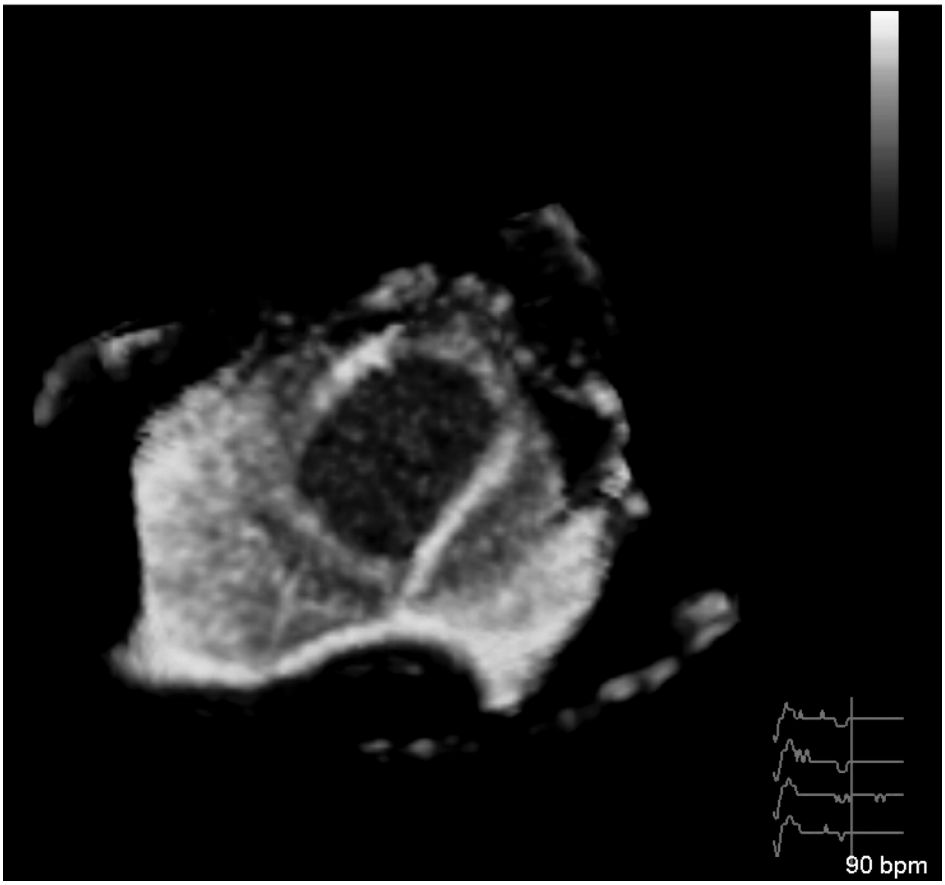


Figure 10. Left atrial view of an atrial septal defect using RT3DE. The size and the localization in relation with the aorta are clearly depicted. More important, the presence of a small rim surrounding the defect can be identified.

FUTURE APPLICATIONS

Considering the abovementioned advantages over conventional 2D echocardiography, it is likely that RT3DE will become a routine part of most echocardiographic examinations. Furthermore, future advances in transducer and computer technology will allow for miniaturized probes with larger scanning volume, higher spatial and temporal resolution and more sophisticated and completely automated quantification software (including 3D speckle tracking analysis for assessment of myocardial strain and torsion mechanics).

Particularly promising is the potential application of RT3DE to guide intracardiac procedures, mainly using the transesophageal approach. In fact, this technique may be useful in various transcatheter interventions: 1) percutaneous MV annuloplasty, for the identification

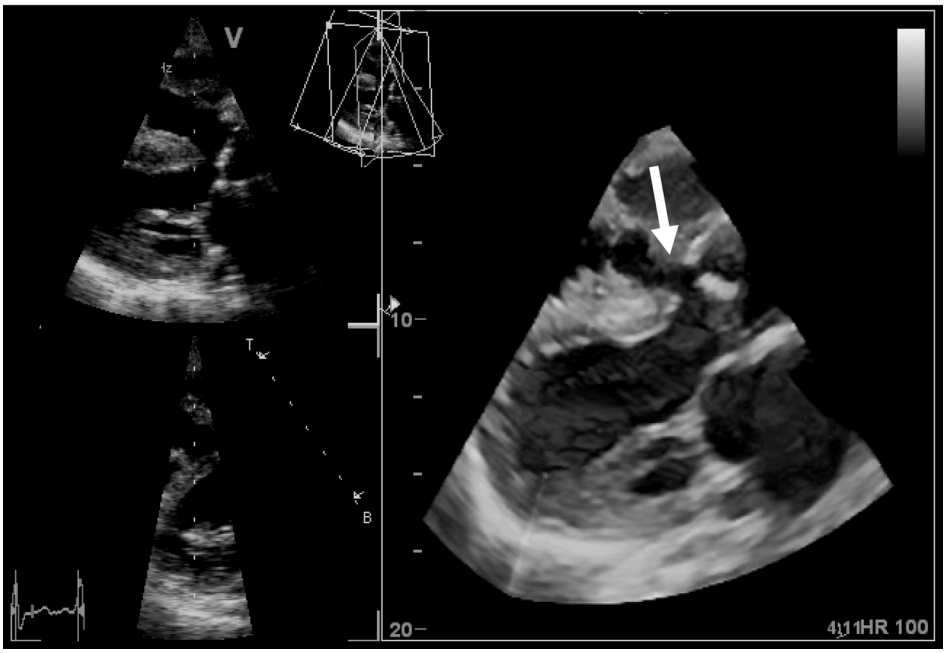


Figure 11. Real-time 3D echocardiogram (sagittal view) of a patient with a double outlet right ventricle with a large ventricular septum defect (see arrow).

of the coronary sinus and quantification of the angle between the aortic orifice and the MV plane; 2) percutaneous aortic valve replacement, for the selection of the correct size and position of the prosthesis and on-line monitoring of the procedure; 3) atrial septal defect and patent foramen ovale closures with occluder devices [53]; 4) elecrophysiological procedures, guiding the transeptal puncture and the positioning of the ablation catheters in the LA, eventually in combination with electroanatomical mapping systems [59]. In all these procedures, transesophageal RT3DE may improve the imaging guidance and reduce the radiation exposure from fluoroscopy.

CONCLUSIONS

RT3DE has made an important transition from a research tool to a clinically applicable imaging technique. Main advantages of this modality over conventional 2D echocardiography are the accurate quantification of cardiac chamber size and function and the possibility of unlimited image plane orientations for better understanding of valvular or congenital heart diseases.

REFERENCES

1. Hung J, Lang R, Flachskampf F et al. 3D echocardiography: a review of the current status and future directions. *J Am Soc Echocardiogr.* 2007;20:213-233.
2. Gill EA, Klas B. Three-dimensional echocardiography: an historical perspective. *Cardiol Clin.* 2007;25:221-229.
3. Sugeng L, Shernan SK, Salgo IS et al. Live 3-dimensional transesophageal echocardiography initial experience using the fully-sampled matrix array probe. *J Am Coll Cardiol.* 2008;52:446-449.
4. Salgo IS. Three-dimensional echocardiographic technology. *Cardiol Clin.* 2007;25:231-239.
5. Lang RM, Bierig M, Devereux RB et al. Recommendations for chamber quantification. *Eur J Echocardiogr.* 2006;7:79-108.
6. Gordon EP, Schnittger I, Fitzgerald PJ, Williams P, Popp RL. Reproducibility of left ventricular volumes by two-dimensional echocardiography. *J Am Coll Cardiol.* 1983;2:506-513.
7. Arai K, Hozumi T, Matsumura Y et al. Accuracy of measurement of left ventricular volume and ejection fraction by new real-time three-dimensional echocardiography in patients with wall motion abnormalities secondary to myocardial infarction. *Am J Cardiol.* 2004;94:552-558.
8. Corsi C, Lang RM, Veronesi F et al. Volumetric quantification of global and regional left ventricular function from real-time three-dimensional echocardiographic images. *Circulation.* 2005;112:1161-1170.
9. Gutierrez-Chico JL, Zamorano JL, Perez de Isla et al. Comparison of left ventricular volumes and ejection fractions measured by three-dimensional echocardiography versus by two-dimensional echocardiography and cardiac magnetic resonance in patients with various cardiomyopathies. *Am J Cardiol.* 2005;95:809-813.
10. Jenkins C, Bricknell K, Hanekom L, Marwick TH. Reproducibility and accuracy of echocardiographic measurements of left ventricular parameters using real-time three-dimensional echocardiography. *J Am Coll Cardiol.* 2004;44:878-886.
11. Kuhl HP, Schreckenberg M, Rulands D et al. High-resolution transthoracic real-time three-dimensional echocardiography: quantitation of cardiac volumes and function using semi-automatic border detection and comparison with cardiac magnetic resonance imaging. *J Am Coll Cardiol.* 2004;43:2083-2090.
12. Mor-Avi V, Jenkins C, Kuhl HP et al. Real-time 3-dimensional echocardiographic quantification of left ventricular volumes: multicenter study for validation with magnetic resonance imaging and investigation of sources of error. *JACC Cardiovasc Imaging. 2008;*1: 413-423.
13. Levy D, Garrison RJ, Savage DD, Kannel WB, Castelli WP. Prognostic implications of echocardiographically determined left ventricular mass in the Framingham Heart Study. *N Engl J Med.* 1990;322:1561-1566.
14. Caiani EG, Corsi C, Sugeng L et al. Improved quantification of left ventricular mass based on endocardial and epicardial surface detection with real time three dimensional echocardiography. *Heart.* 2006;92:213-219.
15. Mor-Avi V, Sugeng L, Weinert L et al. Fast measurement of left ventricular mass with real-time three-dimensional echocardiography: comparison with magnetic resonance imaging. *Circulation.* 2004;110:1814-1818.
16. Takeuchi M, Nishikage T, Mor-Avi V et al. Measurement of left ventricular mass by real-time three-dimensional echocardiography: validation against magnetic resonance and comparison with two-dimensional and m-mode measurements. *J Am Soc Echocardiogr.* 2008;21:1001-1005.

17. Mannaerts HF, van der Heide JA, Kamp O, Stoel MG, Twisk J, Visser CA. Early identification of left ventricular remodelling after myocardial infarction, assessed by transthoracic 3D echocardiography. *Eur Heart J.* 2004;25:680-687.
18. Hare JL, Jenkins C, Nakatani S, Ogawa A, Yu CM, Marwick TH. Feasibility and clinical decision-making with 3D echocardiography in routine practice. *Heart.* 2008;94:440-445.
19. Mor-Avi V, Lang RM. Three-dimensional echocardiographic evaluation of the heart chambers: size, function, and mass. *Cardiol Clin.* 2007;25:241-251.
20. Frielingsdorf J, Franke A, Kuhl HP et al. Evaluation of regional systolic function in hypertrophic cardiomyopathy and hypertensive heart disease: a three-dimensional echocardiographic study. *J Am Soc Echocardiogr.* 1998;11:778-786.
21. Caiani EG, Coon P, Corsi C et al. Dual triggering improves the accuracy of left ventricular volume measurements by contrast-enhanced real-time 3-dimensional echocardiography. *J Am Soc Echocardiogr.* 2005;18:1292-1298.
22. Krenning BJ, Kirschbaum SW, Soliman OI et al. Comparison of contrast agent-enhanced versus non-contrast agent-enhanced real-time three-dimensional echocardiography for analysis of left ventricular systolic function. *Am J Cardiol.* 2007;100:1485-1489.
23. Franke A. Real-time three-dimensional echocardiography in stress testing: bi- and triplane imaging for enhanced image acquisition. *Cardiol Clin.* 2007;25:261-265.
24. Matsumura Y, Hozumi T, Arai K et al. Non-invasive assessment of myocardial ischaemia using new real-time three-dimensional dobutamine stress echocardiography: comparison with conventional two-dimensional methods. *Eur Heart J.* 2005;26:1625-1632.
25. Takeuchi M, Otani S, Weinert L, Spencer KT, Lang RM. Comparison of contrast-enhanced real-time live 3-dimensional dobutamine stress echocardiography with contrast 2-dimensional echocardiography for detecting stress-induced wall-motion abnormalities. *J Am Soc Echocardiogr.* 2006;19:294-299.
26. Bax JJ, Abraham T, Barold SS et al. Cardiac resynchronization therapy: Part 1--issues before device implantation. *J Am Coll Cardiol.* 2005;46:2153-2167.
27. Chung ES, Leon AR, Tavazzi L et al. Results of the Predictors of Response to CRT (PROSPECT) Trial. *Circulation.* 2008;117:2608-2616.
28. Van de Veire NR, Yu CM, Ajmone-Marsan N et al. Triplane tissue Doppler imaging: a novel three-dimensional imaging modality that predicts reverse left ventricular remodelling after cardiac resynchronisation therapy. *Heart.* 2008;94:e9.
29. Kapetanakis S, Kearney MT, Siva A, Gall N, Cooklin M, Monaghan MJ. Real-time three-dimensional echocardiography: a novel technique to quantify global left ventricular mechanical dyssynchrony. *Circulation.* 2005;112:992-1000.
30. Marsan NA, Bleeker GB, Ypenburg C et al. Real-time three-dimensional echocardiography permits quantification of left ventricular mechanical dyssynchrony and predicts acute response to cardiac resynchronization therapy. *J Cardiovasc Electrophysiol.* 2007;19:392-399.
31. Marsan NA, Bleeker GB, Ypenburg C et al. Real-time three-dimensional echocardiography as a novel approach to assess left ventricular and left atrium reverse remodeling and to predict response to cardiac resynchronization therapy. *Heart Rhythm.* 2008;5:1257-1264.
32. Benjamin EJ, D'Agostino RB, Belanger AJ, Wolf PA, Levy D. Left atrial size and the risk of stroke and death. The Framingham Heart Study. *Circulation.* 1995;92:835-841.
33. Rossi A, Cicoira M, Zanolla L et al. Determinants and prognostic value of left atrial volume in patients with dilated cardiomyopathy. *J Am Coll Cardiol.* 2002;40:1425.

34. Khankirawatana B, Khankirawatana S, Lof J, Porter TR. Left atrial volume determination by three-dimensional echocardiography reconstruction: validation and application of a simplified technique. *J Am Soc Echocardiogr.* 2002;15:1051-1056.
35. Poutanen T, Ikonen A, Vainio P, Jokinen E, Tikanoja T. Left atrial volume assessed by transthoracic three dimensional echocardiography and magnetic resonance imaging: dynamic changes during the heart cycle in children. *Heart.* 2000;83:537-542.
36. Anwar AM, Geleijnse ML, Soliman OI, Nemes A, Ten Cate FJ. Left atrial Frank-Starling law assessed by real-time, three-dimensional echocardiographic left atrial volume changes. *Heart.* 2007;93:1393-1397.
37. Poutanen T, Jokinen E, Sairanen H, Tikanoja T. Left atrial and left ventricular function in healthy children and young adults assessed by three dimensional echocardiography. *Heart.* 2003;89:544-549.
38. Spencer KT, Mor-Avi V, Gorcsan J, III et al. Effects of aging on left atrial reservoir, conduit, and booster pump function: a multi-institution acoustic quantification study. *Heart.* 2001;85:272-277.
39. Abhayaratna WP, Seward JB, Appleton CP et al. Left atrial size: physiologic determinants and clinical applications. *J Am Coll Cardiol.* 2006;47:2357-2363.
40. Marsan NA, Tops LF, Holman ER et al. Comparison of left atrial volumes and function by real-time three-dimensional echocardiography in patients having catheter ablation for atrial fibrillation with persistence of sinus rhythm versus recurrent atrial fibrillation three months later. *Am J Cardiol.* 2008;102:847-853.
41. Chen G, Sun K, Huang G. In vitro validation of right ventricular volume and mass measurement by real-time three-dimensional echocardiography. *Echocardiography.* 2006;23:395-399.
42. Kjaergaard J, Petersen CL, Kjaer A, Schaadt BK, Oh JK, Hassager C. Evaluation of right ventricular volume and function by 2D and 3D echocardiography compared to MRI. *Eur J Echocardiogr.* 2006;7:430-438.
43. Tamborini G, Brusoni D, Torres Molina JE et al. Feasibility of a new generation three-dimensional echocardiography for right ventricular volumetric and functional measurements. *Am J Cardiol.* 2008;102:499-505.
44. Sugeng L, Coon P, Weinert L et al. Use of real-time 3-dimensional transthoracic echocardiography in the evaluation of mitral valve disease. *J Am Soc Echocardiogr.* 2006;19:413-421.
45. Zamorano J, Perez de Isla, Sugeng L et al. Non-invasive assessment of mitral valve area during percutaneous balloon mitral valvuloplasty: role of real-time 3D echocardiography. *Eur Heart J.* 2004;25:2086-2091.
46. Zamorano J, Cordeiro P, Sugeng L et al. Real-time three-dimensional echocardiography for rheumatic mitral valve stenosis evaluation: an accurate and novel approach. *J Am Coll Cardiol.* 2004;43:2091-2096.
47. Pepi M, Tamborini G, Maltagliati A et al. Head-to-head comparison of two- and three-dimensional transthoracic and transesophageal echocardiography in the localization of mitral valve prolapse. *J Am Coll Cardiol.* 2006;48:2524-2530.
48. Iwakura K, Ito H, Kawano S et al. Comparison of orifice area by transthoracic three-dimensional Doppler echocardiography versus proximal isovelocity surface area (PISA) method for assessment of mitral regurgitation. *Am J Cardiol.* 2006;97:1630-1637.
49. Kahlert P, Plicht B, Schenk IM, Janosi RA, Erbel R, Buck T. Direct assessment of size and shape of noncircular vena contracta area in functional versus organic mitral regurgitation using real-time three-dimensional echocardiography. *J Am Soc Echocardiogr.* 2008;21:912-921.

50. Kasprzak JD, Salustri A, Roelandt JR, Ten Cate FJ. Three-Dimensional Echocardiography of the Aortic Valve: Feasibility, Clinical Potential, and Limitations. *Echocardiography.* 1998;15:127-138.
51. Ge S, Warner JG, Jr., Abraham TP et al. Three-dimensional surface area of the aortic valve orifice by three-dimensional echocardiography: clinical validation of a novel index for assessment of aortic stenosis. *Am Heart J.* 1998;136:1042-1050.
52. Poh KK, Levine RA, Solis J et al. Assessing aortic valve area in aortic stenosis by continuity equation: a novel approach using real-time three-dimensional echocardiography. *Eur Heart J.* 2008;29:2526-2535.
53. Balzer J, Kuhl H, Rassaf T et al. Real-time transesophageal three-dimensional echocardiography for guidance of percutaneous cardiac interventions: first experience. *Clin Res Cardiol.* 2008;97:565-574.
54. Faletra F, La Marchesina U, Bragato R, De Chiara F. Three dimensional transthoracic echocardiography images of tricuspid stenosis. *Heart.* 2005;91:499.
55. Nii M, Roman KS, Macgowan CK, Smallhorn JF. Insight into normal mitral and tricuspid annular dynamics in pediatrics: a real-time three-dimensional echocardiographic study. *J Am Soc Echocardiogr.* 2005;18:805-814.
56. Sinha A, Nanda NC, Misra V et al. Live three-dimensional transthoracic echocardiographic assessment of transcatheter closure of atrial septal defect and patent foramen ovale. *Echocardiography.* 2004;21:749-753.
57. van den Bosch AE, Ten Harkel DJ, McGhie JS et al. Characterization of atrial septal defect assessed by real-time 3-dimensional echocardiography. *J Am Soc Echocardiogr.* 2006;19:815-821.
58. Del Pasqua A, Sanders SP, de Zorzi A et al. Impact of Three-Dimensional Echocardiography in Complex Congenital Heart Defect Cases: The Surgical View. *Pediatr Cardiol.* 2008.
59. Chierchia GB, Capulzini L, de Asmundis C et al. First experience with real-time three-dimensional transoesophageal echocardiography-guided transseptal in patients undergoing atrial fibrillation ablation. *Europace.* 2008;10:1325-1328.

PART IA

Real-time three-dimensional echocardiography as a novel approach to assess left ventricular size, function and dyssynchrony

CHAPTER 2

Predicting response to CRT. The value of two- and three-dimensional echocardiography

N Ajmone Marsan, O A Breithardt, V Delgado, M Bertini, and L F Tops

Europace 2008;10 Suppl 3:iii73–9.

INTRODUCTION

In patients with severe, symptomatic drug-refractory heart failure and wide QRS complex, cardiac resynchronization therapy (CRT) has been demonstrated to have significant favorable effects on left ventricular (LV) remodeling and function and on clinical outcomes [1]. However, a consistent percentage of patients fail to benefit from CRT when the established clinical and electrocardiographic selection criteria are applied [2]. In particular, 20 to 30% of patients do not experience any clinical improvement after CRT and 40 to 50% of patients do not show any significant LV reverse remodeling or improvement in LV function. Therefore, at present attention has shifted towards a more accurate selection of CRT candidates, beyond the standard use of NYHA functional class, LV ejection fraction and QRS complex. Several contributory factors to CRT non-response have been reported, such as inappropriate LV lead positioning and, in patients with ischemic cardiomyopathy, the extent and location of scar tissue and viable myocardium [3,4]. Furthermore, the presence of significant baseline LV mechanical dyssynchrony has been demonstrated to be predictive for a positive response to CRT [5]. Echocardiography has been extensively used for a direct assessment of LV dyssynchrony with different approaches. In this review, the value of 2D and 3D echocardiographic modalities to predict response to CRT will be discussed, highlighting the advantages and drawbacks of each modality.

TWO-DIMENSIONAL ECHOCARDIOGRAPHY

Two-dimensional (2D) echocardiography is widely applied in the selection and management of CRT patients, due to the low cost, broad availability, non-invasive approach and the extensive information that this technique can provide: 1) 2D echocardiography confirms the presence of an impaired LV systolic function at baseline and can evaluate CRT success at follow-up in terms of LV reverse remodeling and/or improvement of LV function; 2) 2D echocardiography evaluates the presence of other significant cardiac structural abnormalities that might affect therapy success, such as valvular pathologies and the extent of akinetic/thin (probably scar) myocardium; 3) 2D echocardiography can assess the presence of LV dyssynchrony with adequate temporal resolution.

Visual assessment of wall motion synchrony by 2D echocardiography is probably the first and most straightforward step to approach a possible CRT candidate. However, the human eye with its limited temporal resolution is not able to precisely quantify the extent and location of myocardial dyssynchrony [6]. Nevertheless, it is possible to identify typical phenomena that are associated with myocardial dyssynchrony. In the presence of delayed electrical conduction, the interventricular septum typically shows a characteristic multiphasic motion pattern (abnormal relaxation pattern) and the LV often demonstrates a rotating motion (typi-

cally oriented counter-clockwise in late systole, often also referred to as "rocking motion" or "apical shuffle"), as seen in the apical 4-chamber view. In a small study on 53 patients, Jansen et al. were able to demonstrate that the identification of these two phenomena predicted the presence of LV dyssynchrony (defined by tissue Doppler criteria) and LV reverse remodeling after CRT with a sensitivity of more than 90% and a positive predictive value above 85% [7]. The septal multiphasic motion pattern can be also detected and quantified from the M-mode short axis view at the level of the papillary muscles. The 'septal-to-posterior wall motion delay' is calculated as the shortest interval between the maximal posterior displacement of the septum and the maximal inward displacement of the posterior wall [8]. However, this parameter demonstrated a limited predictive value and, more importantly, a poor feasibility especially in ischemic patients [9].

Two-dimensional echocardiography also permits the quantification of myocardial dyssynchrony based on the analysis of endocardial wall motion. Breithardt et al. evaluated a semi-automated contour detection algorithm, which had been originally developed for stress-echocadiography, in a small cohort of CRT patients [10]. Semi-automatically contoured septal and lateral wall motion curves were constructed from digitized video recordings of the apical 4-chamber view and averaged over several cardiac cycles to calculate the phase angle difference between the opposing walls. Patients with significant dyssynchrony, defined by a phase angle difference below -25° or above +25°, were better hemodynamic CRT responders, defined by a >10% increase in LV peak positive dP/dt and/or pulse pressure. This quantitative approach is obviously limited by the restriction to two opposing walls, but similar algorithms have later been transferred to 3D technology.

Kawaguchi et al. quantified LV dyssynchrony before and during CRT with contrast enhanced 2D echocardiography [11]. Temporal and spatial pixel intensity changes were analyzed in up to 50 sequential beats (contrast variability imaging) and demonstrated improved septal inward motion and reduced LV septal-lateral dyssynchrony by CRT. This novel approach is clearly limited by its time-consuming and costly image acquisition which necessitates the intravenous administration of contrast agents and the lack of a widely commercially available software tool.

Modern quantitative analyses, such as tissue Doppler imaging (TDI) and speckle tracking analysis, are also based on 2D echocardiography and are discussed in more detail elsewhere in this Supplement. Briefly, TDI is at present the most frequently used technique for LV dyssynchrony assessment [12]. In particular, this technique allows the measurement of myocardial regional velocities with a very high temporal-resolution and, in relation to the electrical activity (QRS complex), enables the assessment of the electro-mechanical delay of 2 or more LV segments. Both two- and multiple-segmental approaches demonstrated their value for the prediction of clinical and echocardiographic response to CRT with high sensitivity and specificity [13,14]. Recently, tissue synchronization imaging (TSI) has become available to simplify this approach, providing an intuitive color-coded image of the myocardium according to the

automatically detected time-to-peak systolic velocity (Ts) of each LV segment, together with the possibility of an automated quantitative assessment [15]. Furthermore, when myocardial velocities are known, several other parameters can be derived off-line. Integrating velocities over time results in myocardial displacement, i.e. the total amount of tissue movement during systole. Alternatively, the spatial derivative of velocity and displacement leads to strain rate and strain calculation, respectively, as myocardial deformation measurements [16] (Figure 1). However, these parameters have proven not to be as robust as myocardial velocity parameters for predicting response to CRT [14,17], probably due to the relatively poor reproducibility, independent of the operator experience. Furthermore, for all myocardial motion and deformation measurements, angle-dependency of TDI analysis has to be considered a major drawback, limiting the application of this technique to few LV segments and to one component of contraction (longitudinal, radial and circumferential) at a time.

Speckle tracking analysis is a novel echocardiographic technique that allows myocardial deformation measurements (strain and strain rate) from standard 2D gray scale images, track-

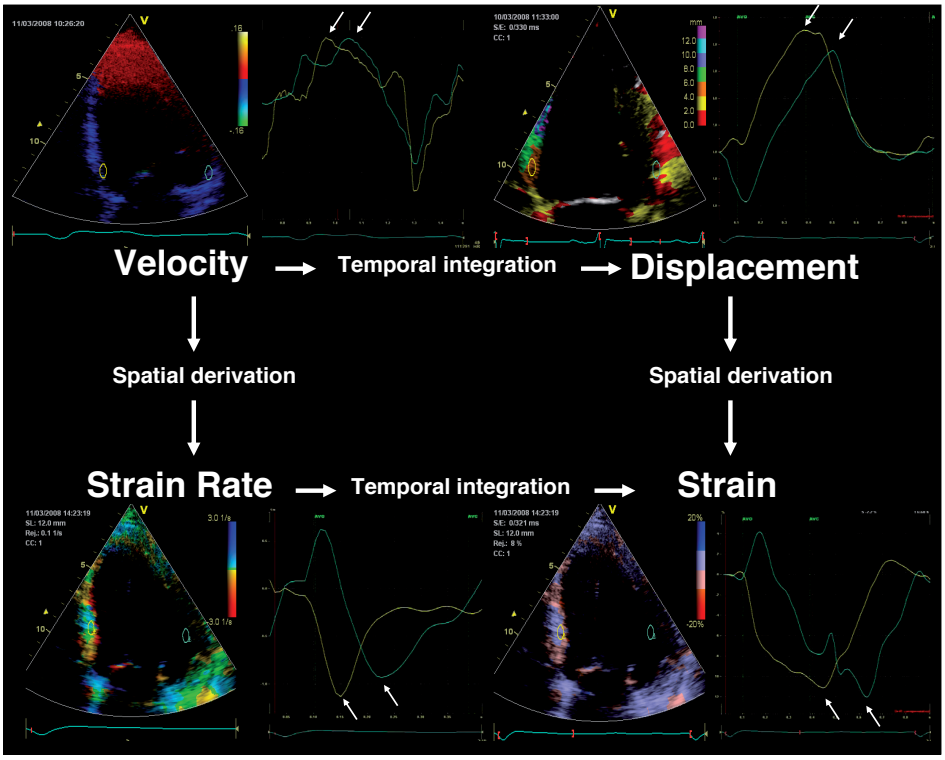


Figure 1. Color-coded apical 4-chamber TDI images with off-line post-processing velocity, displacement, strain rate and strain tracings. The arrows indicate the systolic peak of the septum and lateral wall in each curve. Myocardial displacement is obtained integrating velocity over time. Myocardial strain rate is the spatial derivative of velocity and can be integrated throughout systole to obtain strain

ing frame-to-frame the movement of natural myocardial acoustic markers ('speckles'). The advantage of this technique, compared to TDI, is the angle-independency, allowing for the assessment of the 3 components of myocardial contraction (longitudinal, radial and circumferential direction) in all LV segments. Initial studies have demonstrated the value of radial dyssynchrony, assessed with this technique, to predict response to CRT [18,19]. Furthermore, Gorcsan and colleagues suggested that combining radial dyssynchrony, measured by speckle tracking, with longitudinal dyssynchrony, measured by TDI, predicted echocardiographic response to CRT (88% sensitivity and 80% specificity) significantly better than either technique alone [20].

THREE-DIMENSIONAL ECHOCARDIOGRAPHY

Early approaches to 3D echocardiography were based on the principle that a 3D data set is reconstructed from a series of 2D images obtained using either freehand scanning or a mechanically driven rotating transducer that sequentially recorded images at predefined intervals. This approach was limited by several technical aspects during image acquisition and required significant time-consuming off-line data processing [21]. Nowadays, 3D echocardiography is a real-time technique that permits a rapid (5–7 minutes) post-processing of the 3D dataset off-line or on the scanner itself. In addition, the post-processing of the 3D dataset provides, in one single analysis, highly accurate quantification of LV volumes and function as well as the assessment of LV dyssynchrony with different modalities. In particular, 3D echocardiography, applying a semi-automated contour-tracing algorithm in multiple planes, has been validated against MRI and found to be more accurate and reproducible than 2D echocardiography for the assessment of LV volumes and function [22,23]. These are crucial measurements in the evaluation of CRT success and carry out important prognostic implications [24]. Furthermore, a 3D assessment of LV dyssynchrony has the advantage of a simultaneous acquisition of all LV segments, allowing for more extensive intersegment comparison, as compared with other 2D techniques, and avoiding the problem of heart rate variability during image acquisition.

Tri-plane tissue Doppler imaging

Recently, color-coded TDI has been used in combination with tri-plane imaging, which allows for analysis of the 3D dataset along 3 major planes with a simultaneous visualization of the apical 4-, 2- and 3-chamber views (Figure 2). Sample volumes can be placed simultaneously in 12 LV segments and Ts of any LV segment can be compared during the same heartbeat. Van de Veire et al. applied this technique in 60 patients undergoing CRT and demonstrated that the standard deviation of Ts of 12 (6 basal and 6 mid segments) LV segments (Ts-SD-12), with a cut-off value of ≥33 ms, was able to predict echocardiographic response with a sensitivity

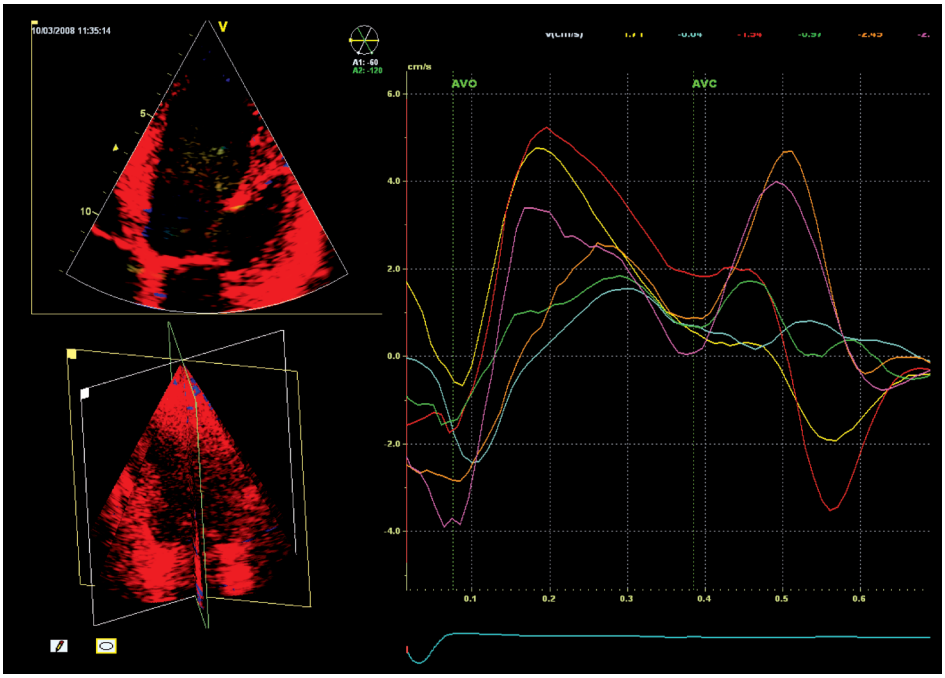


Figure 2. Tri-plane TDI: example of the myocardial velocity curves that can be derived by positioning the sample volume in any LV segment of the tri-plane dataset (in this figure only 6 segments are displayed). This patient has substantial LV dyssynchrony with a wide dispersion of Ts: Ts-SD-12 is 57.5 ms (calculated between the aortic valve opening, AVO, and the aortic valve closure, AVC).

of 90% and a specificity of 83% [25]. These findings further support the previous results of Yu et al. using single-plane TDI [14].

Similarly, it has become possible to apply TSI to the tri-plane view and this approach was found useful to identify the area of latest activation within the LV (Figure 3). Further studies are needed to confirm the feasibility of this technique in the clinical practice and to explore the value to predict response to CRT [25].

Analysis of volumetric changes by real-time three-dimensional echocardiography

Real-time three-dimensional echocardiography (RT3DE) has emerged as a novel echocardiographic technique for the assessment of LV dyssynchrony based on the analysis of regional volumetric changes. Briefly, LV 3D model is subdivided by the software in 17 wedge shaped (apart from the apex) sub-volumes according to standard segmentation (Figure 4). For the whole LV and for each volumetric segment, it is possible to derive time-volume data for the entire cardiac cycle and assess the time taken to reach the minimum systolic volume (Tmsv)

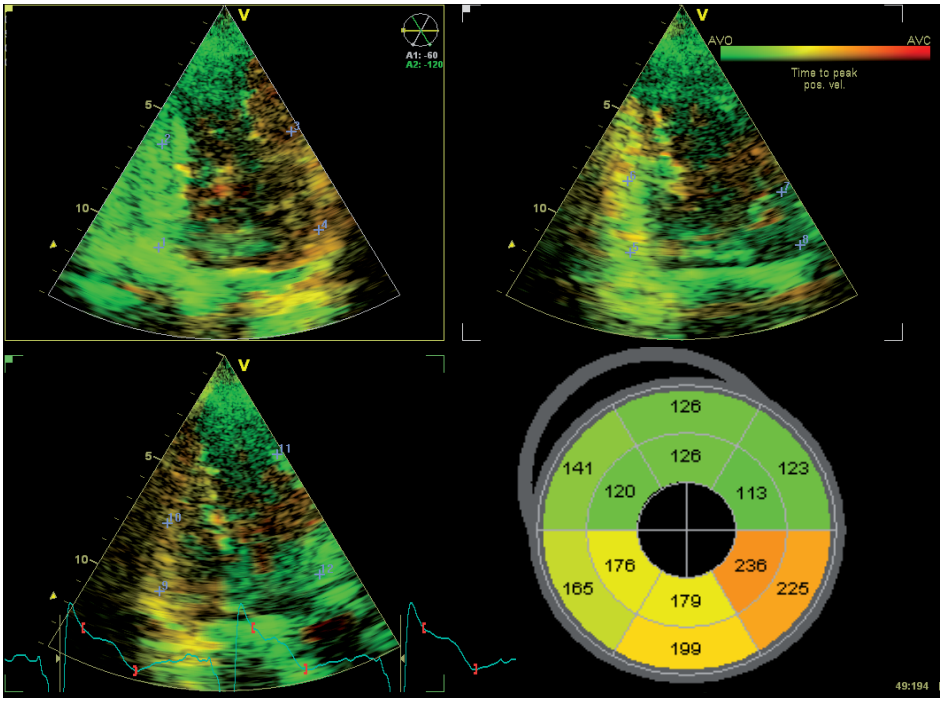


Figure 3. Example of tissue synchronisation imaging (TSI) applied to the tri-plane dataset. The time-to-peak systolic velocity is automatically detected for each LV segment (displayed as numbers in the polar plot) and the software provides an intuitive color-coded image of the myocardium (in yellow/orange the delayed segment), that is useful for the identification of the latest activated segment.

(Figure 4). Segments should achieve the minimum volume at the same point in the cardiac cycle. However, when significant LV dyssynchrony is present, a wide dispersion of the Tmsv of the various segments occurs. The standard deviation of the Tmsv for 16 segments has been proposed as a measure of LV dyssynchrony and expressed as a percentage of the cardiac cycle (the systolic dyssynchrony index, SDI). Furthermore, parametric images, derived from over 800 virtual waveforms, are also provided by the software with a visual summary of LV regional contraction timings as a polar plot. The global Tmsv is used as timing reference and segments with a Tmsv that is approximately the same as global Tmsv are coded in green. Early segments are color-coded in blue, whereas late segments are coded in red/yellow, providing a rapid and intuitive assessment of the area of latest LV activation (Figure 5). This may be of particularly importance to guide an optimal LV lead placement. Kapetanakis et al. demonstrated the feasibility of LV dyssynchrony assessment with RT3DE in a large group of patients and normal subjects using SDI [26]. In 26 patients referred for CRT implantation, the authors observed that clinical responders (reduction in NYHA functional class) had significantly higher SDI at baseline as compared to non-responders (16.6±1.1% vs. 7.1±2.0%, p <0.001). In addition, after a mean follow-up of 10 months, a reduction in SDI was noted in responders,

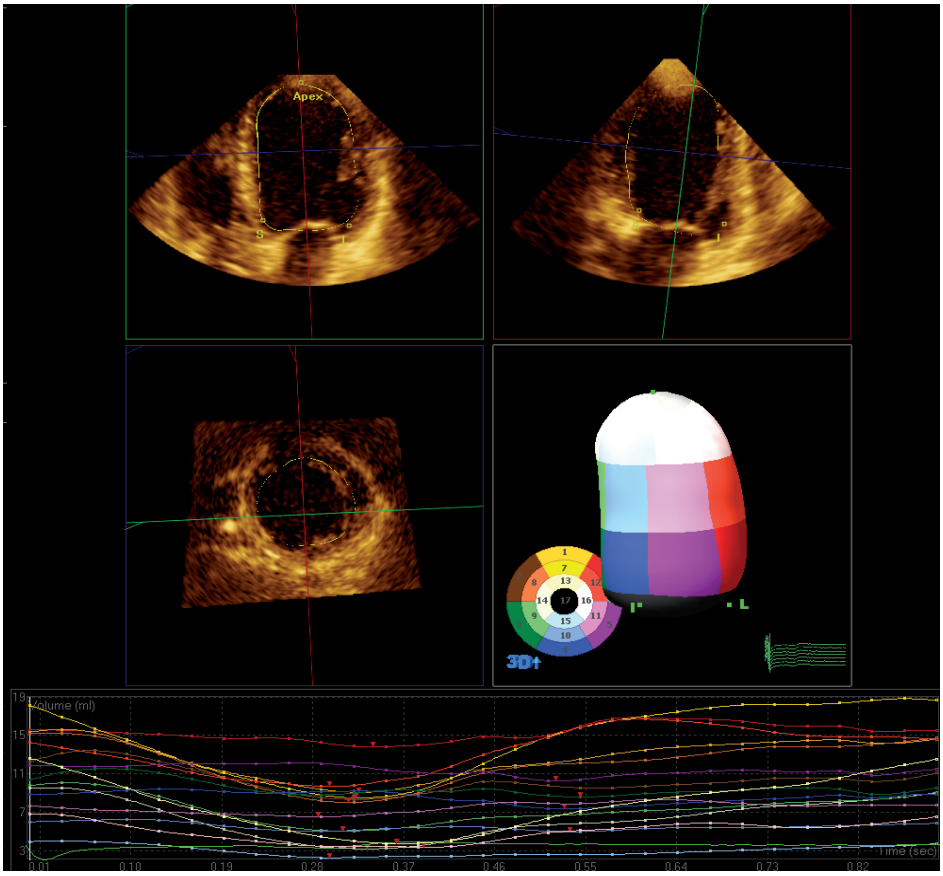


Figure 4. Example of 3D LV volumes generated by post-processing of a RT3DE dataset, acquired in a heart failure patient scheduled for CRT. The LV 3D model is subdivided by the software in 17 wedge shaped (apart from the apex) sub-volumes and for each volumetric segment, it is possible to derive time-volume data (lower panel) and assess the time taken to reach the minimum systolic volume (red dots).

whereas an increase in SDI was observed in non-responders. In a more recent study, Marsan et al. addressed the predictive value of this parameter and found that a SDI ≥5.6% had a sensitivity of 88% and a specificity of 86% to predict acute volumetric response to CRT [27].

Currently, no data are available on the predictive value of long-term response to CRT and the technique needs further validation for this application. Furthermore, RT3DE has still some limitations. First, the temporal resolution is suboptimal, about 30 to 35 ms. Nonetheless, the feasibility of LV dyssynchrony assessment has been demonstrated in a large group of normal individuals and unselected patients with and without QRS prolongation [26]. Furthermore, the image quality is somewhat lower than 2D echocardiography and the incomplete visualization of large ventricles may affect the quantitative analysis. However, several studies have reported a good feasibility in heart failure patients [27].

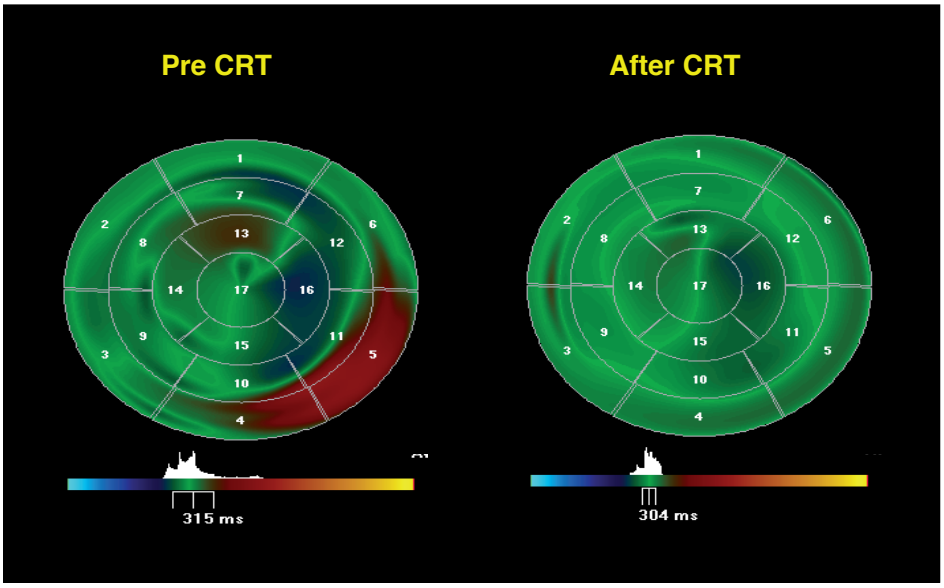


Figure 5. Parametric image derived from 3D dataset of a patient scheduled for CRT. The LV is divided into the standard segments (from 1 to 17). Using color coding (blue indicating early activation and orange-red late activation) representing regional time-to-minimum systolic volumes, the posterior wall is identified as the latest activated before CRT (left panel). Six months after CRT (right panel) the overall green color indicates absence of regions with delayed activation.

CLINICAL IMPLICATIONS AND FUTURE DIRECTIONS

Limitations of current LV dyssynchrony evaluation

Different echocardiographic approaches, with relative strengths and limitations, are available for the assessment of LV dyssynchrony and prediction of response to CRT. However, LV dyssynchrony assessment is a challenging goal, since it can not be considered an all-or-none phenomenon but a dynamic condition that may vary widely and can be dependent on loading conditions [28]. Consequently, it is still not clear which parameters, among those of myocardial motion, myocardial deformation or volume changes, would best reflect the complex pathophysiologic substratum of LV dyssynchrony in heart failure and whether the two-segmental model should be preferred over the multiple-segmental model. Therefore, a consensus on the definition of LV dyssynchrony is still lacking. In addition, the predictive value of these echocardiographic indices have been generated from small, single-center, non-randomized studies that used non-uniform definitions of response to CRT and evaluated a relatively short-term follow-up [5]. Consequently, the results need to be confirmed in larger prospective multi-center studies. Ideally, the optimal predictor of a favourable response to

CRT must have high sensitivity and specificity. In addition, it should also be simple to perform, widely available, easily reproducible and obtainable before and after CRT implantation.

Future directions

The PROSPECT trial is currently evaluating in 426 patients whether specific echocardiographic measurements of dyssynchrony, including M-mode, Doppler and TDI, could be used to better predict a favourable response to CRT [29]. The first, preliminary results revealed that none of the echocardiographic parameters was associated with a relevant additional response rate [30]. However, these findings may be explained by the fact that a marked inter-core lab variability was found for these parameters, highlighting the challenges that the interpretation of these exams offer even to experienced personnel [31]. Importantly, it should be noted that the most recent, 3D and automated imaging techniques were not included in this trial. Furthermore, a combined approach using different and complementary parameters of LV dyssynchrony, rather than using single parameters, may provide better results [20]. More large prospective studies are needed to fully appreciate the role of LV dyssynchrony assessed with echocardiography in the prediction of response to CRT. Consequently, at present LV dyssynchrony assessment is not yet recommended for patient selection for CRT [12]. Furthermore, it should be kept in mind that other pathophysiological issues may also be important to consider before CRT, including extent and location of scar tissue, optimal LV lead position and availability of coronary veins.

REFERENCES

1. Freemantle N, Tharmanathan P, Calvert MJ, Abraham WT, Ghosh J, Cleland JG. Cardiac resynchronisation for patients with heart failure due to left ventricular systolic dysfunction -- a systematic review and meta-analysis. *Eur J Heart Fail.* 2006;8:433-440.
2. Mehra MR, Greenberg BH. Cardiac resynchronization therapy: caveat medicus! *J Am Coll Cardiol.* 2004;43:1145-1148.
3. Becker M, Franke A, Breithardt OA et al. Impact of left ventricular lead position on the efficacy of cardiac resynchronisation therapy: a two-dimensional strain echocardiography study. *Heart.* 2007;93:1197-1203.
4. Bleeker GB, Kaandorp TA, Lamb HJ et al. Effect of posterolateral scar tissue on clinical and echocardiographic improvement after cardiac resynchronization therapy. *Circulation.* 2006;113:969-976.
5. Bax JJ, Abraham T, Barold SS et al. Cardiac resynchronization therapy: Part 1--issues before device implantation. *J Am Coll Cardiol.* 2005;46:2153-2167.
6. Kvitting JP, Wigstrom L, Strotmann JM, Sutherland GR. How accurate is visual assessment of synchronicity in myocardial motion? An In vitro study with computer-simulated regional delay in myocardial motion: clinical implications for rest and stress echocardiography studies. *J Am Soc Echocardiogr.* 1999;12:698-705.
7. Jansen AH, van DJ, Bracke F et al. Qualitative observation of left ventricular multiphasic septal motion and septal-to-lateral apical shuffle predicts left ventricular reverse remodeling after cardiac resynchronization therapy. *Am J Cardiol.* 2007;99:966-969.
8. Pitzalis MV, Iacoviello M, Romito R et al. Cardiac resynchronization therapy tailored by echocardiographic evaluation of ventricular asynchrony. *J Am Coll Cardiol.* 2002;40:1615-1622.
9. Marcus GM, Rose E, Viloria EM et al. Septal to posterior wall motion delay fails to predict reverse remodeling or clinical improvement in patients undergoing cardiac resynchronization therapy. *J Am Coll Cardiol.* 2005;46:2208-2214.
10. Breithardt OA, Stellbrink C, Herbots L et al. Cardiac resynchronization therapy can reverse abnormal myocardial strain distribution in patients with heart failure and left bundle branch block. *J Am Coll Cardiol.* 2003;42:486-494.
11. Kawaguchi M, Murabayashi T, Fetics BJ et al. Quantitation of basal dyssynchrony and acute resynchronization from left or biventricular pacing by novel echo-contrast variability imaging. *J Am Coll Cardiol.* 2002;39:2052-2058.
12. Gorcsan J, III, Abraham T, Agler DA et al. Echocardiography for cardiac resynchronization therapy: recommendations for performance and reporting--a report from the American Society of Echocardiography Dyssynchrony Writing Group endorsed by the Heart Rhythm Society. *J Am Soc Echocardiogr.* 2008;21:191-213.
13. Bax JJ, Bleeker GB, Marwick TH et al. Left ventricular dyssynchrony predicts response and prognosis after cardiac resynchronization therapy. *J Am Coll Cardiol.* 2004;44:1834-1840.
14. Yu CM, Gorcsan J, III, Bleeker GB et al. Usefulness of tissue Doppler velocity and strain dyssynchrony for predicting left ventricular reverse remodeling response after cardiac resynchronization therapy. *Am J Cardiol.* 2007;100:1263-1270.
15. Van de Veire N, Bleeker GB, De Sutter J et al. Tissue synchronisation imaging accurately measures left ventricular dyssynchrony and predicts response to cardiac resynchronisation therapy. *Heart.* 2007;93:1034-1039.

16. Sun JP, Popovic ZB, Greenberg NL et al. Noninvasive quantification of regional myocardial function using Doppler-derived velocity, displacement, strain rate, and strain in healthy volunteers: effects of aging. *J Am Soc Echocardiogr.* 2004;17:132-138.
17. Yu CM, Fung JW, Zhang Q et al. Tissue Doppler imaging is superior to strain rate imaging and postsystolic shortening on the prediction of reverse remodeling in both ischemic and nonischemic heart failure after cardiac resynchronization therapy. *Circulation.* 2004;110:66-73.
18. Delgado V, Ypenburg C, van Bommel R et al. Assessment of left ventricular dyssynchrony by speckle tracking strain imaging. *J Am Coll Cardiol.* 2008.
19. Suffoletto MS, Dohi K, Cannesson M, Saba S, Gorcsan J, III. Novel speckle-tracking radial strain from routine black-and-white echocardiographic images to quantify dyssynchrony and predict response to cardiac resynchronization therapy. *Circulation.* 2006;113:960-968.
20. Gorcsan J, III, Tanabe M, Bleeker GB et al. Combined longitudinal and radial dyssynchrony predicts ventricular response after resynchronization therapy. *J Am Coll Cardiol.* 2007;50:1476-1483.
21. Hung J, Lang R, Flachskampf F et al. 3D echocardiography: a review of the current status and future directions. *J Am Soc Echocardiogr.* 2007;20:213-233.
22. Kuhl HP, Schreckenberg M, Rulands D et al. High-resolution transthoracic real-time three-dimensional echocardiography: quantitation of cardiac volumes and function using semi-automatic border detection and comparison with cardiac magnetic resonance imaging. *J Am Coll Cardiol.* 2004;43:2083-2090.
23. Corsi C, Lang RM, Veronesi F et al. Volumetric quantification of global and regional left ventricular function from real-time three-dimensional echocardiographic images. *Circulation.* 2005;112:1161-1170.
24. Yu CM, Bleeker GB, Fung JW et al. Left ventricular reverse remodeling but not clinical improvement predicts long-term survival after cardiac resynchronization therapy. *Circulation.* 2005;112:1580-1586.
25. Van de Veire N, Yu CM, Ajmone-Marsan N et al. Triplane tissue Doppler imaging: a novel three-dimensional imaging modality that predicts reverse left ventricular remodelling after cardiac resynchronisation therapy. *Heart.* 2008;94:e9.
26. Kapetanakis S, Kearney MT, Siva A, Gall N, Cooklin M, Monaghan MJ. Real-time three-dimensional echocardiography: a novel technique to quantify global left ventricular mechanical dyssynchrony. *Circulation.* 2005;112:992-1000.
27. Marsan NA, Bleeker GB, Ypenburg C et al. Real-time three-dimensional echocardiography permits quantification of left ventricular mechanical dyssynchrony and predicts acute response to cardiac resynchronization therapy. *J Cardiovasc Electrophysiol.* 2008;19:392-399.
28. Kass DA. An epidemic of dyssynchrony: but what does it mean? *J Am Coll Cardiol.* 2008;51:12-17.
29. Yu CM, Abraham WT, Bax J et al. Predictors of response to cardiac resynchronization therapy (PROSPECT)--study design. *Am Heart J.* 2005;149:600-605.
30. Cleland JG, Abdellah AT, Khaleva O, Coletta AP, Clark AL. Clinical trials update from the European Society of Cardiology Congress 2007: 3CPO, ALOFT, PROSPECT and statins for heart failure. *Eur J Heart Fail.* 2007;9:1070-1073.
31. Nagueh SF. Mechanical dyssynchrony in congestive heart failure: diagnostic and therapeutic implications. *J Am Coll Cardiol.* 2008;51:18-22.

CHAPTER 3

Real-time three-dimensional echocardiography permits quantification of left ventricular mechanical dyssynchrony and predicts acute response to cardiac resynchronization therapy

N Ajmone Marsan, G B Bleeker, C Ypenburg, S Ghio, N R van de Veire, E R Holman, E E Van der Wall, L Tavazzi, M J Schalij, and J J Bax

J Cardiovasc Electrophysiol 2008;19:392–9.

ABSTRACT

Objectives: To evaluate the value of real-time 3-dimensional echocardiography (RT3DE) to predict acute response to cardiac resynchronization therapy (CRT).

Methods: 60 consecutive heart failure patients scheduled for CRT were included. RT3DE was performed before and within 48 hours after pacemaker implantation to calculate both left ventricular (LV) volumes and LV dyssynchrony. LV dyssynchrony was defined as the standard deviation of the time taken to reach the minimum systolic volume for 16 LV segments (referred to as the systolic dyssynchrony index, SDI). Patients were subsequently divided into acute responders or non-responders, based on a reduction ≥15% in LV end-systolic volume immediately after CRT.

Results: 4 patients (7%) were excluded from further analysis because either suboptimal apical acquisitions or significant translation artefacts. Out of the remaining 56 patients, 35 patients (63%) were classified as acute responders. Baseline characteristics were similar between responders and non-responders, except for the SDI, which was larger in responders. Moreover, responders demonstrated a significant reduction of SDI immediately after CRT (from 9.7±4.1% to 3.6±1.8%, $p < 0.001$), whereas SDI did not change in non-responders (3.4±1.8% versus 3.1±1.1%, NS). ROC curve analysis revealed that a cut-off value for SDI of 5.6% yielded a sensitivity of 88% with a specificity of 86% to predict acute echocardiographic response to CRT (AUC 0.96).

Conclusions: RT3DE is highly predictive for acute response to CRT (sensitivity 88% and specificity 86%). In addition, RT3DE allows assessment of changes in LV volumes and LV ejection fraction before and after CRT implantation.

INTRODUCTION

In recent years cardiac resynchronization therapy (CRT) has become an established therapy for patients with drug-refractory heart failure and a wide QRS complex [1]. However, close analysis of the large CRT trials revealed that up to 30% of patients did not respond to CRT when the established selection criteria were applied [2]. Several studies addressing this issue have indicated that the presence of baseline left ventricular (LV) dyssynchrony is an important predictor of response to CRT [3]. In the established selection criteria, the presence of a wide QRS complex has been used as a marker of cardiac dyssynchrony; however, recent findings showed that QRS duration correlated poorly with LV dyssynchrony, thereby explaining its poor predictive value for response to CRT [4,5]. Conversely, direct echocardiographic assessment of LV dyssynchrony has been demonstrated highly predictive for response to CRT [3]. Since this observation, various echocardiographic parameters have been proposed to appropriately select CRT candidates ranging from simple M-mode-echocardiography to more advanced techniques such as tissue Doppler imaging (TDI) [6–12].

Recently, real-time 3-dimensional echocardiography (RT3DE) has become available as a novel promising technique for assessment of LV dyssynchrony based on analysis of regional volumetric changes of the LV. A potential advantage of the use of RT3DE in patients undergoing CRT is that it allows both LV dyssynchrony assessment as well as highly accurate three-dimensional quantification of LV volumes and LV function during follow-up which allows assessment of therapy success. An initial study by Kapetenakis et al.[13] demonstrated promising results when RT3DE was applied in a small group of patients undergoing CRT. In the current study, the value of RT3DE for prediction of response to CRT and the assessment LV volumes following CRT implantation was evaluated in a larger group of patients undergoing CRT implantation.

METHODS

Patient population and protocol

Sixty consecutive heart failure patients, scheduled for implantation of a CRT device, were included in this study. Patients were selected for CRT on the following basis:

- LV ejection fraction (EF) ≤35%,
- QRS duration >120 ms and
- NYHA functional class III or IV, despite optimal medical treatment.

Etiology was considered ischemic in the presence of significant coronary artery disease (>50% stenosis in ≥1 major epicardial coronary artery) on coronary angiographic examination and/or a history of myocardial infarction and previous coronary artery revascularizations. Patients with a recent myocardial infarction (<3 months) or decompensated heart failure were excluded.

Before implantation of the CRT device, LV volumes, LVEF and LV dyssynchrony were measured using RT3DE. LV stroke volume (SV) was also calculated using the pulsed-wave Doppler signal in the LV outflow tract. All echocardiographic measurements were repeated immediately (within 48 hours) after CRT implantation and the analysis was performed blinded to the pre-implantation data.

In addition, 20 patients were randomly identified to evaluate the inter- and intra-observer agreement for the analysis of LV volumes, LVEF and dyssynchrony. Bland-Altman analysis was performed to evaluate agreement between observer 1 and observer 2 to assess inter-observer agreement and between 2 measurements by observer 1 to assess intra-observer agreement.

Real-time 3-dimensional echocardiography

Acquisition of 3-dimensional data set

RT3DE was performed before and within 48 hours after CRT implantation. Patients were imaged in the left lateral decubitus position with a commercially available system (iE33, Philips Medical Systems, N.A., Bothell, Washington, USA) equipped with X3, fully sampled matrix transducer. Apical full-volume data sets were obtained in all patients.

For the evaluation of LV volumes and LVEF, the lowest scan line density was used and gain and compression were adjusted to obtain a good image quality and a clear endocardial border. With a specific software (Large Volume size, Vision 2007, Philips Medical Systems) 4 small real-time sub-volumes were acquired from alternate cardiac cycles and combined to provide a larger pyramidal volume (up to 103 x 103 degrees) and to ensure a complete capture of the LV. The acquisition was performed during end-expiratory apnoea within 1 breath hold and with a relatively stable heart rate to minimize translation artefacts between the 4 sub-volumes. A 3D data set was considered unsuitable for analysis if >2 segments could not be visualized or if it contained visible translation artefacts. For the evaluation of LV dyssynchrony the frame rate was optimized by reducing the depth and by the acquisition of a full-volume data set of 7 sub-volumes.

LV volumes and LV ejection fraction

RT3DE data sets were stored digitally and quantitative analysis of the 3D dataset was performed off-line using a semi-automated contour tracing algorithm (Q-Lab, version 5.0, Philips Medical Systems) over a complete heart cycle. The software provides for each frame the apical 4 chamber and 2 chamber views and the parasternal short-axis view. After first identifying the apex and mitral annulus on the end-diastolic and end-systolic frames (using 5 reference points), a preconfigured ellipse is fitted to the endocardial border for each frame (mean number of frames: 16±4) and manually adjusted as required. The three-dimensional model of the LV is generated and LV volumes and LVEF are obtained (Figure 1). Papillary muscles were included in the LV cavity. The post-processing of the images required between 2 and 4 minutes, depending on the manual adjustments needed.

Patients with an acute reduction ≥15% of LV end-systolic volume (reflecting acute improvement in LV systolic function) were considered acute responders to CRT [14]. Additionally, LV SV was calculated before and within 48 hours after pacemaker implantation, using the pulsed-wave Doppler signal in the LV outflow tract from the apical long-axis view.

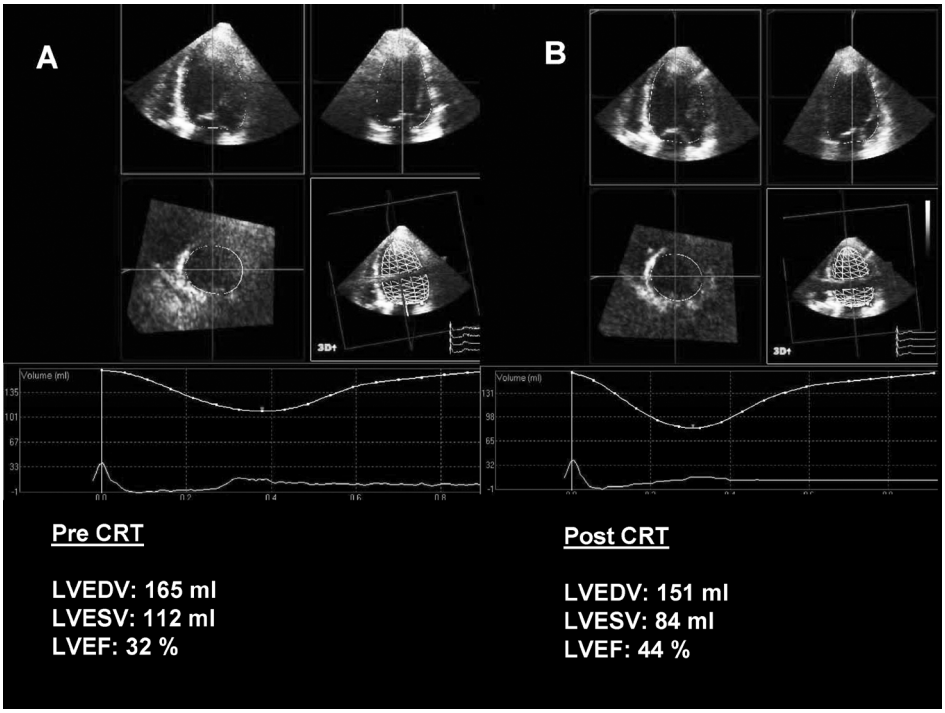


Figure 1. Example of 3D left ventricular (LV) volumes generated by post-processing of a RT3DE dataset, acquired in a patient scheduled for CRT. Panel A: pre CRT. Panel B: immediately post CRT. LV end-systolic volume (LVESV) and LV ejection fraction (LVEF) improved significantly.

Assessment of LV dyssynchrony

The LV 3D model was subdivided in 16 pyramidal sub-volumes (6 basal segments, 6 mid segments and 4 apical segments). For the whole LV and for each volumetric segment, it is possible to derive time-volume data for the entire cardiac cycle and assess the time taken to reach the minimum systolic volume (Tmsv). From this information, as previously described by Kapetanakis et al.[13], the standard deviation of 16 segments Tmsv expressed in percentage of cardiac cycle (the systolic dyssynchrony index, SDI) was calculated as a marker of global dyssynchrony of the LV. Of interest, the time-volume data of an akinetic segment is displayed by the software as a flat curve (excursion = 0) and the minimum systolic volume is identified in the middle of this curve, substantially not affecting the deviation standard of the timings (SDI). A completely dyskinetic segment (positive excursion) is excluded from the SDI calculation. For the baseline SDI calculation 36 out of 896 segments (4%) were discarded because dyskinetic; 232 segments (26%) were defined akinetic. After CRT, the same number of dyskinetic segments was found, whereas the number of akinetic segments decreased to 198 (22%).

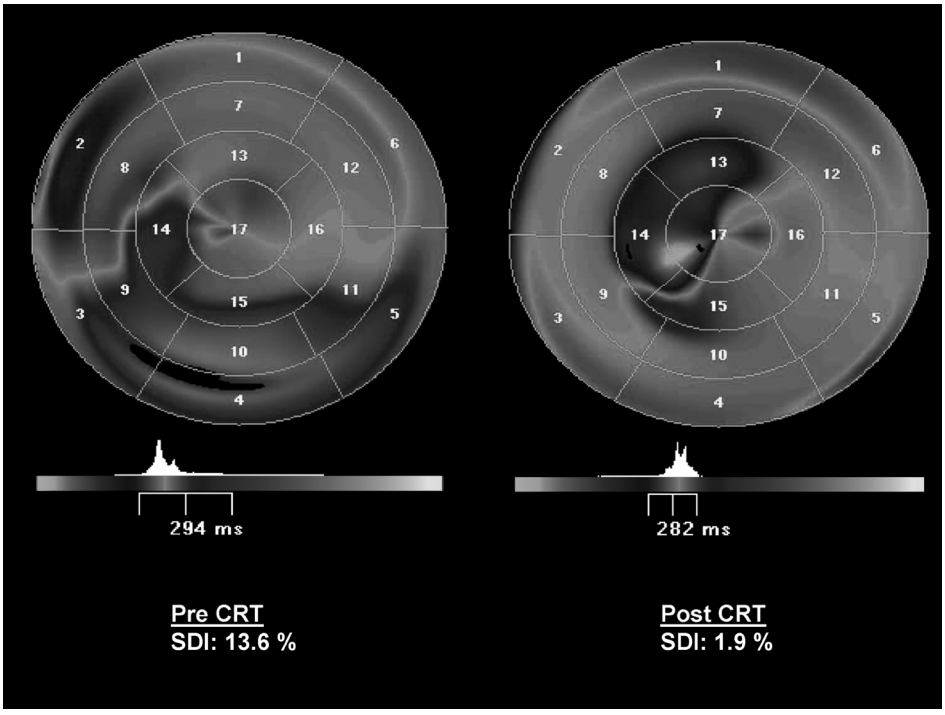


Figure 2. Example of left ventricular (LV) dyssynchrony analysis from a RT3DE data set using parametric images. The global Tmsv is used as timing reference; early segments are coded in blue, whereas late segments are coded in red. Pre CRT: Before CRT, the inferior segments are activated last. Post CRT: the homogeneous color indicates absence of regions with delayed activation, indicating resynchronization after CRT implantation. After implantation the systolic dyssynchrony index (SDI) decreased from 13.6% to 1.9%.

In addition to the time-volume data, parametric images, derived from over 800 virtual waveforms, are provided by the software (Q-Lab, version 5.0, Philips Medical Systems) with a visual summary, as a polar plot, of LV regional contraction timings. The global Tmsv is used as timing reference. Accordingly, segments with a Tmsv about global Tmsv are coded in green. Early segments are coded in blue, whereas late segments are coded in red/yellow (Figure 2). Using both analysis of the regional time-to-minimum systolic volume and the parametric images, the latest activated LV wall (either lateral, posterior, inferior, septal, anteroseptal or anterior) was identified as a marker of regional dyssynchrony.

Reproducibility of the RT3DE measurements

Twenty patients were randomly identified for inter- and intra-observer agreement. Bland-Altman analysis was performed to evaluate agreement between observer 1 and observer 2 to determine inter-observer agreement. Similarly, the 3D measurements derived by the first observer were compared (Bland-Altman analysis) with the results calculated by the same operator 1 month later to determine intra-observer agreement.

The inter-observer agreement was good. According to the Bland-Altman analysis, the mean differences for SDI, LV end-diastolic volume (EDV), end-systolic volume (ESV) and EF were 0.1±1%, 1.3±17 ml, 0.3±17 ml and 0.4±4%, respectively, all not significantly different from zero. The intra-observer agreement was also good. The agreement between the 2 measurements according to the Bland-Altman analysis was excellent with mean differences of 0.03±0.5% for SDI, 0.6±10 ml for LVEDV, 0.7±6 ml for LVESV and 0.8±3% for LVEF, all not significantly different from zero.

Pacemaker implantation

The LV pacing lead was inserted transvenously via the subclavian route. First, a coronary sinus venogram was obtained using a balloon catheter. Next, the LV pacing lead was inserted through the coronary sinus, using an 8Fr-guiding catheter, and positioned as far as possible in the venous system, preferably in the (postero-) lateral vein. The right atrial and ventricular leads were positioned conventionally. When an indication for an internal defibrillator existed, a combined device was implanted. In all patients the implantation of the CRT device was successful without major complications (Contak Renewal, Guidant Corp.; Insync III-CD or Insync Sentry, Medtronic Inc.). Two types of LV leads were used (Easytrak, Guidant Corp., or Attain, Medtronic Inc.). For each patient, the atrio-ventricular interval was adjusted to maximize mitral inflow duration with pulsed-wave Doppler echocardiography [15]. No adjustment of the inter-ventricular delay was made.

Statistical analysis

Continuous data are presented as mean ± standard deviation. Categorical data are presented as absolute numbers or percentages. Comparisons between responders and non-responders were performed using the independent-samples *t*-test; comparisons between pre- and post-implantation characteristics were performed using the paired-samples *t*-test. Before performing a Student's *t*-test, the normal distribution of the continuous variables was verified using the Kolmogorov–Smirnov test and using the Levene's test to check for equality in variances for all comparisons. Correlation analysis was used to compare the relationship between the change of SDI and the change of LVESV, LVEF and LV SV after CRT by the Pearson correlation coefficients. Optimal cut-off value of SDI to predict acute echocardiographic response to CRT was determined by receiver-operating characteristic (ROC) curve analysis. The optimal cut-off value was defined as that providing the maximal accuracy to distinguish between echocardiographic responders/non-responders. For all tests, a p-value <0.05 was considered significant. A statistical software program SPSS 12.0 (SPSS Inc, Chicago, Il, USA) was used for statistical analysis.

RESULTS

Patient population

The study population consisted of 60 consecutive heart failure patients. Four patients (7%) were excluded from further analysis because of suboptimal apical acquisitions or significant translation artefacts. The baseline characteristics of the remaining 56 patients (45 men, mean age 65±9 years) are summarized in Table 1. All patients were in sinus rhythm and most patients were in NYHA class III; 62% of patients had ischemic cardiomyopathy. RT3DE revealed severe LV dilation (mean LVEDV 201±48 ml), with depressed LV function (mean LVEF 28±6%). In addition, substantial LV dyssynchrony was present as indicated by a mean SDI of 7.3±4.6%. The latest activated LV wall was the lateral in 17 patients (30%), the posterior in 16 patients (29%), the inferior in 13 patients (23%), the anterior in 9 patients (16%) and the septum in 1 patient (2%).

Acute echocardiographic response

Immediately after CRT implantation, 35 patients (63%) experienced an acute reduction in LVESV ≥15%; as pre-defined, these patients were classified as acute responders. The acute responders also showed a significant increase in LVEF and LV SV (Table 2). In contrast, LVEDV showed no immediate decrease after CRT implantation (from 201±48 ml to 191±46 ml, NS) (Table 2).

Table 1. Baseline characteristics of the patient population (n = 56).

Age (years)	**65±9**
Gender (M/F)	45/11
NYHA class III/IV (n)	53/3
QRS duration (ms)	148±31
ECG pattern:	
LBBB/IVCD, n (%)	37(66)/19 (34)
Etiology, n (%)	
Ischemic	35 (62)
Idiopathic	21 (38)
Medication, n (%)	
ACE Inhibitors	49 (87)
ß-blockers	41 (73)
Diuretics and /or	
Spironolactone	53 (95)
Amiodarone	8 (14)
LVEDV (ml)	201±48
LVESV (ml)	147±43
LVEF (%)	28±6
LV SV (ml)	38±14
SDI (%)	7.3±4.6

IVCD: non-specific intraventricular conduction delay, LBBB: left bundle branch block, LVEDV: left ventricular end-diastolic volume, LVESV: left ventricular end-systolic volume, LVEF: left ventricular ejection fraction, LV SV: left ventricular stroke volume, NYHA: New York Heart Association, SDI: systolic dyssynchrony index.

Table 2. Responders versus non-responders: echocardiographic variables before and immediately after CRT implantation.

	Non-responders n = 21	**Responders n = 35**	**p-value**
LVEDV (ml)			
Baseline	202±50	201±48	NS
After implantation	200±49	191±46	NS
LVESV (ml)			
Baseline	148±42	147±44	NS
After implantation	145±41	124±38*	0.05
LVEF (%)			
Baseline	27±7	28±6	NS
After implantation	28±6	36±6*	<0.001
LV SV (ml)			
Baseline	37±15	39±13	NS
After implantation	37±14	47±14*	0.01
SDI (%)			
Baseline	3.4±1.8	9.7±4.1	<0.001
After implantation	3.1±1.1	3.6±1.8*	NS

* p <0.001 baseline versus follow-up. Abbreviations see Table 1.

Table 3. Baseline clinical characteristics of responders versus non-responders.

	Non-responders n = 21	Responders n = 35	p-value
Age (years)	66±8	65±10	NS
Gender (M/F)	16/5	29/6	NS
Ischemic/Idiopathic (n)	15/6	20/15	NS
NYHA class III/IV (n)	21/0	32/3	NS
QRS duration (ms)	157±29	147±35	NS
ECG pattern: LBBB/IVCD (n)	9/12	10/25	NS

IVCD: non-specific intraventricular conduction delay, LBBB: left bundle branch block, NYHA: New York Heart Association.

All baseline characteristics were comparable between responders and non-responders, except for LV dyssynchrony as measured with the use of RT3DE (assessing SDI) (Table 2 and Table 3*)*.The SDI was significantly higher in responders as compared to non-responders (9.7±4.1% versus 3.4±1.8%, p <0.001). Moreover, responders demonstrated a significant reduction in SDI immediately after CRT (from 9.7±4.1% to 3.6±1.8%, p <0.001), whereas in non-responders SDI remained unchanged (from 3.4±1.8% to 3.1±1.1%, NS) (Table 2). In addition, the postero-lateral region (where the LV pacing lead is positioned) was latest activated in 74% of responders as compared to 33% of non-responders (p = NS).

Prediction of acute response after CRT implantation by RT3DE

A fair correlation was observed between baseline SDI and the change in LVESV after CRT (r = 0.60, p <0.001), while a good correlation between baseline SDI and the change in LVEF after CRT was demonstrated (r = 0.70, p <0.001) (Figure 3). A fair correlation was also noted between baseline SDI and the change in LV SV after CRT (r = 0.51, p <0.001).

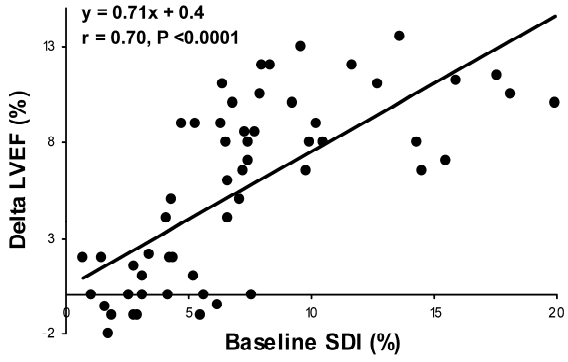


Figure 3. The correlation between the change (delta) in LV ejection fraction (LVEF) after CRT and baseline systolic dyssynchrony index (SDI) is shown.

To define the optimal cut-off value to predict echocardiographic response to CRT, ROC curve analysis was performed. At a cut-off value of 5.6% for LV dyssynchrony (SDI), a sensitivity of 88% with a specificity of 86% were obtained to predict an acute reduction ≥15% of LVESV (area under the curve = 0.96, 95% CI = 0.9 -1.0, p <0.001) (Figure 4). Accordingly, using

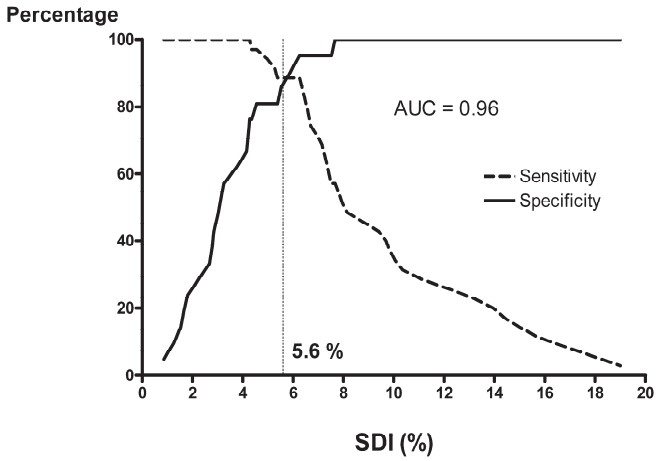


Figure 4. ROC curve analysis demonstrated a sensitivity of 88% with a specificity of 86% to predict an acute reduction of left ventricular end-systolic volume ≥15% after CRT at a cut-off of 5.6% for LV dyssynchrony (SDI). AUC = area under the ROC curve.

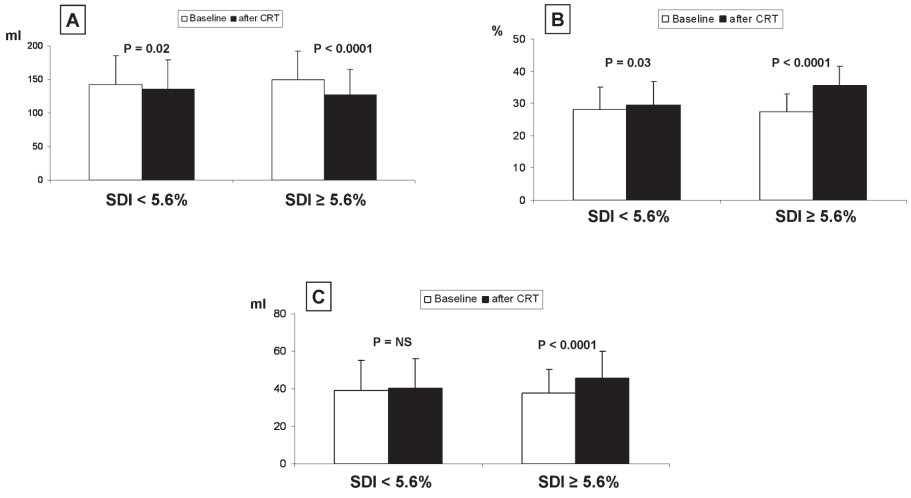


Figure 5. Comparison between patients with substantial versus non-substantial LV dyssynchrony (SDI) (cut-off value of ≥5.6%). The decrease in LV end-systolic volume (Panel A) and the increase in LV ejection fraction (Panel B) and in LV stroke volume (Panel C) are significantly higher in patients with substantial LV dyssynchrony.

this cut-off value, 34 patients (61%) had SDI ≥5.6%; these patients showed a significantly better improvement in LV systolic function (defined as a reduction of LVESV and an increase in LVEF and SV) as compared to patients with SDI <5.6% (Figure 5).

DISCUSSION

The findings in the current study can be summarized as follows: 1) acquisition and analysis of a RT3DE data set is feasible and reproducible in patients with severely dilated left ventricles and provides quantitative information on both LV volumes and LV dyssynchrony; 2) all baseline characteristics were comparable between responders and non-responders to CRT, except for LV dyssynchrony as measured using the SDI, which was larger in responders; 3) a SDI ≥5.6% had a sensitivity of 88% and a specificity of 86% to predict an acute reduction in LVESV after CRT implantation.

Benefit of CRT

Recent large clinical trials have demonstrated the beneficial effects of CRT on symptoms, exercise capacity, LV reverse remodeling and, most important, on clinical outcome.[1] However, despite these impressive results approximately one third of patients fails to improve after CRT when the established selection criteria are being applied (NYHA functional class III or IV, LVEF ≤35% and QRS duration >120 ms) [2]. Several studies have recently emphasized the importance of the presence of significant baseline LV dyssynchrony for the prediction of response to CRT [3]. Traditionally QRS duration has been used as a marker of LV dyssynchrony; however recent data has suggested that QRS duration is a poor marker of LV dyssynchrony, thereby explaining its poor predictive value for response to CRT [4,5]. Since the observation that QRS duration is a poor marker of LV dyssynchrony several echocardiographic methods have been introduced to quantify LV dyssynchrony. Most experience has been obtained with tissue Doppler imaging. For example Bax and colleagues [7] analyzed the electromechanical activation delay in the longitudinal direction among 4 basal LV segments, whereas Yu et al. [8,9] have used the standard deviation of time-to-peak systolic velocity of 12 LV segments. Both studies have identified the TDI parameters of LV dyssynchrony as powerful predictors of clinical response and LV reverse remodeling after CRT. More recently, also radial LV dyssynchrony assessed by speckle tracking strain was able to predict immediate and long-term response to CRT [16]. At present, it is still unclear which technique is the gold standard for LV dyssynchrony since large comparative studies directly comparing the relative merits of the different techniques are lacking [17].

RT3DE has been recently introduced as a promising technique for the assessment of LV dyssynchrony. In theory RT3DE has several potential advantages over other echocardiographic techniques: 1) Next to LV dyssynchrony analysis RT3DE permits highly accurate quantitative measurement of LV size and function which allows for simultaneous evaluation of therapy success, 2) RT3DE measures a composite effect of longitudinal, radial and circumferential contraction which is angle-independent, potentially resulting in more reproducible results and, 3) RT3DE is able to measure all (16) myocardial segments in 1 single recording allowing for a rapid assessment of the area of latest LV activation to guide optimal LV lead placement.

Assessment of LV volumes and LV function by RT3DE

A recent study by Yu et al.[18] demonstrated that a reduction in LV end-systolic volumes is the best predictor of improved survival after CRT, whereas improvement in clinical parameters was not predictive. Therefore improvement in LV volumes after CRT implantation probably provides the most clinical meaningful marker of therapy success. Quantification of LV end-systolic volume before CRT and during follow-up is therefore crucial in order to assess therapy success. In most studies the measurement of LV volumes and LVEF has been performed with echocardiography from a 2D dataset using the Simpson's biplane method. It has been demonstrated however, that the 3D echocardiographic approach is superior compared to the 2D approach and comparable with magnetic resonance imaging for LV volumes estimation [19,20]. RT3DE, which was used in the current study, permits a rapid and accurate quantification of LV size and function with a semi-automated contour-tracing algorithm [21]. Initial studies in CRT patients have used RT3DE to assess both acute changes in LV volumes as well as the effects at mid-term follow-up [13]. In the current study a reduction ≥15% of LVESV immediately after CRT (reflecting improved LV systolic function) was used to define acute response and non-response after CRT. An acute improvement in LV end-systolic volume was noted in 63% of patients; this finding is in agreement with other studies focusing on the acute response to CRT using different 2D echocardiographic parameters including dP/dT, stroke volume, LVESV and LVEF [14,22–26].

Of interest, RT3DE can also provide information on regional LV function (measured as excursion) and consequently information on regional wall motion abnormalities. For instance, an akinetic segment is displayed as a flat curve, a dyskinetic segment as a positive excursion, whereas hypo- and normokinetic segments are displayed as negative excursions. Not only may the presence of baseline wall motion abnormalities (per se or included in wall motion score index) have influence on response to CRT, but also the effect of CRT on regional LV function can be evaluated. However, no studies have validated RT3DE (versus MRI or 2D echocardiography) for this specific analysis. Of note, wall motion abnormalities, such as akinesia and dyskinesia, do not affect the SDI calculation.

Assessment of LV dyssynchrony by RT3DE

In a small group of patients Kapetanakis and coworkers [13] demonstrated that patients with a significant improvement in symptoms and LV reverse remodeling after CRT (responders) had a larger SDI before CRT implantation, as compared to non-responders to CRT. In the current study similar results were found in a group of 56 heart failure patients: a higher SDI value was noted in the responders as compared to non-responders (9.7±4.1% versus 3.4±1.8%, p <0.001). However, the absolute SDI values were somewhat lower in the current study. This difference may partially be explained by the different software packages used for the 3D dataset analysis. In contrast to the Tomtec-software (as used by Kapetanakis et al.[13]), the Q-lab software (used in the current study) does not permit the operator to change the point of time-to-minimum systolic volume which is automatically detected, yielding a better reproducibility of the measurements, which tends to result in lower SDI values. Another difference between both studies is the fact that Kapetanakis et al.[13] used an arbitrary cut-off value for significant mechanical dyssynchrony, which was defined as an SDI >3 SD above the mean for a group of normal subjects (8.3%). In the current study on the other hand, ROC curve analysis was performed to define the optimal cut-off value for SDI to predict response to CRT in a group of heart failure patients undergoing CRT; based on this ROC curve analysis, an SDI ≥5.6% was identified as the optimal cut-off value which yielded a sensitivity of 88% with a specificity of 86% to predict an acute response to CRT. In contrast, the earlier proposed value of 8.3% for SDI yielded an excellent specificity (100%) with a lower sensitivity of 46%. Burgess et al. [27] compared RT3DE and TDI for the assessment of LV dyssynchrony. Applying a cut-off value of 32 ms for the Ts-SD of 12 segments and of 8.3% (cut-off value of Kapetanakis et al.) for the SDI, these authors demonstrated that TDI identified a much greater proportion of patients with significant LV dyssynchrony than RT3DE (64% versus 42%), suggesting that the population derived cut-off value of Kapetenakis is somewhat high.

An important advantage of RT3DE is the simultaneous assessment of 16 LV segments in 1 recording. Through the analysis of each regional time-to-minimum systolic volume and the display of parametric imaging in polar plots (Figure 2), RT3DE permits a rapid identification of the area of latest mechanical activation. Tailoring the LV lead position to the exact area of maximal mechanical delay has recently attracted attention, although the technical limitations of transvenous coronary sinus pacing still exist. Several studies demonstrated that LV pacing at the site of latest activation is associated with the maximal clinical benefit and the greatest LV reverse remodeling [28,29] compared with LV pacing at the standard location (the postero-lateral wall). In line with these results, the current study showed a clear, although not statistically significant, trend of a higher percentage of patients with the postero-lateral wall as the site of latest activation in responders (74%) compared to non-responders (33%).

Study limitations

Echocardiographic or clinical data at mid- or long-term follow-up were not available and the present study focused on acute response to CRT. However, several studies, as discussed above, have already explored the acute beneficial effects of CRT and, recently, Suffoletto et al. demonstrated that acute improvement in systolic function translated in LV reverse remodeling at mid-term follow-up [30]**.** In view of the relatively small study population and the novelty of this technique, the predictive value of RT3DE needs to be further investigated in a multicenter prospective study. Also, the predictive value of RT3DE (SDI) as evaluated in the current study was not compared to other echocardiographic techniques currently available for LV dyssynchrony assessment such as TDI and strain imaging. Further multicenter studies are needed to explore the relative merits of the different techniques for the prediction of response to CRT, in order to define a gold standard for LV dyssynchrony assessment in CRT patients.

Recent studies have indicated that regional scar tissue and global scar burden may also be related to non-response to CRT. Data on scar tissue and/or segmental wall motion abnormalities, however, were not systematically available in the current study. Furthermore, no data were available on the exact position of the LV pacing lead and consequently data on the potential effect of LV lead position in relation to the site of latest activation were not available.

CONCLUSIONS

RT3DE allows quantitative analysis of LV dyssynchrony as well as assessment of LV volumes and ejection fraction in heart failure patients. An SDI ≥5.6% is highly predictive for acute volumetric response to CRT.

REFERENCES

1. Freemantle N, Tharmanathan P, Calvert MJ, Abraham WT, Ghosh J, Cleland JG. Cardiac resynchronization for patients with heart failure due to left ventricular systolic dysfunction – a systematic review and meta-analysis. *Eur Heart J* 2006;8:433-440.
2. Mehra MR, Greenberg BH: Cadiac resynchronization therapy: caveat medicus! *J Am Coll Cardiol* 2004;43:1145-1148.
3. Bax JJ, Abraham T, Barold SS et al. Cardiac resynchronization therapy: Part 1 issues before device implantation. *J Am Coll. Cardiol* 2005;46:2153-2167.
4. Ghio S, Constantin C, Klersy C, et al. Interventricular and intraventricular dyssynchrony are common in heart failure patients, regardless of QRS duration. *Eur Heart J* 2004;25:571-578.
5. Bleeker GB, Schalij MJ, Molhoek SG, et al. Relationship between QRS duration and left ventricular dyssynchrony in patients with end-stage heart failure. *J Cardiovasc Electrophysiol* 2004;15:544-549.
6. Pitzalis MV, Iacoviello M, Romito R et al. Ventricular asynchrony predicts a better outcome in patients with chronic heart failure receiving cardiac resynchronization therapy. *J Am Coll Cardiol* 2005;45:65-69.
7. Bax JJ, Bleeker GB, Marwick TH et al. Left ventricular dyssynchrony predicts response and prognosis after cardiac resynchronization therapy. *J Am Coll Cardiol* 2004;44:1834–1840.
8. Yu CM, Chau E, Sanderson JE et al. Tissue Doppler echocardiographic evidence of reverse remodeling and improved synchronicity by simultaneously delaying regional contraction after biventricular pacing therapy in heart failure. *Circulation* 2002;105:438–445.
9. Yu CM, Fung JW, Zhang Q et al. Tissue Doppler imaging is superior to strain rate imaging and postsystolic shortening on the prediction of reverse remodeling in both ischemic and nonischemic heart failure after cardiac resynchronization therapy. *Circulation* 2004;110:66-73.
10. Sogaard P, Egeblad H, Kim WY et al. Tissue Doppler imaging predicts improved systolic performance and reversed left ventricular remodeling during long-term cardiac resynchronization therapy. *J Am Coll Cardiol* 2002;40:723-730.
11. Breithardt OA, Stellbrink C, Herbots L et al. Cardiac resynchronization therapy can reverse abnormal myocardial strain distribution in patients with heart failure and left bundle branch block. *J Am Coll Cardiol* 2003;42:486-494.
12. Notabartolo D, Merlino JD, Smith AL et al. Usefulness of the peak velocity difference by tissue Doppler imaging technique as an effective predictor of response to cardiac resynchronization therapy. *Am J Cardiol* 2004;94:817-820.
13. Kapetanakis S, Kearney MT, Siva A, Gall N, Cooklin M, Monaghan MJ. Real-time three-dimensional echocardiography. A novel technique to quantify global left ventricular mechanical dyssynchrony. *Circulation* 2005;112: 992-1000.
14. Van de Veire NR, Bleeker GB, Ypenburg C et al. Usefulness of triplane tissue Doppler imaging to predict acute response to cardiac resynchronization therapy. *Am J Cardiol* 2007;100:476-82.
15. Kedia N, Ng K, Apperson-Hansen C et al. Usefulness of atrioventricular delay optimization using Doppler assessment of mitral inflow in patients undergoing cardiac resynchronization therapy. *Am J Cardiol* 2006;98:780-785.
16. Suffoletto MS, Dohi K, Cannesson M, Saba S, Gorcsan J 3rd. Novel speckle-tracking radial strain from routine black-and-white echocardiographic images to quantify dyssynchrony and predict response to cardiac resynchronization therapy. *Circulation* 2006;113:960-968.

17. Yu CM, Abraham WT, Bax JJ et al. PROSPECT Investigators: Predictors of response to cardiac resynchronization therapy (PROSPECT)--study design. *Am Heart J* 2005;149:600-605.
18. Yu CM, Bleeker GB, Fung JW et al. Left ventricular reverse remodeling but not clinical improvement predicts long-term survival after cardiac resynchronization therapy. *Circulation* 2005;112:1580-1586.
19. Kuhl HP, Schreckenberg M, Rulands D et al. High-resolution transthoracic real-time three-dimensional echocardiography: quantification of cardiac volumes and function using semi-automatic border detection and comparison with cardiac magnetic resonance imaging. *J Am Coll Cardiol* 2004;43:2083-2090.
20. Arai K, Hozumi T, Matsumura Y et al. Accuracy of measurement of left ventricular volume and ejection fraction by new real-time three-dimensional echocardiography in patients with wall motion abnormalities secondary to myocardial infarction. *Am J Cardiol* 2004;94:552-558.
21. Corsi C, Lang RM, Veronesi F et al. Volumetric quantification of global and regional left ventricular function from real-time three-dimensional echocardiographic images. *Circulation* 2005;112:1161-1670.
22. Dohi K, Suffoletto MS, Schwartzman D, Ganz L, Pinsky MR, Gorcsan J 3rd. Utility of echocardiographic radial strain imaging to quantify left ventricular dyssynchrony and predict acute response to cardiac resynchronization therapy. *Am J Cardiol* 2005;96:112-116.
23. Gorcsan J 3rd, Kanzaki H, Bazaz R, Dohi K, Schwartzman D. Usefulness of echocardiographic tissue synchronization imaging to predict acute response to cardiac resynchronization therapy. *Am J Cardiol* 2004;93:1178-1181.
24. Breithardt OA, Stellbrink C, Kramer AP et al; PATH-CHF Study Group: Pacing Therapies for Congestive Heart Failure. Echocardiographic quantification of left ventricular asynchrony predicts an acute hemodynamic benefit of cardiac resynchronization therapy. *J Am Coll Cardiol* 2002;40:536-545.
25. Kim WY, Sogaard P, Mortensen PT et al. Three dimensional echocardiography documents haemodynamic improvement by biventricular pacing in patients with severe heart failure. *Heart* 2001;85:514-520.
26. Zhang Q, Yu CM, Fung JW et al. Assessment of the effect of cardiac resynchronization therapy on intraventricular mechanical synchronicity by regional volumetric changes. *Am J Cardiol* 2005;95:126-9.
27. Burgess MI, Jenkins C, Chan J, Marwick TH. Measurement of left ventricular dyssynchrony in patients with ischaemic cardiomyopathy: A comparison of real-time three-dimensional and tissue Doppler echocardiography. *Heart* 2007,93:1191-1196.
28. Murphy RT, Sigurdsson G, Mulamalla S et al. Tissue synchronization imaging and optimal left ventricular pacing site in cardiac resynchronization therapy. *Am J Cardiol* 2006;97:1615-1621.
29. Becker M, Franke A, Breithardt OE et al. Impact of left ventricular lead osition on the efficacy of cardiac resynchronization therapy. A two-Dimensional strain echocardiography study. *Heart*. 2007;93:1197-1203.
30. Suffoletto MS, Cannesson M, Tanabe M, Saba S, Gorcsan J III. Relationship of tissue Doppler dyssynchrony and acute hemodynamic response to later reverse remodelling after resynchronization therapy. *J Am Coll Cardiol* 2006;47:A11 (abstract).

CHAPTER 4

Real-time three-dimensional echocardiography as a novel approach to quantify left ventricular dyssynchrony: a comparison study with phase analysis of gated myocardial perfusion SPECT

N Ajmone Marsan, M M Henneman, J Chen, C Ypenburg, P Dibbets, S Ghio, G B Bleeker, M P Stokkel, E E van der Wall, L Tavazzi, E V Garcia, and J J Bax

J Am Soc Echocardiogr 2008;21:801–7.

ABSTRACT

Objectives: Different imaging modalities have been explored for assessment of left ventricular (LV) dyssynchrony. Gated myocardial perfusion SPECT (GMPS) with phase analysis is a reliable technique to quantify LV dyssynchrony and predict response to cardiac resynchronization therapy. Real time three-dimensional echocardiography (RT3DE) is a novel imaging technique that provides an index of LV systolic dyssynchrony (SDI), based on regional volumetric changes as a function of time and calculated as the standard deviation of time-to-minimum systolic volume of 16-standard myocardial segments expressed in percentage of cardiac cycle. The aim of this study was to compare LV dyssynchrony evaluated with GMPS with LV dyssynchrony assessed with RT3DE.

Methods: The study population consisted of 40 heart failure patients who underwent both GMPS and RT3DE.

Results: Good correlations between LV dyssynchrony assessed with RT3DE and GMPS were demonstrated ($r = 0.76$ for histogram bandwidth, $r = 0.80$ for phase SD, $p < 0.001$). Patients with substantial LV dyssynchrony on GMPS (defined as $\geq 135°$ for histogram bandwidth and $\geq 43°$ for phase SD), had significantly higher SDI than patients without substantial LV dyssynchrony.

Conclusions: The good correlations between LV dyssynchrony assessed with GMPS and with RT3DE provide further support for the use of RT3DE for reliable assessment of LV dyssynchrony.

INTRODUCTION

Patients with heart failure, depressed left ventricular (LV) function and wide QRS complex may benefit from cardiac resynchronization therapy. Previous studies have shown that the presence of LV dyssynchrony is important for the response to cardiac resynchronization therapy (CRT) [1]. Different imaging modalities have been explored for assessment of LV dyssynchrony, including echocardiography [2,3], magnetic resonance imaging [4] and gated myocardial perfusion single photon emission computed tomography (GMPS) with phase analysis [5,6]. A three-dimensional (3D) technique may be preferred since these techniques provide information on LV dyssynchrony in the entire left ventricle. In addition, reliable information on LV ejection fraction (LVEF) can simultaneously be obtained. Recently, a novel echocardiographic technique has emerged for the assessment of LV dyssynchrony: real time three-dimensional echocardiography (RT3DE) [7]. This technique allows accurate quantification of LV volumes and LVEF [8–10] and functional assessment of 16 LV segments. In addition, an index of LV systolic dyssynchrony (SDI), based on analysis of regional volumetric changes, can be derived from RT3DE to quantify the severity of LV dyssynchrony [7].

Initial results with RT3DE for assessment of LV dyssynchrony are promising but further validation is needed. In the current study, assessment of LV dyssynchrony by RT3DE was compared with GMPS using phase analysis. Phase analysis is a count-based method that extracts the phase from the regional LV count changes during the cardiac cycle. Phase information is related to the onset of mechanical contraction in the 3D myocardial wall and therefore provides information on the synchrony of the contraction of the LV [11–13]. This approach provides important information on the presence of LV dyssynchrony in patients with heart failure and can predict response to CRT [5,6]. The aim of the present study was to investigate how LV dyssynchrony as evaluated with phase analysis with GMPS relates with LV dyssynchrony as assessed with RT3DE. Assessment of LVEF with both techniques was also compared.

METHODS

Patients and study protocol

The study population consisted of 40 consecutive patients with drug-refractory heart failure, who were referred to our heart failure out-patient clinic for evaluation of therapeutic options (e.g. medical therapy, surgery, CRT). In all patients, GMPS was performed to exclude inducible ischemia or viability, in order to refer patients to revascularization if indicated [14,15]. In addition, phase analysis was used to evaluate the presence of LV dyssynchrony. All patients also underwent RT3DE for assessment of LV volumes and function, and LV dyssynchrony. Thereafter,

LV dyssynchrony measured with RT3DE was compared with LV dyssynchrony measured with phase analysis.

Patients' clinical status was evaluated by assessment of NYHA functional class, exercise capacity (using the 6-minute walk test) and quality-of-life score (using the Minnesota quality-of-life questionnaire).

Gated myocardial perfusion SPECT

Resting GMPS with technetium-99m tetrofosmin (500 MBq, injected at rest) was performed using a triple head SPECT camera system (GCA 9300/HG, Toshiba Corp.) equipped with low energy high resolution collimators. A 20% window around the 140-KeV energy peak of technetium-99m tetrofosmin was used. A total of 90 projections (step and shoot mode, 35 seconds per projection, imaging time 23 minutes) was obtained over a 360-degree circular orbit. GMPS acquisition involved 16 frames per cardiac cycle with an average temporal resolution of 45 ms. Data were stored in a 64 x 64 matrix. Data were reconstructed by filtered backprojection and then reoriented to yield gated short-axis images. The reconstruction was performed over 360 degrees and took generally 3–5 minutes. LVEF was assessed from the gated short-axis images using previously validated and commercially available automated software (quantitative gated SPECT, QGS, Cedars-Sinai Medical Center, Los Angeles, California) [16].

All studies were then submitted to the Emory Cardiac Toolbox for phase analysis [11]. A phase distribution was extracted from a GMPS study, representing the regional onset of mechanical contraction of the LV. It can be displayed in a polar map or in 3D and used to generate a phase histogram. Two quantitative indices have been recently validated to assess LV dyssynchrony with phase analysis and to predict response to CRT [5,6]: 1. histogram bandwidth, which includes 95% of the elements of the phase distribution; 2. phase SD, which is the SD of the phase distribution. In a normal heart LV contraction is homogeneous and phase distribution is nearly uniform with a highly peaked distribution. As the LV mechanical synchrony worsens, histogram bandwidth and phase SD are expected to increase. Based on previous work [6], we applied a cut-off value of 135° for histogram bandwidth and of 43° for phase SD to define substantial LV dyssynchrony.

Real time three-dimensional echocardiography

Acquisition of the 3-dimensional data set

Patients were imaged in left lateral decubitus position with a commercially available system (iE33, Philips Medical Systems, N.A., Bothell, Washington, USA) equipped with X3, fully sampled matrix transducer. Apical full-volume data sets were obtained in all patients. The acquisition of all images could be completed in approximately 5 minutes in all patients. For the evaluation of LV volumes and LVEF, the lowest scan line density was used and gain and compression were adjusted to obtain a good image quality and a clear endocardial border. With dedicated software (Large Volume Size, Vision 2007, Philips Medical Systems) 4 small real-time sub-volumes were acquired from alternate cardiac cycles and combined to provide a larger pyramidal volume (up to 103 x 103 degrees) and to ensure a complete capture of the LV. The acquisition was performed during end-expiratory phase of 1 breath-hold and with a relatively stable heart rate to minimize translation artefacts between the 4 sub-volumes. For the evaluation of LV dyssynchrony the frame rate was optimized by reducing the depth and by the acquisition of a full-volume data set of 7 sub-volumes with an average temporal resolution of 30 ms.

Assessment of LV volumes and LV ejection fraction

RT3DE data sets were stored digitally and quantitative analysis of the 3D data was performed off-line using a semi-automated contour tracing algorithm (Q-Lab, version 5.0, Philips Medical Systems) over a complete heart cycle. The echocardiographic examination and the off-line analysis were performed by the same experienced echocardiographist, blinded to the GMPS and clinical data.

After first identifying the apex and mitral annulus on end-diastolic and end-systolic slices, a preconfigured ellipse was fitted to the endocardial border for each frame. The endocardial border definition was optimal in most of patients and, in case of a suboptimal automated contour tracing, manual adjustments have been performed (in 12 out of 40 patients). A 3D model of the LV was then generated and LV volumes and LVEF fraction were provided (Figure 1). Papillary muscles were included in the LV cavity. The post-processing of the images required between 2 and 5 minutes.

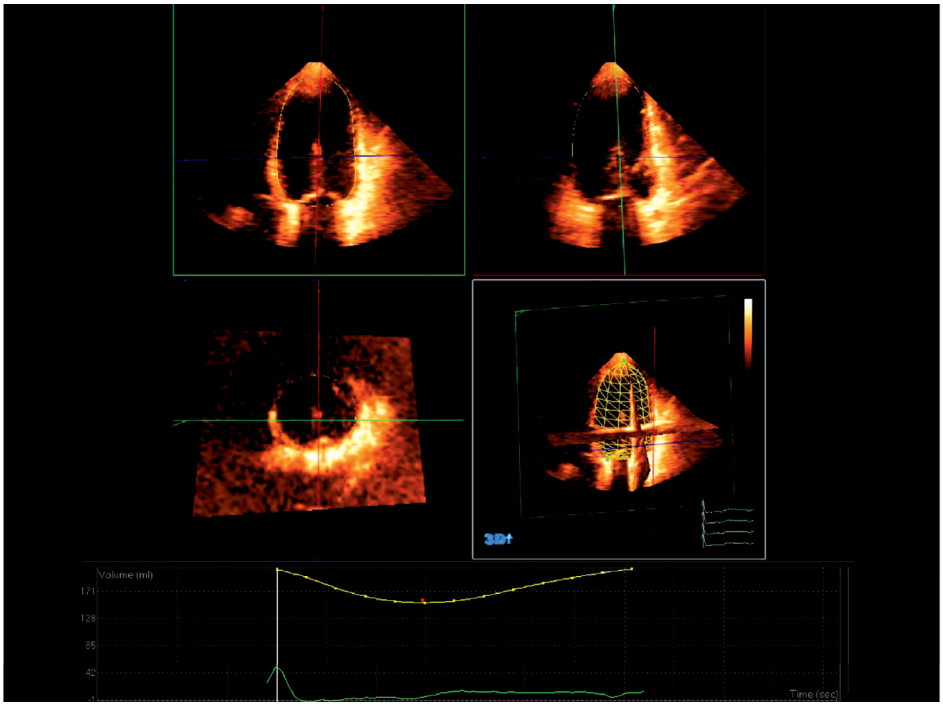


Figure 1. Example of 3D LV volumes and LVEF generated by post-processing of a RT3DE dataset, acquired in a heart failure patient.

Assessment of LV dyssynchrony

The LV 3D model was subdivided in 16 pyramidal sub-volumes (6 basal segments, 6 mid segments and 4 apical segments). For the whole LV and for each volumetric segment, it is possible to derive time-volume data for the entire cardiac cycle and assess the time taken to reach the minimum systolic volume (Tmsv). As previously described by Kapetanakis et al [7], the standard deviation of 16 segments Tmsv expressed in percentage of cardiac cycle (SDI) was calculated. Parametric images, derived from over 800 virtual waveforms, are also provided by the software (Q-Lab, version 5.0, Philips Medical Systems) with a visual presentation (polar plot) of LV regional contraction timings. The global Tmsv is used as timing reference and coded in green. Early segments are coded in blue, whereas late segments are coded in red/yellow (Figure 2) allowing a rapid identification of the area of latest activation.

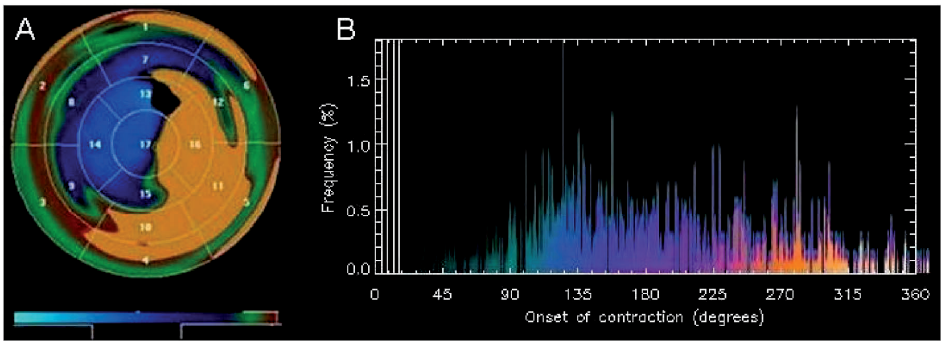


Figure 2. Example of a patient with severe LV dyssynchrony on both RT3DE and phase analysis with GMPS.
Panel A: Polar map generated by post processing of a RT3DE dataset. Early activated segments are coded in blue, whereas late activated segments are coded in red/yellow allowing a rapid identification of the area of latest activation. This patient had an SDI of 16.4%.
Panel B: Histogram distribution generated by phase analysis displaying a non-uniform and wide-spread distribution (early activated segments in blue, late activated segments in yellow) (same patient as panel A). This patient had a histogram bandwidth of 257º and a phase SD of 77.7º

Reproducibility of the RT3DE measurements

Twenty patients were selected to evaluate the inter- and intra-observer agreement for the analysis of LVEF and LV dyssynchrony. Bland-Altman analysis was performed to evaluate agreement between observer 1 and observer 2 to determine inter-observer agreement. An excellent agreement was found with a mean difference for SDI and LVEF of 0.1±2 % (p = NS) and 0.4±3 % (p = NS), respectively. Similarly, the 3D measurements derived by the first observer were compared (Bland-Altman analysis) with the results calculated by the same operator 1 month later. The intra-observer agreement was excellent with average differences of 0.03±0.4 % (p = NS) for SDI and 0.8±2 % (p = NS) for LVEF.

Statistical analysis

Continuous data are presented as mean ± SD. Categorical data are presented as absolute number or percentages. Unpaired and paired Student *t* test, Mann-Whitney test and χ^2 test were used for appropriate comparisons. Pearson's correlation analysis was performed to evaluate the relation between LV dyssynchrony (SDI) by RT3DE and histogram bandwidth and phase SD by the phase analysis of GMPS. A similar approach was used to compare assessment of LVEF by RT3DE and GMPS together with the Bland-Altman analysis that was performed to evaluate the mean difference between the two techniques. A p-value <0.05 was considered to be statistically significant. A statistical software program SPSS 12.0 (SPSS Inc, Chicago, Il, USA) was used for statistical analysis.

RESULTS

Patient characteristics

Baseline characteristics of the study population (32 men; mean age 62±10 years) are summarized in Table 1. Most patients had ischemic etiology of cardiomyopathy (75%) and 68% of patients was in NYHA functional class III. Mean QRS duration was 135±33 ms. Patients had severe LV dysfunction and dilatation (mean LVEF 29±7%, mean LV end-diastolic volume 223±70 ml).

The correlation between LVEF assessed with GMPS and RT3DE was good ($r = 0.84$ ($r^2 = 0.7$, $p < 0.001$). The Bland-Altman analysis revealed a small, but non-significant difference in the value of LVEF measured with RT3DE and GMPS: GMPS LVEF was 0.8±8 % lower than RT3DE LVEF (p = NS) (Figure 3).

Table 1. Baseline characteristics of the study population (n = 40).

Age (yrs)	**62±10**
Gender (M/F)	32/8
NYHA class, n (%)	2.7±0.5
I	0
II	13 (32)
III	27 (68)
IV	0
6-MWT (m)	354±118
QoL score	29±15
QRS duration (ms)	135±33
Etiology, n (%)	
Ischemic	30 (75)
Idiopathic	10 (25)
LVEF (%)	29±7
LVEDV (ml)	223±71
LVESV (ml)	159±61
Histogram bandwidth (°)	149±73
Phase SD (°)	46±22

LVEDV = left ventricular end-diastolic volume; LVEF = left ventricular ejection fraction; LVESV = left ventricular end-systolic volume; 6-MWT = 6 minute walk test; QoL = quality of life score.

LV mechanical dyssynchrony

The mean value of SDI in the study population was 7.8±4.8%, whereas from phase analysis the mean value of histogram bandwidth was 149±73° and the mean value of phase SD was 46.0±21.7°. A good correlation was observed between SDI and LV dyssynchrony assessed with

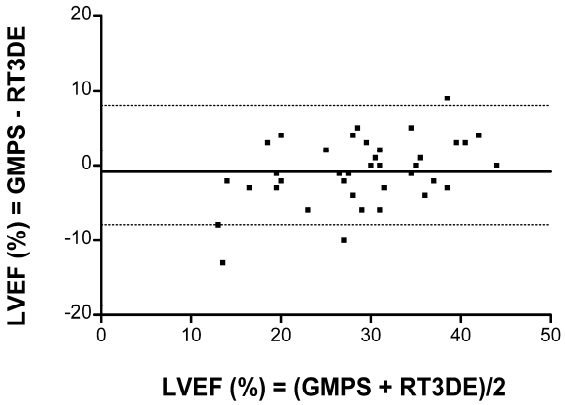


Figure 3. Bland-Altman scatter plot of differences in LVEF between RT3DE and GMPS and the average LVEF between the two techniques: GMPS LVEF is 0.8±8 % lower than RT3DE LVEF (p = NS).

phase analysis. Pearson's correlation coefficient was 0.76 ($r^2 = 0.58$) for histogram bandwidth ($p < 0.001$) and 0.80 ($r^2 = 0.64$) for phase SD ($p < 0.001$) (Figures 4A and 4B). Based on previous work,[6] we applied a cut-off value of 135° for histogram bandwidth and of 43° for phase SD to define substantial LV dyssynchrony. Considering the value of histogram bandwidth, 21 patients (52%) had substantial LV dyssynchrony (defined as ≥135°). No significant differences in baseline echocardiographic characteristics were found between patients with and without substantial LV dyssynchrony (Table 2), except that SDI was higher in patients with histogram bandwidth ≥135°: 10.4±5.1% versus 4.8±1.8% ($p < 0.001$) (Figure 5A). Considering phase SD, 19 patients (48%) had substantial LV dyssynchrony (defined as ≥43°) and these patients had a significantly higher value of SDI as compared to patients without substantial LV dyssynchrony: 11.2±4.8% versus 4.7±1.9% ($p < 0.001$) (Figure 5B).

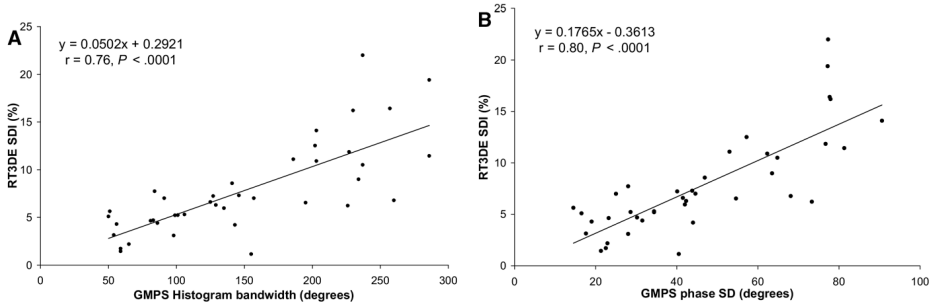


Figure 4A. Correlation between histogram bandwidth assessed with phase analysis of GMPS and LV dyssynchrony assessed with RTDE (SDI).
Figure 4B. Correlation between phase SD by phase analysis of GMPS and LV dyssynchrony assessed with RT3DE (SDI).

The relatively low percentage of patients with substantial LV dyssynchrony may be partially explained by the characteristics of the study population that consists of heart failure patients with varying degrees of LV dysfunction and both wide and narrow QRS complexes.

Table 2. Baseline characteristics of patients with substantial and without substantial LV dyssynchrony assessed by histogram bandwidth and phase SD from phase analysis.

	Histogram bandwidth <135° (n = 19)	**Histogram bandwidth ≥135° (n = 21)**	**p-value**
Ischemic etiology, n (%)	12 (63)	18 (86)	NS
LVEF (%)	29±7	30±8	NS
LVEDV (ml)	229±69	219±74	NS
LVESV (ml)	164±59	155±63	NS
SDI (%)	4.8±1.8	10.4±5.1	<0.001
	Phase SD <43° (n = 21)	**Phase SD ≥43° (n = 19)**	**p-value**
Ischemic etiology, n (%)	13 (62)	17 (89)	NS
LVEF (%)	29±7	30±8	NS
LVEDV (ml)	224±68	223±76	NS
LVESV (ml)	161±59	157±64	NS
SDI (%)	4.7±1.9	11.2±4.8	<0.001

SDI = systolic dyssynchrony index assessed with RT3DE. For other abbreviations see Table 1.

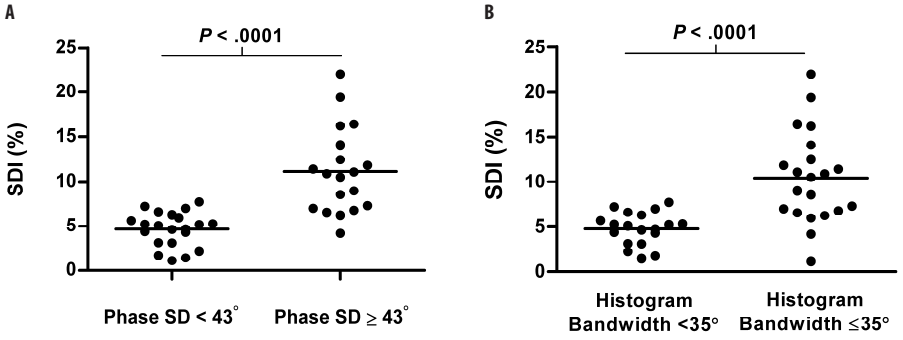


Figure 5A. LV dyssynchrony assessed with RT3DE (SDI) is significantly higher in patients with substantial LV dyssynchrony on phase analysis, using a cut-off value for histogram bandwidth of 135° as previously described.[6]

Figure 5B. LV dyssynchrony assessed with RT3DE (SDI) is significantly higher in patients with substantial LV dyssynchrony on phase analysis, using a cut-off value for phase SD of 43° as previously described.[6]

LV systolic function vs. LV mechanical dyssynchrony

Of the 40 patients included, 22 (55%) had LVEF ≤30%, assessed by RT3DE, whereas 18 (45%) patients had LVEF >30%. No significant difference in LV dyssynchrony, measured with both RT3DE and phase analysis, was noted between the two groups. Histogram bandwidth was 148±67° in patients with LVEF ≤30% and 150±81° in patients with LVEF >30% (p = NS); phase SD was 45.1±18.3° in patients with LVEF ≤30% and 47.0±25.8° in patients with LVEF >30% (p = NS); accordingly SDI was 6.9±3.0% in patients with LVEF ≤30% and 8.8±6.3% in patients with LVEF >30% (p = NS).

Correlations between GMPS variables histogram bandwidth and phase SD, and SDI were slightly better for patients with LVEF >30% (histogram bandwidth: $y = 0.0662x - 1.1875$, $r = 0.85$ ($r^2 = 0.72$); and phase SD: $y = 0.2101x - 1.1238$, $r = 0.86$ ($r^2 = 0.74$)) as compared with patients with LVEF ≤30% (histogram bandwidth: $y = 0.0305x + 2.4374$, $r = 0.69$ ($r^2 = 0.48$); phase SD: $y = 0.1185x + 1.5864$, $r = 0.73$ ($r^2 = 0.53$)).

Discussion

The findings in the current study support the use of RT3DE for assessment of LV dyssynchrony; assessment of LV dyssynchrony according to RT3DE using SDI, correlated well with previously validated nuclear imaging techniques for assessment of LV dyssynchrony. In particular, SDI by RT3DE correlated well with histogram bandwidth and phase SD by GMPS phase analysis.

In addition, both techniques can assess the LVEF with high accuracy, and the correlation between both modalities for assessing LVEF in the current study was good ($r = 0.84$, $p < 0.001$) with a small, non-significant difference (mean difference 0.8±8 %).

LV dyssynchrony appears important in the response to CRT. Many techniques have been used to assess LV dyssynchrony and to predict response to CRT. For example, TDI has been used for assessing longitudinal myocardial velocities and strain, and speckle tracking focuses on the evaluation of radial strain [2,17]. Other non-echocardiographic techniques for assessment of LV dyssynchrony include GMPS with phase analysis [5,6], and velocity encoded magnetic resonance imaging (VE-MRI)[4]. However, all these techniques have their disadvantages: echocardiographic techniques only allow assessment of dyssynchrony in a 2D setting, GMPS with phase analysis involves radiation and VE-MRI cannot be applied after CRT implantation. The optimal modality would be a 3D approach that combined all the different components of myocardial contraction (longitudinal, radial circumferential), that is also suitable for repeated imaging without imposing a radiation burden. RT3DE is a novel echocardiographic technique that appreciates radial, longitudinal and circumferential timing of the myocardium. Moreover, it permits identification of the area of latest mechanical activation and accurate assessment of LV function and size without imposing a radiation burden. Recently, Kapeta-

nakis et al [7] have studied the feasibility of LV dyssynchrony assessment with RT3DE in a large group of patients and normal subjects. The authors developed an index (SDI) to quantify LV dyssynchrony with RT3DE by calculating the time to reach minimum regional volume for each segment as a percentage of the cardiac cycle. The SDI was defined as the SD of the timings of all 16 segments. After classifying patients according to their LV systolic (dys) function (normal with LVEF >50%, mild dysfunction with LVEF 40-49%, moderate dysfunction with LVEF 30-39%, and severe dysfunction with LVEF <30%), the authors were able to show significant differences in SDI between these 4 groups. In addition, 26 patients were referred for CRT implantation. It was observed that responders to CRT had significantly higher SDI at baseline than the non-responders (16.6±1.1% vs 7.1±2.0%, p <0.001). After a mean follow-up of 10±1 months, a reduction in SDI could be demonstrated in the responders to CRT, whereas an increase in SDI was observed in the non-responders. Although these results are promising, only a moderate correlation could be detected for SDI and the SD of the maximum sustained systolic velocity (Ts-SD) as assessed with TDI (r = 0.38). These observations are in line with data reported by Burgess and colleagues [18], who compared RT3DE and TDI for the assessment of LV dyssynchrony in 100 patients with ischemic cardiomyopathy. The authors hypothesized that the poor correlation between these 2 techniques could be in part explained by the respective assessment of longitudinal versus radial timing.

In the current study, the performance of RT3DE for assessment of LV dyssynchrony was compared with phase analysis with GMPS in heart failure patients with varying degrees of LV dysfunction and both wide a narrow QRS complexes. Table 3 provides and head-to-head comparison between the two techniques from a technical point of view. The temporal resolution of GMPS is perceived to be slightly lower as compared with echocardiography. Both techniques use the first harmonic Fourier approximation to improve the temporal resolution. The first harmonic Fourier approximation can enhance phase calculation if it is applied to data with lower temporal resolution by transforming discrete data points into a continuous curve. For GMPS phase analysis only the systolic portion of the data is used to determine the phase. By fitting the curve closely with the systolic data points, the artifactual phase difference resulting from a lower temporal resolution is importantly reduced [6].

Table 3. Head-to head comparison between GMPS and RT3DE from a technical point of view.

	GMPS	RT3DE
Mean imaging time	23 min	5 min
Mean post-processing time	3-5 min	2-5 min
Mean temporal resolution	45 ms	30 ms
Mean frame rate	16 frames per cycle	20-35 frames per sec
LV dyssynchrony assessment	regional time-to-onset of mechanical contraction	regional time-to-minimum systolic volume
LV dyssynchrony parameter	Histogram bandwidth Phase SD	SDI

SDI = systolic dyssynchrony index.

Although phase analysis with GMPS measures the regional onset of mechanical contraction and RT3DE the regional time-to-minimum systolic volume, both techniques evaluate the regional changes with a 3D approach, combining all the different components of myocardial contraction. A good correlation between RT3DE and phase analysis with GMPS was demonstrated for the assessment of LV dyssynchrony (r = 0.76 for histogram bandwidth, r = 0.80 for phase SD). A good correlation between the two techniques was also found for LVEF assessment. However, the correlation coefficient (r = 0.84) was somewhat lower as compared to other validation studies between RT3DE and cardiac magnetic resonance imaging (r = 0.9) [19,20], although Jenkins et al [21] found a correlation coefficient of 0.81, which is fairly in line with our results.

Several limitations of the current study need attention. The patient cohort was relatively small, and larger populations need to be studied. Moreover, as we compared 2 different techniques, the basis of regional myocardial dyssynchrony is fundamentally different: GMPS considers the onset of mechanical contraction whereas RT3DE assesses the timing of minimum systolic volume. Nevertheless this difference, the present study shows that both techniques seem to correlate fairly well (r = 0.76 for histogram bandwidth and r = 0.80 for phase SD). In the present study, follow-up data after CRT implantation were not available.

A more general limitation is the radiation burden of GMPS, which renders the technique less suitable for repeated imaging.

CONCLUSIONS

The current findings demonstrate that LV dyssynchrony assessed by RT3DE correlated well with histogram bandwidth and phase SD derived from phase analysis and GMPS. The correlation between LVEF derived from both techniques was also good. These findings provide further support for the use of RT3DE for reliable assessment of LV dyssynchrony.

REFERENCES

1. Bax JJ, Abraham T, Barold SS et al. Cardiac resynchronization therapy: Part 1--issues before device implantation. *J Am Coll Cardiol.* 2005;46:2153-2167.
2. Bax JJ, Bleeker GB, Marwick TH et al. Left ventricular dyssynchrony predicts response and prognosis after cardiac resynchronization therapy. *J Am Coll Cardiol.* 2004;44:1834-1840.
3. Yu CM, Fung JW, Zhang Q et al. Tissue Doppler imaging is superior to strain rate imaging and postsystolic shortening on the prediction of reverse remodeling in both ischemic and nonischemic heart failure after cardiac resynchronization therapy. *Circulation.* 2004;110:66-73.
4. Westenberg JJ, Lamb HJ, van der Geest RJ et al. Assessment of left ventricular dyssynchrony in patients with conduction delay and idiopathic dilated cardiomyopathy: head-to-head comparison between tissue doppler imaging and velocity-encoded magnetic resonance imaging. *J Am Coll Cardiol.* 2006;47:2042-2048.
5. Henneman MM, Chen J, Ypenburg C et al. Phase analysis of gated myocardial perfusion single-photon emission computed tomography compared with tissue Doppler imaging for the assessment of left ventricular dyssynchrony. *J Am Coll Cardiol.* 2007;49:1708-1714.
6. Henneman M.M, Chen J, Dibbets P et al. Can LV dyssynchrony as assessed with phase analysis on gated myocardial perfusion SPECT predict response to CRT? J Nucl Med 2007;48:1104-1111
7. Kapetanakis S, Kearney MT, Siva A, Gall N, Cooklin M, Monaghan MJ. Real-time three-dimensional echocardiography: a novel technique to quantify global left ventricular mechanical dyssynchrony. *Circulation.* 2005;112:992-1000.
8. Kuhl HP, Schreckenberg M, Rulands D et al. High-resolution transthoracic real-time three-dimensional echocardiography: quantitation of cardiac volumes and function using semi-automatic border detection and comparison with cardiac magnetic resonance imaging. *J Am Coll Cardiol.* 2004;43:2083-2090.
9. Arai K, Hozumi T, Matsumura Y et al. Accuracy of measurement of left ventricular volume and ejection fraction by new real-time three-dimensional echocardiography in patients with wall motion abnormalities secondary to myocardial infarction. *Am J Cardiol.* 2004;94:552-558.
10. Corsi C, Lang RM, Veronesi F et al. Volumetric quantification of global and regional left ventricular function from real-time three-dimensional echocardiographic images. *Circulation.* 2005;112:1161-1170.
11. Chen J, Garcia EV, Folks RD et al. Onset of left ventricular mechanical contraction as determined by phase analysis of ECG-gated myocardial perfusion SPECT imaging: development of a diagnostic tool for assessment of cardiac mechanical dyssynchrony. *J Nucl Cardiol.* 2005;12:687-695.
12. Cooke CD, Garcia EV, Cullom SJ, Faber TL, Pettigrew RI. Determining the accuracy of calculating systolic wall thickening using a fast Fourier transform approximation: a simulation study based on canine and patient data. *J Nucl Med.* 1994;35:1185-1192.
13. Ziffer JA, Cooke CD, Folks RD et al. Quantitative myocardial thickening assessed with sestamibi clinical evaluation of a count-based method. J Nucl Med 1991 (abstract)
14. Levine MG, McGill CC, Ahlberg AW et al. Functional assessment with electrocardiographic gated single-photon emission computed tomography improves the ability of technetium-99m sestamibi myocardial perfusion imaging to predict myocardial viability in patients undergoing revascularization. *Am J Cardiol.* 1999;83:1-5.
15. Udelson JE, Coleman PS, Metherall J et al. Predicting recovery of severe regional ventricular dysfunction. Comparison of resting scintigraphy with 201Tl and 99mTc-sestamibi. *Circulation.* 1994;89:2552-2561.

16. Germano G, Kiat H, Kavanagh PB et al. Automatic quantification of ejection fraction from gated myocardial perfusion SPECT. *J Nucl Med.* 1995;36:2138-2147.
17. Suffoletto MS, Dohi K, Cannesson M, Saba S, Gorcsan J, III. Novel speckle-tracking radial strain from routine black-and-white echocardiographic images to quantify dyssynchrony and predict response to cardiac resynchronization therapy. *Circulation.* 2006;113:960-968.
18. Burgess MI, Jenkins C, Chan J, Marwick TH. Measurement of left ventricular dyssynchrony in patients with ischaemic cardiomyopathy: A comparison of real-time three-dimensional and tissue doppler echocardiography. *Heart* 2007;93:1191-1196
19. Qi X, Cogar B, Hsiung MC et al. Live/real time three-dimensional transthoracic echocardiographic assessment of left ventricular volumes, ejection fraction, and mass compared with magnetic resonance imaging. *Echocardiography.* 2007;24:166-173.
20. Nikitin NP, Constantin C, Loh PH et al. New generation 3-dimensional echocardiography for left ventricular volumetric and functional measurements: comparison with cardiac magnetic resonance. *Eur J Echocardiogr.* 2006;7:365-372.
21. Jenkins C, Chan J, Hanekom L, Marwick TH. Accuracy and feasibility of online 3-dimensional echocardiography for measurement of left ventricular parameters. *J Am Soc Echocardiogr.* 2006;19:1119-1128.

CHAPTER 5

Usefulness of multimodality imaging for detecting differences in temporal occurrence of left ventricular systolic mechanical events in healthy young adults

N Ajmone Marsan, L F Tops, J J M Westenberg, V Delgado, A de Roos, E E van der Wall, M J Schalij, and J J Bax

Am J Cardiol 2009;104:440–6.

ABSTRACT

Objectives: Detailed information about the absolute temporal occurrence of myocardial motion and deformation events during the cardiac cycle is still lacking. However, the normal time-range of these parameters may be of great importance as a reference for detecting and interpreting mechanical dyssynchrony and for identifying a delayed contraction in case of left ventricular (LV) dysfunction. The aim of this study was to determine in young healthy subjects and for different LV segments the value of: 1) time to peak systolic longitudinal velocity, displacement, strain rate and strain, using tissue Doppler imaging (TDI); 2) time to minimum systolic volume, using real-time three-dimensional echocardiography (RT3DE) and 3) time to maximum thickness, using cardiac magnetic resonance imaging (MRI).

Methods: A total of 20 young healthy volunteers (13 men, mean age 32±4 years) underwent both cardiac MRI and echocardiografic examination, including TDI and RT3DE. To define LV ejection time and isovolumic relaxation time (IVRT), aortic valve closure and opening and mitral valve opening were identified.

Results: For all LV segments, longitudinal peak systolic velocity and strain rate were early-systolic events. Peak systolic longitudinal displacement and strain, in turn, occurred in the late systole or, in 20-30% of LV segments, during IVRT, similarly to minimum systolic volume and maximum myocardial thickness.

Conclusions: The current study provides a systematic report of the normal time-range of the measurements obtained by TDI, RT3DE and cardiac MRI. Peak systolic longitudinal velocity and strain rate significantly precede peak longitudinal displacement, strain, minimum systolic volume and maximum thickness.

INTRODUCTION

Tissue Doppler imaging (TDI) has been extensively applied for the assessment of left ventricular (LV) dyssynchrony [1] and systolic function [2–4]. Measurements were mainly based on myocardial velocities [4–7] (expression of myocardial motion), but also on strain and strain rate imaging (which evaluate myocardial deformation) [3,8,9]. A systematic description of the normal temporal occurrence of myocardial motion and deformation events has not been reported. However, this information would be of great interest to better interpret LV dyssynchrony and to define when a segment has a delayed contraction [10–12]. Real-time 3-dimensional echocardiography (RT3DE) has also been proposed as a novel technique for the assessment of LV dyssynchrony and systolic function, based on the analysis of regional volumetric changes [13]. Also for this technique, the normal values of the time taken to reach the minimum systolic volume are not known. This may be of clinical importance for comparison with other imaging techniques. Similarly, cardiac magnetic resonance imaging (MRI) provides accurate information on myocardial deformation (as myocardial thickness) [14], but the normal time-values of this measure have not been extensively explored [15]. Accordingly, the aim of this study was to determine the value of time to peak systolic velocity, strain rate, displacement, strain, minimum systolic volume and maximum thickness for different LV segments, in young healthy subjects using the various techniques.

METHODS

A total of 20 young healthy volunteers (13 men, mean age 32±4 years) underwent, on the same day, both cardiac MRI and an echocardiografic examination, including TDI and RT3DE. All subjects gave informed consent and the protocol was approved by the institutional review board. No subject had a history of cardiac disease or cardiac symptoms and all of them were

Table 1. Baseline characteristics of the study population (n = 20).

Age (years)	32±4
Gender (male/female)	13/7
Body surface area (m2)	1.86±0.14
Heart rate (bpm)	63±10
Diastolic function	
E/A	1.7±0.2
Deceleration time (ms)	163±20
Left ventricular ejection fraction (%)	63±2
Left ventricular end-diastolic volume (ml)	102±18
Left ventricular end-systolic volume (ml)	38±8

normotensive and in sinus rhythm. The resting electrocardiogram (ECG) and the standard 2-dimensional echocardiographic examination were normal (Table 1).

Studies were performed using a commercially available system (Vingmed Vivid Seven, General Electric Healthcare, Horten, Norway) and a 3.5-Mhz transducer. Left ventricular end-diastolic and end-systolic volumes and LV ejection fraction were calculated from the conventional apical 2- and 4-chamber views using the biplane Simpson's technique. Peak velocity in early (E wave) and late (A wave) diastole of the transmitral flow was derived from conventional pulsed-wave Doppler imaging and the ratio was E/A calculated. To define LV ejection time and isovolumic relaxation time (IVRT), aortic valve closure (AVC) and opening (AVO) and mitral valve opening (MVO) were identified on pulsed-wave Doppler traces obtained from LV inflow and outflow tract and expressed as a percentage of the cardiac cycle.

Color Doppler TDI was superimposed on the underlying 2-dimensional grey-scale images (2-, 4- and 3-chamber apical views) to assess longitudinal myocardial regional function. Gain settings, filters and pulse repetition frequency were adjusted to optimize color saturation and to avoid any aliasing within the image. Sector size and depth were optimized for the highest possible frame rate (>150/s). At least 3 consecutive beats were recorded and the

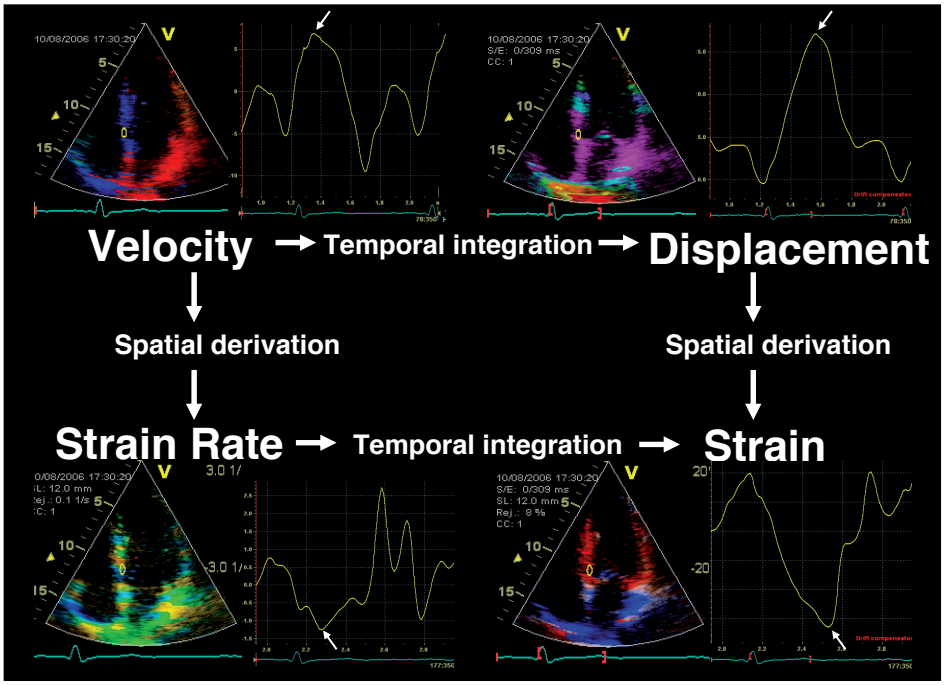


Figure 1. Examples of normal myocardial velocity, displacement, strain rate and strain curves obtained from the basal septum. The small arrows indicate the systolic peak of each curve. Myocardial displacement is obtained integrating velocity over time. Myocardial strain rate is the spatial derivative of velocity and can be integrated throughout systole to obtain strain [3].

images were digitally stored for off-line analysis (EchoPac, GE Vingmed Ultrasound, Horten, Norway). During post-processing, sample areas (8 x 5 mm) were placed at the level of 12 LV segments (basal and mid segments of the septum, lateral, inferior, anterior, posterior and anteroseptal walls) and a semi-automated tissue tracking was used to maintain the sample area in the region of interest throughout the cardiac cycle. For each segment, assessment of regional myocardial velocity, displacement, strain and strain rate were performed. Time from R wave (from the ECG signal) to peak systolic longitudinal velocity (Ts), displacement (Td), strain rate (Tsr) and strain (Tϵ) were calculated (Figure 1) and expressed as a percentage of the cardiac cycle to take the possible difference in heart rate during the echocardiographic and MRI studies into account. In particular, whether peak systolic longitudinal velocity, displacement, strain rate and strain occur after the AVC was noted, and the time from AVC was measured.

Apical full-volume data sets were obtained in all subjects using the iE33 system (Philips Medical Systems, N.A., Bothell, Washington, USA) equipped with X3, fully sampled matrix transducer. Gain and compression were optimized to obtain a good image quality and scan line density was adjusted to ensure a complete capture of the LV (sector width = 90 x 90 degrees). Real-time sub-volumes were acquired from alternate cardiac cycles and combined to provide the larger pyramidal volume during 1 breath-hold. Frame rate was optimized (32 frames/sec) reducing the depth and acquiring a full-volume data set of 7 sub-volumes. RT3DE data sets were stored digitally and quantitative analysis was performed off-line using a semi-automated contour tracing algorithm (Q-Lab, version 5.0, Philips Medical Systems) over a complete heart cycle. After first identifying, with 5 reference points, the apex and mitral annulus on end-diastolic and end-systolic slices, a preconfigured ellipse is fitted to the endocardial border for each frame and manually adjusted as required. Three-dimensional (3D) model of the LV is generated and subdivided in 17 wedge shaped (apart from the apex) sub-volumes. For 12 volumetric segments (6 basal and 6 mid) the time taken to reach the minimum systolic

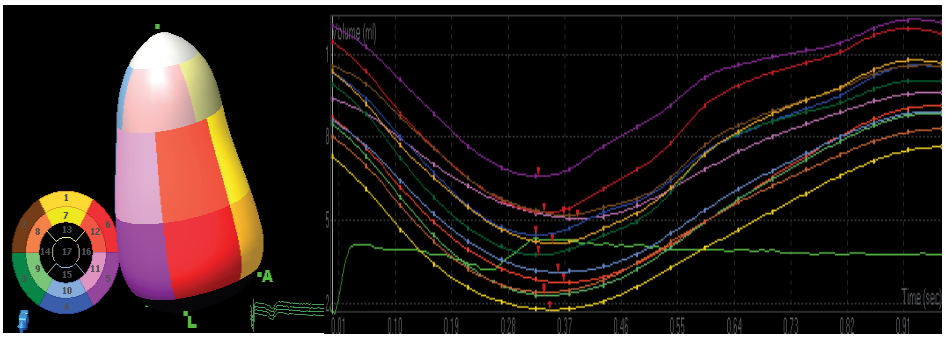


Figure 2. Three-dimensional model of a normal left ventricle (left panel) and time-volume curves derived from the 6 basal and 6 mid segments (right panel). The red dots identify the minimum systolic volume for each segment.

volume (Tmsv) from the R wave of the ECG was calculated (Figure 2). Furthermore, the time from AVC to the minimum systolic volume was assessed. To be comparable with the other imaging techniques, these timings were expressed as a percentage of the cardiac cycle.

MRI data acquisition was performed on a 1.5 T scanner (ACS-NT15 Intera, software release 11, Philips Medical Systems, Best, The Netherlands), using the body coil for transmission and a five element phased array cardiac-coil placed on the chest for signal reception. First, scout images and 2- and 4-chamber acquisitions were performed, needed for planning. A cine-set of 10-12 multi-slice images were acquired in short-axis orientation, covering the complete left ventricle from apex to base. Each slice was acquired in one single breath-hold. Steady-state free-precession was used for optimal image contrast. The following imaging parameters were used: slice thickness of the imaging planes = 10 mm, with no gap; Field-of-View = 350 mm (80% rectangular); scan matrix = 192 × 154, with reconstructed voxels of 1.37 × 1.37 × 8.0 mm; flip angle α = 50°; TR/TE = 3.3/1.7. One signal average was used. Gated cardiac synchronization was applied and 40 phases per cardiac cycle were reconstructed, yielding a temporal resolution of around 20 ms. From the complete short-axis dataset, 2 slices were selected representing the basal and mid-ventricular level and divided into 6 standard segments [16]. In these slices, epicardial and endocardial contours were manually drawn for all phases, using the QMass software package (Medis, Leiden, The Netherlands). For each segment, a radial wall thickness curve was plotted and the time from the R wave (and, in case of post-systolic peak thickness, from the AVC) to maximum wall thickness (Tt) was determined and expressed as a percentage of cardiac cycle (Figure 3).

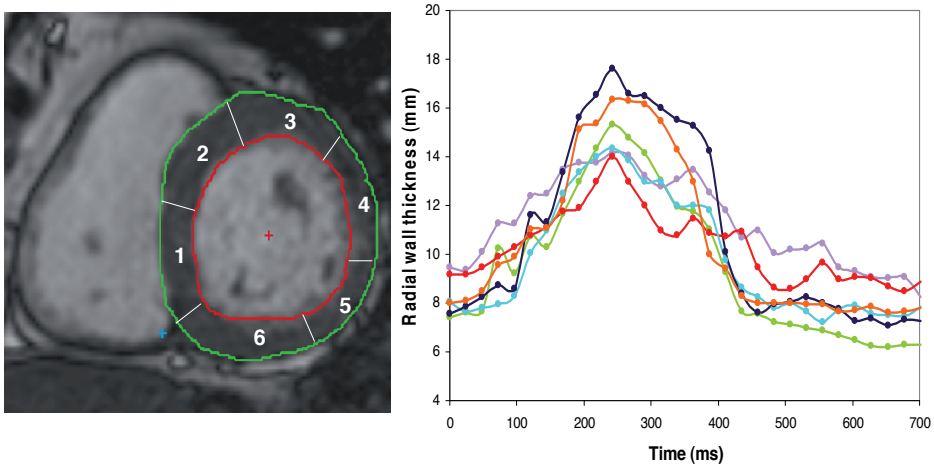


Figure 3. Example of the assessment of myocardial thickness using magnetic resonance imaging in a normal subject. In the slice representing the basal left ventricular level (left panel), epicardial and endocardial contours are drawn for all phases and the radial wall thickness curves for the 6 segments are plotted (right panel) to derive the time to maximum thickness.

Continuous data are presented as mean±SD; dichotomous data are presented as numbers and percentages. For multiple comparison between different LV segments and different timing parameters, parametric analysis of variance (ANOVA) was performed with Scheffe's post hoc analysis, after testing for normal data distribution (Kolmogorov-Smirnov test). The reproducibility of the TDI, RT3DE and MRI measurements was assessed by Bland-Altman analysis using the image dataset of 10 randomly selected subjects (120 segments): mean differences ±2SD are reported. Statistical significance was set at two tailed $p < 0.05$. A statistical software program SPSS 12.0 (SPSS Inc, Chicago, II, USA) was used for statistical analysis.

RESULTS

Tissue Doppler imaging

The mean Ts values for each LV segment are displayed in Table 2. The myocardial peak systolic velocity occurred for all the segments immediately after the AVO (= 7.5±6%, expressed as percentage of cardiac cycle) (Figure 4A) and no significant differences were found between the segments, although a trend toward an earlier Ts for the mid segments compared to the

Table 2. Mean segmental (12-segment model) values of time to peak systolic velocity (Ts), peak displacement (Td), peak systolic strain rate (Tsr) and peak strain (Tε) as derived from TDI. Also summarized are the mean segmental (12-segment model) values of time to minimum systolic volume (Tmsv) as measured by RT3DE and time to maximum thickness (Tt) as measured by MRI. The timings are expressed as a percentage of the cardiac cycle.

	Ts (%)	Td (%)	Tsr (%)	Tε (%)	Tmsv (%)	Tt (%)	p-value (ANOVA)
Septal							
Basal	11.3±2.3	34.0±5.9	11.3±2.4	35.4±7.1	35.4±4.8	33.2±7.2	<0.001
Mid	10.9±2.1	34.3±6.0	10.5±2.5	35.1±6.2	34.5±5.4	31.8±5.1	<0.001
Lateral							
Basal	10.9±1.8	33.1±4.5	11.3±2.1	33.9±5.7	35.6±5.1	32.2±4.4	<0.001
Mid	10.7±1.9	33.0±4.2	10.5±1.9	33.3±4.9	34.5±5.6	32.0±5.2	<0.001
Inferior							
Basal	10.7±1.7	33.6±5.3	11.0±1.7	33.8±6.7	35.5±4.8	34.6±4.9	<0.001
Mid	10.4±1.5	33.9±5.1	10.3±1.8	33.7±6.0	34.1±5.1	33.1±4.6	<0.001
Anterior							
Basal	10.4±2.2	33.1±4.9	10.4±2.2	32.9±6.0	34.3±5.6	31.4±3.6	<0.001
Mid	10.1±1.8	33.3±4.3	10.0±1.7	33.6±4.4	34.3±4.0	31.3±4.5	<0.001
Posterior							
Basal	10.9±1.9	33.7±5.5	11.0±2.2	35.0±6.2	35.8±5.0	35.5±5.0	<0.001
Mid	10.4±1.6	33.5±5.4	10.5±1.6	34.4±5.7	34.7±5.7	33.5±4.5	<0.001
Anteroseptal							
Basal	10.6±2.0	33.2±4.7	10.5±2.1	34.2±5.0	35.1±5.7	32.0±4.3	<0.001
Mid	10.7±2.2	33.6±4.2	10.4±2.3	34.1±5.3	34.8±4.9	31.6±4.6	<0.001

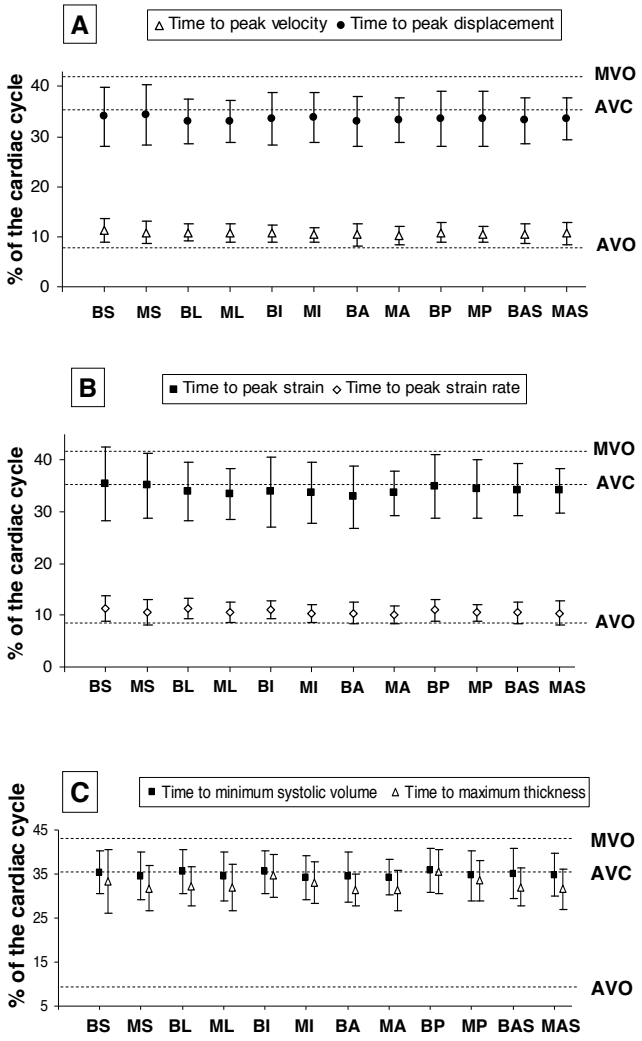


Figure 4. Distribution of time to peak systolic velocity and displacement (panel A) and time to peak systolic strain rate and strain (panel B), all measured with TDI, in relation to the aortic valve opening (AVO) or closing (AVC). Of note, MVO = mitral valve opening. In panel C, distribution of time to minimum systolic volume, measured with RT3DE, and time to maximum wall thickness, measured with MRI. Peak systolic velocity and strain rate are early systolic events, whereas peak displacement and strain occur late in systole. Likewise, minimum systolic volume and maximum myocardial thickness occur late in systole.

On the Y-axis, each of the 12 LV segments analyzed: BA = basal anterior; BAS = basal anteroseptal; BI = basal inferior; BL = basal lateral; BP = basal posterior; BS = basal septum; MA = mid anterior; MAS = mid anteroseptal; MI = mid inferior; ML = mid lateral; MP = mid posterior; MS = mid septum.

basal segments was noted. The intra- and inter-observer agreement for the Ts measurement, calculated on 120 segments, were good: 3±16 ms and 7±28 ms (p = NS), respectively.

The mean Td values for each LV segment are shown in Table 2 and were significantly different from the Ts values (p <0.001, post hoc analysis of ANOVA). Of interest, peak displacement occurred immediately before AVC (= 36.7±5.3%) or during the IVRT (before MVO = 41.2±5.9%) (Figure 4A). Out of 240 segments, 31 (13%) showed a peak displacement 9±6 ms (= 0.9±0.6% of the cardiac cycle) after the AVC. No significant differences for Td values were found between the LV segments (Table 2). The intra- and inter-observer agreement for the Td measurement (120 segments) were good: 2±18 ms and 1±46 ms (p = NS), respectively.

Table 2 shows the mean values of Tsr for each LV segment. Peak systolic strain rate occurred immediately after the AVO (Figure 4B). Subsequently, Tsr was similar to Ts (p = NS) and significantly different from Td (p <0.001, post hoc analysis of ANOVA). The intra- and inter-observer agreement for the Tsr measurement (120 segments) were good: 2±12 ms and 3±34 ms (p = NS), respectively.

Peak strain, in turn, occurred just before AVC or during the IVRT (Figure 4B). In particular, 43 (18%) out of 240 segments showed a peak displacement 16±10 ms (= 16±11% of the cardiac cycle) after AVC. The post hoc analysis of ANOVA revealed that Tε was similar to Td (p = NS) and significantly different (p <0.001) from Ts and Tsr (Table 2). The intra- and inter-observer agreement for the Tε measurement (120 segments) were good: 2±29 ms and 4±56 ms (p = NS), respectively.

No significant differences both for Tsr and Tε were found between the LV segments. However, Tsr and Tε tended to occur earlier in the mid compared to the basal segments (Table 2).

Real-time three-dimensional echocardiography

Table 2 shows the Tmsv values for each LV segment. The minimum systolic volume has been reached before the AVC or during the IVRT (Figure 4C) and therefore Tmsv was similar to Td and Tε (p = NS) and significantly different from Ts and Tsr (p <0.001). Of interest, 75 (31%) out of 240 segments showed a minimum systolic volume 33±27 ms (34±27% of the cardiac cycle) after AVC. No significant differences were found between the LV segments for Tmsv, although Tmsv tended to occur earlier in the mid compared to the basal segments (Table 2). The intra- and inter-observer agreement for the Tmsv measurement (120 segments) were good: 1±11 ms and 1±42 ms (p = NS), respectively.

Magnetic resonance imaging

The maximum myocardial radial thickness was reached before the AVC or during the IVRT (Figure 4C) and therefore Tt was similar (p = NS) to Td, Tε and Tmsv and significantly different (p <0.001) form Ts and Tsr. A total of 49 (20%) segments showed a maximum thickness 23±18 ms (24±18% of the cardiac cycle) after AVC. No significant differences were found between the LV segments, although a trend toward an earlier Ts for the mid segments compared to the basal segments was noted (Table 2). The intra- and inter-observer agreement for the Tt measurement (120 segments) were good: 1±10 ms and 2±33 ms (p = NS), respectively.

DISCUSSION

The present study provides insight into the temporal occurrence of cardiac mechanical events in normal subjects using different imaging techniques. The main findings can be summarized as follows: 1) peak systolic velocity and strain rate are early systolic events; 2) peak displacement and strain occur in the late systole, similarly to minimum systolic volume, measured with RT3DE, and maximum myocardial thickness, measured with MRI.

Different imaging techniques, using either myocardial motion or myocardial deformation measurements, have been applied to evaluate LV function and more recently, to detect the time difference in mechanical events among different LV segments (in order to assess LV dyssynchrony for patients considered for cardiac resynchronization therapy) [4–9]. However, beyond the relative comparison between segments, the absolute temporal occurrence of myocardial motion and deformation events during the cardiac cycle has been reported only occasionally [17] and detailed information on the normal range of these timings is still lacking. Nevertheless, these values may be of great importance and are needed as a reference for detecting and interpreting mechanical LV dyssynchrony. Furthermore, these values may be helpful for identifying a delayed contraction in case of (subclinical) cardiac dysfunction.

The current study provides normal reference values for timing of the different phenomena occurring in cardiac systole. No significant differences in the time-occurrence of these phenomena were found among different LV segments, probably because of the limited temporal-resolution of these imaging techniques. However, the results highlight the difference between these different phenomena, namely that peak velocity and strain rate occur early in systole whereas the resultant action (displacement, strain, minimal LV volume, maximum wall thickness) occur late in systole.

Tissue Doppler imaging, because of the high temporal resolution, is one of the most suitable techniques to detect small differences in myocardial timings [4] and is currently one of the frequently used techniques to assess LV dyssynchrony. In particular, TDI can measure myocardial velocity and displacement (obtained by integration of velocity over time) that both

reflect myocardial motion, but also myocardial strain rate (as the spatial derivative of velocity) and strain (obtained by integration of strain rate over time), both reflecting myocardial deformation [3]. Other echocardiographic modalities, such as RT3DE [13], and non-echocardiographic imaging modalities, such as MRI [18;19], provide further possibilities to evaluate LV dyssynchrony in different manners. RT3DE measures LV regional volumetric changes during the cardiac cycle, reflecting myocardial motion. MRI provides accurate information on changes of regional myocardial thickness, reflecting myocardial deformation. Based on temporal delays in any of these parameters between different regions in the LV, dyssynchrony can be derived. Since these imaging modalities do not assess the same mechanical phenomena, these different echocardiographic and MRI approaches may not be entirely comparable. Only few studies performed a direct comparison between these different techniques. Burgess et al. [20] compared TDI and RT3DE for the assessment of LV dyssynchrony in heart failure patients and reported a poor agreement between the 2 techniques ($r = 0.11$). The different mechanical events and, more important, the different ventricular timings measured by these techniques may be potential explanations for these findings [20]. In normal subjects, as demonstrated in the current study, peak velocity and peak strain rate are reached in early systole, while peak strain, displacement, minimum systolic volume and maximum thickness are end-systolic events. The early-systolic phase of the cardiac cycle corresponds to the peak systolic ventricular pressure, while at the end of the systole and during IVRT, ventricular pressure rapidly declines. Furthermore, these phases of the cardiac cycle may be differently influenced by alterations of myocardial contractility and loading conditions [21]. LV dyssynchrony may therefore affect the abovementioned systolic measurements in a different way and a systematic report of the normal range of these timings for each modality would be of great importance as a reference. For example, Breithardt et al. [10] described in heart failure patients a significant delay between myocardial motion and deformation using TDI. The authors found that peak myocardial velocities significantly preceded (~ 90 ms) peak myocardial strain and suggested that this dissociation might be dependent on the degree of asynchrony and on the underlying disease (ischemic vs. non-ischemic cardiomyopathy). However, no references to normal values were reported to further interpret these findings. The present study provides these values and showed that, also in normal subjects, Ts consistently preceded Tε, although with greater difference (~ 200 ms). Furthermore, Tsr was also found to be significantly earlier than the measurements of total amount of deformation or motion (peak displacement, peak strain, miminum systolic volume and maximum thickness). Consequently, these measurements will not correlate well in direct comparisons, since they represent different parameters, occurring at different timings in systole; in contrast, these parameters may be combined to provide more solid information on LV dyssynchrony [22]. However, further studies, including normal subjects with older age and heart failure patients, are needed to confirm these results.

Cardiac MRI and TDI have been applied to obtain quantitative information on global and regional LV systolic function [2,3,14], avoiding the disadvantages of observer-dependent inter-

pretation. RT3DE has recently become available with the potential of similar application [23]. Beyond the absolute measure of the maximum motion and/or deformation of a LV segment, the time-analysis of these events might be helpful to further interpret myocardial (subclinical) dysfunction. The presence of myocardial dysfunction and/or conduction disturbances may in fact lead to an absolute delay of LV contraction with or without any intra-ventricular relative delay or significant reduction of the global contraction. Several studies proposed the presence of post-systolic (after AVC) shortening as a marker of myocardial dysfunction, mainly during acute/chronic ischemia or in case of myocardial scar [11,12]. In fact, this phenomenon may occur in dyskinetic segments as a passive mechanism, but can also occur in hypokinetic segments as a result of prolonged contraction (active process) or delayed relaxation, and therefore may be related to residual myocardial viability [11,12]. However, post-systolic shortening has also been described as a normal finding in healthy subjects in approximately 20-30% of LV segments [12]. In particular, Kowalski et al. [17] found in 40 normal subjects that both peak radial and longitudinal strain occur either during IVRT (20 to 60 ms after AVC) or shortly before AVC. Zwanenburg et al. [24] obtained similar results for peak circumferential strain. The present study further confirms these findings for peak longitudinal strain and broadened the analysis including measurements of other imaging modalities. Peak displacement, minimum systolic volume and maximum thickness were found to occur during IVRT in 20-30% of LV segments, as well. The precise physiologic basis of this phenomenon is not known but can be related to a reshaping of the LV cavity during IVRT that should facilitate LV filling phase [25]. The presence of post-systolic shortening, besides the technique used to detect it, can therefore not be considered pathognomonic for disease. Further studies are needed to confirm these findings in subjects with older age, in which this phenomenon might be even accentuated, and to compare normal individuals with different type of patients.

REFERENCES

1. Bax JJ, Abraham T, Barold SS et al. Cardiac resynchronization therapy: Part 1--issues before device implantation. *J Am Coll Cardiol* 2005;46:2153-2167.
2. Alam M, Witt N, Nordlander R, Samad BA. Detection of abnormal left ventricular function by Doppler tissue imaging in patients with a first myocardial infarction and showing normal function assessed by conventional echocardiography. *Eur J Echocardiogr* 2007;8:37-41.
3. Sun JP, Popovic ZB, Greenberg NL et al. Noninvasive quantification of regional myocardial function using Doppler-derived velocity, displacement, strain rate, and strain in healthy volunteers: effects of aging. *J Am Soc Echocardiogr* 2004;17:132-138.
4. Sutherland GR, Stewart MJ, Groundstroem KW et al. Color Doppler myocardial imaging: a new technique for the assessment of myocardial function. *J Am Soc Echocardiogr* 1994;7:441-458.
5. Bax JJ, Bleeker GB, Marwick TH et al. Left ventricular dyssynchrony predicts response and prognosis after cardiac resynchronization therapy. *J Am Coll Cardiol* 2004;44:1834-1840.
6. Sade LE, Kanzaki H, Severyn D, Dohi K, Gorcsan J, III. Quantification of radial mechanical dyssynchrony in patients with left bundle branch block and idiopathic dilated cardiomyopathy without conduction delay by tissue displacement imaging. *Am J Cardiol* 2004;94:514-518.
7. Yu CM, Chau E, Sanderson JE et al. Tissue Doppler echocardiographic evidence of reverse remodeling and improved synchronicity by simultaneously delaying regional contraction after biventricular pacing therapy in heart failure. *Circulation* 2002;105:438-445.
8. Sogaard P, Egeblad H, Pedersen AK et al. Sequential versus simultaneous biventricular resynchronization for severe heart failure: evaluation by tissue Doppler imaging. *Circulation* 2002;106:2078-2084.
9. Yu CM, Fung JW, Zhang Q et al. Tissue Doppler imaging is superior to strain rate imaging and postsystolic shortening on the prediction of reverse remodeling in both ischemic and nonischemic heart failure after cardiac resynchronization therapy. *Circulation* 2004;110:66-73.
10. Breithardt OA, Stellbrink C, Herbots L et al. Cardiac resynchronization therapy can reverse abnormal myocardial strain distribution in patients with heart failure and left bundle branch block. *J Am Coll Cardiol* 2003;42:486-494.
11. Skulstad H, Edvardsen T, Urheim S et al. Postsystolic shortening in ischemic myocardium: active contraction or passive recoil? *Circulation* 2002;106:718-724.
12. Voigt JU, Lindenmeier G, Exner B et al. Incidence and characteristics of segmental postsystolic longitudinal shortening in normal, acutely ischemic, and scarred myocardium. *J Am Soc Echocardiogr* 2003;16:415-423.
13. Kapetanakis S, Kearney MT, Siva A, Gall N, Cooklin M, Monaghan MJ. Real-time three-dimensional echocardiography: a novel technique to quantify global left ventricular mechanical dyssynchrony. *Circulation* 2005;112:992-1000.
14. van der Geest RJ, Reiber JH. Quantification in cardiac MRI. *J Magn Reson Imaging* 1999;10:602-608.
15. Herbots L, Maes F, D'hooge J et al. Quantifying myocardial deformation throughout the cardiac cycle: a comparison of ultrasound strain rate, grey-scale M-mode and magnetic resonance imaging. *Ultrasound Med Biol* 2004;30:591-598.
16. Cerqueira MD, Weissman NJ, Dilsizian V et al. Standardized myocardial segmentation and nomenclature for tomographic imaging of the heart: a statement for healthcare professionals from the Cardiac Imaging Committee of the Council on Clinical Cardiology of the American Heart Association. *Circulation* 2002;105:539-542.

17. Kowalski M, Kukulski T, Jamal F et al. Can natural strain and strain rate quantify regional myocardial deformation? A study in healthy subjects. *Ultrasound Med Biol* 2001;27:1087-1097.
18. Chalil S, Stegemann B, Muhyaldeen S et al. Intraventricular dyssynchrony predicts mortality and morbidity after cardiac resynchronization therapy: a study using cardiovascular magnetic resonance tissue synchronization imaging. *J Am Coll Cardiol* 2007;50:243-252.
19. Lardo AC, Abraham TP, Kass DA. Magnetic resonance imaging assessment of ventricular dyssynchrony: current and emerging concepts. *J Am Coll Cardiol* 2005;46:2223-2228.
20. Burgess MI, Jenkins C, Chan J, Marwick TH. Measurement of left ventricular dyssynchrony in patients with ischaemic cardiomyopathy: A comparison of real-time three-dimensional and tissue doppler echocardiography. *Heart* 2007;93:1191-6
21. Borlaug BA, Melenovsky V, Redfield MM et al. Impact of arterial load and loading sequence on left ventricular tissue velocities in humans. *J Am Coll Cardiol* 2007;50:1570-1577.
22. Gorcsan J, III, Tanabe M, Bleeker GB et al. Combined longitudinal and radial dyssynchrony predicts ventricular response after resynchronization therapy. *J Am Coll Cardiol* 2007;50:1476-1483.
23. Jaochim NH, Sugeng L, Corsi C et al. Volumetric analysis of regional left ventricular function with real-time three-dimensional echocardiography: validation by magnetic resonance and clinical utility testing. *Heart* 2007;93:572-578.
24. Zwanenburg JJ, Gotte MJ, Kuijer JP, Heethaar RM, Van Rossum AC, Marcus JT. Timing of cardiac contraction in humans mapped by high-temporal-resolution MRI tagging: early onset and late peak of shortening in lateral wall. *Am J Physiol Heart Circ Physiol* 2004;286:H1872-H1880.
25. Sengupta PP, Khandheria BK, Korinek J et al. Apex-to-base dispersion in regional timing of left ventricular shortening and lengthening. *J Am Coll Cardiol* 2006;47:163-172.

CHAPTER 6

Tri-plane tissue Doppler imaging: a novel 3-dimensional imaging modality that predicts reverse left ventricular remodeling after cardiac resynchronization therapy

N R van de Veire, C M Yu, **N Ajmone Marsan**, G B Bleeker, C Ypenburg, J de Sutter, Q Zhang, J W H Fung, J Y S Chan, E R Holman, E E van der Wall, M J Schalij, J J Bax

Heart 2008;94:e9.

ABSTRACT

Objectives: Several 2-dimensional TDI echocardiographic techniques have proven useful to identify CRT responders. Recently a 3-dimensional probe allowing simultaneous acquisition of TDI data in 3 imaging planes became available. The present study evaluated the value of tri-plane tissue Doppler imaging (TDI) to predict reverse left ventricular (LV) remodeling after cardiac resynchronization therapy (CRT).

Methods: Sixty heart failure patients, scheduled for CRT, underwent tri-plane echocardiography with simultaneous TDI acquisition before and 6 months after implantation. From the tri-plane dataset a 3-dimensional left ventricular (LV) volume was generated and LV volumes and ejection fraction were calculated. Intraventricular dyssynchrony was quantitatively analyzed by evaluating time from onset QRS to peak myocardial systolic velocity in 12 LV segments from the tri-plane dataset and calculation of the standard deviation (Ts-SD-12). Clinical response was defined as an improvement of at least 1 New York Heart Association class. Reverse LV remodeling was defined as ≥15% decrease of LV end-systolic volume at 6 months follow-up.

Results: Responders to CRT had significantly more LV dyssynchrony at baseline than non-responders; Ts-SD-12: 42±14 versus 22±12 ($P<0.0001$). A cut-off value of 33 for baseline Ts-SD-12, acquired from the tri-plane TDI dataset, yielded a sensitivity of 89% with a specificity of 82% to predict clinical response to CRT; sensitivity and specificity to predict reverse LV remodeling were 90% and 83%.

Conclusions: Tri-plane TDI echocardiography predicts clinical response and reverse LV remodeling 6 months after CRT implantation.

INTRODUCTION

Cardiac resynchronization therapy (CRT) is now accepted as an alternative therapeutic option in heart failure patients who remain highly symptomatic despite optimized medical treatment [1]. However, using classic selection criteria for CRT including New York Heart Association (NYHA) Class III or IV, impaired left ventricular (LV) systolic function and conduction delay on the surface electrocardiogram (i.e. wide QRS complex >120 ms), up to 30% of CRT patients do not respond favourably [2]. The presence of LV dyssynchrony is considered a key issue in the identification of potential responders to CRT [3,4]. Numerous 2-dimensional (2-D) echocardiographic methods, often using tissue Doppler imaging (TDI), have been proposed to quantify LV dyssynchrony and predict response to CRT [5–10]. The TDI method originally described by Yu and co-workers is a standard deviation of electromechanical activation times (Ts-SD-12) based on a 12-segment model of the LV [7,11]. To calculate this dyssynchrony parameter, 3 different apical views need to be acquired separately, non-simultaneously, thus neglecting heart rate variability. Recently, a 3-dimensional (3D) TDI imaging modality, tri-plane TDI, became available which permits simultaneous acquisition of TDI from all LV segments during the same heartbeat. In addition, the tri-plane technique allows calculation of 3-D volumes and LV ejection fraction. There are no published data available on the potential role of tri-plane TDI to predict response to CRT.

In the present study, this novel 3-D echocardiographic technique, tri-plane TDI, was applied to 60 heart failure patients to quantify LV volumes, ejection fraction and LV dyssynchrony at baseline and at 6 months follow-up. Aim of the study was to assess the value of this tri-plane approach to predict clinical response and reverse LV remodeling, 6 months after CRT implantation.

METHODS

Patient population

The study population comprised of 60 consecutive heart failure patients scheduled for CRT. Inclusion criteria were severely symptomatic heart failure despite optimal medical treatment (NYHA class III or IV), depressed LV ejection fraction and wide QRS complex (>120 ms, with left bundle branch block or interventricular conduction delay) on the surface electrocardiogram. Patients with atrial fibrillation or a previously implanted pacemaker were excluded.

Study protocol

Within 24 hours before CRT implantation, all patients underwent the following examinations: 12-lead electrocardiogram and extensive tri-plane transthoracic echocardiography as described below. NYHA functional class was assessed by a clinician blinded to all other data. Subjects completed the Minnesota living-with-heart-failure questionnaire, a 21-question self-administered instrument with scores ranging from 0 to 5 for each question; higher scores indicate poorer quality of life [12]. Exercise capacity was assessed using the 6-minute hall walk test [13]. Six months after implantation of the CRT device, all patients underwent the same examinations including tri-plane echocardiography.

Tri-plane TDI echocardiography

Acquisition of the 3D dataset

Studies were performed with a commercially available echocardiographic platform (VIVID 7, GE Vingmed Ultrasound, Horten, Norway), equipped with a 3V-probe for tri-plane acquisition. Patients were scanned in left lateral decubitus position, from the apical window. Care was taken to visualize the true LV apex allowing simultaneous acquisition of the apical 4-, 2- and 3-chamber views. Color-coded TDI was applied to the tri-plane view to assess longitudinal myocardial regional function. Gain settings, filters and pulse repetition frequency were adjusted to optimize color saturation. Sector size and depth were optimized for the highest possible frame rate. At least three consecutive beats were recorded and the images were digitally stored for offline analysis (EchoPac, GE Vingmed Ultrasound, Horten, Norway).

Quantification of LV volumes and ejection fraction

During post-processing, the tri-plane dataset was frozen in end-diastole and the endocardial border was manually traced in the apical 4-, 2- and 3-chamber views respectively. Then, using the same heartbeat, the tri-plane dataset was frozen in end-systole and again the endocardial border was manually traced in the apical 4-, 2- and 3-chamber views. A 3-D LV end-diastolic and end-systolic volume was generated automatically by the software and LV volumes and ejection fraction were reported accordingly (Figure 1).



Figure 1. Example of 3-D LV volumes, generated from a tri-plane dataset, at baseline (Panel A) and at 6 months follow-up (Panel B) Note the significant decrease of LV volumes and the increase in LV ejection fraction.

Quantitative analysis of LV dyssynchrony

During post-processing, the tri-plane color-coded TDI dataset was used to analyze myocardial velocity curves from 12 LV segments derived from information acquired during the same heartbeat. Sample volumes were placed in the basal and mid segments of the septal, lateral, inferior, anterior, posterior and anteroseptal LV walls of the tri-plane dataset to calculate time from the beginning of QRS to peak myocardial systolic velocity (Ts). From these 12 measurements a standard deviation was calculated (Ts-SD-12) as a measure of intraventricular dyssynchrony. A patient example is provided in Figure 2. Additionally, peak myocardial systolic velocities were measured pre- and post-implantation at the basal septal, lateral, inferior and anterior LV walls.

Implantation of CRT device

The LV pacing lead was inserted transvenously via the subclavian route. First, a coronary sinus venogram was obtained during occlusion of the coronary sinus with a balloon catheter. Next, the LV pacing lead was inserted into the coronary sinus with the help of an 8F guiding catheter and positioned as far as possible in the venous system, preferably in the (postero-) lateral vein. The right atrial and ventricular leads were positioned conventionally. When a conventional indication for an internal defibrillator existed, a CRT-D device was implanted. At implantation, both the sensing and pacing thresholds (at pulse duration of 0.5 ms) of the LV pacing lead were measured.

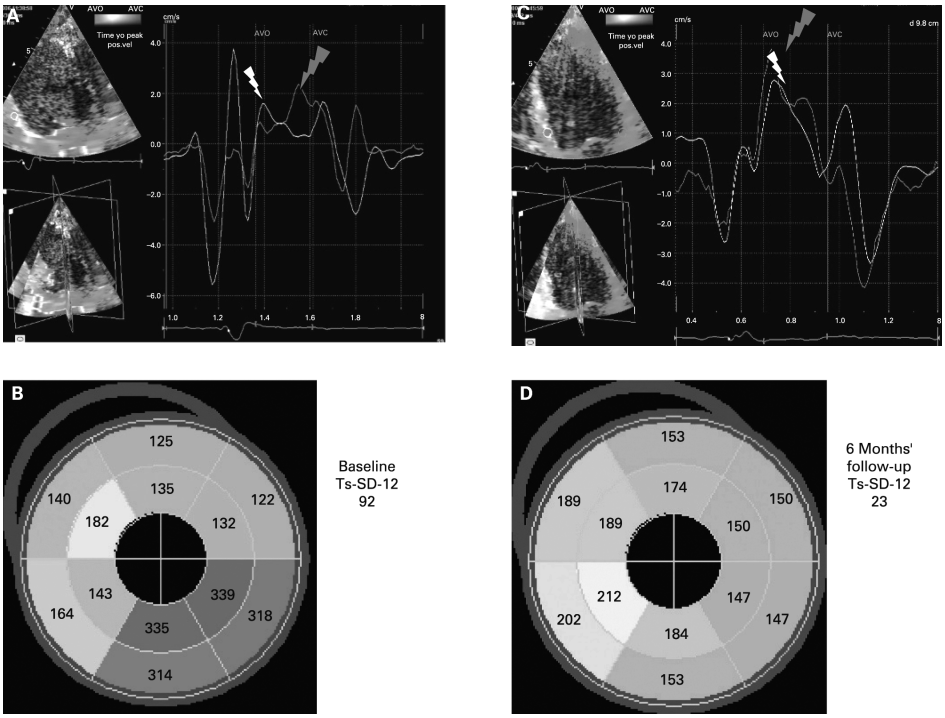


Figure 2. Example of myocardial velocity curves at the basal septum and lateral wall of the left ventricle derived from a tri-plane dataset. At baseline there is a significant delay between the septum and lateral wall (Panel A). The standard deviation (Panel B) of all 12 LV segments is 92, indicating severe LV dyssynchrony. At 6 months follow-up, the septum and lateral wall are activated simultaneously (Panel C) and LV dyssynchrony has significantly improved (Panel D).

Definition of response to CRT

Patients were subsequently divided into clinical responders and non-responders, based on an improvement in NYHA functional class by ≥1 score, 6 months post implantation. Echocardiographic response was defined as a reduction of at least 15% in LV end-systolic volume (reverse LV remodeling) at 6 months follow-up [14].

Statistical analysis

All analyses were performed with the statistical software program SPSS 12.0.1 (SPSS Inc, Chicago, Il, USA). Continuous data are presented as mean (standard deviation). Categorical data are presented as absolute numbers or percentages. Comparisons between responders and non-responders were performed using the independent-samples T test; comparisons between pre- en post-implantation characteristics were performed using the paired-samples

T test. Correlations between changes in dyssynchrony or changes in myocardial velocities and LV end-systolic volume and ejection fraction were evaluated with Spearman correlations test. Receiver-operating characteristic (ROC) curves were also analyzed to determine the value of Ts-SD-12 to predict clinical response and reverse LV remodeling after CRT. From these ROC curves, the area under the curve was calculated and presented with 95% confidence intervals (95% CI). A p-value <0.05 was considered significant.

RESULTS

Patient population

A total of 60 consecutive patients (47 men, 13 women) undergoing CRT implantation were included in the study. Mean age was 66 (11) years, 37 patients (62%) had ischemic cardiomyopathy, 23 (38%) had non-ischemic cardiomyopathy. Moreover, 54 patients (90%) were in NYHA class III and 6 (10%) in NYHA class IV. All patients were on optimized medical treatment including beta-blockers (62%), angiotensin converting enzyme inhibitors (85%), diuretics (84%) and aldactone (39%). Mean QRS width was 146 (32) ms. Using tri-plane technology, mean LV end-diastolic volume was 207 (74) ml, mean LV end-systolic volume 160 (71) ml and mean LV ejection fraction 25 (10) %.

Validation of the tri-plane technique

Consistent correlations were found between the Ts data measured using a conventional 2-D method and Ts data measured using triplane technology; r ranging between 0.94 and 0.98 (p <0.001). Bland–Altman analysis shows excellent limits of agreement between LV dyssynchrony (Ts-SD-12) measured by 2-D analysis and LV dyssynchrony measured by triplane technology (Figure 3).

Clinical response 6 months post CRT implantation

At 6 months follow-up, 63% of the patients showed clinical improvement as defined by an increase of NYHA class by at least 1 score. The only pre-implantation characteristic differing significantly between responders and non-responders was the extent of LV dyssynchrony as assessed with tri-plane TDI (42 (14) vs 22 (12), p <0.001). Besides an improvement of NYHA class (3.1 (0.3) at baseline, 1.7 (0.5) at follow-up, p <0.0001), clinical responders also showed

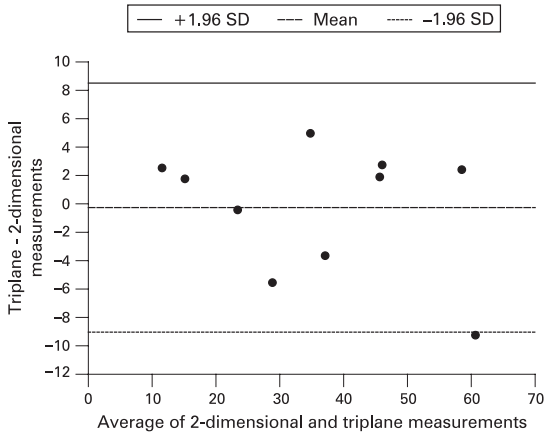


Figure 3. Bland–Altman plot comparing left ventricular dyssynchrony (Ts-SD-12) measured by a conventional two-dimensional method and triplane technology. SD, standard deviation.

improvement in 6-minute walking distance (335 (104) m at baseline, 388 (79) m at follow-up, p = 0.001), quality of life score (32 (19) at baseline, 22 (17) at follow-up, p = 0.001) LV end-diastolic volume (197 (62) ml at baseline, 172 (56) ml at follow-up, p <0.001), LV end-systolic volume (150 (60) ml at baseline, 108 (41) ml at follow-up, p <0.001) and LV ejection fraction (26 (9) % at baseline, 37 (9) % at follow-up, p <0.001). Moreover LV dyssynchrony Ts-SD-12 improved from 42 (14) to 23 (12) (p <0.001).

Reverse LV remodeling at 6 months follow-up

A total of 58% of patients exhibited a reduction of LV end-systolic volume ≥15% within 6 months after CRT implantation (Figure 4). Patients with reverse LV remodeling did not only show improvement of LV end-systolic volume (- 48.6 ml on average) but also a significant decrease of LV end-diastolic diameter (- 31.9 ml on average) and an increase of LV ejection fraction (+ 13.4% on average). Baseline clinical and echocardiographic characteristics of patients without and with reverse LV remodeling are reported in Table 1. The only pre-implantation characteristic differing significantly between patients with and without reverse LV remodeling was the extent of LV dyssynchrony as assessed with tri-plane TDI. Figure 5 shows a relation between the decrease in LV dyssynchrony and the decrease in LV end-systolic volume or the increase in LV ejection fraction.

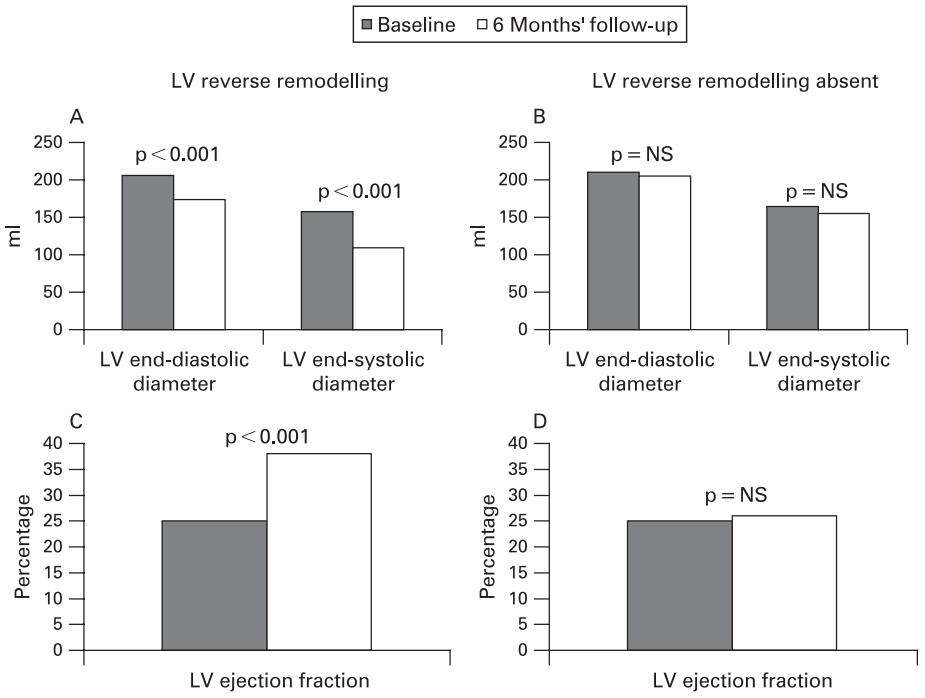


Figure 4. Change in LV volumes and LV ejection fraction at baseline (grey) and at 6 months follow-up (white) in patients exhibiting reverse remodeling (Panels A and C) and those without reverse remodeling (Panels B and D).

Table 1. Baseline characteristics of patients without and with reverse LV remodeling at 6 months follow-up.

	No reverse LV remodeling n = 25	Reverse LV remodeling n = 35	p-value
Age (years)	65 (10)	67 (12)	NS
Gender (M/F)	83% / 17%	77% / 25%	NS
Ischemic/Idiopathic	50% / 50%	31% / 69%	NS
NYHA III/IV	88% / 12%	94% / 6%	NS
6-min walking (m)	331 (119)	326 (101)	NS
Quality of life	37 (19)	32 (20)	NS
QRS width (ms)	142 (37)	149 (28)	NS
LVEDV (ml)	210 (91)	206 (61)	NS
LVESV (ml)	164 (89)	158 (59)	NS
LVEF (%)	25 (11)	25 (9)	NS
Ts-SD-12	20 (10)	44 (12)	< 0.001

Results are shown as mean (SD) unless stated otherwise.

LVEDV: left ventricular end-diastolic volume; LVEF: left ventricular ejection fraction; LVESV: left ventricular end-systolic volume; NYHA: New York Heart Association; Ts-SD-12: standard deviation of time to peak systolic myocardial velocity measured at 12 left ventricular segments derived from a triplane dataset.

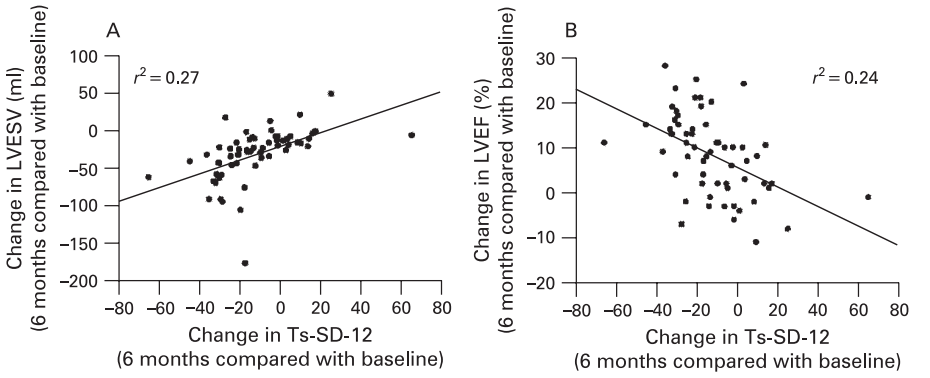


Figure 5. Scatter plots showing the relation between the decrease in left ventricular dyssynchrony (quantified as Ts-SD-12) and (A) decrease in left ventricular end-systolic volume (LVESV); (B) increase in left ventricular ejection fraction (LVEF), 6 months after cardiac resynchronisation therapy. A line is fitted using simple regression analysis and the r2 values are reported, respectively.

Prediction of clinical response after CRT by tri-plane TDI

Overall, Ts-SD-12 measured with tri-plane technology, was significantly larger in clinical responders than in non-responders, indicating severe LV dyssynchrony in the clinical responders. Figure 6A shows the ROC curve illustrating the excellent ability of Ts-SD-12, measured with tri-plane TDI technology, to predict clinical response. An ideal cut-off value for Ts-SD-12 to predict clinical response 6 months after CRT implantation, was defined at 33 ms based on the highest possible sensitivity (89%) and specificity (82%).

Prediction of reverse LV remodeling after CRT by tri-plane TDI

Overall, Ts-SD-12 measured with tri-plane technology, was significantly larger in patients with reverse LV remodeling as compared to patients without reverse LV remodeling, indicating severe LV dyssynchrony in patients with reverse remodeling. Figure 6B shows the ROC curve illustrating the excellent value of Ts-SD-12, measured with tri-plane TDI technology, to predict reverse LV remodeling. An ideal cut-off value for Ts-SD-12 to predict reverse LV remodeling at 6 months follow-up, was defined at 33 ms based on the highest possible sensitivity (90%) and specificity (83%).

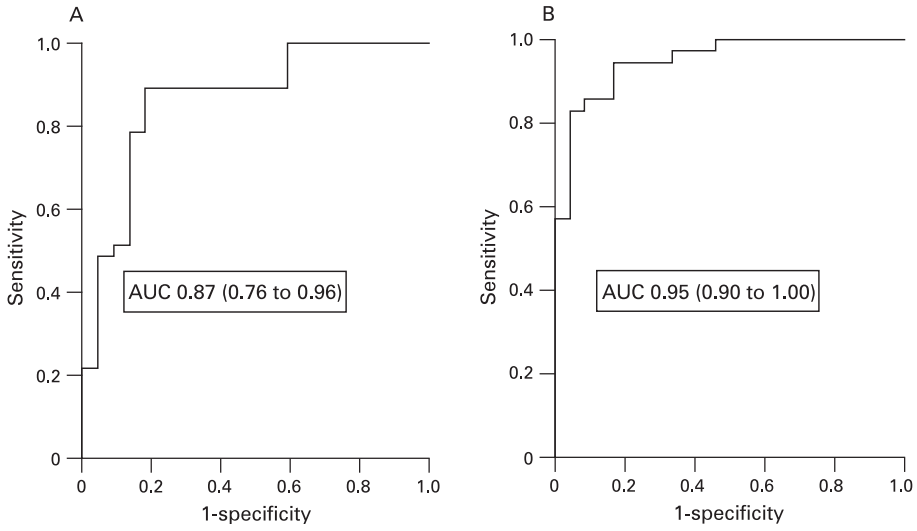


Figure 6. Panel A: ROC curve for Ts-SD-12 predicting clinical response 6 months after CRT implantation; the area under the curve is indicated with the 95% confidence interval. Panel B: ROC curve for Ts-SD-12 predicting reverse LV remodeling (defined as at least 15% reduction in LV end-systolic volume) 6 months post CRT implantation; the area under the curve is indicated with the 95% confidence interval.

DISCUSSION

The findings in the current study can be summarized as follows: 1) the 3-D echo approach permits integrated assessment of LV volumes, LV ejection fraction and LV dyssynchrony; 2) in patients undergoing CRT, LV dyssynchrony was the only predictor of clinical response to CRT; 3) the standard deviation of time to peak myocardial systolic velocity in 12 LV segments (Ts-SD-12) ≥33, calculated from the tri-plane TDI dataset, had a sensitivity of 90% with a specificity of 83% to predict reverse LV remodeling, at 6 months post CRT implantation.

Several authors have emphasized the importance of quantifying the degree of LV dyssynchrony in CRT candidates, to identify potential responders. Earlier studies proposed methods using M-mode [5] or pulsed-wave TDI [15,16], but recently, color-coded TDI [6,7,10] and techniques derived from color-coded TDI such as TSI [17] and strain rate imaging [8,9] have gained interest. The majority of color-coded TDI techniques are based on the measurement of time intervals between onset of the QRS complex and peak myocardial systolic velocity. Some authors have compared the activation times of the septal and lateral LV segments; for this approach TDI registration of the apical 4-chamber view, using 2-D technology, is sufficient [6].

Others used information derived from various LV segments. Yu and co-workers originally described the model (derived from 2D data) using electromechanical activation times of 12 LV segments to quantify LV dyssynchrony [7,11]. A potential problem with the 2D approach if

one uses the 12-segment model, is the cumbersome data acquisition. At least three separate color-coded 2D datasets are to be acquired, non-simultaneously. This implies that heart-rate variability is often neglected, resulting in non-simultaneous comparison of segmental coordination. Moreover, in all CRT studies assessing LV remodeling, LV volumes and LV ejection fraction were estimated from 2-D datasets with Simpson's biplane method.

Tri-plane imaging is a 3-D technique that integrates data from 3 conventional apical views. Validation studies have demonstrated that the tri-plane approach is superior to the bi-plane method and comparable to magnetic resonance imaging for LV volume estimation [18,19]. Recently a 3D probe became commercially available (GE Vingmed Ultrasound, Horten, Norway) allowing simultaneous acquisition of a tri-plane dataset and color-coded TDI. In the present study, we have demonstrated the multi-purpose of this tri-plane TDI dataset in 60 heart failure patients scheduled for CRT implantation. A 3D LV volume was generated allowing evaluation of volumetric changes 6 months post-implantation, showing reverse LV remodeling in responders.

Furthermore an established 2-D TDI-based method [7,11] to quantify LV dyssynchrony using a 12-segment LV model was successfully applied to the tri-plane dataset. Sample volumes were placed in 12 LV segments and myocardial peak systolic velocities or time to peak systolic velocities of any LV segment could be compared during the same heartbeat. From these data, the Ts-SD-12 was calculated. Using 2D technology, Yu et al applied the Ts-SD-12 in 30 CRT patients and reported that a cut-off value >32.6 ms permitted separation of responders and non-responders to CRT [7,11] In a subsequent study the same authors used TSI in a 2-D dataset to quantify LV dyssynchrony [17]. The Ts-SD-12 was most powerful to predict reverse LV remodeling; ROC curve analysis revealed an area of 0.90 with a sensitivity of 87% and a specificity of 81% employing a cut-off value of 34.4 ms. In the present study, the Ts-SD-12 was calculated from the tri-plane dataset. A ROC curve area of 0.95 was shown with a sensitivity of 90% and a specificity of 87% for a cut-off value of 33 ms, well in line with the above-mentioned 2-D studies. The advantage of the tri-plane method is that acquisition of a single tri-plane dataset allows simultaneous comparison of 12 LV segments during the same heartbeat whereas the 2-D method requires at least 3 acquisitions.

Experience with 3D echocardiographic evaluation of CRT patients is limited. Kapetanakis et al used real-time 3D echocardiography and calculated a systolic dyssynchrony index derived from dispersion of time to minimal regional volume in 26 patients undergoing CRT implantation [20]. The authors noted that patients with a large systolic dyssynchrony index before implantation experienced the greatest reduction in mechanical dyssynchrony after CRT, whereas patients without symptomatic improvement had a statistically lower systolic dyssynchrony index before CRT implantation. The method described by Kapetanakis et al [20] is based on identification of the last LV region reaching minimum regional volume; the tri-plane method is based on the assessment of LV dyssynchrony from TDI velocity curves, currently the most frequently used echocardiographic method to predict benefit from CRT [4].

Study limitations

Patients with atrial fibrillation and previous pacemakers were excluded; further studies are needed in these specific patient populations to explore the value of 3-D TDI.

CONCLUSIONS

In the present study, a novel 3-D echocardiographic application, allowing simultaneous acquisition of a tri-plane TDI dataset, was successfully applied in 60 heart failure patients scheduled for CRT. From the tri-plane TDI dataset, quantitative analysis of LV dyssynchrony could be derived as well as LV volumes and ejection fraction. LV dyssynchrony, derived from the tri-plane TDI dataset, was highly predictive for clinical response and LV reverse remodeling after 6 months of CRT.

REFERENCES

1. Freemantle N, Tharmanathan P, Calvert MJ et al. Cardiac resynchronization for patients with heart failure due to left ventricular systolic dysfunction – a systematic review and meta-analysis. *Eur Heart J* 2006;8:433-440.
2. Mehra MR, Greenberg BH. Cadiac resynchronization therapy: caveat medicus! *J Am Coll Cardiol* 2004;43:1145-1148.
3. Bax JJ, Abraham T, Barold SS et al. Cardiac resynchronization therapy: Part 1 issues before device implantation. *J Am Coll Cardiol* 2005;46:2153-2167.
4. Bank AJ, Kelly AS. Tissue Doppler imaging and left ventricular dyssynchrony in heart failure. *J Card Failure* 2006;12:154-162.
5. Pitzalis MV, Iacoveillo M, Romito R et al. Ventricular asynchrony predicts a better outcome in patients with chronic heart failure receiving cardiac resynchronization therapy. *J Am Coll Cardiol* 2005;45:65-69.
6. Bax JJ, Bleeker GB, Marwick TH et al. Left ventricular dyssynchrony predicts response and prognosis after cardiac resynchronization therapy, *J Am Coll Cardiol* 2004;44:834–1840.
7. Yu CM, Chau E, Sanderson JE et al. Tissue Doppler echocardiographic evidence of reverse remodeling and improved synchronicity by simultaneously delaying regional contraction after biventricular pacing therapy in heart failure. *Circulation* 2002;105:438–445.
8. Sogaard P, Egeblad H, Kim WY et al. Tissue Doppler imaging predicts improved systolic performance and reversed left ventricular remodeling during long-term cardiac resynchronization therapy. *J Am Coll Cardiol* 2002;40:723-730.
9. Breithardt OA, Stellbrink C, Herbots L et al. Cardiac resynchronization therapy can reverse abnormal myocardial strain distribution in patients with heart failure and left bundle branch block. *J Am Coll Cardiol* 2003;42:486-494.
10. Notabartolo D , Merlino JD, Smith AL et al. Usefulness of the peak velocity difference by tissue Doppler imaging technique as an effective predictor of response to cardiac resynchronization therapy, *Am J Cardiol* 2004;94:817-820.
11. Yu CM, Fung WH, Lin H et al. Predictors of left ventricular reverse remodeling after cardiac resynchronization therapy for heart failure secondary to idiopathic dilated or ischemic cardiomyopathy. *Am J Cardiol* 2002;91:684–688.
12. Rector TS, Cohn JN. Assessment of patient outcome with the Minnesota Living with Heart Failure questionnaire: reliability and validity during a randomized, double-blind, placebo-controlled trial of pimobendan. Pimobendan Multicenter Research Group. *Am Heart J*. 1992;24:1017-25.
13. Refsgaard J. This is a walking test not a talking test: the six minute walking test in congestive heart failure. *Eur Heart J* 2005;26:749-750.
14. Yu CM, Abraham WT, Bax JJ et al on behalf of the PROSPECT investigators. Predictors of response to cardiac resynchronization therapy (PROSPECT) – study design. *Am J Cardiol* 2005;49:600-605.
15. Ansalone G, Giannantoni P, Ricci R et al. Doppler myocardial imaging to evaluate the effectiveness of pacing sites in patients receiving biventricular pacing. *J Am Coll Cardiol* 2002;39:489-499.
16. Penicka M, Bartunek J, De Bruyne B et al. Improvement of left ventricular function after cardiac resynchronization therapy is predicted by tissue Doppler imaging echocardiography. *Circulation* 2004;109:978-983.
17. Yu CM, Zhang Q, Wing-Hong Fung J et al. A novel tool to assess systolic asynchrony and identify responders of cardiac resynchronization therapy by tissue synchronization imaging. *J Am Coll Cardiol* 2005;45:677-684.

18. Rodevand O, Bjornerheim R, Aakhus S, Kjekshus J. Left ventricular volumes assessed by different new three-dimensional echocardiographic methods and ordinary biplane technique. *Int J Cardiovasc Imaging* 1998;14:55-63.
19. Iwase M, Kondo T, Hasegawa K et al. Three-dimensional echocardiography by semi-automatic border detection in assessment of left ventricular volume and ejection fraction: comparison with magnetic resonance imaging. *J Cardiol* 1997;30:97-105.
20. Kapetanakis S, Kearny MT, Siva A et al. Real-time three-dimensional echocardiography. A novel technique to quantify global left ventricular mechanical dyssynchrony. *Circulation* 2005;112:992-1000.

CHAPTER 7

Left ventricular dyssynchrony assessed by two 3-dimensional imaging modalities: phase analysis of gated myocardial perfusion SPECT and tri-plane tissue Doppler imaging

N Ajmone Marsan, M M Henneman, J Chen, C Ypenburg, P Dibbets, S Ghio, G B Bleeker, M P Stokkel, E E van der Wall, L Tavazzi, E V Garcia, and J J Bax

Eur J Nucl Med Mol Imaging 2008;35:166–73.

ABSTRACT

Objectives: To compare left ventricular (LV) dyssynchrony assessment by phase analysis from gated myocardial perfusion SPECT (GMPS) with LV dyssynchrony assessment by tri-plane tissue Doppler imaging (TDI). Baseline LV dyssynchrony assessed with standard deviation (SD) of time-to-peak systolic velocity of 12 LV segments (Ts-SD) with TDI has proven to be a powerful predictor of response to CRT. Information on LV dyssynchrony can also be provided by GMPS with phase analysis of regional LV maximal count changes throughout the cardiac cycle.

Methods: Forty heart failure patients, referred for evaluation of potential eligibility for CRT, underwent both 3D echocardiography, with tri-plane TDI, and resting GMPS. From tri-plane TDI, Ts-SD was used as a validated parameter of LV dyssynchrony and compared with different indices (histogram bandwidth, phase SD, histogram skewness and kurtosis) derived from phase analysis of GMPS.

Results: Histogram bandwidth and phase SD showed good correlation with Ts-SD ($r = 0.77$ and $r = 0.74$, $p < 0.001$ respectively). Patients with substantial LV dyssynchrony assessed with tri-plane TDI (Ts-SD ≥33 ms) had also significantly higher values of histogram bandwidth and phase SD.

Conclusions: The results of this study support the use of phase analysis by GMPS to evaluate LV dyssynchrony. Histogram bandwidth and phase SD showed the best correlation with Ts-SD assessed with tri-plane TDI and appeared the most optimal variables for assessment of LV dyssynchrony with GMPS.

INTRODUCTION

Cardiac resynchronization therapy (CRT) has become an established therapy for patients with end-stage heart failure [1]. However, up to 30% of the patients do not respond to CRT when selection is based on the traditional clinical and electrocardiographic criteria (New York Heart Association (NYHA) functional class III or IV, left ventricular ejection fraction (LVEF) <35%, and QRS duration >120 ms) [2]. In the search for better selection criteria for CRT, it has been shown that patients with LV dyssynchrony have a higher likelihood of a positive response to CRT [3–8]. Over the past few years, the assessment of LV dyssynchrony has been studied extensively with echocardiography.

The most frequently used technique is tissue Doppler imaging (TDI) which permits evaluation of timing of regional myocardial velocity, and comparison of different regions yields information on LV dyssynchrony.

Bax et al. [3] have used a 4-segment model to assess LV dyssynchrony (4 basal LV segments: anterior, lateral, inferior and septal) and reported that a delay ≥65 ms among the 4 segments was a strong predictor of response to CRT. Other authors extended the analysis by evaluating the activation pattern of the entire LV. This method, originally described by Yu and co-workers [6–8], uses the standard deviation (SD) of electromechanical activation times based on a 12-segment model of LV (Ts-SD). The authors investigated 56 patients with heart failure who underwent CRT implantation and demonstrated that a cut-off value of 34.4 ms for Ts-SD could predict reverse LV remodeling after CRT with a sensitivity of 87% and a specificity of 81% [7]. However, to calculate this parameter of LV dyssynchrony, 3 apical views need to be acquired separately. A 3-dimensional (3D) TDI imaging modality (tri-plane TDI) has become available to overcome this limitation. Tri-plane TDI allows simultaneous acquisition of all LV segments during the same heartbeat rendering the technique more precise than the 2-dimensional (2D) TDI equivalent. Another recent development is the use of gated myocardial perfusion single photon emission computed tomography (GMPS) for assessment of LV dyssynchrony [9,10]. A count-based method has been developed to extract phase information from the regional LV count changes throughout the cardiac cycle, and this phase information is related to the time interval when a region, in the 3D LV wall, starts to contract (phase analysis). This technique has recently been implemented to the Emory Cardiac Toolbox as a diagnostic tool for assessment of LV mechanical dyssynchrony [9].

To further validate the use of GMPS with phase analysis for the assessment of LV dyssynchrony, a direct comparison with tri-plane TDI was performed in a cohort of heart failure patients.

METHODS

Patients population and data collection

Forty consecutive patients with heart failure, referred for evaluation of potential eligibility for CRT, were included in this study. Traditional selection criteria for CRT were applied, including moderate-to-severe drug refractory heart failure (NYHA class III or IV), depressed LVEF (<35%) and prolonged QRS duration (>120 ms). Patients with a recent myocardial infarction (<3 months) or decompensated heart failure were excluded. Evaluation of the clinical status included assessment of NYHA functional class, quality-of-life score (using the Minnesota quality-of-life questionnaire) and exercise capacity (using the 6-minute walk test). Extensive echocardiographic analysis, using 3D transthoracic echocardiography, was performed to assess LV dyssynchrony. Resting GMPS with technetium-99m tetrofosmin was clinically performed to exclude extensive ischemia and/or viability [11,12], in order to refer patients to revascularization if indicated. Thereafter, all scans were subjected to phase analysis to evaluate LV dyssynchrony. The results of the phase analysis with GMPS to assess LV dyssynchrony were subsequently compared with LV dyssynchrony derived from tri-plane TDI.

Echocardiography

3D data set acquisition

All patients underwent transthoracic echocardiography performed with a commercially available echocardiographic platform (VIVID 7, GE Vingmed Ultrasound, Horten, Norway), and equipped with a 3V-probe for 3D acquisition.

Patients were scanned in left lateral decubitus position, from the apical window in tri-plane modus, acquiring simultaneously the apical 4-, 2- and 3-chamber views. Care was taken to visualize the true LV apex. Color-coded TDI was applied to the tri-plane view to assess longitudinal myocardial regional function. Gain settings, filters and pulse repetition frequency were adjusted to optimize color saturation. Sector size and depth were optimized for the highest possible frame rate. At least two consecutive beats were recorded from each view and the images were digitally stored for off-line analysis (EchoPac, GE Vingmed Ultrasound, Horten, Norway). The echocardiographic examination and the off-line analysis were performed by the same experienced echocardiographist, blinded to the GMPS and clinical data.

3D analysis of LV dyssynchrony

During post-processing, the tri-plane TDI dataset was used to analyze myocardial velocity curves as previously described with 2D TDI echocardiography [6–8]. Sample volumes were placed in the basal and mid segments of the septal, lateral, inferior, anterior, posterior and anteroseptal LV walls to calculate the time from the beginning of the QRS complex to peak systolic velocity (Ts), using the same heart beat (Figure 1). Subsequently, the standard deviation of Ts (Ts-SD) of the 12 myocardial segments was calculated and used as a parameter of LV dyssynchrony [6-8]. A cut-off value of Ts-SD ≥33 ms was used to define the presence of substantial LV dyssynchrony.

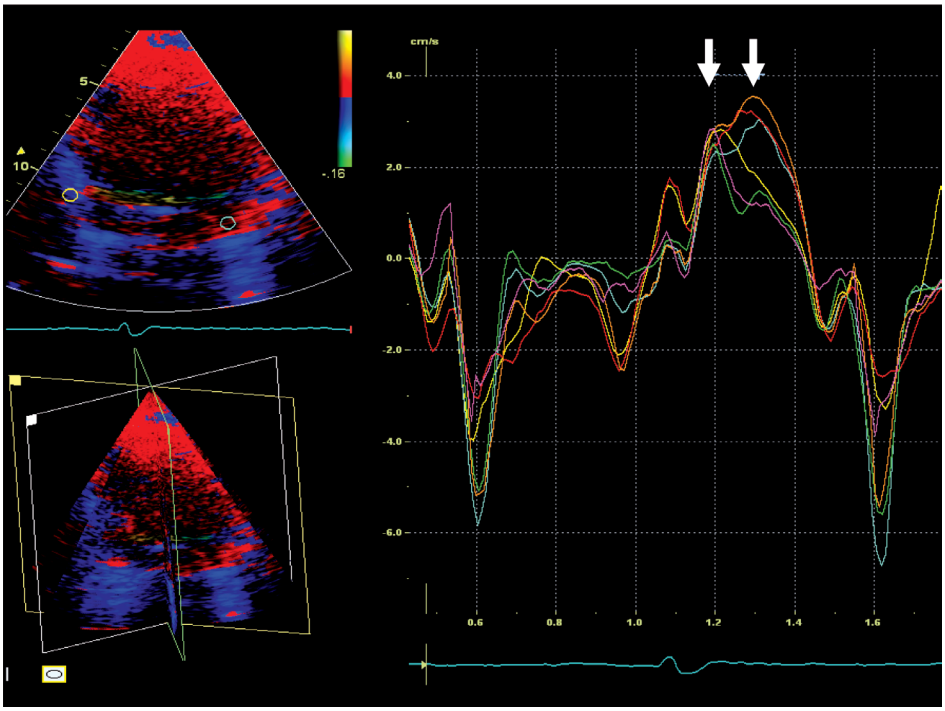


Figure 1. Example of the myocardial velocity curves that can be derived by positioning the sample volume in any LV segment of the tri-plane dataset. This patient has substantial LV dyssynchrony: the postero-lateral and anterior walls (orange, light blue and red curves) are activated later than the septal and inferior walls (yellow and green curves); standard deviation of 12 LV segments Ts is 57.5 ms.

Gated myocardial perfusion SPECT

Resting GMPS with technetium-99m tetrofosmin (500 MBq, injected at rest) was performed using a triple head SPECT camera system (GCA 9300/HG, Toshiba Corp.) equipped with low

energy high resolution collimators. Around the 140-KeV energy peak of technetium-99m tetrofosmin, a 20% window was used. A total of 90 projections (step and shoot mode, 35 seconds per projection, imaging time 23 minutes) were obtained over a 360-degrees circular orbit. GMPS acquisition involved 16 frames per cardiac cycle. Data were reconstructed by filtered backprojection and then re-oriented to yield gated short-axis images. Data reconstruction was performed over 360 degrees. These images were then submitted to the Emory Cardiac Toolbox for phase analysis [9]. GMPS images were analyzed at the department of radiology of Emory University School of Medicine by J.C. and E.V.G., who were blinded to the echocardiographic and clinical data. A phase distribution was extracted from a GMPS study, representing the regional onset of mechanical contraction of the LV. It can be displayed in a polar map or in 3D and used to generate a phase histogram. An example of a patient without LV dyssynchrony is shown in Figure 2a, whereas an example of a patient with substantial LV dyssynchrony as assessed with phase analysis by GMPS is shown in Figure 2b. The following 4 quantitative indices were obtained from the phase analysis of all patients: 1. histogram bandwidth, which includes 95% of the elements of the phase distribution; 2. phase SD, which is the SD of the phase distribution; 3. phase histogram skewness, which indicates the symmetry of the histogram; 4. histogram kurtosis, which indicates the degree to which the histogram is peaked [9]. In a healthy individual the LV contracts in a coordinated manner and the phase distribution is nearly uniform with a highly peaked distribution of the histograms. As the LV contraction becomes dyssynchronous the phase SD and histogram bandwidth are expected to increase (Figure 2b).

Statistical analysis

Continuous data are presented as mean±SD; dichotomous data are presented as numbers and percentages. Comparison of data was performed using the unpaired Student *t* test or χ^2 test when appropriate. Pearson's correlation analysis was performed to evaluate the relation between histogram bandwidth, phase SD, histogram skewness and histogram kurtosis by the phase analysis of GMPS and LV dyssynchrony (Ts-SD) by tri-plane TDI. A p-value <0.05 was considered to be statistically significant. A statistical software program SPSS 12.0 (SPSS Inc, Chicago, Il, USA) was used for statistical analysis.

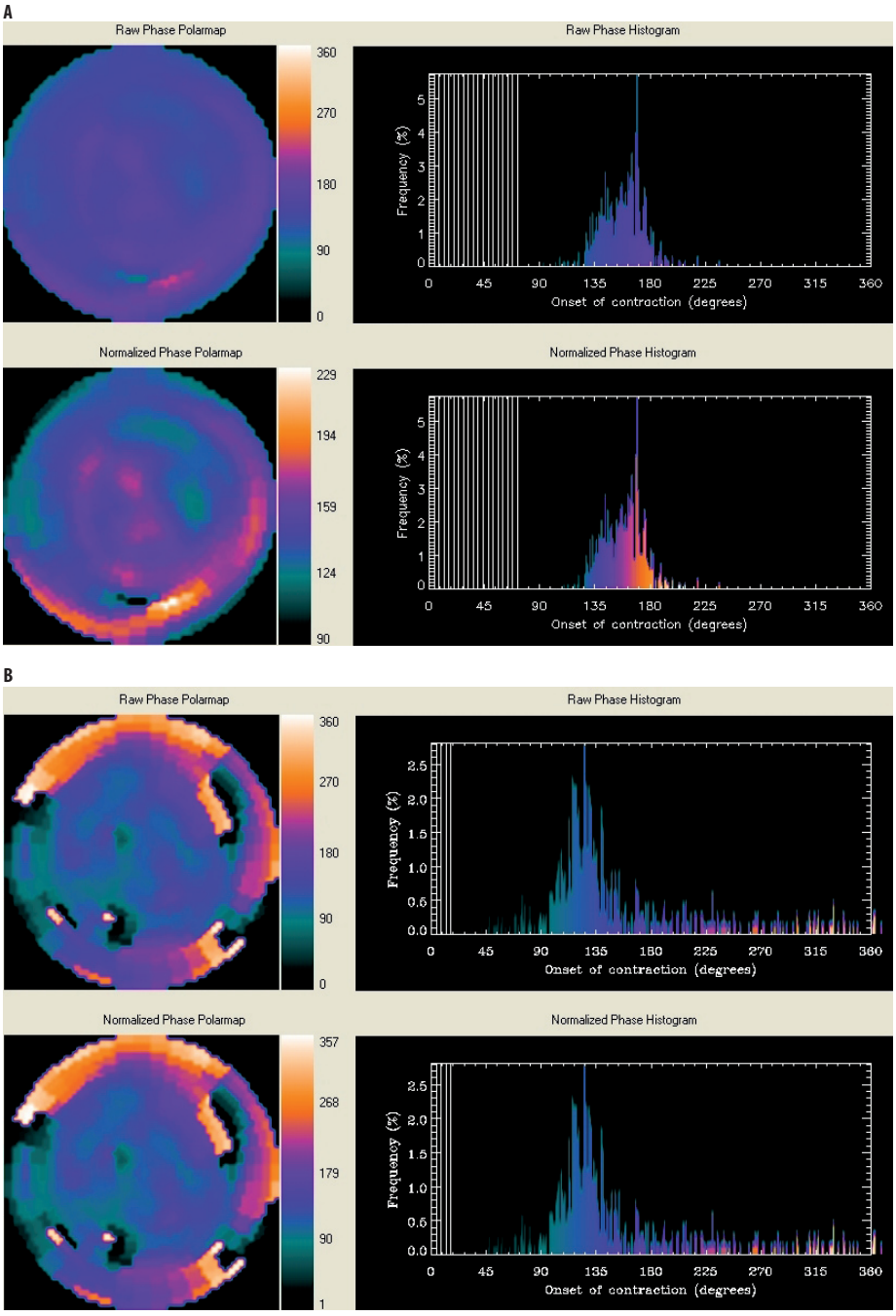


Figure 2A: Example of a patient without LV dyssynchrony on GMPS. The non-normalized (upper panel) and normalized (lower panel) phase distributions are nearly uniform and the corresponding phase histograms are highly-peaked, narrow distributions.

Figure 2B: Example of a patient (same as in Figure 1) with LV dyssynchrony on GMPS. The non-normalized (upper panel) and normalized (lower panel) phase distributions show significant non-uniformity and the corresponding phase histograms have widespread distributions.

RESULTS

Patient population

A total of 40 consecutive patients with heart failure were included in this study (29 (72%) men; mean age 66±10 years). Baseline characteristics are summarized in Table 1. Patients had severe LV dysfunction (mean LVEF 26±7%), with extensive LV dilatation (mean LV end-diastolic volume 210±48 ml). LV dyssynchrony assessment with tri-plane TDI demonstrated a mean value of Ts-SD of 34±15 ms.

Table 1. Baseline characteristics of the study population (n = 40).

Age (yrs)	**66±10**
Gender (M/F)	29/11
NYHA class	3.0±0.4
6-MWT (m)	282±126
QoL score	38±17
QRS duration (ms)	147±33
Etiology, n (%)	
Ischemic	25 (62)
Idiopathic	15 (38)
LVEF (%)	26±7
LVEDV (ml)	210±48
LVESV (ml)	157±43
Medication, n (%)	
ACE Inhibitors	34 (85)
B-blockers	28 (70)
Diuretics and/or spironolactone	36 (90)

LVEDV=left ventricular end-diastolic volume; LVEF=left ventricular ejection fraction; LVESV=left ventricular end-systolic volume; 6-MWT=6 minute walk test; QoL=quality of life score; Ts-SD=standard deviation of time to peak systolic velocity of 12 LV segments.

Histogram bandwidth

The mean histogram bandwidth was 130°±69° (range 41° to 260°); the normal value is 38.7°±11.8° for men and 30.6°±9.6° for women [9]. A good correlation between histogram bandwidth and LV dyssynchrony, assessed with tri-plane TDI, was observed ($r = 0.77$, $p < 0.001$, Figure 3).

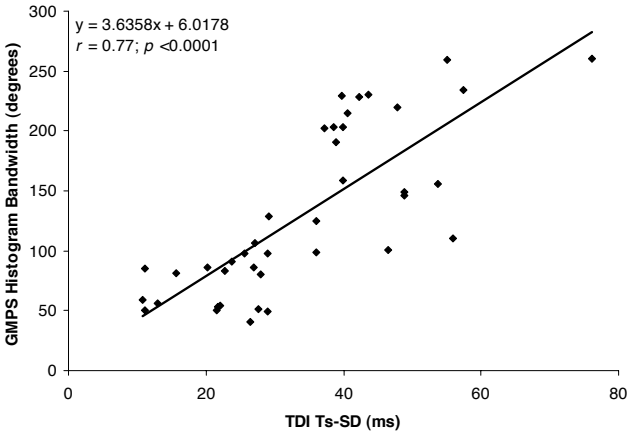


Figure 3. Correlation between histogram bandwidth assessed with GMPS and LV dyssynchrony assessed with tri-plane TDI (Ts-SD).

Phase SD

The mean phase SD was 40.2°±18.8° (range 14.5° to 77.9°), whereas the normal value is 14.2°±5.1° for men and 11.8°±5.2° for women [9]. Pearson's correlation showed a good correlation between phase SD and Ts-SD (r = 0.74, p <0.001, Figure 4).

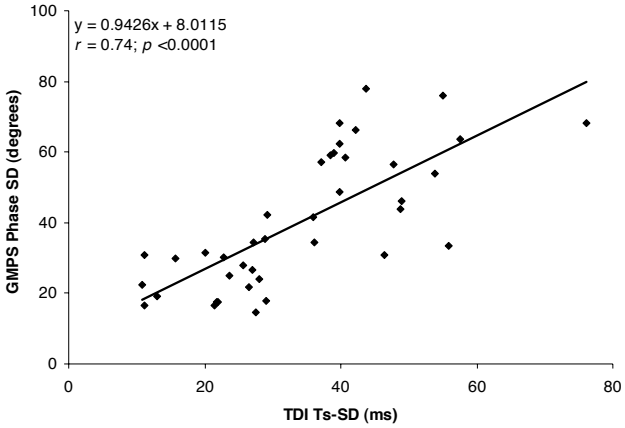


Figure 4. Phase SD assessed with GMPS versus LV dyssynchrony assessed with tri-plane TDI (Ts-SD).

Histogram skewness

The mean histogram skewness was 2.50±0.81 (range 1.16 to 5.49), whereas the normal value is 4.19±0.68 for men and 4.60±0.72 for women [9]. A poor correlation with LV dyssynchrony assessed with tri-plane TDI was demonstrated by Pearson's correlation (r = -0.30, p = 0.06).

Histogram kurtosis

The mean histogram kurtosis was 7.38±6.23 (range 1.08 to 37.42), whereas the normal value is 19.72±7.68 for men and 23.21±8.16 for women [9]. No correlation between histogram kurtosis and Ts-SD was shown by Pearson's correlation (r = -0.14, p = 0.38).

Substantial versus no substantial LV dyssynchrony

Of the 40 patients included, 20 (50%) had a substantial LV dyssynchrony (defined as Ts-SD ≥33 ms) [7,8]. No significant differences in baseline characteristics were noted between the two patient groups (Table 2). Histogram bandwidth and phase SD were significantly higher in patients with Ts-SD ≥33 ms compared to patients with Ts-SD <33 ms: 186°±52° versus 74°±24° (p <0.001) and 55.3°±13.6° versus 25.1°±7.6° (p <0.001), respectively (Figure 5a and b). In addition, histogram skewness was significantly lower in patients with Ts-SD ≥33 ms than in

Table 2. Baseline characteristics of patients with substantial (≥33 ms) and no substantial LV dyssynchrony (<33 ms) assessed by SD of time to peak systolic velocity of 12 LV segments (Ts-SD).

	Ts-SD ≥33 ms (n = 20)	Ts-SD <33 ms (n = 20)	p-value
Age (yrs)	67±10	66±9	NS
Gender (M/F)	14/6	15/5	NS
QRS duration (ms)	145±31	149±36	NS
NYHA class	3.0±0.4	3.0±0.4	NS
Etiology, n (%)			
Ischemic	14 (70)	11 (55)	NS
Idiopathic	6 (30)	9 (45)	NS
LVEF (%)	25±7	26±7	NS
LVEDV (ml)	209±47	207±50	NS
LVESV (ml)	159±46	153±42	NS
Histogram bandwidth (°)	186±52	74±24	<0.001
Phase SD (°)	55.3±13.6	25.1±7.6	<0.001
Histogram skewness	2.23±0.93	2.78±0.55	0.03
Histogram kurtosis	6.36±7.94	8.40±3.79	NS

For abbreviations see Table 1.

patients with Ts-SD <33 ms (2.23±0.93 versus 2.78±0.55, p = 0.03). No significant difference between the 2 groups was observed for histogram kurtosis (6.36±7.94 versus 8.4±3.79, p = NS) (Figure 5c and 5d). An example of a patient with substantial LV dyssynchrony on both tri-plane TDI as on phase analysis with GMPS is provided in Figure 1 and 2b.

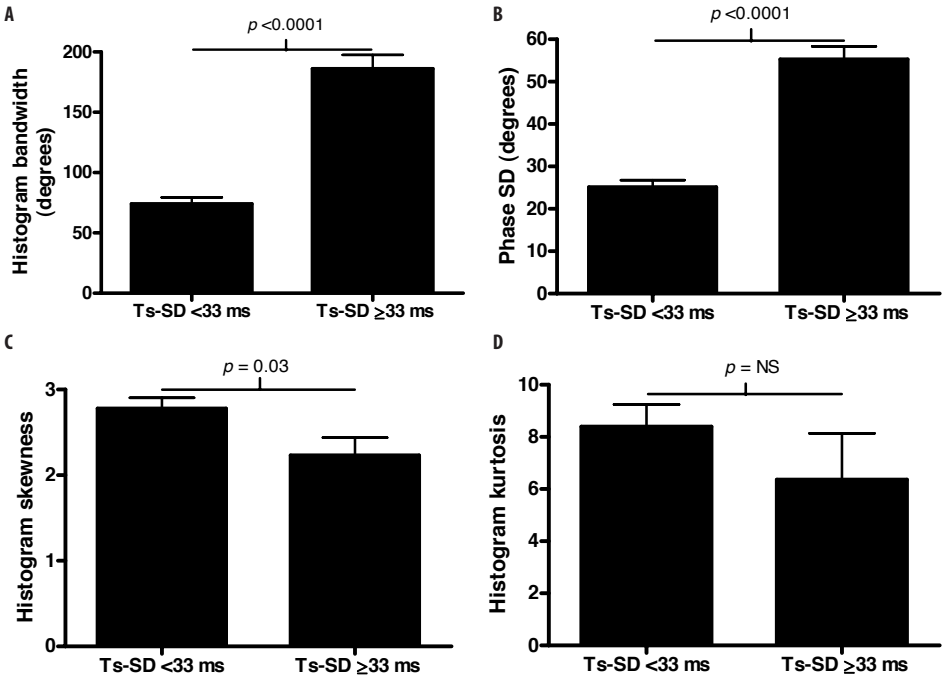


Figure 5. Figure 5A: Patients with substantial versus no substantial LV dyssynchrony (Ts-SD), using a cut-off value ≥33 ms. Histogram bandwidth is significantly higher in patients with substantial LV dyssynchrony. Figure 5B: Patients with substantial versus no substantial LV dyssynchrony (Ts-SD), using a cut-off value ≥33 ms. Phase SD is significantly higher in patients with substantial LV dyssynchrony. Figure 5C: Patients with substantial versus no substantial LV dyssynchrony (Ts-SD), using a cut-off value ≥33 ms. Histogram skewness is significantly lower in patients with substantial LV dyssynchrony. Figure 5D: Patients with substantial versus no substantial LV dyssynchrony (Ts-SD), using a cut-off value ≥33 ms. No significant difference in histogram kurtosis was demonstrated between patients without and patients with substantial LV dyssynchrony as assessed with tri-plane echocardiography.

Ischemic versus idiopathic dilated cardiomyopathy

In total, 25 patients (62%) had an ischemic cardiomyopathy and 15 patients (38%) had an idiopathic dilated cardiomyopathy. No differences in echocardiographic variables, including LV dyssynchrony assessed by tri-plane TDI, or GMPS phase analysis indices were found between ischemic and non-ischemic patients. No significant differences in correlation coefficients were observed between patients with ischemic cardiomyopathy and patients with idiopathic dilated cardiomyopathy for the 4 different GMPS variables (Table 3).

Table 3. Correlation coefficients of LV dyssynchrony, assessed with tri-plane TDI, versus the different LV dyssynchrony parameters, derived from phase analysis of GMPS (idiopathic dilated cardiomyopathy versus ischemic cardiomyopathy).

	Ischemic cardiomyopathy (n = 25)	Idiopathic dilated cardiomyopathy (n = 15)	p-value
Histogram Bandwidth	r = 0.79	r = 0.78	NS
Phase SD	r = 0.77	r = 0.75	NS
Histogram skewness	r = -0.22	r = -0.48	NS
Histogram kurtosis	r = -0.07	r = -0.35	NS

DISCUSSION

The main findings of the present study can be summarized as follows:

1) LV dyssynchrony assessment with phase analysis on GMPS is feasible in heart failure patients screened for eligibility for CRT implantation. The phase analysis variables histogram bandwidth and phase SD show good correlation with LV dyssynchrony as measured with tri-plane TDI (Ts-SD), suggesting that GMPS phase analysis can be used to quantify LV dyssynchrony. 2) Patients with substantial LV dyssynchrony on tri-plane TDI have significantly higher values of histogram bandwidth and phase SD derived from phase analysis with GMPS (histogram bandwidth: 186º±52º versus 74º±24º, p <0.001), and phase SD: 55.3º±13.6º versus 25.1º±7.6º (p <0.001).

CRT is now considered an important therapeutic option in the treatment of patients with end-stage heart failure [1]. Although encouraging beneficial effects have been reported, including improvement in LVEF and reduction in heart failure symptoms, it has also been demonstrated that up to 30% of patients do not have a favorable response to CRT. The presence of LV dyssynchrony is considered a key issue in the identification of potential responders to CRT [3–6]. Echocardiography and in particular TDI have been extensively used to assess LV dyssynchrony. Several parameters derived from myocardial velocity curves of different LV segments have been proposed to quantify LV dyssynchrony and predict response to CRT [3–8]. Yu and coworkers described a model (derived from 2D TDI data) to quantify global LV dyssynchrony using Ts-SD of 12 LV segments [6–8]. The authors reported a cut-off value >32.6 ms to distinguish between responders and non-responders [8] and a cut-off value >34.4 ms as the most powerful predictor of LV reverse remodeling [7]. In this study LV dyssynchrony was evaluated by Ts-SD from tri-plane TDI and compared with LV dyssynchrony assessment with phase analysis by GMPS. The tri-plane TDI technique avoids the problem of heart rate variability since simultaneous acquisition of the 3 apical views is possible; in the present study a cut-off value ≥33 ms was used to define substantial LV dyssynchrony on tri-plane TDI.

Information on cardiac dyssynchrony can also be derived from nuclear imaging. Kerwin et al. [13] evaluated interventricular dyssynchrony in 13 heart failure patients using multi-gated equilibrium blood pool scintigraphy and phase analysis. Patients were imaged during biven-

tricular pacing and in sinus rhythm. During biventricular pacing, a significant improvement in interventricular synchrony was observed. Moreover, an improvement in LVEF was reported for all 13 patients during biventricular pacing (17.2±7.9% to 22.5±8.3%, p <0.001) and the increase in LVEF correlated significantly with the improvement in interventricular synchrony (r = 0.86; p <0.001). Fauchier et al. [14] used equilibrium radionuclide angiography and phase analysis to evaluate the prognostic value of interventricular and intraventricular dyssynchrony in 103 patients with idiopathic dilated cardiomyopathy. Phase images were generated from the scintigraphic data, and mean phase angles and SDs were calculated for the right and left ventricle. During a follow-up period of 27±23 months, 18 major cardiac events occurred. Multivariate analysis revealed that LV intraventricular dyssynchrony and elevated pulmonary capillary wedge pressure were the only independent predictors of cardiac events.

GMPS is currently used in patients with heart failure to exclude ischemia and/or viability before referring for CRT implantation, and to assess total scar burden in patients with ischemic cardiomyopathy [11,12]. Indeed, various studies have shown that the presence of severe resting perfusion defects, as assessed with GMPS, limit the response to CRT [15–17]. Recently, Chen et al. [9] developed with GMPS a count-based method to extract phase information from the regional LV count changes throughout the cardiac cycle. The phase information is related to the regional onset of mechanical contraction of the LV (phase analysis) and provides information on the synchronicity of the LV contraction. The authors assessed in 90 normal individuals the normal range for 4 quantitative indices which can be used as markers of LV dyssynchrony (histogram bandwidth, phase SD, histogram skewness and histogram kurtosis) [9]. Recently, these 4 GMPS indices have been compared with LV dyssynchrony assessment by TDI in 75 patients with severe heart failure. It was shown that among the 4 quantitative indices of phase analysis, the variables histogram bandwidth and phase SD correlated best with LV dyssynchrony as assessed by TDI [10]. The current study involved a different patient subset, and provides further support that phase analysis with GMPS can be useful in the evaluation of LV dyssynchrony.

The value of GMPS to assess LV dyssynchrony has been analyzed and the indices derived from phase analysis were compared with Ts-SD measured by tri-plane TDI. It was shown that histogram bandwidth and phase SD correlated well with Ts-SD as evaluated by tri-plane TDI (histogram bandwidth: r = 0.77 and phase SD: r = 0.74). In addition, significantly higher values for histogram bandwidth and phase SD were observed in patients with substantial LV dyssynchrony on tri-plane TDI compared with patients without substantial LV dyssynchrony on tri-plane TDI.

Study limitations

In the present study, follow-up data after CRT implantation were not available. Therefore the value of phase analysis to predict response to CRT could not be determined. Furthermore, GMPS may be less suitable for repeated analysis during the follow-up after CRT implantation, due to radiation burden of the technique.

CONCLUSIONS

The results of this study confirm the feasibility to evaluate LV dyssynchrony with phase analysis by GMPS and its applicability in the clinical setting. In particular, histogram bandwidth and phase SD showed a good correlation with LV dyssynchrony measured with Ts-SD as assessed with tri-plane TDI. Future prospective studies in larger patient populations with follow-up after CRT implantation are needed to elucidate the potential role of GMPS with phase analysis for prediction of response to CRT.

REFERENCES

1. Freemantle N, Tharmanathan P, Calvert MJ, Abraham WT, Ghosh J, Cleland JG. Cardiac resynchronisation for patients with heart failure due to left ventricular systolic dysfunction -- a systematic review and meta-analysis. *Eur J Heart Fail* 2006;8:433-440.
2. Abraham WT, Fisher WG, Smith AL et al. Cardiac resynchronization in chronic heart failure. *N Engl J Med* 2002;346:1845-1853.
3. Bax JJ, Bleeker GB, Marwick TH et al. Left ventricular dyssynchrony predicts response and prognosis after cardiac resynchronization therapy. *J Am Coll Cardiol* 2004;44:1834-1840.
4. Sogaard P, Egeblad H, Kim WYet al. Tissue Doppler imaging predicts improved systolic performance and reversed left ventricular remodeling during long-term cardiac resynchronization therapy. *J Am Coll Cardiol* 2002;40:723-730.
5. Notabartolo D, Merlino JD, Smith AL et al. Usefulness of the peak velocity difference by tissue Doppler imaging technique as an effective predictor of response to cardiac resynchronization therapy. *Am J Cardiol* 2004;94:817-820.
6. Yu CM, Chau E, Sanderson JE et al. Tissue Doppler echocardiographic evidence of reverse remodeling and improved synchronicity by simultaneously delaying regional contraction after biventricular pacing therapy in heart failure. *Circulation* 2002;105:438-445.
7. Yu CM, Zhang Q, Fung JW et al. A novel tool to assess systolic asynchrony and identify responders of cardiac resynchronization therapy by tissue synchronization imaging. *J Am Coll Cardiol* 2005;45:677-684.
8. Yu CM, Fung WH, Lin H, Zhang Q, Sanderson JE, Lau CP. Predictors of left ventricular reverse remodeling after cardiac resynchronization therapy for heart failure secondary to idiopathic dilated or ischemic cardiomyopathy. *Am J Cardiol* 2003;91:684-688.
9. Chen J, Garcia EV, Folks RD et al. Onset of left ventricular mechanical contraction as determined by phase analysis of ECG-gated myocardial perfusion SPECT imaging: development of a diagnostic tool for assessment of cardiac mechanical dyssynchrony. *J Nucl Cardiol* 2005;12:687-695.
10. Henneman MM, Chen J, Ypenburg C et al. Phase analysis of gated myocardial perfusion SPECT compared to tissue Doppler imaging for the assessment of left ventricular dyssynchrony. *J Am Coll Cardiol* 2007;49:1708-1714.
11. Levine MG, McGill CC, Ahlberg AW et al. Functional assessment with electrocardiographic gated single-photon emission computed tomography improves the ability of technetium-99m sestamibi myocardial perfusion imaging to predict myocardial viability in patients undergoing revascularization. *Am J Cardiol* 1999;83:1-5.
12. Udelson JE, Coleman PS, Metherall J et al. Predicting recovery of severe regional ventricular dysfunction. Comparison of resting scintigraphy with 201Tl and 99mTc-sestamibi. *Circulation* 1994;89:2552-2561.
13. Kerwin WF, Botvinick EH, O'Connell JW et al. Ventricular contraction abnormalities in dilated cardiomyopathy: effect of biventricular pacing to correct interventricular dyssynchrony. *J Am Coll Cardiol* 2000;35:1221-1227.
14. Fauchier L, Marie O, Casset-Senon D, Babuty D, Cosnay P, Fauchier JP. Interventricular and intraventricular dyssynchrony in idiopathic dilated cardiomyopathy: a prognostic study with fourier phase analysis of radionuclide angioscintigraphy. *J Am Coll Cardiol* 2002;40:2022-2030.
15. Sciagra R, Giaccardi M, Porciani MC et al. Myocardial perfusion imaging using gated SPECT in heart failure patients undergoing cardiac resynchronization therapy. *J Nucl Med* 2004;45:164-168.

16. Ypenburg C, Schalij MJ, Bleeker GB et al. Impact of viability and scar tissue on response to cardiac resynchronization therapy in ischaemic heart failure patients. *Eur Heart J* 2007;28:33-41.
17. Adelstein EC, Saba S. Scar burden by myocardial perfusion imaging predicts echocardiographic response to cardiac resynchronization therapy in ischemic cardiomyopathy. *Am Heart J* 2007;153:105-112.

CHAPTER 8

Noninvasive imaging of cardiac venous anatomy with 64-slice computed tomography and noninvasive assessment of LV dyssynchrony by 3D tissue synchronization imaging in patients with heart failure scheduled for CRT

N R van de Veire, **N Ajmone Marsan**, J D Schuijf, G B Bleeker, M C E F Wijffels, L van Erven, E R Holman, J de Sutter, E E van der Wall, M J Schalij, and J J Bax

Am J Cardiol 2008;101:1023–9.

ABSTRACT

Objectives: Objectives of this study were to perform a prospective head-to-head comparison between multi-slice computed tomography (MSCT) venography and invasive venography in cardiac resynchronization therapy (CRT) candidates as well as to evaluate the relation between left ventricular (LV) lead position and effect on LV dyssynchrony and immediate response to CRT.

Methods: Twenty-one consecutive heart failure patients scheduled for CRT implantation were prospectively enrolled to undergo 64-slice MSCT to visualize the venous system, invasive venography during device implantation, and tri-plane tissue synchronization imaging (TSI) before and after implantation.

Results: Excellent agreement between MSCT and invasive venography was noted. No significant differences were observed between both techniques regarding vessel diameters. In 12 patients, a match was observed between the area of latest mechanical activation (on TSI) and LV lead position. These patients showed a significant decrease in LV dyssynchrony (43±7 ms to 11±9 ms, $p < 0.001$) with acute reduction in LV end-systolic volume (188±54 ml to 162±48 ml, $p < 0.01$) and improvement in LV ejection fraction (22%±9% to 34%±9%, $p < 0.01$). Patients with a mismatch between area of latest activation and LV lead position remained dyssynchronous without improvement in LV function.

Conclusions: Visualization of major tributaries of the coronary sinus was comparable between invasive venography and MSCT venography. Optimal LV lead positioning in a vein draining the area of latest mechanical activation (determined from tri-plane TSI) resulted in acute improvement of LV dyssynchrony and systolic function after CRT implantation.

INTRODUCTION

Cardiac resynchronization therapy (CRT) is an attractive treatment for highly symptomatic heart failure patients with wide QRS complex and depressed left ventricular (LV) systolic function [1]. In large randomized clinical trials, up to 30% of patients do not respond favourably to CRT [2,3]. Two major issues need to be addressed during the selection process of potential candidates to improve the success rate [3]. First, LV dyssynchrony appears an important predictor of response to CRT [4]. The amount of intraventricular dyssynchrony can be reliably assessed noninvasively with tissue Doppler echocardiography [5]. Second, attention to venous anatomy ensures the area of latest activation can be reached through a suitable vein. Particularly in patients with ischemic cardiomyopathy, lack of a suitable branch of the coronary sinus may hamper successful endovascular LV lead implantation [6]. In 2005, preliminary data suggested that the cardiac venous system could be depicted noninvasively using 16-slice multi-slice computed tomography (MSCT) [7]. Recently, the feasibility of 64-slice MSCT to evaluate the cardiac veins was confirmed in a retrospective analysis of 100 patients [8]. However, prospective comparisons between MSCT and invasive venography for assessment of venous anatomy are lacking. Moreover, information on location of LV dyssynchrony and venous anatomy should be integrated to determine whether a transvenous or a surgical approach should be selected for LV lead positioning. In the present study, 21 consecutive patients with heart failure scheduled for CRT underwent 64-slice CT of the cardiac venous system, invasive venography during device implantation, and 3-dimensional tissue synchronization imaging (TSI) echocardiography before CRT to assess location and extent of LV dyssynchrony. Study aims were (1) to perform a head-to-head comparison between MSCT venography and invasive venography in CRT candidates (to further validate the use of MSCT for assessing venous anatomy), and (2) to evaluate the effect of CRT when the LV lead is positioned inside or outside a vein draining the area of latest mechanical activation.

METHODS

A total of 21 consecutive patients with heart failure scheduled for CRT, underwent 64-slice MSCT before, and invasive venography during CRT implantation. Exclusion criteria were atrial fibrillation, documented contrast allergy, and reduced renal function (serum creatinine >140 µmol/L).

Imaging was performed with a 64-detector row Toshiba Multislice Aquilion 64 system (Toshiba Medical Systems, Otawara, Japan) with a collimation of 64 x 0.5 mm and a rotation time of 0.4 seconds. Between 95 and 140 ml (mean 108±11 ml) of contrast material (Iomeron 400, Bracco Altana Pharma GmbH, Konstanz, Germany) at an injection rate of 5 ml/min was used with an automatic bolus triggering technique. To optimize the scan for

venous visualization, an additional 2-second delay was applied after the contrast bolus reached the descending aorta before triggering the scan. For optimal filling of the cardiac venous system, the use of saline chasing was omitted. Tube voltage was 120 kV at 300 mA. A segmental reconstruction algorithm allowed inclusion of patients with a range of heart rates. The majority of the patients were already taking low-dose β-blockers; additional β blockade was considered contra-indicated because of the presence of heart failure. During the MSCT examination, electro-cardiography was performed simultaneously for retrospective gating of the data. An initial data set was reconstructed at 75% of the RR interval, with a slice thickness of 0.5 mm and a reconstruction interval of 0.3 mm. Data reconstruction was performed on a Vitrea post-processing workstation (Vital Images, Plymouth, Minnesota).

Three-dimensional volume-rendered reconstructions were used to obtain general information on the anatomy of the cardiac veins. Thereafter, the course of the veins was evaluated in three orthogonal planes using multi-planar reformatting. The tributaries of the coronary sinus evaluated [9] include posterior interventricular vein, posterior vein of the LV, and left marginal vein. First-degree side branches were also noted, if present. The diameter of the coronary sinus ostium was measured in 2 directions (anteroposterior and superoinferior), and the diameters of the tributaries were measured close to their origin.

Retrograde venography was performed after implantation of the right atrial and right ventricular leads in all 21 patients. The coronary sinus was cannulated from a subclavian entry site by an 8F guiding catheter. A balloon occlusion catheter (Arrow model 6714; Arrow International Inc., Reading, Pennsylvania, or Medtronic model 6215, Medtronic Inc., Minneapolis, Minnesota) was advanced to the proximal part of the coronary sinus. Three venograms (right anterior oblique 30°, anteroposterior and left anterior oblique 30° views) were then obtained with an acceptable occlusion balloon position. A non-ionic contrast agent with low osmolarity (Iomeron 350; Bracco Altana Pharma GmbH) was used. Next, the balloon occlusion catheter was withdrawn and the LV pacing lead was positioned, preferably in the (postero)lateral vein. The choice of LV lead position was made independently by the implanting cardiologist, who was blinded to the MSCT and dyssynchrony data. At implantation, both the sensing and pacing thresholds (at pulse duration of 0.5 ms) of the LV pacing lead were measured. The final position of the LV pacing lead was assessed by fluoroscopy.

The different image series were stored digitally and analyzed by an experienced observer without knowledge of the MSCT data, at a separate workstation using commercially available software (QCA-CMS version 6.0; Medis, Leiden, The Netherlands). Images were first analyzed to identify the tributaries of the coronary sinus and presence of 1st degree side branches. The proximal vein diameters of the coronary sinus, posterior interventricular vein, posterior vein of the left ventricle, and left marginal vein were measured after catheter-based image calibration.

All patients underwent a transthoracic echocardiogram before and within 72 hours after CRT implantation. Studies were performed with a commercially available echocardiographic platform (VIVID 7; GE Vingmed Ultrasound, Horten, Norway), equipped with a 3V-probe for

3-dimensional acquisition. Patients were scanned in left lateral decubitus position, from the apical window in tri-plane modus. Care was taken to visualize the true LV apex, allowing simultaneous acquisition of the apical 4-, 2-, and 3-chamber views. Color-coded TSI was applied to the tri-plane view to assess longitudinal myocardial regional function. Gain settings, filters, and pulse repetition frequency were adjusted to optimize color saturation. Sector size and depth were optimized for the highest possible frame rate. At least 2 consecutive beats were recorded from each view, and the images were digitally stored for offline analysis (EchoPac; GE Vingmed Ultrasound). During post-processing, the tri-plane data set was frozen in end-diastole, and the endocardial border was manually traced in the apical 4-, 2- and 3-chamber views, respectively. Then, using the same heartbeat, the tri-plane data set was frozen in end-systole, and again the endocardial border was manually traced in the apical 4-, 2-, and 3-chamber views. Three-dimensional LV end-diastolic and end-systolic volumes were generated automatically by the software (Echopac), and LV ejection fraction was reported accordingly [10].

During post-processing, the tri-plane TSI data set was used to analyze myocardial velocity curves as previously described.5 TSI automatically calculates the time from the beginning of the QRS complex to peak systolic velocity in every position in the image with reference to the QRS interval. The TSI algorithm detects positive velocity peaks within a specified time interval, and the color coding ranges from green (earliest), over yellow-orange to red (latest) within this interval. By using surface mapping and manual tracing of the endocardial borders, a 3-dimensional rendered volume was automatically generated, allowing for a spatial representation of electromechanical activation times. Sample volumes were placed in the basal and mid segments of the septal, lateral, inferior, anterior, posterior, and anteroseptal LV walls to measure the time between onset of QRS complex and peak systolic myocardial velocity. From these 12 measurements, the LV dyssynchrony parameters calculated include delay between septum and lateral wall [11,12] and standard deviation of all 12 LV segments [13,14]. The severity of mitral regurgitation was graded semiquantitatively from color-flow Doppler in the conventional parasternal long-axis and apical 2- and 4-chamber images. Mitral regurgitation was characterized as mild, 1+ (jet area/left atrial area <10%); moderate, 2+ (jet area/left atrial area 10% to 20%); moderately severe, 3+ (jet area/left atrial area 20% to 45%); and severe, 4+ (jet area/left atrial area >45%) [15].

All analyses were performed with the statistical software program SPSS 12.0.1 (SPSS, Inc., Chicago, Illinois). Continuous data are presented as mean±SD. Categorical data are presented as absolute numbers or percentages. Comparisons between MSCT and invasive venography were performed using the independent samples t test and Pearson's correlation analysis; comparisons between characteristics before and after implantation were performed using the paired samples t test. Comparisons between categorical variables were performed with Chi-Square testing. A p-value <0.05 was considered significant.

RESULTS

There were 13 (62%) men and 8 (38%) women with a mean age of 67±11 years; all were in New York Heart Association (NYHA) class III despite optimized medical therapy (86% used diuretics, 95% angiotensin-converting enzyme inhibitors, 71% β-blockers, 48% spironolactone). Patients with ischemic (12, 57%) and those with nonischemic cardiomyopathy (9, 43%) were both included; 6 (29%) had a history of percutaneous coronary intervention, and 6 (29%) had a history of coronary artery bypass grafting (combined with mitral valve annuloplasty in 2 patients). MSCT was successfully performed in all included patients. Average heart rate during scanning was 65±14 beats/min, scan time 21±11 seconds, helical pitch 14.3±0.7. On average, 108±11 ml of contrast was used. CRT device and transvenous LV lead implantation were successful in all but 1 patient (absence of suitable veins on venography, and this patient was referred for surgical LV lead implantation), without major complications. All remaining 20 patients received a combined CRT-implantable cardioverter defibrillator device (Contak Renewal 4 CRT-D, Guidant, and Insync Marquis or Sentry CRT-D, Medtronic Inc.). Two types of LV leads were used, Easytrack 4517-90 (Guidant) or Attain OTW bipolar 4194 (Medtronic Inc.). Five patients underwent upgrading of a previously implanted implantable cardioverter defibrillator to a CRT-debrillator device. During implantation, invasive balloon occlusion venography was performed in all 21 patients.

Table 1. Prevalence of the major cardiac veins and number of side branches using multi-slice computed tomography (MSCT) and invasive venography.

	n/Total (%)	
	MSCT	Invasive Venography
Coronary sinus	21/21 (100%)	21/21 (100%)
Posterior interventricular vein	21/21 (100%)	18/21 (86%)
0 side branches	14/21 (67%)	12/18 (66%)
1 side branch	2/21 (9%)	3/18 (17%)
2 side branches	4/21 (19%)	3/18 (17%)
3 side branches	0/21 (0%)	0/18 (0%)
4 side branches	1/21 (5%)	0/18 (0%)
Posterior vein of LV	20/21 (95%)	20/21 (95%)
0 side branches	15/20 (75%)	12/20 (60%)
1 side branch	2/20 (10%)	1/20 (5%)
2 side branches	3/20 (15%)	6/20 (30%)
3 side branches	0/20 (0%)	0/20 (0%)
4 side branches	0/20 (0%)	1/20 (5%)
Left marginal vein	12/21 (57%)	13/21 (62%)
0 side branches	6/12 (50%)	5/13 (38%)
1 side branch	2/12 (17%)	3/13 (23%)
2 side branches	3/12 (25%)	4/13 (31%)
3 side branches	0/12 (0%)	0/13 (0%)
4 side branches	1/12 (8%)	1/13 (8%

Identification of the coronary sinus and its major tributaries on MSCT and invasive venography in the entire study population is reported in Table 1. The posterior interventricular vein was not observed with invasive venography in 3 patients (14%), whereas on MSCT this vein was observed in all patients. The left marginal vein was observed in 12 patients (57%) on MSCT and in 13 patients (62%) with invasive venography. The number of visible side branches of the major tributaries is reported in Table 1. Figure 1 illustrates the excellent agreement between MSCT and invasive venography in a patient with heart failure with a history of coronary artery bypass grafting. The diameters of the coronary sinus and tributaries, measured with MSCT and invasive venography are depicted in Figure 2. No significant differences in measured diameters were observed between MSCT and invasive venography, and excellent correlations were observed between noninvasively and invasively measured diameters (Figure 2).

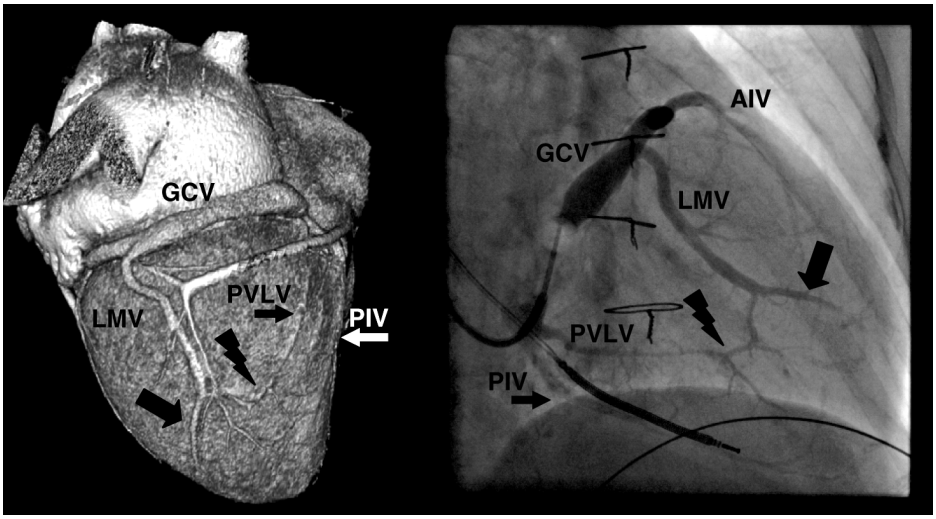


Figure 1. Cardiac venous anatomy of an 80-year-old man with severe heart failure and history of coronary artery bypass grafting. The left panel is a 3-dimensional volume-rendered reconstruction from 64-slice MSCT data. The right panel is a fluoroscopic image from invasive venography. All major tributaries of the coronary sinus are visualized using both techniques, specifically, a small posterior interventricular vein (PIV), a posterior vein of the left ventricle (PVLV), and a large left marginal vein (LMV). Note the prominent side branch of the LMV (block arrow) and the connection between the LMV and PVLV (lightning flash). The left ventricular lead was successfully implanted in the LMV.

At baseline, all patients had severe LV dilatation with depressed LV function, accompanied by functional mitral regurgitation (Table 2); also, a significant extent of LV dyssynchrony was observed [11–14]. Immediately after implantation, LV end-diastolic volume remained unchanged, whereas LV endsystolic volume decreased significantly with an improvement in LV ejection fraction and mitral regurgitation. The extent of LV dyssynchrony was significantly reduced after CRT implantation.

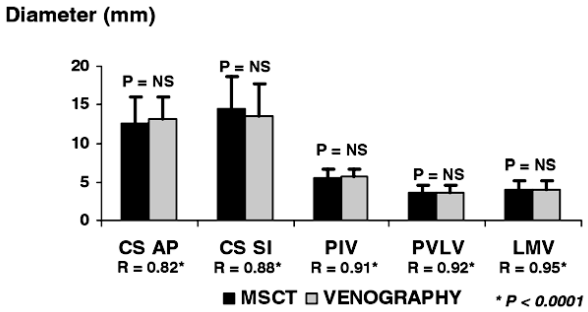


Figure 2. No significant differences are observed between invasive venography or MSCT in quantitative assessment of the diameters of the CS in the anteroposterior (AP) and superoinferior (SI) direction, the posterior interventricular vein (PIV), the posterior vein of the left ventricle (PVLV), and the left marginal vein (LMV). Correlation coefficients between invasively and noninvasively measured diameters are mentioned below the X-axis.

Table 2. Echocardiographic observations before and after cardiac resynchronization therapy (CRT) implantation.

	Before CRT	After CRT	p-value
Mitral regurgitation grade	1.5±0.9	1.1±0.9	<0.001
3-dimensional volumetric parameters:			
LV end-diastolic volume (ml)	239±56	239±55	NS
LV end-systolic volume (ml)	183±50	168±50	<0.05
LV ejection fraction (%)	24±9	31±10	<0.05
LV dyssynchrony indexes:			
Septal-to-lateral delay (ms)	84±19	45±50	0.001
Standard deviation 12 LV segments (ms)	43±8	26±21	0.001

Using a 12-segment LV model with 3-dimensional TSI imaging, the area of latest mechanical activation was lateral in 8 patients (38%), anterolateral in 9 (43%), posterolateral in 2 (9.5%), and inferolateral in 2 (9.5%). From the fluoroscopic images obtained during CRT implantation, the precise LV lead position was determined. If the LV lead was positioned in a cardiac vein draining the area of latest mechanical activation, this was considered a match between LV lead position and area of latest activation. In 12 patients (57%), a match was noted between the area of latest mechanical activation on tri-plane TSI and the final LV lead position. In these patients, a significant decrease in LV dyssynchrony was observed (Figure 3). Moreover, positioning the LV lead in a vein draining the area of latest mechanical activation (match) resulted in an acute decrease in LV end-systolic volume (average reduction of 26 ml or 13.3%) with an increase in LV ejection fraction (average increase of 12%) after CRT implantation. In contrast, LV dyssynchrony persisted in the 8 patients (38%) with a mismatch between the LV lead position and the area of latest mechanical activation, and improvement in LV ejection fraction and reduction in LV end-systolic volume were not observed in these patients (Figure 3). Figure 4 shows pre-implantation venograms and MSCT images of an 85-year-old patient with heart failure. A large left marginal vein is identified and used for LV lead implantation.

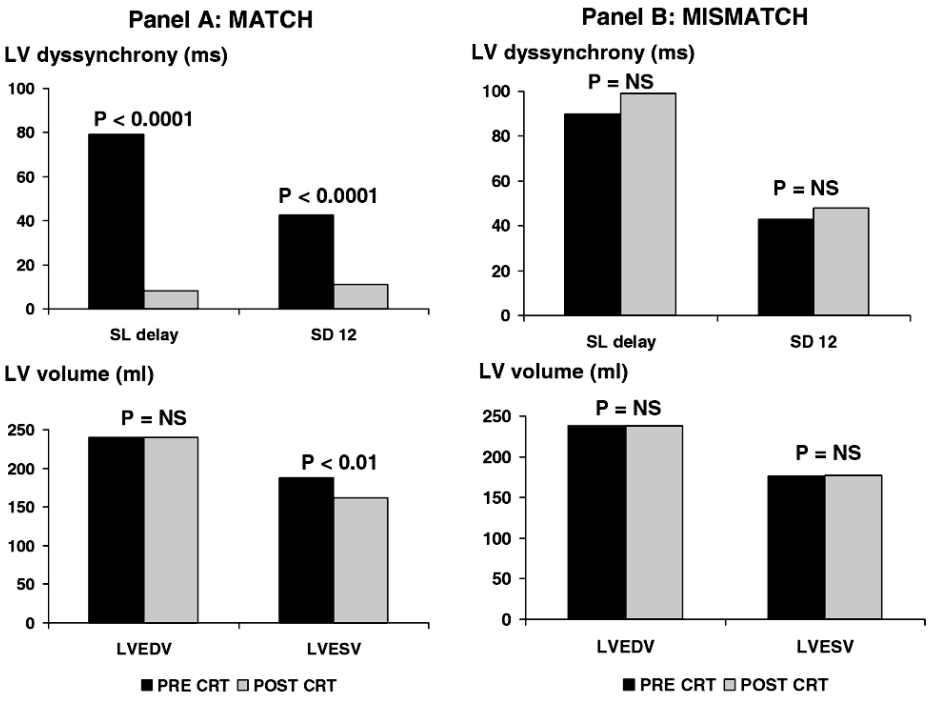


Figure 3. (A) The favorable effects of positioning the left ventricular lead within the area of latest mechanical activation (match). (B) Absence of these effects in patients showing a mismatch between lead position and area of latest mechanical activation. The upper graphs depict dyssynchrony parameters calculated from tri plane TSI data, specifically, septal-to-lateral delay (SL delay) and standard deviation of time to peak myocardial systolic velocity in 12 LV segments (SD12). The lower graphs depict LV-end systolic volume (LVESV) and LV end-diastolic volume (LVEDV) before and after CRT implantation.

This LV lead position matched the area of latest mechanical activation (identified with 3-dimensional TSI), and synchrony was restored acutely after CRT (septal-to lateral delay 90 ms at baseline, 10 ms after implantation, standard deviation of 12 LV segments 45 ms at baseline, 5 ms after implantation). In addition, a reduction of LV end-systolic volume from 191 to 153 ml was observed with an increase in LV ejection fraction from 13% to 28%.

DISCUSSION

Until recently, invasive venography was the only technique enabling clinicians to evaluate the coronary sinus and its major tributaries. In several preliminary studies, 16-slice MSCT was proposed as a valid non-invasive alternative [7,16,17]. These findings were recently confirmed in a retrospective analysis of 100 patients using 64 slice MSCT technology [8]. All studies report a significant variability in the cardiac venous system, particularly in patients with a history of myocardial infarction [7,8,16,17]. These results may have important implications for the decision of transvenous or surgical LV lead positioning [8,18]. In contrast to previous reports on MSCT venography, the present study included exclusively patients with heart failure who were actually scheduled for CRT implantation, allowing for a direct comparison between MSCT venography and invasive venography during CRT implantation. In agreement with previously published series, the left marginal vein was not observed in a large percentage of patients [7,8,9]. Moreover, all tributaries of the coronary sinus that were eventually used for LV lead insertion during CRT implantation were visualized on MSCT. Furthermore, no significant differences were observed between invasive venography and 64-slice MSCT venography regarding diameters of the different vessels, in line with a preliminary comparison between 16-slice MSCT and invasive venography [17].

In selected patients, CRT reduced symptoms, improved exercise capacity, and reduced morbidity and mortality [19,20,21]. In these large randomized trials, CRT is successful in approximately 70% of patients. Positioning the LV lead in a vein draining the area of latest mechanical activation may be a valuable strategy to further improve the success rate.3 Tissue Doppler techniques have proven their efficacy to identify the area of latest mechanical activation [4,5,12,13,14,22]. In the present study, tri-plane TSI was used to locate the area of latest mechanical activation. This approach may be particularly useful because it provides a true 3-dimensional representation of the left ventricle with a 3-dimensional dyssynchrony map obtained during a single heartbeat. Moreover, automated dyssynchrony calculations are possible that may potentially reduce observer variability. In 57% of patients, a match between area of latest mechanical activation and final LV lead position was noted, and CRT resulted in acute resynchronization with acute reduction in LV end-systolic volume and improvement in LV ejection fraction. These favourable effects were not observed in patients with a mismatch between area of latest mechanical activation and LV lead position. These observations agree with recent studies highlighting the importance of matching the LV lead position with the site of latest activation [23,24,25]. This relation between the response to CRT and the match between area of latest mechanical activation and LV lead position underscores the important role of non invasive imaging to determine LV lead implantation strategy. With tri-plane TSI, the precise area of latest mechanical activation can be derived, whereas MSCT depicts the cardiac venous system on a 3-dimensional LV volume set. Transvenous LV lead implantation is preferred if a suitable tributary of the coronary sinus matches the area of latest mechanical activation. In

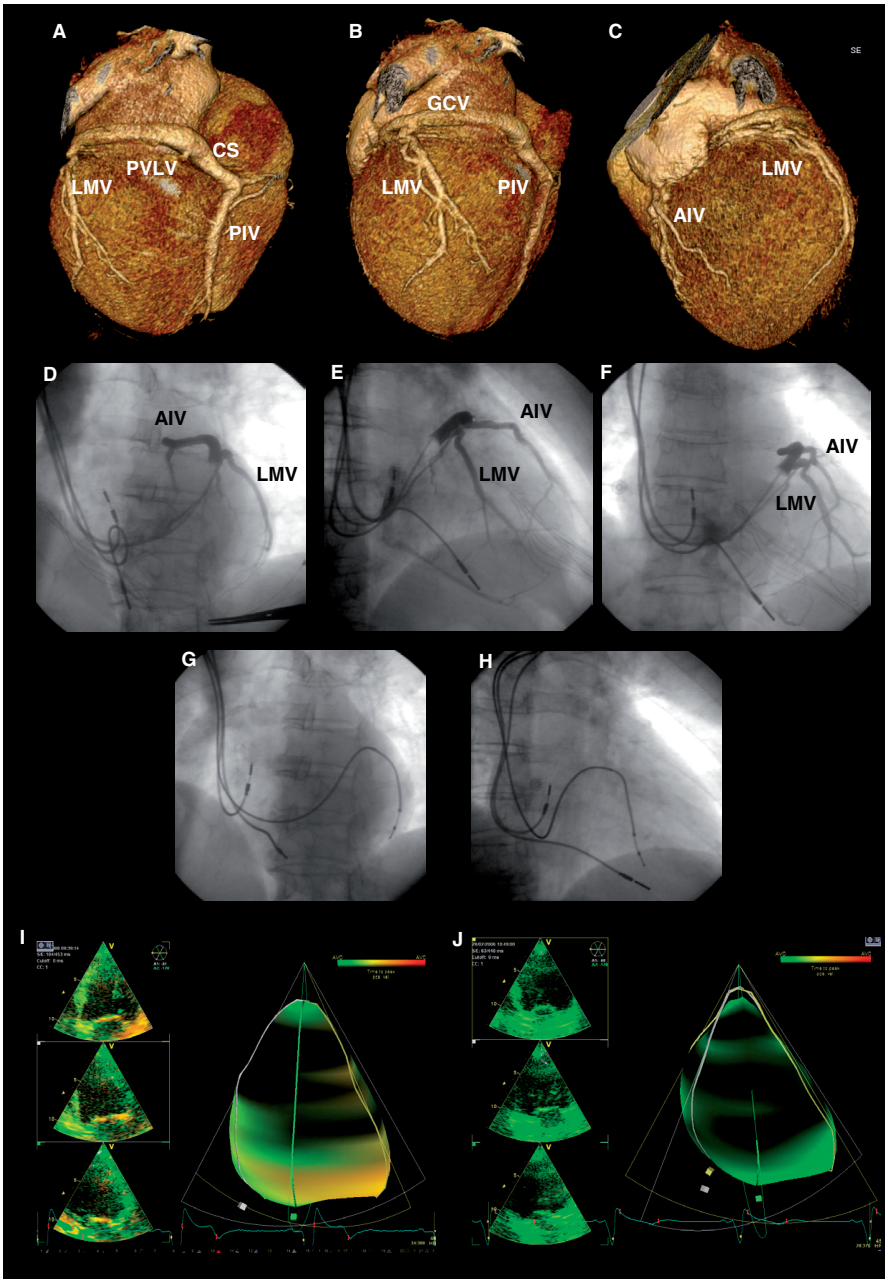


Figure 4. Case example of an 85-year-old patient with idiopathic dilated cardiomyopathy, NYHA class III heart failure and wide QRS complex (157 ms, LBBB-configuration). MSCT shows a large left marginal vein with prominent side branches (A, B, C). These findings are confirmed by invasive venography (D, E, F). In the 3-dimensional LV dyssynchrony assessment with TSI (I), the late mechanical activation (yellow) is located in the lateral wall. The LV lead is positioned in the left marginal vein (G, H), resulting in synchronous activation of the LV, represented (green) on TSI, obtained immediately after CRT (J). In addition, a reduction of LV end-systolic volume from 191 to 153 ml was observed, with an increase in LV ejection fraction from 13% to 28%.

the absence of a suitable coronary sinus tributary in the area of latest mechanical activation, a surgical approach may be preferred. In the present study, the LV lead was positioned without taking the LV dyssynchrony information into account. Accordingly, only 57% of patients exhibited a match between LV lead position and area of latest mechanical activation. These patients had substantial benefit from CRT. The remaining 43% of patients, however, had a mismatch between LV lead position and area of latest activation and did not benefit from CRT. Potentially, superior results could have been obtained if the pre-implantation information provided by tri-plane TSI and MSCT had influenced the implantation strategy in these patients. At present, CT venography is still associated with substantial radiation, but further technological development will most likely result in reduction of radiation burden.

REFERENCES

1. Abraham WT. Cardiac resynchronization therapy. *Prog Cardiovasc Dis* 2006;48:232–238.
2. Mehra MR, Greenberg BH, Cardiac resynchronization therapy. Caveat medicus! *J Am Coll Cardiol* 2004;43:1145–1148.
3. Bax JJ, Abraham T, Barold SS, Breithardt OA et al. Cardiac resynchronization therapy: part 1 issues before device implantation. *J Am Coll Cardiol* 2005;46:2152–2167.
4. Yu CM, Bax JJ, Monaghan M, Nihoyannopoulos P. Echocardiographic evaluation of cardiac dyssynchrony for predicting a favourable response to cardiac resynchronization therapy. *Heart* 2004;90(suppl 6):vi17–vi22.
5. Bank AJ, Kelly AS. Tissue Doppler imaging and left ventricular dyssynchrony in heart failure. *J Cardiac Fail* 2006;12:154 –162.
6. Goitein O, Lacomis JM, Gorcsan J III, Schwartman D. Left ventricular pacing lead implantation: potential utility of multimodal image integration. *Heart Rhythm* 2006;3:91–94.
7. Jongbloed MR, Lamb HJ, Bax JJ et al. Noninvasive visualization of the cardiac venous system using multislice computed tomography. *J Am Coll Cardiol* 2005;45:749 –753.
8. Van de Veire N, Schuijf J, De Sutter J et al. Non-invasive visualization of the cardiac venous system in coronary artery disease patients using 64-slice computed tomography. *J Am Coll Cardiol* 2006;48:1832–1838.
9. von Lüdinghausen M. The venous drainage of the human myocardium. *Adv Anat Embryol Cell Biol* 2003;168(suppl I):1–105.
10. Rodevand O, Bjornerheim R, Aakhus S, Kjekshus J. Left ventricular volumes assessed by different new three-dimensional echocardiographic methods and ordinary biplane technique. *Int J Cardiovasc Imaging* 1998;14:55– 63.
11. Bax JJ, Bleeker GB, Marwick TH et al. Left ventricular dyssynchrony predicts response and prognosis after cardiac resynchronization therapy. *J Am Coll Cardiol* 2004;44:1834 –1840.
12. Van de Veire N, Bleeker G, De Sutter J et al. Tissue synchronization imaging accurately measures left ventricular dyssynchrony and predicts response to cardiac resynchronization therapy. *Heart* 2007;93:1034 –1039.
13. Yu CM, Chau E, Sanderson JE et al. Tissue Doppler echocardiographic evidence of reverse remodeling and improved synchronicity by simultaneously delaying regional contraction after biventricular pacing therapy in heart failure. *Circulation* 2002;105:438–445.
14. Yu CM, Zhang Q, Wing-Hong Fung J et al. A novel tool to assess systolic asynchrony and identify responders of cardiac resynchonization therapy by tissue synchronization imaging. *J Am Coll Cardiol* 2005;45:677– 684.
15. Thomas JD. How leaky is that mitral valve? Simplified Doppler methods to measure regurgitant orifice area. *Circulation* 1997;95:548–550.
16. Abbara S, Cury RC, Nieman K et al. Noninvasive evaluation of cardiac veins with 16-MDCT angiography. *Am J Roentgenol* 2005;185:1001–1006.
17. Mühlenbruch G, Koos R, Wildberger JE, Günther R, Mahnken AH. Imaging of the cardiac venous system: comparison of MDCT and conventional angiography. *Am J Roentgenol* 2005;185:1252–1257.
18. Singh JP, Houser S, Heist EK, Ruskin JN. The coronary venous anatomy. A segmental approach to aid cardiac resynchronization therapy. *J Am Coll Cardiol* 2005;46:68 –74.

19. Freemantle N, Tharmanathan P, Calvert MJ, Abraham WT, Ghosh J, Cleland JG. Cardiac resynchronization for patients with heart failure due to left ventricular systolic dysfunction–a systematic review and meta-analysis. *Eur Heart J* 2006;8:433– 440.
20. Cleland JGF, Daubert J-C, Erdmann E et al on behalf of the CARE-HF Study Investigators. Longer-term effects of cardiac resynchronization therapy on mortality in heart failure (the CARE-HF trial extension phase). *Eur Heart J* 2006;27:1928 –1932.
21. Rivero-Ayerza M, Theuns DAMJ, Garcia-Garcia HM, Boersma E, Simoons M, Jordaens L. Effects of cardiac resynchronization therapy on overall mortality and mode of death: a meta-analysis of randomized controlled trials. *Eur Heart J* 2006;27:2682–2688.
22. Van de Veire N, De Sutter J, Van Camp G et al on behalf of the Belgian Multicenter Registry on Dyssynchrony. Global and regional parameters of dyssynchrony in ischemic and non-ischemic cardiomyopathy. *Am J Cardiol* 2005;95:1020 –1023.
23. Murphy RT, Sigurdsson G, Mullamalla S et al. Tissue synchronization imaging and optimal left ventricular pacing site in cardiac resynchronization therapy. *Am J Cardiol* 2006;97:1615–1621.
24. Becker M, Franke A, Breithardt O et al. Impact of left ventricular lead position on the efficacy of cardiac resynchronization therapy. A two-dimensional strain echocardiography study. *Heart* 2007;93:1197–1203.
25. Becker M, Kramann R, Franke A et al. Impact of left ventricular lead position in cardiac resynchronization therapy on left ventricular remodelling. A circumferential strain analysis based on 2D echocardiography. *Eur Heart J* 2007;28:1211–1220.

PART IB

Real-time three-dimensional echocardiography for the assessment of left atrium volumes and function

CHAPTER 9

Real-time three-dimensional echocardiography as a novel approach to assess left ventricular and left atrium reverse remodeling and to predict response to CRT

N Ajmone Marsan, G B Bleeker, C Ypenburg, R J van Bommel, S Ghio, N R van de Veire, V Delgado, E R Holman, E E van der Wall, M J Schalij, and J J Bax

Heart Rhythm 2008;5:1257-64.

ABSTRACT

Objectives: Real-time 3-dimensional echocardiography (RT3DE) is a novel promising technique for the assessment of left ventricular (LV) dyssynchrony. Aim of this study was to explore the value of RT3DE to assess LV and left atrium (LA) reverse remodeling and to predict response to cardiac resynchronization therapy (CRT).

Methods: A total of 57 consecutive heart failure patients scheduled for CRT were included and RT3DE was performed before and 6 months after implantation. LV dyssynchrony was defined as the standard deviation of the time to reach the minimum systolic volume for 16 LV segments, expressed in percentage of cardiac cycle (systolic dyssynchrony index, SDI). Patients were divided in responders or non-responders, based on a reduction ≥15% in LV end-systolic volume after CRT.

Results: Six patients (10%) were excluded from further analysis because of suboptimal images. Out of the remaining 51 patients, 34 (67%) were classified as responders. Baseline characteristics were similar between responders and non-responders, except for the SDI, which was larger in responders (9.7±3.6% vs. 5.1±1.8%, $p < 0.001$). ROC curve analysis revealed that a cut-off value for SDI of 6.4% yielded a sensitivity of 88% with a specificity of 85% to predict response to CRT. In responders, RT3DE also demonstrated beneficial effects of CRT on LA: 1) significant LA reverse remodeling; 2) significant improvement in LA total emptying fraction and in LA conduit and reservoir function.

Conclusions: RT3DE allows assessment of changes in LV and LA volumes and function after CRT and it is highly predictive for response to CRT.

INTRODUCTION

Cardiac resynchronization therapy (CRT) is considered an additional therapeutic option in heart failure patients who remain highly symptomatic despite optimized medical treatment [1]. Large studies have demonstrated a significant improvement in clinical and echocardiographic endpoints [2]. However, up to 30% of the patients do not respond to CRT when selection is based on the traditional clinical and electrocardiographic criteria [3]. In the search for better selection criteria for CRT, it has been demonstrated that a direct echocardiographic assessment of left ventricular (LV) dyssynchrony is highly predictive for response to CRT [4]. A novel echocardiographic technique has emerged for the assessment of LV dyssynchrony based on the analysis of regional volumetric changes: real time three-dimensional echocardiography (RT3DE). Promising results for the assessment of LV dyssynchrony have been shown when RT3DE was applied in patients with varying degrees of LV dysfunction and in normal subjects [5]. Furthermore, we have recently shown the value of RT3DE to predict acute echocardiographic response to CRT [6]. Clinically more important however, is the response at long-term follow-up. In the current study, the value of RT3DE both to assess LV reverse remodeling and to predict echocardiographic response to CRT was evaluated at 6 months follow-up.

In addition, it has been recently demonstrated that RT3DE provides a highly accurate evaluation of left atrium (LA) size and function [7,8] that are established markers of adverse cardiovascular outcomes [9–11]. Only few data are available about the effect of CRT on LA remodeling and function [12]. In the current study, it was hypothesized that a favorable response to CRT would also lead to an improvement in LA size and function.

METHODS

Patient population and protocol

The study population consisted of 57 consecutive patients with heart failure scheduled for CRT implantation. Traditional selection criteria for CRT were applied: New York Heart Association (NYHA) functional class III-IV, LV ejection fraction (EF) ≤35%, and QRS duration >120ms. Patients with atrial fibrillation were excluded to allow a complete evaluation of LA function. Of note, acute results after CRT in 42 of these patients have been reported recently [6]. Before CRT implantation and at 6 months follow-up, clinical status (including NYHA class, 6-minute walking distance and Minnesota quality-of-life score) was assessed and LV and LA size and function were measured using RT3DE. Assessment of mitral regurgitation and LV filling pattern was performed using 2D Color-Doppler echocardiography. The echocardiographic analysis was performed by an experienced observer blinded to pre- and post-implantation data.

Real-time 3-dimensional echocardiography

Patients were imaged with a commercially available system (iE33, Philips Medical Systems, Bothell, Washington, USA) equipped with an X3, fully sampled matrix transducer. Apical full-volume data sets were obtained combining, within 1 breath-hold, 7 small real-time sub-volumes to provide a larger pyramidal volume. Frame rate ranged from 20 to 35 frames/sec. A 3D data set was considered unsuitable for analysis if >2 segments could not be visualized or if it contained visible translation artifacts. RT3DE data sets were stored digitally and quantitative analysis was performed off-line using a semi-automated contour tracing algorithm (Q-Lab, version 5.0, Philips Medical Systems); post-processing of the images required 5-7 minutes.

Assessment of LV volumes and ejection fraction

During post-processing of the 3D data set, the software automatically displays the apical 4- and 2-chamber views and the parasternal short-axis view. After initial identification of the apex and the mitral annulus with 5 reference points on the end-diastolic and end-systolic frames, a preconfigured ellipse is fitted to the endocardial border for each frame. A manual adjustment of the endocardial border was performed if required. A LV 3D model is automatically generated and LV volumes and LVEF are calculated.

Patients with a reduction ≥15% of LV end-systolic volume (ESV) at 6 months follow-up were considered responders to CRT [13].

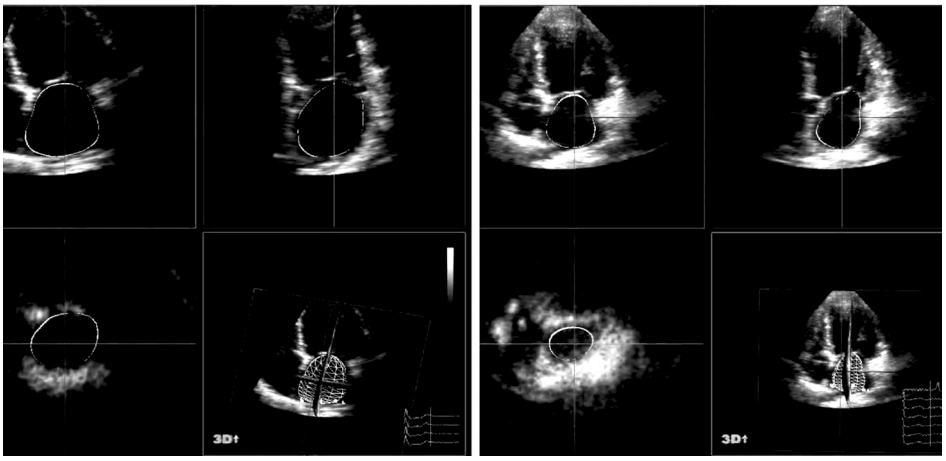


Figure 1. Example of 3D LA volumes obtained by post-processing of a 3D dataset, acquired in a patient scheduled for CRT. Left panel: before CRT (LA maximum volume = 40 ml/m2; LA minimum volume = 18 ml/m2). Right panel: 6 months after CRT (LA maximum volume = 21 ml/m2, LA minimum volume = 12 ml/m2).

Assessment of LA volumes and function

Analysis of 3D images was performed using the same semi-automated contour tracing algorithm as for the LV, marking 5 atrial reference points (Figure 1). Manual corrections of the automatic trace were made to exclude LA appendage and pulmonary veins entrance. LA volume was measured at 3 phases of the cardiac cycle: 1) maximum volume (LAmax) at end-systole, just before mitral valve opening; 2) minimum volume (LAmin) at end-diastole, just before mitral valve closure; 3) volume before atrial active contraction (LApreA), obtained from the last frame before mitral valve reopening or at the end of P wave on ECG. As recommended [14], LA volumes were indexed to the body surface area (BSA). According to previous studies[8,15,16], LA function was explored assessing the following indices:

1) Total atrial emptying fraction (LAEF) = [(LAmax - LAmin)/LAmax] x100
2) Active atrial emptying fraction (LAactive) = [(LApreA - LAmin)/LApreA] x100, as an index of LA booster pump function.
3) Passive atrial emptying fraction (LApassive) = [(LAmax - LApreA)/LAmax] x100, as an index of LA conduit function.
4) Atrial expansion index (LAreservoir) = [(LAmax - Lamin)/LAmin] x100, which is considered an index of LA reservoir function.

Assessment of LV dyssynchrony

The LV 3D model was subdivided by the software in 17 standard wedge shaped (apart from the apex) sub-volumes. For each volumetric segment the time taken to reach the minimum systolic volume (Tmsv) was calculated (Figure 2). As previously described by Kapetanakis et al [5], the standard deviation of the Tmsv for 16 segments (excluding the true apex) was expressed as a percentage of cardiac cycle (obtaining the systolic dyssynchrony index, SDI) and used as a marker of global LV dyssynchrony. Parametric images are also provided by the software with a visual summary, as a polar plot, of LV regional contraction timings and a rapid identification of the latest activated LV wall (Figure 2).

Reproducibility of the RT3DE measurements

Twenty patients were randomly identified for inter- and intra-observer agreement. According to the Bland-Altman analysis, inter-observer agreement was good. The mean differences for SDI, LVESV and LVEF were 0.1±1%, 0.3±17 ml and 0.4±4%, respectively (p = NS). The mean differences for LAmax, LAmin and LApreA were 4.2±6.4 ml, 0.52±3.4 ml and 2.8±4.4 ml, respectively (p = NS).

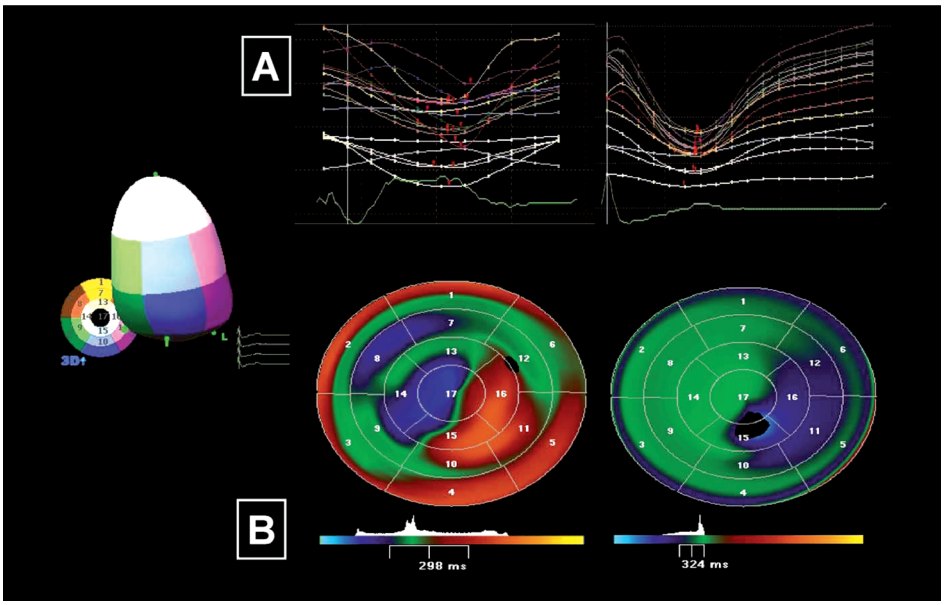


Figure 2. Example of the 3D LV model generated by post-processing of a RT3DE dataset and subdivided by the software in 17 sub-volumes (left panel). Panel A: for each volumetric segment, it is possible to derive time-volume curves and assess the time needed to reach the minimum systolic volume (Tmsv, red dots). In this example, the dispersion of Tmsv is high (SDI 12.4%) at baseline (graph on the left), while after CRT (graph on the right) the segmental time-volume curves are more synchronous (SDI 2.2%). Panel B: parametric image, using color-coding (blue indicating early activation and orange-red late activation) representing Tmsv, showing that the inferior and posterior LV regions are the latest activated before CRT (polar plot on the left). Six months after CRT (polar plot on the right) the overall green color indicates absence of regions with delayed activation.

The intra-observer agreement was also excellent with mean differences of 0.7±6 ml for LVESV, 0.8±3% for LVEF, 1.8±3.9 ml for LAmax, 0.16±2.1 ml for LAmin and 0.9±1.7 ml for LApreA (p = NS).

Color-Doppler echocardiography

The severity of mitral regurgitation was graded semi-quantitatively from color-Doppler in the parasternal long-axis and apical 4-chamber view and characterized as follows: absent, mild (ratio jet area/LA area<20%), moderate (jet area/LA area 20% to 40%) and severe (jet area/LA area>40%) [17].

Doppler measurements of LV diastolic function were performed according to the Canadian Consensus recommendations [18] and the patients were divided in 2 groups, namely those with and those without restrictive filling pattern defined as follows: ratio of early (E) to late (A) diastolic filling velocities (E/A) >2 and deceleration time (DT) of E <150 ms.

Pacemaker implantation

The LV pacing lead was inserted transvenously via the subclavian route and positioned as far as possible in a lateral or postero-lateral vein. The right atrial and ventricular leads were positioned in the right atrial appendage (or on the right atrium lateral wall) and in the right ventricular apex, respectively. All patients received a combined device (CRT-D; Contak Renewal, Guidant Corp.; Insync III-CD or Insync Sentry, Medtronic Inc.) without major complications. Two types of LV leads were used (Easytrak, Guidant Corp.; Attain, Medtronic Inc.). For each patient, the device was programmed in DDD mode (lower rate 40 bpm) and the atrio-ventricular interval was adjusted to maximize mitral inflow duration with pulsed-wave Doppler echocardiography. No adjustment to the inter-ventricular delay was made.

Statistical analysis

Continuous data are presented as mean±standard deviation. Categorical data are presented as absolute numbers or percentages. T-test and χ^2-test were used for appropriate comparisons. Changes in NYHA class, LV filling pattern and mitral regurgitation before and after CRT have been evaluated with Wilcoxon ranks test. To determine the relationship between baseline variables and echocardiographic response to CRT, logistic regression analysis was applied. First, univariate analysis was performed, followed by a multivariate analysis including those variables who had a p-value ≤0.25 at univariate analysis. Linear regression analysis was performed to study the relationship between the changes in LVESV and in LA volumes after CRT. Optimal cut-off value of SDI to predict echocardiographic response to CRT was determined by receiver operating characteristic (ROC) curve analysis. For all tests, a p-value<0.05 was considered significant. A statistical software program SPSS 12.0 (SPSS Inc, Chicago, USA) was used for statistical analysis.

RESULTS

Patient population

Six patients (10.5%) were excluded from further analysis because of suboptimal images; baseline characteristics of the remaining 51 patients are summarized in Table 1. RT3DE revealed severe LV dilatation (mean LVEDV 200±47 ml), with depressed LV function (mean LVEF 28±6%). Furthermore, a moderate-severe LA dilatation (LAmax 40±18 ml/m2) and dysfunction (LAEF 36±14%) was observed [19,20].

Mean LV dyssynchrony (SDI) was 8.4±3.9% and the latest activated LV wall was the lateral in 17 patients (33%), the posterior in 15 patients (29%), the inferior in 12 patients (24%) and the anterior in 7 patients (14%).

Table 1. Baseline characteristics of study population (n = 51)

Age (years)	**66±9**
Gender (M/F)	41/10
NYHA class	3.0±0.5
6-MWT (m)	335±119
Quality of life score	30±19
QRS duration (ms)	146±30
Etiology, n (%)	
Ischemic	31 (61)
Idiopathic	20 (39)
Medication, n (%)	
ACE Inhibitors	46 (90)
ß-blockers	37 (72)
Diuretics and /or Spironolactone	47 (92)
LVEDV (ml)	200±47
LVESV (ml)	145±40
LVEF (%)	28±6
MR, n (absent/mild/moderate/severe)	11/21/14/5
Restrictive LV filling pattern, n (%)	12 (24%)
SDI (%)	8.4±3.9

EDV: end-diastolic volume, EF: ejection fraction, ESV: end-systolic volume, LV: left ventricular, MR: mitral regurgitation, NYHA: New York Heart Association, SDI: systolic dyssynchrony index, 6-MWT: 6 minutes walk test.

Clinical response to CRT

At 6 months follow-up evaluation, significant improvement in NYHA functional class (from 3±0.5 to 1.9±0.8, p <0.001), 6-minute walk distance (from 335±119m to 385±117m, p <0.001) and Minnesota quality-of-life questionnaire (from 30±19 to 23±18, p <0.05) was observed.

Echocardiographic response to CRT

LV volumes and function

Reverse LV remodeling was observed on RT3DE at 6 months follow-up: LVEDV decreased from 200±47 ml to 179±47 ml (p <0.001) and LVESV from 145±40 ml to 117±40 ml (p <0.001). Furthermore, a significant improvement in LVEF was observed, from 28±6% to 35±8% (p <0.001).

LA volumes and function

After 6 months follow-up, a significant reduction of LA volumes was observed on RT3DE: LAmax decreased from 40±18 ml/m2 to 35±16 ml/m2 (p <0.001); LAmin decreased from 26±18 ml/m2 to 22±15 ml/m2 (p <0.001) and LApreA from 31±18 ml/m2 to 26±15 ml/m2 (p <0.001). In addition, a significant improvement in LA function was observed: LAEF increased from 36±14% to 40±14% (p <0.01), LApassive from 24±9% to 26±10% (p = 0.01) and LAreservoir from 66±39% to 76±43% (p = 0.02). No significant improvement was observed in LAactive (from 17±11% to 19±11%, p = NS).

Table 2. Responders (≥15% reduction in LVESV) versus non-responders: clinical and echocardiographic variables before and 6 months after CRT implantation.

	Responders n = 34	Non-responders n = 17	p–value (responders vs. non-responders)
Age (years)	65±8	67±10	NS
Gender (M/F)	28/6	13/4	NS
Ischemic/idiopathic (n)	18/16	13/4	NS
QRS duration (ms)	142±28	154±31	NS
NYHA class			
Baseline	3.0±0.5	3.0±0.4	NS
After implantation	1.9±0.7*	2.4±0.5*	<0.05
6-MWT (m)			
Baseline	351±159	307±155	NS
After implantation	398±175*	337±154*	NS
Quality of life score			
Baseline	28±16	31±24	NS
After implantation	19±14*	27±20	NS
LVEDV (ml)			
Baseline	196±51	208±35	NS
After implantation	162±45*	213±26	<0.001
LVESV (ml)			
Baseline	140±44	156±30	NS
After implantation	98±32*	154±28	<0.001
LVEF (%)			
Baseline	29±5	26±7	NS
After implantation	38±8*	28±8	<0.001
MR, n (absent/mild/moderate/severe)			
Baseline	8/14/8/4	3/7/6/1	NS
After implantation	12/14/5/3	4/8/4/1	NS
Restrictive LV filling pattern, n (%)			
Baseline	5 (15)	7 (41)	NS
After implantation	3 (9)	6 (35)	NS
SDI (%)			
Baseline	9.7±3.6	5.1±1.8	<0.001
After implantation	3.0±1.6*	4.8±2.7	<0.01

* = p <0.001 baseline versus follow-up. Abbreviations see Table 1.

Responders and non-responders

Six months after CRT implantation, 34 patients (67%) experienced a reduction in LVESV ≥15% and were classified as responders. Compared to non-responders, these patients also showed a significantly larger reduction in LVEDV and a larger increase in LVEF (Table 2).

Similarly, at 6 months follow-up, a significant improvement in LA size (LAmax decreased from 38±21 to 32±16 ml/m2, p <0.001) and LA function (except for LAactive) was detected in responders, whereas non-responders showed stable or slightly worse LA volumes and function (Table 3). Linear regression analysis demonstrated a significant relationship between the changes in LVESV and in LA volumes at 6 months after CRT. Of interest, when patients showed a reduction in LVESV ≥15% (responders), most of them also demonstrated a significant reduction (≥10%) in LAmax and LAmin (Figure 3).

Table 3. Left atrium size and function, before and 6 months after CRT implantation, in the total study population and in responders (≥15% reduction in LVESV) versus non-responders.

	Responders n = 34	Non-responders n = 17	p–value (responders vs non-responders)
LAmax (ml/m2)			
Baseline	38±21	42±13	NS
After implantation	32±16*	42±12	0.03
LAmin (ml/m2)			
Baseline	25±20	28±11	NS
After implantation	19±16*	28±10	0.04
LApreA (ml/m2)			
Baseline	30±20	32±11	NS
After implantation	24±16*	33±10	0.03
LAEF (%)			
Baseline	38±15	35±12	NS
After implantation	43±15*	33±10	0.01
LApassive (%)			
Baseline	24±10	24±10	NS
After implantation	28±10*	22±8	0.03
LAactive (%)			
Baseline	18±12	15±8	NS
After implantation	21±13	14±7	0.05
LAreservoir (%)			
Baseline	70±43	58±29	NS
After implantation	87±47*	53±23	<0.01

* = p <0.01 baseline versus follow-up. LA: left atrium; LAactive: active atrial emptying fraction; LAEF: total atrial emptying fraction; LAmax: maximum volume; LAmin: minimum volume; LApassive: passive atrial emptying fraction; LApreA: volume before atrial contraction; LAreservoir: atrial expansion index.

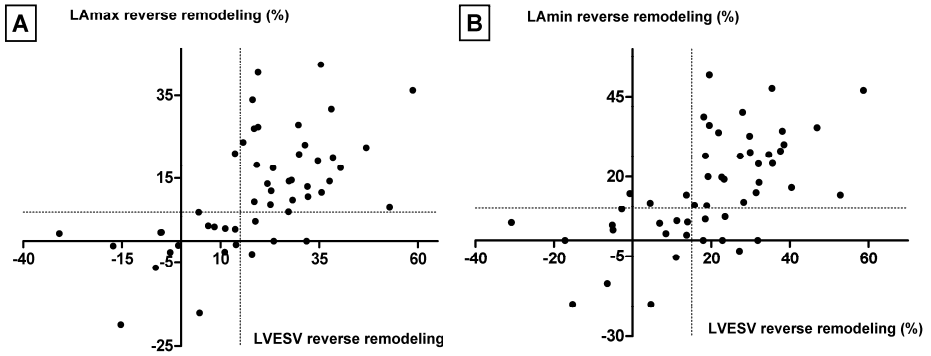


Figure 3. Relationship between reverse remodeling of LV end-systolic volume (LVESV) and reverse remodeling of LA maximum volume (LAmax; Panel A; y = 0.46x+2.66, r = 0.6, p <0.001) and of LA minimum volume (LAmin; Panel B; y = 0.56x+4.72, r = 0.6, p <0.001) at 6 months follow-up.

Of interest, when patients showed a reduction in LVESV ≥15% (responders, see dotted vertical line in Figures), a significant reduction (≥10%, see dotted horizontal line) in LAmax and LAmin was also observed in 88% and 82% of responders, respectively.

Prediction of echocardiographic response to CRT

All baseline clinical and echocardiographic characteristics were comparable between responders and non-responders, except for LV dyssynchrony assessed with SDI (Table 2), which was significantly higher in responders compared to non-responders (9.7±3.6% versus 5.1±1.8%, p <0.001). Moreover, responders demonstrated a significant reduction in SDI after CRT (from 9.7±3.6% to 3.0±1.6%, p <0.001), whereas in non-responders the SDI remained unchanged (5.1±1.8 versus 4.8±2.7%, p = NS).

At the univariate analysis baseline SDI was significantly associated with echocardiographic response to CRT (Table 4). After correction for other baseline characteristics in the multivariate analysis, SDI remained the only variable significantly correlated with response to CRT (p = 0.006, OR = 1.58, 95% CI = 1.14-2.20). To define the optimal cut-off value for SDI for prediction of echocardiographic response to CRT, ROC curve analysis was performed. The area under the curve was 0.92, which indicates a good predictive value, and a cut-off value of 6.4% yielded a sensitivity of 88% and a specificity of 85% to predict LV reverse remodeling at 6 months follow-up.

Table 4. Univariate analysis: estimates of correlation between clinical and echocardiographic variables and response to CRT, defined as a reduction ≥15% of LV end-systolic volume. In bold the p-value of the baseline variables included in the multivariate analysis.

	Odds ratio (95% CI)	p–value
Age	0.98 (0.91-1.05)	0.51
Etiology	0.35 (0.09-1.28)	0.10
QRS duration	0.98 (0.96-1.00)	0.19
LVEDV	0.99 (0.98-1.01)	0.37
LVEF	1.09 (1.00-1.23)	0.06
SDI	1.65 (1.18-2.32)	0.004
LAmax	1.01 (0.97-1.02)	0.47
LAEF	1.02 (0.97-1.07)	0.34

For abbreviations see Tables 1 and 3.

DISCUSSION

In the current study, RT3DE demonstrated a significant improvement in LV remodeling and function at 6 months after CRT associated with a significant improvement in LA volumes and function. In addition, LV dyssynchrony (as measured with SDI) was the only predictor of echocardiographic response to CRT with high sensitivity and specificity.

Use of RT3DE to assess therapy success after CRT

Left ventricle

In the current study, RT3DE has been used to measure LV volumes and function before and after CRT. Response to CRT has been differently defined, using both clinical and echocardiographic parameters. Since Yu et al demonstrated that a reduction in LVESV is the best predictor of improved survival after CRT [21], quantification of LVESV before implantation and during follow-up became crucial in order to assess therapy success. Overcoming the drawbacks of geometric assumptions and cut-plane reproducibility in sequential studies, RT3DE has been validated against MRI and found to be far more accurate and reproducible than 2-dimensional echocardiography for LV volumes assessment [22,23]. Furthermore, RT3DE, in the same acquisition and analysis, integrates this information with a quantitative assessment of LV dyssynchrony.

Left atrium

RT3DE provides an accurate and geometric assumption-free quantification of LA volume, which has been suggested the most reliable index of LA size [14], and allows for an extensive assessment of LA function through the analysis of phasic LA volume changes during the cardiac cycle [7,8]. Only one study thus far examined how LA size and function change after CRT. Yu et al evaluated with 2D echocardiography, tissue Doppler and strain imaging, LA size and function before and shortly after CRT [12]. The authors noted a reduction only in LA minimum volume due to an improvement in LA active function and an increase in systolic atrial strain (suggesting an improvement of atrial compliance).

In the current study, with longer follow-up, clear LA reverse remodeling was observed only in responders, with a significant reduction of all LA volumes. This result probably reflects LA structural changes that require a long-lasting reduction in LA volume- and pressure-overload to be highlighted [24].

Moreover, significant improvement in LA conduit and reservoir functions was observed in responders. LA conduit function is mainly related to LV diastolic function that has been demonstrated to improve after CRT [8,16]. Although a significant improvement in LV filling pattern was not observed (Table 2), the analysis was limited to the presence/absence of an advanced diastolic dysfunction and by the use only of Doppler measurements.

LA reservoir function reflects the ability of the LA to fill during ventricular systole and it is mainly influenced by LA wall stiffness and mitral annulus systolic displacement [16,25]. The improvement of LA reservoir function after CRT can be subsequently explained by the improvement in LV systolic function and the increase in LA compliance. Of note, the major determinants of LA active function are heart rhythm and LApreA (Frank-Starling effect) [8]. All the patients of the study were in sinus rhythm with a fairly normal baseline LA active function [16] and did not show significant changes in LApreA after CRT; accordingly, no significant improvement in LAactive was observed.

The improvement in LA size and function after CRT demonstrated in the present study may also have important clinical implications, since there is strong evidence that in heart failure patients LA enlargement is a robust predictor of adverse cardiovascular outcomes such as atrial fibrillation occurrence, worsening heart failure and thromboembolic events [9,10].

Assessment of LV dyssynchrony by RT3DE and prediction of echocardiographic response to CRT

Several studies demonstrated the importance of the presence of significant baseline LV dyssynchrony to predict response to CRT [4]. Echocardiography and in particular tissue Doppler and strain imaging have been extensively used to assess LV dyssynchrony and to predict

response to CRT[4,26]. Nevertheless, the results of PROSPECT trial recently suggested that TDI and conventional echocardiographic measures have limited value for prediction of response to CRT, when these techniques are applied in the community rather than in expert centers, indicating the need for sufficient training in data acquisition and analysis [13]. In addition, novel techniques, such as 2D strain imaging and RT3DE, were not included in the PROSPECT trial and may provide complete and accurate information on LV dyssynchrony. In particular, RT3DE measures LV regional volumetric changes during the cardiac cycle, as a composite effect of longitudinal, radial and circumferential contraction. Kapetanakis et al demonstrated the feasibility of LV dyssynchrony assessment (SDI) with RT3DE in a large group of patients and normal subjects [5]; 26 patients underwent CRT implantation and responders to CRT had significantly higher SDI at baseline than non-responders (16.6±1.1% vs. 7.1±2.0%, p <0.001). We obtained similar results: a higher baseline SDI was found in responders as compared to non-responders (9.7±3.6% vs. 5.1±1.8%, p <0.001), although the absolute SDI values were somewhat lower in the current study. This difference may be explained by the different software packages used for the 3D dataset analysis. In contrast to the TomTec software (used by Kapetanakis et al), the Q-Lab software uses a different contour tracing algorithm and does not permit the operator to change the point of Tmsv which is automatically detected, yielding a better reproducibility of the measurements but with a trend towards a lower SDI values. Direct comparisons are needed to elucidate these findings.

Furthermore, the cut-off value used by Kapetanakis et al for significant mechanical dyssynchrony was arbitrarily derived as an SDI >3SD above the mean value obtained in normal subjects (8.3%). We recently reported a cut-off value for SDI of 5.6% to optimally predict acute echocardiographic response after CRT implantation [6], and a similar cut-off value (6.4%) was obtained in the current study to predict response at 6 months follow-up.

Study limitations

The patient cohort was relatively small and the predictive value of RT3DE needs to be assessed for clinical endpoints and confirmed in larger prospective studies.

Data on scar tissue and the exact LV lead position were not systematically available, which have been shown to affect response to CRT [27,28]. Also, the contribution of reduction in mitral regurgitation on LA size and function after CRT should be explored in a larger group of patients.

CONCLUSIONS

RT3DE allows assessment of the effects of CRT on LV and LA volumes and function. Baseline LV dyssynchrony (as measured with SDI) is predictive for echocardiographic response to CRT.

REFERENCES

1. Freemantle N, Tharmanathan P, Calvert MJ, Abraham WT, Ghosh J, Cleland JG. Cardiac resynchronisation for patients with heart failure due to left ventricular systolic dysfunction -- a systematic review and meta-analysis. *Eur J Heart Fail.* 2006;8:433-440.
2. Cleland JG, Daubert JC, Erdmann E et al. The effect of cardiac resynchronization on morbidity and mortality in heart failure. *N Engl J Med.* 2005;352:1539-1549.
3. Mehra MR, Greenberg BH. Cardiac resynchronization therapy: caveat medicus! *J Am Coll Cardiol.* 2004;43:1145-1148.
4. Bax JJ, Abraham T, Barold SS et al. Cardiac resynchronization therapy: Part 1--issues before device implantation. *J Am Coll Cardiol.* 2005;46:2153-2167.
5. Kapetanakis S, Kearney MT, Siva A, Gall N, Cooklin M, Monaghan MJ. Real-time three-dimensional echocardiography: a novel technique to quantify global left ventricular mechanical dyssynchrony. *Circulation.* 2005;112:992-1000.
6. Marsan NA, Bleeker GB, Ypenburg C et al. Real-time three-dimensional echocardiography permits quantification of left ventricular mechanical dyssynchrony and predicts acute response to cardiac resynchronization therapy. *J Cardiovasc Electrophysiol.* 2007;19:399.
7. Anwar AM, Soliman OI, Geleijnse ML, Nemes A, Vletter WB, Ten Cate FJ. Assessment of left atrial volume and function by real-time three-dimensional echocardiography. *Int J Cardiol.* 2007;123:161.
8. Anwar AM, Geleijnse ML, Soliman OI, Nemes A, Ten Cate FJ. Left atrial Frank-Starling law assessed by real-time, three-dimensional echocardiographic left atrial volume changes. *Heart.* 2007;93:1393-1397.
9. Abhayaratna WP, Seward JB, Appleton CP et al. Left atrial size: physiologic determinants and clinical applications. *J Am Coll Cardiol.* 2006;47:2357-2363.
10. Rossi A, Cicoira M, Zanolla L et al. Determinants and prognostic value of left atrial volume in patients with dilated cardiomyopathy. *J Am Coll Cardiol.* 2002;40:1425.
11. Matsuda Y, Toma Y, Ogawa H et al. Importance of left atrial function in patients with myocardial infarction. *Circulation.* 1983;67:566-571.
12. Yu CM, Fang F, Zhang Q et al. Improvement of atrial function and atrial reverse remodeling after cardiac resynchronization therapy for heart failure. *J Am Coll Cardiol.* 2007;50:778-785.
13. Chung ES, Leon AR, Tavazzi L et al. Results of the Predictors of Response to CRT (PROSPECT) Trial. *Circulation.* 2008;117:2608-2616.
14. Lang RM, Bierig M, Devereux RB et al. Recommendations for chamber quantification. *Eur J Echocardiogr.* 2006;7:79-108.
15. Poutanen T, Jokinen E, Sairanen H, Tikanoja T. Left atrial and left ventricular function in healthy children and young adults assessed by three dimensional echocardiography. *Heart.* 2003;89:544-549.
16. Spencer KT, Mor-Avi V, Gorcsan J, III et al. Effects of aging on left atrial reservoir, conduit, and booster pump function: a multi-institution acoustic quantification study. *Heart.* 2001;85:272-277.
17. Bonow RO, Carabello BA, Kanu C et al. ACC/AHA 2006 guidelines for the management of patients with valvular heart disease: a report of the American College of Cardiology/American Heart Association Task Force on Practice Guidelines (writing committee to revise the 1998 Guidelines for the Management of Patients With Valvular Heart Disease): developed in collaboration with the Society of Cardiovascular Anesthesiologists: endorsed by the Society for Cardiovascular Angiography and Interventions and the Society of Thoracic Surgeons. *Circulation.* 2006;114:e84-231.

18. Rakowski H, Appleton C, Chan KL et al. Canadian consensus recommendations for the measurement and reporting of diastolic dysfunction by echocardiography: from the Investigators of Consensus on Diastolic Dysfunction by Echocardiography. *J Am Soc Echocardiogr.* 1996;9:736-760.
19. Pritchett AM, Jacobsen SJ, Mahoney DW, Rodeheffer RJ, Bailey KR, Redfield MM. Left atrial volume as an index of left atrial size: a population-based study. *J Am Coll Cardiol.* 2003;41:1036-1043.
20. Gutman J, Wang YS, Wahr D, Schiller NB. Normal left atrial function determined by 2-dimensional echocardiography. *Am J Cardiol.* 1983;51:336-340.
21. Yu CM, Bleeker GB, Fung JW et al. Left ventricular reverse remodeling but not clinical improvement predicts long-term survival after cardiac resynchronization therapy. *Circulation.* 2005;112:1580-1586.
22. Corsi C, Lang RM, Veronesi F et al. Volumetric quantification of global and regional left ventricular function from real-time three-dimensional echocardiographic images. *Circulation.* 2005;112:1161-1170.
23. Kuhl HP, Schreckenberg M, Rulands D et al. High-resolution transthoracic real-time three-dimensional echocardiography: quantitation of cardiac volumes and function using semi-automatic border detection and comparison with cardiac magnetic resonance imaging. *J Am Coll Cardiol.* 2004;43:2083-2090.
24. Casaclang-Verzosa G, Gersh BJ, Tsang TS. Structural and functional remodeling of the left atrium: clinical and therapeutic implications for atrial fibrillation. *J Am Coll Cardiol.* 2008;51:1-11.
25. Barbier P, Solomon SB, Schiller NB, Glantz SA. Left atrial relaxation and left ventricular systolic function determine left atrial reservoir function. *Circulation.* 1999;100:427-436.
26. Suffoletto MS, Dohi K, Cannesson M, Saba S, Gorcsan J, III. Novel speckle-tracking radial strain from routine black-and-white echocardiographic images to quantify dyssynchrony and predict response to cardiac resynchronization therapy. *Circulation.* 2006;113:960-968.
27. Becker M, Franke A, Breithardt OA et al. Impact of left ventricular lead position on the efficacy of cardiac resynchronisation therapy: a two-dimensional strain echocardiography study. *Heart.* 2007;93:1197-1203.
28. Bleeker GB, Kaandorp TA, Lamb HJ et al. Effect of posterolateral scar tissue on clinical and echocardiographic improvement after cardiac resynchronization therapy. *Circulation.* 2006;113:969-976.

CHAPTER 10

Comparison of left atrial volumes and function by RT3DE in patients having catheter ablation for atrial fibrillation with persistence of sinus rhythm versus recurrent atrial fibrillation three months later

N Ajmone Marsan, L F Tops, E R Holman, N R van de Veire, K Zeppenfeld, E Boersma, E E van der Wall, M J Schalij, and J J Bax

Am J Cardiol 2008;102:847-53.

ABSTRACT

Objectives: Real-time 3-dimensional echocardiography (RT3DE) can provide a unique combination of accurate left atrium (LA) volume quantification and rapid, automatic assessment of LA function. The aim of the study was to evaluate the changes in LA volumes and function in patients with atrial fibrillation (AF) undergoing radiofrequency catheter ablation (RFCA), using RT3DE.

Methods: Fifty-seven consecutive patients referred for RFCA were studied. Paroxysmal AF was present in 43 patients (75%), and persistent AF in 14 (25%). After a mean follow-up of 7.9±2.7 months, patients were divided into 2 groups: successful RFCA (SR group) and recurrence of AF (AF group). RT3DE was performed before, within 3 days and 3 months after RFCA to assess LA volumes (maximum, minimum and preA) and LA functions (passive, active and reservoir).

Results: A total of 38 patients (67%) had successful RFCA (SR group). Immediately after RFCA, no significant changes in LA volumes and function were observed. After 3 months, a significant reduction in LA volumes (maximum: from 26±8 to 23±7 mL/m2, $p < 0.01$) was noted only in the SR group, together with a significant improvement in LA active (from 22±8 to 33±9%, <0.01) and reservoir functions (from 116±45 to 152±54%, $p < 0.01$). Conversely, the AF group showed a trend towards a deterioration of LA volumes and function.

Conclusions: In patients who maintain sinus rhythm after RFCA, a significant reverse remodeling and functional improvement of the LA is observed using RT3DE.

INTRODUCTION

Recently, real-time 3-dimensional echocardiography (RT3DE) has been validated against magnetic resonance imaging and it has been shown to be more accurate and reproducible than 2-dimensional (2D) echocardiography for the quantification of left atrial (LA) volumes [1,2]. Furthermore, RT3DE may be a novel, reliable technique for the assessment of LA function, providing unique information about phasic changes of LA volumes during the cardiac cycle [3,4]. In the present study, RT3DE was used to evaluate the changes in LA volumes and function in atrial fibrillation (AF) patients treated with radiofrequency catheter ablation (RFCA).

METHODS

Over a 10 months period, 57 consecutive patients (44 men; age 56±9 years) with symptomatic drug-refractory AF, referred to our institution for RFCA in accordance to the current guidelines criteria, were included in this study. According to the ACC/AHA/ESC Guidelines definition [5], paroxysmal AF was present in 43 patients (75%), while persistent AF was present in the remaining 14 patients (25%); none of the patients had permanent AF. Mean AF duration (calculated from the time of the first episode) was 4.6±4.1 years and the patients had an unsuccessful treatment with 3±1 anti-arrhythmic drugs (mainly flecainide, propafenone, sotalol and amiodarone).

After RFCA, the patients were evaluated at the out-patient clinic on a regular basis. During follow-up, all medication, including anti-arrhythmic drugs, were continued in all patients for 3 months after the RFCA procedure. Afterwards, anti-arrhythmic drugs were discontinued at discretion of the physician. At the latest follow-up, successful RFCA was defined as the absence of symptomatic recurrences lasting more than 3 minutes [6] and/or the absence of AF episodes lasting more than 30 seconds (detected with 24-hours Holter ECG recording and surface ECG) during follow-up, after a blanking period of 1 month [5,7]. Accordingly, the study population was divided into 2 groups: patients with successful RFCA (SR group) and patients who had recurrence of AF (AF group).

Before, and within 3 days after the ablation procedure, RT3DE was performed to assess LA and left ventricular (LV) size and function. In addition, conventional 2D color-Doppler echocardiography was performed to assess mitral regurgitation (MR) and LV filling pattern. After 3 months follow-up, the echocardiograms were repeated to assess the effect of the RFCA on LA volumes and function.

Patients were imaged with a commercially available system (iE33, Philips Medical Systems, Bothell, Washington) equipped with X3, fully sampled matrix transducer. Apical full-volume data sets were obtained in all patients, combining 7 small real-time sub-volumes to provide a larger pyramidal volume. The acquisition was performed during end-expiratory apnea within

1 breath hold. Frame rate ranged from 20 to 35 frames/sec. The RT3DE data sets were stored digitally and quantitative analyses were performed off-line using a semi-automated contour tracing algorithm (Q-Lab, version 5.0, Philips Medical Systems) based on 5 reference points. In all patients the image quality was sufficient for quantitative analysis and the post-processing of the images was performed within 10 minutes. Left ventricular volumes and function were assessed as previously described in detail [8].

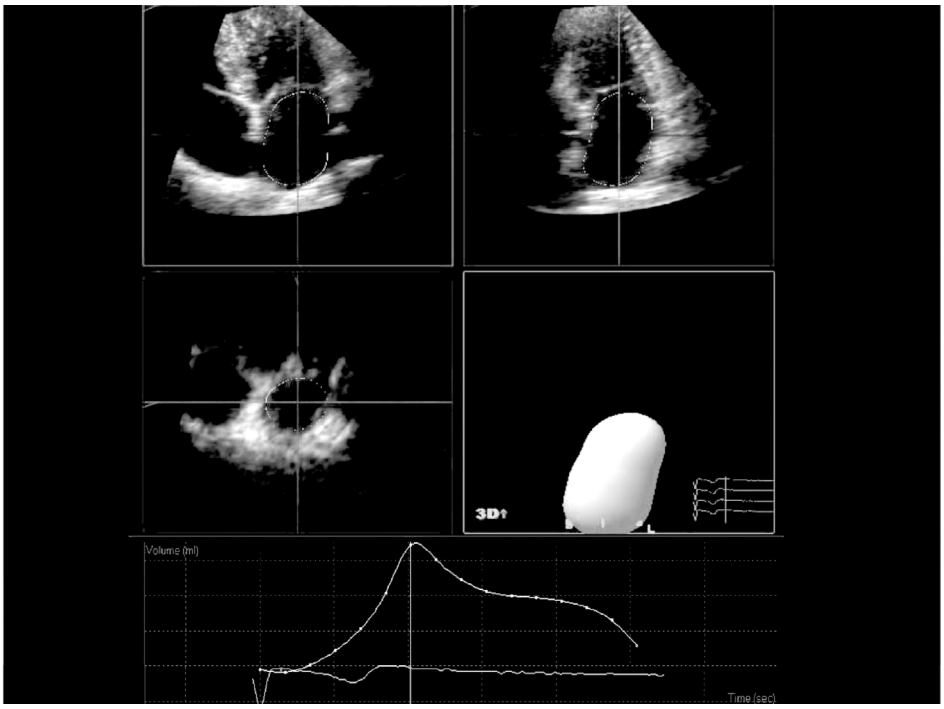


Figure 1. Assessment of LA volumes using RT3DE. An automatic border detection is obtained marking 5 reference points in the apical 2- and 4-chamber views (upper panel) and the LA 3D model is provided by the software. The changes of LA volumes during the heart cycle are plotted as a curve (lower panel).

Quantification of LA volumes was performed using the semi-automated contour tracing algorithm developed for the LV, but marking 5 atrial reference points: 4 at the anterior, inferior, lateral and septal part of atrial dome and 1 at the level of the mitral annulus (Figure 1). The position of the reference points was chosen to avoid changes in the view orientation that the software automatically generates, since the position of the dome of the LA is opposite of the apex of the LV. Manual corrections of the automatic trace were made to exclude the LA appendage and the pulmonary vein ostia. Left atrial volumes were measured at 3 time points during the cardiac cycle:

1) maximum volume (LA_{max}) at end-systole, just before mitral valve opening;
2) minimum volume (LA_{min}) at end-diastole, just before mitral valve closure;
3) volume before atrial active contraction (LA_{preA}) obtained from the last frame before mitral valve reopening or at time of the P wave on the surface ECG. All LA volumes were indexed to the body surface area, as recommended [9].

Twenty patients were randomly identified for inter- and intra-observer agreement. According to the Bland-Altman analysis, intra-observer variability was excellent with a mean differences of 1.2±2.9 mL for LA_{max}, 0.1±1.1 mL for LA_{min} and 0.8±2.3 mL for LA_{preA} (p = NS). Inter-observer variability was also good with a mean difference for LA_{max}, LA_{min} and LA_{preA} of 3.6±5.6 mL, 0.7±5.4 mL and 1.9±3.4 mL, respectively (p = NS).

The LA function was derived from the LA volumes and expressed with the following parameters [10,11]:

1) Total atrial emptying fraction: $LA_{EF} = [(LA_{max} - LA_{min})/LA_{max}] \times 100$
2) Active atrial emptying fraction: $LA_{active} = [(LA_{preA} - LA_{min})/LA_{preA}] \times 100$, which is considered an index of LA active contraction.
3) Passive atrial emptying fraction: $LA_{passive} = [(LA_{max} - LA_{preA})/LA_{max}] \times 100$, which is considered an index of LA conduit function.
4) Atrial expansion index: $LA_{reservoir} = [(LA_{max} - LA_{min})/LA_{min}] \times 100$, which is considered an index of LA reservoir function.

The severity of MR was graded semi-quantitatively from color-Doppler images in the conventional parasternal long-axis and apical 4-chamber view and characterized as follows: absent, mild (ratio jet area/LA area <20%), moderate (jet area/LA area 20% to 40%) and severe (jet area/LA area >40%) [12]. Left ventricular diastolic function was evaluated according to the Canadian Consensus recommendations [13] through the following Doppler measurements: ratio of early (E) to late (A) diastolic filling velocities (E/A) and deceleration time (DT) of the E wave.

The RFCA procedure was aimed at electrical isolation of all pulmonary veins from the LA. Endocardial mapping was performed with a 4-mm quadripolar mapping/ablation catheter (7Fr Thermocool, Biosense Webster, Diamond Bar, California, USA), using a 3D electroanatomic mapping system (CARTO, BiosenseWebster). A 6Fr diagnostic catheter placed in the right atrium served as a temporal reference. Radiofrequency current was applied outside the ostia of all pulmonary veins, using the ablation catheter with a 4-mm open loop irrigated tip. The following power and temperature settings were used: irrigation rate 20 ml/min, maximum temperature 50º C, and maximum radiofrequency energy 30W. At each point, the radiofrequency current was applied until a voltage of <0.1 mV was achieved, with a maximum of 60 s/point. The procedure was considered successful when pulmonary vein isolation was confirmed by the recording of entrance block during SR or pacing in the coronary sinus. All

patients received heparin intravenously (activated clotting time >300 sec) to avoid thromboembolic complications during the catheter ablation procedure. After RFCA, the rhythm was continuously monitored until discharge.

Continuous data are presented as mean±standard deviation. Categorical data are presented as absolute numbers or percentages. Independent-samples T test and Wilcoxon rank-test were used to compare continuous variables, as appropriate, and χ^2 test was used to compare categorical variables. Sequential data measurements were analyzed by the general linear model (GLM) procedure for repeated measures. For all tests, a p-value <0.05 was considered significant. A statistical software program SPSS 15.0 (SPSS Inc, Chicago, II, USA) was used for statistical analysis.

RESULTS

Baseline clinical characteristics of the study population are summarized in Table 1. At baseline, RT3DE revealed a mild enlargement of LA volume and a moderate reduction in LA_{EF}, LA_{active} and $LA_{reservoir}$ (Table 2), as compared to the reference values for a normal LA [9,14]. Left ventricular systolic and diastolic functions were normal and in 27 patients MR was present (mild n = 24; moderate n = 3) (Table 3). Six patients were in AF at the baseline evaluation and all had a recurrence of AF during follow-up. In these patients, LA_{preA}, LA_{active}, $LA_{passive}$ and LV diastolic function could therefore not be assessed.

After a mean follow-up of 7.9±2.7 months, 38 patients (67%) had successful RFCA (SR group), whereas 19 patients (33%) had recurrence of AF (AF group). Of note, these patients

Table 1. Baseline clinical characteristics of the total study population and of patients with and without recurrence of atrial fibrillation after radiofrequency catheter ablation.

Variable	Total study population n = 57	Sinus rhythm group n = 38	Atrial fibrillation group n = 19
Age (years)	56±9	57±9	53±9
Male/Female	44/13	28/10	16/3
Body surface area (m2)	2.1±0.2	2.1±0.3	2.1±0.1
Atrial fibrillation Paroxysmal/Persistent	45 (79%)/12 (21%)	34 (89%)/4 (11%)	11 (58%)/8 (42%)*
Duration atrial fibrillation (years)	4.6±4.1	4.5±4.1	4.6±4.1
Number of anti-arrhythmic drugs per patient	3±1	3±1	3±1
Angiotensin converting enzyme-inhibitor and/or Angiotensin receptor blocker,	26 (46%)	17 (45%)	9 (47%)
Heart rate (beats/minute)	62±20	60±13	66±36
Hypertension	25 (44%)	13 (34%)	11 (58%)
Diabetes mellitus	6 (11%)	6 (15%)	0 (0%)
Coronary artery disease	3 (5%)	2 (5%)	1 (5%)

*: p <0.05 sinus rhythm group versus atrial fibrillation group.

Table 2. Left atrium (LA) volumes and function at baseline, immediately after and 3 months after the ablation procedure in the total study population and in patients with or without recurrence of atrial fibrillation.

Variable	Total study population n = 57	Sinus rhythm group n = 38	Atrial fibrillation group n = 19	p-value (Sinus rhythm vs. atrial fibrillation)
LA VOLUMES				
LA maximum volume (mL/m2)				<0.01§
Baseline	28±9	26±8	31±8	<0.05
After ablation		26±8	31±8	<0.05
3 months follow-up		23±7*	32±8	<0.001
LA minimum volume (mL/m2)				<0.01§
Baseline	14±6	13±5	16±7	NS
After ablation		12±5	17±6	<0.01
3 months follow-up		10±4*	18±6	<0.001
LA volume preA (mL/m2)				<0.01§
Baseline	16±5	16±5	18±6	NS
After ablation		16±5	18±4	NS
3 months follow-up		14±5*	20±6*	<0.01
LA FUNCTION				
LA total emptying fraction (%)				<0.01§
Baseline	50±11	52±10	47±13	NS
After ablation		52±10	44±12	<0.05
3 months follow-up		58±10*	42±11*	<0.001
LA passive emptying fraction (%)				NS§
Baseline	39±9	39±9	38±10	NS
After ablation		39±9	35±10	NS
3 months follow-up		38±9	35±9	NS
LA active emptying fraction (%)				<0.001§
Baseline	22±8	22±8	24±7	NS
After ablation		21±6	17±7	NS
3 months follow-up		33±9*	15±9*	<0.001
LA expansion index (%)				<0.01§
Baseline	110±48	116±45	101±55	NS
After ablation		117±43	92±49	NS
3 months follow-up		152±54*	78±35*	<0.001

*: p <0.01 (GLM for repeated measures within subjects).

§: p value derived from GLM for repeated measures between subjects (sinus rhythm vs. atrial fibrillation)

were classified in the same group also at 3 months follow-up evaluation. No significant differences were found in the baseline clinical characteristics between the AF and SR groups, except for the percentage of patients with persistent AF (Table 1). At baseline, RT3DE showed larger LA_{max} in the AF group than in the SR group (31±8 vs. 26±8 mL/m^2, p <0.05), but no significant differences in LA and LV function (Table 2 and 3). Conventional 2D color-Doppler echocardiography revealed a comparable LV diastolic function and prevalence of MR (mild/moderate) between the 2 groups (Table 3). Immediately after the RFCA procedure, no significant changes in LA volumes were observed (Table 2). However, after 3 months of follow-up, a significant decrease in LA volumes was noted in the SR group, involving LA_{max}, LA_{min} and LA_{preA} volumes. Conversely, the AF group showed a trend towards an increase in LA volumes during

follow-up (Table 2). An example of a patient in the SR group with a significant reduction of LA_{max} and LA_{min} is shown in Figure 2. In both groups, no significant changes in LA function were noted immediately after the RFCA procedure. However, after 3 months of follow-up, a significant improvement of LA_{active} and $LA_{reservoir}$ was noted in the SR group, whereas in the AF group these parameters showed a significant deterioration (Figure 3). In contrast, $LA_{passive}$ function did not change significantly in both groups. In concordance with the changes in LA_{active}, a significant improvement in LA_{EF} was observed in the SR group, while a significant deterioration in LA_{EF} was observed in the AF group (Table 2).

Mean LV ejection fraction was 58±9% in the SR group and 57±11% in the AF group (p = NS) and no significant changes were observed during follow-up. Similarly, LV diastolic function was normal in both groups before the RFCA procedure and did not change during follow-up (Table 3). However, 12 patients in the SR group and 3 patients in the AF group had an abnormal LV relaxation based on E/A <1. For these patients an improvement in LV filling pattern was noted in the SR group only (E/A ratio from 0.7±0.2 to 1.6±0.5, p <0.01). Only 3 patients had clinically relevant MR (moderate or severe) and a significant improvement in the degree of MR after RFCA was only observed in the SR group (Table 3).

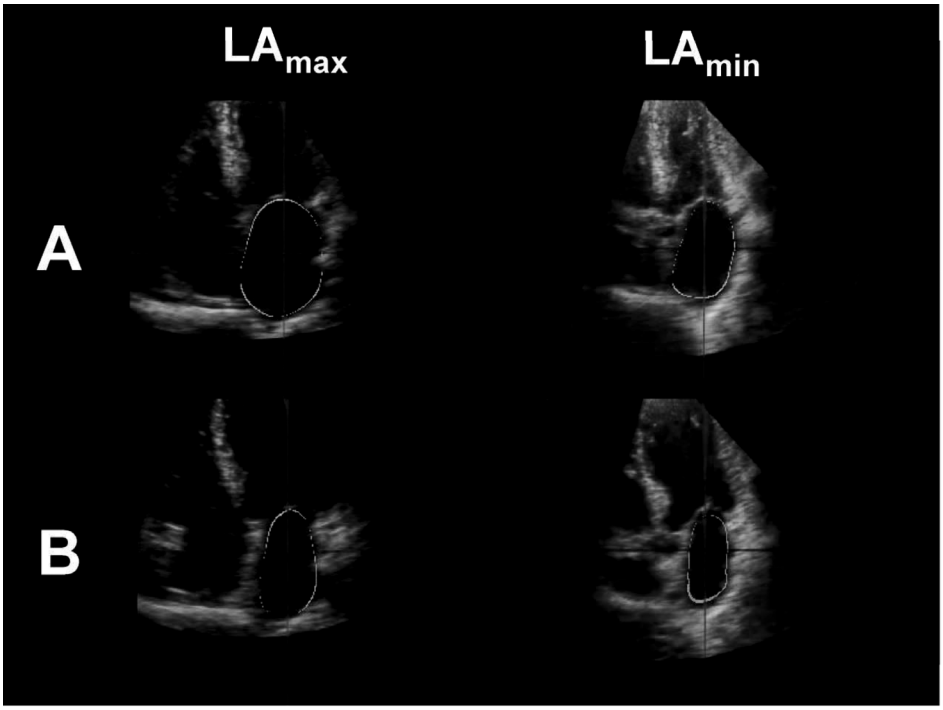


Figure 2. Example of a patient with significant reduction of LA_{max} and LA_{min}, 3 months after the RFCA (panel B vs. panel A). LA_{max} decreased from 83 to 66 mL/m^2 and LA_{min} decreased from 44 to 33mL/m^2.

Table 3. Left ventricular function at baseline and 3 months after the ablation procedure in the total study population and in patients with or without recurrence of atrial fibrillation.

Variable	Total study population n = 57	Sinus rhythm group n = 38	Atrial fibrillation group n = 19
LEFT VENTRICULAR FUNCTION			
Left ventricular ejection fraction (%)			
Baseline	57±9	58±9	57±11
3 months follow-up		59±10	57±8
E/A			
Baseline	1.2±0.6	1.1±0.4	1.4±0.6
3 months follow-up		1.2±0.2	1.3±0.7
Deceleration time (ms)			
Baseline	194±53	196±51	192±48
3 months follow-up		199±40	195±42
Mitral regurgitation, n (absent/mild/moderate/severe)			
Baseline	30/24/3/0	21/16/1/0	9/8/2/0
3 months follow-up		25/13/0/0*	9/8/2/0

*: $p < 0.01$ baseline versus follow-up.

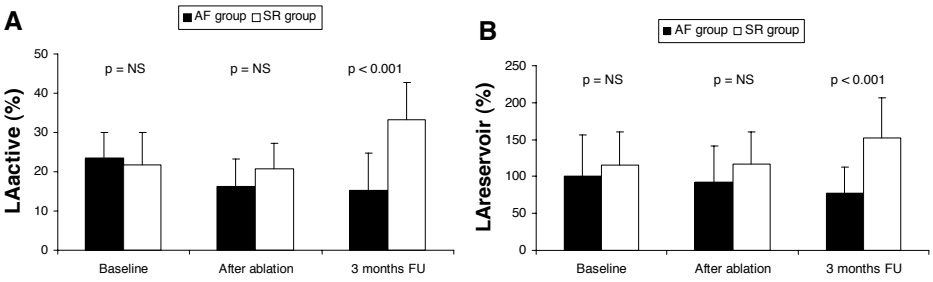


Figure 3. Left atrium active emptying fraction (LA_{active}; panel A) and expansion index ($LA_{reservoir}$; panel B) at baseline, immediately after catheter ablation and at 3 months follow-up (FU) in SR and AF groups.

DISCUSSION

The main findings of the current study can be summarized as follows: 1) three months after RFCA, a significant reduction in LA volumes and a clear improvement of LA active contraction and LA reservoir function was observed in patients with a successful RFCA procedure; 2) patients with recurrence of AF after RFCA showed a trend towards a worsening of LA volumes and function.

In the present study, RT3DE was used to assess LA volumes and function in patients treated with RFCA for AF. The assessment of LA size is fundamental in the management of patients with AF, since it has important prognostic value and is used as a surrogate marker of therapy success [15–18]. The most recent recommendations for cardiac chamber quantification indicate LA volume as the preferred measurement of LA size [9]. However, the majority of the previous

studies only evaluated LA diameter and LA area, using conventional 2D echocardiography [16,18,19]. Although most frequently used, 2D echocardiography is limited for the assessment of LA volume by significant geometric assumptions and low reproducibility due to diverging position and orientation of imaging planes. RT3DE has been demonstrated to be more accurate for LA volumes quantification, with the most favorable test-retest variation [1,2,4]. In addition to LA volumes, assessment of LA function is of particular significance in patients treated with RFCA for AF. However, accurate non-invasive measurements for LA function are still lacking. Recently, initial studies have proposed tissue Doppler imaging (TDI) and 2D strain as new modalities to assess LA myocardial function [20,21]. However, these techniques need to be further validated for this purpose and have some limitations related to the angle dependency of TDI [21] and the difficult analysis of LA systole with 2D strain [20]. In contrast, RT3DE is well validated [3,4,22] and provides a unique combination of an accurate measurement of LA volumes together with a rapid and automatic detection of phasic changes of LA volumes that provides detailed information of the different LA functions.

The relationship between LA enlargement and AF is complex: structural changes of the LA may be related several factors including 1) pressure or volume overload due to underlying structural heart disease; 2) the increased LV filling pressure induced by the tachyarrhythmia; 3) AF itself [23,24]. Supporting the latter hypothesis, abnormal atrial histology (fibrosis, necrosis and inflammation) has been found uniformly in patients with lone AF [25]. Furthermore, LA dilatation has been directly correlated with the duration of AF, as a result of LA electrical and structural remodeling [18]. In the present study, mild dilatation of the LA was noted at baseline using RT3DE. This may be explained by the relatively low prevalence of patients with persistent AF and with structural heart disease (Table 1). Of note, the AF group, compared to the SR group, demonstrated larger baseline LA volumes, probably related to the higher percentage of persistent AF. Furthermore, after 3 months a significant decrease in LA volumes was noted in patients with successful RFCA. These results are in agreement with previous studies that showed a significant reduction in LA volumes after conversion of AF to SR, either by electrical cardioversion or RFCA [6,14,26]. The reduction in LA_{min} as observed in the present study is most probably the direct result of the improvement of LA active contraction; whereas the reduction in LA_{max} is reflecting a true reverse remodeling that is related with the long-lasting restoration of SR. Although LA reverse remodeling may also be ascribed to atrial scarring caused by RFCA, this is very unlikely since LA volumes tended to worsen in patients with recurrence of AF during follow-up.

In addition, an improvement in LA function was observed in patients who maintained SR after RFCA. The LA serves multiple functions. During LV systole and isovolumic relaxation, it operates as a "reservoir" that receives blood from pulmonary veins and stores energy in the form of pressure; during the early diastole, it operates as a "conduit" for transfer blood into the LV after mitral valve opening; during the late diastole the "active" contraction of LA contributes to LV stroke volume by 20-30% [22,23]. To interpret the baseline and follow-up find-

ings of the present study, it is important to consider that the major determinants of LA_{active} are the heart rhythm, the atrial contractility and the LA_{preA} (Frank-Starling effect) [3,11]. The $LA_{reservoir}$ is rather influenced by LV systolic function (mitral annulus displacement) and by LA wall stiffness [11,27]. On the contrary, $LA_{passive}$ is mainly related to LV diastolic function [11,28].

In the present study, a moderate reduction of LA_{active} and $LA_{reservoir}$ was noted at baseline evaluation. Conversely, no significant impairment of $LA_{passive}$ was observed. Since LV systolic and diastolic functions were normal on average and LA_{preA} was even decreased compared to the normal values, the reduction in LA_{active} and $LA_{reservoir}$ is most probably related to the effect of AF itself on the contractility and the stiffness of atrial walls.

Immediately after RFCA, no significant changes in LA functions were found, but LA_{active} tended to worsen. This finding occurred in both the SR and AF groups and can be related to the phenomenon of atrial "stunning" [29]. After 3 months of follow-up, a significant improvement in LA_{active} and $LA_{reservoir}$ was noted in the SR group, whereas in the AF group these parameters showed a significant deterioration. Since LV systolic and diastolic functions did not change after RFCA and LA_{preA} was even decreased, the functional improvement in the SR group is most probably related to a favorable effect of the long-lasting restoration of SR on the intrinsic characteristics of the atrial myocardium [24]. These findings are in line with previous studies [6,14] and carry important clinical implications, since they may translate into a reduced risk of AF recurrences and thrombo-embolic complications at long-term follow-up [24]. However, the exact impact of LA reverse remodeling and improvement of LA function on cardiovascular outcomes remains to be determined.

The results of the present study need to be confirmed in a larger population with longer clinical and echocardiographic follow-up. In addition, in patients with paroxysmal AF, asymptomatic recurrences cannot be excluded and may have influenced the success rate in the present study.

REFERENCES

1. Khankirawatana B, Khankirawatana S, Lof J, Porter TR. Left atrial volume determination by three-dimensional echocardiography reconstruction: validation and application of a simplified technique. *J Am Soc Echocardiogr.* 2002;15:1051-1056.
2. Poutanen T, Ikonen A, Vainio P, Jokinen E, Tikanoja T. Left atrial volume assessed by transthoracic three dimensional echocardiography and magnetic resonance imaging: dynamic changes during the heart cycle in children. *Heart.* 2000;83:537-542.
3. Anwar AM, Geleijnse ML, Soliman OI, Nemes A, Ten Cate FJ. Left atrial Frank-Starling law assessed by real-time, three-dimensional echocardiographic left atrial volume changes. *Heart.* 2007;93:1393-1397.
4. Anwar AM, Soliman OI, Geleijnse ML, Nemes A, Vletter WB, ten Cate FJ. Assessment of left atrial volume and function by real-time three-dimensional echocardiography. *Int J Cardiol.* 2007;123:161.
5. Fuster V, Ryden LE, Cannom DS et al. ACC/AHA/ESC 2006 guidelines for the management of patients with atrial fibrillation--executive summary: a report of the American College of Cardiology/American Heart Association Task Force on Practice Guidelines and the European Society of Cardiology Committee for Practice Guidelines (Writing Committee to Revise the 2001 Guidelines for the Management of Patients With Atrial Fibrillation). *J Am Coll Cardiol.* 2006;48:854-906.
6. Reant P, Lafitte S, Jais P et al. Reverse remodeling of the left cardiac chambers after catheter ablation after 1 year in a series of patients with isolated atrial fibrillation. *Circulation.* 2005;112:2896-2903.
7. Calkins H, Brugada J, Packer DL et al. HRS/EHRA/ECAS expert Consensus Statement on catheter and surgical ablation of atrial fibrillation: recommendations for personnel, policy, procedures and follow-up. A report of the Heart Rhythm Society (HRS) Task Force on catheter and surgical ablation of atrial fibrillation. *Heart Rhythm.* 2007;4:816-861.
8. Soliman OI, Krenning BJ, Geleijnse ML et al. A comparison between QLAB and TomTec full volume reconstruction for real time three-dimensional echocardiographic quantification of left ventricular volumes. *Echocardiography.* 2007;24:967-974.
9. Lang RM, Bierig M, Devereux RB et al. Recommendations for chamber quantification. *Eur J Echocardiogr.* 2006;7:79-108.
10. Poutanen T, Jokinen E, Sairanen H, Tikanoja T. Left atrial and left ventricular function in healthy children and young adults assessed by three dimensional echocardiography. *Heart.* 2003;89:544-549.
11. Spencer KT, Mor-Avi V, Gorcsan J, III et al. Effects of aging on left atrial reservoir, conduit, and booster pump function: a multi-institution acoustic quantification study. *Heart.* 2001;85:272-277.
12. Bonow RO, Carabello BA, Kanu C et al. ACC/AHA 2006 guidelines for the management of patients with valvular heart disease: a report of the American College of Cardiology/American Heart Association Task Force on Practice Guidelines (writing committee to revise the 1998 Guidelines for the Management of Patients With Valvular Heart Disease): developed in collaboration with the Society of Cardiovascular Anesthesiologists: endorsed by the Society for Cardiovascular Angiography and Interventions and the Society of Thoracic Surgeons. *Circulation.* 2006;114:e84-231.
13. Rakowski H, Appleton C, Chan KL et al. Canadian consensus recommendations for the measurement and reporting of diastolic dysfunction by echocardiography: from the Investigators of Consensus on Diastolic Dysfunction by Echocardiography. *J Am Soc Echocardiogr.* 1996;9:736-760.

14. Thomas L, Thomas SP, Hoy M, Boyd A, Schiller NB, Ross DL. Comparison of left atrial volume and function after linear ablation and after cardioversion for chronic atrial fibrillation. *Am J Cardiol.* 2004;93:165-170.
15. Benjamin EJ, D'Agostino RB, Belanger AJ, Wolf PA, Levy D. Left atrial size and the risk of stroke and death. The Framingham Heart Study. *Circulation.* 1995;92:835-841.
16. Berruezo A, Tamborero D, Mont L et al. Pre-procedural predictors of atrial fibrillation recurrence after circumferential pulmonary vein ablation. *Eur Heart J.* 2007;28:836-841.
17. Kirchhof P, Auricchio A, Bax J et al. Outcome parameters for trials in atrial fibrillation: executive summary: Recommendations from a consensus conference organized by the German Atrial Fibrillation Competence NETwork (AFNET) and the European Heart Rhythm Association (EHRA). *Eur Heart J.* 2007;28:2803-2817.
18. Petersen P, Kastrup J, Brinch K, Godtfredsen J, Boysen G. Relation between left atrial dimension and duration of atrial fibrillation. *Am J Cardiol.* 1987;60:382-384.
19. Beukema WP, Elvan A, Sie HT, Misier AR, Wellens HJ. Successful radiofrequency ablation in patients with previous atrial fibrillation results in a significant decrease in left atrial size. *Circulation.* 2005;112:2089-2095.
20. D'Andrea A, Caso P, Romano S et al. Different effects of cardiac resynchronization therapy on left atrial function in patients with either idiopathic or ischaemic dilated cardiomyopathy: a two-dimensional speckle strain study. *Eur Heart J.* 2007;28:2738-2748.
21. Yu CM, Fang F, Zhang Q et al. Improvement of atrial function and atrial reverse remodeling after cardiac resynchronization therapy for heart failure. *J Am Coll Cardiol.* 2007;50:778-785.
22. Thomas L. Assessment of atrial function. *Heart Lung Circ.* 2007;16:234-242.
23. Abhayaratna WP, Seward JB, Appleton CP et al. Left atrial size: physiologic determinants and clinical applications. *J Am Coll Cardiol.* 2006;47:2357-2363.
24. Casaclang-Verzosa G, Gersh BJ, Tsang TS. Structural and functional remodeling of the left atrium: clinical and therapeutic implications for atrial fibrillation. *J Am Coll Cardiol.* 2008;51:1-11.
25. Frustaci A, Chimenti C, Bellocci F, Morgante E, Russo MA, Maseri A. Histological substrate of atrial biopsies in patients with lone atrial fibrillation. *Circulation.* 1997;96:1180-1184.
26. Tops LF, Bax JJ, Zeppenfeld K, Jongbloed MR, van der Wall EE, Schalij MJ. Effect of radiofrequency catheter ablation for atrial fibrillation on left atrial cavity size. *Am J Cardiol.* 2006;97:1220-1222.
27. Barbier P, Solomon SB, Schiller NB, Glantz SA. Left atrial relaxation and left ventricular systolic function determine left atrial reservoir function. *Circulation.* 1999;100:427-436.
28. Nikitin NP, Witte KK, Thackray SD, Goodge LJ, Clark AL, Cleland JG. Effect of age and sex on left atrial morphology and function. *Eur J Echocardiogr.* 2003;4:36-42.
29. Khan IA. Atrial stunning: basics and clinical considerations. *Int J Cardiol.* 2003;92:113-128.

PART II

Contrast-enhanced echocardiography

CHAPTER 11

Safety of contrast-enhanced echocardiography within 24 h after acute myocardial infarction

G Nucifora, **N Ajmone Marsan**, HM J Siebelink, J M van Werkhoven, J D Schuijf, M J Schalij, D Poldermans, E R Holman, and J J Bax

Eur J Echocardiogr 2008;9:816-18.

ABSTRACT

Objectives: Contrast-enhanced echocardiography is widely used to enhance left ventricular (LV) endocardial border delineation in stable patients with known or suspected coronary artery disease. In patients with acute myocardial infarction, accurate assessment of LV function and size is important, but data on the safety of contrast-enhanced echocardiography in the early stage of myocardial infarction (within 24 hours) are lacking. In the current study, the experience on the safety of contrast-enhanced echocardiography within 24 hours of acute myocardial infarction is reported.

Methods: A total of 115 consecutive patients (58±11 years; 77% male) admitted to the coronary care unit for ST-elevation acute myocardial infarction underwent clinically indicated contrast-enhanced echocardiography within 24 hours of hospital admission to assess LV size and function. Perflutren (Luminity®, Bristol-Myers Squibb Pharma, Bruxelles, Belgium) was used as contrast agent. Safety was determined evaluating vital signs, physical examination, ECG and adverse events.

Results: On contrast-enhanced echocardiography, mean LV ejection fraction was 44±11% and 56% of patients had a LV ejection fraction ≤45%. Administration of echo contrast did not induce any significant change in vital signs, physical examination and ECG. Major adverse events were not observed whereas minor events occurred in 4% of patients (hypersensitivity at the injection site in 3 and transient back pain in 2).

Conclusions: These data provide evidence on the safety of contrast-enhanced echocardiography in the first 24 hours of myocardial infarction; larger patient cohorts are needed to confirm these findings.

INTRODUCTION

Contrast-enhanced echocardiography is widely used to provide cardiac chamber opacification and to improve left ventricular (LV) endocardial border delineation in patients with known or suspected coronary artery disease [1], but data on the safety of contrast-enhanced echocardiography in patients in the first 24 hours after acute myocardial infarction are lacking. It is however particularly important in this subset of patients to have accurate information on LV function and LV dimensions, both for therapeutic and prognostic reasons. In this article, we report the experience on the safety of contrast-enhanced echocardiography with Perflutren (Luminity®, Bristol-Myers Squibb Pharma, Bruxelles, Belgium) performed the first day after acute myocardial infarction.

METHODS

Patient population

Over a 6 months period, a total of 115 consecutive patients admitted to the coronary care unit for ST-elevation acute myocardial infarction underwent urgent coronary angiography and primary percutaneous coronary intervention. Contrast-enhanced echocardiography was clinically performed in the coronary care unit within 24 hours from patients' admission to optimally evaluate LV dimensions, LV regional and global function and to exclude LV thrombus formation and mechanical complications of infarction.

Contrast-enhanced echocardiography

Patients were imaged in the left lateral decubitus position with a commercially available system (Vivid 7 Dimension, GE Healthcare, Horten, Norway) equipped with a M3S phased array transducer (3.5 MHz). Luminity® was used as contrast agent. Each patient received an infusion of 1.3 mL of echo contrast diluted in 50 mL of 0.9% NaCl solution through a 20 gauge intravenous catheter in a proximal forearm vein. Infusion rate was initially set at 4.0 mL/min and then titrated to achieve optimal LV cavity enhancement without attenuation artifacts [2]. Contrast-enhanced echocardiography was performed using harmonic imaging at low mechanical index (0.26). Images were obtained in the standard 4-, 2- and 3-chamber apical views and care was taken to record the images at a phase when the contrast agent flow was relatively stable with absent or minimal swirling in the apex. LV end-diastolic (EDV) and end-systolic (ESV) volumes were measured according to the Simpson's biplane method [3] and

LV ejection fraction was calculated as [(EDV-ESV)/EDV] x100. Qualitative assessment of the regional wall motion was performed according to the 16-segment model of the American Society of Echocardiography and the global wall motion score index was calculated for each patient [3]. The three LV apical views were also systematically checked for the presence of LV thrombi and mechanical complications of infarction.

Safety monitoring

The safety of contrast-enhanced echocardiography was assessed by evaluating the vital signs (blood pressure and heart rate), physical examination, ECG and occurrence of adverse events. Vital signs were assessed within 10 minutes before the administration of echo contrast and repeated after 2, 15, 30 and 60 minutes. Physical examination was performed before and after contrast-enhanced echocardiography and daily until discharge. Furthermore, during hospitalization, all patients had continuous 12-lead ECG monitoring for the occurrence of arrhythmias and ischemia and an additional standard single-lead ECG was monitored during the examination. All patients were evaluated for the occurrence of adverse events during echo contrast administration and the following days of hospitalization. The investigators characterized the intensity of potential adverse events.

Statistical analysis

Continuous variables are expressed as mean and standard deviation. Categorical data are presented as absolute numbers and percentages.

RESULTS

Patient population

Clinical characteristics of the patients are summarized in Table 1. Mean age of the patients was 58±11 years; 88 (77%) were male. The infarct-related artery was the left anterior descending coronary artery in 48 (42%) patients and obstructive multi-vessel disease (i.e. more than 1 vessel with a luminal narrowing ≥70%) was present in 39 (34%) patients.

Table 1. Clinical and echocardiographic characteristics of the patient population (n = 115).

Age (years)	**58±11**
Gender (male/female)	88/27
Diabetes, n (%)	10 (9)
Family history of coronary artery disease, n (%)	48 (42)
Hypercholesterolemia, n (%)	18 (16)
Hypertension, n (%)	40 (35)
Current or previous smoking, n (%)	73 (63)
Previous myocardial infarction, n (%)	11 (10)
Previous myocardial revascularization, n (%)	7 (6)
Body mass index (kg/m^2)	27±4
Anterior myocardial infarction, n (%)	47 (41)
Infarct-related artery, n (%)	
- left anterior descending coronary artery	48 (42)
- left circumflex coronary artery	16 (14)
- right coronary artery	51 (44)
Multi-vessel disease, n (%)	39 (34)
Left ventricular end-diastolic volume (mL)	97±25
Left ventricular end-systolic volume (mL)	54±19
Left ventricular ejection fraction (%)	44±11
- <35%, n (%)	24 (21)
- 35-45%, n (%)	40 (35)
- >45%, n (%)	51 (44)
Wall motion score index	1.9±0.4

Contrast-enhanced echocardiography

The mean infusion rate of echo contrast during echocardiography was 3.0±0.6 mL/min and the total infusion dose was on average 16 µL/kg. As shown in Table 1, the mean LV ejection fraction was 44±11%, with 64 (56%) patients having HAD a LV ejection fraction ≤45%. In all the patients, contrast-enhanced echocardiography excluded the presence of LV thrombi and mechanical complications of infarction, including 7 patients in whom an apical thrombus was suspected based on non-enhanced 2D echocardiography.

Safety monitoring

Administration of echo contrast did not induce any significant change in vital signs, physical examination and ECG. No death, acute myocardial infarction or other cardiovascular events occurred during the echocardiographic examination or the remaining hospitalization period. The only adverse events observed were transient hypersensitivity at the injection site (in 3 patients) and transient back pain (in 2 patients); all these adverse events were rated as mild in intensity and required no treatment.

DISCUSSION

Echocardiography is readily available, can be quickly performed at bedside and is frequently the primary test to evaluate LV size and function in patients with known or suspected coronary artery disease [3]. In patients with suboptimal acoustic windows, intravenous echo contrast is administered to improve endocardial border delineation and to increase accuracy and reproducibility of regional and global LV function assessment [4–6]. Contrast-enhanced echocardiography may be particularly important in patients presenting with acute myocardial infarction. Urgent and repeated echocardiographic examinations are indeed crucial in these patients, in order to evaluate regional and global LV function and to exclude LV thrombi and mechanical complications of infarction [7–9]. Contrast-enhanced echocardiography, providing more accurate and reproducible data, as compared to non-enhanced echocardiography, is therefore more reliable for the following therapeutic decision-making [10]. Moreover, potential alternative diagnostic imaging techniques (i.e. transesophageal echocardiography, radionuclide ventriculography and cardiac magnetic resonance) are more invasive or expensive [10].

Luminity® is a second-generation contrast agent that comprises a perfluoropropane microbubble coated with a particularly flexible bilipid shell [11]. This contrast agent has a microvascular rheology similar to that of the red blood cells, with a transient and hemodynamically insignificant microbubble entrapment in the pulmonary microcirculation [12]. Moreover, it does not require cellular uptake, and the fluorocarbon gas is filtered out by the lungs within minutes [12]. Preclinical and clinical studies demonstrated a high safety index of this echo contrast agent in animal models, healthy humans and patients with suspected cardiac disease [4,13]. Post-marketing surveillance data confirmed these results, with a very low reported risk of major events (1:10,000 risk of serious cardiopulmonary events and 1:500,000 risk of death) [14,15]. Although a clear relationship of these events with contrast injection has not been proven, non-immunoglobulin E-mediated or anaphylactoid reactions from local complement activation, as well as sudden increase of pulmonary artery pressure in patients with impaired pulmonary function, have been proposed as potential explanatory mechanisms [14].

Overall, the safety profile of Luminity® seems to be quite similar to that reported for another commercially available hexafluoride-based agent (SonoVue®, Bracco, Milan, Italy), but with a lower incidence of allergic reactions [11,16]. Hypersensitivity to the shell component polyethylene glycol, not present in Luminity®, could in part account for this difference [16].

Therefore, substantial safety data already exist for the use of Luminity® in stable patients with known or suspected cardiac disease [4,17], but safety data on its use in patients within 24 hours of acute myocardial infarction are lacking. In the current clinical report, administration of Luminity® shortly after acute myocardial infarction (within 24 hours) was safe and well tolerated, even in the presence of LV dysfunction. No significant changes in vital signs, physical examination and ECG were observed, while possible transient increase of serum cardiac biomarkers indicating micro-damage to cardiomyocytes could not be detected due to the

confounding effect of the recent acute myocardial infarction. No major adverse events were observed and minor adverse events occurred in 4% of patients and were mild in intensity and required no treatment. These findings were quite similar to that reported by previous clinical studies (minor events in 6.8% of 1558 patients) [17]. In particular, in the present case series no patient referred headache (the most common side effect of Luminity®), while 3 and 2 patients, respectively, complained hypersensitivity at the injection site and transient back pain.

CONCLUSIONS

Current data provide evidence on the safety of using Luminity® in the acute phase of myocardial infarction, even if these findings need further confirmation in larger cohorts of patients. In this specific clinical setting, the risk/benefit ratio associated to the use of this echo contrast agent seems to be particularly favorable, considering the provided advantages for the diagnostic process and the therapeutic management.

REFERENCES

1. Kaufmann BA, Wei K, Lindner JR. Contrast echocardiography. *Curr Probl Cardiol.* 2007;32:51-96.
2. Weissman NJ, Cohen MC, Hack TC, Gillam LD, Cohen JL, Kitzman DW. Infusion versus bolus contrast echocardiography: a multicenter, open-label, crossover trial. *Am Heart J.* 2000;139:399-404.
3. Schiller NB, Shah PM, Crawford M et al. Recommendations for quantitation of the left ventricle by two-dimensional echocardiography. American Society of Echocardiography Committee on Standards, Subcommittee on Quantitation of Two-Dimensional Echocardiograms. *J Am Soc Echocardiogr.* 1989;2:358-367.
4. Kitzman DW, Goldman ME, Gillam LD, Cohen JL, Aurigemma GP, Gottdiener JS. Efficacy and safety of the novel ultrasound contrast agent perflutren (definity) in patients with suboptimal baseline left ventricular echocardiographic images. *Am J Cardiol.* 2000;86:669-674.
5. Malm S, Frigstad S, Sagberg E, Larsson H, Skjaerpe T. Accurate and reproducible measurement of left ventricular volume and ejection fraction by contrast echocardiography: a comparison with magnetic resonance imaging. *J Am Coll Cardiol.* 2004;44:1030-1035.
6. Hoffmann R, von Bardeleben S, Kasprzak JD et al. Analysis of regional left ventricular function by cineventriculography, cardiac magnetic resonance imaging, and unenhanced and contrast-enhanced echocardiography: a multicenter comparison of methods. *J Am Coll Cardiol.* 2006;47:121-128.
7. Galema TW, Geleijnse ML, Yap SC et al. Assessment of left ventricular ejection fraction after myocardial infarction using contrast echocardiography. *Eur J Echocardiogr.* 2008;9.250-254.
8. Mansencal N, Nasr IA, Pilliere R et al. Usefulness of contrast echocardiography for assessment of left ventricular thrombus after acute myocardial infarction. *Am J Cardiol.* 2007;99:1667-1670.
9. Grayburn PA. Product safety compromises patient safety (an unjustified black box warning on ultrasound contrast agents by the Food and Drug Administration). *Am J Cardiol.* 2008;101:892-893.
10. Olszewski R, Timperley J, Szmigielski C et al. The clinical applications of contrast echocardiography. *Eur J Echocardiogr.* 2007;8:S13-S23.
11. Bouakaz A, de JN. WFUMB Safety Symposium on Echo-Contrast Agents: nature and types of ultrasound contrast agents. *Ultrasound Med Biol.* 2007;33:187-196.
12. Lindner JR, Song J, Jayaweera AR, Sklenar J, Kaul S. Microvascular rheology of Definity microbubbles after intra-arterial and intravenous administration. *J Am Soc Echocardiogr.* 2002;15:396-403.
13. Fritz TA, Unger EC, Sutherland G, Sahn D. Phase I clinical trials of MRX-115. A new ultrasound contrast agent. *Invest Radiol.* 1997;32:735-740.
14. Douglas PS, Weyman AE, Lindner JR, Wei K. Contrast echocardiography: past, present, and... future? *J Am Coll Cardiol Img.* 2008;1:107-110.
15. Main ML, Goldman JH, Grayburn PA. Thinking Outside the "Box" - The Ultrasound Contrast Controversy. *J Am Coll Cardiol.* 2007;50:2434-2437.
16. Van Camp G, Droogmans S, Cosyns B. Bio-effects of ultrasound contrast agents in daily clinical practice: fact or fiction? *Eur Heart J.* 2007;28:1190-1192.
17. European Medicines Agency (EMEA). European public assessment reports for authorised medicinal products for human use - Luminity scientific discussion. http://www.emea.europa.eu/humandocs/PDFs/EPAR/luminity/065406en6.pdf . 2006.

CHAPTER 12

Real-time 3-dimensional echocardiography early after acute myocardial infarction: incremental value of echo-contrast for assessment of left ventricular function

G Nucifora, **N Ajmone Marsan**, E R Holman, HM J Siebelink, J M van Werkhoven, A J Scholte, E E van der Wall, M J Schalij, and J J Bax

Am Heart J 2009;157:882.e1-8.

ABSTRACT

Objectives: Accurate and reproducible assessment of left ventricular (LV) systolic function is important in patients with acute myocardial infarction (AMI). Real time three-dimensional echocardiography (RT3DE) is an accurate technique, but it relies heavily on good image quality. Aim of the present study was to evaluate the incremental value of contrast-enhanced RT3DE.

Methods: A total of 140 consecutive patients (58±11 years; 78% men) with ST-elevation AMI clinically underwent non-enhanced and contrast-enhanced RT3DE within 24 hours from AMI to evaluate global and regional LV systolic function. Endocardial border definition was graded for each of the 16 LV segments as: 0 = border invisible; 1 = border visualized only partially and 2 = complete visualization of the border. Three image quality groups (good, fair and uninterpretable) were identified. LV volumes and ejection fraction were measured off-line. Wall motion was graded for each visible segment as: 1 = normal; 2 = hypokinetic; 3 = akinetic and 4 = dyskinetic.

Results: During contrast-enhanced RT3DE, as compared to non-enhanced RT3DE, the number of segments with complete visualization of the endocardial border increased from 66% to 84% ($p < 0.001$) and the number of patients with a good quality echocardiogram increased from 59% to 94% ($p < 0.001$). Intra- and inter-observer agreement for assessment of global and regional LV systolic function improved during contrast-enhanced RT3DE, as compared to non-enhanced RT3DE.

Conclusions: Assessment of LV systolic function in AMI patients with RT3DE is frequently hampered by suboptimal echocardiographic quality. Contrast-enhanced RT3DE is of incremental value, improving the endocardial border visualization and the reproducibility of LV function assessment.

INTRODUCTION

The assessment of global and regional left ventricular (LV) systolic function is extremely important among patients with acute myocardial infarction (AMI), since it carries significant therapeutic and prognostic implications [1–6]. Recently, real time three-dimensional echocardiography (RT3DE) has been introduced for assessment of LV function and volumes. RT3DE has been validated against magnetic resonance imaging and found to be more accurate and reproducible as compared to two-dimensional echocardiography (2DE) [7–13]. However, even more than 2DE, RT3DE relies heavily on the presence of good image quality [14;15].

The use of intravenous contrast agents during 2DE has been shown to be of incremental value, improving LV endocardial border visualization among patients with suboptimal image quality and increasing the accuracy and reproducibility of LV systolic function measurements [16–22]. In contrast, data regarding the use of echo contrast during RT3DE are scarce [14;23–25]. In particular, no specific data exist about the efficacy of contrast-enhanced RT3DE performed early after AMI; the safety of contrast-enhanced echocardiography early after AMI was reported recently with 2DE [26]. Aim of the present study was therefore to investigate, in a large cohort of consecutive patients with AMI, the potential incremental value of contrast-enhanced RT3DE over non-enhanced RT3DE for assessment of LV function and volumes.

METHODS

Patient population

The patient population consisted of 140 patients admitted to the coronary care unit because of ST-elevation AMI.The diagnosis of ST-elevation AMI was made on the basis of typical ECG changes and/or ischemic chest pain associated with elevation of cardiac biomarkers [27].

All patients underwent immediate coronary angiography and primary percutaneous coronary intervention. As part of the clinical work-up, RT3DE (with echo contrast) was performed in the coronary care unit within 24 hours from patients' admission to accurately evaluate global and regional LV systolic function.

Echocardiography

Patients were imaged in left lateral decubitus position with a commercially available system (Vivid 7, GE Healthcare, Horten, Norway) equipped with a 3V phased array transducer (2.5 MHz). First, apical full volume 3D data sets were acquired in harmonic mode, integrating,

during a brief breath-hold, 8 R-wave-triggered sub-volumes into a larger pyramidal volume (90° by 90°) with a complete capture of the LV. Thereafter, the same acquisition was repeated during echo contrast administration (Luminity®, Bristol-Myers Squibb Pharma, Bruxelles, Belgium) to optimize LV border delineation. Each patient received an intravenous infusion of 1.3 ml of echo contrast diluted in 50 ml of 0.9% NaCl solution; the rate of infusion was initially set at 4.0 ml/min and then titrated to achieve optimal LV chamber opacification and endocardial border delineation [28]. Contrast-enhanced RT3DE was performed in harmonic mode at low mechanical index (0.26), and care was taken to record the images at a phase when echo contrast flow was relatively stable with absent or minimal swirling in the apex. The 3D data sets were digitally stored for the off-line analysis.

Echocardiographic analysis

The 3D data sets were analyzed on-line for the analysis of LV chamber opacification and off-line for the analysis of LV endocardial border definition and LV volumes and function. The off-line analysis was performed using a dedicated software (4D LV-Analysis©; TomTec, Munich, Germany) by an observer who had no knowledge of the patient's identity, medical history and symptom status. As described elsewhere [29], the software automatically displays in a quad-screen the 4-chamber view, as a reference view, the 2- and 3- chamber views with default interplane angles at 60 degrees and a short-axis view (Figure 1). The interplane angles can be manually modified in order to obtain adequate orientation of the 3 apical views and their meeting point can be adjusted in the middle of the LV cavity in order to avoid LV foreshortening. This procedure can also be used to evaluate regions between the 3 adjacent conventional apical views.

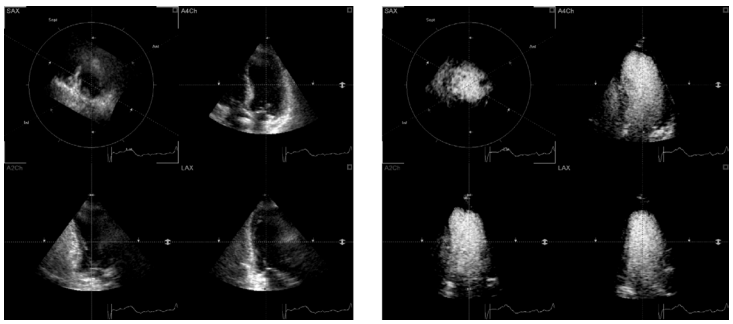


Figure 1. Left panel. Example of fair quality echocardiogram during non-enhanced RT3DE. **Right panel.** Optimal left ventricular chamber opacification and improved endocardial border definition during contrast-enhanced RT3DE in the same patient. The 3 apical views are shown with the 4-chamber as a reference view in the top right and the 2- and 3-chamber views in the bottom left and bottom right, respectively. Top left: short-axis view.

LV chamber opacification

The degree of LV chamber opacification during echo contrast administration was graded according to 5 points rating scale [17;28]: 0 = no contrast enhancement; 1 = weak or little contrast enhancement; 2 = adequate contrast enhancement that facilitates image interpretation; 3 = full contrast enhancement that definitely aids image interpretation; 4 = excessive contrast enhancement that hampers interpretation. The percentage of patients with adequate-to-full contrast enhancement was calculated. The mean time needed to achieve adequate-to-full contrast enhancement was measured.

LV endocardial border definition

Qualitative assessment of the endocardial border was performed both in non-enhanced and contrast-enhanced images. A standard 16-segment model was used [30]. Adequacy of LV endocardial border definition was graded for each of the 16 cardiac segments as follows [22]: 0 = border invisible; 1 = border visualized only partially throughout the cardiac cycle and/or incomplete segment length, and 2 = complete visualization of the border. A global endocardial visualization score was calculated as the sum of each LV segment's score.

On basis of the global score, 3 image quality groups were defined: good (score 25-32), fair (score 17-24) and uninterpretable (score ≤16) [15;22]. Uninterpretable echocardiograms were deemed non-diagnostic and further analyses of LV volumes and global and regional LV functions were considered not feasible.

LV volumes and global systolic function

The algorithm used by the software to calculate LV end-diastolic volume (EDV), LV end-systolic volume (ESV) and LVEF is described in detail elsewhere [29]. Briefly, the endocardial border is manually traced in the 3 apical views (including LV trabeculations and papillary muscles within the cavity) in both the end-diastolic and end-systolic frames. Subsequently, the software automatically identifies the endocardial border in the entire 3D dataset; further manual adjustments are possible in approximately 30 coronal and sagittal planes. Finally, a reconstruction of the LV model is generated and LV volumes and LVEF are obtained.

LV regional function

Qualitative assessment of the regional wall motion was performed both in non-enhanced and contrast-enhanced images, according to the same 16-segment model used for the evaluation of LV endocardial border definition [30]. Segments with invisible endocardial border were excluded from this analysis. Wall motion was graded for each of the visualized segments as follows: 1 = normal; 2 = hypokinetic; 3 = akinetic and 4 = dyskinetic. A global wall motion score index (WMSI) was calculated as the sum of each LV segment's score divided by the number of visualized segments.

Reproducibility of RT3DE measurements

The datasets of 20 patients with a good quality echocardiogram and 20 patients with a fair quality echocardiogram during non-enhanced RT3DE were randomly selected and analyzed again 1 month later by the original observer and by a second observer who was blinded to the results of the previous analysis. Intra- and inter-observer agreement was assessed for the measurements of LV volumes and LVEF and the grading of regional wall motion.

Statistical analysis

Continues variables are expressed as mean and standard deviation. Categorical data are presented as absolute numbers and percentages.

The global endocardial visualization score and the measurements of LV volumes, LVEF and WMSI were compared between the 2 imaging techniques with the paired *t*-test. To determine whether there was a statistically significant difference in the comparison between categorical variables, the McNemar test was performed for binary data and the marginal homogeneity test for multinomial response data. Intra- and inter-observer agreement in the measurements of LV volumes and LVEF were assessed using Bland-Altman analysis and expressed as the mean difference between the 2 measurements ±2 standard deviations. To evaluate intra- and inter-observer agreement in the grading of regional wall motion, weighted Kappa test was used and the level of agreement was interpreted as follows: 0 to 0.2 = poor to slight; 0.21 to 0.4 = fair; 0.41 to 0.6 = moderate; 0.61 to 0.8 = substantial; and 0.81 to 1.0 = nearly perfect. A p-value <0.05 was considered statistically significant. Statistical analysis was performed using the SPSS software package (SPSS 15.0, Chicago, Illinois).

RESULTS

Patient population

Baseline characteristics of the patient population are summarized in Table 1. Mean age of the patients was 58±11 years; 109 (78%) were male. Fifteen (11%) patients had a history of myocardial infarction and 12 (9%) had previous surgical or percutaneous myocardial revascularization. The infarct-related artery was the left anterior descending coronary artery in 60 (43%) patients, the left circumflex coronary artery in 19 (13%) and the right coronary artery in 61 (44%). Obstructive multi-vessel disease (i.e. more than 1 vessel with a luminal narrowing ≥70%) was present in 51 (36%) patients.

Table 1. Clinical and echocardiographic patient characteristics (n = 140).

Age (years)	**58±11**
Gender (male/female)	109/31
Diabetes	16 (11%)
Family history of coronary artery disease	54 (39%)
Hypercholesterolemia	26 (19%)
Hypertension	50 (36%)
Current or previous smoking	85 (61%)
Previous myocardial infarction	15 (11%)
Previous myocardial revascularization	12 (9%)
Body mass index (kg/m^2)	27±4
Current anterior myocardial infarction	60 (43%)
Current infarct-related artery	
- left anterior descending coronary artery	60 (43%)
- left circumflex coronary artery	19 (13%)
- right coronary artery	61 (44%)
Multi-vessel coronary artery disease	51 (36%)

Echocardiography

The mean infusion rate of echo contrast was 3.0±0.6 ml/min and the total infusion dose was on average 16 µl/kg.

LV chamber opacification

Adequate-to-full enhancement during echo contrast infusion was noted in 130 (93%) patients. Weak or little contrast enhancement was observed in 9 (6%) patients and excessive

contrast enhancement in 1 (1%) patient. The mean time needed to achieve adequate-to-full LV contrast enhancement was 65±20 sec.

LV endocardial border definition

During non-enhanced RT3DE, from the total number of 2240 LV segments, the endocardial border was invisible in 243 (11%) and visualized only partially in 509 (23%). A complete visualization of the border was possible in 1488 (66%) segments (Table 2). The mean global endocardial visualization score was 25±6. A total of 82 (59%) patients had a good quality echocardiogram, while 44 (31%) and 14 (10%) had a fair quality and uninterpretable echocardiogram, respectively (Figure 2).

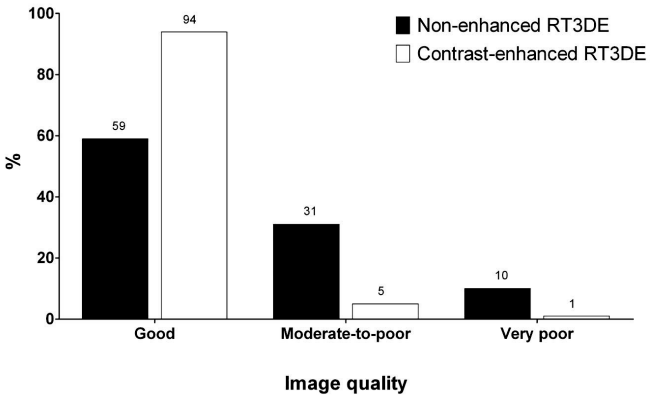


Figure 2. Image quality during non-enhanced and contrast-enhanced RT3DE.
p <0.001 for comparison between the 2 imaging techniques.

During contrast-enhanced RT3DE, a complete visualization of the border was possible in 1890 (84%) segments (p <0.001 as compared to non enhanced RT3DE) (Table 2). The LV endocardial border definition significantly improved in the segments of each LV wall (Table 2). As compared to non-enhanced RT3DE, the mean global endocardial visualization score improved to 29±3 (p <0.001). A total of 131 (94%) patients had a good quality echocardiogram, while 7 (5%) and 2 (1%) had a fair quality and uninterpretable echocardiogram, respectively (p <0.001 in comparison to non-enhanced RT3DE) (Figure 2).

An example of LV chamber opacification and improved endocardial border definition during contrast-enhanced RT3DE, as compared to non-enhanced RT3DE is displayed in Figure 1.

Table 2. Left ventricular endocardial border definition with non-enhanced and contrast-enhanced RT3DE.

	Non-enhanced RT3DE	Contrast-enhanced RT3DE	p-value
Overall segments (n = 2240)			<0.001
- border invisible	243 (11%)	16 (1%)	
- border visualized only partially	509 (23%)	334 (15%)	
- complete visualization of the border	1488 (66%)	1890 (84%)	
Anterior wall segments (n = 420)			<0.001
- border invisible	118 (28%)	4 (1%)	
- border visualized only partially	145 (35%)	139 (33%)	
- complete visualization of the border	157 (37%)	277 (66%)	
Antero-lateral wall segments (n = 420)			<0.001
- border invisible	40 (10%)	1 (0%)	
- border visualized only partially	151 (36%)	46 (11%)	
- complete visualization of the border	229 (54%)	373 (89%)	
Anterior septum segments (n = 280)			<0.001
- border invisible	55 (20%)	5 (2%)	
- border visualized only partially	64 (23%)	57 (20%)	
- complete visualization of the border	161 (57%)	218 (78%)	
Inferior wall segments (n = 420)			0.04
- border invisible	13 (3%)	2 (1%)	
- border visualized only partially	52 (12%)	52 (12%)	
- complete visualization of the border	355 (85%)	366 (87%)	
Infero-lateral wall segments (n = 280)			<0.001
- border invisible	7 (2%)	2 (1%)	
- border visualized only partially	67 (24%)	29 (10%)	
- complete visualization of the border	206 (74%)	249 (89%)	
Inferior septum segments (n = 420)			<0.001
- border invisible	10 (2%)	2 (1%)	
- border visualized only partially	30 (7%)	11 (2%)	
- complete visualization of the border	380 (91%)	407 (97%)	

RT3DE: real-time three-dimensional echocardiography.

LV volumes and global systolic function

Non-enhanced RT3DE provided significantly lower values of LVEDV as compared to contrast-enhanced RT3DE (107±28 ml vs.113±27 ml, p <0.001). The values of LVESV were not statistically different between the 2 techniques (59±21 ml vs. 61±20 ml, p = ns). Accordingly, non-enhanced RT3DE provided slightly, but significantly lower values of LVEF (45±9% vs. 47±9%, p = 0.003).

LV regional systolic function

WMSI assessed on non-enhanced and contrast-enhanced images were 1.8±0.4 and 1.7±0.4, respectively (p = 0.04).

Reproducibility of RT3DE measurements

Intra- and inter-observer agreement for the measurements of LV volumes, LVEF and the grading of regional wall motion obtained with the 2 techniques are shown in Tables 3 and 4. The weakest agreements were observed among patients with a fair quality echocardiogram. Contrast-enhanced RT3DE improved intra- and inter-observer agreement both in good and fair echocardiograms.

Table 3. Intra- and inter-observer agreements for the measurements of left ventricular volumes and left ventricular global function, in relation to image quality during non-enhanced RT3DE.

	Good quality echocardiogram during non-enhanced RT3DE		**Fair quality echocardiogram during non-enhanced RT3DE**	
Intra-observer agreement				
	Non-enhanced	Contrast-enhanced	Non-enhanced	Contrast-enhanced
LVEDV	-1.5±28.0	-0.7±6.8	-4.5±42	4.0±12.8
LVESV	-1.0±17.0	0.2±5.4	-2.7±24.8	3.1±5.6
LVEF	-0.1±10.0	-0.4±4.6	1.7±14.8	-0.8±5.0
Inter-observer agreement				
	Non-enhanced	Contrast-enhanced	Non-enhanced	Contrast-enhanced
LVEDV	-6.1±36.2	-0.6±13.8	-6.6±44.2	4.8±17.4
LVESV	-4.2±20.2	0.5±9.2	-6.4±36.2	3.8±12.6
LVEF	1.0±12.8	-0.7±7.4	2.2±22.4	-1.4±8.8

Intra- and inter-observer agreements for the measurements of LV volumes and LVEF were assessed using the method proposed by Bland and Altman and expressed as the mean difference between the 2 measurements±2 standard deviations. EDV: end-diastolic volume; EF: ejection fraction; ESV: end-systolic volume; LV: left ventricle; RT3DE: real-time three-dimensional echocardiography.

Table 4. Intra- and inter-observer agreements for the grading of left ventricular regional wall motion, in relation to image quality during non-enhanced RT3DE.

	Good quality echocardiogram during non-enhanced RT3DE		**Fair quality echocardiogram during non-enhanced RT3DE**	
Intra-observer agreement				
	Non-enhanced	Contrast-enhanced	Non-enhanced	Contrast-enhanced
LV RWM	0.77	0.95	0.69	0.92
Inter-observer agreement				
	Non-enhanced	Contrast-enhanced	Non-enhanced	Contrast-enhanced
LV RWM	0.65	0.87	0.54	0.85

Intra- and inter-observer agreements for the grading of LV RWM were assessed using the weighted Kappa test and expressed as weighted Kappa value. LV: left ventricle; RT3DE: real-time three-dimensional echocardiography: RWM: regional wall motion.

DISCUSSION

The current results show that, among unselected patients in the early stage of AMI, contrast-enhanced RT3DE has a high feasibility (93%), and is of incremental value for the assessment of LV systolic function. Specifically, as compared to non-enhanced RT3DE, 1) it significantly increased the number of LV segments with a complete visualization of the endocardial border (from 66% to 84%); 2) it increased the number of good quality echocardiograms (from 59% to 94%); and 3) it reduced the number of fair quality and uninterpretable echocardiograms (from 41% to 6%). Moreover, intra- and inter-observer agreement for the measurements of global and regional LV systolic function improved during contrast-enhanced RT3DE, particularly among patients with fair quality echocardiogram during non-enhanced RT3DE.

Advantages and limitations of RT3DE

The most commonly used imaging modality for the evaluation of global and regional LV systolic function is 2DE. However, 2DE relies on significant geometric assumptions, resulting in modest agreement with reference methods and fair reproducibility [17;31].

More recently, RT3DE has been proposed to overcome the above mentioned limitations of 2DE; RT3DE correlated well with magnetic resonance imaging for assessment of LV volumes and LV ejection fraction [8–11]. In addition, it has been suggested that RT3DE has potential advantages for the evaluation of regional LV function in regions/planes that could not be adequately visualized with 2DE [7;13].

Because of its higher accuracy and reproducibility, RT3DE could be extremely useful for serial assessment of systolic function [32]. RT3DE would be particularly useful in AMI patients, in whom accurate assessment of LV function and volumes is important for prediction of future adverse events [2;3].

However, RT3DE has still several limitations; particularly, RT3DE image quality is highly dependent on the acoustic window, due to a lower spatial and temporal resolution as compared to 2DE [11;24]. Accordingly, adequate endocardial border delineation may be difficult on RT3DE still frames, even in the presence of relatively good quality 2DE [33]. Due to this limitation, most of the previous RT3DE studies included only patients with an optimal acoustic window [8–10]. Few studies explored the feasibility of RT3DE, in relation to the image quality, for the assessment of LV systolic function in unselected population and reported a prevalence of uninterpretable or poor quality RT3DE images in the range of 35% [15;24]. This issue may be even more prominent in patients with AMI, in whom adequate assessment of LV function and volumes is important for prognosis, but in whom RT3DE data acquisition may be hampered by reduced patient mobility [12;34]. In the present study, 41% of 140 consecutive patients referred to RT3DE within 24 hours from AMI had a fair quality or uninterpretable echocardiogram. This

percentage is in line with previous studies [15;24] and may also be related to technical limitations associated to the performance of RT3DE in the coronary care unit, as well as the high body mass index of our study population.

Incremental value of contrast-enhanced RT3DE

In the subset of patients with inadequate RT3DE images, contrast agents could improve LV endocardial border visualization, increasing the feasibility, accuracy and reproducibility of LV function assessment as previously reported with 2DE [16–22].

Thus far, few small studies [14;23–25] (16, 20, 39 and 50 patients, respectively) previously assessed the accuracy of contrast-enhanced RT3DE, reporting a good agreement between contrast-enhanced RT3DE and magnetic resonance imaging for assessment of LV function and volumes. However, data regarding the feasibility of contrast-enhanced RT3DE and its incremental value over non-enhanced RT3DE (in terms of improved image quality) have not been shown. In the present study, we reported our experience on the feasibility and efficacy of contrast-enhanced RT3DE in a large, unselected cohort of patients in the early stage of AMI. Echo contrast infusion ensured optimal LV opacification in 93% of the patients. Moreover, the definition of the endocardial border significantly increased with the use of echo contrast, allowing more reliable and reproducible assessment of regional wall motion abnormalities. Of note, visualization of the anterior and anterolateral walls particularly improved with the use of echo contrast.

Overall, the prevalence of good quality echocardiograms increased from 59% to 94% with the intravenous contrast. The prevalence of fair image quality and uninterpretable echocardiograms decreased from 31% to 5% and from 10% to 1%, respectively.

Study limitations

The present study has some limitations that should be acknowledged. First, the semi-automated algorithm used for LV volume analysis requires manual tracing of the endocardial border in the 3 apical planes, which is a subjective procedure that could alter the reproducibility of the technique. Second, an independent gold standard (e.g. magnetic resonance imaging) was not performed and therefore data about accuracy of contrast-enhanced RT3DE could not be provided.

CONCLUSIONS

In patients with recent AMI, the use of echo contrast significantly improved the endocardial border visualization and the reproducibility of measurements of global and regional LV systolic function.

REFERENCES

1. Nishimura RA, Reeder GS, Miller FA, Jr. et al. Prognostic value of predischarge 2-dimensional echocardiogram after acute myocardial infarction. *Am J Cardiol* 1984;53:429-432.
2. Serruys PW, Simoons ML, Suryapranata H et al. Preservation of global and regional left ventricular function after early thrombolysis in acute myocardial infarction. *J Am Coll Cardiol* 1986;7:729-742.
3. White HD, Norris RM, Brown MA, Brandt PW, Whitlock RM, Wild CJ. Left ventricular end-systolic volume as the major determinant of survival after recovery from myocardial infarction. *Circulation* 1987;76:44-51.
4. Berning J, Steensgaard-Hansen F. Early estimation of risk by echocardiographic determination of wall motion index in an unselected population with acute myocardial infarction. *Am J Cardiol* 1990;65:567-576.
5. Volpi A, De Vita C, Franzosi MG et al. Determinants of 6-month mortality in survivors of myocardial infarction after thrombolysis. Results of the GISSI-2 data base. The Ad hoc Working Group of the Gruppo Italiano per lo Studio della Sopravvivenza nell'Infarto Miocardico (GISSI)-2 Data Base. *Circulation* 1993;88:416-429.
6. Oh JK, Gibbons RJ, Christian TF et al. Correlation of regional wall motion abnormalities detected by two-dimensional echocardiography with perfusion defect determined by technetium 99m sestamibi imaging in patients treated with reperfusion therapy during acute myocardial infarction. *Am Heart J* 1996;131:32-37.
7. Collins M, Hsieh A, Ohazama CJ et al. Assessment of regional wall motion abnormalities with real-time 3-dimensional echocardiography. *J Am Soc Echocardiogr* 1999;12:7-14.
8. Jenkins C, Bricknell K, Hanekom L, Marwick TH. Reproducibility and accuracy of echocardiographic measurements of left ventricular parameters using real-time three-dimensional echocardiography. *J Am Coll Cardiol* 2004;44:878-886.
9. Sugeng L, Mor-Avi V, Weinert L et al. Quantitative assessment of left ventricular size and function: side-by-side comparison of real-time three-dimensional echocardiography and computed tomography with magnetic resonance reference. *Circulation* 2006;114:654-661.
10. Jenkins C, Bricknell K, Chan J, Hanekom L, Marwick TH. Comparison of two- and three-dimensional echocardiography with sequential magnetic resonance imaging for evaluating left ventricular volume and ejection fraction over time in patients with healed myocardial infarction. *Am J Cardiol* 2007;99:300-306.
11. Badano LP, Dall'Armellina E, Monaghan MJ et al. Real-time three-dimensional echocardiography: technological gadget or clinical tool? *J Cardiovasc Med (Hagerstown)* 2007;8:144-162.
12. Arruda-Olson AM, Bursi F, Gerber Y, May RH, Roger VL, Pellikka PA. Three-Dimensional Echocardiography for Evaluating Left Ventricular Function in Patients With ST Elevation Myocardial Infarction: A Pilot Study. *Mayo Clin Proc* 2008;83:372-373.
13. Jaochim Nesser H, Sugeng L, Corsi C et al. Volumetric analysis of regional left ventricular function with real-time three-dimensional echocardiography: validation by magnetic resonance and clinical utility testing. *Heart* 2007;93:572-578.
14. Corsi C, Coon P, Goonewardena S et al. Quantification of regional left ventricular wall motion from real-time 3-dimensional echocardiography in patients with poor acoustic windows: effects of contrast enhancement tested against cardiac magnetic resonance. *J Am Soc Echocardiogr* 2006;19:886-893.

15. Tighe DA, Rosetti M, Vinch CS et al. Influence of image quality on the accuracy of real time three-dimensional echocardiography to measure left ventricular volumes in unselected patients: a comparison with gated-SPECT imaging. *Echocardiography* 2007;24:1073-1080.
16. Hundley WG, Kizilbash AM, Afridi I, Franco F, Peshock RM, Grayburn PA. Administration of an intravenous perfluorocarbon contrast agent improves echocardiographic determination of left ventricular volumes and ejection fraction: comparison with cine magnetic resonance imaging. *J Am Coll Cardiol* 1998;32:1426-1432.
17. Kitzman DW, Goldman ME, Gillam LD, Cohen JL, Aurigemma GP, Gottdiener JS. Efficacy and safety of the novel ultrasound contrast agent perflutren (definity) in patients with suboptimal baseline left ventricular echocardiographic images. *Am J Cardiol* 2000;86:669-674.
18. Thomson HL, Basmadjian AJ, Rainbird AJ et al. Contrast echocardiography improves the accuracy and reproducibility of left ventricular remodeling measurements: a prospective, randomly assigned, blinded study. *J Am Coll Cardiol* 2001;38:867-875.
19. Malm S, Frigstad S, Sagberg E, Larsson H, Skjaerpe T. Accurate and reproducible measurement of left ventricular volume and ejection fraction by contrast echocardiography: a comparison with magnetic resonance imaging. *J Am Coll Cardiol* 2004;44:1030-1035.
20. Hoffmann R, von Bardeleben S, ten Cate F et al. Assessment of systolic left ventricular function: a multi-centre comparison of cineventriculography, cardiac magnetic resonance imaging, unenhanced and contrast-enhanced echocardiography. *Eur Heart J* 2005;26:607-616.
21. Hoffmann R, von Bardeleben S, Kasprzak JD et al. Analysis of regional left ventricular function by cineventriculography, cardiac magnetic resonance imaging, and unenhanced and contrast-enhanced echocardiography: a multicenter comparison of methods. *J Am Coll Cardiol* 2006;47:121-128.
22. Galema TW, Geleijnse ML, Yap SC et al. Assessment of left ventricular ejection fraction after myocardial infarction using contrast echocardiography. *Eur J Echocardiogr* 2008;9:250-254.
23. Caiani EG, Coon P, Corsi C et al. Dual triggering improves the accuracy of left ventricular volume measurements by contrast-enhanced real-time 3-dimensional echocardiography. *J Am Soc Echocardiogr* 2005;18:1292-1298.
24. Krenning BJ, Kirschbaum SW, Soliman OI et al. Comparison of contrast agent-enhanced versus non-contrast agent-enhanced real-time three-dimensional echocardiography for analysis of left ventricular systolic function. *Am J Cardiol* 2007;100:1485-1489.
25. Jenkins C, Moir S, Chan J, Rakhit D, Haluska B, Marwick TH. Left ventricular volume measurement with echocardiography: a comparison of left ventricular opacification, three-dimensional echocardiography, or both with magnetic resonance imaging. *Eur Heart J* 2008.
26. Nucifora G, Marsan NA, Siebelink HM et al. Safety of contrast-enhanced echocardiography within 24 h after acute myocardial infarction. *Eur J Echocardiogr* 2008;9:816-818.
27. Thygesen K, Alpert JS, White HD et al. Universal definition of myocardial infarction. *Circulation* 2007;116:2634-2653.
28. Weissman NJ, Cohen MC, Hack TC, Gillam LD, Cohen JL, Kitzman DW. Infusion versus bolus contrast echocardiography: a multicenter, open-label, crossover trial. *Am Heart J* 2000;139:399-404.
29. Soliman OI, Krenning BJ, Geleijnse ML et al. A comparison between QLAB and TomTec full volume reconstruction for real time three-dimensional echocardiographic quantification of left ventricular volumes. *Echocardiography* 2007;24:967-974.
30. Lang RM, Bierig M, Devereux RB et al. Recommendations for chamber quantification: a report from the American Society of Echocardiography's Guidelines and Standards Committee and the Chamber Quantification Writing Group, developed in conjunction with the European Association

of Echocardiography, a branch of the European Society of Cardiology. *J Am Soc Echocardiogr* 2005;18:1440-1463.

31. McGowan JH, Cleland JG. Reliability of reporting left ventricular systolic function by echocardiography: a systematic review of 3 methods. *Am Heart J* 2003;146:388-397.
32. Chan J, Jenkins C, Khafagi F, Du L, Marwick TH. What is the optimal clinical technique for measurement of left ventricular volume after myocardial infarction? A comparative study of 3-dimensional echocardiography, single photon emission computed tomography, and cardiac magnetic resonance imaging. *J Am Soc Echocardiogr* 2006;19:192-201.
33. Nemes A, Geleijnse ML, Krenning BJ et al. Usefulness of ultrasound contrast agent to improve image quality during real-time three-dimensional stress echocardiography. *Am J Cardiol* 2007;99:275-278.
34. Olszewski R, Timperley J, Szmigielski C et al. The clinical applications of contrast echocardiography. *Eur J Echocardiogr* 2007;8:S13-S23.

CHAPTER 13

Impact of left ventricular dyssynchrony early on left ventricular function after first acute myocardial infarction

G Nucifora, M Bertini, **N Ajmone Marsan**, V Delgado, A J Scholte, A CT Ng, J M van Werkhoven, HM J Siebelink, E R Holman, M J Schalij, E E van der Wall, and J J Bax

Am J Cardiol 2010;105:306-11.

ABSTRACT

Objectives: The impact of left ventricular (LV) dyssynchrony after acute myocardial infarction (AMI) on LV ejection fraction (EF) is unknown.

Methods: One hundred twenty-nine patients with a first ST-elevation AMI (58±11 years, 78% men) and QRS duration <120 ms were included. All patients underwent primary percutaneous coronary intervention. Real-time 3-dimensional echocardiography and myocardial contrast echocardiography were performed to assess LV function, LV dyssynchrony, and infarct size. LV dyssynchrony was defined as the standard deviation of the time to reach the minimum systolic volume for 16 LV segments, expressed in percent cardiac cycle (systolic dyssynchrony index [SDI]). Myocardial perfusion at myocardial contrast echocardiography was scored (1 = normal/homogenous; 2 = decreased/patchy; 3 = minimal/absent) using a 16-segment model; a myocardial perfusion index, expressing infarct size, was derived by summing segmental contrast scores and dividing by the number of segments.

Results: SDI in patients with AMI was 5.24±2.23% compared to 2.02±0.70% of controls (p <0.001). Patients with AMI and LVEF <45% had significantly higher SDI compared to patients with LVEF >45% (4.29±1.44 vs 6.95±2.40, p <0.001). At multivariate analysis, SDI was independently related to LVEF; in addition, the impact of SDI on LV systolic function was incremental to infarct size and anterior location of AMI (F change 16.9, p <0.001).

Conclusions: LV synchronicity is significantly impaired soon after AMI. LV dyssynchrony is related to LVEF and has an additional detrimental effect on LV function, beyond infarct size and the anterior location of AMI.

INTRODUCTION

Advances in echocardiographic techniques, i.e., tissue Doppler echocardiography, speckle-tracking echocardiography, and real-time 3-dimensional echocardiography (RT3DE) have recently demonstrated an impaired left ventricular (LV) synchronicity in patients with acute myocardial infarction (AMI) [1–3]. In the setting of chronic heart failure, LV dyssynchrony is a phenomenon extensively described and related to impaired LV systolic function and poor prognosis [4–8]. In the setting of AMI, however, it is unclear whether LV dyssynchrony is independently associated with LV ejection fraction (EF). Moreover, the detrimental effect of LV dyssynchrony on LV systolic function in addition to other variables remains unknown. Accordingly, the aim of the present study was twofold: (1) to assess the decrease in LV synchronicity after AMI (compared to normal values) and (2) to explore the relation between this decrease in LV synchronicity and LV systolic function. In particular, the effect of LV dyssynchrony on LVEF in addition to other variables was assessed.

METHODS

The population consisted of 159 consecutive patients admitted to the coronary care unit because of a first ST-segment elevation AMI. Patients with a QRS complex duration >120 ms were excluded from the study.

The diagnosis of AMI was made on the basis of typical ECG changes and/or ischemic chest pain associated with elevation of cardiac biomarkers [9]. All patients underwent immediate coronary angiography and primary percutaneous coronary intervention (PCI). The infarct-related artery was identified by the site of coronary occlusion during coronary angiography and ECG criteria. During PCI, the final TIMI (Thrombolysis In Myocardial Infarction) flow was assessed. In addition, the time from onset of symptoms to first balloon dilatation (symptoms-to-balloon time) was determined.

Using the ECGs acquired on admission and 1 h after PCI, the ST-segment resolution was assessed, as previously described [10]. The sum of ST-segment elevation was measured 60 ms after the J point in leads I, aVL, and V1 to V6 for anterior AMI and leads II, III, aVF, V5, and V6 for non-anterior AMI. The percentage of resolution of ST-segment elevation from before to after PCI was then calculated.

RT3DE was performed 48 hours after PCI to assess global LV systolic function and LV dyssynchrony; immediately after RT3DE, myocardial contrast echocardiography was performed to assess infarct size. These echocardiographic examinations are part of the routine, comprehensive assessment of patients presenting with AMI in our clinics.

In addition, 30 subjects without evidence of structural heart disease and without known risk factors for coronary artery disease, matched for age, gender and body surface area, who

underwent RT3DE, were included as a normal control group. These individuals were derived from the echo database and were clinically referred for echocardiographic evaluation because of atypical chest pain, palpitations or syncope without murmur.

To determine the impairment of LV synchronicity after AMI, the patient data were compared with the data from the normal controls. In addition, the relation between LV systolic function and other clinical and echocardiographic variables (including LV dyssynchrony, infarct size, and infarct location) was evaluated.

Patients were imaged in left lateral decubitus position with a commercially available system (Vivid 7, GE Healthcare, Horten, Norway) equipped with a 3V phased array transducer (2.5 MHz). Apical full volume 3D data sets were acquired in harmonic mode, integrating, during a brief breath-hold, 8 R-wave-triggered sub-volumes into a larger pyramidal volume (90° by 90°) with a complete capture of the LV. The 3D data sets were digitally stored for the off-line analysis.

Off-line analysis was performed by an observer who had no knowledge of the patient's identity and standard 2DE and MCE results. A dedicated software (4D LV-Analysis©; TomTec, Munich, Germany) was used. The algorithm used by the software to calculate LV end-diastolic volume, LV end-systolic volume and LVEF is described in detail elsewhere [11]. Briefly, a semi-automated method for the detection of the apical 4-chamber view and the 60° and 120° incremental views and for the tracing of the endocardial border in the entire 3D dataset (including LV trabeculations and papillary muscles within the LV volume) is used. Subsequently, a final reconstruction of the LV model is generated and LV volumes and LVEF are obtained. In addition, the same LV model was used for the assessment of LV dyssynchrony, as previously described [12]. Briefly, the

LV model was automatically divided in 16 pyramidal subvolumes (6 basal segments, 6 mid segments, and 4 apical segments) based around a nonfixed central point. For each volumetric segment, the time–volume curve for the entire cardiac cycle was derived and the time taken to reach the minimum systolic volume was calculated. The standard deviation of the time taken to reach the minimum systolic volume expressed as percent cardiac cycle (systolic dyssynchrony index [SDI]) was then calculated as a marker of global LV dyssynchrony [12].

Immediately after RT3DE, myocardial contrast echocardiography was performed to evaluate myocardial perfusion, to assess infarct size after AMI. The same ultrasound system equipped with a 3.5-MHz transducer was used. The 3 standard apical views were acquired using a low-power technique (mechanical index 0.10 to 0.26). Background gains were set so that minimal tissue signal was seen, and the focus was set at the level of the mitral valve. Luminity® (Bristol-Myers Squibb Pharma, Brussels, Belgium) was used as contrast agent. Each patient received an infusion of 1.3 mL of echo contrast diluted in 50 mL of 0.9% NaCl solution through a 20 gauge intravenous catheter in a proximal forearm vein. Infusion rate was initially set at 4.0 mL/min and then titrated to achieve optimal myocardial enhancement without attenuation artifacts [13]. Machine settings were optimized to obtain the best pos-

sible myocardial opacification with minimal attenuation. At least 15 cardiac cycles after high mechanical index (1.7) microbubble destruction [14] were stored in cine-loop format.

Analysis of myocardial contrast echocardiograms was performed off-line using EchoPAC version 7.0.0 (GE Healthcare, Horten, Norway). To evaluate myocardial perfusion, the LV was divided according to the same 16-segment model of the American Society of Echocardiography [15]. A semiquantitative scoring system was used to assess contrast intensity after microbubble destruction: 1) normal/homogenous opacification; 2) reduced/patchy opacification; 3) minimal or absent contrast opacification [14,16]. A myocardial perfusion index, expressing infarct size, was derived by adding contrast scores of all segments and dividing by the total number of segments [14,16].

Continues variables are expressed as mean±standard deviation, when normally distributed, and as median and interquartile range, when not normally distributed. Categorical data are presented as absolute numbers and percentages. Differences in continuous variables between control subjects and AMI patients were assessed using the Student *t* test or the Mann-Whitney *U* test, if appropriate. *Chi*-square test or Fisher exact test, if appropriate, were computed to assess differences in categorical variables. Univariate and multivariate linear regression analysis were performed to evaluate the relationship between LVEF in patients with AMI and the characteristics of age, gender, coronary risk factors, infarct location, multi-vessel disease, symptoms-to-balloon time, TIMI flow grade 3 after PCI, QRS duration, ST-segment resolution, peak troponin T, LV dyssynchrony (expressed as SDI) and infarct size (expressed as myocardial perfusion index) Only variables with p-value <0.1 at univariate analysis were entered as covariates in the multivariate model. To determine the potential incremental value of SDI over the other variables, the R^2 of the multivariate model was compared to the R^2 of the same model without SDI. A p-value <0.05 was considered statistically significant. Statistical analysis was performed using the SPSS software package (SPSS 15.0, Chicago, Illinois).

RESULTS

Reliable RT3DE and myocardial contrast echocardiographic data were obtained in 129 patients; consequently, 30 patients were excluded from further analysis. All control subjects had reliable RT3DE data.

Clinical and echocardiographic characteristics of AMI patients are listed in Table 1. A total of 60 (46%) patients had an anterior AMI; obstructive multi-vessel disease (i.e. > 1 vessel with a luminal narrowing ≥70%) was present in 46 (36%) patients.

As compared to control subjects, AMI patients had significantly lower LVEF (64±6% vs. 46±9%, p <0.001) and significantly higher SDI (2.02±0.70% vs. 5.24±2.23%, p <0.001). The observed impairment of LV synchronicity in AMI patients is shown in Figure 1.

Table 1. Clinical and echocardiographic characteristics of control subjects and patients with acute myocardial infarction (AMI)

	Control subjects (n = 30)	AMI patients (n = 129)	p- value
Age (years)	57±11	58±11	0.53
Male gender	23 (77%)	100 (78%)	0.92
Body surface area (m2)	1.96±0.58	1.98±0.22	0.76
Diabetes	-	14 (11%)	-
Family history of coronary artery disease*	-	49 (38%)	-
Hypercholesterolemia†	-	19 (15%)	-
Hypertension‡	-	47 (36%)	-
Current or previous smoking	-	76 (59%)	-
Anterior myocardial infarction	-	60 (46%)	-
Infarct-related artery			
- left anterior descending coronary artery	-	60 (46%)	-
- left circumflex coronary artery	-	22 (18%)	-
- right coronary artery	-	46 (36%)	-
Multi-vessel disease	-	46 (36%)	-
TIMI flow 3		109 (85%)	-
Symptoms-to-balloon time (min)	-	177 (134-219)	-
QRS duration	-	96±13	-
ST-segment resolution (%)	-	62±31	-
Peak troponin T (μg/l)	-	3.10 (1.52-6.89)	-
LVEDV (ml)	90±23	110±30	0.01
LVESV (ml)	35±14	60±23	<0.001
LVEF (%)	64±6	46±9	<0.001
SDI (%)	2.02±0.70	5.24±2.23	<0.001
MPI	-	1.25 (1.09-1.50)	-

EF: ejection fraction; EDV: end-diastolic volume; ESV: end-systolic volume; LV: left ventricular; MPI: myocardial perfusion index; SDI: systolic dyssynchrony index; TIMI: Thrombolysis In Myocardial Infarction. Data are expressed as mean±SD, median (interquartile range), or number of subjects (percentage).

* Defined when close relatives had premature coronary artery disease
(men <55 years old and women <65 years old).

† Defined as total cholesterol level ≥240 mg/dl.

‡ Defined as systolic blood pressure ≥140 mm Hg and/or diastolic blood pressure ≥90 mm Hg. Table 2. Clinical and echocardiographic characteristics of patients with acute myocardial infarction in relation to left ventricular systolic function.

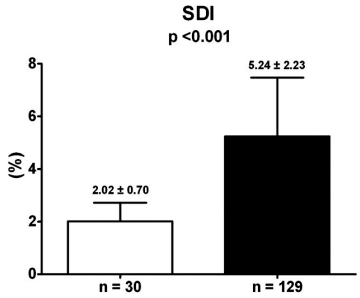


Figure 1. Systolic dyssynchrony index in control subjects (white bars) and acute myocardial infarction (AMI) patients (black bars) (p <0.001).

Table 2. Clinical and echocardiographic characteristics of patients with acute myocardial infarction in relation to left ventricular systolic function

Variable	LVEF ≥45%	LVEF <45%	p-value
	(n = 83)	(n = 46)	
Age (years)	57±11	60±11	0.090
Male gender	60 (72%)	40 (87%)	0.056
Diabetes	9 (11%)	5 (11%)	1.00
Family history of coronary artery disease	31 (37%)	18 (39%)	0.84
Hypercholesterolemia	12 (15%)	7 (15%)	0.91
Hypertension	35 (42%)	12 (26%)	0.069
Current or previous smoker	47 (57%)	29 (63%)	0.48
Anterior myocardial infarction	34 (41%)	26 (57%)	0.090
Multivessel-disease	24 (29%)	22 (48%)	0.032
TIMI flow 3	74 (89%)	35 (76%)	0.049
Symptoms-to-balloon time (min)	170 (127–215)	184 (150–231)	0.16
QRS duration (ms)	94±13	99±13	0.027
ST-segment resolution (%)	65±31	56±30	0.13
Peak troponin T (µg/l)	2.69 (1.23–5.39)	4.82 (1.85–1.02)	0.006
LVEDV (ml)	105±25	118±38	0.042
LVESV (ml)	51±14	75±28	<0.001
LVEF (%)	51±5	37±6	<0.001
SDI (%)	4.29±1.44	6.95±2.40	<0.001
MPI	1.19 (1.00–1.38)	1.56 (1.23–1.81)	<0.001

Abbreviations as in Table 1. Data are expressed as mean±SD, median (interquartile range), or number of subjects (percentage).

Patients with AMI were subdivided into 2 groups according to LV systolic function (LVEF ≥45%, n = 83; LVEF <45%, n = 46). Clinical and echocardiographic characteristics of these 2 groups are presented in Table 2. Patients with LVEF <45% had more frequently multivessel disease (p = 0.032), less frequently TIMI flow grade 3 after primary PCI (p = 0.049) and higher peak troponin T (p = 0.006) compared to patients with LVEF ≥45% (Table 2).

Regarding LV synchronicity, patients with LVEF <45% had significantly higher SDI (p <0.001) compared to patients with LVEF ≥45% (Table 2). Figure 2 shows the impairment of

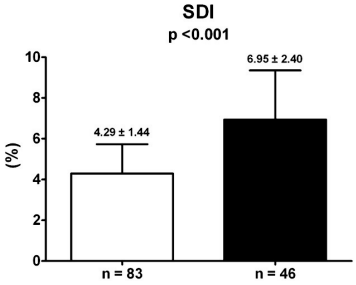


Figure 2. Systolic dyssynchrony index in patients with AMI in relation to LV systolic function, namely LVEF ≥45% (white bars) and LVEF <45% (black bars) (p <0.001).

LV synchronicity in patients with AMI and LVEF <45% compared to those with LVEF ≥45%. Indeed, a significant relation (r = 0.69, p <0.001) was noted between LVEF and SDI.

Table 3 shows the results of the univariate and multivariate linear regression analysis performed to determine the factors related to LV systolic function. At univariate analysis, several variables were significantly related to LVEF. However, at multivariate analysis, only anterior location of AMI (beta -0.16, p = 0.037), SDI (beta -0.52, p <0.001), and myocardial perfusion index (beta -0.28, p = 0.034) were independent factors associated with LVEF. Adding SDI to the multivariate model significantly increased R^2 from 0.45 to 0.52 (F change 16.9, p <0.001).

Figure 3 shows an example of a patient with severe impairment of LV systolic function and synchronicity after AMI.

Table 3. Univariate and multivariate linear regression analyses to determine the independent correlates of left ventricular systolic function in patients with acute myocardial infarction.

	Univariate		Multivariate	
	β	p-value	β	p-value
Age	-0.17	0.058	0.025	0.72
Male gender	-0.14	0.10	-	-
Diabetes	0.017	0.85	-	-
Family history of coronary artery disease	0.092	0.30	-	-
Hypercholesterolemia	-0.031	0.73	-	-
Hypertension	0.051	0.57	-	-
Current or previous smoker	-0.005	0.96	-	-
Anterior myocardial infarction	-019	0.036	-0.16	0.037
Multi-vessel disease	-0.19	0.032	-0.94	0.35
TIMI flow	0.15	0.092	0.001	0.99
Symptoms-to-balloon time	-0.077	0.38	-	-
QRS duration	-0.17	0.061	-0.0079	0.24
ST-segment resolution	0.21	0.015	0.028	0.69
Peak troponin T	-0.28	0.001	0.037	0.62
SDI	-0.69	<0.001	-0.52	<0.001
MPI	-0.65	<0.001	-0.28	0.034

The R2 of the model selected at multivariate analysis was 0.52.
Abbreviations as in Table 1.

DISCUSSION

The results of the present study show that LV synchronicity (assessed by RT3DE) is significantly impaired soon after AMI. The severity of this impairment is related to LV systolic function. In addition, the impact of SDI on LV systolic function was incremental to infarct size and anterior location of AMI.

The presence and clinical relevance of LV dyssynchrony in the setting of chronic heart failure has been extensively investigated in the previous decade; in this group of patients, loss of LV

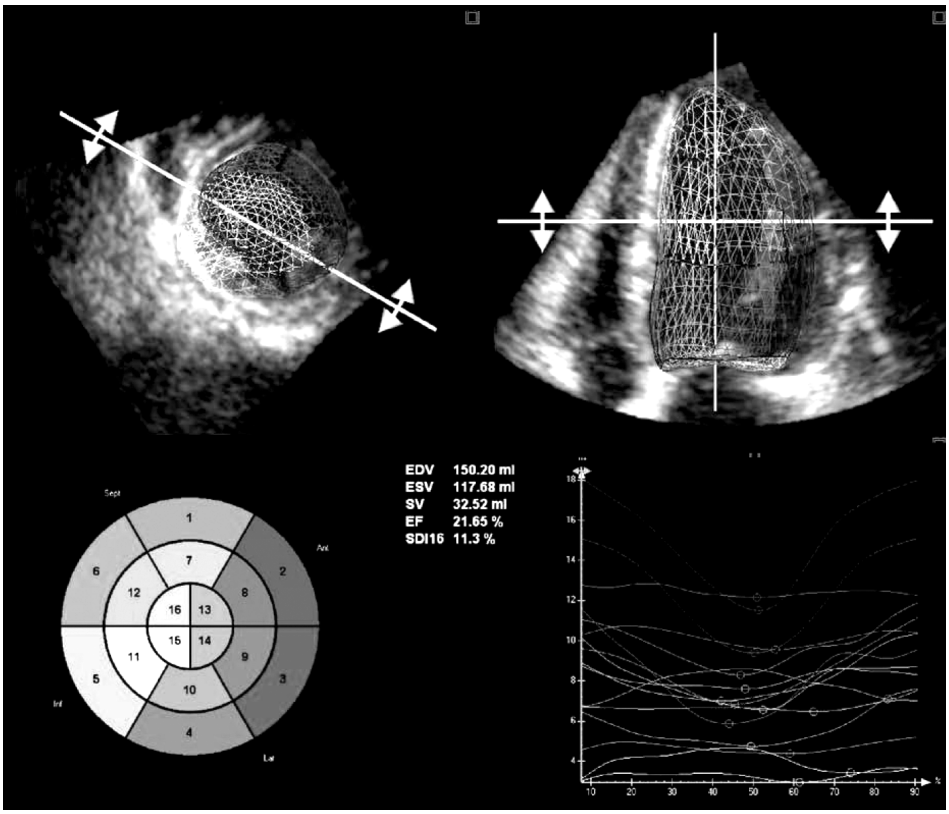


Figure 3. Example of a patient showing severe impairment of LV systolic function (LVEF 22%) and synchronicity (SDI 11.3%) after AMI.

synchronous contraction is related to impaired LV systolic function and poor hemodynamic status and is a predictor of worse outcome [4–8]. In addition, restoration of LV synchronicity, by cardiac resynchronization therapy, has been shown to reverse LV remodeling and to improve LV function and prognosis [17–19].

More recently, LV dyssynchrony has been described to occur also in patients with AMI [1–3,20]. However, the clinical meaning of this phenomenon has not been yet fully elucidated. In particular, it is unclear whether the presence of LV dyssynchrony after AMI independently influences LV function in these patients. Moreover, the detrimental effect of LV dyssynchrony in addition to other variables (e.g., infarct size and anterior location of AMI) on LV systolic function remains unknown.

In the present study, RT3DE was used to assess LV systolic function and LV synchronicity after AMI. This approach has been documented to provide highly accurate measurements of LVEF[21]; in addition, it is more robust than tissue Doppler echocardiography for the evaluation of LV dyssynchrony, being more reproducible and more consistent in differentiating healthy subjects from those affected by LV dyssynchrony [22]. Moreover, myocardial contrast

echocardiography was used to obtain information about myocardial perfusion abnormalities after AMI and, hence, infarct size [23].

In line with previous observations [1], impairment of LV synchronicity (expressed as SDI) was observed in patients with AMI compared to control subjects. In addition, LV dyssynchrony was significantly associated to LV systolic function. Importantly, this relation remained after adjustment for infarct size and anterior location of AMI, being incremental over these variables in determining LVEF. LV dyssynchrony results in a non-homogenous distribution of myocardial load and deformation and thus increases myocardial energy demand [24]; this may negatively influence the contractility of residual viable myocardium, thus further impairing LV function. The results of the present study suggest that LV dyssynchrony soon after AMI has an additional detrimental impact on LV performance, beyond the infarct size itself; moreover, it may potentially contribute to the vicious circle of progression of LV dysfunction [2]. In this perspective, therapeutic approaches aiming to recover a more synchronous LV contraction (e.g., with cardiac resynchronization therapy) may be beneficial and improve LV systolic function, thus preventing LV remodeling. However, further studies are needed to support this hypothesis.

REFERENCES

1. Zhang Y, Chan AK, Yu CM et al. Left ventricular systolic asynchrony after acute myocardial infarction in patients with narrow QRS complexes. *Am Heart J* 2005;149:497–503.
2. Mollema SA, Liem SS, Suffoletto MS et al. Left ventricular dyssynchrony acutely after myocardial infarction predicts left ventricular remodeling. *J Am Coll Cardiol* 2007;50:1532–1540.
3. Delgado V, Sitges M, Vidal B et al. Assessment of left ventricular dyssynchrony by real-time three-dimensional echocardiography. *Rev Esp Cardiol* 2008;61:825– 834.
4. Baldasseroni S, Opasich C, Gorini M et al. Left bundle-branch block is associated with increased 1-year sudden and total mortality rate in 5517 outpatients with congestive heart failure: a report from the Italian network on congestive heart failure. *Am Heart J* 2002;143:398–405.
5. Fauchier L, Marie O, Casset-Senon D, Babuty D, Cosnay P, Fauchier JP. Interventricular and intraventricular dyssynchrony in idiopathic dilated cardiomyopathy: a prognostic study with Fourier phase analysis of radionuclide angioscintigraphy. *J Am Coll Cardiol* 2002;40:2022–2030.
6. Yu CM, Lin H, Zhang Q, Sanderson JE. High prevalence of left ventricular systolic and diastolic asynchrony in patients with congestive heart failure and normal QRS duration. *Heart* 2003;89:54–60.
7. Bader H, Garrigue S, Lafitte S et al. Intra-left ventricular electromechanical asynchrony. A new independent predictor of severe cardiac events in heart failure patients. *J Am Coll Cardiol* 2004;43:248 –256.
8. Penicka M, Bartunek J, Lang O et al. Severe left ventricular dyssynchrony is associated with poor prognosis in patients with moderate systolic heart failure undergoing coronary artery bypass grafting. *J Am Coll Cardiol* 2007;50:1315–1323.
9. Thygesen K, Alpert JS, White HD et al. Universal definition of myocardial infarction. *Circulation* 2007;116:2634 –2653.
10. Nijveldt R, Beek AM, Hirsch A et al. Functional recovery after acute myocardial infarction: comparison between angiography, electrocar-diography, and cardiovascular magnetic resonance measures of microvascular injury. *J Am Coll Cardiol* 2008;52:181–189.
11. Soliman OI, Krenning BJ, Geleijnse ML et al. A comparison between QLAB and TomTec full volume reconstruction for real time three-dimensional echocardiographic quantification of left ventricular volumes. *Echocardiography* 2007;24:967–974.
12. Kapetanakis S, Kearney MT, Siva A, Gall N, Cooklin M, Monaghan MJ. Real-time three-dimensional echocardiography: a novel technique to quantify global left ventricular mechanical dyssynchrony. *Circulation* 2005;112:992–1000.
13. Weissman NJ, Cohen MC, Hack TC, Gillam LD, Cohen JL, Kitzman DW. Infusion versus bolus contrast echocardiography: a multicenter, open-label, crossover trial. *Am Heart J* 2000;139:399–404.
14. Dwivedi G, Janardhanan R, Hayat SA, Swinburn JM, Senior R. Prognostic value of myocardial viability detected by myocardial contrast echocardiography early after acute myocardial infarction. *J Am Coll Cardiol* 2007;50:327–334.
15. Lang RM, Bierig M, Devereux RB et al. Recommendations for chamber quantification: a report from the American Society of Echocardiography's Guidelines and Standards Committee and the Chamber Quantification Writing Group, developed in conjunction with the European Association of Echocardiography, a branch of the European Society of Cardiology. *J Am Soc Echocardiogr* 2005;18:1440 –1463.

16. Main ML, Magalski A, Kusnetzky LL, Morris BA, Jones PG. Usefulness of myocardial contrast echocardiography in predicting global left ventricular functional recovery after anterior wall acute myocardial infarction. *Am J Cardiol* 2004;94:340 –342.
17. Yu CM, Chau E, Sanderson JE et al. Tissue Doppler echocardiographic evidence of reverse remodeling and improved synchronicity by simultaneously delaying regional contraction after biventricular pacing therapy in heart failure. *Circulation* 2002;105:438–445.
18. Bleeker GB, Mollema SA, Holman ER et al. Left ventricular resynchronization is mandatory for response to cardiac resynchronization therapy: analysis in patients with echocardiographic evidence of left ventricular dyssynchrony at baseline. *Circulation* 2007;116:1440–1448.
19. Ypenburg C, van Bommel RJ, Borleffs CJ et al. Long-term prognosis after cardiac resynchronization therapy is related to the extent of left ventricular reverse remodeling at midterm follow-up. *J Am Coll Cardiol* 2009;53:483– 490.
20. Chang SA, Chang HJ, Choi SI et al. Usefulness of left ventricular dyssynchrony after acute myocardial infarction, assessed by a tagging magnetic resonance image derived metric, as a determinant of ventricular remodeling. *Am J Cardiol* 2009;104:19 –23.
21. Badano LP, Dall'Armellina E, Monaghan MJ et al. Real-time three-dimensional echocardiography: technological gadget or clinical tool? *J Cardiovasc Med* 2007;8:144–162.
22. Conca C, Faletra FF, Miyazaki C et al. Echocardiographic parameters of mechanical synchrony in healthy individuals. *Am J Cardiol* 2009;103:136 –142.
23. Hayat SA, Senior R. Myocardial contrast echocardiography in ST elevation myocardial infarction: ready for prime time? *Eur Heart J* 2008;29:299 –314.
24. Prinzen FW, Hunter WC, Wyman BT, McVeigh ER. Mapping of regional myocardial strain and work during ventricular pacing: experimental study using magnetic resonance imaging tagging. *J Am Coll Cardiol* 1999;33:1735–1742.

CHAPTER 14

Reduced left ventricular torsion early after myocardial infarction is related to left ventricular remodeling

G Nucifora, **N Ajmone Marsan**, M Bertini, V Delgado, HM J Siebelink, J M van Werkhoven, A J Scholte, M J Schalij, E E van der Wall, E R Holman, and J J Bax

C*irc Cardiovasc Imaging* 2010;3:433-42.

ABSTRACT

Objectives: Left ventricular (LV) torsion is emerging as a sensitive parameter of LV systolic myocardial performance. The aim of the present study was to explore the effects of acute myocardial infarction (AMI) on LV torsion, and to determine the value of LV torsion early after AMI in predicting LV remodeling at 6-month follow-up.

Methods: A total of 120 patients with a first ST-elevation AMI (59±10 years, 73% male) were included. All patients underwent primary percutaneous coronary intervention. After 48 hours, speckle tracking echocardiography was performed to assess LV torsion; infarct size was assessed by myocardial contrast echocardiography. At 6-month follow-up, LV volumes and LV ejection fraction were reassessed, in order to identity patients who developed LV remodeling (defined as ≥15% increase in LV end-systolic volume).

Results: As compared to control subjects, peak LV torsion in AMI patients was significantly impaired (1.54±0.64°/cm vs 2.07±0.27°/cm; p <0.001). At multivariate linear regression analysis, only LV ejection fraction (β = 0.36, p <0.001) and infarct size (β = -0.47, p <0.001), were independently associated with peak LV torsion. At 6-month follow-up, 19 patients showed LV remodeling. At multivariate logistic regression analysis, only peak LV torsion (OR = 0.77; 95% CI 0.65-0.92; p = 0.003) and infarct size (OR = 1.04; 95% CI, 1.01–1.07; p = 0.021) were independently related to LV remodeling. Peak LV torsion provided modest but significant incremental value over clinical, echocardiographic, and myocardial contrast echocardiography variables in predicting LV remodeling. By receiver-operating characteristic curve analysis, peak LV torsion ≤1.44°/cm provided the highest sensitivity (95%) and specificity (77%) to predict LV remodeling.

Conclusions: LV torsion is significantly impaired early after AMI. The amount of impairment of LV torsion predicts LV remodeling at 6-month follow-up.

INTRODUCTION

Remodeling of the left ventricle (LV) after acute myocardial infarction (AMI) is associated to the development of heart failure and to poor survival rate [1,2]. Accordingly, identification of patients prone to develop post-infarction LV remodeling represents an important issue in clinical cardiology. These considerations have stimulated the research of new parameters able to provide a quantitative and objective estimation of the myocardial damage post-AMI and to identify the patients at risk of LV remodeling [3].

The systolic twisting motion of the LV along its longitudinal axis, resulting from the opposite rotation of the LV apex compared to the base, is emerging as an important, sensitive parameter of LV systolic function [4]. Recently, echocardiographic assessment of LV rotational mechanics based on speckle-tracking analysis has been introduced and validated against sonomicrometry and magnetic resonance imaging [5,6]. In the clinical setting however, not much data on changes in LV torsion after AMI are available [7,8], and no specific data exist concerning the role of LV torsion in predicting post-infarction LV remodeling.

Accordingly, the aim of the present evaluation was twofold. First, we sought to determine the correlates of LV torsion after AMI, and second, we aimed to explore the relation between LV torsion and the development of LV remodeling at 6-month follow-up.

METHODS

Patient population and data collection

The population consisted of 146 consecutive patients admitted to the coronary care unit because of a first ST-segment elevation AMI. The diagnosis of AMI was made on the basis of typical ECG changes and/or ischemic chest pain associated with elevation of cardiac biomarkers [9]. All patients underwent immediate coronary angiography and primary percutaneous coronary intervention (PCI). The infarct-related artery was identified by the site of coronary occlusion during coronary angiography and ECG criteria. During PCI, final TIMI (Thrombolysis In Myocardial Infarction) flow was assessed.

Clinical evaluation included 2-dimensional echocardiography with speckle-tracking analysis to assess LV global longitudinal strain and torsion, and myocardial contrast echocardiography (MCE) was performed 48 hours after PCI to assess the extent of perfusion abnormalities and infarct size. At 6-month follow-up, 2-dimensional echocardiography was performed to re-assess LV volumes and LV ejection fraction (EF). These echocardiographic examinations are part of the routine, comprehensive assessment of AMI patients in our clinics.

In addition, 20 subjects without evidence of structural heart disease and without known risk factors for coronary artery disease, matched for age, gender and body surface area, who underwent 2-dimensional echocardiography, were included as a normal control group. These individuals were derived from the echo database and were clinically referred for echocardiographic evaluation because of atypical chest pain, palpitations or syncope without murmur.

To determine the reduction in LV torsion after AMI, the patient data were compared with the data from the normal controls. In addition, the independent correlates of LV torsion after AMI were investigated and the role of LV torsion in predicting LV remodeling (defined as ≥15% increase in LV end-systolic volume [ESV]) at 6-month follow-up was assessed [1,10].

Two-dimensional echocardiography

All AMI patients and control subjects were imaged in left lateral decubitus position with a commercially available system (Vivid 7 Dimension, GE Healthcare, Horten, Norway) equipped with a 3.5-MHz transducer. Standard 2-dimensional images and Doppler and color-Doppler data were acquired from the parasternal and apical views (4-, 2- and 3-chamber) and digitally stored in cine-loop format; analyses were subsequently performed offline using EchoPAC version 7.0.0 (GE Healthcare, Horten, Norway). LV end-diastolic volume (EDV) and LVESV were measured according to the Simpson's biplane method and LVEF was calculated as [(EDV-ESV)/EDV] x100 [11].

Qualitative assessment of regional wall motion was performed according to the 16-segment model of the American Society of Echocardiography and the global wall motion score index (WMSI) was calculated for each patient [11]. As previously described [12], transmitral and pulmonary vein pulsed-wave Doppler tracings were used to classify diastolic function as *1)* normal; *2)* diastolic dysfunction grade 1 (mild); *3)* diastolic dysfunction grade 2 (moderate); *4)* diastolic dysfunction grade 3 (severe); *5)* diastolic dysfunction grade 4 (severe).

Speckle-tracking analysis

Longitudinal strain analysis

Longitudinal strain analysis of the LV was performed by speckle-tracking imaging (EchoPAC version 7.0.0). Gray-scale 2D apical images of the LV (4-, 2-, and 3-chamber views) were used with a frame rate ranging from 60 to 100 frames per second. From an end-systolic frame, the endocardial border was manually traced, and the software automatically traces 2 more concentric regions of interest (ROIs) to include the entire myocardial wall. Speckle-tracking

analysis detects and tracks the unique myocardial ultrasound patterns frame by frame. The in-plane frame-to-frame displacement of each pattern over time is used to derive strain. The software automatically validates the segmental tracking throughout the cardiac cycle and allows the operator further adjustment of the ROI to improve tracking quality. As previously described [13], GLS was calculated, as an index of global LV systolic function, by averaging the GLSs obtained automatically from each apical view.

Torsional mechanics analysis

Speckle tracking analysis was applied to evaluate LV basal and apical rotations, LV twist and LV torsion. Parasternal short-axis images of the LV were acquired at 2 different levels: *1)* basal level, identified by the mitral valve and *2)* apical level, as the smallest cavity achievable distally to the papillary muscles (moving the probe down and slightly laterally, if needed). Frame rate was 60-100 frames/s and 3 cardiac cycles for each short-axis level were stored in cine-loop format for the offline analysis (EchoPAC version 7.0.0). The endocardial border was traced at an end-systolic frame and the ROI was chosen to fit the whole myocardium. The software allows the operator to check and validate the tracking quality and to adjust the endocardial border or modify the width of the ROI, if needed. Each short-axis image was automatically divided into 6 standard segments: septal, anteroseptal, anterior, lateral, posterior, and inferior. The software calculated LV rotation from the apical and basal short-axis images as the average angular displacement of the 6 standard segments referring to the ventricular centroid, frame by frame. Counterclockwise rotation was marked as positive value and clockwise rotation as negative value when viewed from the LV apex. LV twist was defined as the net difference (in degrees) of apical and basal rotation at isochronal time points. LV torsion as then calculated as the ratio between LV twist (in degrees) and the LV diastolic longitudinal length (in cm) between the LV apex and the mitral plane [14].

Twenty patients were randomly selected for the assessment of reproducibility of peak LV twist. Bland-Altman analysis was performed to evaluate the intra- and inter-observer agreement repeating the analysis 1 month later by the same observer and by a second independent observer. The intra-observer agreement was excellent. According to the Bland-Altman analysis, the mean difference±2 standard deviations (SD) for peak LV twist was 0.05±0.35º. The inter-observer agreement was also good. According to the Bland-Altman analysis, the mean difference±2 SD for peak LV twist was 0.16±1.50º.

Myocardial contrast echocardiography

Immediately following 2-dimensional echocardiography, MCE was performed to evaluate myocardial perfusion, in order to assess infarct size after AMI. The same ultrasound system was used and the 3 standard apical views were acquired using a low-power technique (0.1-0.26 mechanical index). Background gains were set so that minimal tissue signal was seen, and the focus was set at the level of the mitral valve. Luminity® (Bristol-Myers Squibb Pharma, Brussels, Belgium) was used as contrast agent. Each patient received an infusion of 1.3 mL of echo contrast diluted in 50 mL of 0.9% NaCl solution through a 20 gauge intravenous catheter in a proximal forearm vein. Infusion rate was initially set at 4.0 mL/min and then titrated to achieve optimal myocardial enhancement without attenuation artifacts [15]. Machine settings were optimized to obtain the best possible myocardial opacification with minimal attenuation. At least 15 cardiac cycles after high mechanical index (1.7) microbubble destruction [16] were stored in cine-loop format for the offline analysis (EchoPAC version 7.0.0). The LV was divided according to a standard 16-segment model and a semiquantitative scoring system was used to assess contrast intensity after microbubble destruction: *1)* normal/homogenous opacification; *2)* reduced/patchy opacification; *3)* minimal or absent contrast opacification [11,16]. A myocardial perfusion index (MPI), indicating the extent of infarct size, was derived by adding contrast scores of all segments and dividing by the total number of segment [16].

Twenty patients were randomly selected for the assessment of reproducibility of perfusion scoring. Weighted Kappa test was performed to evaluate the intra- and inter-observer agreement repeating the analysis 1 month later by the same observer and by a second independent observer. Both intra- and inter-observer agreements were good (weighted Kappa = 0.86 and = 0.84, respectively)**.**

Statistical analysis

Continues variables are expressed as mean±SD, when normally distributed, and as median and interquartile range, when not normally distributed. Categorical data are presented as absolute numbers and percentages. Differences in continuous variables between 2 groups were assessed using the Student *t* test or the Mann-Whitney *U* test, if appropriate. *Chi*-square test or Fisher exact test, where appropriate, were computed to assess differences in categorical variables.

Differences in continuous variables between >2 groups were assessed by 1-way ANOVA or Kruskal-Wallis test, where appropriate; when the result of the analysis was significant, a post hoc test with Bonferroni's correction was applied.

Univariate and multivariate linear regression analysis (with an automatic stepwise selection procedure with backward elimination) were performed to evaluate the relationship be-

tween peak LV torsion among AMI patients and the following clinical and echocardiographic variables: age, gender, infarct location (anterior vs. non-anterior), multi-vessel disease, TIMI flow grade 3 after PCI, peak troponin T, LVEDV, LVESV, LVEF, WMSI, presence of diastolic dysfunction, peak LV GLS and MPI. Age and sex were entered into the multivariate model independently of their probability value by univariate analysis and were kept fixed throughout the stepwise selection procedure. Regarding the remaining variables, only those with a probability value <0.20 by univariate analysis were entered as covariates in the multivariate model. Linear-regression analyses were performed to evaluate the relation between peak LV torsion at baseline and LVESV at 6-month follow-up, as well as the change in LVESV after 6-month follow-up compared with the baseline value.

Univariate and multivariate logistic regression analysis (with an automatic stepwise selection procedure with backward elimination) were performed to evaluate the relationship between the occurrence of LV remodeling at 6-month follow-up and the following baseline clinical and echocardiographic variables: age, gender, infarct location (anterior vs. non-anterior), multi-vessel disease, TIMI flow grade 3 after PCI, peak troponin T, LVEDV, LVESV, LVEF, WMSI, presence of diastolic dysfunction, peak LV GLS, MPI and peak LV torsion. Age, gender, and LVESV were entered into the multivariate model independently of their probability value by univariate analysis and were kept fixed throughout the stepwise selection procedure. Regarding the remaining variables, only those with a probability value <0.20 by univariate analysis were entered as covariates in the multivariate model. The incremental predictive value of peak LV torsion over clinical, echocardiographic, and MCE variables was assessed by calculating the global chi-square values.

Receiver operator characteristic curve analysis was performed to determine the accuracy of baseline peak LV torsion to predict LV remodeling at 6-month follow-up in the overall patient population and among anterior and non-anterior AMI patients. A p-value <0.05 was considered statistically significant. Statistical analysis was performed using the SPSS software package (SPSS 15.0, Chicago, Illinois).

RESULTS

Reliable speckle-tracking curves for rotation analysis and diagnostic MCE data were obtained in 120 patients; consequently, 26 patients were excluded from further analysis. Of note, no significant difference was observed between included and excluded patients with regard to age (59±10 versus 57±10 years, p = 0.31), male sex (87 [73%] versus 17 [65%], p = 0.47), anterior location of AMI (55 [46%] vsus 13 [50%], p =), and peak value of troponin T 3.04 µg/L [1.65 to 7.03] versus 3.18 µg/L [1.74 to 12.62], p = 0.58). All control subjects had reliable speckle-tracking curves.

Clinical and echocardiographic characteristics

Clinical and echocardiographic characteristics of control subjects and AMI patients are listed in Table 1. By definition, control subjects and AMI patients did not differ in age or gender. Among AMI patients, the infarct-related artery was the left anterior descending coronary artery in 55 (46%) patients and obstructive multi-vessel disease (i.e. more than 1 vessel with a luminal narrowing ≥70%) was present in 41 (34%) patients. The peak value of troponin T was 3.04 (1.65-7.03 μg/l). The mean LVEF was 48±9%.

Table 1. Baseline clinical and echocardiographic characteristics of control subjects and AMI patients

	Control subjects (n = 20)	AMI patients (n = 120)	p-value
Age (years)	56±10	59±10	0.37
Male gender	15 (75%)	87 (73%)	0.82
Diabetes	-	13 (11%)	
Family history of coronary artery disease	-	45 (37%)	
Hypercholesterolemia	-	16 (13%)	
Hypertension	-	43 (36%)	
Current or previous smoking	-	67 (56%)	
Anterior myocardial infarction	-	55 (46%)	
Infarct-related artery			
- left anterior descending coronary artery	-	55 (46%)	
- left circumflex coronary artery	-	21 (17%)	
- right coronary artery	-	44 (37%)	
Multi-vessel disease	-	41 (34%)	
TIMI flow grade 3	-	101 (84%)	
Peak troponin T (μg/l)	-	3.04 (1.65-7.03)	
LVEDV (ml)	103±22	104±27	0.91
LVESV (ml)	40±10	55±21	<0.001
LVEF (%)	61±7	48±9	<0.001
LV diastolic longitudinal length (cm)	8.6±0.6	8.3±0.8	0.18
WMSI	-	1.72±0.34	
Diastolic function			<0.001
- grade 0	20 (100%)	47 (39%)	
- grade 1	-	63 (52%)	
- grade 2	-	8 (7%)	
- grade 3	-	2 (2%)	
Peak LV GLS (%)	-19.4±1.7	-14.0±3.8	<0.001
Peak LV basal rotation (°)	-6.8±2.7	-5.1±2.7	0.013
Peak LV apical rotation (°)	11.6±2.8	8.4±4.6	<0.001
Peak LV twist (°)	17.7±2.1	12.7±5.2	<0.001
Peak LV torsion (°/cm)	2.07±0.27	1.54±0.64	<0.001
MPI	-	1.28 (1.08-1.50)	

EF: ejection fraction; EDV: end-diastolic volume; ESV: end-systolic volume; GLS: global longitudinal strain; LV: left ventricular; MPI: myocardial perfusion index; WMSI: wall motion score index

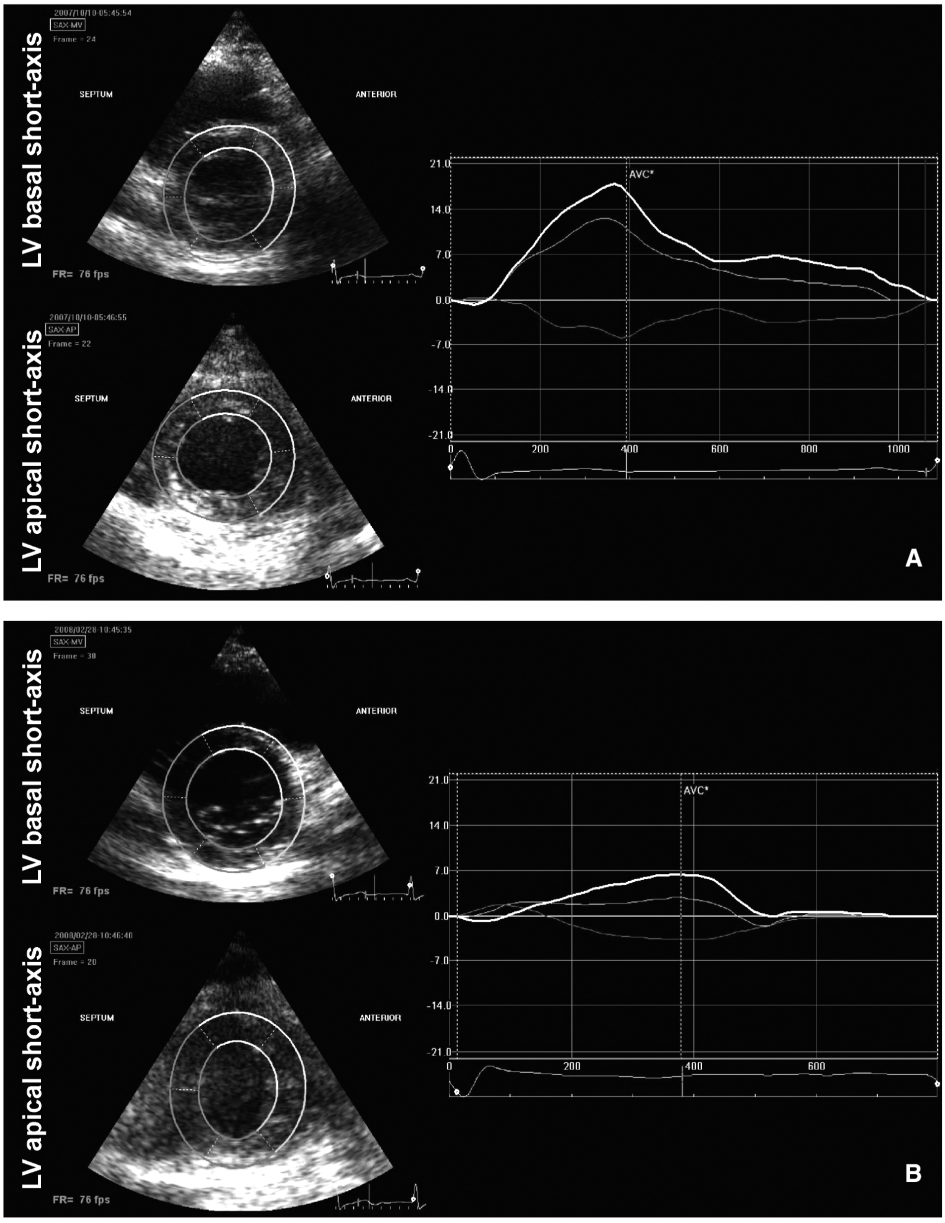


Figure 1. Left ventricular (LV) rotational mechanics curves of a control subject (panel **A**) and of a patient with anterior acute myocardial infarction (panel **B**). Panel **A.** Speckle-tracking analysis shows normal peak LV basal and apical rotations and consequently normal peak LV twist (18.4˚; white line). Panel **B**. Speckle-tracking analysis shows impaired peak LV basal and apical rotations and consequently reduced peak LV twist (6.8˚; white line).

Compared to control subjects, AMI patients had significantly reduced peak LV basal rotation (-5.1±2.7˚ vs. -6.8±2.7˚, p = 0.013), reduced peak LV apical rotation (8.4±4.6˚ vs. 11.6±2.8˚, p <0.001), and consequently decreased peak LV twist (12.7±5.2˚ vs. 17.7±2.1˚, p <0.001) and peak LV torsion (1.54±0.64°/cm versus 2.07±0.27°/cm,p <0.001). Among AMI patients, those with an anterior AMI had significantly lower peak LV apical rotation, LV twist, and LV torsion compared with the remaining AMI patients (6.5±4.3° versus 10.1±4.2°, p <0.001; 11.1±5.4° versus 14.0±4.7°, p = 0.002; and 1.35±0.65°/cm versus 1.70±0.58°/cm, p = 0.003, respectively), whereas peak LV basal rotation was not different (-5.4±2.6° versus -4.9±2.8°, p = 0.31). Of note, no significant difference was observed in peak LV basal rotation, apical rotation, LV twist, and LV torsion between patients (n = 37) with anterior AMI due to proximal LAD occlusion versus patients (n = 18) with anterior AMI due to mid or distal LAD occlusion (-5.2±2.5° versus -5.8±2.7°, p = 0.38; 6.9±4.3° versus 5.6±4.2°, p = 0.30; 11.4±5.2° versus 10.7±5.8°, p = 0.67; and 1.36±0.63°/cm versus 1.35±0.72°/cm, p = 0.95, respectively). Examples of LV rotational mechanics curves obtained by speckle-tracking analysis in a control subject and in a patient with AMI are shown in Figure 1.

Determinants of LV twist among AMI patients

Table 2 shows the results of the univariate and multivariate linear regression analyses performed to determine the factors related to peak LV torsion among AMI patients. By univariate analysis, several variables were significantly related to peak LV torsion: anterior AMI, TIMI flow grade 3 after PCI, peak troponin T, LVEDV, LVESV, LVEF, WMSI, presence of diastolic dysfunc-

Table 2. Univariate and multivariate linear regression analyses to determine the independent correlates of peak LV torsion in AMI patients.

	Univariate		Multivariate	
	β	p-value	β	p-value
Age	-0.080	0.38	0.057	0.37
Male gender	-0.048	0.61	-0.046	0.46
Anterior myocardial infarction	-0.27	0.003	-	-
Multi-vessel disease	-0.13	0.17	-	-
TIMI flow grade 3	0.25	0.005	-	-
Peak troponin T	-0.40	<0.001	-	-
LVEDV	-0.25	0.007	-	-
LVESV	-0.51	<0.001	-	-
LVEF	0.65	<0.001	0.36	<0.001
WMSI	-0.66	<0.001	-	-
Presence of diastolic dysfunction	-0.23	0.011	-	-
Peak LV GLS	-0.56	<0.001	-	-
MPI	-0.69	<0.001	-0.47	<0.001

Abbreviations as in Table 1.

tion, peak LV GLS and MPI. However, by multivariate analysis, only LVEF (β = 0.36, p <0.001) and MPI (β = -0.47, p <0.001) were independently associated with peak LV torsion.

The relationships between peak LV torsion and MPI is shown in Figure 2. Patients without myocardial segments with minimal or absent contrast opacification had higher peak LV torsion compared with patients with ≥1 myocardial segment with minimal or absent contrast opacification (1.84±0.49°/cm versus 1.27±0.63°/cm; p <0.001). In addition, a progressive reduction of peak LV torsion with increasing number of myocardial segments with minimal or absent contrast opacification was observed (Figure 3).

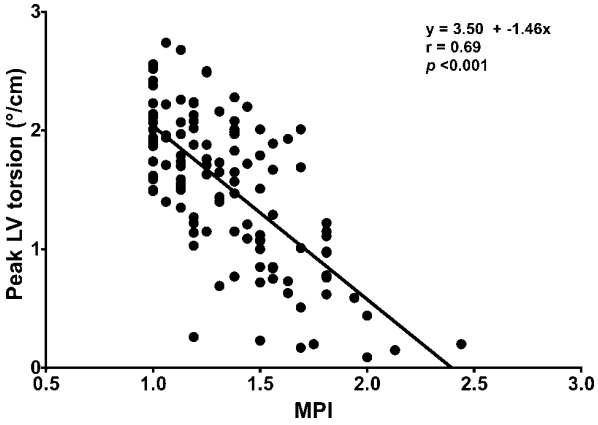


Figure 2. Linear regression analysis illustrating the relation between peak LV torsion and MPI.

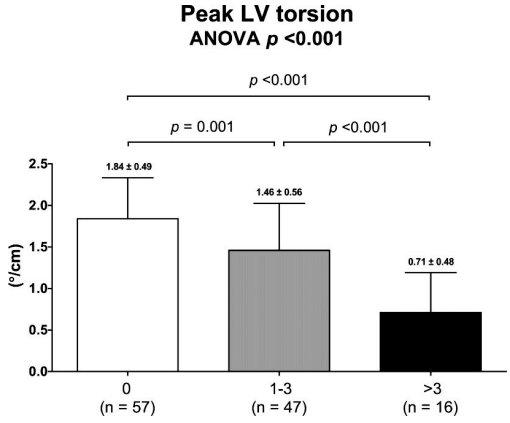


Figure 3. Relation between peak LV torsion and number of myocardial segments with minimal or absent contrast opacification.

LV remodeling at 6-month follow-up

A total of 8 out of 120 AMI patients included in the initial population did not complete the 6-month follow-up; consequently, data at baseline and at 6-month follow-up were available for 112 patients. At 6-month follow-up, mean LVEDV was 114±37 ml whereas mean LVESV was 54±29 ml with a mean LVEF of 55±10%. A total of 19 patients developed LV remodeling.

Baseline clinical and echocardiographic characteristics of AMI patients with versus without LV remodeling are summarized in Table 3. At baseline, patients who developed LV remodeling had larger LVESV (p = 0.036), lower LVEF (p <0.001), and higher MPI (p <0.001), indicating larger infarct size. Regarding LV rotational mechanics parameters, at baseline patients with LV remodeling had significantly lower peak LV apical rotation (p <0.001) and peak LV twist (p <0.001), and peak LV torsion (p <0.001) as compared to patients without LV remodeling; con-

Table 3. Baseline clinical and echocardiographic characteristics of AMI patients without versus with LV remodeling

	No LV remodeling (n = 93)	LV remodeling (n = 19)	p-value
Age (years)	58±10	61±9	0.20
Male gender	66 (71%)	15 (79%)	0.48
Diabetes	9 (10%)	2 (11%)	0.91
Family history of coronary artery disease	36 (39%)	7 (37%)	0.88
Hypercholesterolemia	13 (14%)	2 (11%)	0.74
Hypertension	34 (37%)	6 (32%)	0.68
Current or previous smoking	54 (58%)	9 (47%)	0.39
Anterior myocardial infarction	35 (38%)	13 (68%)	0.013
Multi-vessel disease	29 (31%)	9 (47%)	0.18
TIMI flow grade 3	81 (87%)	14 (74%)	0.16
Peak troponin T (μg/l)	2.54 (1.29-5.25)	9.63 (4.96-12.51)	<0.001
LVEDV (ml)	101±23	106±34	0.59
LVESV (ml)	51±15	63±24	0.036
LVEF (%)	50±8	40±8	<0.001
LV diastolic longitudinal length (cm)	8.2±0.7	8.3±0.6	0.76
WMSI	1.63±0.30	2.05±0.21	<0.001
Presence of diastolic dysfunction	52 (56%)	16 (84%)	0.021
MPI	1.19 (1.00-1.41)	1.75 (1.38-1.81)	<0.001
Peak LV GLS (%)	-15.0±3.3	-11.1±3.3	<0.001
Peak LV basal rotation (°)	-5.4±2.6	-4.6±2.5	0.20
Peak LV apical rotation (°)	9.7±4.1	3.5±3.0	<0.001
Peak LV twist (°)	14.4±4.3	6.6±3.5	<0.001
Peak LV torsion (°/cm)	1.75±0.51	0.80±0.44	<0.001
Medical therapy at discharge			
Antiplatelet agents	93 (100%)	19 (100%)	1.00
Angiotensin-convertin enzyme inhibitors and/or angiotensin receptor blockers	93 (100%)	19 (100%)	1.00
Beta-blockers	89 (96%)	18 (95%)	1.00
Statins	93 (100%)	19 (100%)	1.00

Abbreviations as in Table 1.

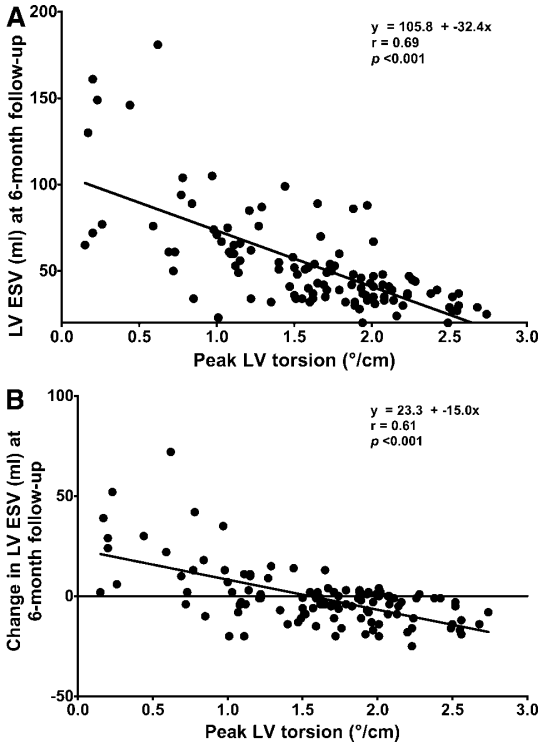


Figure 4. Relation between peak LV torsion at baseline and LVESV at 6-month follow-up (**A**) and the change in LVESV after 6-month follow-up compared with baseline value (**B**).

versely, no difference in peak LV basal rotation was observed between the 2 groups. Patients with more impaired peak LV torsion at baseline had larger LVESV at 6-month follow-up and a higher change in LVESV in the 6-month follow-up period (Figure 4).

Table 4 shows the results of the univariate and multivariate logistic regression analysis performed to determine the relationship between clinical and echocardiographic characteristics at baseline and LV remodeling at 6-month follow-up. By univariate analysis, several variables were significantly related to LV remodeling: anterior AMI, peak troponin T, LVESV, LVEF, WMSI, presence of diastolic dysfunction, peak LV GLS, MPI and peak LV torsion. However, by multivariate analysis, only peak LV torsion (OR = 0.77; 95% CI 0.65-0.92; p = 0.003) and MPI (OR = 1.04, 95% CI, 1.01-1.07; p = 0.021) were independently related to the development of LV remodeling. Furthermore, peak LV torsion provided modest but significant incremental value over clinical, echocardiographic, and MCE variables in predicting LV remodeling (Figure 5).

By recever-operator-characteristics curve analysis (Figure 6), peak LV torsion ≤1.44°/cm provided the highest sensitivity (95%) and specificity (77%) to predict LV remodeling; diagnostic accuracy was high in both anterior and non-anterior AMI patients (Figure 6).

Table 4. Univariate and multivariate logistic regression analyses to determine the independent predictors of LV remodeling at 6-month follow-up.

	Univariate		Multivariate	
	OR (95% CI)	**p-value**	**OR (95% CI)**	**p-value**
Age	1.03 (0.98-1.09)	0.20	1.00 (0.93-1.08)	0.94
Male gender	1.53 (0.47-5.04)	0.48	3.62 (0.66-19.8)	0.14
Anterior myocardial infarction	3.59 (1.25-10.3)	0.017	-	-
Multi-vessel disease	1.99 (0.73-5.40)	0.18	-	-
TIMI flow grade 3	0.42 (0.13-1.36)	,0.001	-	-
Peak troponin T	1.23 (1.11-1.36)	<0.001	-	-
LVEDV	1.01 (0.99-1.03)	0.47	-	-
LVESV	1.04 (1.01-1.07)	0.006	0.99 (0.94-1.04)	0.77
LVEF	0.85 (0.78-0.92)	<0.001	-	-
WMSI	1.73 (1.34-2.24)	<0.001	-	-
Presence of diastolic dysfunction	4.21 (1.15-15.4)	0.030	-	-
Peak LV GLS	1.43 (1.19-1.71)	<0.001	-	-
Peak LV torsion*	0.72 (0.62-0.82)	<0.001	0.77 (0.65-0.92)	0.003
MPI*	1.79 (1.39-2.31)	<0.001	1.29 (0.84-1.97)	0.24

Abbreviations as in Table 1. OR indicates odds ratio. C-statistic = 0.93

*OR and 95% CI are intended for a 0.1-unit increase.

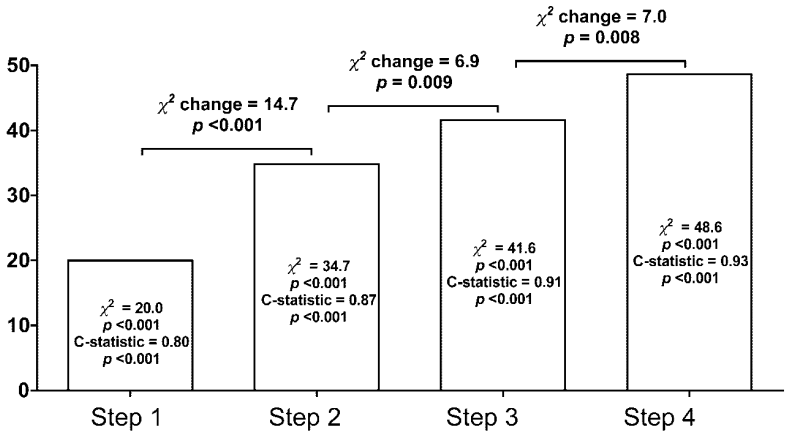


Figure 5. Incremental value of peak LV torsion over clinical, echocardiographic, and MCE variables in predicting LV remodeling at 6-month follow-up.

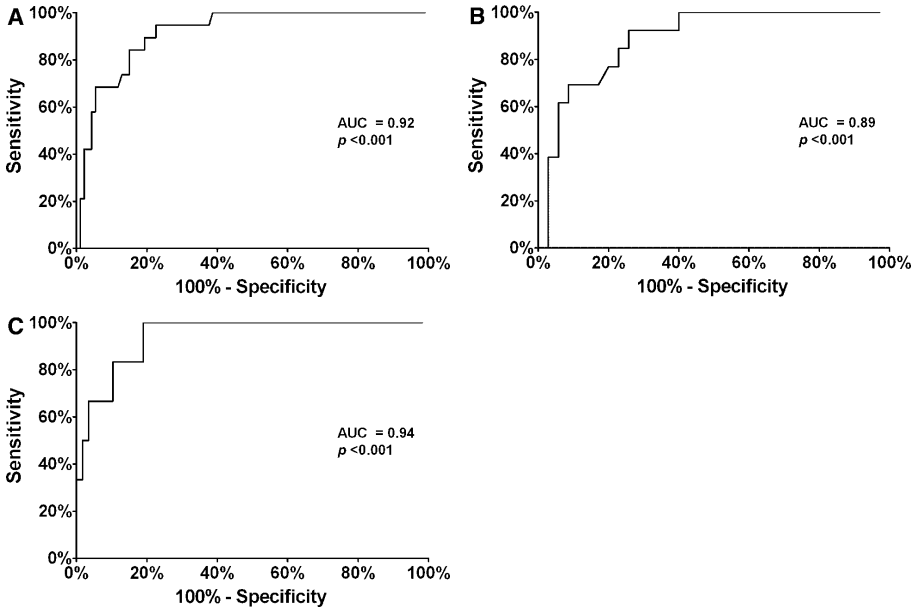


Figure 6. Receiver-operator characteristic (ROC) curve, testing the accuracy of peak LV torsion to predict LV remodeling at 6-month follow-up. A, In the overall patient population, peak LV torsion ≤1.44°/cm provided the highest sensitivity (95%) and specificity (77%) to predict LV remodeling. B, Among patients with anterior AMI, peak LV torsion ≤1.29°/cm provided the highest sensitivity (92%) and specificity (74%) to predict LV remodeling. C, Among patients with nonanterior AMI, peak LV torsion ≤1.44°/cm provided the highest sensitivity (100%) and specificity (81%) to predict LV remodeling. AUC indicates area under the curve.

DISCUSSION

The results of the present evaluation show that LV torsion is significantly impaired early after AMI, due to a reduction of both basal and apical rotation. Infarct size (assessed by MCE) was independently related to LV torsion. In addition, LV torsion early after AMI was significantly and independently related to the occurrence of LV remodeling at 6-month follow-up.

Impact of AMI on LV rotational mechanics

Previous experimental and clinical studies have consistently shown an impairment of LV torsional deformation in the setting of acute and chronic myocardial infarction [7,8,18–21]. In addition, LV torsion was related to global LV systolic function and the extent of wall motion abnormalities [7,8,21]. The present evaluation confirms and extends these previous observations. LV systolic function was indeed significantly related to the LV torsion. More important, an independent correlation between infarct size (assessed by MCE and expressed as MPI) and LV

torsion was noted on multivariate analysis. The larger damage of the LV subepicardial myofibers and the greater disarrangement of the typical architecture of LV myofibers secondary to larger infarcts may explain the observed relation between infarct size and LV torsion.

Epicardial myofibers are indeed extremely important to maintain LV torsional deformation [4]. Epicardial myofibers (as compared to the endocardial fibers) produce larger torque (related to the larger radius), and determine the overall direction of rotation [4]. Damage of the epicardial fibers appears therefore mandatory for an impairment of LV rotational mechanics. Accordingly, the present evaluation underscores that larger infarcts (as indicated by higher MPI values), leading to more extensive, transmural damage (spreading to the epicardial myofibers) [17], result in a larger impairment of LV torsion. Previous experimental studies using an occlusion-reperfusion model provided evidence for this hypothesis, by showing that LV torsion was impaired in the presence of transmural ischemia, while LV torsion was preserved in the presence of subendocardial ischemia only [22,23]. In addition, LV myofibers have a typical spiral architecture that is also extremely important in determining the LV systolic wringing motion. Large infarcts may be associated with extensive distortion of the typical architecture of the LV myofibers, altering their obliquity and eventually impairing LV torsion [24].

Role of LV twist in predicting LV remodeling

Besides being strictly related to the myocardial damage after AMI, LV torsion at baseline was found to be a strong predictor of LV remodeling at 6-month follow-up; interestingly, this relation remained even after adjustment for other univariate predictors of LV remodeling, including infarct size (expressed as MPI). Peculiar properties of the LV systolic twisting motion may explain this finding.

LV torsion indeed is not simply an index of global LV systolic function; previous mathematical models revealed the essential role of LV torsion in optimizing LV oxygen demand and the efficiency of LV systolic thickening by uniformly distributing myofiber stress across the myocardial wall [25]. A significant impairment of LV torsion after AMI will therefore result in an increased myofiber stress and oxygen demand of the remaining non-infarcted myocardium. This low-efficiency state would further impair myocardial contractility, possibly representing the initial step of a vicious circle of progressive LV dilatation and decline in LV systolic function [18,24].

Clinical implications

The present evaluation underscores the value of LV torsion as a sensitive global parameter of LV systolic myocardial performance. Its impairment early after AMI is strictly related to the

extent myocardial damage and possibly plays an important role in the development of LV remodeling. Accordingly, this parameter may be used in clinical practice as an early marker for risk stratification. Early assessment of LV torsion after AMI using speckle-tracking echocardiography could identify patients (with reduced LV torsion) who may benefit from aggressive medical therapy to prevent LV remodeling, heart failure and poor outcome.

Study limitations

Some limitations should be acknowledged. First, only patients with ST-segment elevation AMI were included; consequently, the results cannot be extrapolated to patients with non–ST-segment elevation AMI. Another important limitation concerns the acquisition of the short-axis images. The acquisition of true LV apical short-axis images is indeed dependent on the acoustic window (more than the basal short-axis view) and may be technically difficult to acquire in some patients. In addition, transducer position has a strong impact on the assessment of apical rotation by speckle-tracking echocardiography. It should, however, be emphasized that the most caudal transducer position was used to acquire the parasternal short-axis apical view; moreover, all patients without true LV apical short-axis images were not included in the present evaluation. Furthermore, motion throughout the planes at the basal level may reduce the accuracy of measurement of LV basal rotation. Finally, the impairment of LV torsion observed early after AMI may be partially related to the presence of myocardial stunning; further studies are needed to assess the evolution of LV torsion after the acute phase of AMI.

CONCLUSIONS

LV torsion is significantly impaired early after AMI. The amount of impairment of LV torsion is related to infarct size. In addition, LV torsion at baseline predicts the occurrence of LV remodeling at 6-month follow-up, with modest but significant incremental value over clinical, echocardiographic and MCE variables.

REFERENCES

1. White HD, Norris RM, Brown MA, Brandt PW, Whitlock RM, Wild CJ. Left ventricular end-systolic volume as the major determinant of survival after recovery from myocardial infarction. *Circulation* 1987; 76:44 –51.
2. St John Sutton M, Pfeffer MA, Plappert T et al. Quantitative two-dimensional echocardiographic measurements are major predictors of adverse cardiovascular events after acute myocardial infarction: the protective effects of captopril. *Circulation* 1994;89:68 –75.
3. Bolognese L, Cerisano G. Early predictors of left ventricular remodeling after acute myocardial infarction. *Am Heart J* 1999;138:S79 –S83.
4. Sengupta PP, Khandheria BK, Narula J. Twist and untwist mechanics of the left ventricle. *Heart Fail Clin* 2008;4:315–324.
5. Notomi Y, Lysyansky P, Setser RM et al Measurement of ventricular torsion by two-dimensional ultrasound speckle tracking imaging. *J Am Coll Cardiol* 2005;45:2034 –2041.
6. Helle-Valle T, Crosby J, Edvardsen T et al. New noninvasive method for assessment of left ventricular rotation: speckle tracking echocardiography. *Circulation* 2005;112:3149 –3156.
7. Takeuchi M, Nishikage T, Nakai H, Kokumai M, Otani S, Lang RM. The assessment of left ventricular twist in anterior wall myocardial infarction using two-dimensional speckle tracking imaging. *J Am Soc Echocardiogr* 2007;20:36–44.
8. Bansal M, Leano RL, Marwick TH. Clinical assessment of left ventricular systolic torsion: effects of myocardial infarction and ischemia. *J Am Soc Echocardiogr* 2008;21:887– 894.
9. Thygesen K, Alpert JS, White HD et al. Universal definition of myocardial infarction. *Circulation* 2007;116:2634 –2653.
10. Himelman RB, Cassidy MM, Landzberg JS, Schiller NB. Reproducibility of quantitative two-dimensional echocardiography. *Am Heart J* 1988;115:425– 431.
11. Lang RM, Bierig M, Devereux RB et al. Recommendations for chamber quantification: a report from the American Society of Echocardiography's Guidelines and Standards Committee and the Chamber Quantification Writing Group, developed in conjunction with the European Association of Echocardiography, a branch of the European Society of Cardiology. *J Am Soc Echocardiogr* 2005;18:1440 –1463.
12. Lester SJ, Tajik AJ, Nishimura RA, Oh JK, Khandheria BK, Seward JB. Unlocking the mysteries of diastolic function: deciphering the Rosetta Stone 10 years later. *J Am Coll Cardiol* 2008;51:679–689.
13. Reisner SA, Lysyansky P, Agmon Y, Mutlak D, Lessick J, Friedman Z. Global longitudinal strain: a novel index of left ventricular systolic function. *J Am Soc Echocardiogr* 2004;17:630–633.
14. Kim HK, Sohn DW, Lee SE et al. Assessment of left ventricular rotation and torsion with two-dimensional speckle tracking echocardiography. *J Am Soc Echocardiogr* 2007;20:45–53.
15. Weissman NJ, Cohen MC, Hack TC, Gillam LD, Cohen JL, Kitzman DW. Infusion versus bolus contrast echocardiography: a multicenter, open-label, crossover trial. *Am Heart J* 2000;139:399–404.
16. Dwivedi G, Janardhanan R, Hayat SA, Swinburn JM, Senior R. Prognostic value of myocardial viability detected by myocardial contrast echocardiography early after acute myocardial infarction. *J Am Coll Cardiol* 2007;50:327–334.
17. Janardhanan R, Moon JC, Pennell DJ, Senior R. Myocardial contrast echocardiography accurately reflects transmurality of myocardial necrosis and predicts contractile reserve after acute myocardial infarction. *Am Heart J* 2005;149:355–362.

18. Tibayan FA, Rodriguez F, Langer F et al Alterations in left ventricular torsion and diastolic recoil after myocardial infarction with and without chronic ischemic mitral regurgitation. *Circulation* 2004;110(suppl II):II-109–II-114.
19. Sun JP, Niu J, Chou D et al. Alterations of regional myocardial function in a swine model of myocardial infarction assessed by echocardiographic 2-dimensional strain imaging. *J Am Soc Echocardiogr* 2007;20: 498–504.
20. Nagel E, Stuber M, Lakatos M, Scheidegger MB, Boesiger P, Hess OM. Cardiac rotation and relaxation after anterolateral myocardial infarction. *Coron Artery Dis* 2000;11:261–267.
21. Garot J, Pascal O, Diebold B et al. Alterations of systolic left ventricular twist after acute myocardial infarction. *Am J Physiol Heart Circ Physiol* 2002;282:H357–H362.
22. Kroeker CA, Tyberg JV, Beyar R. Effects of ischemia on left ventricular apex rotation: an experimental study in anesthetized dogs. *Circulation* 1995;92:3539 -3548.
23. Knudtson ML, Galbraith PD, Hildebrand KL, Tyberg JV, Beyar R. Dynamics of left ventricular apex rotation during angioplasty: a sensitive index of ischemic dysfunction. *Circulation* 1997;96:801–808.
24. Buchalter MB, Rademakers FE, Weiss JL, Rogers WJ, Weisfeldt ML, Shapiro EP. Rotational deformation of the canine left ventricle measured by magnetic resonance tagging: effects of catecholamines, ischaemia, and pacing. *Cardiovasc Res* 1994;28:629–635.
25. Beyar R, Sideman S. Left ventricular mechanics related to the local distribution of oxygen demand throughout the wall. *Circ Res* 1986;58:664–677.

PART III

Magnetic resonance imaging

PART IIIA

Magnetic resonance imaging for the assessment of left ventricular dyssynchrony and myocardial viability

CHAPTER 15

Comparison between TDI and velocity-encoded magnetic resonance imaging for measurement of myocardial velocities, assessment of LV dyssynchrony, and estimation of LV filling pressures in patients with ischemic cardiomyopathy

N Ajmone Marsan, J JM Westenberg, L F Tops, C Ypenburg, E R Holman, J H C Reiber, A de Roos, E E van der Wall, M J Schalij, J R Roelandt, and J J Bax

Am J Cardiol 2008;102:1366-72.

ABSTRACT

Objectives: Velocity-encoded magnetic resonance imaging (VE-MRI), commonly used to perform flow measurements, can be applied for myocardial velocity analysis, similar to tissue Doppler imaging (TDI). In this study, a comparison between VE-MRI and TDI was performed for the assessment of LV dyssynchrony and LV filling pressures.

Methods: Ten healthy volunteers and 22 patients with heart failure secondary to ischemic cardiomyopathy underwent both VE-MRI and TDI. Longitudinal myocardial peak systolic (PSV) and diastolic (PDV) velocities and time to PSV (Ts) were measured with both techniques at the level of LV septum and lateral wall. To quantify LV dyssynchrony, the delay in Ts between basal septum and lateral wall was calculated (SLD) and patients were categorized in 3 groups: minimal (SLD <30 ms), intermediate (30-60 ms) and extensive (>60 ms) LV dyssynchrony. The E/E' ratio was also assessed and patients were divided in 3 groups: normal (E/E' <8), probably abnormal (E/E' = 8-15) and elevated (E/E' >15) LV filling pressures.

Results: Excellent correlations were observed for PSV and PDV ($r = 0.95$, $p < 0.001$) measured with TDI and VE-MRI. A small bias ($p < 0.001$) of -1.1±1.1 cm/s for PSV and of -0.45±1.03 cm/s for PDV was noted between the 2 techniques. A strong correlation was also noted between Ts measured with TDI and VE-MRI ($r = 0.97$, $p < 0.001$) without a significant difference. TDI and VE-MRI showed an excellent agreement for LV dyssynchrony and LV filling pressures classification with a weighted κ of 0.96 and 0.91, respectively.

Conclusion: TDI and VE-MRI are highly concordant and can be used interchangeably for the assessment of LV dyssynchrony and filling pressures.

INTRODUCTION

Velocity-encoded magnetic resonance imaging (VE-MRI), commonly used to perform flow measurements, can be applied for myocardial velocity analysis, similar to tissue Doppler imaging (TDI). Preliminary studies have compared TDI and VE-MRI in patients with hypertensive heart disease [1] and in patients scheduled for cardiac resynchronization therapy (CRT) [2,3]. Good correlations between the 2 techniques were reported for the assessment of left ventricular (LV) myocardial velocities and timings. The aim of this study was to compare TDI and VE-MRI in patients with heart failure secondary to ischemic cardiomyopathy, including the measurement of systolic and diastolic velocities and time to peak systolic velocity for different LV segments. Furthermore, the applicability of VE-MRI was evaluated for assessment of LV dyssynchrony and estimation of LV filling pressures, using validated indices derived from TDI.

METHODS

A total of 10 healthy volunteers (5 men, 31±5 years) and 22 consecutive patients with heart failure secondary to ischemic cardiomyopathy (16 men, 58±11 years) underwent both cardiac MRI and echocardiographic evaluation including TDI, on the same day. The patients were clinically referred for echocardiography and cardiac MRI. All healthy volunteers gave informed consent and the protocol was approved by the institutional review board.

Echocardiography was performed using a commercially available system (Vingmed Vivid Seven, General Electric Healthcare, Horten, Norway) equipped with a 3.5-Mhz transducer. Left ventricular end-diastolic (EDV) and end-systolic (ESV) volumes and LV ejection fraction (EF) were calculated using the biplane Simpson's technique [4]. Peak velocity in early diastole (E wave) of the transmitral flow was derived from conventional pulsed-wave Doppler imaging.

For TDI images, the sector width was narrowed to visualize one myocardial wall at a time, to obtain a good alignment between the wall and the ultrasound beam and to reach a frame rate of at least 130 frames/second. At least 3 consecutive beats were recorded and the images were digitally stored for off-line analysis (EchoPac 6.1, GE Vingmed Ultrasound, Horten, Norway). During post-processing, the color-coded TDI dataset was used to analyze longitudinal myocardial velocities: regions of interest (5 x 5 mm) were placed at the basal and mid level [5] of LV septum and lateral wall. Semi-automated tissue tracking was used to maintain the sample area in the region of interest throughout the cardiac cycle. Subsequently, the following variables were measured:

1) peak systolic velocity (PSV)
2) peak diastolic E' velocity (E'PDV)
3) peak diastolic A' velocity (A'PDV)
4) time from R wave (from the ECG signal) to PSV (Ts)

The Ts is expressed as a percentage of the cardiac cycle, to take the possible difference in heart rate during the echocardiographic and MRI studies into account. To quantify LV dyssynchrony, the delay in Ts between the basal septum and lateral wall was calculated (referred to as septal-to-lateral delay, SLD, Figure 1) [6] and the patients were categorized into 3 groups according to the extent of LV dyssynchrony: minimal (SLD <30 ms), intermediate (SLD 30 to 60 ms) and extensive (SLD >60 ms) [6]. Inter- and intra-observer agreement for the assessment of the SLD were 90% and 96% respectively, as previously reported [7].

In addition, the ratio of transmitral E wave velocity and mitral annulus septal early velocity (E/E') was calculated. This ratio correlates closely with LV filling pressures[8], and is therefore used in the evaluation of LV diastolic function [9]. The patient population was divided into 3 groups: normal LV filling pressures/LV diastolic function (E/E' <8), probably abnormal LV filling pressures/LV diastolic function (E/E' = 8-15) and elevated LV filling pressure/ LV diastolic dysfunction (E/E' >15) [9;10].

MRI data acquisition was performed on a 1.5 T scanner (ACS-NT15 Intera, software release 11, Philips Medical Systems, Best, The Netherlands). Scout images preceded the 2- and 4-chamber acquisitions, conform standard cardiac MR protocols [11], using steady-state free precession [12]. To obtain the transmitral blood flow, a spoiled gradient-echo phase-contrast acquisition was performed [13] with one-directional through-plane velocity-encoding. The acquisition plane was positioned at the mitral annulus in end-systole perpendicular to the expected transmitral flow [14]. The maximum velocity sensitivity was set to 150 cm/s. Slice thickness of the imaging plane was 8 mm, Field-of-View = 370 mm, scan matrix = 128´102, with voxels of 2.89´3.21´8.0 mm; flip angle a = 20°, TR/TE = 5.0/3.1; 4 signal averages (NSA) were used to increase the signal-to-noise ratio. Retrospective cardiac synchronization was used and 40 cardiac phases were reconstructed for one cardiac cycle. From the velocity curves, the maximum velocity of transmitral E wave was derived. A VE acquisition for the longitudinal velocity parallel to the long-axis of the LV, in a 4-chamber orientation, was performed with the following imaging parameters: slice thickness = 8 mm, Field-of-View = 370 mm, scan matrix = 128×76, with reconstructed voxels of 1.45×1.45×8.0 mm, flip angle α = 50°, TR/TE = 6.9/4.9; four NSA; velocity sensitivity was 20 cm/s. Retrospective cardiac triggering was used. Acquisition was performed with free breathing. The maximal number of phases was reconstructed, yielding a temporal resolution of 6-12 ms. Image analysis was performed off-line, as previously described [3], using the extended version of QMass software (Medis, Leiden, The Netherlands). Regions of interest (5 x 5 mm) were positioned at the basal and mid level of the septum and lateral wall in all phase images as for echocardiography [5]. Since the basal and mid levels move constantly, manual correction for the placement of the regions of interest is needed throughout the cardiac cycle. The mean velocity over the sample area was measured resulting in myocardial wall motion velocity graphs over one average cycle (Figure 1). Longitudinal velocity toward the apex was defined as positive. The post-processing of the images required 3-5 minutes. Similar to echocardiography, peak systolic and diastolic velocities and

Ts (corrected for heart rate) were measured. To quantify LV dyssynchrony, the SLD was derived from the basal segments of the septum and lateral wall. The patients were subsequently classified using the same cut-off values as applied to TDI. The coefficient of variation for SLD assessment with VE-MRI (defined as the standard deviation of the differences between the 2 series of measurements divided by the mean of both measurements) was less than 10% for both intra- and inter-observer variation as previously reported [3]. LV diastolic function was evaluated by estimation of LV filling pressures, using the septal E/E′ ratio [8]. Patients were categorized in 3 groups according to the cut-off values validated for TDI echocardiography [10].

Continuous data are presented as mean±SD; dichotomous data are presented as numbers and percentages. Comparison of data was performed using the paired or unpaired Student *t* test. Pearson's correlation analysis was performed to evaluate the relation between TDI and VE-MRI measurements. Bland-Altman analysis was performed to evaluate the differences in PSV, PDV and in time-to-peak velocities assessed with VE-MRI and TDI. The mean differences, trends and limits of agreement are reported. Agreement for LV dyssynchrony and diastolic function classification with TDI versus VE-MRI was assessed from a 3×3 table using weighted

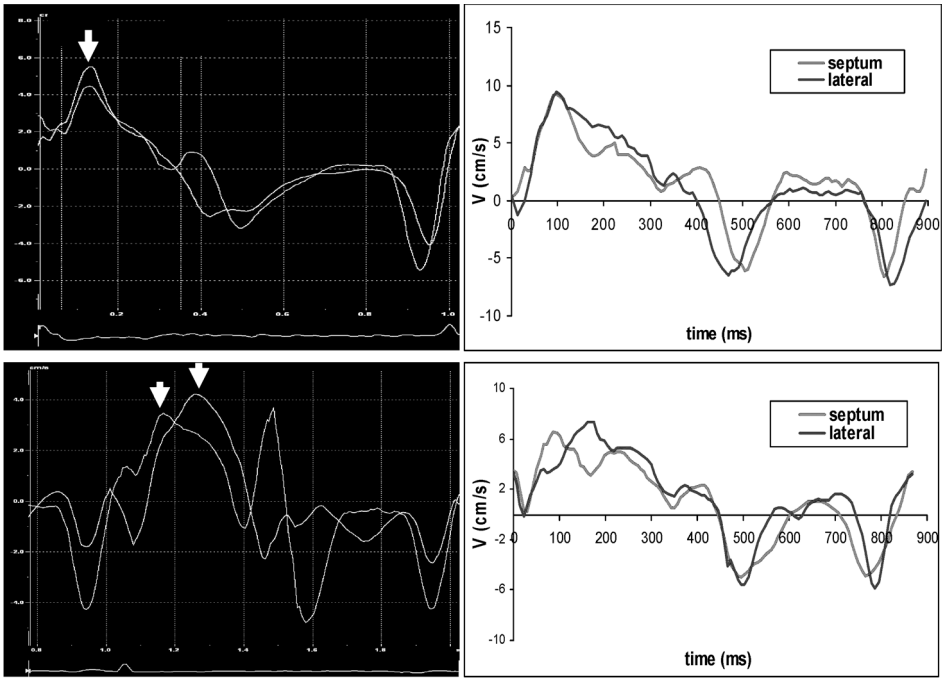


Figure 1. Left ventricular (LV) dyssynchrony assessment from myocardial velocity curves (of the septum and lateral wall) with tissue Doppler imaging (left panels) and velocity-encoded magnetic resonance imaging (right panels). White arrows indicate peak systolic myocardial velocities of the basal segments of septum and lateral wall. In the upper panels an example of a heart failure patient without significant LV dyssynchrony (no septal-to-lateral delay) is shown. The lower panels demonstrate examples of a heart failure patient with extensive LV dyssynchrony (septal-to-lateral delay = 90 ms).

κ statistics (Fleiss-Cohen weighting). A p-value <0.05 was considered to be statistically significant. A statistical software program SPSS 12.0 (SPSS Inc, Chicago, Il, USA) was used for statistical analysis.

RESULTS

Baseline individual characteristics of the study population are summarized in Table 1. In the heart failure patients, the echocardiographic examination revealed severe LV dilatation (LVEDV 222±58 ml) and depressed LV ejection fraction (30±6 %). The majority of the patients were in NYHA functional class III (n = 16, 73%).

For the overall study population, the PSV measured with VE-MRI showed a very good correlation with PSV measured with TDI (r = 0.95, p <0.001) (Figure 2). Bland-Altman analysis revealed a mean difference between TDI and VE-MRI of -1.1±1.1 cm/s, with a significant trend (p <0.01); limits of agreement ranged from -3.4 cm/s to 1.1 cm/s (Figure 3). The PSV (at basal and mid segments of LV septum and lateral wall) were higher in normal subjects than in heart failure patients, both measured with TDI (7.6±3.1 vs. 2.5±1.4 cm/s, p <0.001) and with VE-MRI (8.6±3.2 vs. 3.7±2.1 cm/s, p <0.001). Of interest, the correlation coefficient between TDI and VE-MRI was higher for normal individuals (r = 0.97, p <0.001) than for heart failure patients (r = 0.82, p <0.001).

The values of time to peak systolic velocities for each LV segment are shown in Table 2. An excellent correlation was observed in the overall study population between Ts measured with TDI and Ts measured with VE-MRI (r = 0.97, p <0.001) (Figure 4). Bland-Altman analysis showed a non-significant difference between both techniques of -0.26±1.71% (limits of agreement from -3.6% to 3.1%). The Ts, measured with both methods at the level of LV septum and lateral wall, were longer in heart failure patients than in normal individuals (Table 2). Of note, Pearson's correlation analysis revealed comparable correlation coefficients for time to peak systolic velocities in heart failure patients (r = 0.96, p <0.001) and controls (r = 0.90, p <0.001). A strong correlation between TDI and VE-MRI was also observed for the assessment of LV dyssynchrony (r = 0.95, p <0.001). On TDI, according to the above mentioned classification, 10 patients had minimal LV dyssynchrony (SLD <30 ms), 4 had intermediate (SLD 30 to 60 ms) and 8 had extensive (SLD >60 ms) LV dyssynchrony. Similarly on VE-MRI, 9 patients had minimal, 5 had intermediate and 8 had extensive LV dyssynchrony (weighted κ for TDI vs. VE-MRI was 0.96). Of note, none of the controls showed LV dyssynchrony on both techniques.

In the total study population, the PDV (E'PDV and A'PDV) measured with VE-MRI showed an excellent correlation with PDV measured with TDI (r = 0.95, p <0.001) (Figure 2). The PDV measured with VE-MRI consistently exceeded the PDV measured with TDI. Bland-Altman analysis (using absolute values) revealed a mean difference of -0.45±1.03 cm/s between the 2 techniques (p <0.001, limits of agreement from -2.5 to 1.5 cm/sec) (Figure 3). Both E' PDV and

Table 1. Individual characteristics of the study population (22 patients with heart failure secondary to ischemic cardiomyopathy and 10 healthy control subjects), including the measurements of left ventricular dyssynchrony and left ventricular filling pressures (E/E') assessed by tissue Doppler Imaging (TDI) and velocity-encoded magnetic resonance imaging (VE-MRI).

Subject	Age (years)	Gender	QRS duration (ms)	New York Heart Association class	Left ventricular end-diastolic volume (ml)	Left ventricular end-systolic volume (ml)	Left ventricular ejection fraction (%)	Left ventricular dyssynchrony by TDI (ms)	Left ventricular dyssynchrony by VE-MRI (ms)	E/E' by TDI	E/E' by VE-MRI
Patient 1	39	Female	132	3	152	94	38	110	138	13.2	12.1
Patient 2	42	Male	152	3	240	153	36	40	32	10.8	11.0
Patient 3	45	Female	147	3	291	218	25	112	84	17.3	18.4
Patient 4	45	Male	186	2	214	150	30	33	51	30.9	26.7
Patient 5	48	Male	90	3	220	155	29	21	9	14.2	17.4
Patient 6	50	Male	120	2	197	141	28	48	55	24.8	22.5
Patient 7	50	Male	90	4	184	120	35	7	0	9.7	8.1
Patient 8	51	Male	90	3	205	145	29	10	15	29.0	31.2
Patient 9	52	Male	140	3	306	200	34	95	95	11.3	18.7
Patient 10	54	Male	120	2	140	88	37	14	8	11.4	11.8
Patient 11	57	Male	138	3	332	278	16	130	117	25.0	23.3
Patient 12	61	Male	160	2	276	198	28	80	85	28.0	17.3
Patient 13	64	Male	180	3	135	85	37	0	0	12.8	11.9
Patient 14	64	Male	120	3	200	145	27	25	38	37.1	50
Patient 15	64	Male	120	2	265	199	25	110	95	18	20.8
Patient 16	65	Female	124	3	310	235	24	28	21	33.2	20.6
Patient 17	67	Female	200	3	220	163	26	120	121	27.9	20.3
Patient 18	68	Male	143	3	214	149	30	51	34	20.4	24.4
Patient 19	69	Male	96	3	126	87	31	8	5	20.0	14.3
Patient 20	73	Female	150	3	230	151	34	10	14	9.0	9.1
Patient 21	74	Male	156	3	245	158	35	7	0	12.3	13.7
Patient 22	75	Female	150	3	186	147	21	70	76	20.3	27.9
Control 1	26	Female	90	-	83	30	64	8	5	3.2	2.1
Control 2	26	Male	80	-	116	48	59	3	7	1.4	3.0
Control 3	28	Female	82	-	85	30	65	9	18	4.6	2.2
Control 4	28	Male	102	-	105	41	61	25	13	7.1	6.6
Control 5	30	Female	93	-	81	30	62	0	0	4.4	5.6
Control 6	30	Female	91	-	70	27	62	8	5	6.8	6.5
Control 7	36	Male	100	-	109	40	61	7	10	3.3	2.3
Control 8	36	Male	98	-	100	36	64	11	0	5.4	5.5
Control 9	36	Male	100	-	110	41	62	5	5	7.7	7.8
Control 10	37	Female	76	-	75	27	64	20	11	3.8	4.1

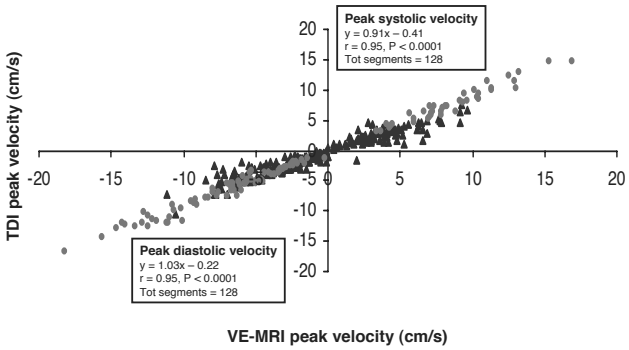


Figure 2. Correlation between peak systolic and diastolic velocities (at basal and mid segments of LV septum and lateral wall) measured with tissue Doppler imaging (TDI) and velocity-encoded magnetic resonance imaging (VE-MRI) in normal individuals (gray dots) and in heart failure patients (black triangles).

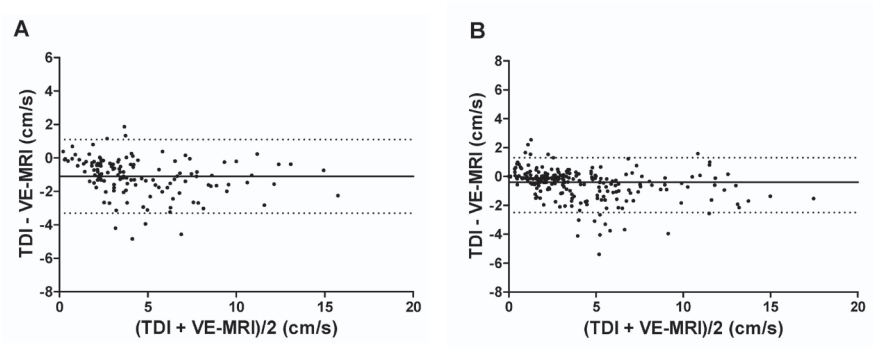


Figure 3. Bland-Altman scatter plot of differences in peak systolic velocity (Panel A) and peak diastolic velocity (using absolute values, Panel B) between TDI and VE-MRI and the average peak systolic velocity and peak diastolic velocity (using absolute values) between the 2 techniques.

Table 2. Time to peak systolic velocity (Ts) of 4 LV segments, expressed as a percentage of cardiac cycle, measured with velocity-encoded magnetic resonance imaging (VE-MRI) and tissue Doppler imaging (TDI) in normal subjects (controls) and in heart failure (HF) patients.

	VE-MRI	TDI
Basal septum Ts (%)		
HF patients	15.6±6.2	15.1±5.2
Controls	9.8±2.0*	9.5±1.5*
Mid septum Ts (%)		
HF patients	15.4±6.5	15.2±6.1
Controls	9.2±2.3*	8.7±1.2*
Basal lateral Ts (%)		
HF patients	19.6±8.4	19.5±7.3
Controls	9.0±1.2*	9.2±1.1*
Mid lateral Ts (%)		
HF patients	18.8±8.6	18.7±8.2
Controls	8.8±1.4*	8.7±1.2*

*: p <0.001: normal subjects versus HF patients

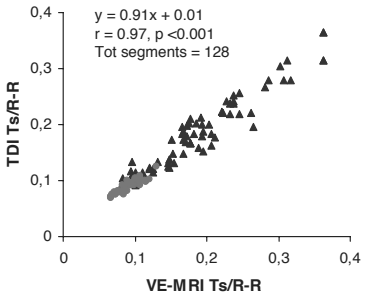


Figure 4. Correlation between time to peak systolic velocities (Ts, at basal and mid segments of LV septum and lateral wall), corrected for the R-R interval, measured with tissue Doppler imaging (TDI) and velocity-encoded magnetic resonance imaging (VE-MRI) in normal individuals (grey dots) and in heart failure patients (black triangles).

A' PDV, measured at the level of LV septum and lateral wall, were higher in normal individuals than in heart failure patients. Mean E' PDV in the controls vs. heart failure patients: -9.1±3.0 vs. -3.2±1.8 cm/s with TDI ($p < 0.001$) and -9.6±3.3 vs. -3.7±2.3 cm/s with VE-MRI ($p < 0.001$). Mean A' PDV in the controls vs. heart failure patients: -3.7±1.6 vs. -2.1±1.4 cm/s with TDI ($p < 0.01$) and -4.3±2.1 vs. -2.6±1.5 cm/s with VE-MRI ($p < 0.01$). Interestingly, the correlation coefficient was higher for controls than for heart failure patients both for E'PDV ($r = 0.96$ vs. $r = 0.87$) and for A'PDV ($r = 0.96$ vs. $r = 0.89$).

For the evaluation of the maximum velocity of transmitral E wave, Doppler echocardiography and MRI showed a strong correlation ($r = 0.94$, $p < 0.001$). With Bland-Altman analysis a mean difference of -0.32±6.8 cm/sec (limits of agreement from -13.6 to 12.9 cm/sec) was observed, with a non-significant trend (p = NS). A strong correlation between MRI and echocardiography was observed for the assessment of E/E' ratio ($r = 0.95$, $p < 0.001$). Interestingly on TDI, 9 patients had an E/E' between 8 and 15, and 13 had E/E' >15. On VE-MRI, 8 patients had E/E' between 8 and 15, and 14 had E/E' >15 (weighted κ for TDI vs. VE-MRI was 0.91).

DISCUSSION

The main findings of the current study can be summarized as follows: 1) a strong correlation was found between TDI and VE-MRI for the assessment of myocardial peak systolic and diastolic velocities, with a small difference between the 2 techniques; 2) a strong correlation was also found between TDI and VE-MRI for the assessment of Ts and the agreement between the 2 techniques was excellent when patients were categorized according to the severity of LV dyssynchrony; 3) excellent correlation and agreement was also found between the 2 techniques for LV filling pressures estimation (using the E/E' ratio).

Tissue Doppler imaging has been used in several studies [15–18] to measure longitudinal myocardial peak systolic velocities, providing quantitative information on regional LV systolic function and avoiding the disadvantages of observer-dependent interpretation. In addition, this technique plays a fundamental role in the diagnostic algorithm for LV diastolic dysfunction [9]. In particular, the E/E' ratio has been demonstrated to correlate closely with LV filling pressures [8;10] and to be a powerful predictor of survival [19]. Cardiac MRI is widely accepted as the gold standard for the assessment of LV volumes and function. However, beyond the analysis of transmitral flow pattern [20], an accurate and clinically applicable method to assess LV diastolic function with MRI is still lacking. When applied for myocardial wall motion measurement, VE-MRI may obtain similar data to that provided by TDI, without the limitations of the acoustical window, and can be used for the assessment of myocardial velocities and the E/E' ratio. An initial study by Delfino et al [2] compared TDI and VE-MRI for the assessment of longitudinal myocardial velocities (PSV and E'PDV) in 10 normal volunteers and in 10 patients scheduled for CRT. The authors reported a good correlation (r = 0.86) between the 2 techniques, but a large bias in the value of peak velocities was found (-4.4±3.7 cm/sec). In the present study an excellent correlation between both methods was confirmed (r = 0.95 for PSV and PDV), including a larger sample size, both basal and mid LV segments and using optimized image acquisition and analysis. A much smaller difference was noted between the 2 techniques: -1.1±1.1 cm/s for PSV and -0.45±1.03 cm/s for PDV, probably due to technical differences between the 2 studies. First, Delfino and co-workers positioned the sample area in the VE-MRI acquisition on a short-axis view at 70% of the distance from apex, while in the TDI acquisition velocities were acquired at the basal level of the apical 4-chamber view. This may lead to potential errors due to the shifting of the myocardial wall, especially during systole. In the present study the sample area was placed in a 4-chamber orientation in both TDI and VE-MRI and the position of the samples was manually corrected in each phase in the VE-MRI. Second, in the current study the temporal resolution of VE-MRI was optimized and was comparable to that of TDI, whereas in the previous study the temporal resolution of VE-MRI was lower (30-40 ms). The residual small bias between the 2 techniques can be explained by acoustical window limits and non-optimal alignment between the wall and the ultrasound beam for TDI and potential phase errors and partial volume effects for MRI. These results need to be confirmed in larger studies that should test the applicability of MRI for these measurements in different centers. Unfortunately, at present a non-invasive gold standard is not available for the assessment of myocardial velocities. However, both VE-MRI and TDI have been previously validated in phantom models [21;22] and the strong correlation between the 2 techniques observed in the present study allows a reciprocal validation. More important, the excellent agreement found in the present study for the assessment of LV diastolic function (using the E/E' ratio), supports the interchangeable use of both techniques in this clinical setting. However, the lack of a direct comparison with invasive measurements of LV filling pressures is a study limitation.

Several single-center studies suggested that LV dyssynchrony may play an important role in the prediction of a favourable response to CRT [23], thereby improving the selection of candidates to CRT. The most frequently used technique to assess LV dyssynchrony is TDI and various parameters derived from myocardial velocity curves have been proposed for this purpose [6;24–26]. However, recently published results of the first multi-center trial suggested that TDI and conventional echocardiographic measures have limited value for prediction of response to CRT, mainly due to a marked inter-laboratory variability for the assessment of these parameters [27]. Cardiac MRI provides important information for the selection of potential candidates for CRT [28]. In addition to an accurate quantification of LV size and function, MRI allows a precise assessment of the location and extent of scar tissue, which has been demonstrated to be important for prediction of response to CRT [28]. Reliable and reproducible quantification of LV dyssynchrony would strengthen the role of cardiac MRI in the evaluation of potential candidates for CRT especially in patients with ischemic cardiomyopathy. Preliminary studies compared TDI and VE-MRI for the assessment of LV dyssynchrony. Delfino et al [2] evaluated 10 patients scheduled for CRT and reported an excellent correlation between both techniques without any significant bias in the measurement of Ts. However, only 2 patients of the study population exhibited significant LV dyssynchrony. Westenberg et al [3] confirmed the good correlation and agreement between TDI and VE-MRI in LV dyssynchrony classification of 20 non-ischemic patients. The present study extended previous findings [2;3] to a larger group of patients with heart failure secondary to ischemic cardiomyopathy and noted similar good results. These results confirm that MRI may be a valuable tool for patient selection prior to CRT, providing a comprehensive evaluation of LV size and function, extent of scar tissue and LV dyssynchrony.

However, several limitations for the applicability of cardiac MRI should be addressed. First, claustrophobia, cardiac arrhythmias, and cardiac devices limit the use of this technique. Second, MRI can not provide follow-up information after CRT implantation and is not as readily available as TDI echocardiography.

REFERENCES

1. Paelinck BP, de Roos A, Bax JJ et al. Feasibility of tissue magnetic resonance imaging: a pilot study in comparison with tissue Doppler imaging and invasive measurement. *J Am Coll Cardiol* 2005;45:1109-1116.
2. Delfino JG, Bhasin M, Cole R et al. Comparison of myocardial velocities obtained with magnetic resonance phase velocity mapping and tissue Doppler imaging in normal subjects and patients with left ventricular dyssynchrony. *J Magn Reson Imaging* 2006;24:304-311.
3. Westenberg JJ, Lamb HJ, van der Geest RJ et al. Assessment of left ventricular dyssynchrony in patients with conduction delay and idiopathic dilated cardiomyopathy: head-to-head comparison between tissue doppler imaging and velocity-encoded magnetic resonance imaging. *J Am Coll Cardiol* 2006;47:2042-2048.
4. Schiller NB, Shah PM, Crawford M et al. Recommendations for quantitation of the left ventricle by two-dimensional echocardiography. American Society of Echocardiography Committee on Standards, Subcommittee on Quantitation of Two-Dimensional Echocardiograms. *J Am Soc Echocardiogr* 1989;2:358-367.
5. Cerqueira MD, Weissman NJ, Dilsizian V et al. Standardized myocardial segmentation and nomenclature for tomographic imaging of the heart: a statement for healthcare professionals from the Cardiac Imaging Committee of the Council on Clinical Cardiology of the American Heart Association. *Circulation* 2002;105:539-542.
6. Bax JJ, Marwick TH, Molhoek SG et al. Left ventricular dyssynchrony predicts benefit of cardiac resynchronization therapy in patients with end-stage heart failure before pacemaker implantation. *Am J Cardiol* 2003;92:1238-1240.
7. Bleeker GB, Schalij MJ, Molhoek SG et al. Relationship between QRS duration and left ventricular dyssynchrony in patients with end-stage heart failure. *J Cardiovasc Electrophysiol* 2004;15:544-549.
8. Nagueh SF, Middleton KJ, Kopelen HA, Zoghbi WA, Quinones MA. Doppler tissue imaging: a noninvasive technique for evaluation of left ventricular relaxation and estimation of filling pressures. *J Am Coll Cardiol* 1997;30:1527-1533.
9. Paulus WJ, Tschope C, Sanderson JE et al. How to diagnose diastolic heart failure: a consensus statement on the diagnosis of heart failure with normal left ventricular ejection fraction by the Heart Failure and Echocardiography Associations of the European Society of Cardiology. *Eur Heart J* 2007;28:2539-2550.
10. Ommen SR, Nishimura RA, Appleton CP et al. Clinical utility of Doppler echocardiography and tissue Doppler imaging in the estimation of left ventricular filling pressures: A comparative simultaneous Doppler-catheterization study. *Circulation* 2000;102:1788-1794.
11. Steenbeck J, Pruessmann K. Technical developments in cardiac MRI: 2000 update. *Rays* 2001;26:15-34.
12. Van Rossum AC, Visser FC, Van Eenige MJ, Valk J, Roos JP. Oblique views in magnetic resonance imaging of the heart by combined axial rotations. *Acta Radiol* 1987;28:497-503.
13. Pelc NJ, Bernstein MA, Shimakawa A, Glover GH. Encoding strategies for three-direction phase-contrast MR imaging of flow. *J Magn Reson Imaging* 1991;1:405-413.
14. Sondergaard L, Thomsen C, Stahlberg F et al. Mitral and aortic valvular flow: quantification with MR phase mapping. *J Magn Reson Imaging* 1992;2:295-302.

15. Alam M, Witt N, Nordlander R, Samad BA. Detection of abnormal left ventricular function by Doppler tissue imaging in patients with a first myocardial infarction and showing normal function assessed by conventional echocardiography. *Eur J Echocardiogr* 2007;8:37-41.
16. Bountioukos M, Schinkel AF, Bax JJ, Lampropoulos S, Poldermans D. The impact of hypertension on systolic and diastolic left ventricular function. A tissue Doppler echocardiographic study. *Am Heart J* 2006;151:1323-12.
17. Strotmann JM, Hatle L, Sutherland GR. Doppler myocardial imaging in the assessment of normal and ischemic myocardial function--past, present and future. *Int J Cardiovasc Imaging* 2001;17:89-98.
18. Sun JP, Popovic ZB, Greenberg NL et al. Noninvasive quantification of regional myocardial function using Doppler-derived velocity, displacement, strain rate, and strain in healthy volunteers: effects of aging. *J Am Soc Echocardiogr* 2004;17:132-138.
19. Hillis GS, Moller JE, Pellikka PA et al. Noninvasive estimation of left ventricular filling pressure by E/e' is a powerful predictor of survival after acute myocardial infarction. *J Am Coll Cardiol* 2004;43:360-367.
20. Paelinck BP, Lamb HJ, Bax JJ, van der Wall EE, de Roos A. Assessment of diastolic function by cardiovascular magnetic resonance. *Am Heart J* 2002;144:198-205.
21. Lee VS, Spritzer CE, Carroll BA et al. Flow quantification using fast cine phase-contrast MR imaging, conventional cine phase-contrast MR imaging, and Doppler sonography: in vitro and in vivo validation. *AJR Am J Roentgenol* 1997;169:1125-1131.
22. Fleming AD, McDicken WN, Sutherland GR, Hoskins PR. Assessment of colour Doppler tissue imaging using test-phantoms. *Ultrasound Med Biol* 1994;20:937-951.
23. Bax JJ, Abraham T, Barold SS et al. Cardiac resynchronization therapy: Part 1--issues before device implantation. *J Am Coll Cardiol* 2005;46:2153-2167.
24. Bax JJ, Bleeker GB, Marwick TH et al. Left ventricular dyssynchrony predicts response and prognosis after cardiac resynchronization therapy. *J Am Coll Cardiol* 2004;44:1834-1840.
25. Yu CM, Chau E, Sanderson JE et al. Tissue Doppler echocardiographic evidence of reverse remodeling and improved synchronicity by simultaneously delaying regional contraction after biventricular pacing therapy in heart failure. *Circulation* 2002;105:438-445.
26. Sanderson JE. Systolic and diastolic ventricular dyssynchrony in systolic and diastolic heart failure. *J Am Coll Cardiol* 2007;49:106-108.
27. Chung ES, Leon AR, Tavazzi L et al. Results of the Predictors of Response to CRT (PROSPECT) Trial. *Circulation* 2008;117:2608-2616.
28. Bleeker GB, Kaandorp TA, Lamb HJ et al. Effect of posterolateral scar tissue on clinical and echocardiographic improvement after cardiac resynchronization therapy. *Circulation* 2006;113:969-976.

CHAPTER 16

Magnetic resonance imaging and response to cardiac resynchronization therapy: relative merits of left ventricular dyssynchrony and scar tissue

N Ajmone Marsan, J JM Westenberg, C Ypenburg, R J van Bommel, S Roes, V Delgado, L F Tops, R J van der Geest, E Boersma, A de Roos, M J Schalij, and J J Bax

Eur Heart J 2009;30:2360-7.

ABSTRACT

Objectives: To assess the relative value of a novel measure of left ventricular (LV) dyssynchrony derived from magnetic resonance imaging (MRI) and the extent of scar tissue for prediction of response to cardiac resynchronization therapy (CRT).

Methods: A total of 35 heart failure patients scheduled for CRT were included. LV dyssynchrony was defined as the standard deviation of 16 segment time-to-maximum radial wall thickness (SDt-16) obtained from a cine-set of short-axis slices. Delayed-enhanced MRI was performed for scar analysis. Echocardiography was used to determine response to CRT (reduction ≥15% in LV end-systolic volume 6 months after implantation).

Results: At follow-up, 21 patients (60%) were classified as responders. On MRI, SDt-16 was significantly higher in responders compared to non-responders (median 97 ms vs. 60 ms, $p < 0.001$) while the total extent of scar was larger in non-responders (median 35% vs. 3% in responders, $p < 0.001$). At the logistic regression analysis, SDt-16 was directly associated (OR = 6.3, 95%CI 3.1-9.9, $p < 0.001$) and the total extent of scar was inversely associated (OR = 0.52, 95%CI 0.43-0.87, $p < 0.001$) with response to CRT.

Conclusions: MRI offers the unique opportunity to assess LV dyssynchrony and scar extent in a single session. Both these parameters are important predictors of echocardiographic response to CRT.

INTRODUCTION

Magnetic resonance imaging (MRI) can provide a comprehensive assessment of cardiac morphology and function. Accordingly, MRI has been applied extensively for the evaluation of heart failure patients. In addition, MRI may be important for selection of candidates for cardiac resynchronization therapy (CRT). It has been demonstrated that a favorable response to CRT may depend on different factors, including the severity of left ventricular (LV) dyssynchrony, and the extent and location of scar tissue in the LV [1]. Various methods for assessment of LV dyssynchrony by MRI have recently been reported [2–5] and MRI is particularly suited for assessment of scar tissue. [6] Which of these parameters (dyssynchrony, scar tissue) is more important for response to CRT is still unclear.

In the present study, a novel approach to detect LV dyssynchrony with MRI is evaluated in patients undergoing CRT. In addition, the extent and location of scar tissue is assessed using contrast-enhanced MRI. Subsequently, the relative merits of LV dyssynchrony and scar tissue for prediction of response to CRT are evaluated.

METHODS

Patient population and protocol

The study population consisted of 50 consecutive heart failure patients scheduled for CRT according to the current guidelines: New York Heart Association (NYHA) functional class III-IV despite optimal medical therapy, LV ejection fraction (EF) ≤35% and QRS duration ≥120 ms. Patients with recent myocardial infarction (<3 months), decompensated heart failure, previous cardiac pacemaker/ICD or intracranial clips were excluded. Six patients did not undergo MRI because of atrial fibrillation and 5 patients could not complete the image acquisition because of claustrophobia. The image quality was not considered good enough for further analysis in 4 patients, due to the poor compliance of the patient during the breath-holding procedure or frequent ectopic beats. The remaining 35 patients constituted the current study population and were enrolled within 6 months. Etiology was considered ischemic in the presence of significant coronary artery disease (>50% stenosis in ≥1 major epicardial coronary artery) on coronary angiography and/or history of myocardial infarction or previous revascularization.

Magnetic resonance imaging was performed before CRT to assess LV dyssynchrony using a novel approach (details see below). Normal values for this novel MRI technique to assess LV dyssynchrony were derived from 20 subjects without echocardiographic evidence of structural heart disease and matched for age and gender. For comparison, LV dyssynchrony was also evaluated at baseline by radial strain speckle tracking analysis.

In the patients, the extent and location of scar tissue was derived from contrast-enhanced MRI. In addition, as part of the routine clinical work-up, echocardiography and assessment of clinical status (including NYHA class, 6-minute walking distance and Minnesota quality-of-life score) were performed at baseline and 6 months (±2 weeks) after CRT implantation, to evaluate response to CRT.

For MRI dyssynchrony analysis, all subjects gave informed consent and the protocol was approved by the institutional review board.

Magnetic resonance imaging

Data acquisition

Data acquisition was performed on a 1.5 T scanner equipped with powertrack 6000 gradients (Gyroscan ACS-NT/Intera, Philips Medical Systems, Best, The Netherlands), using the body coil for transmission and a 5 element phased array cardiac-coil placed on the chest for signal reception. Scout images and 2- and 4-chamber acquisitions were performed (conform standard cardiac MR protocols [7]) needed for planning. A cine-set of 10-12 multi-slice images were acquired in short-axis orientation, covering the complete LV from apex to base. Each slice was acquired in a single breath-hold. Segmented gradient-echo (turbo field echo) was used, with parallel imaging (Sensitivity Encoding, acceleration factor 2) [8] and steady-state free-precession [9] for fast imaging and optimal image contrast. The following imaging parameters were used: slice thickness of the imaging planes = 10 mm, with no gap; Field-of-View = 440 mm; 80% scan percentage, scan matrix = 256 × 256, with reconstructed voxels of 1.56 × 1.56 × 10.0 mm; flip angle α = 35°; TR/TE = 3.6/1.7. One signal average was used. Gated cardiac synchronization was applied and 40 phases per cardiac cycle were reconstructed, yielding a temporal resolution of around 20 ms.

In the patients, contrast-enhanced images were acquired 15 minutes after bolus injection of gadolinium diethylenetriamine pentaacetetic acid (Magnevist, Schering/Berlex, Berlin, Germany; 0.15 mmol/Kg) with an inversion recovery gradient echo sequence (400 x 400 mm^2 Field-of-View; 256 x 256 matrix size, 5-mm slice thickness with gap of -5mm, 15° flip angle, echo time 1.36 ms and 4.53-ms repetition time) [10]. The inversion time was determined with a Look-Locker sequence [11] and was typically in the range of 250-300 ms. Depending on the patient's heart rate and heart size, 20 to 24 slices in the short-axis orientation were obtained in 2 breath-hold acquisitions of approximately 15 seconds (Figure 1).

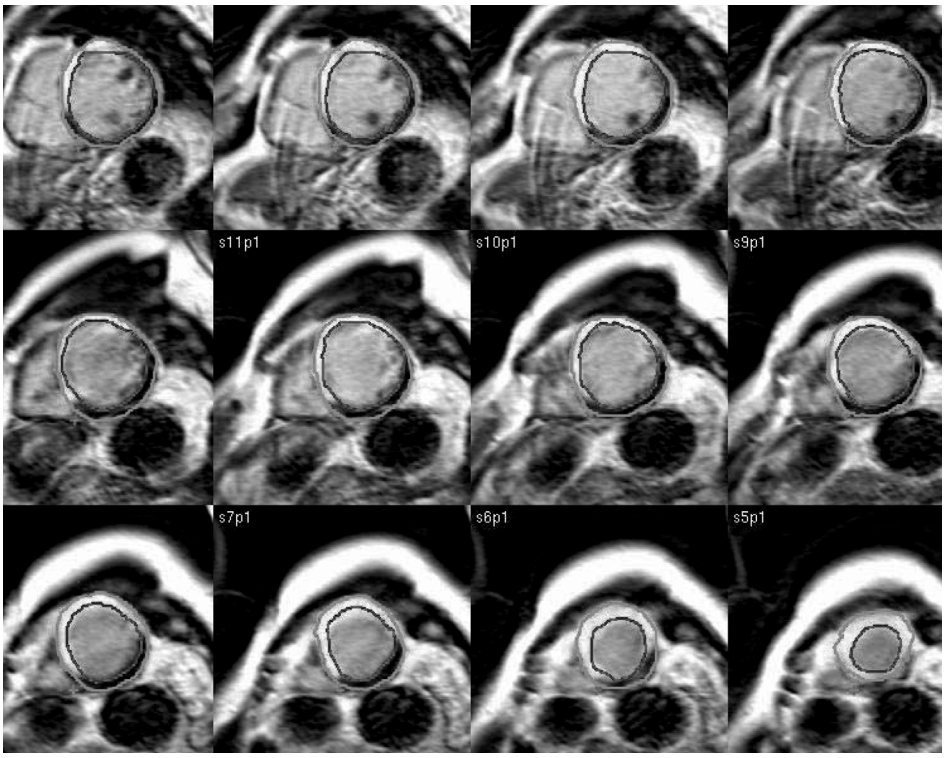


Figure 1. Short-axis slices obtained with contrast-enhanced magnetic resonance imaging showing a large transmural area of scarred myocardium (bright/white) at the level of the left ventricular septum, anterior wall and apex.

LV dyssynchrony analysis

From the complete short-axis dataset, 3 slices were selected representing the basal, mid-ventricular and apical level. In these slices, epicardial and endocardial contours (excluding trabeculations and papillary muscles) were drawn for all phases, using QMass analytical software package (Medis, Leiden, the Netherlands). According to the standard 16-segment model [12], the basal and mid-ventricular short-axis slices were divided into 6 segments, while the apical short-axis slice was divided into 4 segments. For each segment, a radial wall thickness curve was automatically plotted and the time from the R wave on the ECG to maximum wall thickness on MRI (Tt) was determined (Figure 2). The analysis of LV dyssynchrony included also a maximum wall thickness eventually occurring after the systolic phase. The standard deviation of 16 segments Tt (SDt-16) was calculated as a marker of global LV dyssynchrony. The post-processing of the images required between 6 and 10 minutes.

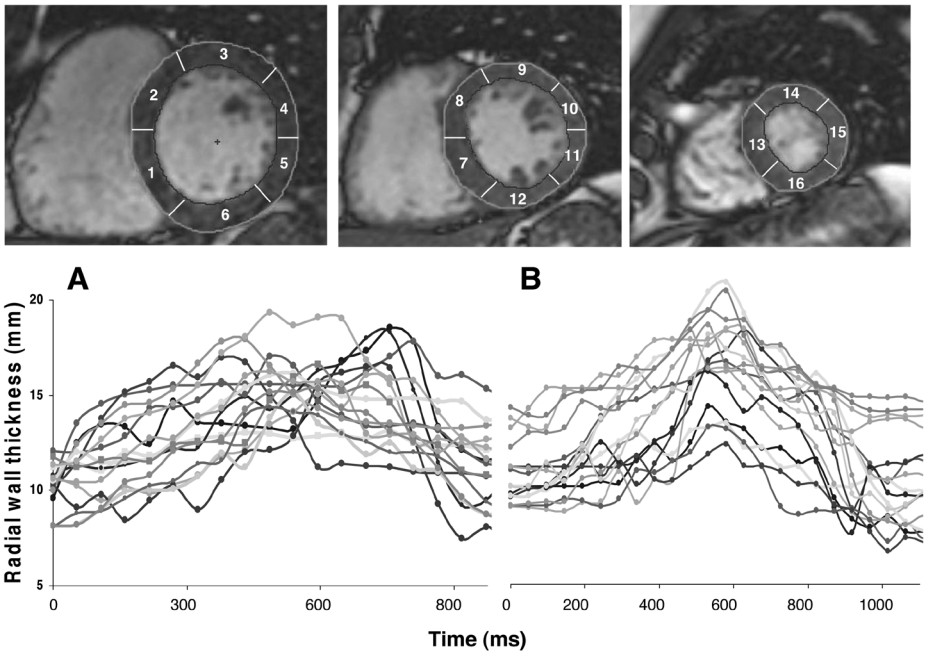


Figure 2. Assessment of left ventricular (LV) dyssynchrony using magnetic resonance imaging. From the complete LV short-axis dataset, 3 slices are selected representing the basal, mid-ventricular and apical level and divided into 16 standard segments. In these slices, epicardial and endocardial contours are drawn for all phases (upper panel). For each segment a radial wall thickness curve is plotted and the time from the R wave on the ECG to maximum wall thickness (Tt) is measured. The standard deviation of 16 segments Tt (SDt-16) was calculated as a marker of global LV dyssynchrony. **Panel A** shows an example of a patient with a significant LV dyssynchrony (SDt-16 = 98 ms), while **Panel B** shows an example of a patient with synchronous LV contraction (SDt-16 = 40 ms).

Myocardial scar analysis

The endocardial and the epicardial borders were traced on short-axis slices (from the contrast-enhanced MRI dataset) and each slice was divided according to the standard myocardial segmentation [12]. Hyperenhanced regions were defined by selecting a region-of-interest inside the normal myocardium and thresholding the window setting at 5 SD above the mean signal intensity, as previously reported [13]. Normal myocardium was defined by the absence of any regional contrast enhancement on visual inspection. The total LV myocardial mass and the amount of scar tissue (expressed in grams) were quantified using QMass (Medis). The following parameters were derived: 1) total extent of scar, expressed as percentage of LV mass; 2) scar transmurality, defined as scar exceeding >50% of the myocardial wall, in any of the 16 segments [14]; 3) scar location, considering both transmural and non-transmural scar. In particular, scar location was classified in 3 groups according to the typical coronary artery territories [15]: antero-septum/anterior/apex (LAD), infero-septum/inferior (RCA) and postero-lateral (LCX). The typical non-ischemic mid-wall pattern was also considered as a fourth group.

Echocardiography

All patients were imaged in left lateral decubitus position using a commercially available system (Vingmed Vivid 7, General Electric Healthcare, Horten, Norway). Images were obtained using a 3.5-MHz transducer and digitally stored in cine-loop format. The analysis was performed offline using EchoPAC version 6.0.1 (General Electric-Vingmed). From the conventional apical 2- and 4-chamber views, LV end-diastolic (EDV), LV end-systolic volume (ESV) and LVEF were calculated using the biplane method of discs (modified Simpson's rule) [15]. In addition, from the short axis image of the LV at the level of the papillary muscles, LV dyssynchrony was evaluated by radial strain speckle tracking analysis, measuring the anteroseptal-to-posterior wall delay and the standard deviation of time to peak radial strain of 6 segments (SD-6s), as previously described [16;17].

At 6 months follow-up, patients were divided into responders or non-responders, based on a reduction ≥15% in LVESV [18].

Reproducibility of LVESV measurement was assessed on 20 randomly selected patients, using Bland-Altman analysis and repeating the measurement few days later by the same observer and by a second independent observer. According to the Bland-Altman analysis, the results were expressed as mean difference±2 standard deviation. The intra-observer agreement was 0.6±8.3 ml ($p = 0.12$), whereas the inter-observer agreement was 1.1±10.1 ml ($p = 0.078$).

The severity of mitral regurgitation was graded semi-quantitatively from color-Doppler images obtained in the parasternal long-axis and apical 4-chamber views and characterized as follows: absent, mild (ratio jet area/LA area <20%), moderate (jet area/LA area 20% to 40%) and severe (jet area/LA area >40%) [19].

CRT implantation

The LV pacing lead was inserted transvenously via the subclavian route. First, a coronary sinus venogram was obtained during occlusion of the coronary sinus with a balloon catheter. Next, the LV pacing lead (Easytrak, Boston Scientific, St. Paul, Minnesota, or Attain-SD, Medtronic, Minneapolis, Minnesota) was inserted into the coronary sinus with the help of an 8F guiding catheter and positioned as far as possible in the venous system, preferably in the (postero-) lateral vein. The final position of the LV pacing lead was assessed with cine fluoroscopy as previously described [20] and the relation between LV lead position and location of transmural scar was assessed. The right atrial and right ventricular leads were positioned conventionally. All patients received a biventricular pacemaker with cardioverter-defibrillator back-up (Contak Renewal 4RF, Boston Scientific; or InSync Sentry, Medtronic Inc.).

Statistical analysis

Clinical and echocardiographic (including speckle tracking analysis) continuous variables are presented as mean±standard deviation. The MRI continuous variables were not normally distributed (as evaluated by Kolmogorov-Smirnov tests) and therefore presented as medians and corresponding 25th and 75th percentiles. Categorical data are summarized as frequencies and percentages, and Wilcoxon-Mann-Whitney tests, chi-square tests with Yates' correction or Fisher exact tests were used for appropriate comparisons. Pearson's correlation analysis was performed to evaluate the relation between LV dyssynchrony measured by MRI and speckle tracking strain analysis. To determine the relationship between patients' characteristics at baseline and echocardiographic response to CRT, univariable logistic regression analysis was applied (odds ratios with their corresponding 95% confidence intervals [CI] are reported).

The reproducibility of SDt-16 measurement was assessed by Bland-Altman analysis for repeated measures (mean differences and 95% limits of agreement are reported) using a randomly selected dataset of 10 patients and 5 normal subjects (total of 240 segments). The measurements derived by a first observer were compared with the results calculated 1 month later by the same operator (intra-observer agreement) and by a second independent observer (inter-observer agreement). For all tests, a p-value <0.05 was considered significant. A statistical software program SPSS 12.0 (SPSS Inc, Chicago, Illinois) was used for statistical analysis.

Table 1. Baseline characteristics of the study population: patients versus control subjects.

	Control subjects (n = 20)	Patients (n = 35)	p-value
Age, years	62±8	63±11	0.61
Gender, male/female	15/5	26/9	0.47
NYHA class	-	3.0±0.5	-
QRS duration, ms	91±9	145±33	<0.001
Etiology, n (%)			
Ischemic/Non-ischemic	-	20 (57)/15 (43)	-
Medication, n (%)			
ACE Inhibitors	-	32 (91)	-
ß-blockers	-	30 (86)	-
Diuretics and /or Spironolactone	-	32 (91)	-
LVEDV, ml	87±30	230±70	<0.001
LVESV, ml	35±13	177±70	<0.001
LVEF, %	62±7	24±8	<0.001
MR moderate/severe, n (%)	-	11 (31)	-

EDV: end-diastolic volume, EF: ejection fraction, ESV: end-systolic volume, LV: left ventricle, MR: mitral regurgitation, NYHA: New York Heart Association.

RESULTS

Baseline characteristics of the 35 patients are summarized in Table 1. The etiology of cardiomyopathy was ischemic in 20 (57%) patients. Mean QRS duration was 145±33 ms. Standard echocardiography revealed severe LV dilatation (mean LVEDV 230±70 ml) with depressed LV systolic function (mean LVEF 24±8%).

Magnetic resonance imaging

LV dyssynchrony

Reliable radial wall thickness curves were obtained in 793 (91%) of 880 segments. Intra- and inter-observer agreements for SDt-16 measurement were good: 1.75 ms (95% limits of agreement 18.6/-15.15 ms; p = 0.62) and 2.23 ms (95% limits of agreement 27.8/-23.3 ms; p = 0.56), respectively (Figure 3).

Left ventricular dyssynchrony, as measured by SDt-16, was significantly larger in patients (median 88 ms [25th and 75th percentiles 67 and 99 ms]) as compared to control subjects (median 26 ms [25th and 75th percentiles 22 and 31 ms], p <0.001).

Similarly, echocardiographic radial strain speckle tracking analysis showed a significant LV dyssynchrony in the patients: the anteroseptal-to-posterior wall delay was 175±90 ms and SD-6s 90±52 ms.

Of note, according to the previously reported definition of significant LV dyssynchrony [16;17], 24 patients (68.5%) showed an anteroseptal-to-posterior wall delay ≥130 ms and 19 patients (54%) a SD-6s ≥76 ms. Furthermore, a good correlation was found between LV dyssynchrony

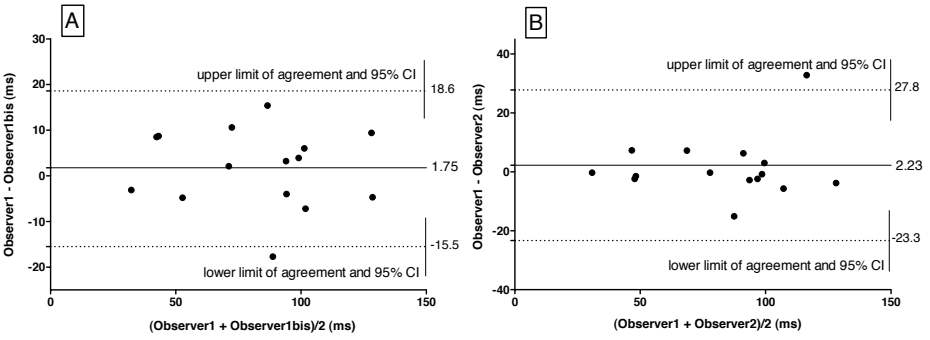


Figure 3. Intra- (Panel A) and inter-observer (Panel B) agreements for SDt-16 measurement calculated with Bland-Altman analysis for repeated measures. The mean bias, the 95% limits of agreement and their associated 95% confidence intervals are reported.

measured by MRI (SDt-16) and LV dyssynchrony derived from speckle tracking strain analysis ($r = 0.60$, $p < 0.001$ for anteroseptal-to-posterior wall delay, and $r = 0.77$, $p < 0.001$ for SD-6s).

Myocardial scar

Of the 35 patients, 24 (69%) had scar tissue on contrast-enhanced MRI. In these patients, the median total extent of scar was 12% (25^{th} and 75^{th} percentiles 4 and 36%) and transmural scar was present in 14 (40%) patients. In particular, scar involved most frequently the septum/anterior/apex region (8 patients, 40%) and the inferior wall (7 patients, 35%), while a postero-lateral scar was detected in 5 (25%) patients. Of interest, in 4 (27%) patients with non-ischemic cardiomyopathy, a mid-wall scar pattern was detected.

Prediction of response to CRT

Six months after CRT implantation, a reduction in LVESV ≥15% was noted in 21 patients (60%) who were classified as responders to CRT. Responders showed a significant improvement in clinical parameters (NYHA class, 6-minute walking distance, quality-of-life score) after 6 months of CRT, whereas non-responders did not improve, except for a modest improvement in NYHA class (Table 2). Responders also exhibited an improvement in echocardiographic parameters (LVESV by definition, but also an improvement in LVEDV and LVEF), whereas non-responders did not improve (Table 2).

No significant differences in baseline clinical and echocardiographic characteristics were noted between responders and non-responders (Table 2), except for a higher prevalence of ischemic etiology of heart failure in non-responders (86% vs. 38%, $p = 0.007$).

On MRI, the SDt-16 was significantly larger in responders compared to non-responders (median 97 ms [25^{th} and 75^{th} percentiles 90 and 106 ms] vs. 60 ms [25^{th} and 75^{th} percentiles 47 and 71 ms], $p < 0.001$) (Table 3). Similarly, on echocardiography the anteroseptal-to-posterior wall delay (212.4±76.5 ms vs. 97.6±64.6 ms, $p < 0.001$) and SD-6s (110.7±46.9 ms vs. 47.7±31.9 ms, $p < 0.001$) were larger in responders as compared to non-responders.

Furthermore, the total extent of scar tissue was significantly larger in non-responders as compared to responders to CRT, with a median of 35% (25^{th} and 75^{th} percentiles 12 and 48%) for non-responders and a median of 3% (25^{th} and 75^{th} percentiles 0 and 8%) for responders ($p < 0.001$). Similarly, a transmural scar was present in 71% of non-responders and in 19% of responders ($p = 0.003$) (Table 3).

No significant difference was found between responders and non-responders for scar location (Table 3). However, a match between LV lead position and a transmural scar was found in 8 (57%) non-responders and in 3 (14%) responders ($p = 0.002$, Table 3).

Table 2. Responders versus non-responders: clinical and echocardiographic characteristics before and 6 months after CRT implantation.

	Responders n = 21	Non-responders n = 14	p–value
Age, years	64±9	62±12	0.47
Gender, male/female	16/5	10/4	0.32
Ischemic/Non-ischemic, n (%)	8(38)/13(62)	12(86)/2(14)	0.007
QRS duration, ms	154±29	142±25	0.23
NYHA class			
Baseline	3.2±0.6	3.0±0.4	0.41
After implantation	1.7±0.9*	2.3±0.7*	0.036
6-MWT, m			
Baseline	349±158	322±140	0.25
After implantation	402±71*	336±160	0.21
Quality of life score			
Baseline	30±13	32±23	0.53
After implantation	16±12*	30±20	0.029
LVEDV, ml			
Baseline	243±100	207±54	0.065
After implantation	195±83*	206±67	<0.001
LVESV, ml			
Baseline	187±92	158±50	0.066
After implantation	129±72*	158±53	<0.001
LVEF, %			
Baseline	23±7	24±9	0.31
After implantation	34±10*	23±10	<0.001
MR (moderate/severe), n (%)			
Baseline	6 (28)	5 (36)	0.44
After implantation	2 (10)	5 (36)	0.28

*= p <0.001 baseline versus follow-up. 6-MWT: 6 minutes walk test. For the rest of abbreviations see Table 1.

Table 3. Responders versus non-responders: left ventricular dyssynchrony and myocardial scar assessed by cardiac magnetic resonance imaging.

	Responders n = 21	Non-responders n = 14	p-value
Total scar extent, % (25th,75th percentiles)	3 (0-8)	35 (12-48)	<0.001
Patients with scar, n (%)	11 (52)	13 (93)	<0.001
Transmural scar, n (%)	4 (19)	10 (71)	0.003
Non transmural scar, n (%)	7 (33)	3 (21)	0.079
Scar location, n (%)			0.064
Septum/anterior/apex	1 (5)	7 (50)	
Inferior	6 (28)	1 (7)	
Postero-lateral	1 (5)	4 (29)	
Mid-wall	3 (14)	1 (7)	
Match LV lead/transmural scar, n (%)	3 (14)	8 (57)	0.002
SDt-16, ms (25th, 75th percentiles)	97 (90-106)	60 (47-71)	<0.001

SDt-16: standard deviation of 16 segment time-to-peak radial thickness.

Importantly at the univariable logistic regression analysis, SDt-16 was strongly associated with response to CRT (OR = 6.3, 95% CI 3.1-9.9, p <0.001), while the total extent of scar was significantly associated with non-response to CRT (OR = 0.52, 95% CI 0.43-0.87, p <0.001). The presence of a match between the LV lead position and a transmural scar was also a significantly associated with non-response to CRT (OR = 0.125, 95% CI 0.031-0.630, p = 0.012). Among the other clinical and echocardiographic variables, only the QRS duration was significantly associated with response to CRT (OR = 1.03, 95% CI 1.01-1.05, p = 0.048).

DISCUSSION

The main findings of the current study can be summarized as follows: 1) LV dyssynchrony, measured by SDt-16, was significantly larger in heart failure patients as compared to normal individuals and showed a good correlation with LV dyssynchrony measured by speckle tracking strain analysis; 2) SDt-16, total extent of scar and the presence of a match between LV lead position and a transmural scar were strongly associated with response to CRT.

MRI for the assessment of LV dyssynchrony

Several single-center studies have suggested that the presence of significant baseline LV dyssynchrony may predict favorable response to CRT and thereby improve selection of potential candidates [1]. Echocardiography, and in particular tissue Doppler imaging (TDI), has been used extensively to directly assess LV mechanical dyssynchrony [1]. However, the recently published results of the PROSPECT trial suggested that standard echocardiography and TDI have limited value for prediction of response to CRT, mainly due to high inter-corelab variability [18]. However, measurements of LV dyssynchrony derived from novel echocardiographic techniques and non-echocardiographic imaging modalities were not included in this trial. In particular, several techniques to assess LV dyssynchrony using MRI are emerging. Myocardial tissue tagging provides highly reproducible data on myocardial strain not only in the longitudinal, but also in the radial and circumferential direction [2;3]. However, the clinical applicability of this method is limited by the time-consuming post-processing of the dataset. Also, velocity-encoded MRI has demonstrated good reproducibility and excellent agreement with TDI for assessment of the electromechanical delay between the LV septum and lateral wall [4]. However, this method is mainly limited by the fact that it can include in the analysis only the basal and mid LV segments and it evaluates myocardial velocities and not measurements of active deformation. More recently, MRI tissue synchronization imaging has been proposed by Chalil et al. as a novel technique for the assessment of LV dyssynchrony and the prediction of mortality and morbidity after CRT [5]. This is a relatively simple and clinically applicable

approach that tracks only the endocardium using standard short-axis views and includes the whole LV in the analysis. However, it quantifies radial wall motion and therefore is still limited by the incapability to distinguish between active deformation, passive motion and noise.

In the present study, a novel MRI method that involves both endocardial and epicardial border detection, was used. By analyzing myocardial wall thickness instead of myocardial motion, it provides accurate information on LV regional active deformation (even when it occurs after the systolic phase) and therefore may reflect true LV dyssynchrony. Furthermore, this method does not require specific acquisitions, but only involves the standard cine-set of LV short-axis slices, from which radial wall thickness is derived.

Recent studies, using speckle tracking echocardiography, suggested that LV dyssynchrony measured by radial strain analysis is a good predictor of response to CRT and appeared superior over longitudinal and circumferential strain [16;17]. Similarly, in the current study, SDt-16 demonstrated to be strongly associated with significant LV reverse remodeling at mid-term follow-up after CRT implantation. Future studies need to compare this approach with other MRI approaches for the assessment of LV dyssynchrony.

In addition, this measurement demonstrated an excellent reproducibility, although assessed in a single-center study and on the same dataset (instead of repeating the MRI scan in the same patient).

MRI for the assessment of myocardial scar

In addition to LV dyssynchrony, other factors may play a significant role in the prediction of response to CRT [1]. Initial single-center studies suggested that the amount and spatial distribution of myocardial scar may be important determinants of response to CRT [14;21–23]. In particular, the presence of extensive scar tissue seems to be associated with limited LV remodeling and improvement in function after CRT [14;23]. However, whether the scar extent has a predictive value for response to CRT in addition to the degree of LV dyssynchrony is still unknown, since the previous studies only focused on myocardial scar analysis without considering the potential interaction with LV dyssynchrony [14;23]. In the present study, the total extent of scar was found to be strongly associated with echocardiographic response to CRT as well as LV dyssynchrony (measured with MRI). These findings confirm and support the evaluation of both parameters (myocardial scar and LV dyssynchrony) for the selection of the candidates to CRT. However, the results of the present study are not sufficient to solve more complicate clinical cases, in which the analysis of LV dyssynchrony and scar extent may provide discordant indication for CRT implantation (substantial LV dyssynchrony but extensive scar or small scar with no substantial LV dyssynchrony). Consequently, an individual and comprehensive evaluation of each patient that undergoes to CRT, including clinical, echocardiographic and MRI variables, is fundamental.

In addition, the location of a transmural scar in the postero-lateral region, where the LV pacing lead is usually positioned, seems to play an important role in the efficacy of CRT [21]. However, White et al. have also demonstrated that a septal scar larger than 40% of the total mass was associated with unfavorable response to CRT [23]. In the current study, the scar location per se did not show a significant effect on CRT efficacy. However, a significant inverse relation was noted between the response to CRT and the presence of a match between the LV lead position and a transmural scar location.

Clinical implications

The MRI approach proposed in the present study offers the potential advantage to obtain accurate measurements of both LV dyssynchrony and myocardial scar in a single session, without requiring multiple imaging investigations and specific MRI acquisitions, beyond the standard protocol. Furthermore, MRI provides detailed information about cardiac morphology and function as well as quantification of trans-valvular flows. This comprehensive approach is particularly useful in heart failure patients and, according to the current results, seems to be capable to improve the selection of candidates to CRT. However, larger patient cohorts and multicenter studies are needed to confirm these findings and a longer follow-up is necessary to perform a survival analysis.

CONCLUSIONS

MRI offers the unique opportunity to assess LV dyssynchrony and the total extent of scar in a single session. Both these parameters showed to be strongly associated with echocardiographic response to CRT.

REFERENCES

1. Bax JJ, Abraham T, Barold SS et al. Cardiac resynchronization therapy: Part 1--issues before device implantation. *J Am Coll Cardiol* 2005;46:2153-2167.
2. Helm RH, Leclercq C, Faris OP et al. Cardiac dyssynchrony analysis using circumferential versus longitudinal strain: implications for assessing cardiac resynchronization. *Circulation* 2005;111:2760-2767.
3. Lardo AC, Abraham TP, Kass DA. Magnetic resonance imaging assessment of ventricular dyssynchrony: current and emerging concepts. *J Am Coll Cardiol* 2005;46:2223-2228.
4. Westenberg JJ, Lamb HJ, van der Geest RJ et al. Assessment of left ventricular dyssynchrony in patients with conduction delay and idiopathic dilated cardiomyopathy: head-to-head comparison between tissue doppler imaging and velocity-encoded magnetic resonance imaging. *J Am Coll Cardiol* 2006;47:2042-2048.
5. Chalil S, Stegemann B, Muhyaldeen S et al. Intraventricular dyssynchrony predicts mortality and morbidity after cardiac resynchronization therapy: a study using cardiovascular magnetic resonance tissue synchronization imaging. *J Am Coll Cardiol* 2007;50:243-252.
6. Kim RJ, Fieno DS, Parrish TB et al. Relationship of MRI delayed contrast enhancement to irreversible injury, infarct age, and contractile function. *Circulation* 1999;100:1992-2002.
7. Van Rossum AC, Visser FC, Van Eenige MJ, Valk J, Roos JP. Oblique views in magnetic resonance imaging of the heart by combined axial rotations. *Acta Radiol* 1987;28:497-503.
8. Pruessmann KP, Weiger M, Scheidegger MB, Boesiger P. SENSE: sensitivity encoding for fast MRI. *Magn Reson Med* 1999;42:952-962.
9. Steenbeck J, Pruessmann K. Technical developments in cardiac MRI: 2000 update. *Rays* 2001;26:15-34.
10. Kaandorp TA, Bax JJ, Schuijf JD et al. Head-to-head comparison between contrast-enhanced magnetic resonance imaging and dobutamine magnetic resonance imaging in men with ischemic cardiomyopathy. *Am J Cardiol* 2004;93:1461-1464.
11. Messroghli DR, Radjenovic A, Kozerke S, Higgins DM, Sivananthan MU, Ridgway JP. Modified Look-Locker inversion recovery (MOLLI) for high-resolution T1 mapping of the heart. *Magn Reson Med* 2004;52:141-146.
12. Cerqueira MD, Weissman NJ, Dilsizian V et al. Standardized myocardial segmentation and nomenclature for tomographic imaging of the heart: a statement for healthcare professionals from the Cardiac Imaging Committee of the Council on Clinical Cardiology of the American Heart Association. *Circulation* 2002;105:539-542.
13. Bondarenko O, Beek AM, Hofman MB et al. Standardizing the definition of hyperenhancement in the quantitative assessment of infarct size and myocardial viability using delayed contrast-enhanced CMR. *J Cardiovasc Magn Reson* 2005;7:481-485.
14. Chalil S, Foley PW, Muyhaldeen SA et al. Late gadolinium enhancement-cardiovascular magnetic resonance as a predictor of response to cardiac resynchronization therapy in patients with ischaemic cardiomyopathy. *Europace* 2007;9:1031-1037.
15. Lang RM, Bierig M, Devereux RB et al. Recommendations for chamber quantification. *Eur J Echocardiogr* 2006;7:79-108.
16. Delgado V, Ypenburg C, van Bommel RJ et al. Assessment of left ventricular dyssynchrony by speckle tracking strain imaging comparison between longitudinal, circumferential, and radial strain in cardiac resynchronization therapy. *J Am Coll Cardiol* 2008;51:1944-1952.

17. Suffoletto MS, Dohi K, Cannesson M, Saba S, Gorcsan J, III. Novel speckle-tracking radial strain from routine black-and-white echocardiographic images to quantify dyssynchrony and predict response to cardiac resynchronization therapy. *Circulation* 2006;113:960-968.
18. Chung ES, Leon AR, Tavazzi L et al. Results of the Predictors of Response to CRT (PROSPECT) Trial. *Circulation* 2008;117:2608-2616.
19. Bonow RO, Carabello BA, Kanu C et al. ACC/AHA 2006 guidelines for the management of patients with valvular heart disease: a report of the American College of Cardiology/American Heart Association Task Force on Practice Guidelines (writing committee to revise the 1998 Guidelines for the Management of Patients With Valvular Heart Disease): developed in collaboration with the Society of Cardiovascular Anesthesiologists: endorsed by the Society for Cardiovascular Angiography and Interventions and the Society of Thoracic Surgeons. *Circulation* 2006;114:e84-231.
20. Albertsen AE, Nielsen JC, Pedersen AK, Hansen PS, Jensen HK, Mortensen PT. Left ventricular lead performance in cardiac resynchronization therapy: impact of lead localization and complications. *Pacing Clin Electrophysiol* 2005;28:483-488.
21. Bleeker GB, Kaandorp TA, Lamb HJ et al. Effect of posterolateral scar tissue on clinical and echocardiographic improvement after cardiac resynchronization therapy. *Circulation* 2006;113:969-976.
22. Ypenburg C, Roes SD, Bleeker GB et al. Effect of total scar burden on contrast-enhanced magnetic resonance imaging on response to cardiac resynchronization therapy. *Am J Cardiol* 2007;99:657-660.
23. White JA, Yee R, Yuan X et al. Delayed enhancement magnetic resonance imaging predicts response to cardiac resynchronization therapy in patients with intraventricular dyssynchrony. *J Am Coll Cardiol* 2006;48:1953-1960.

CHAPTER 17

Agreement and disagreement between contrast-enhanced magnetic resonance imaging and nuclear imaging for assessment of myocardial viability

S D Roes, T A M Kaandorp, **N Ajmone Marsan**, J J M Westenberg, P Dibbets-Schneider, M P Stokkel, H J Lamb, E E van der Wall, A de Roos, and J J Bax

Eur J Nucl Med Mol Imaging 2009;36:594-601.

ABSTRACT

Objectives: The purpose of this study was to compare contrastenhanced MRI and nuclear imaging with 99mTc-tetrofosmin and 18F-fluorodeoxyglucose (18F-FDG) single photon emission computed tomography (SPECT) for assessment of myocardial viability.

Methods: Included in the study were 60 patients with severe ischaemic left ventricular (LV) dysfunction, who underwent contrast-enhanced MRI, 99mTc-tetrofosmin and 18F-FDG SPECT. Myocardial segments were assigned a wall motion score from 0 (normokinesia) to 4 (dyskinesia) and a scar score from 0 (no scar) to 4 (76–100% transmural extent). Furthermore, 99mTc-tetrofosmin and 18F-FDG segmental tracer uptake was categorized from 0 (tracer activity >75%) to 3 (tracer activity <25%). Dysfunctional segments were classified into viability patterns on SPECT: normal perfusion/18F-FDG uptake, perfusion/18F-FDG mismatch, and mild or severe perfusion/18F-FDG match.

Results: Minimal scar tissue was observed on contrast-enhanced MRI (scar score 0.4±0.8) in segments with normal perfusion/18F-FDG uptake, whereas extensive scar tissue (scar score 3.1±1.0) was noted in segments with severe perfusion/18F-FDG match ($p < 0.001$). High agreement (91%) for viability assessment between contrast-enhanced MRI and nuclear imaging was observed in segments without scar tissue on contrast-enhanced MRI as well as in segments with transmural scar tissue (83%). Of interest, disagreement was observed in segments with subendocardial scar tissue on contrast-enhanced MRI.

Conclusions: Agreement between contrast-enhanced MRI and nuclear imaging for assessment of viability was high in segments without scar tissue and in segments with transmural scar tissue on contrast-enhanced MRI. However, evident disagreement was observed in segments with subendocardial scar tissue on contrast-enhanced MRI, illustrating that the non-enhanced epicardial rim can contain either normal or ischaemically jeopardized myocardium.

INTRODUCTION

Assessment of viability is essential for optimization of treatment in patients with ischaemic left ventricular (LV) dysfunction, since dysfunctional but viable myocardium is likely to improve after revascularization, whereas dysfunctional but nonviable myocardium will not benefit [1]. Furthermore, patients with viable myocardium have better survival after revascularization than after medical treatment [2]. At the present time, several noninvasive imaging modalities are available for the assessment of viability, including dobutamine echocardiography, single photon emission computed tomography (SPECT) and positron emission tomography (PET) [3–5]. Nuclear imaging using tracers such as 99mTc-tetrofosmin and 18F- fluorodeoxyglucose (18F-FDG) allows evaluation of viability by assessment of myocardial perfusion and glucose utilization [4]. Contrast-enhanced magnetic resonance imaging (MRI) has been more recently introduced for assessment of viability [6–8]. This technique offers visualization of scar tissue with high spatial resolution, enabling distinction between subendocardial and transmural scar [9]. Kim et al. reported that in segments without contrast-enhancement on MRI, recovery of function is highly likely to occur after revascularization, whereas improvement of function is unlikely in segments with extensive, transmural contrast-enhancement [6]. However, difficulties arise in dysfunctional segments with subendocardial scar tissue, which show an intermediate extent of recovery, since contrast-enhanced MRI provides only information on scar tissue, whereas the non-enhanced (viable) tissue can contain either normal or ischaemically jeopardized myocardium [10]. Hence, the two imaging modalities discussed above provide different information on viability.

To our knowledge, only a few, relatively small studies have evaluated patients using both contrast-enhanced MRI and nuclear imaging to determine viability [11–14]. Consequently, the exact relationship between viability assessed with contrast-enhanced MRI and nuclear imaging is still largely unknown. Therefore, the purpose of the present study was to compare contrast-enhanced MRI and nuclear imaging with 99mTc-tetrofosmin and 18F-FDG SPECT for the assessment of viability in patients with severe ischaemic LV dysfunction.

METHODS

Patient population

The study population consisted of 60 patients with severe ischaemic LV dysfunction who underwent MRI, 99mTctetrofosmin SPECT and 18F-FDG SPECT. Patients with myocardial infarction (MI) <3 months before MRI or SPECT were excluded. Other exclusion criteria were (supra-)ventricular arrhythmias, pacemakers, intracranial clips and claustrophobia. Patient

characteristics are presented in Table 1. The local ethics committee approved the study and all patients gave informed consent.

MRI: data acquisition

A 1.5-T Gyroscan ACS-NT/Intera MRI scanner (Philips Medical Systems, Best, The Netherlands) equipped with a five-element cardiac synergy coil was used. Images were acquired during breath-holds of approximately 15 s using vector electrocardiographic gating. The heart was imaged from apex to base [15] with 10–12 imaging levels (dependent on the heart size) in the short-axis view using a balanced turbofield echo sequence with parallel imaging (SENSE, acceleration factor 2). Typical parameters were a field of view of 400×320 mm2, matrix of 256×206 pixels, slice thickness of 10.00 mm, no slice gap, flip angle of 35°, time to echo of 1.67 ms, and time to repeat of 3.3 ms. Temporal resolution was 25 to 39 ms. The geometric settings of the baseline scans were stored and repeated for the contrast-enhanced images to ensure matching of the same slices (and hence, myocardial segments). Contrast-enhanced images were acquired approximately 15 min after bolus injection of gadolinium diethylenetriamine pentaacetic acid (Magnevist, Schering, Berlin, Germany; 0.15 mmol/kg) with an inversion-recovery 3-D turbofield echo sequence; the inversion time was determined with a real-time plan scan. Typical parameters were a field of view of 400×300 mm2, matrix of 256×192 pixels, slice thickness of 5.00 mm, flip angle of 15°, time to echo of 1.1 ms, and time to repeat of 3.00 ms.

MRI: data analysis

To determine global function, endocardial borders were outlined manually on short-axis cine images with previously validated software (MASS; Medis, Leiden, The Netherlands) [16]. Papillary muscles were regarded as part of the ventricular cavity, and epicardial fat was excluded. LV end-systolic volume (ESV) and LV end-diastolic volume (EDV) were calculated. Subsequently, ESV was subtracted from EDV and LV ejection fraction (LVEF) was calculated. To determine regional wall motion, cine MR images were visually interpreted by two experienced observers using a 17-segment model [17]. Each segment was assigned a wall motion/thickening score using the following five-point scale: 0 normal wall motion, 1 mild hypokinesia, 2 severe hypokinesia, 3 akinesia, and 4 dyskinesia. Wall thickening was taken into account for this classification, preempting the problem of postoperative paradoxical septal motion in patients with previous coronary artery bypass grafting. Contrast-enhanced images were scored visually by two experienced observers using the 17-segment model described above

[17]. Segmental scarring was graded on each segment using the following five-point scale: 0 absence of hyperenhancement, 1 hyperenhancement of 1% to 25% of

LV wall thickness, 2 hyperenhancement extending from 26% to 50%, 3 hyperenhancement extending from 51% to 75%, and 4 hyperenhancement extending from 76% to 100% [18].

99mTc-tetrofosmin SPECT: data acquisition

Imaging was performed at rest, with 99mTc-tetrofosmin (500 MBq) using a triple-head SPECT camera (GCA 9300/HG, Toshiba Corporation) equipped with low-energy, general-purpose collimators. A 20% window was used around the 140-keV energy peak of 99mTc-tetrofosmin. A total of 90 projections (step-and-shoot mode of 35 s/projection, total imaging time 23 min) were obtained over a 360° circular orbit. Data were stored in a 64×64, 16-bit matrix. The raw scintigraphic data were reconstructed with filtered back projection using a Butterworth filter (cut-off frequency 0.26 cycles per pixel, order 9). No attenuation correction was used.

99mTc-tetrofosmin SPECT: data analysis

Additional reconstruction yielded standard long- and shortaxis projections perpendicular to the heart axis. Reconstructed slices were 6 mm in all directions. The short-axis slices were displayed in polar map format, adjusted for peak myocardial activity (100%). The myocardium was divided into 17 segments [17]. Segmental tracer activity was categorized visually by two experienced observers on a four-point scale (0 normal tracer activity >75%, 1 mildly reduced tracer activity 50–75%, 2 moderately reduced tracer activity 25–50%, and 3 severely reduced tracer activity <25%).

18F-FDG SPECT: data acquisition

18F-FDG imaging, to evaluate myocardial glucose utilization, was performed on a separate day, after administration of acipimox (a nicotinic acid derivative, 500 mg, oral dose; Byk, Zwanenberg, The Netherlands) [19]. Acipimox enhances myocardial 18F-FDG uptake by reducing the plasma level of free fatty acids [20]. After acipimox administration, the patients received a low-fat, carbohydrate-rich meal. This small meal further enhances myocardial 18F-FDG uptake by stimulating endogenous insulin release [21]. A blood sample was taken 60 min after acipimox administration to assess plasma glucose levels, and insulin was administered if needed. Then, 185 MBq 18F-FDG was injected at rest. Data were acquired 45 min later at rest using the same SPECT system as described for perfusion imaging, with commercially

available 511-KeV collimators. Data were acquired over 360° and stored in a 64×64, 16-bit matrix. From the raw scintigraphic data, transaxial slices were reconstructed by filtered back projection using a Butterworth filter (cut-off frequency 0.17 cycles per pixel, order 8). Attenuation correction was not applied.

18F-FDG SPECT: data analysis

Further reconstruction yielded standard short- and long-axis projections perpendicular to the heart axis. 18F-FDG shortaxis slides were displayed in polar map format, normalized to the maximum activity (set at 100%); the polar maps were divided into 17 segments [17]. Segmental tracer activity was categorized visually by two experienced observers on a four-point scale (0 normal tracer activity >75%, 1 mildly reduced tracer activity 50–75%, 2 moderately reduced tracer activity 25–50%, and 3 severely reduced tracer activity <25%).

Definition of viability on nuclear imaging

The dysfunctional segments on cine MRI (wall motion score ≥1) were divided into four groups with different patterns of viability. Group I (normal perfusion/18F-FDG uptake) consisted of segments with normal 99mTc-tetrofosmin activity (score 0) and normal 18F-FDG activity (score 0). Group II (perfusion/18F-FDG mismatch) consisted of segments with reduced 99mTc-tetrofosmin activity (score 1, 2 or 3) and preserved/relatively increased 18F-FDG activity (18FFDG score <99mTc-tetrofosmin score). Group III (mild perfusion/18F-FDG match) consisted of segments with a mild reduction in 99mTc-tetrofosmin activity (score 1) and a concordant mild reduction in 18F-FDG activity (score 1). Finally, group IV (severe perfusion/18F-FDG match) consisted of segments with a moderate or severe reduction in 99mTc-tetrofosmin activity (score 2 or 3) and a concordant reduction in 18F-FDG activity.

Statistical analysis

Continuous data are expressed as means±standard deviation (SD). One-way ANOVA was used to compare scar score between the groups with different viability patterns. Proportions were compared using chi-squared ($\chi 2$) analysis. P-values <0.05 were considered statistically significant.

RESULTS

Patient population

Clinical data are presented in Table 1. The mean age of the study population was 65±11 years and 50 patients (83%) were men. All patients had evidence of coronary artery disease (CAD) on coronary angiography. No clinical events or interventions were reported between MRI and SPECT examinations.

Table 1. Clinical characteristics of the study population

Clinical variable	Mean±SD	No. (%) of patients (n = 60)
Age (years)	65±11	
Men		50 (83)
Diabetes mellitus		16 (27)
Hypertension		14 (23)
Hypercholesterolaemia		23 (38)
Smoking		25 (42)
Previous MI		60 (100)
Prior revascularization		34 (57)
Percutaneous coronary intervention		20 (33)
Coronary artery bypass grafting		14 (23)
Extent of CAD (on coronary angiography)		
One-vessel disease		11 (18)
Two-vessel disease		18 (30)
Three-vessel disease		31 (52)
Medications:		
β-Blockers		48 (82)
Calcium channel blockers		10 (17)
ACE inhibitors		55 (92)
Oral anticoagulants		59 (98)
Statins		48 (80)
Nitrates		28 (47)
Diuretics		56 (93)

Magnetic resonance imaging

Mean LVEF in the total study population was 27±9%. The mean LVESV and mean LVEDV were 250±110 ml and 335±114 ml, respectively. A total of 1020 segments were analysed, of which 692 (68%) showed abnormal wall motion. Of these dysfunctional segments, 91 (13%) showed mild hypokinesia, 248 (36%) showed severe hypokinesia, and 298 (43%) segments were

akinetic and 55 (8%) were dyskinetic. Of the 692 dysfunctional segments, 484 (70%) revealed hyperenhancement, 105 (15%) showed minor hyperenhancement (scar score 1), 107 (15%) had a scar score of 2, 130 (19%) a scar score of 3, and 142 (21%) a scar score of 4.

99mTc-tetrofosmin SPECT

Of the 692 dysfunctional segments, 182 (26%) showed normal 99mTc-tetrofosmin activity (score 0), 91 (13%) showed mildly reduced tracer activity (score 1), 147 (21%) showed moderately reduced tracer activity (score 2), and 272 (39%) showed severely reduced tracer activity (score 3).

18F-FDG SPECT

Normal 18F-FDG activity was observed in 220 segments (32%) of the 692 dysfunctional segments. Mildly reduced tracer activity (score 1) was seen in 157 segments (23%), moderately reduced tracer activity (score 2) in 108 segments (16%), and severely reduced tracer activity (score 3) in 207 segments (30%).

Viability patterns assessed with nuclear imaging

Of the 692 dysfunctional segments, 183 (26%) showed normal perfusion/18F-FDG uptake, 145 (21%) showed perfusion/18F-FDG mismatch, 73 (11%) showed mild perfusion/18F-FDG match, and 291 (42%) showed severe perfusion/ 18F-FDG match. Of the 353 akinetic and dyskinetic segments, 40 (11%) showed normal perfusion/18F-FDG uptake, 78 (22%) showed perfusion/18F-FDG mismatch, 35 (10%) showed mild perfusion/18F-FDG match, and 200 (57%) showed severe perfusion/18F-FDG match.

Viability: nuclear imaging versus contrast-enhanced MRI

The mean scar scores measured in the segments grouped according to viability pattern on nuclear imaging are presented in Figure 1. Minimal scar tissue was observed on contrast-enhanced MRI in segments with normal perfusion/18F-FDG uptake on nuclear imaging (scar score 0.4±0.8), whereas extensive scar tissue (scar score 3.1±1.0) was noted in segments showing severe perfusion/18F-FDG match on nuclear imaging ($p < 0.001$). Next (Figure 2), the dysfunctional segments were grouped according to the transmural extent of the scar

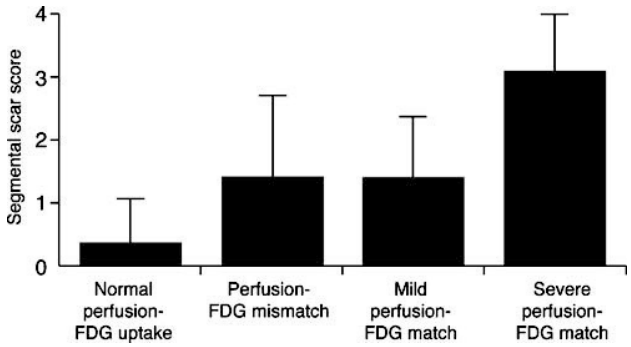


Figure 1. Mean scar scores on contrast-enhanced MRI for segments grouped according to viability pattern on nuclear imaging. (one-way ANOVA: p <0.001). Error bars represent standard deviations.

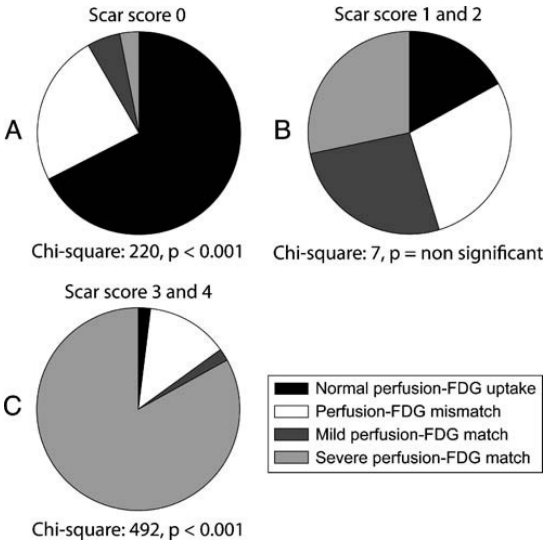


Figure 2. Relationship between contrast-enhanced MRI and nuclear imaging for dysfunctional segments showing the frequency of the four viability patterns assessed with nuclear imaging in segments without scar tissue (a), with subendocardial scar tissue (b) and with transmural scar tissue (c) on contrast-enhanced MRI.

tissue on contrast-enhanced MRI. The majority of segments without scar tissue on contrast-enhanced MRI (scar score 0, Figure 2a) showed normal perfusion/18F-FDG uptake (67%) or perfusion/18F-FDG mismatch (24%). Considering viability, agreement in these segments was high (91%), since segments without scar tissue on contrast-enhanced MRI as well as segments with normal perfusion/18F-FDG uptake or perfusion/18F-FDG mismatch on nuclear imaging are regarded as viable tissue. Conversely, the majority (83%) of segments with transmural scar tissue on contrast-enhanced MRI (scar scores 3 and 4, Figure 2c) showed severe

perfusion/18F-FDG match on nuclear imaging. Accordingly, agreement in these segments was also high (83%), since segments with transmural scar tissue on contrast-enhanced MRI and segments with severe perfusion/18F-FDG match on nuclear imaging represent nonviable tissue. Of note, in segments with subendocardial scar tissue on contrast-enhanced MRI (scar scores 1 and 2, Figure 2b), the various viability patterns assessed with nuclear imaging were evenly distributed, indicating that segments with subendocardial scar tissue on contrast-enhanced MRI, may have normal perfusion/18F-FDG uptake, perfusion/18F-FDG mismatch, mild perfusion/18F-FDG match or severe perfusion/18F-FDG match. Figure 3 shows an example of a patient with subendocardial scar tissue on contrast-enhanced MRI and perfusion/18F-FDG mismatch on nuclear imaging.

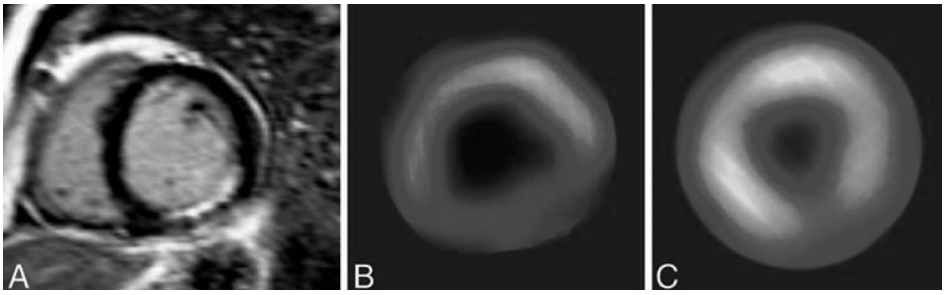


Figure 3. Patient with inferior subendocardial scar tissue on contrast-enhanced MRI (a) and a severe reduction in 99mTc-tetrofosmin activity (b) but preserved 18F-FDG activity (c) on SPECT (perfusion/18F-FDG mismatch), indicating ischaemically jeopardized myocardium, highlighting the discrepancy between information derived from contrast-enhanced MRI and nuclear imaging.

Finally (Figure 4), the akinetic and dyskinetic segments were analysed separately. The majority of these segments without scar tissue on contrast-enhanced MRI (scar score 0, Figure 4a) showed normal perfusion/18F-FDG uptake (47%) or perfusion/18F-FDG mismatch (39%) on nuclear imaging. Consequently, agreement between the two techniques for assessment of viability was high (86%). Conversely, in the majority of segments with transmural scar tissue on contrast-enhanced MRI (scar scores 3 and 4, Figure 4c), severe perfusion/18F-FDG match was observed on nuclear imaging (84%). Accordingly, agreement was also high (84%) in this category. Of interest, in segments with subendocardial scar tissue on contrast-enhanced MRI (scar scores 1 and 2, Figure 4b), the viability pattern on nuclear imaging varied highly between normal perfusion/18F-FDG uptake, perfusion/18FFDG mismatch, mild perfusion/18F-FDG match and severe perfusion/18F-FDG match.

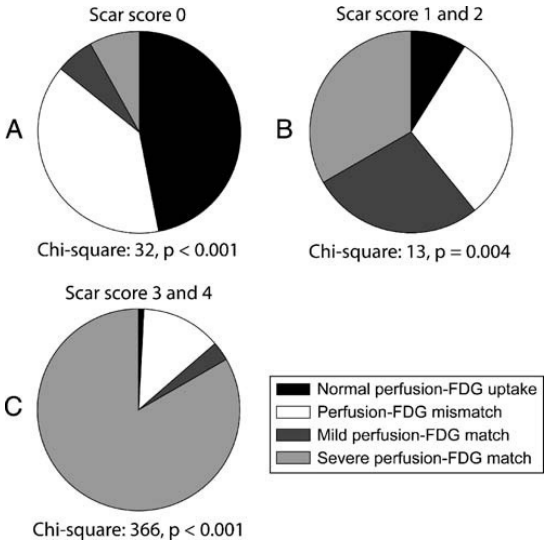


Figure 4. Relationship between contrast-enhanced MRI and nuclear imaging for akinetic and dyskinetic segments showing the frequency of the four viability patterns assessed with nuclear imaging in segments without scar tissue (a), with subendocardial scar tissue (b) and transmural scar tissue (c) on contrast-enhanced MRI.

DISCUSSION

The major finding in this study is that agreement between contrast-enhanced MRI and nuclear imaging for assessment of viability is high in segments without scar tissue as well as in segments with transmural scar tissue on contrast-enhanced MRI. Disagreement between the two imaging modalities regarding viability assessment was observed in segments with subendocardial scar tissue on contrast-enhanced MRI.

Contrast-enhanced MRI has been introduced as a reliable noninvasive technique for visualization of scar tissue in patients with previous MI [6,18] and in patients with clinical suspicion of CAD but without a history of MI [22]. Kim et al. evaluated the accuracy of contrast-enhanced MRI for the assessment of scar tissue in dogs with previous MI and reported excellent agreement between the extent of scar tissue on contrast-enhanced MRI and the histological extent of necrosis [23].

Subsequently, Kim et al. studied the value of scar tissue assessed with contrast-enhanced MRI for prediction of functional recovery after revascularization in 41 patients with chronic CAD [6]. They reported that the majority of segments (78%) without scar tissue improved in function after revascularization, whereas improvement was virtually absent in segments with transmural scar tissue [6]. Importantly, difficulties arise in segments with subendocardial scar tissue (transmural extent 1–50%), with only 53% of segments showing functional recovery [6].

Pooling of four studies in patients (n = 132) undergoing revascularization revealed a high sensitivity (95%), but a relatively low specificity (45%) of contrast-enhanced MRI for predicting improvement in function [10]. The suboptimal specificity is related to segments with subendocardial scar tissue (transmural extent 1–50%), that do not improve in function. These findings highlight the fact that contrast-enhanced MRI is an excellent technique to delineate scar tissue (anatomical imaging), but the technique does not provide information on the pathophysiological substrate of the non-scarred tissue, which results in suboptimal prediction of functional recovery after revascularization.

Combined perfusion-18F -FDG imaging, as used in the current study, permits delineation of viability based on integration of perfusion and glucose utilization [24]. This approach has been widely validated (both with PET and with SPECT imaging) for detection of viable myocardium and prediction of functional recovery [13,25,26]. Different patterns of perfusion/18F-FDG uptake can be observed. Dysfunctional but viable myocardium can be divided into normal perfusion and 18F-FDG uptake representing repetitively stunned myocardium, whereas reduced perfusion with preserved 18F-FDG uptake represents hibernation. Scar tissue can be divided (based on the concordant reduction in perfusion and 18F-FDG uptake) into subendocardial scar tissue and transmural scar tissue. Based on these different patterns, with integration of perfusion and glucose utilization (assessed by 18F-FDG imaging), it is possible to better characterize the substrate of the dysfunctional myocardium. Few studies have compared contrast-enhanced MRI with perfusion-18F-FDG imaging [11–14,27]. Kühl et al. performed contrast-enhanced MRI and perfusion-18F-FDG imaging in 29 patients with chronic CAD [13]. Comparison between the techniques showed that viable segments on perfusion-18F-FDG imaging contained minimal scar tissue, whereas the extent of scar tissue on contrast-enhanced MRI increased in parallel with the abnormalities on perfusion-18F-FDG imaging; segments with severe matches on perfusion-18F-FDG imaging showed transmural scar tissue on contrast-enhanced MRI [13].

Knuesel et al. studied 19 patients with chronic CAD who underwent 13N-ammonia PET to evaluate perfusion and 18F-FDG PET to evaluate glucose utilization; scar tissue was analysed with contrast-enhanced MRI [11]. The authors reported a good correlation (ranging from r = 0.62 to r = 0.82) between segmental 18F-FDG uptake and the transmural extent of scar tissue on contrast-enhanced MRI. In particular, segments with 18F-FDG uptake ≥50% corresponded well with small areas of subendocardial scar tissue on contrast-enhanced MRI (and extensive non-scar tissue, 4.5 mm of the myocardial wall, on contrast-enhanced MRI). Ten patients also underwent revascularization, and the segments with preserved 18F-FDG uptake and minimal scar tissue improved in function after revascularization; conversely, the segments with severely reduced 18F-FDG uptake and extensive, transmural scar tissue, did not improve in function.

Of interest, the segments with severely reduced 18F-FDG uptake, but non-transmural scar tissue on contrast-enhanced MRI, did not improve in function after revascularization. This is

precisely the issue highlighted in the current study. The problem is that contrast-enhanced MRI provides excellent information on the extent and transmural extent of scar tissue (better than any other imaging technique), but it does not provide information on the pathophysiology of the non-scarred myocardium. As shown by Knuesel et al., segments with a small amount of scar tissue on contrast-enhanced MRI, but severely reduced 18F-FDG uptake do not improve in function [11]. These observations underscore the need to better characterize the non-scarred myocardium, as can be done with 18F-FDG imaging (in combination with perfusion imaging). Indeed, the findings of the current study illustrate that segments with an intermediate transmural extent of scar tissue (score 1 or 2) can exhibit a wide range of patterns on perfusion-18F-FDG imaging (see Figure 2b).

An important limitation of the current study was the lack of outcome data after revascularization, and therefore the study did not provide information on the functional fate of the segments after revascularization (recovery or not). Additional studies in patients undergoing revascularization are needed to further explore the actual outcome of segments with intermediate amounts of scar tissue on contrast-enhanced MRI and different perfusion-18F-FDG uptake patterns.

CONCLUSIONS

Comparison of contrast-enhanced MRI and perfusion-18F-FDG imaging for assessment of viability in patients with severe ischaemic LV dysfunction revealed high agreement in segments without scar tissue on contrast-enhanced MRI as well as in segments with transmural scar tissue. However, evident disagreement was noted in segments with subendocardial scar tissue on contrast-enhanced MRI, illustrating that the non-enhanced epicardial rim can contain either normal or ischaemically jeopardized myocardium. This differentiation is potentially important for prediction of outcome after revascularization. Indeed, Bove et al. have demonstrated in 15 patients that further refinement of the non-scar tissue (in this particular study assessment of contractile reserve by low-dose dobutamine challenge was used) resulted in superior prediction of outcome after revascularization [28]. Further studies, comparing various imaging techniques in patients undergoing revascularization including information on segmental functional outcome are needed to better define the contribution of scar tissue and viable tissue to functional recovery after revascularization.

REFERENCES

1. Rahimtoola SH. The hibernating myocardium. *Am Heart J* 1989;117:211–21.
2. Allman KC, Shaw LJ, Hachamovitch R, Udelson JE. Myocardial viability testing and impact of revascularization on prognosis in patients with coronary artery disease and left ventricular dysfunction: a meta-analysis. *J Am Coll Cardiol* 2002;39:1151–8.
3. Bax JJ, Cornel JH, Visser FC et al. Prediction of recovery of myocardial dysfunction after revascularization. Comparison of fluorine-18 fluorodeoxyglucose/thallium-201 SPECT, thallium-201 stress-reinjection SPECT and dobutamine echocardiography. *J Am Coll Cardiol* 1996;28:558–64.
4. Bax JJ, van der Wall EE, Harbinson M. Radionuclide techniques for the assessment of myocardial viability and hibernation. *Heart* 2004;90(Suppl 5):v26–33.
5. Cornel JH, Bax JJ, Fioretti PM. Assessment of myocardial viability by dobutamine stress echocardiography. *Curr Opin Cardiol* 1996;11:621–6.
6. Kim RJ, Wu E, Rafael A et al. The use of contrast-enhanced magnetic resonance imaging to identify reversible myocardial dysfunction. *N Engl J Med* 2000;343:1445–53.
7. Isbell DC, Kramer CM. Cardiovascular magnetic resonance: structure, function, perfusion, and viability. *J Nucl Cardiol* 2005;12:324–36.
8. Isbell DC, Kramer CM. Magnetic resonance for the assessment of myocardial viability. *Curr Opin Cardiol* 2006;21:469–72.
9. Lee VS, Resnick D, Tiu SS et al. MR imaging evaluation of myocardial viability in the setting of equivocal SPECT results with (99m) Tc sestamibi. *Radiology* 2004;230:191–7.
10. Kaandorp TA, Lamb HJ, van der Wall EE, de Roos A, Bax JJ. Cardiovascular MR to access myocardial viability in chronic ischaemic LV dysfunction. *Heart* 2005;91:1359–65.
11. Knuesel PR, Nanz D, Wyss C et al. Characterization of dysfunctional myocardium by positron emission tomography and magnetic resonance: relation to functional outcome after revascularization. *Circulation* 2003;108:1095–100.
12. Kühl HP, Beek AM, van der Weerdt AP et al. Myocardial viability in chronic ischemic heart disease: comparison of contrast-enhanced magnetic resonance imaging with (18)F-fluorodeoxyglucose positron emission tomography. *J Am Coll Cardiol* 2003;41:1341–48.
13. Kühl HP, Lipke CS, Krombach GA et al. Assessment of reversible myocardial dysfunction in chronic ischaemic heart disease: comparison of contrastenhanced cardiovascular magnetic resonance and a combined positron emission tomography-single photon emission computed tomography imaging protocol. *Eur Heart J* 2006;27:846–53.
14. Wu YW, Tadamura E, Yamamuro M et al. Comparison of contrast-enhanced MRI with (18)F-FDG PET/201Tl SPECT in dysfunctional myocardium: relation to early functional outcome after surgical revascularization in chronic ischemic heart disease. *J Nucl Med* 2007;48:1096–03.
15. Lamb HJ, Doornbos J, van der Velde EA, Kruit MC, Reiber JH, de Roos A. Echo planar MRI of the heart on a standard system: validation of measurements of left ventricular function and mass. *J Comput Assist Tomogr* 1996;20:942–9.
16. van der Geest RJ, Buller VG, Jansen E et al. Comparison between manual and semiautomated analysis of left ventricular volume parameters from short-axis MR images. *J Comput Assist Tomogr* 1997;21:756–65.
17. Cerqueira MD, Weissman NJ, Dilsizian V et al. American Heart Association Writing Group on Myocardial Segmentation and Registration for Cardiac Imaging. Standardized myocardial segmentation and nomenclature for tomographic imaging of the heart: a statement for healthcare

professionals from the Cardiac Imaging Committee of the Council on Clinical Cardiology of the American Heart Association. *Circulation* 2002;105:539–42.

18. Wu E, Judd RM, Vargas JD, Klocke FJ, Bonow RO, Kim RJ. Visualisation of presence, location, and transmural extent of healed Q-wave and non-Q-wave myocardial infarction. *Lancet* 2001;357:21–8.
19. Schinkel AF, Bax JJ, Valkema R et al. Effect of diabetes mellitus on myocardial 18FFDG SPECT using acipimox for the assessment of myocardial viability. *J Nucl Med* 2003;44:877–83.
20. Nuutila P, Knuuti MJ, Raitakari M et al. Effect of antilipolysis on heart and skeletal muscle glucose uptake in overnight fasted humans. *Am J Physiol* 1994;267:E941–6.
21. Bax JJ, Veening MA, Visser FC et al. Optimal metabolic conditions during fluorine-18 fluorodeoxyglucose imaging; a comparative study using different protocols. *Eur J Nucl Med* 1997;24:35–41.
22. Kwong RY, Chan AK, Brown KA et al. Impact of unrecognized myocardial scar detected by cardiac magnetic resonance imaging on event-free survival in patients presenting with signs or symptoms of coronary artery disease. *Circulation* 2006;113:2733–43.
23. Kim RJ, Fieno DS, Parrish TB et al. Relationship of MRI delayed contrast enhancement to irreversible injury, infarct age, and contractile function. *Circulation* 1999;100:1992–2002.
24. Bax JJ, Visser FC, Elhendy A et al. Prediction of improvement of regional left ventricular function after revascularization using different perfusion- metabolism criteria. *J Nucl Med* 1999;40:1866–73.
25. Bax JJ, Cornel JH, Visser FC et al. Prediction of improvement of contractile function in patients with ischemic ventricular dysfunction after revascularization by fluorine-18 fluorodeoxyglucose single-photon emission computed tomography. *J Am Coll Cardiol* 1997;30:377–83.
26. Bax JJ, Patton JA, Poldermans D, Elhendy A, Sandler MP. 18-Fluorodeoxyglucose imaging with positron emission tomography and single photon emission computed tomography: cardiac applications. *Semin Nucl Med* 2000;30:281–98.
27. Klein C, Nekolla SG, Bengel FM et al. Assessment of myocardial viability with contrast-enhanced magnetic resonance imaging: comparison with positron emission tomography. *Circulation* 2002;105:162–7.
28. Bove CM, Dimaria JM, Voros S, Conaway MR, Kramer CM. Dobutamine response and myocardial infarct transmurality: functional improvement after coronary artery bypass grafting –initial experience. *Radiology* 2006;240:835–41.

CHAPTER 18

Three-dimensional echocardiography for the preoperative assessment of patients with left ventricular aneurysm

N Ajmone Marsan, J JM Westenberg, S D Roes, R J van Bommel, V Delgado, R J van der Geest, A de Roos, R J Klautz, J C Reiber, and J J Bax

Ann Thoracic Surg 2011;91:113-21.

ABSTRACT

Objectives: Surgical ventricular reconstruction has been proposed as a treatment option in heart failure patients with left ventricular (LV) aneurysm. The feasibility of this procedure has some limitations and extensive pre-operative evaluation is necessary in order to give the correct indication. For this purpose, magnetic resonance imaging (MRI) is currently considered the gold standard, providing accurate quantification of LV shape, size, global and regional function together with the assessment of myocardial scar and mitral regurgitation severity. The aim of this study was to evaluate the accuracy of real-time three-dimensional echocardiography (RT3DE) as a potential alternative to MRI for this evaluation.

Methods: A total of 52 patients with ischemic cardiomyopathy and LV aneurysm underwent a comprehensive analysis with 2D echocardiography, RT3DE and MRI.

Results: Excellent correlation ($r = 0.97$, $p < 0.001$) and agreement were found between RT3DE and MRI for quantification of LV volumes, ejection fraction and sphericity index; in a segment-to-segment comparison, RT3DE showed to be accurate also for the analysis of wall motion abnormalities ($k = 0.62$) and LV regional thickness ($k = 0.56$) as a marker of myocardial scar. In turn, 2D echocardiography showed to underestimate significantly these parameters. Furthermore, mitral regurgitant volume assessed by RT3DE showed excellent correlation ($r = 0.93$) with regurgitant volume measured by MRI, without significant bias (= -0.7ml/beat).

Conclusions: In the management of heart failure patients with LV aneurysm, RT3DE provides an accurate and comprehensive assessment, including quantification of LV size, shape, global systolic function, regional wall motion and myocardial scar together with a precise evaluation of the severity of mitral regurgitation.

INTRODUCTION

Left ventricular (LV) remodeling after acute myocardial infarction is defined as a progressive LV dilation and dysfunction, accompanied by an expansion of myocardial scar [1;2]. This process was demonstrated to be associated with a poor prognosis [3;4] and several treatments are now available to attenuate or partially reverse this phenomenon. Particularly, in the presence of a LV aneurysm surgical ventricular reconstruction (SVR) has been proposed to improve LV size, shape, wall-stress and function [5]. However, the feasibility of this procedure has some limitations and an extensive pre-operative evaluation is necessary in order to give the correct indication, to plan the operation and to estimate the peri-operative and post-operative mortality. In particular, accurate values of LV size, shape and function are crucial to evaluate the impact of surgery; precise identification of LV regional dysfunction, myocardial scar site and extent is also fundamental to determine the feasibility of the procedure. In addition, reliable quantification of mitral regurgitation is important to evaluate the possibility to perform concomitant mitral valve repair [6].

Magnetic resonance imaging (MRI) is currently considered the gold standard for this comprehensive assessment, providing highly accurate and reproducible data [6]. However, this technique is not widely available and is not compatible with cardiac devices. As an alternative, conventional 2-dimensional (2D) echocardiography has been applied, although with significant inaccuracy due to assumptions about LV cavity geometry. Real-time three-dimensional echocardiography (RT3DE) is now available to overcome these limitations and showed to be more accurate than 2D echocardiography for quantification of LV volumes [7]. The aim of this study was therefore to evaluate, in comparison with MRI, feasibility and accuracy of RT3DE for the complex assessment of patients with LV aneurysm, including LV volumes, LV shape, LV ejection fraction, LV wall motion abnormalities, identification of myocardial scar and quantification of the severity of mitral regurgitation.

METHODS

The study population consisted of 60 consecutive patients with ischemic cardiomyopathy and LV akinetic/dyskinetic aneurysm, who were referred from July 2006 to September 2008 to evaluate the possibility of a SVR. The evaluation included, in the same day, conventional 2D echocardiography, RT3DE and cardiac MRI. Using these imaging modalities, LV size and shape and LV global and regional systolic function were evaluated. The presence of a LV thrombus was also assessed. Since echocardiography can not provide a precise identification of myocardial scar, RT3DE and MRI were compared for the measure of LV regional thickness, as a well-known marker of transmural scar. Finally, these 2 imaging modalities were compared for

the assessment of mitral regurgitation severity. All the variables included in the analysis are summarized in Table 1.

All patients gave informed consent and the protocol was approved by the institutional review board.

Table 1. List of the measures and of the imaging modalities included in the study.

	MRI	RT3DE	2DE
Left ventricular end-diastolic volume (LVEDV)	X	X	X
Left ventricular end-systolic volume (LVESV)	X	X	X
Left ventricular ejection fraction (LVEF)	X	X	X
Left ventricular sphericity index (LVSI)	X	X	X
Left ventricular wall motion score index (LVWMSI)	X	X	X
Left ventricular thrombus detection	X	X	X
Left ventricular regional thickness	X	X	-
Mitral regurgitant volume	X	X	-

2DE:2-dimensional echocardiography, MRI: magnetic resonance imaging, RT3DE:real-time three-dimensional echocardiography

Standard 2D echocardiography

Patients were imaged in the left lateral decubitus position using a commercially available system (iE33, Philips Medical Systems, N.A., Bothell, Washington, USA) equipped with a 3.5-MHz transducer. LV end-systolic volume (ESV) and LV end-diastolic volume (EDV) were determined from the conventional apical 2- and 4-chamber views and LV ejection fraction (EF) was calculated using the biplane Simpson's technique [8].

As a measure of LV shape, sphericity index (SI) was calculated by dividing LVEDV by the volume of a sphere whose diameter was derived from the major end-diastolic LV long-axis. The LV long-axis was obtained as the longest distance between the centre of the mitral annulus and the endocardial apex in the 4-chamber view [6;9].

Qualitative assessment of the regional wall motion was performed according to the standard 16-segment model[10] and was graded as follows: 1 = normal; 2 = hypokinetic; 3 = akinetic and 4 = dyskinetic. A global wall motion score index (WMSI) was calculated as the sum of each LV segment's score divided by the number of visualized segments [8].

Finally, the presence of a LV thrombus, especially in the apical region, was evaluated without contrast administration, using standard and off-axis views.

Real-time three-dimensional echocardiography

Patients were imaged with the same system (iE33, Philips Medical Systems) equipped with an X3, fully sampled matrix transducer. Apical full-volume data sets were obtained combining,

within 1 breath-hold, 7 small real-time sub-volumes to provide a larger pyramidal volume (up to 101×104 degrees) and to ensure a complete capture of the LV. A 3D data set was considered unsuitable for analysis if >2 segments could not be visualized or if it contained visible stitch artefacts due to irregular heart rate or breathing movements. To assess the severity of mitral regurgitation, apical full-volume Color Doppler data sets were also acquired with a Nyquist limit set between 30 and 50 cm/sec. All 3D data sets were stored digitally and quantitative analysis was performed off-line using a semi-automated contour tracing algorithm (Q-Lab, version 6.0, Philips Medical Systems).

During post-processing of the 3D data set, the software automatically displays the apical 4- and 2-chamber views and the parasternal short-axis view. After initial identification of the apex and mitral annulus with 5 reference points on the end-diastolic and end-systolic frames, a preconfigured ellipse is fitted to the endocardial border for each frame. A manual adjustment of the endocardial border was performed if required. A LV 3D model is automatically generated and LV volumes and LVEF are calculated.

The SI of the LV 3D model was calculated as with 2D echocardiography; however, the use of 2 near-orthogonal cut-planes within the 3D dataset allowed for the exact location of the endocardial apex, avoiding any foreshortening (Figure 1). Furthermore, by slicing the 3D dataset, multiple LV short- and long-axes can be obtained (at the basal, mid-ventricular and apical level) and analysed to assess the 3D WMSI as for 2D echocardiography [11]. With the same approach, the presence of a LV thrombus, particularly at the apical level, was also evaluated. From the same short-axis slices, the endocardial and epicardial contours were traced manually at end-diastole, with the papillary muscles included in the cavity. The traced contours

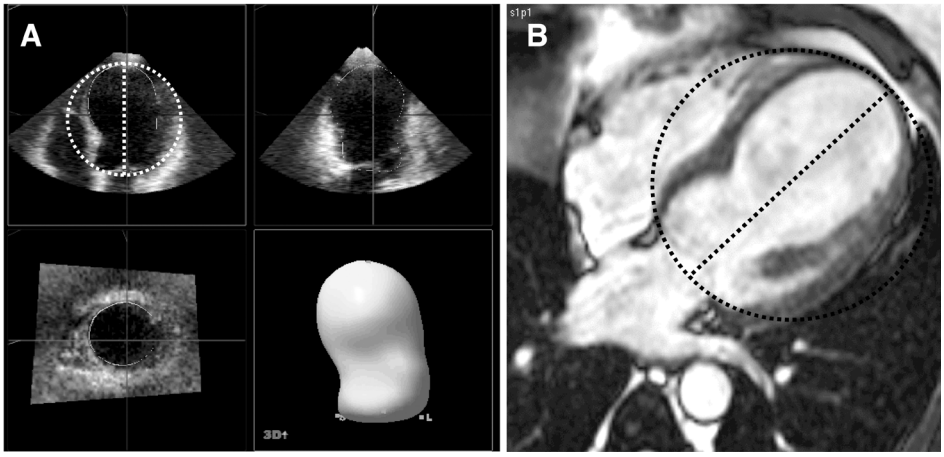


Figure 1. Schematic example of calculation of sphericity index with RT3DE (left panel) and MRI (right panel) in a patient with LV aneurysm. The major end-diastolic LV long axis was obtained as the longest distance between the centre of the mitral annulus and the endocardial apex, identified by cropping the 3D dataset (panel A) or selecting the best slice in the MRI acquisition (panel B). Sphericity index was calculated by dividing LV end-diastolic volume by the volume of a sphere whose diameter was derived from the LV long-axis.

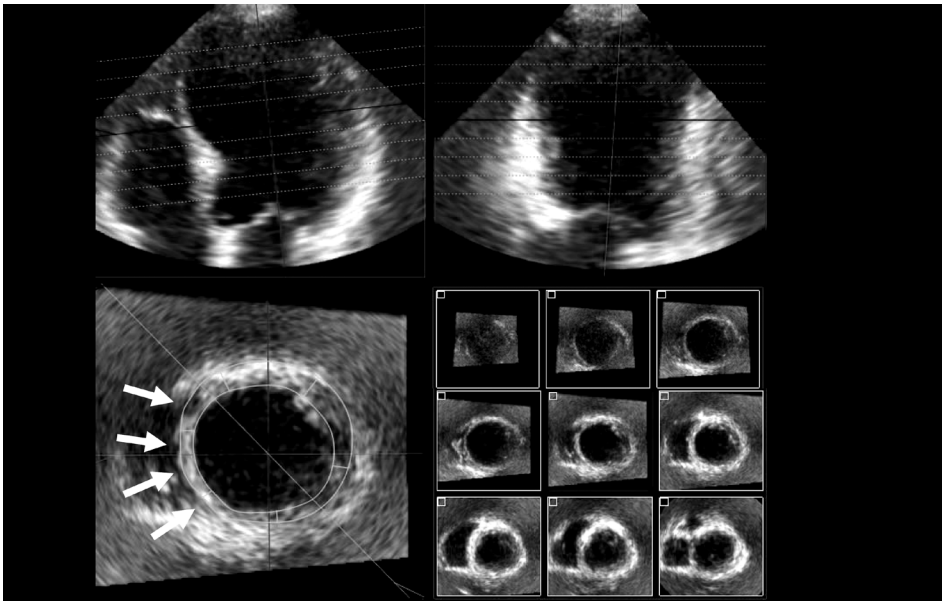


Figure 2. An example of RT3DE assessment of LV regional thickness. After slicing the 3D dataset in 9 LV short-axes (3 at the basal, 3 at the mid-ventricular and 3 at the apical level), the endocardial and epicardial contours were traced manually at the end-diastolic frame. The traced contours were then used to calculate LV regional thickness according to the standard 16-segment model. The white arrows indicate the septum at mid-ventricular level that most likely contains transmural scar tissue (end-diastolic thickness <6mm). The LV apical segments are also significantly thinned (see right bottom panel).

were then used to calculate LV regional thickness according to the standard 16-segment model [10] (Figure 2). In particular as previously described [12], severely thinned regions (end-diastolic thickness <6mm) were considered to be representative for transmural scar.

To evaluate the severity of mitral regurgitation, the effective regurgitant orifice area (EROA) was calculated [13–15]. In particular, the 3D Color Doppler dataset was manually cropped by an image plane perpendicularly oriented to the jet direction until the narrowest cross-sectional area of the jet. The EROA was measured by manual planimetry of the color Doppler signal, tilting the image in an 'en face' view (Figure 3); the regurgitant volume was estimated as EROA multiplied by the velocity time integral of the regurgitant jet on the continuous-wave Doppler.

Image acquisition required approximately 5 min, while post processing required 10 to 15 min, including the measurement of LV volumes, LVEF, LVSI and LV wall motion abnormalities, the evaluation of mitral regurgitation severity and the assessment of LV thrombus

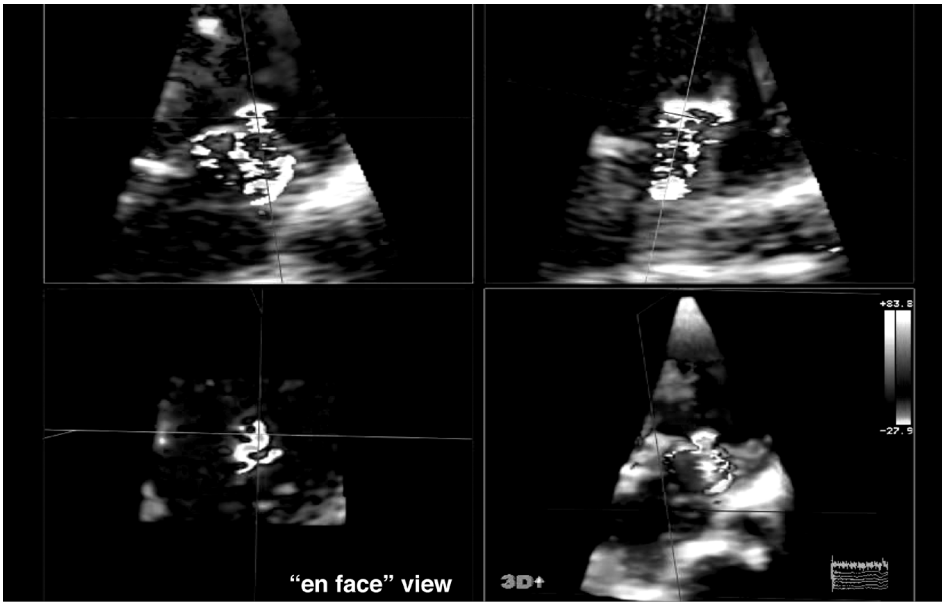


Figure 3. An example of RT3DE assessment of mitral effective regurgitant orifice area. The 3D dataset is manually cropped by an image plane perpendicularly oriented to the jet direction until the narrowest cross-sectional area of the jet. The effective regurgitant orifice area is measured (= 0.26 cm2) by manual planimetry of the color Doppler signal tilting the image in an 'en face' view.

Magnetic resonance imaging

Data acquisition

Data acquisition was performed on a 1.5 T scanner equipped with powertrack 6000 gradients (Gyroscan ACS-NT/Intera, Philips Medical Systems, Best, The Netherlands). Scout images and 2- and 4-chamber acquisitions were performed to identify the intrinsic long-axis of the heart and for further planning. A cine-set of 12-16 multi-slice images were acquired in short-axis orientation, covering the complete LV from apex to base. Segmented gradient-turbo field echo was used, with parallel imaging (Sensitivity Encoding, acceleration factor 2) and steady-state free-precession. The following imaging parameters were used: slice thickness of the imaging planes=10 mm, with no gap; Field-of-View=440 mm; 80% scan, scan-matrix=256 × 256, reconstructed voxels of 1.56×1.56×10.0 mm; α=35°; TR/TE=3.6/1.7.

To evaluate the severity of mitral regurgitation, a true 3D MRI acquisition was applied with velocity-encoding in 3 orthogonal directions (field-of-view 370 mm, 3D volume scan with slab thickness 48 mm, reconstructed into 12 slices of 4 mm, TE/TR=3.3/14, α=10°, acquisi-

tion voxel size 2.9×3.8×4.0 mm^3, reconstructed into 1.4×1.4×4.0 mm^3, NSA 1, with 30 phases reconstructed, EPI factor 5) [16–18].

Data analysis

Quantification of LVESV, LVEDV and LVEF was performed on the short-axis series using MASS analytical software (Medis, Leiden, The Netherlands) and manual contour tracing of the epicardial and endocardial borders, as previously described [19].

The SI was calculated from the 4-chamber acquisition as abovementioned for 2D echocardiography and RT3DE (Figure 1). Qualitative assessment of the regional wall motion was performed using both long- and short-axis acquisitions and the WMSI was based on a 16-segment model as for the echocardiographic analysis. From the same acquisitions, the presence of a LV thrombus was evaluated.

In addition, from the complete short-axis dataset 3 slices were selected representing the basal, mid-ventricular and apical level. From the epicardial and endocardial contours drawn in these slices, LV end-diastolic regional thickness was calculated according to the standard 16-segment model [10] (Figure 4). As previously described in various studies, an end-diastolic thickness <6 mm was considered as a marker of transmural scar [20;21].

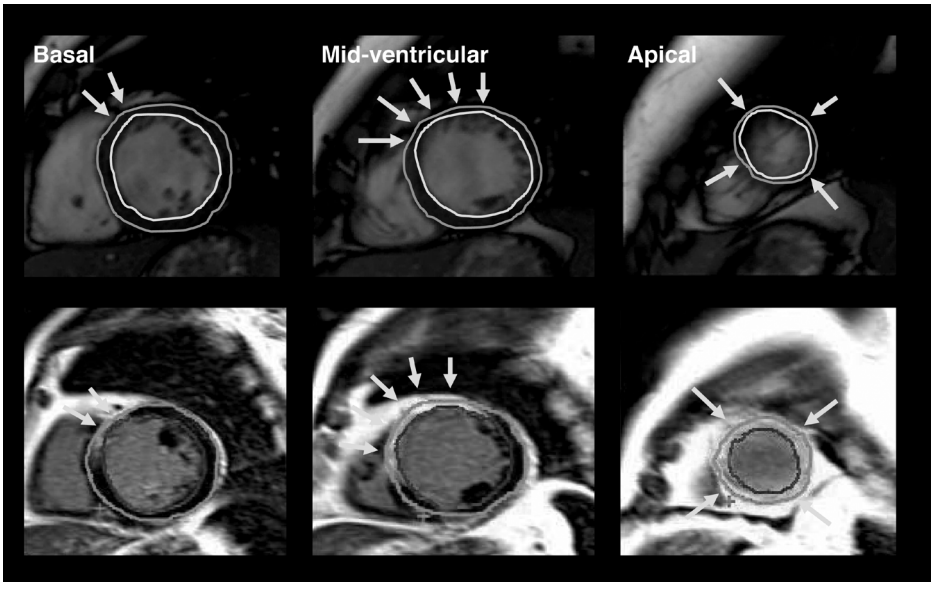


Figure 4. A set of MRI short-axis slices at basal, mid-ventricular and apical level acquired for the assessment of LV wall thickness (upper panel), using gradient-echo acquisitions, and for the analysis of myocardial scar (lower panel), using delayed contrast-enhanced images. In this example, the antero-septum, the anterior wall and the apex are significantly thinned and contain transmural scar (see arrows).

To confirm the site and the extent of scar tissue, contrast-enhanced images (20-24 short-axis slices) were acquired 15 minutes after bolus injection of gadolinium diethylenetriamine pentaacetetic acid (Magnevist, Schering/Berlex, Berlin, Germany; 0.15 mmol/Kg) with an inversion recovery gradient echo sequence (400×400 mm^2 Field-of-View; 256×256 matrix size, 5-mm slice thickness with gap of -5mm, α=15°, TE/TR=1.36/4.53) [22]. Hyperenhanced regions were defined by selecting a region-of-interest inside the normal myocardium and thresholding the window setting at 5SD above the mean signal intensity [23] (Figure 4). The total extent of scar, expressed as percentage of LV mass, was quantified using QMass (Medis) and the number of segments with transmural scar was calculated.

The 3D velocity-encoded MRI acquisitions were analyzed using in-house developed image processing software. The procedure was performed as previously described [17;18]. In summary, from the velocity-encoded MRI data, the 3 velocity vector components of blood flow at the level of the mitral valve plane needs to be reformatted, using the LV 4- and 2-chamber views. The velocities measured perpendicularly to the reconstructed MV plane need to be corrected for the motion of the myocardium in basal/apical direction in order to obtain the true trans-valvular velocity of the blood flow. The trans-valvular volume flow was obtained by integrating the resulting velocities over the annulus area. The regurgitant volume was obtained by calculating the Riemann sum of backward flow during systole in the flow graph. The reproducibility of this analysis was also previously reported [16–18].

Statistical analysis

Continuous data are presented as mean±SD; dichotomous data are presented as numbers and percentages. Comparison of data was performed using the paired Student *t* test. Pearson's correlation analysis was performed to evaluate the relation between echocardiographic and MRI measurements. In addition, Bland-Altman analysis was performed to evaluate the differences between echocardiographic and MRI measurements and the mean bias±2SD are reported. Agreement between these imaging techniques was assessed using weighted κ statistics (Fleiss-Cohen weighting). The reproducibility of the RT3DE measures was assessed with Pearson's correlation and Bland-Altman analysis. A p-value <0.05 was considered to be statistically significant. A statistical software program SPSS16.0 (SPSS Inc, Chicago, Il, USA) was used for statistical analysis.

RESULTS

Three patients (5%) did not undergo cardiac MRI because of major contraindications (atrial fibrillation and cardiac devices). Another 5 patients (8.5%) were excluded from further analysis because of inadequate RT3DE images. Clinical characteristics of the remaining 52 patients are

summarized in Table 2. All patients had symptoms of heart failure despite optimal medical therapy. The presence of a LV aneurysm (with at least 2 contiguous dyskinetic segments) was observed in all patients and in most of the cases (81%) involved the antero-septum, anterior and apical segments, as a result of a previous myocardial infarction in the LAD territory.

Table 2. Clinical characteristics of the study population (n = 52).

Age (years)	62±10
Male/Female	37/15
NYHA class	
II	4(8%)
III	40(77%)
IV	8(15%)
Medication	
ACE-inhibitors	48(92%)
ß-blockers	41(79%)
Diuretics and/or spironolactone	49(94%)
Amiodarone	11(21%)
Anticoagulants	43(82%)
Myocardial infarction/aneurysm location	
Antero-septum/anterior/apex	42(81%)
Infero-septum/inferior	9(17%)
Postero-lateral	1(2%)
Previous percutaneous revascularization	46(88%)
Multi-vessel disease	35(67%)
Single-vessel disease	11(21%)
Time from myocardial infarction (months)	19±11

NYHA: New York Heart Association functional class

Left ventricular size and shape

Mean values of LVEDV, LVESV and SI measured with 2D echocardiography, RT3DE and MRI are displayed in Table 3. According to all these techniques, a severe LV dilatation with a remodeling towards a spherical shape was observed.

Considering MRI the gold standard, RT3DE showed an excellent correlation for the measurements of LVEDV, LVESV and SI ($r = 0.97$, $r = 0.98$ and $r = 0.96$, respectively, $p < 0.001$). However, Bland-Altman analysis (Figure 5) revealed a systematic bias between MRI and RT3DE of 21.6±40.4 ml for LVEDV, of 19.8±40.1 ml for LVESV and of 0.01±0.05 for SI ($p < 0.01$), which tended to increase for larger and more spherical LV volumes.

Similarly, 2D echocardiography showed a good correlation with MRI for the measures of LVEDV, LVESV and SI ($r = 0.94$, $r = 0.95$ and $r = 0.94$, respectively, $p < 0.001$). However, Bland-Altman analysis showed a significantly larger bias between these 2 techniques with a mean difference of 40.9±48.8 ml for LVEDV, of 32.7±44.9 ml for LVESV and of 0.03±0.07 for SI ($p < 0.001$).

Table 3. Mean values of LV size and function measured by 2D echocardiography (2DE), RT3DE and MRI.

	MRI	RT3DE	2DE
LVEDV (ml)	288.4±87.2	266.8±75.3*	247.4±70.5*
LVESV (ml)	212.7±91.4†	192.9±70.8*	180.0±73.7*
LVEF (%)	28.0±12.2	29.0±10.4†	28.8±11.2†
LVSI	0.54±0.17	0.53±0.15†	0.51±0.14*
LVWMSI	2.0±0.6	2.2±0.5†	2.4±0.5*

*=p<0.001 compared to MRI.

†=p<0.05 compared to MRI

EDV: end-diastolic volume, EF: ejection fraction, ESV: end-systolic volume, LV: left ventricle, SI: sphericity index, WMSI: wall motion score index

Left ventricular global and regional systolic function

Mean values of LVEF and WMSI measured with 2D echocardiography, RT3DE and MRI are displayed in Table 3. Considering MRI the gold standard, RT3DE showed an excellent correlation for the measure of LVEF (r = 0.97, p <0.001); a mean bias between MRI and RT3DE of -0.9±4.6% (p <0.05) was found at the Bland-Altman analysis (Figure 5). Similarly, a good correlation for the measure of LVEF (r = 0.96, p <0.001) was observed between 2D echocardiography and MRI with a mean bias of -0.7±5.2% (p <0.05).

A significant difference in the value of WMSI was found both with RT3DE and 2D echocardiography as compared to MRI. However, in a segment-to-segment comparison (for a total of 821 segments that could be satisfactorily visualized by the 3 techniques) a better agreement was observed between RT3DE and MRI (k = 0.62) than between 2D echocardiography and MRI (k = 0.58).

Of note, a LV thrombus was detected by MRI in 4 (8%) patients. A LV thrombus was identified in the same 4 patients by RT3DE, while 2D echocardiography was not able to detect a small thrombus adjacent to the apical anterior wall in one of these patients.

Identification of LV segments with transmural scar

Using RT3DE, LV endocardial and epicardial borders could be both visualized in 779 (93%) segments and a mean of 6.0±1.7 segments per patient showed a thickness <6 mm and were considered as transmural scar. Similarly using MRI, a mean of 5.8±2.2 segments per patient (p <0.001) were defined as transmural scar (thickness <6 mm). In a segment-to-segment comparison, RT3DE and MRI showed a good agreement (k = 0.56) for the identification of LV segments with transmural scar, based on the measure of LV regional thickness. A good agreement was observed also between RT3DE and contrast-enhanced MRI (k = 0.54), which showed a mean of 5.1±1.9 segments per patient with a transmural scar. Of note, using contrast-enhanced MRI mean total scar extent was 29.9±8.2%.

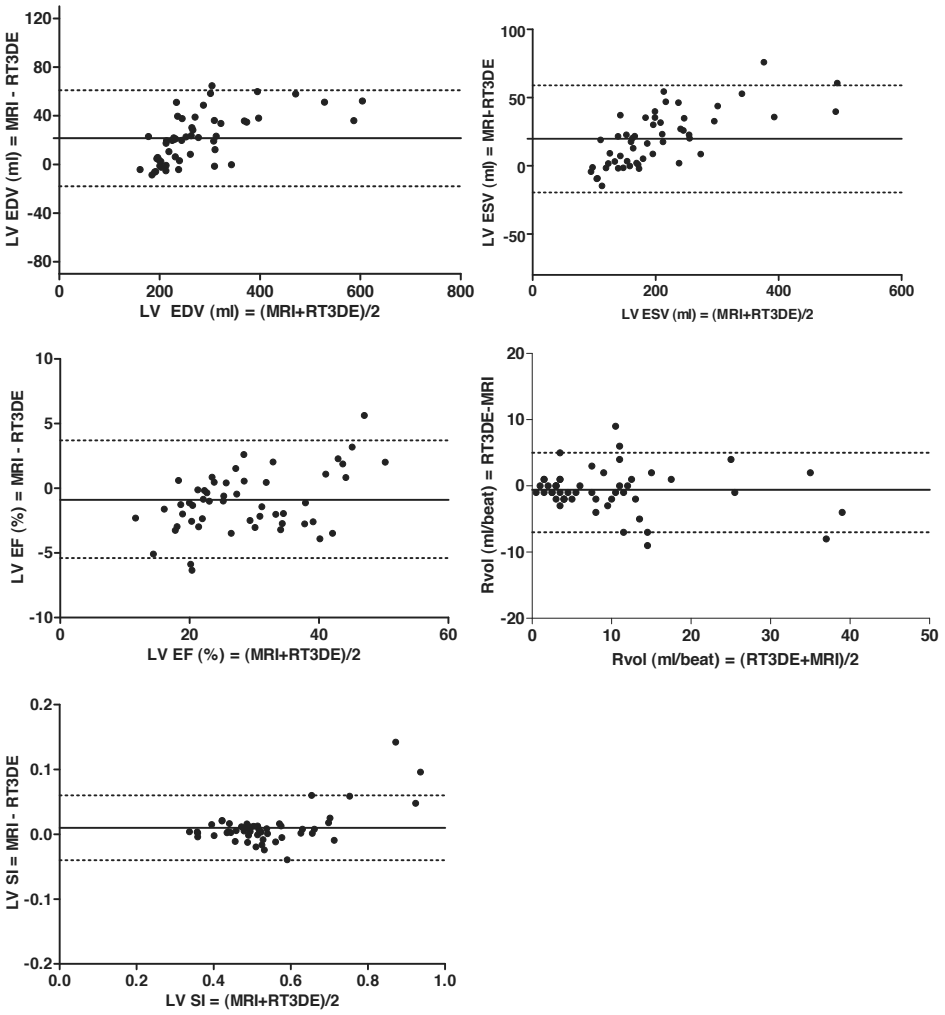


Figure 5. Bland-Altman scatter plot of differences (Y-axis) in LV end-diastolic volume (EDV), LV end-systolic volume (ESV), LV ejection fraction (EF), LV sphericity index (SI) and mitral regurgitant volume (Rvol) between RT3DE and MRI, plotted against the average between these techniques (X-axis). The mean bias (full line) and the 95% limits of agreement (dotted lines) are displayed.

Mitral regurgitation

From RT3DE analysis, the mean mitral regurgitant volume was 9.2±8.8 ml/beat, ranging from 2 to 37 ml/beat. Similarly from the 3D velocity encoded MRI analysis, the mean mitral regurgitant volume was 9.8±9.4 ml/beat, ranging from 2 to 42 ml/beat. RT3DE and MRI showed an excellent correlation for the assessment of mitral regurgitant volume ($r = 0.93$, $p < 0.001$)

and the Bland-Altman analysis (Figure 5) revealed a non significant bias between these techniques (RT3DE–VE MRI = -0.7 ml/beat, limits of agreement from -7.1 to 5.8 ml/beat, p = 0.71).

Reproducibility of RT3DE measures

Reproducibility of RT3DE measures of LVEDV, ESV and EF were previously reported [24;25] by our group and were in line with other studies [26]. Reproducibility of RT3DE assessment of mitral effective regurgitant orifice and regurgitant volume was also previously reported by our group [15].

Inter-observer reproducibility for SI and WMSI was obtained analyzing the 3D dataset of 15 patients at different times by 2 independent observers, each without knowledge of the results obtained by the other. The agreement was good: mean bias was 0.00±0.07 (p = 0.32) and 0.2±0.03 (p = 0.24), respectively. The correlation between the measures of the 2 observers was also excellent (both r = 0.97, p <0.001). Similarly, inter-observer variability for LV regional thickness was tested on 7 patients (112 segments): mean bias was 0.7±0.3 mm (p = 0.11, r = 0.91).

DISCUSSION

The main findings of the current study can be summarized as follows: 1) in patients with LV aneurysm, evaluation of LV size, shape and function by RT3DE is feasible and reproducible; 2) in this group of patients, RT3DE provides highly accurate quantification of LV volumes, EF, SI and WMSI, in a direct comparison with MRI; 3) RT3DE can be also applied for the identification of transmural scar and for the assessment of mitral regurgitation severity.

Heart failure and LV aneurysm

Surgical treatment

Surgical ventricular reconstruction, and in particular endoventricular circular patch plasty (Dor procedure), has been proposed as a treatment for heart failure patients with an extensive myocardial infarction and LV aneurysm. Aim of this procedure is to restructure the curvature of the LV wall back to its original geometric configuration, excluding the scarred portion of the ventricle from the adjacent viable myocardium. Scar exclusion prompts a return to a systolic concentric contraction and was demonstrated to decrease LV volume and to increase LV systolic function [5;27;28]. However, the impact of this procedure on survival is still controversial [27] and accurate patient selection should be performed. In particular, to set the

indication for SVR, accurate quantitative evaluations are necessary to determine the feasibility and the impact of surgery, considering the complicated postoperative LV geometric changes. Accurate quantification of LV size and shape is fundamental to avoid an excessive volume reduction and/or cavity deformation that lead to a progressive diastolic dysfunction and to a restrictive filling pattern [6]. Furthermore, the precise extent of myocardial scar and the wall motion abnormalities is crucial to evaluate whether a "viable" contractile LV cavity can be reshaped. Also, the presence of a LV thrombus is often a decision point for aneurysmecutomy and estimate of peri- and post-operative mortality is mainly based on a reliable assessment of LV global and regional systolic function [5]. In addition, SVR is often accompanied by mitral valve repair and the severity of mitral regurgitation should be therefore carefully evaluated.

Use of imaging for an extensive evaluation

As mentioned above, patients with heart failure and LV aneurysm need an extensive evaluation before SVR. Currently, MRI is considered the gold standard for this comprehensive analysis. This imaging technique in fact was proven to be far more accurate than other techniques for quantification of LV shape and volumes, for the analysis of LV global systolic function and wall motion abnormalities, for identifying the precise extent of transmural scar and for the evaluation of mitral valve apparatus [6]. However, MRI is not widely available, due to the high equipment costs and the need for special facilities, and can not be applied in the presence of cardiac devices and atrial fibrillation, often present in heart failure patients. Furthermore, MRI can not be performed at the bedside or in the operating room, where an immediate assessment of SVR results is of great importance. In a head-to-head comparison with MRI, the current study demonstrated the accuracy of RT3DE as a potential alternative technique for the study of heart failure patients with significantly abnormal LV geometry due to the presence of a LV aneurysm. In particular, excellent correlation and a good agreement were found between these 2 techniques for the calculation of LVEDV, ESV, EF and SI. Of note, a trend towards an increased disagreement between RT3DE and MRI for the measurements of larger LV volumes and for more spherical LV shape was noted, probably due to the challenges (limited sector width and lateral resolution) of obtaining an appropriate echo acquisition in the presence of a very dilated ventricle with geometrical alterations. In a segment-to segment comparison with MRI, RT3DE showed to be accurate also for the analysis of wall motion abnormalities and identification of non-viable segments. In turn, conventional 2D echocardiography showed to be less accurate, with a significant underestimation of these LV parameters probably due to inappropriate geometric assumptions and to the difficulty of obtaining true apical views.

These findings confirmed in a large population the results of initial studies [1;26;29] that applied the old free-hand 3D rotating probe or the novel real-time acquisition in small groups

of patients with LV aneurysm. For the first time however, RT3DE was applied in this study also for the calculation of WMSI and the analysis of LV regional thickness, which contains crucial information for the identification of myocardial transmural scar. Several studies demonstrated that the extent of myocardial scar, more than the type of asynergy (dyskinesia versus akinesia), has an important prognostic value for SVR outcomes [5,6]. Furthermore, RT3DE showed to be an accurate approach also for the assessment of the severity of mitral regurgitation, which is of great prognostic importance and is necessary to plan the surgical treatment. Mitral regurgitant volume assessed by RT3DE showed an excellent correlation with regurgitant volume measured by 3D MRI, without a significant difference between the 2 techniques. In fact, color Doppler RT3DE, allowing for an unlimited plan orientation and in particular for an "en face" view of the mitral valve, provides a direct planimetry of the regurgitant orifice, obviating the geometric assumptions not applicable in patients with functional mitral regurgitation, in which the EROA is typically elongated along the semilunar-shaped leaflet coaptation line [13;15].

This comprehensive approach makes RT3DE particularly suitable for the management of heart failure patients with LV aneurysm. Further studies are needed to demonstrate the accuracy of RT3DE measures using the transesophageal approach, in view of a potential application in the operating room for an immediate assessment of SVR results.

Study limitations

Although the RT3DE measures showed a good reproducibility, further multi-center studies with larger population are needed to confirm the results of the current study. Furthermore, short- and long-term follow-up data are necessary to explore the accuracy and prognostic value of RT3DE for the assessment of progressive LV remodeling or, in case of SVR, for the evaluation of the surgical outcome.

CONCLUSIONS

For the management of heart failure patients with LV aneurysm and in order to determine the best treatment for these patients, RT3DE provides an accurate and comprehensive assessment, including quantification of LV size, shape, global systolic function and extension of wall motion abnormalities together with the identification of transmural scar and a precise evaluation of the severity of mitral regurgitation.

REFERENCES

1. Mannaerts HF, van der Heide JA, Kamp O, Stoel MG, Twisk J, Visser CA. Early identification of left ventricular remodelling after myocardial infarction, assessed by transthoracic 3D echocardiography. *Eur Heart J* 2004;25:680-687.
2. Opie LH, Commerford PJ, Gersh BJ, Pfeffer MA. Controversies in ventricular remodelling. *Lancet* 2006;367:356-367.
3. Cohn JN, Ferrari R, Sharpe N. Cardiac remodeling--concepts and clinical implications: a consensus paper from an international forum on cardiac remodeling. Behalf of an International Forum on Cardiac Remodeling. *J Am Coll Cardiol* 2000;35:569-582.
4. Mangschau A. Akinetic versus dyskinetic left ventricular aneurysms diagnosed by gated scintigraphy: difference in surgical outcome. *Ann Thorac Surg* 1989;47:746-751.
5. Dor V, Sabatier M, Montiglio F, Civaia F, DiDonato M. Endoventricular patch reconstruction of ischemic failing ventricle. a single center with 20 years experience. advantages of magnetic resonance imaging assessment. *Heart Fail Rev* 2004;9:269-286.
6. Dor V, Civaia F, Alexandrescu C, Montiglio F. The post-myocardial infarction scarred ventricle and congestive heart failure: the preeminence of magnetic resonance imaging for preoperative, intraoperative, and postoperative assessment. *J Thorac Cardiovasc Surg* 2008;136:1405-1412.
7. Mor-Avi V, Jenkins C, Kuhl HP, Nesser H, Marwick TH, Franke A et al. Real-time 3-dimensional echocardiographic quantification of left ventricular volumes: multicenter study for validation with magnetic resonance imaging and investigation of sources of error. *JACC Cardiovasc Img* 1, 413-423. 2008;1:413-423.
8. Lang RM, Bierig M, Devereux RB et al. Recommendations for chamber quantification. *Eur J Echocardiogr* 2006;7:79-108.
9. Di Donato M, Dabic P, Castelvecchio S et al. Left ventricular geometry in normal and post-anterior myocardial infarction patients: sphericity index and 'new' conicity index comparisons. *Eur J Cardiothorac Surg* 2006;29 Suppl 1:S225-S230.
10. Cerqueira MD, Weissman NJ, Dilsizian V et al. Standardized myocardial segmentation and nomenclature for tomographic imaging of the heart: a statement for healthcare professionals from the Cardiac Imaging Committee of the Council on Clinical Cardiology of the American Heart Association. *Circulation* 2002;105:539-542.
11. Ahmad M, Xie T, McCulloch M, Abreo G, Runge M. Real-time three-dimensional dobutamine stress echocardiography in assessment stress echocardiography in assessment of ischemia: comparison with two-dimensional dobutamine stress echocardiography. *J Am Coll Cardiol* 2001;37:1303-1309.
12. Schinkel AF, Bax JJ, Boersma E et al. Assessment of residual myocardial viability in regions with chronic electrocardiographic Q-wave infarction. *Am Heart J* 2002;144:865-869.
13. Kahlert P, Plicht B, Schenk IM, Janosi RA, Erbel R, Buck T. Direct assessment of size and shape of noncircular vena contracta area in functional versus organic mitral regurgitation using real-time three-dimensional echocardiography. *J Am Soc Echocardiogr* 2008;21:912-921.
14. Khanna D, Vengala S, Miller AP et al. Quantification of mitral regurgitation by live three-dimensional transthoracic echocardiographic measurements of vena contracta area. *Echocardiography* 2004;21:737-743.
15. Marsan NA, Westenberg JJ, Ypenburg C, et al. Quantification of mitral regurgitation by real-time three-dimensional echocardiography: head-to-head comparison with 3D velocity-encoded magnetic resonance imaging. *JACC Cardiovasc Img.* 2009;2:1245-1252

16. Roes SD, Hammer S, van der Geest RJ et al. Flow Assessment Through Four Heart Valves Simultaneously Using 3-Dimensional 3-Directional Velocity-Encoded Magnetic Resonance Imaging With Retrospective Valve Tracking in Healthy Volunteers and Patients With Valvular Regurgitation. *Invest Radiol* 2009;44:669-675
17. Westenberg JJ, Danilouchkine MG, Doornbos J et al. Accurate and reproducible mitral valvular blood flow measurement with three-directional velocity-encoded magnetic resonance imaging. *J Cardiovasc Magn Reson* 2004;6:767-776.
18. Westenberg JJ, Roes SD, Marsan NA et al. Mitral valve and tricuspid valve blood flow: accurate quantification with 3D velocity-encoded MR imaging with retrospective valve tracking. *Radiology* 2008;249:792-800.
19. Westenberg JJ, Braun J, Van de Veire N et al. Magnetic resonance imaging assessment of reverse left ventricular remodeling late after restrictive mitral annuloplasty in early stages of dilated cardiomyopathy. *J Thorac Cardiovasc Surg* 2008;135:1247-1252.
20. Baer FM, Voth E, Schneider CA, Theissen P, Schicha H, Sechtem U. Comparison of low-dose dobutamine-gradient-echo magnetic resonance imaging and positron emission tomography with [18F]fluorodeoxyglucose in patients with chronic coronary artery disease. A functional and morphological approach to the detection of residual myocardial viability. *Circulation* 1995;91:1006-1015.
21. Kaandorp TA, Lamb HJ, van Der Wall EE, de Roos A, Bax JJ. Cardiovascular MR to access myocardial viability in chronic ischaemic LV dysfunction. *Heart* 2005;91:1359-1365.
22. Kaandorp TA, Bax JJ, Schuijf JD et al. Head-to-head comparison between contrast-enhanced magnetic resonance imaging and dobutamine magnetic resonance imaging in men with ischemic cardiomyopathy. *Am J Cardiol* 2004;93:1461-1464.
23. Bondarenko O, Beek AM, Hofman MB et al. Standardizing the definition of hyperenhancement in the quantitative assessment of infarct size and myocardial viability using delayed contrast-enhanced CMR. *J Cardiovasc Magn Reson* 2005;7:481-485.
24. Marsan NA, Bleeker GB, Ypenburg C et al. Real-time three-dimensional echocardiography as a novel approach to assess left ventricular and left atrium reverse remodeling and to predict response to cardiac resynchronization therapy. *Heart Rhythm* 2008;5:1257-1264.
25. Marsan NA, Bleeker GB, Ypenburg C et al. Real-time three-dimensional echocardiography permits quantification of left ventricular mechanical dyssynchrony and predicts acute response to cardiac resynchronization therapy. *J Cardiovasc Electrophysiol* 2008;19:392-399.
26. Qin JX, Jones M, Shiota T et al. Validation of real-time three-dimensional echocardiography for quantifying left ventricular volumes in the presence of a left ventricular aneurysm: in vitro and in vivo studies. *J Am Coll Cardiol* 2000;36:900-907.
27. Jones RH, Velazquez EJ, Michler RE et al. Coronary bypass surgery with or without surgical ventricular reconstruction. *N Engl J Med* 2009;360:1705-1717.
28. Zhong L, Sola S, Tan RS et al. Effects of surgical ventricular restoration on left ventricular contractility assessed by a novel contractility index in patients with ischemic cardiomyopathy. *Am J Cardiol* 2009;103:674-679.
29. Buck T, Hunold P, Wentz KU, Tkalec W, Nesser HJ, Erbel R. Tomographic three-dimensional echocardiographic determination of chamber size and systolic function in patients with left ventricular aneurysm: comparison to magnetic resonance imaging, cineventriculography, and two-dimensional echocardiography. *Circulation* 1997;96:4286-4297.

PART IIIB

Magnetic resonance imaging for the assessment of valvular heart disease

CHAPTER 19

Mitral valve and tricuspid valve blood flow: accurate quantification with 3D velocity-encoded MR imaging with retrospective valve tracking

J JM Westenberg, S D Roes, **N Ajmone Marsan**, N M J Binnendijk, J Doornbos, J J Bax, J H C Reiber, A de Roos, R J van der Geest

Radiology 2008;249:792-800.

ABSTRACT

Objectives: To validate flow assessment performed with three-dimensional (3D) three-directional velocity-encoded (VE) magnetic resonance (MR) imaging with retrospective valve tracking and to compare this modality with conventional two-dimensional (2D) one-directional VE MR imaging in healthy subjects and patients with regurgitation.

Methods: Patients and volunteers gave informed consent, and local medical ethics committee approval was obtained. Patient data were selected retrospectively and randomly from a database of MR studies obtained between July 2006 and July 2007. The 3D three-directional VE MR images were first validated in vitro and compared with 2D one-directional VE MR images. Mitral valve (MV) and tricuspid valve (TV) flow were assessed in 10 volunteers without valve insufficiency and 20 patients with valve insufficiency, with aortic systolic stroke volume (ASSV) as the reference standard.

Results: Phantom validation showed less than 5% error for both techniques. In volunteers, 3D three-directional VE MR images showed no bias for MV or TV flow when compared with ASSV, whereas 2D one-directional VE MR images showed significant bias for MV flow (15% overestimation, $p < 0.01$). TV flow showed 25% overestimation; however, this was insignificant because of the high standard deviation. Correlation with ASSV was strong for 3D three-directional VE MR imaging ($r = 0.96$, $p < 0.01$ for MV flow; $r = 0.88$, $p < 0.01$ for TV flow) and between MV and TV flow ($r = 0.91$, $p < 0.01$); however, correlation was weaker for 2D one-directional VE MR imaging ($r = 0.80$, $p < 0.01$ for MV flow; $r = 0.22$, $p = 0.55$ for TV flow) and between MV flow and TV flow ($r = 0.34$, $p = 0.34$). In patients (mean regurgitation fractions of 13% and 10% for MV flow and TV flow, respectively), correlation between MV flow and TV flow for 3D three-directional VE MR imaging was strong ($r = 0.97$, $p < 0.01$).

Conclusions: Use of 3D three-directional VE MR imaging enables accurate MV and TV flow quantification, even in patients with valve regurgitation.

INTRODUCTION

Mitral valve (MV) and tricuspid valve (TV) regurgitation is a common complication of ischemic heart disease. Both the timing and the type of surgical intervention depend on the severity of symptoms leading to left ventricle dysfunction [1–3]. Echocardiography is commonly used to classify the severity of MV and TV regurgitation [4–7]. The quality of the acoustic window, attenuation from overlying structures such as ribs and lungs, and operator experience affect echo Doppler image quality and can influence classification of regurgitation [8,9]. Besides having measurement restrictions, semiquantitative approaches—such as assessment of the regurgitant jet area and width on color Doppler images [10,11] and the proximal isovelocity surface area technique [12,13]—rely on modeling assumptions, which are not valid in all subjects. Only flow in the same direction aligned with the ultrasound beam can be quantified, and the sample volume can not be adapted to the motion of the annulus [14,15], thereby limiting accurate quantification with echo Doppler ultrasonography.

Velocity-encoded (VE) magnetic resonance (MR) imaging is a noninvasive imaging modality already extensively used for blood flow assessment [15–19]. In all previous attempts to quantify blood flow with VE MR imaging of atrioventricular valves, heart motion during contraction and relaxation was encountered as the main obstacle. Kayser et al [20] showed that correction for throughplane motion (ie, motion in the longitudinal direction through the acquisition plane positioned at the heart valve of interest) is indispensable for accurate transvalvular flow assessment. With three-directional VE MR imaging [21], intraventricular blood flow patterns can be assessed [22–25] to enable quantification of MV regurgitation [26]. The purpose of our study was to validate flow assessment performed with three-dimensional (3D) three-directional VE MR imaging with retrospective valve tracking and to compare this modality with conventional two-dimensional (2D) one-directional VE MR imaging in healthy subjects and patients with regurgitation.

METHODS

Patient population

Ten healthy volunteers (six men, four women; mean age, 33 years±9 and 26 years±7, respectively; overall mean age, 30 years±8) with no history of cardiac disease were included to validate 3D three-directional VE MR imaging for simultaneous MV and TV flow quantification. Volunteers underwent imaging between April and August 2006. Twenty patients (14 men, six women; mean age, 64 years±12 and 60 years±15, respectively; overall mean age, 63 years±13) with ischemic cardiomyopathy, who were suspected of having MV regurgitation,

TV regurgitation, or both, were evaluated. Patient data were selected retrospectively and at random from a database of MR studies acquired between July 2006 and July 2007. All patients and volunteers gave informed consent, and local medical ethics committee approval was obtained.

MR imaging methods

MR images were acquired with a 1.5-T pulsar gradient system (Intera, release 11; Philips Medical Systems, Best, the Netherlands) with 33 mT/m amplitude, 100 mT/m/msec slew rate, and 0.33-msec rise time. A five-element cardiac coil placed on the chest was used for signal reception. After acquisition of a series of thoracic scout images that were used for planning purposes, two-chamber views of the left and right ventricles were obtained, and four-chamber acquisition was performed with a steadystate free precession sequence (repetition time msec/echo time msec, 3.0/1.5; 350-mm field of view; 8-mm section thickness; 50° flip angle; 1.8 x 2.0 x 8.0-mm acquisition voxel reconstructed into a 1.4 x 1.4 x 8.0-mm voxel; one signal acquired; 30 phases reconstructed during one average cardiac cycle) that lasted 10–15 seconds and covered one breath hold at end expiration.

Aortic flow was assessed with 2D one-directional VE MR imaging perpendicular to the ascending aorta [17]; these images served as the reference standard because this flow acquisition was not affected by errors caused by through-plane motion. In volunteers and phantoms, 2D one-directional VE MR imaging was applied for comparison (8.9/5.7; 350-mm field of view; 8-mm section thickness; 20° flip angle; 2.7 x 3.4 x 8.0-mm acquisition voxel size reconstructed into a 1.4 x 1.4 x 8.0-mm voxel; two signals acquired; retrospective gating with 10% acceptance window, with 30 phases reconstructed during one average cardiac cycle; 150 cm/sec maximal velocity encoding, with the encoding direction perpendicular to the acquisition plane; in vivo free breathing was allowed). In vivo 2D one-directional E MR imaging was used to assess aortic low at the ascending aorta and at the V and TV; this examination was performed a the location of the valve, presented in the two- and four-chamber views at the moment of end systole, with the acquisition plane perpendicular to the diastolic inflow direction.

For three-directional VE MR imaging, a true 3D MR acquisition was designed with velocity encoding in three orthogonal directions (14/3.3; 370-mm field of view; 3D volume imaging with 48-mm slab thickness reconstructed into 12 4-mm sections; 10° flip angle; 2.9 x 3.8 x 4.0-mm acquisition voxel reconstructed into a 1.4 x 1.4 x 4.0-mm voxel; one signal acquired; retrospective gating with 10% acceptance window, with 30 phases reconstructed during one average cardiac cycle; 150 cm/sec maximal velocity encoding in all three directions). To reduce acquisition time, echo planar imaging [27] was used with a factor of five.

Image processing

The 2D one-directional VE MR images were analyzed with the QFlow software package (Medis, Leiden, the Netherlands) by using manual contour segmentation (J.J.M.W., 13 years of experience in cardiac MR imaging). Segmentation took 5–10 minutes. For MV and TV flow, through-plane motion correction from the velocity of the myocardium was performed as suggested by

Kayser et al [20]. In a blinded manner, the same observer compared the 3D three-directional VE MR images with the 2D one-directional VE MR images by using image-processing software developed in-house. A schematic illustration of this procedure is shown in Figure 1. First, from the 3D three-directional VE MR data, blood flow velocity at both locations of the valves (ie, MV and TV) needed to be reformatted. The left ventricular and right ventricular two- and four-chamber views were used as reformation guides for the MV plane and TV plane, respectively. In the four-chamber view, the location of the valve was manually indicated by placing

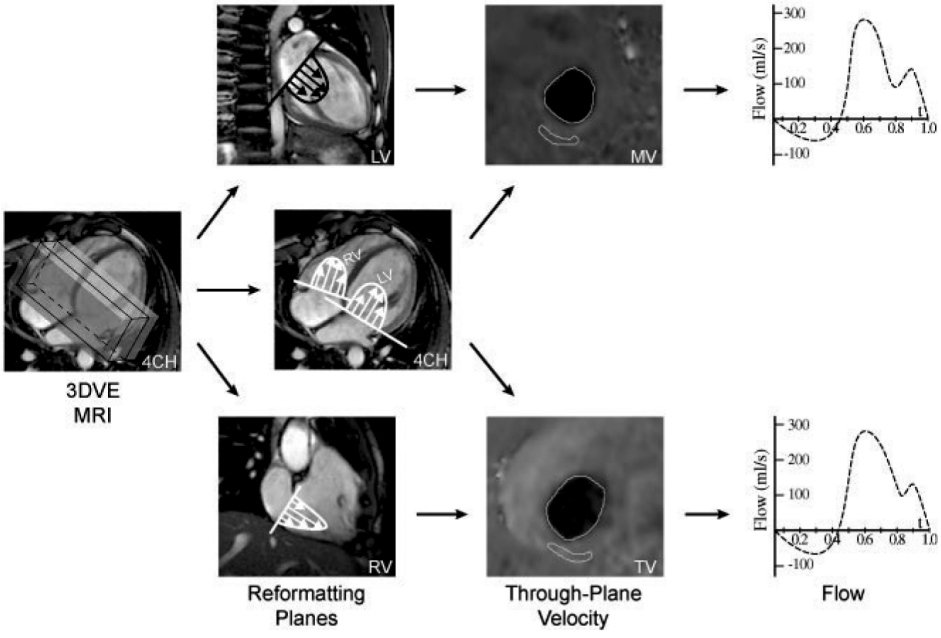


Figure 1. Schematic representation of the reformation of MV flow and TV flow with 3D three-directional VEMR imaging. The 3D acquisition volume for three -directional VE MR imaging is placed at the basal level of the heart. Special attention is paid to the position of the MV and TV remaining inside this 3D volume during the whole cycle. The positions of the respective valvular planes are indicated manually in each of the phases of the cardiac cycle in the two- and four-chamber (4CH) views. The through-plane velocities in the MV plane and the TV plane are reconstructed. Integration of the velocities over the annulus, subtracted by the through-plane velocity acquired in the myocardium, results in the flow graph of the respective valve. Arrows indicate the order in which the steps of the procedure for flow assessment at the particular valves are performed. LV = left ventricle, RV = right ventricle.

a line over the annulus in each of the 30 phases. Reformation of the valvular plane needs to be angulated in two orthogonal directions; thus, angulation in the orthogonal direction of the four-chamber view (ie, the two-chamber view) is manually set and projected onto this two-chamber view. For each phase, all three velocity vector components were reformatted consecutively. Not only were velocities at the valvular plane reformatted, but also reformations of velocities at five planes (two planes on both sides and parallel to the valvular plane) with an interplane distance of 5 mm were constructed. In each plane, the three reformatted velocity components constructed velocity vectors. The through-plane velocity values perpendicular to the reformatted planes were determined from the dot product of the normal vector of these planes and the velocity vectors. The resulting through-plane velocity values were presented for each voxel, each phase, and each of the five reformatted planes.

The central plane (ie, the valvular plane) was generally used for analysis similar to that performed with the 2D one-directional VE MR sequence, with through-plane motion correction from the velocity of the myocardium taken into account. When a high-velocity regurgitant jet occurs, phase dispersion can result in signal loss at the location of the valve [28], with possible underestimation of regurgitation. In such cases, phases with regurgitant flow were analyzed in the first or second plane next to the center plane inside the atrium. The reformatting procedure took 5 minutes for each valve, and subsequent image analysis took 5–10 minutes.

In vitro validation

Validation of the MR technique was performed in vitro with flow phantoms. A constant flow phantom setup was used (Figure 2). Water was pumped through a flexible tube (8-mm inner diameter) with a pump (Verder, Vleuten, the Netherlands) at five constant flow rates (5.8, 8.7, 10.5, 12.0, and 13.7 mL/sec).

The set flow rates were checked with volumetric measurement distal to the phantom. The tube ran through a water tank, which was placed inside the gantry of the MR imager. We compared 2D one-directional VE MR imaging (with the acquisition plane perpendicular to the tube) with 3D three-directional VE MR imaging. In these constant flow experiments, cardiac synchronization to MR acquisition was turned off.

Also, flow experiments in a dynamic left ventricular flow phantom setup (Figure 2) were performed by using a computer-controlled pump (CardioFlow 1000; Shelley Medical Imaging Technologies, London, Ontario, Canada). A harmonic flow was applied to harmonically fill and empty a latex balloon (ie, 3-second period of motion) with the following equation: $V = 20 * \sin(2\pi t/3)$, where V is volume (measured in milliliters) and t is time. The balloon was prefilled with 100 mL of water before sinusoidal flow was applied and placed inside a closed water tank that was connected to a measurement column from which the amplitude of sinusoidal flow was read. At the inlet of the balloon (ie, an 8-mm-diameter tube) and perpendicular to the

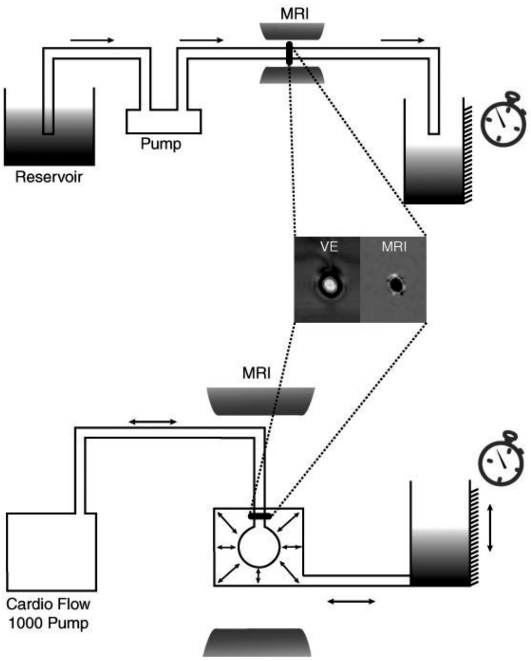


Figure 2. Schematic drawing shows the in vitro setup for MR imaging with constant flow validation (top) and inconstant flow validation (bottom). A pump is used to apply flow (constant flow in the top image, harmonic sinusoidal flow in the bottom image) via tubes to the phantom placed inside the MR gantry. In the top image, flow is determined through a straight tube and compared with volumetric measurement distal to the phantom. In the bottom image, harmonic flow fills and empties a balloon. The balloon is prefilled with 100 mL of water before sinusoidal flow is applied and placed inside a closed water tank that is connected to a measurement column from which the amplitude of sinusoidal flow is read. The flow is assessed with MR imaging at the inlet of the balloon.

flow direction, 2D one-directional VE MR imaging and 3D three-directional VE MR imaging were performed. Triggering was controlled by the same computer that controlled the pump.

Validation in volunteers

In a previous study [22], the net flow volume at the MV was determined in healthy volunteers and compared with aortic systolic stroke volume (ASSV) by using 2D one-directional and 2D three-directional VE MR imaging. For 2D one-directional

VE MR imaging, a significant difference of 25 mL±22 was found ($p < 0.01$): for 2D three-directional VE MR imaging, an insignificant difference of 5 mL±7 was found. Assuming similar differences for the 3D three-directional VE MR technique, comparison between the techniques requires 10 subjects for a power of 90% and a p-value of less than .05. In the current study, 10 healthy volunteers were recruited. MV flow and TV flow were measured with

2D one-directional VE MR imaging and 3D three-directional VE MR imaging, respectively. The ASSV measured with 2D one-directional VE MR imaging in the ascending aorta was used as a reference standard. Correlation between stroke volumes was determined, and differences were studied by using Bland-Altman plots [29].Intra- and inter-observer variation of the image-processing procedure (ie, reformatting and image analysis) was tested with repeated analysis by two observers (J.J.M.W., S.D.R.; 13 and 4 years of experience with cardiac MR imaging, respectively) with an inter-examination time of more than 1 week. Signal-to-noise ratio was determined in peak diastole with 2D one-directional and 3D three-directional VE MR imaging.

Application in patients

Twenty patients with ischemic cardiomyopathy who were suspected of having mitral regurgitation, tricuspid regurgitation, or both at echocardiography were included. The net flow volumes per cycle (defined as stroke volume minus regurgitant flow volume) at the MV and TV were compared, correlation was examined, and Bland-Altman plots were used to study the differences. The regurgitant flow volume was determined on the basis of the flow from the ventricle toward the atrium during systole. The regurgitant flow fraction, representing the severity of regurgitation, was determined on the basis of the ratio between the regurgitant flow volume and the ventricular inflow volume during diastole. Possible aortic regurgitation was corroborated by echocardiographic findings.

Statistical analysis

Continuous variables are expressed as means±standard deviations. Correlation between MR flow acquisitions was evaluated with the Pearson correlation coefficient (r) under the assumption that data were distributed normally. This assumption was tested with the Kolmogorov-Smirnov test. Correlation was classified as strong (r = 0.85), good (r = 0.70–0.85), or fair (r = 0.70). p <0.05 indicated a significant difference. The approach described by Bland and Altman [29] was used to study systematic differences. Mean signed differences and confidence intervals (ie, the limits of agreement) and the mean relative unsigned difference were determined, and significance was tested by using paired-samples *t* tests. Intra- and inter-observer variation was determined by studying not only the significance of differences between measurements but also the intra-class correlation for absolute agreement and the coefficients of variance (defined as the standard deviation of the differences between the two series of measurements divided by the mean of both measurements). P-value <0.05 indicated a significant difference.

RESULTS

In vitro validation

MR flow acquisition was validated at five constant flow rates (Figure 3a). Strong correlation was found between both MR sequences and volumetric measurements (Table 1). The agreement between 3D three-directional VE MR imaging and volumetric measurements was lower than the agreement between 2D one-directional VE MR imaging and volumetric measurements, with a difference of 0.23 mL/sec ($p > 0.05$). The confidence intervals (ie, limits of agreement) for 3D three-directional VE MR imaging and 2D one-directional VE MR imaging were similar. Figure 3b reveals that both MR sequences resulted in underestimation for low flow and overestimation for high flow.

The harmonic flow volume (set at 40 mL) from 2D one-directional VE MR imaging and 3D three-directional VE MR imaging ranged from 41.3 mL (an overestimation of 3%) to 38.7 mL (an underestimation of 3%), respectively.

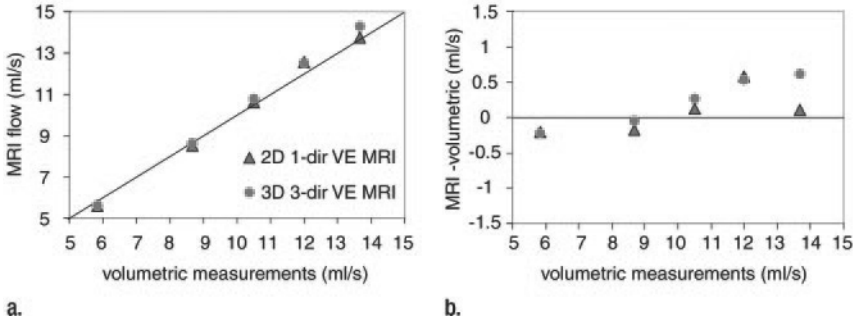


Figure 3. Graphs show in vitro flow validation. (a) Flow is measured with two MR techniques (2D one-directional VE MR imaging and 3D VE MR imaging) and compared with volumetric flow assessment. (b) Differences between the techniques are presented on a Bland-Altman plot.

Validation in volunteers

No distortion or susceptibility artifacts caused by echo-planar imaging were seen in the image data. Mean signal-to-noise ratio was 187±116 for 2D one-directional VE MR imaging and 84±60 for 3D three-directional VE MR imaging. The signal-to-noise ratio for 3D three-directional VE MR imaging was 55% lower than that for 2D one-directional VE MR imaging, but it was still sufficient for accurate image analysis.

A bias was found for 2D one-directional VE MR imaging of MV flow (overestimation, 11 mL per cycle [15%]; $p<0.01$) in the healthy volunteers (Figure 4a). We found that 2D one-

Table 1. Statistics for constant flow experiments performed to compare two MR sequences for flow assessment.

Statistic	2D One-Directional	3D Three-Directional
	VE MR Imaging	VE MR Imaging
Pearson correlation coefficient	1.00 (p <0.01)	1.00 (p <0.01)
Mean signed difference (mL/sec)	0.08	0.23
Mean relative unsigned difference (%)	4	4
P value*	0.58	0.23
Confidence interval (mL/sec)	-0.55, 0.72	-0.50, 0.96

* p- values were calculated with the paired-samples t test.

directional VE MR imaging of TV flow resulted in an overestimation of 12 mL per cycle (25%); however, this was not significant because of the high standard deviation. Use of 3D three-directional VE MR imaging resulted in smaller non significant bias and smaller confidence intervals (ie, limits of agreement) compared with use of 2D one-directional VE MR imaging for both MV flow and TV flow. Correlation with ASSV was strong for 3D three-directional VE MR imaging (for MV, r = 0.96 and p <0.01; for TV, r = 0.88 and p <0.01) and strong between MV and TV (r = 0.91, p <0.01) (Figure 4b). Correlation with ASSV was weaker for 2D one-directional VE MR imaging (for MV, r = 0.80 and p <0.01; for TV, r = 0.22 and p = 0.55) and weak between MV

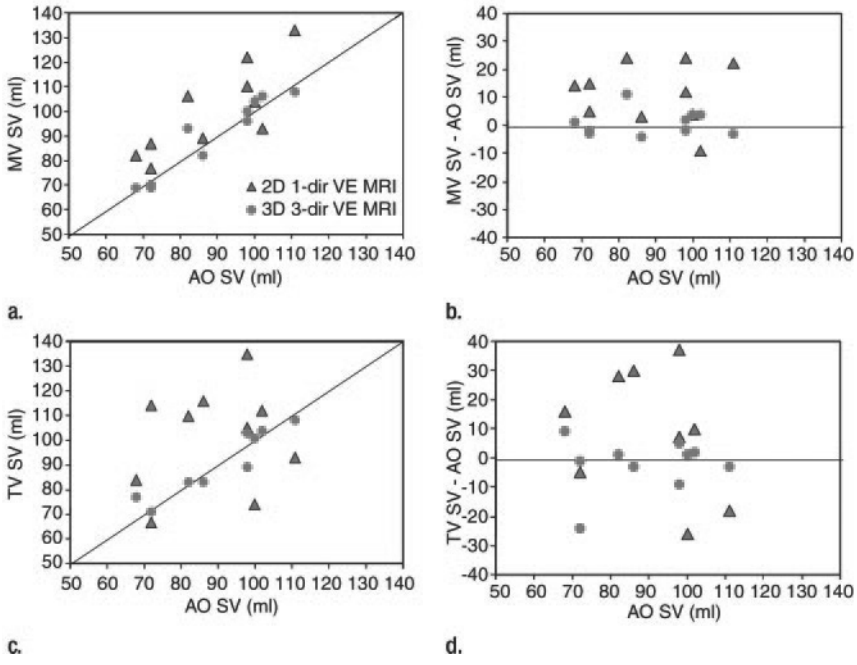


Figure 4. Graphs show net flow volumes measured with two techniques (2D one-directional VE MR imaging and 3D VE MR imaging) at the MV and TV in healthy volunteers and compared with 2D one-directional VE MR ASSV (a and c). Differences between the techniques are presented on Bland-Altman plots (b and d). AO = aortic valve, SV = net stroke volume.

and TV (r = 0.34, p = 0.34) (Figure 5, Table 2). Kolmogorov-Smirnov tests showed that the data were distributed normally. These results indicate that 3D three-directional VE MR imaging provides accurate results for MV flow and TV flow, whereas 2D one-directional VE MR imaging is less accurate.

Intra-observer coefficient of variation was less than or equal to 4%, with an intra-class cor-

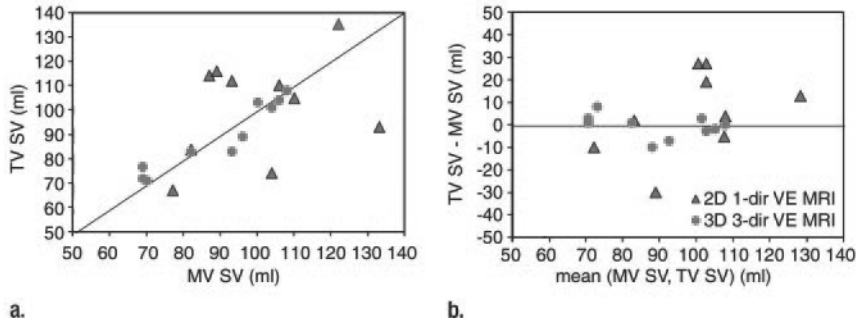


Figure 5. (a) Graph shows net flow volumes measured with two techniques (2D one-directional VE MR imaging and 3D three-directional VE MR imaging) at the MV and TV in healthy volunteers. (b) Differences between the techniques are presented on a Bland-Altman plot. SV = net stroke volume.

Table 2. Statistics for transvalvular flow volumes assessed in healthy volunteers with two MR techniques

	MV vs AO		TV vs AO		MV vs TV	
Statistic	2D 1-Dir VE MRI	3D 3-Dir VE MRI	2D 1-Dir VE MRI	3D 3-Dir VE MRI	2D 1-Dir VE MRI	3D 3-Dir VE MRI
Pearson correlation coef	0.80 (p <0.01)	0.96 (p <0.01)	0.22 (p = 0.55)	0.88 (p <0.01)	0.34 (p = 0.34)	0.91 (p <0.01)
Mean signed difference (mL)	11	1	12	-2	1	-1
Mean relative unsigned difference (%)	15	4	25	7	18	4
p-value*	<0.01	0.60	0.13	0.46	0.92	0.72
Confidence interval (mL)	-10, 32	-8, 10	-33, 57	-20, 16	-44, 45	-11, 10

Note. AO = aortic valve.

* p-values were calculated with the paired-samples t test.

relation coefficient of 0.98 (p <0.01 for both MV flow and TV flow). Inter-observer coefficient of variation was less than or equal to 8%, with intra-class correlation coefficients of 0.94 (p <0.01) and 0.93 (p <0.01) for MV flow and TV flow, respectively (Table 3).

Table 3. Statistics for intra- and inter-observer study for transvalvular flow volume assessed with 3D three-directional VE MR imaging.

	Intra-observer		Inter-observer	
Statistic	MV	TV	MV	TV
Intra-class correlation coefficient	0.98 (p <0.01)	0.98 (p <0.01)	0.94 (p <0.01)	0.93 (p <0.01)
Mean signed difference (mL)	1	1	1	3
Mean relative unsigned difference (%)	3	3	6	6
p-value*	0.61	0.28	0.60	0.27
Confidence interval (mL)	-6, 5	-6, 9	-11, 12	-17, 12
Coefficient of variance (%)	<3	<4	<6	<8

* p-values were calculated with the paired-samples t test.

Application in patients

In the 20 patients, the mean regurgitant fraction was 13%±9 (range, 3%–32%) for MV and 10%±6 (range, 0%–23%) for TV. Kolmogorov-Smirnov test results proved that the data were distributed normally. Correlation between net flow volumes at MV and TV was examined (Figure 6). The statistics are summarized in Table 4.

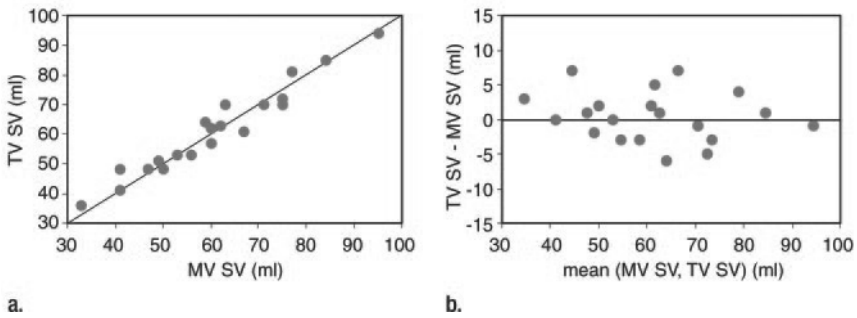


Figure 6, (a) Graph shows net flow volumes measured with two techniques (2D one-directional VE MR imaging and 3D three-directional VE MR imaging) in patients with valve regurgitation assessed at the MV(MV SV) and TV (TV SV). (b) Differences between the techniques are presented on a Bland-Altman plot. SV = net stroke volume.

Correlation between MV flow volume and TV flow volume at 3D three-directional VE MR imaging was strong and showed no significant bias. As expected, correlation between MV flow volume and TV flow volume with ASSV was good; however, these showed a significant bias (15%, p <0.01), as several patients had substantial aortic valve regurgitation as well, which is not accounted for in the ASSV. For 3D three-directional VE MR imaging in 20 patients and 10 volunteers, mean examination time was 4.2 minutes±0.8 at an average heart rate of 67 beats per minute±12.

Table 4. Statistics for transvalvular flow volume assessment with 3D three-directional VE MR imaging in patients.

Statistic	MV vs AO	TV vs AO	MV vs TV
Pearson correlation coefficient	0.82 (p <0.01)	0.74 (p <0.01)	0.97 (p <0.01)
Mean signed difference (mL)	-11	-11	1
Mean relative unsigned difference (%)	15	15	5
p-value*	<0.01	<0.01	0.58
Confidence interval (mL)	-33, 11	-37, 15	-7, 8

Note.AO = aortic valve.

* p-values were calculated with the paired-samples t test.

DISCUSSION

The main findings of the current study are as follows: First, both 2D one-directional VE MR imaging and 3D three-directional VE MR imaging are accurate for in vitro flow assessment when the plane of interest remains fixed in the same location and no through-plane motion is present. Second, in vivo 2D one-directional VE MR imaging shows 15% and 25% overestimation of MV flow and TV flow, respectively. Third, 3D three-directional VE MR imaging yields accurate MV flow and TV flow values in the presence of valve regurgitation, with smaller limits of agreement when compared with 2D one-directional VE MR imaging.

The severity of regurgitation, expressed in the regurgitation fraction determined from the quotient between the regurgitant backward flow during systole and diastolic inflow, is an important determinant of mortality in patients with ischemic cardiomyopathy [30]; therefore, knowledge about the severity of regurgitation is desired for optimal surgical decision making. The value of indirect quantification of regurgitation by measuring left and right ventricular end-systolic and end-diastolic volumes [31] is limited to assessment of isolated valve regurgitation. The use of 2D one-directional VE MR imaging [18–20] for consecutive flow assessment of MV and TV is routine in clinical practice, although this technique has been proved to be inaccurate [22]. Our in vitro validation study has shown that the accuracy of 2D one-directional VE MR imaging is comparable to that of 3D three-directional VE MR imaging when flow assessment takes place at a plane that does not show through-plane motion. In vivo, 2D one-directional VE MR imaging does not adapt to heart motion during relaxation. Thus, with this technique, flow acquisition does not take place at the valve of interest for the complete cardiac cycle, whereas with 3D three-directional VE MR imaging, flow at the valve can be assessed with retrospective adaptation of the reformation plane to the valvular plane.

In a previous study, MV flow was measured with a 2D three-directional VE MR protocol by using a radial stack of acquisition planes positioned on the left ventricle [22]. The current approach with 3D three-directional VE MR imaging shows two important improvements to the 2D three-directional VE MR imaging approach with radial acquisition stack: The first

improvement is that in-plane data sampling is almost isotropic over the MV and TV annuli, with sufficient spatial resolution to ensure accurate flow acquisition over the annuli [18], whereas radial sampling implies dense sampling at the center of the annulus but sparse sampling at the outside region, resulting in underestimation of eccentric regurgitant jets. The second improvement is that MV flow and TV flow are assessed with one acquisition, thereby excluding possible inter-examination variation in heart rate, whereas 2D three-directional VE MR imaging with radial sampling requires a repeated acquisition when both valves are studied. Retrospective gating [32] was used for both flow acquisition techniques. Arrhythmia, often present in patients with ischemic heart disease, has a degrading effect on the overall image quality and therefore on the accuracy of the flow acquisitions. Arrhythmia rejection was used during data acquisition (with an acceptance window of 10% from the value chosen in advance). This prolonged acquisition time but had a positive effect on accuracy. Data acquisition was performed during free breathing. This also degraded image quality compared with that achieved with breathhold techniques or navigator-based acquisitions [33]. However, navigator-based techniques require prospective triggering, which is not suitable when acquisition at both systole and diastole is required with sufficient temporal resolution.

In this study, 20 patients with ischemic cardiomyopathy and suspected of having mitral regurgitation, tricuspid regurgitation, or both were examined. MV flow and TV flow measured with 3D three-directional VE MR imaging were in agreement. Regurgitant fractions ranged from 3% to 32% for MV and from 0% to 23% for TV. This information is essential for surgical decision making. At our institute, 3D three-directional VE MR imaging is now routinely used to test valvular insufficiency in patients eligible for the procedure described by Dor et al [34].

Our study had some limitations. Echo-planar imaging was used with the 3D three-directional VE MR sequence and an echo-planar imaging factor of five to accelerate image acquisition and to make this examination clinically applicable. No distortions or susceptibility artifacts were seen, and although signal-to-noise ratio was 55% lower with 3D three-directional VE MR imaging than with 2D one-directional VE MR imaging, this technique was still sufficient for accurate image analysis. Background phase correction was not performed [35], but by correcting for through-plane motion by subtracting the mean velocity from nearby myocardium from the velocity through the annulus, it can be assumed that local phase offset errors are eliminated. These errors may introduce systematic errors in flow assessment with some MR imagers, and these are also more pronounced in short breath-hold acquisitions [28]. In this study, 2D one-directional VE MR imaging was performed without acceleration, 3D three-directional VE MR imaging was performed with an echo-planar imaging factor of five, and both examinations were performed with free breathing. Both MR sequences were validated extensively in phantoms, and the volunteer data did not indicate systematic differences between MV flow and TV flow.

The image processing needed for assessment of MV flow and TV flow with 3D three-directional VE MR imaging (ie, reformatting and image analysis) still requires manual interaction,

but it showed good reproducibility. MV flow showed 4% or less variation, and TV flow showed 8% or less variation, which is considered acceptable in clinical practice. Compared with the time required for reformatting in 2D one-directional VE MR imaging, another technique in which manual image analysis is mandatory, additional time for the reformatting procedure in 3D three-directional VE MR imaging is 5 minutes per valve.

In healthy volunteers, ASSV was used as the reference standard to compare MV and TV stroke volumes. There was some underestimation with ASSV because of the distensibility of the aorta and the coronary flow. Also, possible variation in heart rate between 2D one-directional VE MR imaging in the ascending aorta, 2D one-directional VE MR imaging at the MV and TV, and 3D three-directional VE MR imaging, respectively, was a potential source of error.

We tested and applied 3D three-directional VE MR imaging in relatively small groups of volunteers and patients within a small age range. A larger study should be performed to prove the accuracy and reproducibility of this technique.

CONCLUSIONS

3D three-directional VE MR imaging is a noninvasive quantification tool used to assess the severity of regurgitation at multiple valves in a single acquisition.

REFERENCES

1. Peterson KL. Timing of surgical intervention in chronic regurgitation. *Herz* 1986;11:63–73.
2. Enriquez-Sarano M. Timing of mitral valve surgery. *Heart* 2002;87:79–85.
3. Bech-Hanssen O, Ryde´n T, Schertse´n H, Ode´n A, Nilsson F, Jeppson A. Mortality after mitral regurgitation surgery: importance of clinical and echocardiographic variables. *Eur J Cardiothorac Surg* 2003;24:723–730.
4. Ascah KJ, Stewart WJ, Jiang L, et al. A Doppler-two-dimensional echocardiographic method for quantification of mitral regurgitation. *Circulation* 1985;72:377–383.
5. Miyatake K, Izumi S, Okamoto M, et al. Semiquantitative grading of severity of mitral regurgitation by real-time two-dimensional Doppler flow imaging technique. *J Am Coll Cardiol* 1986;7:82–88.
6. Hellemans IM, Pieper EG, Ravelli AC, et al. Prediction of surgical strategy in mitral valve regurgitation based on echocardiography. *Am J Cardiol* 1997;79:334–338.
7. Shah PM, Raney AA, Duran CM, Oury JH. Multiplane transesophageal echocardiography: a roadmap for mitral repair. *J Heart Valve Dis* 1999;8:625–629.
8. Gottdiener JS, Bednarz J, Devereux R, et al. American Society of Echocardiography recommendations for use of echocardiography in clinical trials. *J Am Soc Echocardiogr* 2004;17:1086–1119.
9. Rajappan K, Bellenger NG, Melina G, et al. Assessment of left ventricular mass regression after aortic valve replacement: cardiovascular magnetic resonance versus M-mode echocardiography. *Eur J Cardiothorac Surg* 2003;24:59–65.
10. Tribouilloy C, Shen WF, Quere JP, et al. Assessment of severity of mitral regurgitation by measuring regurgitant jet width at its origin with transesophageal Doppler color flow imaging. *Circulation* 1992;85:1248–1253.
11. Hall SA, Bricker ME, Willett DL, Irani WN, Afridi J, Grayburn PA. Assessment of mitral regurgitation severity by Doppler color flow mapping of the vena contracta. *Circulation* 1997;95:636–642.
12. Grossmann G, Giesler M, Schmidt A, et al. Quantification of mitral regurgitation by colour flow Doppler imaging: value of the 'proximal isovelocity surface area' method. *Int J Cardiol* 1993;42:165–173.
13. Enriquez-Sarano M, Sinak LJ, Tajik AJ, Bailey KR, Seward JB. Changes in effective regurgitant orifice throughout systole in patients with mitral valve prolapse: a clinical study using the proximal isovelocity surface area method. *Circulation* 1995;92:2951–2958.
14. Sahn DJ. Instrumentation and physical factors related to visualization of stenotic and regurgitant jets by Doppler color flow mapping. *J Am Coll Cardiol* 1988;12:1354–1365.
15. Fyrenius A, Wigstro¨m L, Bolger AF, et al. Pitfalls in Doppler evaluation of diastolic function: insights from 3-dimensional magnetic resonance imaging. *J Am Soc Echocardiogr* 1999;12:817–826.
16. Rebergen SA, van der Wall EE, Doornbos J, de Roos A. Magnetic resonance measurement of velocity and flow: technique, validation, and cardiovascular applications. *Am Heart J* 1993;126:1439–1456.
17. van der Geest RJ, Niezen RA, van der Wall EE, de Roos A, Reiber JH. Automated measurement of volume flow in the ascending aorta using MR velocity maps: evaluation on inter- and intraobserver variability in healthy volunteers. *J Comput Assist Tomogr* 1998;22:904–911.
18. Chai P, Mohiaddin R. How we perform cardiovascular magnetic resonance flow assessment using phase-contrast velocity mapping. *J Cardiovasc Magn Reson* 2005;7:705–716.
19. Gatehouse PD, Keegan J, Crowe LA, et al. Applications of phase-contrast flow and velocity imaging in cardiovascular MRI. *Eur Radiol* 2005;15:2172–2184.
20. Kayser HW, Stoel BC, van der Wall EE, van der Geest RJ, de Roos A. MR velocity mapping of tricuspid flow: correction for through-plane motion. *J Magn Reson Imaging* 1997;7:669–673.

21. Pelc NJ, Bernstein MA, Shimakawa A, Glover GH. Encoding strategies for three-direction phase-contrast MR imaging of flow. *J Magn Reson Imaging* 1991;1:405–413.
22. Westenberg JJ, Danilouchkine MG, Doornbos J, et al. Accurate and reproducible mitral valvular blood flow measurement with three-directional velocity-encoded magnetic resonance imaging. *J Cardiovasc Magn Reson* 2004;6:767–776.
23. Mohiaddin RH. Flow patterns in the dilated ischemic left ventricle with velocity vector mapping. J Magn Reson Imaging 1995;5:493–498.
24. Bogren HG, Buonocore MH. 4D magnetic resonance velocity mapping of blood flow patterns in the aorta in young vs elderly normal subjects. *J Magn Reson Imaging* 1999;10:861–869.
25. Wigstro¨m L, Ebbers T, Fyrenius A, et al. Particle trace visualization of intracardiac flow using time-resolved 3D phase contrast MRI. *Magn Reson Med* 1999;41:793–799.
26. Westenberg JJ, Doornbos J, Versteegh MI, et al. Accurate quantitation of regurgitant volume with MRI in patients selected for mitral valve repair. *Eur J Cardiothorac Surg* 2005;27:462–467.
27. DeLaPaz RL. Echo-planar imaging. *Radio-Graphics* 1994;14:1045–1058.
28. Kilner PJ, Gatehouse PD, Firmin DN. Flow measurement by magnetic resonance: a unique asset worth optimising. *J Cardiovasc Magn Reson* 2007;9:723–728.
29. Bland JM, Altman DG. Statistical methods for assessing agreement between two methods of clinical measurement. *Lancet* 1986;1:307–310.
30. Grigioni F, Enriquez-Sarano M, Zehr HJ, Bailey KR, Tajik AJ. Ischemic mitral regurgitation: long-term outcome and prognostic implications with quantitative Doppler assessment. *Circulation* 2001;103:1759–1764.
31. Sechtem U, Pflugfelder PW, Cassidy MM, et al. Mitral or aortic regurgitation: quantification of regurgitant volumes with cine MR imaging. *Radiology* 1988;167:425–430.
32. Søndergaard L, Ståhlberg F, Thomsen C, et al. Comparison between retrospective gating and ECG triggering in magnetic resonance velocity mapping. *Magn Reson Imaging*1993;11:533–537.
33. Felmlee JP, Ehman RL, Riederer SJ, Korin HW. Adaptive motion compensation in MRI:accuracy of motion measurement. *Magn Reson Med* 1991;18:207–213.
34. Dor V, Saab M, Coste P, Kornaszewska M, Montiglio F. Left ventricular aneurysm: a new surgical approach. *Thorac Cardiovasc Surg* 1989;37:11–19.
35. Chernobelsky A, Shubayev O, Comeau CR, Wolff SD. Baseline correction of phase contrast images improves quantification of blood flow in the great vessels. *J Cardiovasc Magn Reson* 2007;9:681–685.

CHAPTER 20

Quantification of functional mitral regurgitation by real-time 3D echocardiography: comparison with 3D velocity-encoded cardiac magnetic resonance

N Ajmone Marsan, J JM Westenberg, C Ypenburg, V Delgado, R J van Bommel, S D Roes, G Nucifora, R J van der Geest, A de Roos, J C Reiber, M J Schalij, and J J Bax

JACC Cardiovasc Imaging 2009;2:1245-52.

ABSTRACT

Objectives: Accurate grading of mitral regurgitation (MR) severity is crucial for appropriate patient management, but remains challenging. Velocity-encoded magnetic resonance imaging (MRI) with three-dimensional (3D) 3-directional acquisition has been recently proposed as the reference method. Aim of this study was to evaluate feasibility and accuracy of real-time 3D echocardiography for quantification of MR, in a head-to-head comparison with velocity-encoded MRI.

Methods: A total of 64 patients with functional MR were included. A 3D 3-directional velocity-encoded MRI acquisition was applied to quantify mitral regurgitant volume (Rvol). Color Doppler 3D-echocardiography was applied for direct measurement, in 'en face' view, of mitral effective regurgitant orifice area (EROA); Rvol was subsequently calculated as EROA multiplied by the velocity-time integral of the regurgitant jet on the continuous-wave Doppler. To assess the relative potential error of the conventional approach, color Doppler 2D-echocardiography was performed: vena contracta width was measured in the 4-chamber view and EROA calculated as circular (EROA-4CH); EROA was also calculated as elliptical (EROA-elliptical), measuring vena contracta also in the 2-chamber view. From these 2D measurements of EROA, the regurgitant volumes were also calculated.

Results: the EROA measured by 3D-echocardiography was significantly higher than EROA-4CH ($p<0.001$) and EROA-elliptical ($p<0.001$) with a significant bias between these measurements (0.10 cm2 and 0.06 cm2, respectively). Rvol measured by 3D-echocardiography showed excellent correlation with Rvol measured by MRI ($r = 0.94$) without a significant difference between these techniques (mean difference = -0.08 ml/beat). Conversely, 2D echocardiographic approach from the 4-chamber view significantly underestimated Rvol ($p=0.006$) as compared to MRI (mean difference = 2.9 ml/beat). The 2D elliptical approach demonstrated a better agreement with MRI (mean difference = -1.6 ml/beat, $p=0.04$).

Conclusions: Quantification of EROA and Rvol of functional MR using 3D-echocardiography is feasible and accurate as compared to 3D 3-directional velocity-encoded MRI; the currently recommended 2D-echocardiographic approach significantly underestimate both EROA and Rvol.

INTRODUCTION

Functional mitral regurgitation (MR) is a common and serious complication in patients with global and/or regional left ventricular (LV) dilatation and dysfunction, and is associated with relatively high morbidity and mortality [1–4]. Consequently, timely diagnosis and accurate grading of MR severity are crucial for appropriate patient management and timing of surgical intervention [2,5,6]. However, quantitative assessment of MR remains challenging, and different echocardiographic modalities or semiquantitave angiographic grading have been proposed, but a true gold standard technique is still lacking [7,8]. Evaluation of the effective regurgitant orifice area (EROA) and regurgitant volume (Rvol) is currently recommended, applying 2-dimensional (2D) echocardiography with the proximal isovelocity surface area (PISA) or pulsed Doppler quantitative flow methods [8]. However, both methods have several limitations due to indirect measurements based on imprecise hemodynamic assumptions and multiple computational steps [9–12].

In addition, an accepted direct assessment of EROA is the vena contracta width (VCW), as the narrowest cross-section of the regurgitant jet [8,13,14]. However, this method assumes the orifice as nearly circular and the exact shape and size may not be accurately assessed due to the limited scan plane orientation of 2D echocardiography. Real-time 3-dimensional echocardiography (RT3DE) is now available to overcome this limitation, which is particularly relevant in patients with functional MR, in whom EROA geometry is usually complex and asymmetric [15,16]. In fact, RT3DE provides unlimited image plane orientation and, using color Doppler, allows for a direct EROA quantification [15,17,18].

Recently, velocity encoded magnetic resonance imaging (MRI) has been proposed as a reference method for transvalvular flow quantification [19,20]; in particular, the use of a 3D 3-directional acquisition showed to be able to optimize the conventional 2D one-directional acquisition [21–24], providing independent MR flow quantification. Therefore, the aim of the current study was to explore in patients with functional MR, the feasibility and the accuracy of direct measurement of EROA and quantification of Rvol with RT3DE, in a head-to-head comparison with VE MRI. To assess the relative potential error of 2D echocardiography for these measurements, 2D echocardiography was also performed in the same patient cohort.

METHODS

Patient population and protocol

The patient population consisted of 70 consecutive patients who were clinically referred for cardiac MRI and had functional mild-to-severe MR on color Doppler echocardiography. Functional MR was defined as leaflet tethering and incomplete leaflet coaptation in the presence

of normal mitral valve anatomy and regional or global LV remodeling [25].

Patients with atrial fibrillation, irregular heart rhythm or absolute contraindications (including cardiac devices) for MRI were excluded. The standard MRI protocol was applied to assess LV size and function. A 3D 3-directional velocity encoded MRI acquisition was added to quantify MR. On the same day, patients underwent also 2D color Doppler echocardiography and RT3DE to quantify MR and for comparison with MRI measurements. All patients gave informed consent and the protocol was approved by the institutional review board.

Magnetic resonance imaging

Data acquisition

Data acquisition was performed on a 1.5T MRI scanner equipped with Powertrack 6000 gradients (ACS-NT15 Intera, Philips Medical Systems, Best, The Netherlands; software release 11), using a 5-element cardiac coil placed on the chest for signal reception. LV volumes were determined by planimetry from a series of short-axis acquisitions covering the complete LV from apex to base, following a standardized protocol described previously [26]. The spatial resolution of the acquired images was 1.56×1.56 mm^2.

For 3-directional velocity encoded MRI, a true free breathing 3D MRI acquisition was designed with velocity encoding in 3 orthogonal directions (field-of-view 370 mm, 3D volume scan with slab thickness 48 mm, reconstructed into 12 slices of 4 mm, TE 3.3 ms, TR 14 ms, α 10^o, acquisition voxel size $2.9\times3.8\times4.0$ mm^3, reconstructed into $1.4\times1.4\times4.0$ mm^3, NSA 1, Venc 150 cm/s in all 3 directions) and with 30 phases reconstructed during one average cardiac cycle from the retrospectively gated acquisition (temporal resolution between 25 and 40ms, depending on the patient's heart rate). To reduce acquisition time, echo planar imaging was used with EPI factor 5. Scan time was less than 5 minutes, depending on the subject's heart rate.

LV volumes and function analysis

Quantification of LV end-systolic and end-diastolic volumes and ejection fraction was performed on the short-axis series using MASS analytical software (Medis, Leiden, the Netherlands) and manual contour segmentation of the epicardial and endocardial borders. In the presence of significant mitral regurgitation, LV ejection fraction does not represent the true systolic stroke volume. To correct for this effect, the "forward LV ejection fraction" was calculated as the ratio of the forward stroke volume (obtained from aortic flow measurements derived from velocity encoded MRI) and LV end-diastolic volume [27].

Mitral valve flow quantification

The 3D 3-directional velocity encoded MRI acquisitions were analyzed using in-house developed image processing software. The procedure was performed as previously described [24] and is schematically illustrated in Figure 1. In summary, from the MRI data, the 3 velocity vector components of blood flow at the level of the mitral valve plane needs to be reformatted, using the LV 4- and 2-chamber views; this procedure required 5 to 10 minutes. The velocities measured perpendicularly to the reconstructed mitral valve plane need to be corrected for the motion of the myocardium in basal/apical direction in order to obtain the true trans-valvular velocity of the blood flow [21]. Therefore, the through-plane velocity of the mitral valve annulus was determined in the lateral wall and subtracted from the through-plane MV flow velocities. The trans-valvular volume flow was obtained by integrating the resulting velocities over the annulus area. The regurgitant volume (Rvol-MRI) was obtained by calculating the Riemann sum of backward flow during systole in the flow graph. This analysis required approximately 5 minutes and its reproducibility was previously reported [24]: intraobserver variation was less than 3%, while inter-observer variation was less than 6%.

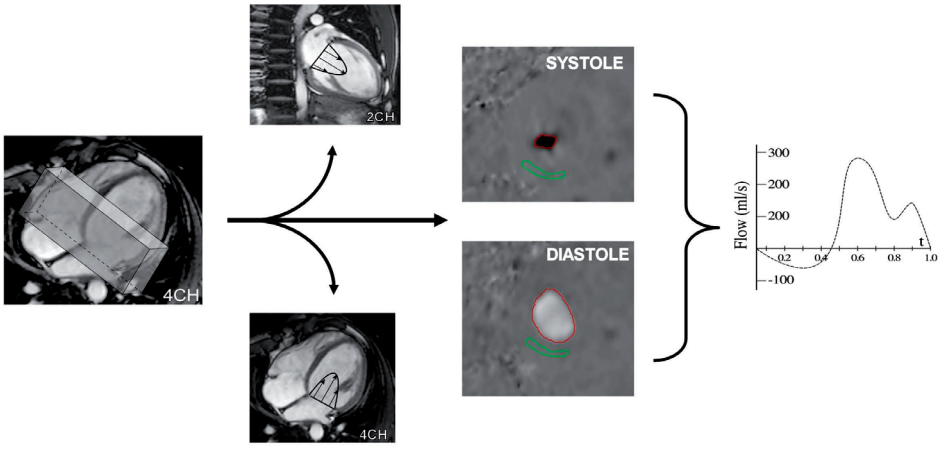


Figure 1. Reformat procedure of mitral valve flow from 3-dimensional (3D) 3-directional velocity encoded magnetic resonance imaging data. Schematic representation of reformat procedure of mitral valve flow from 3-dimensional (3D) 3-directional velocity encoded magnetic resonance imaging data. The acquisition is performed in a volume positioned at the basal level of the heart (left panel), covering the full excursion of the mitral valve during contraction and relaxation. From the 3D velocity vector field, the trans-mitral flow is retrospectively quantified by multi-planar reformatting of mitral valve in 2- and 4-chamber views (second panel). The through-plane velocity is constructed from the dot product with the normal vector (third panel). During systole, regurgitant flow can be identified and quantified. During diastole, mitral valve inflow is acquired. Through-plane motion correction is performed from the longitudinal velocity measured in the lateral wall (green lines). The regurgitant volume was obtained by calculating the Riemann sum of backward flow during systole in the flow graph (right panel).

Echocardiography

Standard 2D echocardiography

Patients were imaged in the left lateral decubitus position using a commercially available system (iE33, Philips Medical Systems, N.A., Bothell, Washington, USA) equipped with a 3.5-Mhz transducer. VCW was measured as the narrowest portion of the MR color Doppler jet in a zoomed optimized apical 4-chamber (4CH) view. In addition, VCW was also measured in the apical 2-chamber (2CH) view to allow a more accurate calculation in case of asymmetric EROA. The systolic frame with the most relevant lesion size was selected for the measurement. Nyquist limits were always set between 30 and 50 cm/sec to avoid any over- or under-estimation and a color gain was used that just eliminates random color speckles from non-moving regions. From the VCW measurements, estimates of EROA were obtained as circular (EROA-4CH = [π x (VCW-4CH/2)]^2) as well as biplane elliptical (EROA-elliptical = [π x (VCW-4CH/2) x (VWC-2CH/2)]) [15]. The Rvol can be estimated as EROA multiplied by the velocity time integral of the regurgitant jet on the continuous-wave Doppler.

Real-time 3-dimensional echocardiography

RT3DE was performed using the same ultrasound system and with an X3, fully sampled matrix transducer. Apical full-volume color Doppler datasets were obtained within 1 breath hold, combining 7 small real-time sub-volumes in a larger pyramidal volume (approximately 60 x 60 degrees). Nyquist limits (aliasing velocity) and color gain were set as for 2D echocardiography. Analysis of the 3D images was performed off-line (Q-Lab, version 6.0, Philips Medical Systems). To measure EROA (-3D), the 3D dataset was manually cropped by an image plane perpendicularly oriented to the jet direction until the narrowest cross-sectional area of the jet [15,18] (Figure 2). EROA-3D was measured by manual planimetry of the color Doppler signal, tilting the image in an 'en face' view and selecting the systolic frame with the most relevant lesion size (Figure 2) . The Rvol (-3D) was derived as for 2D echocardiography. On the cropped images, the ratio of the longest and shortest diameter of EROA (L/S) was also calculated as an index of orifice shape [28]. The image post-processing required 3 to 5 minutes.

Twenty patients were randomly identified to evaluate the inter- and intra-observer agreement for the EROA-3D. According to the Bland-Altman analysis, inter-observer agreement was good: EROA-3D mean difference (±2SD) = 0.06±0.04 cm^2 (p = 0.43). The intra-observer agreement was also good with a mean difference (±2SD) of 0.04±0.04 cm^2 (p = 0.55).

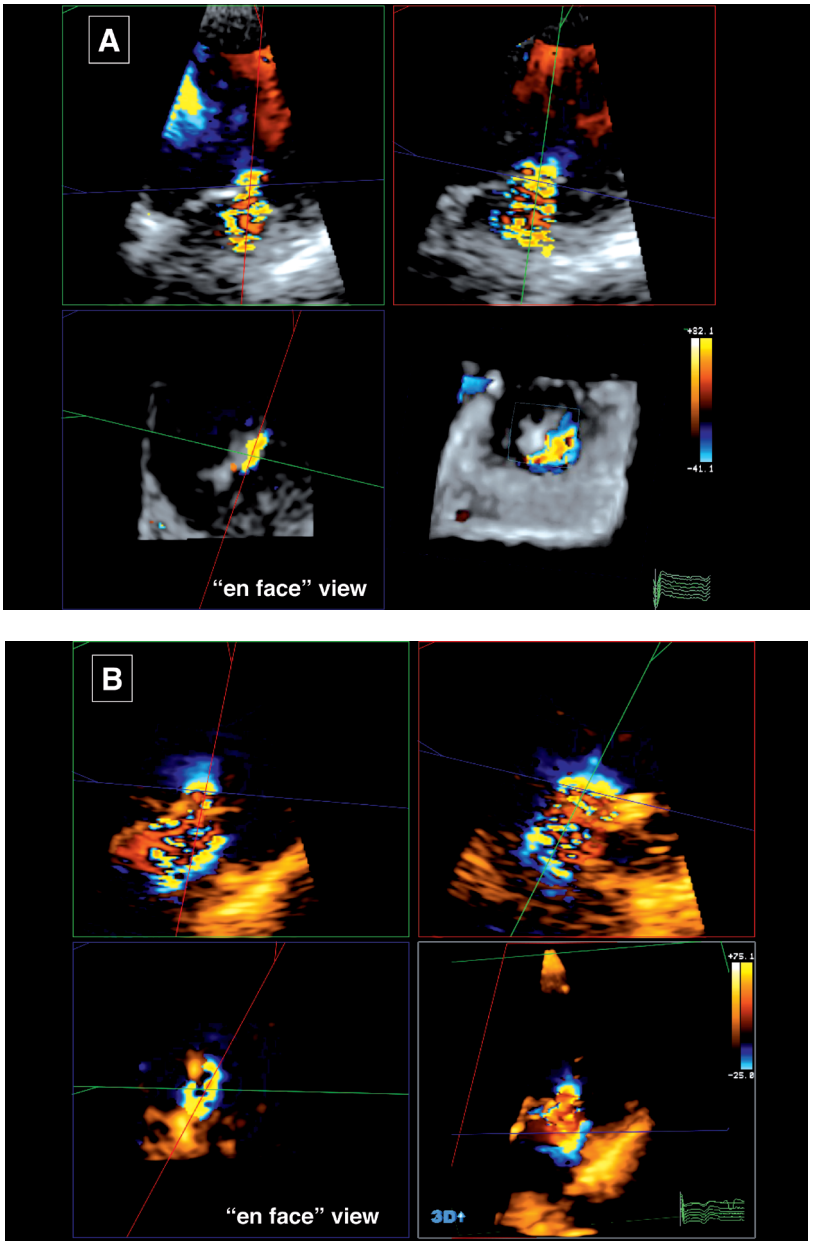


Figure 2. Real-time 3-dimensional (3D) echocardiographic technique for assessment of vena contracta area (EROA-3D). The 3D dataset is manually cropped by an image plane perpendicularly oriented to the jet direction until the narrowest cross-sectional area of the jet. EROA-3D is measured by manual planimetry of the color Doppler signal tilting the image in an 'en face' view. Panel A: example of a patient with moderate functional mitral regurgitation (MR) and asymmetric EROA-3D (= 0.23 cm^2) elongated along the leaflet coaptation line. Panel B: example of a patient with severe functional MR and extremely irregular EROA-3D (= 0.48 cm^2), for which geometric assumptions may not be applicable.

Statistical analysis

Continuous data are presented as mean±standard deviation (the range, when of interest). Categorical data are presented as absolute numbers or percentages. T-test and χ^2-test were used for appropriate comparisons. For Rvol and EROA, that were not normally distributed as evaluated by the Kolmogorov-Smirnov test, a log-transformation has been performed. Pearson's correlation analysis was performed to evaluate the relation between velocity encoded MRI, RT3DE and 2D echocardiographic measurements of EROA and Rvol. Bland-Altman analysis was performed to evaluate the differences in Rvol and EROA assessed with MRI, RT3DE and 2D echocardiography. The mean differences, trends and limits of agreement are reported. A p-value <0.05 was considered to be statistically significant. A statistical software program SPSS 16.0 (SPSS Inc, Chicago, Il, USA) was used for statistical analysis.

RESULTS

Six patients (8.5%) were excluded from further analysis because inadequate RT3DE color Doppler images. Among the remaining 64 patients (44 men, 60±11 years), 48 (75%) were referred because of ischemic cardiomyopathy with a previous myocardial infarction (31 patients with anterior myocardial infarction and 17 with infero-posterior myocardial infarction) and 16 (25%) patients because of idiopathic dilated cardiomyopathy.

MRI analysis revealed severe LV dilatation (mean LV end-diastolic volume 273±66 ml), with depressed LV systolic function (mean forward LV ejection fraction 29±10%). From the 3-directional velocity encoded MRI analysis, the mean mitral Rvol was 12.9±12.6 ml/beat, ranging from 2 to 63 ml/beat. No significant (more than mild) regurgitation of the other cardiac valves was detected by 3-directional velocity encoded MRI.

RT3DE versus 2D echocardiography

The mean values and the ranges of the EROA measurements with 2D echocardiography and RT3DE are displayed in Table 1. EROA-3D was significantly higher than EROA-4CH (p <0.001) and EROA-elliptical (p <0.001), and Bland-Altman analysis confirmed a significant systematic bias between these measurements (Table 2).

From the RT3DE analysis, EROA was considered significantly asymmetric when the L/S ratio was >1.5 [28]. In patients with an asymmetric orifice shape (18, 28%), 4CH was significantly smaller as compared to patients with L/S ≤1.5 (p = 0.02, Table 1), indicating a regurgitant orifice elongated along the leaflet coaptation line with the 4CH view representing the nar-

Table 1. Mean values and range (minimum-maximum) of EROA measured by 2 different 2D echocardiographic approaches (from the 4CH view and with the elliptical formula) and measured by RT3DE, in the total population and among patients with (L/S >1.5) and without (L/S ≤1.5) an asymmetrical regurgitant orifice.

	Total population (n = 64)	L/S >1.5 (n = 18)	L/S ≤1.5 (n = 46)
2D: EROA-4CH, cm2			
Mean (±SD)	0.11±0.12†	0.06±0.06*	0.14±0.13
Range (min-max)	0.008-0.64	0.008-0.27	0.008-0.64
2D: EROA-elliptical, cm2			
Mean (±SD)	0.14±0.15†	0.15±0.14	0.14±0.16
Range (max-min)	0.008-0.75	0.02-0.55	0.008-0.75
RT3DE: EROA-3D, cm2			
Mean (±SD)	0.22±0.14	0.23±0.14	0.20±0.16
Range (max-min)	0.04-0.78	0.07-0.41	0.04-0.78

* = p <0.05 between patients with L/S >15 and with L/S ≤1.5.

† = p <0.001 between 2D echocardiography and RT3DE.

EROA: effective regurgitant orifice area; elliptical: elliptical formula; L/S: ratio of the longest and shortest diameter of EROA-3D; SD: standard deviation; 2D: 2-dimensional; 4CH: 4 chamber view: RT3DE: real-time 3-dimensional echocardiography

Table 2. Summary of the results of the Bland-Altman analysis applied for the EROA and Rvol measurements performed with 2D echocardiography (4CH view and elliptical approaches), RT3DE and 3D 3-directional velocity encoded MRI. The mean difference and the limits of agreements are reported.

	RT3DE: EROA-3D, cm2
2D echo: EROA-4CH, cm2	-0.10 (-0.26 to 0.08)*
2D echo: EROA-elliptical, cm2	-0.06 (-0.17 to 0.04)*
	MRI: Rvol, ml/beat
2D echo: Rvol-4CH, ml/beat	-2.9 (-18.0 to 12.5)†
2D echo: Rvol-elliptical, ml/beat	-1.6 (-11.9 to 8.8)†
RT3DE: Rvol-3D, ml/beat	-0.08 (-7.7 to 7.6)

* = p <0.001

† = p <0.05

MRI: magnetic resonance imaging; Rvol: regurgitant volume. For other abbreviations see Table 1.

rowest and the 2CH view the widest VCW. EROA-elliptical and EROA-3D however, were not significantly different between patients with asymmetric or non-asymmetric EROA (Table 1).

RT3DE versus VE-MRI

The mean Rvol-3D was 12.8±12.7 ml/beat, ranging from 2 to 67 ml/beat. The mean Rvol-4CH was 10.1±11.9 ml/beat (from 1 to 51 ml/beat) and Rvol-elliptical was 11.3±12.1 ml/beat (from 1 to 55 ml/beat).

Rvol-3D showed an excellent correlation with Rvol-MRI (r = 0.94, Figure 3) and the Bland-Altman analysis revealed a non significant bias between these techniques (Figure 3): mean

difference (RT3DE – MRI) = -0.08 ml/beat (p = 0.87), limits of agreement from -7.7 to 7.6 ml/beat (Table 2).

Conversely, the 2D echocardiographic approach from the 4CH view (Rvol-4CH) significantly underestimated Rvol (p = 0.006) as compared to MRI (Rvol-MRI) (Table 2). However, the 2D elliptical approach demonstrated a better agreement with MRI: mean difference (Rvol-elliptical – Rvol-MRI) = -1.6 ml/beat (p = 0.04), limits of agreement from -11.9 to 8.8 ml/beat (Table 2).

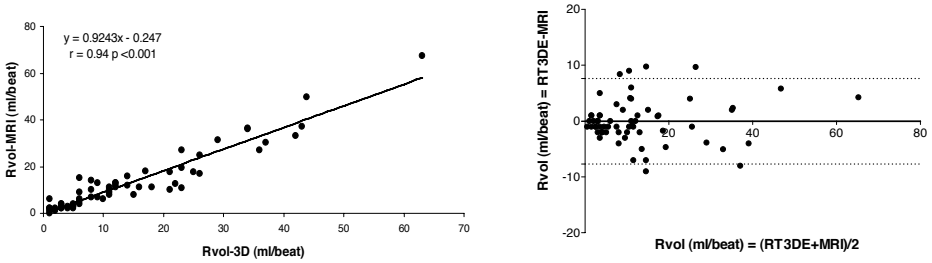


Figure 3. Comparison between mitral regurgitant volume (Rvol) assessed with real-time 3-dimensional echocardiography (RT3DE, Rvol-3D) and by 3-directional velocity encoded magnetic resonance imaging (MRI, Rvol-MRI). Left panel: correlation between mitral regurgitant volume (Rvol) assessed with real-time 3-dimensional echocardiography (RT3DE, Rvol-3D) and by 3-directional velocity encoded magnetic resonance imaging (MRI, Rvol-MRI). Right panel: Bland-Altman scatter plot of differences in Rvol between RT3DE and MRI and the average Rvol between the 2 techniques: Rvol-3D is 0.08 ml/beat lower than Rvol-MRI (p = 0.87), limits of agreement from -7.7 to 7.6 ml/beat.

DISCUSSION

The main findings of the current study can be summarized as follows: 1) in patients with functional MR direct assessment of EROA by RT3DE was feasible and reproducible; 2) 2D echocardiography systematically underestimated the EROA as compared to RT3DE and the difference between these 2 techniques was more accentuated in the presence of an asymmetric regurgitant orifice; 3) a strong correlation was observed between RT3DE and MRI for the measurement of Rvol, with no significant bias between these 2 techniques; conversely, 2D echocardiography significantly underestimated Rvol as compared to MRI.

Quantification of mitral regurgitation

RT3DE versus 2D echocardiography

Accurate grading of MR severity is an important but still controversial issue. Currently, conventional 2D echocardiography is the method of choice for the assessment of MR [8], although

the limitations of this technique are well known. One of the most commonly used measures is the ratio between the regurgitant jet area and the left atrial area. However, this method is semiquantitative and rather subjective. In turn, quantitative approaches, such as PISA and pulsed Doppler quantitative flow methods, are limited by hemodynamic and geometric assumptions that introduce inaccuracies, and by complicated and time-consuming acquisitions and calculations [8–11]. For estimation of MR severity, 2D echocardiographic measurement of VCW has also been proposed as a direct representation of the EROA [8,13,14]. This approach assumes the EROA shape to be either circular or elliptical. However, these assumptions may not be applicable when mitral valve geometry is significantly altered [29] and the regurgitant orifice shows an irregular shape. Particularly in patients with functional MR, EROA is typically elongated along the semilunar-shaped leaflet coaptation line, which contributes to a significant underestimation of the regurgitant orifice when measured from the 4-chamber or parasternal long-axis views [15,16]. In this group of patients, lower thresholds to define severe MR and to identify patients with poor prognosis have been proposed (EROA ≥0.2 cm^2 instead of 0.4 cm^2 and Rvol ≥30 ml/beat instead of ≥60 ml/beat) [2,3,30]. This difference may be explained by the changes in LV and left atrium function and compliance [2,3], but the difference is probably also related to a significant underestimation of MR severity by conventional 2D echocardiographic methods in the presence of an asymmetric regurgitant orifice.

Color Doppler RT3DE, allowing for an unlimited plan orientation and in particular for an "en face" view of the mitral valve, provides a direct assessment of size and shape of regurgitant orifice, obviating the geometric assumptions applied by 2D echocardiography [15,17,18,28]. Initial studies showed the incremental value of RT3DE measurements of EROA over 2D PISA and VCW. In particular, the studies by Iwakura et al [28] and Kahlert et al [15] emphasized the importance of a 3D approach in patients with functional MR, in whom 2D echocardiography significantly underestimated the size of the regurgitant orifice. Similarly, in the current study a significant difference in the measurement of EROA was observed between RT3DE and 2D echocardiography (-0.10 cm^2 for EROA-4CH and -0.06 cm^2 for EROA-elliptical); also, 2D echocardiography underestimated EROA particularly in patients with an asymmetric regurgitant orifice (L/S >1.5). Thus far, a true validation study of RT3DE measurement of EROA is lacking, since previous studies were limited to comparisons between different echocardiographic techniques or used semiquantitative angiographic grading as a reference [15,18,28]. The present study is the first systematic comparison between RT3DE and velocity encoded MRI, which has been recently proposed as the reference method for quantification of MR.

RT3DE versus VE MRI

Velocity encoded MRI is particularly suitable for determining trans-valvular blood flow, providing quantitative information on moving spins [31], and has been recently proposed as a ref-

erence method [19,20]. However, conventional single-slice one-directional velocity encoded MRI showed some limitations [21], in particular due to the fact that the acquisition plane can not be adapted to the motion of the valve, and currently the most accurate approach is considered the 3D 3-directional velocity encoded MRI with retrospective valve tracking. This technique is able to cover the complete velocity vector field of the blood flow and to correct for the through-plane myocardial motion in the apical-basal direction [22,23]. Furthermore, it has been validated in vitro with flow phantoms and in vivo, and showed excellent reproducibility [24].

In the current study, RT3DE measurement of Rvol was compared against 3D 3-directional velocity encoded MRI. An excellent correlation between the 2 techniques was found without a significant bias. The residual non-significant difference between RT3DE and MRI may be explained by 2 sources of errors: the fixed position and the eventual misalignment of the continuous-wave Doppler ultrasound beam to the flow direction. Furthermore, imaging the region of interest with RT3DE can be complicated by acoustic attenuation from cardiac and thoracic structures.

The currently recommended 2D approach, providing a less accurate measurement of the EROA and presenting the same limitations of the Doppler acquisitions, showed a significant underestimation of the Rvol when compared to 3D 3-directional velocity encoded MRI. In particular, a mean bias between these 2 techniques of -2.9 ml/beat ($p<0.05$, limits of agreement from -18.0 to 12.5 ml/beat) may easily lead to a misdiagnosis of the severity of MR (mild instead of moderate or moderate instead of mild).

Clinical implications

The presence of functional MR has important prognostic value and accurate assessment of its severity is crucial for risk stratification and clinical decision making [1–6]. In the present study, quantification of Rvol by RT3DE demonstrated to be feasible and highly accurate compared to 3D 3-directional velocity encoded MRI and, consequently, may be proposed as a better alternative to conventional 2D echocardiographic measurements. In addition, RT3DE will probably overcome the need for 2 different cut-off values to define severity of organic and functional MR, providing direct and accurate quantification of the EROA. Further multi-center studies are needed to confirm the present results and follow-up data are necessary to explore the prognostic implications of these measures.

Of note, RT3DE technology is in continuous progress and will lead to further improvement in the image quality (allowing for a direct assessment of the regurgitant orifice without Color Doppler) and in the temporal resolution (higher frame rate).

CONCLUSIONS

Quantification of the regurgitant orifice and volume of functional MR using RT3DE is feasible and accurate and demonstrated to be superior to the currently recommended 2D echocardiographic approach in a head-to-head comparison with 3D 3-directional velocity encoded MRI.

REFERENCES

1. Bursi F, Enriquez-Sarano M, Nkomo VT et al. Heart failure and death after myocardial infarction in the community: the emerging role of mitral regurgitation. *Circulation.* 2005;111:295-301.
2. Grigioni F, Enriquez-Sarano M, Zehr KJ, Bailey KR, Tajik AJ. Ischemic mitral regurgitation: long-term outcome and prognostic implications with quantitative Doppler assessment. *Circulation.* 2001;103:1759-1764.
3. Grigioni F, Detaint D, Avierinos JF, Scott C, Tajik J, Enriquez-Sarano M. Contribution of ischemic mitral regurgitation to congestive heart failure after myocardial infarction. *J Am Coll Cardiol.* 2005;45:260-267.
4. Iung B, Baron G, Butchart EG et al. A prospective survey of patients with valvular heart disease in Europe: The Euro Heart Survey on Valvular Heart Disease. *Eur Heart J.* 2003;24:1231-1243.
5. Enriquez-Sarano M, Avierinos JF, Messika-Zeitoun D et al. Quantitative determinants of the outcome of asymptomatic mitral regurgitation. *N Engl J Med.* 2005;352:875-883.
6. Rosenhek R, Rader F, Klaar U et al. Outcome of watchful waiting in asymptomatic severe mitral regurgitation. *Circulation.* 2006;113:2238-2244.
7. Enriquez-Sarano M, Seward JB, Bailey KR, Tajik AJ. Effective regurgitant orifice area: a noninvasive Doppler development of an old hemodynamic concept. *J Am Coll Cardiol.* 1994;23:443-451.
8. Zoghbi WA, Enriquez-Sarano M, Foster E et al. Recommendations for evaluation of the severity of native valvular regurgitation with two-dimensional and Doppler echocardiography. *J Am Soc Echocardiogr.* 2003;16:777-802.
9. Enriquez-Sarano M, Miller FA, Jr., Hayes SN, Bailey KR, Tajik AJ, Seward JB. Effective mitral regurgitant orifice area: clinical use and pitfalls of the proximal isovelocity surface area method. *J Am Coll Cardiol.* 1995;25:703-709.
10. Schwammenthal E, Chen C, Benning F, Block M, Breithardt G, Levine RA. Dynamics of mitral regurgitant flow and orifice area. Physiologic application of the proximal flow convergence method: clinical data and experimental testing. *Circulation.* 1994;90:307-322.
11. Utsunomiya T, Ogawa T, Doshi R et al. Doppler color flow "proximal isovelocity surface area" method for estimating volume flow rate: effects of orifice shape and machine factors. *J Am Coll Cardiol.* 1991;17:1103-1111.
12. Zoghbi WA, Quinones MA. Determination of cardiac output by Doppler echocardiography: a critical appraisal. *Herz.* 1986;11:258-268.
13. Hall SA, Brickner ME, Willett DL, Irani WN, Afridi I, Grayburn PA. Assessment of mitral regurgitation severity by Doppler color flow mapping of the vena contracta. *Circulation.* 1997;95:636-642.
14. Mascherbauer J, Rosenhek R, Bittner B et al. Doppler echocardiographic assessment of valvular regurgitation severity by measurement of the vena contracta: an in vitro validation study. *J Am Soc Echocardiogr.* 2005;18:999-1006.
15. Kahlert P, Plicht B, Schenk IM, Janosi RA, Erbel R, Buck T. Direct assessment of size and shape of noncircular vena contracta area in functional versus organic mitral regurgitation using real-time three-dimensional echocardiography. *J Am Soc Echocardiogr.* 2008;21:912-921.
16. Otsuji Y, Handschumacher MD, Schwammenthal E et al. Insights from three-dimensional echocardiography into the mechanism of functional mitral regurgitation: direct in vivo demonstration of altered leaflet tethering geometry. *Circulation.* 1997;96:1999-2008.
17. Irvine T, Li XN, Rusk R, Lennon D, Sahn DJ, Kenny A. Three dimensional colour Doppler echocardiography for the characterisation and quantification of cardiac flow events. *Heart.* 2000;84 Suppl 2:II2-II6.

18. Khanna D, Vengala S, Miller AP et al. Quantification of mitral regurgitation by live three-dimensional transthoracic echocardiographic measurements of vena contracta area. *Echocardiography.* 2004;21:737-743.
19. Buck T, Plicht B, Kahlert P, Schenk IM, Hunold P, Erbel R. Effect of dynamic flow rate and orifice area on mitral regurgitant stroke volume quantification using the proximal isovelocity surface area method. *J Am Coll Cardiol.* 2008;52:767-778.
20. Stewart RA, Raffel OC, Kerr AJ et al. Pilot study to assess the influence of beta-blockade on mitral regurgitant volume and left ventricular work in degenerative mitral valve disease. *Circulation.* 2008;118:1041-1046.
21. Kayser HW, Stoel BC, van der Wall EE, van der Geest RJ, de Roos A. MR velocity mapping of tricuspid flow: correction for through-plane motion. *J Magn Reson Imaging.* 1997;7:669-673.
22. Westenberg JJ, Danilouchkine MG, Doornbos J et al. Accurate and reproducible mitral valvular blood flow measurement with three-directional velocity-encoded magnetic resonance imaging. *J Cardiovasc Magn Reson.* 2004;6:767-776.
23. Westenberg JJ, Doornbos J, Versteegh MI et al. Accurate quantitation of regurgitant volume with MRI in patients selected for mitral valve repair. *Eur J Cardiothorac Surg.* 2005;27:462-466.
24. Westenberg JJ, Roes SD, Marsan NA et al. Mitral valve and tricuspid valve blood flow: accurate quantification with 3D velocity-encoded MR imaging with retrospective valve tracking. *Radiology.* 2008;249:792-800
25. Gillam LD. Is it time to update the definition of functional mitral regurgitation?: structural changes in the mitral leaflets with left ventricular dysfunction. *Circulation.* 2008;118:797-799.
26. Westenberg JJ, van der Geest RJ, Lamb HJ et al. MRI to evaluate left atrial and ventricular reverse remodeling after restrictive mitral annuloplasty in dilated cardiomyopathy. *Circulation.* 2005;112:I437-I442.
27. Westenberg JJ, Braun J, Van de Veire N et al. Magnetic resonance imaging assessment of reverse left ventricular remodeling late after restrictive mitral annuloplasty in early stages of dilated cardiomyopathy. *J Thorac Cardiovasc Surg.* 2008;135:1247-1252.
28. Iwakura K, Ito H, Kawano S et al. Comparison of orifice area by transthoracic three-dimensional Doppler echocardiography versus proximal isovelocity surface area (PISA) method for assessment of mitral regurgitation. *Am J Cardiol.* 2006;97:1630-1637.
29. Kwan J, Qin JX, Popovic ZB, Agler DA, Thomas JD, Shiota T. Geometric changes of mitral annulus assessed by real-time 3-dimensional echocardiography: becoming enlarged and less nonplanar in the anteroposterior direction during systole in proportion to global left ventricular systolic function. *J Am Soc Echocardiogr.* 2004;17:1179-1184.
30. Vahanian A, Baumgartner H, Bax J et al. Guidelines on the management of valvular heart disease: The Task Force on the Management of Valvular Heart Disease of the European Society of Cardiology. *Eur Heart J.* 2007;28:230-268.
31. Wigstrom L, Ebbers T, Fyrenius A et al. Particle trace visualization of intracardiac flow using time-resolved 3D phase contrast MRI. *Magn Reson Med.* 1999;41:793-799.

PART IV

Incremental value of advanced imaging modalities in cardiac resynchronization therapy

CHAPTER 21

Left ventricular rotational mechanics in acute myocardial infarction and in chronic (ischemic and nonischemic) heart failure patients

M Bertini, G Nucifora, **N Ajmone Marsan**, V Delgado, R J van Bommel, G Boriani, M Biffi, E R Holman, E E Van der Wall, M J Schalij, and J J Bax

Am J Cardiol 2009;103:1506-12.

ABSTRACT

Objectives: Left ventricular (LV) twist and untwisting rate are emerging as global and thorough parameters for assessment of LV function. This study explored differences of LV twist and untwisting rate in patients with acute myocardial infarction (AMI) and patients with ischemic and nonischemic chronic heart failure (HF).

Methods: Fifty patients with AMI, 49 with ischemic HF, and 38 with nonischemic HF were studied. As a control group, 28 subjects without evidence of structural heart disease were included. Speckle-tracking analysis was applied to LV short-axis images at basal and apical levels. LV twist was defined as the net difference of apical and basal rotations at isochronal time points. The first time derivative of LV untwist was defined as the LV untwisting rate.

Results: Compared with control subjects, peak LV twist was decreased in patients with AMI and extremely decreased in those with HF ($p < 0.001$, analysis of variance). A strong correlation ($r = 0.87$, $p < 0.001$) was found between peak LV twist and LV ejection fraction in the overall study population. LV untwisting rate was progressively decreased in patients with AMI and HF compared with control subjects ($p < 0.001$, analysis of variance). A moderate correlation ($r = 0.56$, $p < 0.001$) was noted between peak LV untwisting rate and grade of diastolic dysfunction in the overall study population.

Conclusions: LV twist and untwisting rate are strongly related to LV systolic and diastolic functions, respectively. Impairment of LV function observed in patients with AMI and HF is associated with a decrease of LV twist and untwisting rate.

INTRODUCTION

Recently, a novel speckle-tracking analysis has become available as a simple echocardiographic method to assess left ventricular (LV) twist and untwisting rate. This technique has been validated against sonomicrometry and tagged magnetic resonance imaging, which are currently considered the gold standards for assessment of rotational parameters [1,2]. Initial studies evaluated LV twist and untwisting rate in patients with myocardial infarction (MI) and heart failure (HF) [3–5], but thus far, the impact of these different diseases on rotational mechanics has never been systematically evaluated.

The present study assessed differences of LV twist and untwisting rate between patients with acute MI (AMI) and chronic HF.

METHODS

One hundred thirty-seven consecutive patients were enrolled; 50 patients had AMI, 49 had chronic ischemic HF, and 38 had nonischemic HF. Diagnosis of AMI was based on the presence of symptoms consistent with myocardial ischemia lasting ≥30 minutes and ≥2-mm ST-segment elevation in ≥2 contiguous electrocardiographic leads [6]. All patients with AMI underwent urgent coronary angiography, followed by primary percutaneous coronary intervention, and echocardiographic examination was performed within 48 hours after AMI. Cause of HF was considered ischemic in the presence of significant coronary artery disease (>50% stenosis in ≥1 major epicardial coronary artery) on coronary angiogram and/or history of AMI or previous revascularization.

In addition, 28 subjects without evidence of structural heart disease, matched for age and gender, were included as a control group. Clinical echocardiographic analysis included standard 2-dimensional echocardiography to assess LV systolic and diastolic functions. Furthermore, speckle-tracking analysis was applied to assess LV rotational parameters (twist and untwisting rate).

All patients were imaged in the left lateral decubitus position with a commercially available system (Vingmed Vivid 7, General Electric Medical Systems, Milwaukee, Wisconsin) equipped with a 3.5-MHz transducer. Standard 2-dimensional images and Doppler and color Doppler data acquired from parasternal and apical views (2, 3, and 4 chambers) were digitally stored in cine-loop format; analyses were subsequently performed off-line using EchoPac 7.0.0 (General Electric Medical Systems).

LV end-diastolic volume (EDV) and end-systolic volume (ESV) were measured according to the Simpson biplane method and LV ejection fraction (EF) was calculated as ([EDV – ESV]/end-diastolic volume) X 100 [7]. Transmitral and pulmonary vein (PV) pulse-wave Doppler tracings, obtained in accordance to recommendations of the American Society of Echocardiography

[8], were used to classify diastolic function as (1) normal, when the E/A ratio was equal to 0.9 to 1.5, deceleration time was equal to 160 to 240 ms, and PV systolic velocity ≥PV diastolic velocity; (2) diastolic dysfunction grade 1 (mild), when the E/A ratio <0.9, deceleration time >240 ms, and PV systolic velocity was >> PV diastolic velocity; (3) diastolic dysfunction grade 2 (moderate), when the E/A ratio was equal to 0.9 to 1.5, deceleration time was equal to 160 to 240 ms, and PV systolic velocity was <PV diastolic velocity; (4) diastolic dysfunction grade 3 (severe), when the E/A ratio >2.0, deceleration time <160 ms, and PV systolic velocity was <<PV diastolic velocity; or (5) diastolic dysfunction grade 4 (severe), when the E/A ratio >2.5, deceleration time <130 ms, and PV systolic velocity was <<PV diastolic velocity [9].

Speckle-tracking analysis is based on tracking of natural acoustic markers, or speckles, on standard gray-scale images. This novel technique is angle independent and permits evaluation of myocardial contraction/relaxation along the circumferential, longitudinal, and radial directions [10,11].

In the present evaluation, speckle-tracking analysis was applied to determine the LV twist and LV untwisting rate. Parasternal short-axis images were acquired at 2 distinct levels: (1) basal level, identified by the mitral valve, and (2) apical level, defined as the smallest cavity achievable distal to the papillary muscles (moving the probe down and slightly laterally, if needed). The frame rate was 45 to 100 frames/s and 3 cardiac cycles for each parasternal short-axis level were stored in cine-loop format for off-line analysis. The endocardial border was traced at an end-systolic frame and the region of interest was chosen to fit the entire myocardium. The software allows the operator to check and validate the tracking quality and to adjust the endocardial border or modify the width of the region of interest, if needed. Furthermore, each short-axis image was automatically divided into 6 standard segments, i.e., septal, anteroseptal, anterior, lateral, posterior, and inferior. Subsequently, the speckle-tracking software calculated LV rotation from the apical and basal short-axis images as the average angular displacement of the 6 standard segments referring to the ventricular centroid, frame by frame. Counter-clockwise rotation was marked as a positive value and clockwise rotation as a negative value when viewed from the LV apex. The software automatically calculated LV twist, defined as the net difference (in degrees) of apical and basal rotations at isochronal time points. The opposite rotation after LV twist was defined as LV untwist and the time derivative of LV untwist was defined as LV untwisting rate (degrees per second; Figure 1).

The following measurements were obtained: (1) peak apical and basal rotations, (2) peak LV twist and peak LV untwisting rate, (3) time to peak apical and basal rotations, and (4) time to peak LV twist and untwisting rate. A pulse-wave Doppler tracing obtained from the LV outflow tract was used to identify timing of aortic valve opening and closure. All timings were expressed as percent systolic phase.

To assess the reproducibility of peak LV twist and peak LV untwisting rate measurements, 20 patients were randomly selected. Bland-Altman analysis was performed to evaluate intra- and inter-observer agreements, repeating the analysis 1 week later by the same ob-

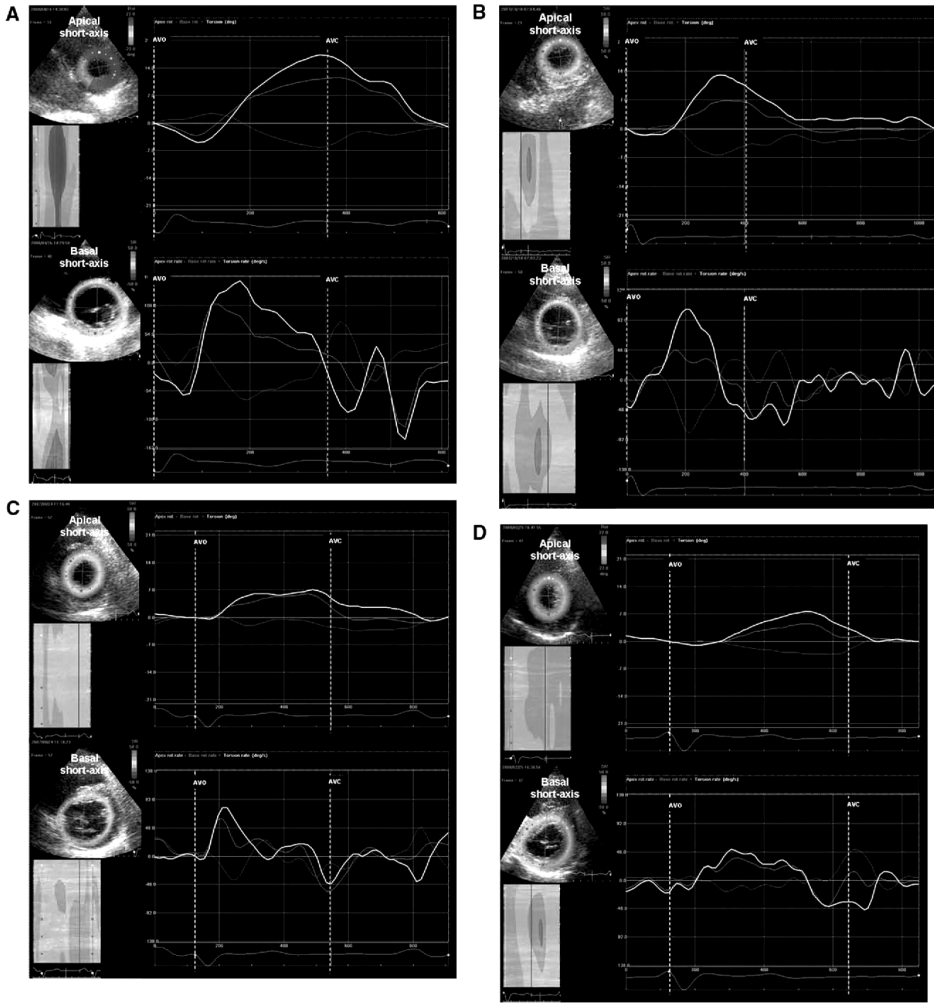


Figure 1 Left ventricular twist and untwisting rate in a normal control (Panel A), patient with AMI (Panel B), patient with ischemic HF (Panel C) and a patient with nonischemic HF(Panel D). Apical rotation (upper green line), apical rotation rate (lower green line), basal rotation (upper purple line), basal rotation rate (lower purple line), LV twist/untwist (upper white line), and LV twisting/untwisting rate (lower white line) are displayed.

AVC = aortic valve closure; AVO = aortic valve opening.

server and by a second independent observer. Bland-Altman analysis demonstrated good intra-observer and inter-observer agreements, with a small bias not significantly different from 0. Mean differences±2 SDs for peak LV twist and peak LV untwisting rate were 0.05±0.43 and -1.93±15.97°/s for intra-observer agreement and 0.17±1.51 and -3.97±35.63°/s for inter-observer agreement.

Continuous variables are expressed as mean±SD. Categorical data are presented as absolute numbers and percentages. One-way analysis of variance test was used to assess differences in continuous variables across different groups of patients; if the result of the analysis was significant, Bonferroni post hoc test was applied. Differences in categorical variables were analyzed using chi-square tests or Fischer's exact tests, as appropriate. Linear regression analysis was used to determine relations between peak LV twist and LVEF, between peak LV untwisting rate and grade of diastolic dysfunction, and between peak LV untwisting rate and LVESV. To identify independent determinants of peak LV untwisting rate, a multivariable linear regression analysis was performed including LVESV and grade of diastolic dysfunction as covariates. All statistical tests were 2-sided, and a p-value <0.05 was considered statistically significant. Statistical analysis was performed using SPSS 14.0 (SPSS, Inc., Chicago, Illinois).

RESULTS

Table 1 presents clinical and echocardiographic characteristics of the different patient groups and the control group.

Compared with controls, patients with AMI had significantly lower values of LV apical rotation (9.8±3.0 vs 7.6±3.8°, p = 0.007), LV basal rotation (-6.3±2.4 vs -4.9±2.1°, p = 0.04), and LV twist (15.7±3.1 vs 11.6±3.8°, p <0.001).

LV rotational parameters were not significantly different between patients with ischemic HF and those with nonischemic HF but were significantly impaired compared with patients with AMI; peak apical rotations were 2.5±1.9 and 2.4±1.8°, respectively (p <0.001 compared with patients with AMI) and peak basal rotations were -3.4±2.0 and -2.8±2.2°, respectively (p = 0.003 and p <0.001, respectively, compared with patients with AMI). Consequently, peak LV twists were 5.2±2.2 and 4.0±2.9°, respectively (p <0.001 compared with patients with AMI; Table 1).

Figure 2 shows the progressive decrease of peak LV twist and LVEF among the 4 different groups. In particular, a strong correlation (r = 0.87, p <0.001) was found between peak LV twist and LVEF (Figure 3) and between peak LV apical rotation and LVEF (r = 0.79, p <0.001) in the overall study population; conversely, only a modest relation was found between peak LV basal rotation and LVEF (r = -0.48, p <0.001). Furthermore, time to peak LV twist occurred sooner in patients with AMI, ischemic HF, and nonischemic HF compared with controls (p <0.001, analysis of variance; Table 1).

Peak LV untwisting rate was not significantly different between patients with ischemic HF and those with nonischemic HF, with lower values compared with patients with AMI (-58±34°/s in patients with ischemic HF, p = 0.018; -59±32°/s in patients with nonischemic HF, p = 0.036; Table 1).

Table 1. Clinical, echocardiographic and rotational parameters of controls and patients with acute myocardial infarction, ischemic heart failure (HF) and nonischemic HF.

	Normal controls (n = 28)	AMI patients (n = 50)	Patients with ischemic HF (n = 49)	Patients with nonischemic HF (n = 38)	ANOVA p-value
Age (years)	60±11	60±11	64±11	65±13	0.084
Gender male, n (%)	21 (75)	38 (76)	43 (88)	28 (74)	0.16
LVEDV (ml)	87±26*	103±28*	179±67	214±74¶	<0.001
LVESV (ml)	34±11*	55±21*	130±52	164±61¶	<0.001
LVEF (%)	62±6‡	47±10*	28±5	24±6¶	<0.001
Diastolic function, n (%)	‡	†			
Grade 0	28 (100)	7 (14)	0 (0)	0 (0)	<0.001
Grade 1	0 (0)	19 (38)	12 (24)	8 (21)	0.002
Grade 2	0 (0)	14 (28)	13 (26)	6 (16)	0.014
Grade 3-4	0 (0)	10 (20)	24 (49)	24 (63)	<0.001
Peak LV twist (°)	15.7±3.1‡	11.6±3.8*	5.2±2.2	4.0±2.9	<0.001
Peak LV untwisting rate (°/s)	-108±30*§	-75±35ll¶	-58±34	-59±33	<0.001
Time peak LV twist (% systole)	98±8‡§	83±14	83±19	75±27	<0.001
Time peak LV untwisting (% systole)	114±9	118±17	116±17	116±23	0.75

* p <0.001;

† p <0.01 versus ischemic and nonischemic HF.

‡ p <0.001 versus AMI, ischemic HF, and nonischemic HF.

§ p <0.01 versus AMI.

ll p <0.05 versus ischemic HF.

¶ p <0.05 versus nonischemic HF.

ANOVA = analysis of variance; AMI = acute myocardial infarction; EDV = end-diastolic volume; EF = ejection fraction; ESV = end-systolic volume; HF = heart failure; LV = left ventricular.

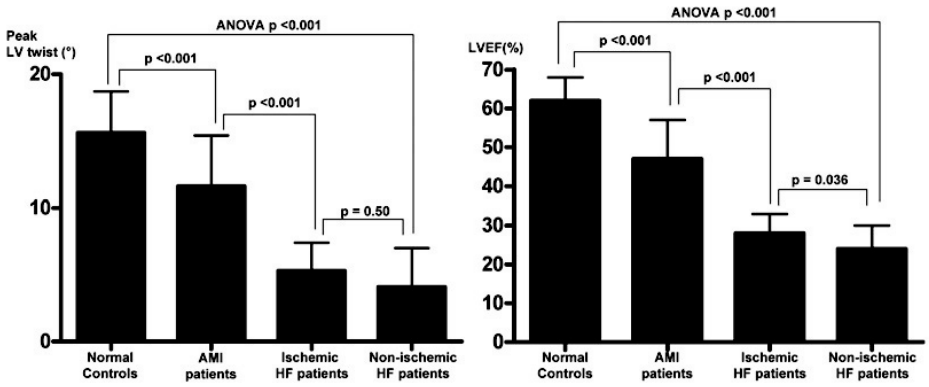


Figure 2. Peak LV twist (left) and LVEF (right) in controls, patients with AMI, patients with ischemic HF, and patients with nonischemic HF. ANOVA = analysis of variance.

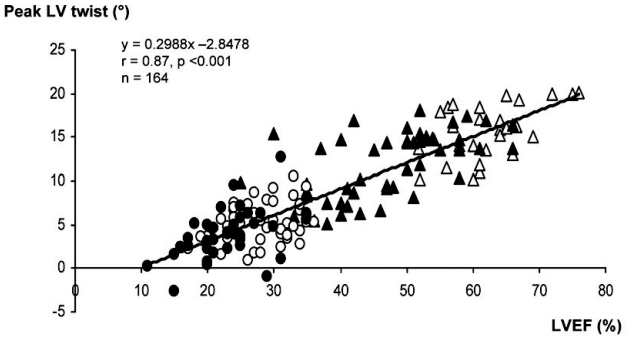


Figure 3. Correlation between LVEF and peak LV twist in the entire study population including controls (white triangles), patients with AMI (black triangles), patients with ischemic HF (white circles), and patients with nonischemic HF (black circles).

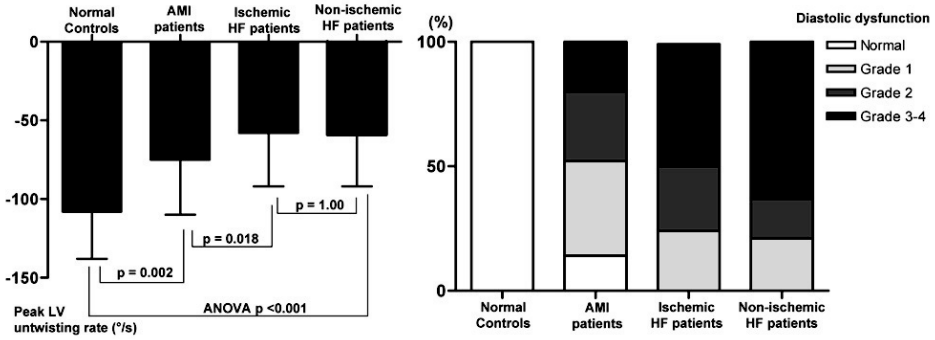


Figure 4. (Left) A decreased peak LV untwisting rate is observed in patients with AMI, those with ischemic HF, and those with nonischemic HF compared with controls. (Right) Distribution of normal diastolic function (white bars) and grades 1 (light gray bars), 2 (dark gray bars), and 3 to 4 (black bars) of diastolic dysfunction in controls and patients with AMI, ischemic HF, and nonischemic HF.

Peak LV untwisting rate and grade of diastolic dysfunction among the 4 groups are shown in Figure 4. A moderate correlation ($r = 0.56$, $p < 0.001$) was noted between peak LV untwisting rate and grade of diastolic dysfunction in the overall study population (Figure 5). Furthermore, peak LV untwisting rate was significantly related to LVESV ($r = 0.42$, $p < 0.001$). At multivariable linear regression analysis LVESV (beta 0.16, $p = 0.047$) and grade of diastolic dysfunction (beta 0.47, $p < 0.001$) were independently related to peak LV untwisting rate.

No significant differences were found among the different groups for time to peak LV untwisting rate (Table 1).

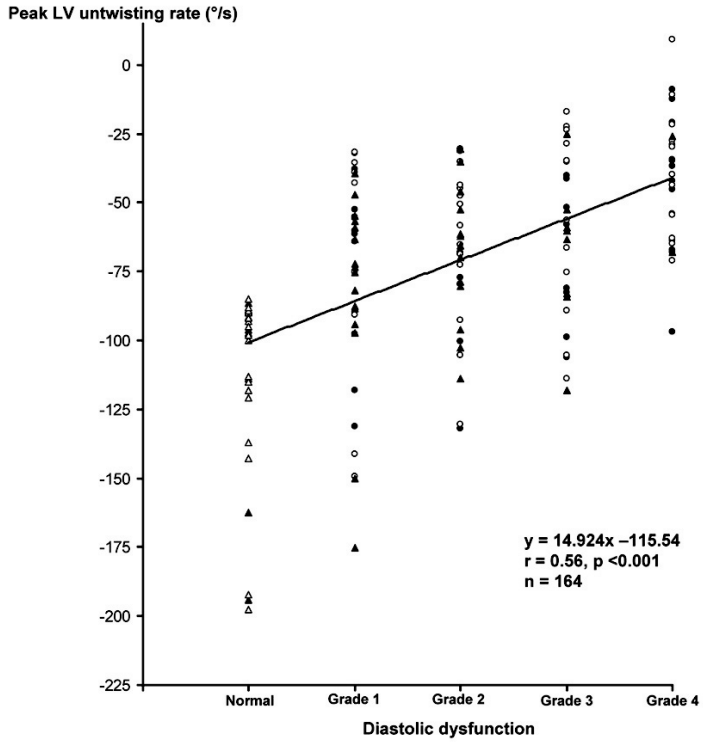


Figure 5. Correlation between grades of diastolic dysfunction (see definition in text) and peak LV untwisting rate in controls (white triangles), patients with AMI (black triangles), patients with ischemic HF (white circles), and patients with nonischemic HF (black circles).

DISCUSSION

The present study comprehensively evaluated differences in LV twist and untwisting rate in patients with AMI, ischemic HF, and nonischemic HF, providing new insight in the relation between LV rotational mechanics and LV function. The main findings can be summarized as follows: (1) LV twist is strongly related to LV systolic function and LV untwisting rate is modestly, but significantly, related to diastolic function; (2) impairment of LV function is associated not only with a decrease of LV twist and untwisting rate but also with an earlier peak of LV twist during systole.

As previously demonstrated in a mathematical model, LV twist distributes equally LV fiber stress and shortening across the LV wall [12]. Accordingly, LV twist increases the efficiency of sarcomere shortening and improves myocardial deformation during LV ejection [12]. In the present study, a significant impairment of LV twist was observed in patients with AMI and HF compared with controls. Moreover, a strong relation between degree of impairment of LV twist and observed impairment of LVEF was noted, confirming previous findings demonstrating a relation between LV twist and LVEF [4,5,13]. The strong correlation found between LV apical

rotation and LVEF is not surprising, because LV apical rotation contributes more to LV twist than LV basal rotation [14]. The different effects of AMI and long-term LV remodeling (in HF) on LV twist were also explored. LV twist was more decreased in patients with chronic HF compared with AMI. These findings may be explained by different mechanisms underlying a decrease in LV twist. In patients with HF, LV twist impairment is probably the result of a long-lasting process, with a rearrangement of LV myofibers with a consequent loss of the specific LV architecture responsible for the wringing motion [4,15,16]. Conversely, in patients with AMI the decrease of LV twist may result from an acute impairment in rotation of the LV region involved in the infarction [3,17]. Severity of this impairment appears related to transmurality of the infarction and to extent of dysfunctional myocardial segments[13,18].

Intriguingly, time to peak LV twist occurred sooner in patients with AMI and those with HF compared with controls. The impaired LV rotational mechanics observed in AMI and HF most likely explains this finding; less time is needed to reach peak LV twist because of the decreased contraction and rotation of LV myofibers. In addition, diseased LV myofibers are not able to fully counteract systolic ventricular pressure, preventing further myocardial shortening and, consequently, leading to sooner peak LV twist [18].

LV systolic twist consists of a deformation of the interstitial matrix resulting in storage of potential energy; the rapid release of potential energy stored during systole in isovolumic relaxation time leads to LV untwisting [19]. In turn LV untwisting generates an intraventricular pressure gradient facilitating diastolic LV filling [19]. Indeed, LV untwisting rate is emerging as an index of diastolic function [20–22]. In particular, LV untwisting rate was related to the time constant of LV pressure decay (tau) and the intraventricular pressure gradient [21]. In the present study, a good relation between LV untwisting rate and global diastolic function was observed. The relation was not perfect, probably because LV untwisting rate is a marker of diastolic suction rather than global diastolic function. LV untwisting rate was also independently related to LVESV; however, on multivariable linear regression analysis, grade of diastolic dysfunction was the strongest determinant of LV untwisting rate.

A significant impairment of LV untwisting rate was observed in patients with AMI and HF compared with control subjects. In patients with AMI, impairment in LV untwisting rate may be related to increased ventricular stiffness and consequent diastolic dysfunction due to recent acute ischemia and infarction [23]. In patients with HF, LV untwisting rate was even more decreased compared with patients with AMI. This observation may be explained by the presence of extensive, diffuse LV fibrosis as encountered in patients with HF, which is not (yet) present soon after AMI [24].

Although groups of patients with different grades of diastolic dysfunction were studied, no significant differences in time to peak LV untwisting rate were noted. This finding is in line with previous experimental and clinical studies in which only peak of untwisting rate but not time to peak untwisting rate was affected by grade of diastolic dysfunction [21,25].

As limitations, acquisition of LV apical short-axis images (highly dependent on the acoustic window) and through-plane motion, particularly at the basal level, could have affected the accuracy of the measurement of LV rotational parameters.

REFERENCES

1. Helle-Valle T, Crosby J, Edvardsen T et al. New noninvasive method for assessment of left ventricular rotation: speckle tracking echocardiography. *Circulation* 2005;112:3149 –3156.
2. Notomi Y, Lysyansky P, Setser RM et al. Measurement of ventricular torsion by two-dimensional ultrasound speckle tracking imaging. *J Am Coll Cardiol* 2005;45:2034–2041.
3. Bansal M, Leano RL, Marwick TH. Clinical assessment of left ventricular systolic torsion: effects of myocardial infarction and ischemia. *J Am Soc Echocardiogr* 2008;21:887– 894.
4. Kanzaki H, Nakatani S, Yamada N, Urayama S, Miyatake K, Kitakaze M. Impaired systolic torsion in dilated cardiomyopathy: reversal of apical rotation at mid-systole characterized with magnetic resonance tagging method. *Basic Res Cardiol* 2006;101:465– 470.
5. Sade LE, Demir O, Atar I, Muderrisoglu H, Ozin B. Effect of mechanical dyssynchrony and cardiac resynchronization therapy on left ventricular rotational mechanics. *Am J Cardiol* 2008;101:1163–1169.
6. Thygesen K, Alpert JS, White HD et al. Universal definition of myocardial infarction. *Circulation* 2007;116:2634 –2653.
7. Lang RM, Bierig M, Devereux RB et al. Recommendations for chamber quantification: a report from the American Society of Echocardiography's Guidelines and Standards Committee and the Chamber Quantification Writing Group, developed in conjunction with the European Association of Echocardiography, a branch of the European Society of Cardiology. *J Am Soc Echocardiogr* 2005;18:1440 –1463.
8. Quinones MA, Otto CM, Stoddard M, Waggoner A, Zoghbi WA. Recommendations for quantification of Doppler echocardiography: a report from the Doppler Quantification Task Force of the Nomenclature and Standards Committee of the American Society of Echocardiography. *J Am Soc Echocardiogr* 2002;15:167–184.
9. Lester SJ, Tajik AJ, Nishimura RA, Oh JK, Khandheria BK, Seward JB. Unlocking the mysteries of diastolic function: deciphering the Rosetta Stone 10 years later. *J Am Coll Cardiol* 2008;51:679–689.
10. Leitman M, Lysyansky P, Sidenko S et al. Two-dimensional strain-a novel software for real-time quantitative echocardiographic assessment of myocardial function. *J Am Soc Echocardiogr* 2004;17:1021–1029.
11. Reisner SA, Lysyansky P, Agmon Y, Mutlak D, Lessick J, Friedman Z. Global longitudinal strain: a novel index of left ventricular systolic function. *J Am Soc Echocardiogr* 2004;17:630–633.
12. Beyar R, Sideman S. Left ventricular mechanics related to the local distribution of oxygen demand throughout the wall. *Circ Res* 1986;58:664–677.
13. Garot J, Pascal O, Diebold B et al. Alterations of systolic left ventricular twist after acute myocardial infarction. *Am J Physiol Heart Circ Physiol* 2002;282:H357–H362.
14. Opdahl A, Helle-Valle T, Remme EW et al. Apical rotation by speckle tracking echocardiography: a simplified bedside index of left ventricular twist. *J Am Soc Echocardiogr* 2008;21.1121-1128
15. Setser RM, Kasper JM, Lieber ML, Starling RC, McCarthy PM, White RD. Persistent abnormal left ventricular systolic torsion in dilated cardiomyopathy after partial left ventriculectomy. *J Thorac Cardiovasc Surg* 2003;126:48 –55.
16. Athanasuleas CL, Buckberg GD. Surgical restoration of the postinfarction dilated ventricle. *Heart Fail Clin* 2008;4:361–370.
17. Sun JP, Niu J, Chou D et al. Alterations of regional myocardial function in a swine model of myocardial infarction assessed by echocardiographic 2-dimensional strain imaging. *J Am Soc Echocardiogr* 2007; 20:498 –504.

18. Knudtson ML, Galbraith PD, Hildebrand KL, Tyberg JV, Beyar R. Dynamics of left ventricular apex rotation during angioplasty: a sensitive index of ischemic dysfunction. *Circulation* 1997;96:801–808.
19. Sengupta PP, Khandheria BK, Narula J. Twist and untwist mechanics of the left ventricle. *Heart Fail Clin* 2008;4:315–324.
20. Notomi Y, Martin-Miklovic MG, Oryszak SJ et al. Enhanced ventricular untwisting during exercise: a mechanistic manifestation of elastic recoil described by Doppler tissue imaging. *Circulation* 2006;113:2524 –2533.
21. Notomi Y, Popovic ZB, Yamada H et al. Ventricular untwisting: a temporal link between left ventricular relaxation and suction. *Am J Physiol Heart Circ Physiol* 2008;294:H505–H513.
22. Wang J, Khoury DS, Yue Y, Torre-Amione G, Nagueh SF. Left ventricular untwisting rate by speckle tracking echocardiography. *Circulation* 2007;116:2580 –2586.
23. Ross J Jr. Is there a true increase in myocardial stiffness with acute ischemia? *Am J Cardiol* 1989;63:87E–91E.
24. Weber KT. Extracellular matrix remodeling in heart failure: a role for de novo angiotensin II generation. *Circulation* 1997;96:4065– 4082.
25. Park SJ, Miyazaki C, Bruce CJ, Ommen S, Miller FA, Oh JK. Left ventricular torsion by two-dimensional speckle tracking echocardiography in patients with diastolic dysfunction and normal ejection fraction. *J Am Soc Echocardiogr* 2008;21:1129 –1137.

CHAPTER 22

Effects of cardiac resynchronization therapy on left ventricular twist

M Bertini, **N Ajmone Marsan**, V Delgado, R J van Bommel, G Nucifora, C. JW Borleffs, G Boriani, M Biffi, E R Holman, E E van der Wall, M J Schalij, and J J Bax

J Am Coll Cardiol 2009;54:1317-25.

ABSTRACT

Objectives: Left ventricular (LV) twist is emerging as a comprehensive index of LV function. This study explored the effects of cardiac resynchronization therapy (CRT) on LV twist, particularly in relation to LV lead position.

Methods: Eighty heart failure (HF) patients were included. 2D-echocardiography was performed at baseline, immediately after CRT, and at 6 months follow-up. Speckle-tracking analysis was applied to assess LV twist. LV lead was placed preferably in a (postero-)lateral vein and at fluoroscopy, the position was classified as basal, mid-ventricular or apical. Response to CRT was defined as reduction of LV end-systolic volume ≥15% at 6 months follow-up. A control group comprised 30 normal subjects.

Results: Peak LV twist in HF patients was 4.8±2.6° compared to 15.0±3.6° of the controls ($p < 0.001$). At 6 months follow-up, peak LV twist significantly improved only in responders (56%), from 4.3±2.4° to 8.5±3.2° ($p < 0.001$). The strongest predictor of response to CRT was the improvement of peak LV twist immediately after CRT (odds ratio 1.899, 95% confidence intervals 1.334-2.703, $p < 0.001$). Furthermore, LV twist significantly improved in patients with an apical (from 4.3±3.1° to 8.6±3.0°, $p = 0.001$) and mid-ventricular (from 4.8±2.2° to 6.4±3.9°, $p = 0.038$) but not with a basal (5.0±3.3 vs. 4.1±3.2, $p = 0.28$) LV lead position. Similarly LVEF significantly increased in patients with an apical (from 26±7% to 37±7%, $p < 0.001$) and mid-ventricular (from 26±6% to 33±8%, $p < 0.001$) but not with a basal (26±5% vs. 28±8%, $p = 0.30$) LV lead position.

Conclusions: An immediate improvement of LV twist after CRT predicts LV reverse remodeling at 6 months follow-up.

INTRODUCTION

The human heart has a specific helical arrangement of the myofibers with a right-hand orientation from the base towards the apex in the endocardial layers and a left-hand orientation in the epicardial layers. This spiral architecture of the myofibers leads to a left ventricular (LV) systolic wringing motion as a result of an opposite rotation of LV apex and base [1, 2]. The gradient between apex and base in the rotation angle along LV longitudinal axis is called twist and contributes significantly to LV systolic function, in addition to myocardial shortening and thickening [3–5].

In heart failure (HF) patients, LV twist is significantly reduced [6]. Cardiac resynchronization therapy (CRT) is considered a major therapeutic breakthrough for HF patients, and recent large randomized trials have shown that CRT has beneficial effects on HF symptoms, LV systolic function and survival [7, 8]. At present, minimal data are available about the effect of CRT on LV twist [9, 10].

In the current study, the effect of CRT on LV twist was assessed using speckle-tracking echocardiography. Furthermore, the relationship between the change in LV twist and LV reverse remodeling at 6 months follow-up was investigated. Finally, the influence of the LV lead position on the improvement in LV twist and response to CRT was explored.

METHODS

Patient population and protocol

A total of 87 consecutive HF patients scheduled for CRT were prospectively included. According to current guidelines, the inclusion criteria were: New York Heart Association (NYHA) functional class III-IV, sinus rhythm, LV ejection fraction (LVEF) ≤35%, QRS duration ≥120 ms [11]. Etiology of HF was considered ischemic in the presence of significant coronary artery disease (>50% stenosis in ≥1 major epicardial coronary artery) on coronary angiography and/or a history of myocardial infarction or revascularization.

The clinical evaluation consisted of: 1) assessment of clinical status: NYHA functional class, quality of life (using the Minnesota Living with Heart Failure questionnaire) [12] and 6-minute walk distance[13] at baseline and 6 months follow-up; 2) assessment of LV volumes, function, dyssynchrony and twist, using standard echocardiography and speckle-tracking analysis at baseline, within 48 hours (immediately after CRT) and at 6 months follow-up.

In addition, 30 subjects without evidence of structural heart disease, frequency-matched for age, gender and body surface area, were included as a normal control group, selected

from an echocardiographic data base. These subjects were referred for the echocardiographic evaluation because of atypical chest pain, palpitations or syncope without murmur.

Standard echocardiography

All patients were imaged in left lateral decubitus position using a commercially available system (Vingmed Vivid 7, General Electric-Vingmed, Milwakee, Wisconsin, USA). Standard 2-dimensional images were obtained using a 3.5-MHz transducer and digitally stored in cine-loop format; the analysis was performed offline using EchoPAC version 6.0.1 (General Electric-Vingmed).

From the standard apical views (4- and 2-chamber) LV volumes and LVEF were calculated according to the American Society of Echocardiography guidelines [14]. At 6 months follow-up, patients were classified as echocardiographic responders based on a reduction ≥15% of LV end-systolic volume (LVESV) [15].

Segmental wall motion was assessed according to American Society of Echocardiography in order to evaluate the presence of scarred segments within ischemic HF patients [14]. Akinetic and diskinetic segments (wall motion score 3 and 4) were classified as scarred segments [16].

Speckle-tracking analysis

The speckle-tracking software tracks frame-to-frame the movement of natural myocardial acoustic markers, or speckles, on standard gray scale images. Speckles are randomly distributed and each region of the myocardium has a distinguishing pattern, a fingerprint. Furthermore, speckle-tracking analysis is angle independent and allows the evaluation of myocardial contraction/relaxation along the circumferential, longitudinal and radial direction [17, 18].

In the current study, speckle-tracking analysis was applied to evaluate LV dyssynchrony (based on radial strain analysis) and LV twist. Parasternal short-axis images were acquired at 3 distinct levels: 1) basal level, identified by the mitral valve; 2) papillary muscle level; 3) apical level (the smallest cavity achievable distally to the papillary muscles, moving the probe down and slightly laterally, if needed). Frame rate ranged from 45 to 100 frame/s and 3 cardiac cycles for each parasternal short-axis level were stored in cine-loop format for the offline analysis (EchoPAC). The endocardial border was traced at an end-systolic frame and the region of interest (ROI) was chosen to fit the whole myocardium. The software allows the operator to check and validate the tracking quality and to adjust the endocardial border or modify the width of the ROI, if needed. Furthermore, each short-axis image was automatically divided into 6 standard segments: septal, anteroseptal, anterior, lateral, posterior, and inferior.

Aortic valve opening and closure were identified on pulsed-wave Doppler tracings obtained from the LV outflow tract.

LV dyssynchrony analysis

LV dyssynchrony was derived from the radial strain curves obtained from the papillary muscle short-axis view. As previously described, LV dyssynchrony was defined as the time difference of peak radial strain between the anteroseptal and posterior segments [19].

LV twist analysis

The speckle-tracking software calculates LV rotation from the apical and basal short-axis images as the average angular displacement of the 6 standard segments referring to the ventricular centroid, frame by frame. Counterclockwise rotation was marked as positive value and clockwise rotation as negative value when viewed from the LV apex. LV twist was defined as the net difference (in degrees) of apical and basal rotation at isochronal time points. For the calculation of LV twist, averaged apical and basal rotation data were exported to a spreadsheet program (Excel 2003; Microsoft Corporation, Redmond, Washington) (Figure 1) [20, 21]. The following measurements were derived: peak apical and basal rotation, peak LV twist.

Reproducibility

Reproducibility of LV end-diastolic volume (LVEDV), LVESV, LVEF and peak LV twist was assessed on 20 randomly selected HF patients. Bland-Altman analysis was performed to evaluate the intra- and inter-observer agreement repeating the analysis few days later by the same observer and by a second independent observer. The results were expressed as absolute mean difference±2 standard deviation (SD).

The intra-observer agreement for LVEDV, LVESV, LVEF and peak LV twist were 7.4±11.2 ml, 7.0±10.1 ml, 1.9±4.4%, and 0.2±0.3º, respectively.

The inter-observer agreement for LVEDV, LVESV, LVEF and peak LV twist were 12.9±14.7 ml, 11.3±13.9 ml, 2.5±4.9%, and 0.7±0.8º, respectively.

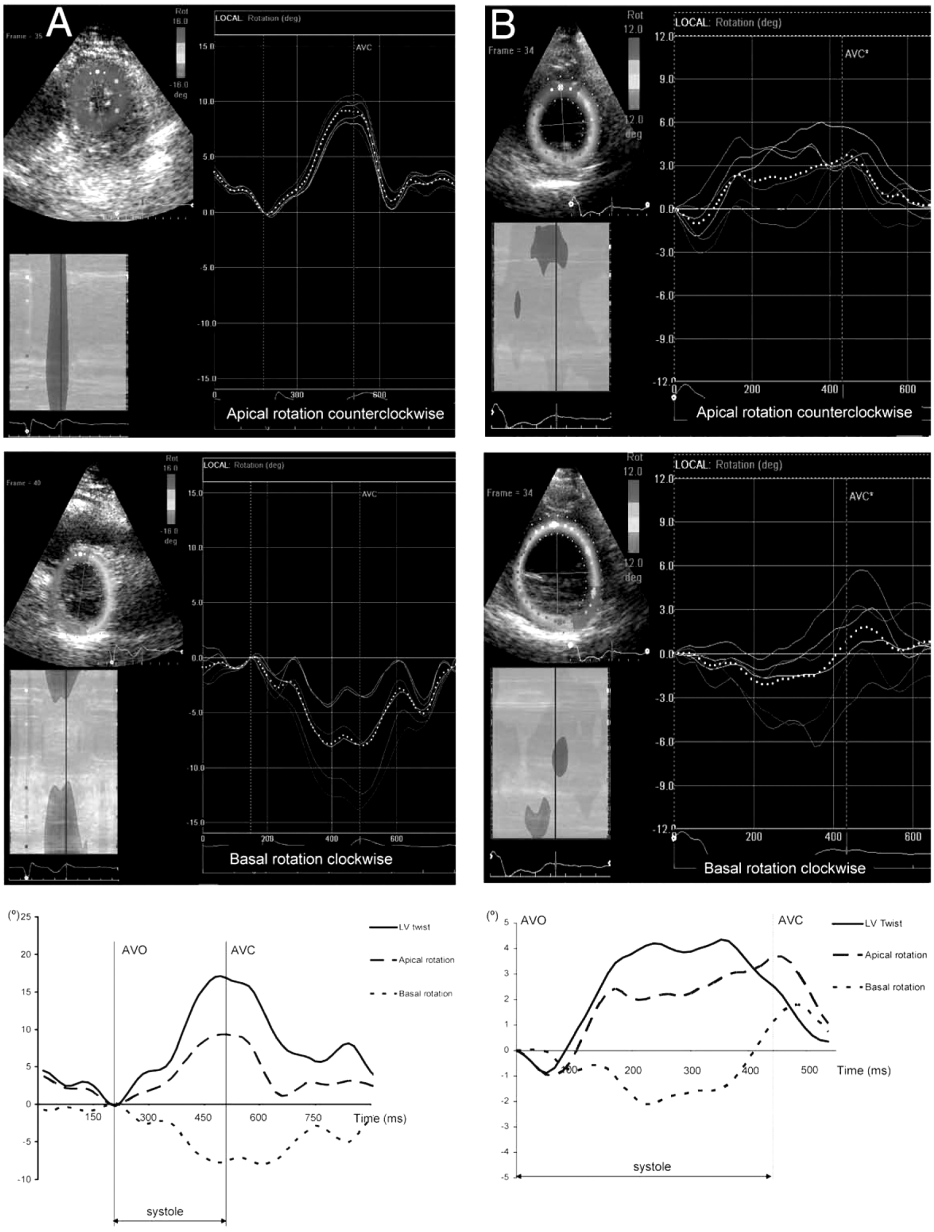


Figure 1 (Assessment of LV twist). Examples of left ventricular (LV) twist in normal control (panel A) and in heart failure patient (panel B). In both panels, the upper parts represent apical and basal rotations and the lower parts represent LV twist calculation after exporting the data to a spreadsheet program (Excel 2003; Microsoft Corporation, Redmond, Washington). AVC: aortic valve closure. AVO: aortic valve opening.

CRT implantation

All patients received a biventricular pacemaker with cardioverter-defibrillator function (Contak Renewal 4RF, Boston Scientific St. Paul, Minnesota; or InSync Sentry, Medtronic Inc. Minneapolis, Minnesota; Lumax 340 HF-T, Biotronik, Berlin). The right atrial and ventricular leads were positioned conventionally. All LV leads were implanted transvenously, and positioned preferably in a (postero)lateral vein. A coronary sinus venogram was obtained using a balloon catheter, followed by the insertion of the LV pacing lead. An 8-F guiding catheter was used to place the LV lead (Easytrak, Boston Scientific, or Attain-SD, Medtronic, or Corox OTW Biotronik) in the coronary sinus.

LV lead position

Target veins were lateral or postero-lateral veins. The LV lead position was determined using biplane fluoroscopy classification [22]. In the right anterior oblique view and/or in the postero-anterior view, the distance between the coronary sinus/mitral plane and the cardiac apex was divided in 3 parts and the LV lead position was classified in 3 groups: basal, mid-ventricular and apical.

Statistical analysis

All continuous variables had a normal distribution (as evaluated with Kolmogorov-Smirnov tests). Summary statistics for these data are therefore presented as mean±SD. Categorical data are presented as numbers and percentages. Paired T test was used for the comparison between continuous variables at baseline and immediately after CRT and between baseline and at 6 months follow-up. Unpaired T test was performed to compare continuous variables between normal controls and HF patients and between CRT responders and non-responders. Chi-square/Fischer's exact tests were computed to test for differences in categorical variables. Linear regression analysis was performed to determine the relations between LV twist, LVEF and LV dyssynchrony. In order to identify independent determinants of LV twist, a multivariable linear regression analysis using the enter model was performed including as covariates LVEF and LV dyssynchrony. Linear regression analysis was used to assess the relation between the Δ (difference between immediately after CRT and baseline) peak LV twist and Δ LVEF. The differences in peak LV twist during follow-up in responders and non-responders were assessed using ANOVA for repeated measurements. In order to identify variables related to a positive response to CRT, univariable and multivariable logistic regression analysis were performed including clinical (age, gender, etiology, QRS duration at baseline and 6-minute walk

distance at baseline) and echocardiographic (LVESV at baseline, ΔLVESV, LV dyssynchrony at baseline, ΔLV dyssynchrony, peak LV twist at baseline, Δpeak LV twist) characteristics of the patients. Only, significant ($p < 0.05$) univariable predictors were entered as covariates in the multivariable logistic regression analysis which was performed using the enter model. Odds ratio (OR) and 95% confidence intervals (CI) were calculated. Model discrimination was assessed using c-statistic and model calibration was assessed using Hosmer-Lemeshow statistic. The differences in peak LV twist and LVEF between the groups of patients with different LV lead position were assessed by one-way ANOVA. All statistical tests were 2-sided, and a p-value <0.05 was considered significant. A statistical software program SPSS 14.0 (SPSS Inc, Chicago, IL, USA) was used for statistical analysis.

RESULTS

Patient population

Reliable speckle-tracking for rotation analysis was obtained in all normal controls and in 80 (92%) HF patients. Consequently, 7 (8%) patients were excluded from the study. Of the 80 HF patients enrolled, 9 did not complete the 6 months follow-up; 3 patients died of worsening HF, 1 had LV pacing switched off due to intolerable phrenic stimulation, 1 had CRT device explantation secondary to infection, and 4 were lost to follow-up. Therefore, data at baseline and immediately after CRT were collected for 80 patients and data at 6 month follow-up were collected for 71 patients. Baseline characteristics of normal controls and the HF patients are listed in Table 1.

LV twist baseline

As shown in Table 1, peak apical rotation, peak basal rotation and peak LV twist were severely reduced in HF patients compared to normal controls: 2.4±1.8° vs. 9.4±3.2° ($p < 0.001$), -3.3±2.0° vs. -6.1±2.4° ($p < 0.001$) and 4.8±2.6° vs. 15.0±3.6° ($p < 0.001$), respectively.

A significant relation ($r = 0.53$, $p < 0.001$) was observed between peak LV twist and LVEF in HF patients. This relation was stronger in non-ischemic ($r = 0.60$, $p < 0.001$) than in ischemic HF patients ($r = 0.34$, $p = 0.020$) (Figure 2A). Moreover, a modest relation ($r = -0.33$, $p = 0.003$) was observed between peak LV twist and LV dyssynchrony in HF patients. At multivariable linear regression analysis, LVEF ($\beta = 0.47$, $p < 0.001$) and LV dyssynchrony ($\beta = -0.21$, $p = 0.032$) were independent determinants of LV twist.

Table 1. Baseline characteristics of normal controls and heart failure (HF) patients.

	Normal controls (n = 30)	HF patients (n = 80)	p-value
Age (years)	61±11	64±11	0.091
Gender (male/female)	22/8	61/19	0.46
NYHA class	-	3.0±0.4	-
QoL	-	34±20	-
6-minute walk distance (m)	-	321±109	-
QRS duration (ms)	91±9	148±30	<0.001
Etiology, n (%)			
Ischemic	-	45 (56)	-
Non-ischemic	-	35 (44)	-
Medication, n (%)			
ACE Inhibitors	-	74 (92)	-
ß-blockers	-	69 (86)	-
Diuretics and/or Spironolactone	-	67 (84)	-
LVEDV (ml)	86±26	196±74	<0.001
LVESV (ml)	34±11	146±60	<0.001
LVEF (%)	62±7	26±6	<0.001
LV dyssynchrony (ms)	14±9	146±81	<0.001
Peak apical rotation (°)	9.4±3.2	2.4±1.8	<0.001
Peak basal rotation (°)	-6.1±2.4	-3.3±2.0	<0.001
Peak LV twist (°)	15.0±3.6	4.8±2.6	<0.001

LVEDV: left ventricular end-diastolic volume, LVEF: left ventricular ejection fraction; LVESV: left ventricular end-systolic volume, NYHA: New York Heart Association, QoL: Score on the Minnesota Living with Heart Failure Questionnaire

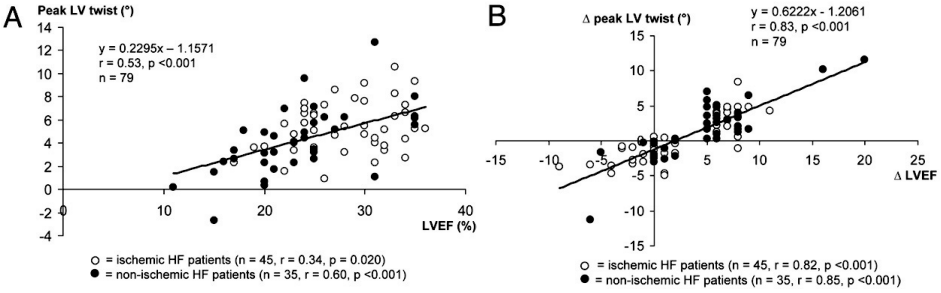


Figure 2 (LV twist and LV systolic function). Panel A: Correlation between baseline peak LV twist and LVEF in heart failure patients (ischemic, white circles, and non-ischemic, black circles). Panel B: Correlation between Δ peak LV twist and Δ LVEF immediately after CRT in heart failure patients (ischemic, white circles, and non-ischemic, black circles).

LV twist after CRT

Immediately after CRT

Immediately after CRT, peak LV twist increased from 4.8±2.6º to 5.9±3.2º (p = 0.007). In particular, Δ peak LV twist was strongly related to Δ LVEF (r = 0.83, p <0.001) and this relation was good in both non-ischemic (r = 0.85, p <0.001) and ischemic HF patients (r = 0.82, p <0.001) (Figure 2B). Furthermore, the relations between Δ peak LV twist and Δ LV dyssynchrony (r = -0.57, p <0.001) and between Δ LV dyssynchrony and Δ LVEF (r = -0.63, p <0.001) were good but less strong than the previous relation between Δ peak LV twist and Δ LVEF.

Six months follow-up

At 6 months follow-up, 40 of 71 (56%) patients were classified as echocardiographic responders to CRT (defined as a decrease in LVESV ≥15%).

No significant differences in the baseline clinical characteristics were found between responders and non-responders (Table 2). At 6 months follow-up, significant improvement in

Table 2. Clinical characteristics of responders vs. non-responders at baseline and 6 months follow-up.

	Responders (n = 40)	Non-responders (n = 31)	p-value
Age (years)	66±10	66±11	0.88
Gender (male/female)	32/8	20/11	0.18
Medication, n (%)			
ACE Inhibitors	37 (92)	29 (93)	0.77
ß-blockers	35 (87)	27 (86)	0.82
Diuretics and/or Spironolactone	34 (84)	26 (84)	0.82
Etiology, n (%)			
Ischemic	20 (50)	18 (58)	
Non-ischemic	20 (50)	13 (42)	0.63
QRS duration (ms)	149±32	149±30	0.97
NYHA class			
Baseline	3.0±0.5	3.0±0.5	0.92
6 months follow-up	2.0±0.7*	2.7±0.6†	<0.001
QoL			
Baseline	35±23	32±15	0.51
6 months follow-up	20±20*	29±19	0.065
6-minute walk distance (m)			
Baseline	306±106	330±107	0.34
6 months follow-up	363±109*	327±110	0.17

* = p <0.001 baseline vs. 6 month follow-up; † = p<0.05 baseline vs. 6 month follow-up. Abbreviations see Table 1.

NYHA class (from 3.0±0.5 to 2.0±0.7, p <0.001), quality of life (from 35±23 to 20±20, p <0.001), and 6-minute walk distance (from 306±106 m to 363±109 m, p <0.001) were observed in CRT responders only (Table 2).

Baseline echocardiographic characteristics were also similar between the 2 groups, except for LV dyssynchrony (Table 3) that was larger in responders compared to non-responders (182±71 ms vs. 116±83 ms, p = 0.003). A trend towards lower values of peak LV twist were noted in responders as compared to non-responders (4.3±2.4° vs. 5.4±2.9°, p = 0.072). At 6 months follow-up, LV dyssynchrony improved in CRT responders (from 182±71 ms to 60±45 ms, p <0.001), whereas in non-responders LV dyssynchrony did not change (116±83 ms vs. 136±89 ms, p = 0.30) (Table 3). Importantly, within ischemic HF patients, CRT responders presented significantly lower number of scarred segments at 2D-echocardiography as compared to non-responders (2.7±0.9 vs. 4.2±2.2, p = 0.016).

Table 3. Standard echocardiographic variables and rotational parameters in responders vs. non-responders at baseline and 6 months follow-up.

	Responders (n = 40)	Non-responders (n = 31)	p-value (responders vs. non-responders)
LVESV (ml)			
Baseline	144±58	153±67	0.56
6 months follow-up	110±43*	164±72‡	0.001
LVEF (%)			
Baseline	26±6	26±6	0.91
6 months follow-up	37±7*	26±6	<0.001
LV dyssynchrony (ms)			
Baseline	182±71	116±83	0.003
6 months follow-up	60±45*	136±89	<0.001
Peak apical rotation (°)			
Baseline	2.3±1.7	2.8±2.1	0.32
6 months follow-up	5.0±3.0*	2.1±2.3	<0.001
Peak basal rotation (°)			
Baseline	-3.2±2.2	-3.5±1.7	0.51
6 months follow-up	-4.3±1.9†	-2.1±2.2†	<0.001
Peak LV twist (°)			
Baseline	4.3±2.4	5.4±2.9	0.072
6 months follow-up	8.5±3.2*	3.3±2.2*	<0.001

* = p <0.001 baseline vs. 6 month follow-up; † = p <0.01 baseline vs. 6 month follow-up; ‡ = p<0.05 baseline vs. 6 month follow-up.
Abbreviations see Table 1.

Concerning the rotational parameters, in responders peak LV twist progressively improved during follow-up (ANOVA p-value <0.001), whereas in non-responders a progressive deterioration of peak LV twist was noted (ANOVA p-value <0.001) (Figure 3). Particularly, both apical and basal rotation significantly improved in responders (from 2.3±1.7° to 5.0±3.0°, p <0.001 and from -3.2±2.2° to -4.3±1.9°, p = 0.006), whereas only basal rotation significantly deteriorated in non-responders (from -3.5±1.7 to -2.1±2.2, p = 0.001) (Table 3).

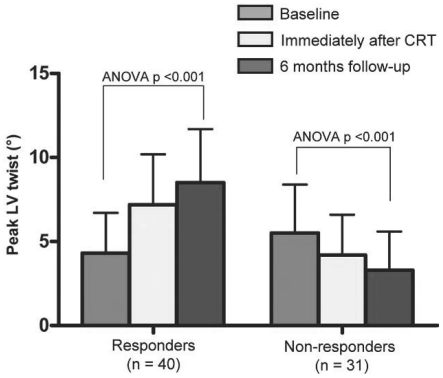


Figure 3 (LV twist in responders and non-responders). Peak LV twist in responders and non-responders at baseline, immediately after CRT and at 6 months follow-up.

Prediction of LV reverse remodeling

At univariable logistic regression, LV dyssynchrony at baseline, Δ LV dyssynchrony, Δ LVESV and Δ peak LV twist were significantly related to LV reverse remodeling at 6 months follow-up (Table 4). At multivariable logistic regression analysis, Δ peak LV twist was the strongest predictor of response to CRT at 6 months follow-up (OR = 1.899, 95%CI = 1.334-2.703, p <0.001) (Table 4).

Table 4. Univariable and multivariable logistic regression analysis for prediction of response to CRT (defined as reduction in LVESV ≥15%).

Dependent variable:	**Univariable analysis**		**Multivariable analysis**	
Response to CRT at 6 months follow-up	OR (95% CI)	p-value	OR (95% CI)	p-value
Independent variables				
Age	1.003 (0.958-1.050)	0.90		
Female gender	2.198 (0.756-6.404)	0.15		
Ischemic etiology	0.722 (0.281-1.858)	0.50		
QRS width at baseline	1.000 (0.985-1.016)	0.97		
6 minutes walking test at baseline	0.998 (0.993-1.002)	0.34		
LVESV at baseline	0.998 (0.990-1.005)	0.56		
Δ LVESV immediately after CRT	0.949 (0.915-0.984)	0.005	0.998 (0.950-1.049)	0.94
LV dyssynchrony at baseline	1.013 (1.005-1.021)	0.002	1.011 (1.001-1.022)	0.037
Δ LV dyssynchrony immediately after CRT	0.992 (0.986-0.998)	0.010	1.007 (0.996-1.017)	0.21
Peak LV twist at baseline	0.844 (0.698-1.019)	0.078		
Δ peak LV twist immediately after CRT	1.837 (1.378-2.449)	<0.001	1.899 (1.334-2.703)	<0.001

c-statistic: 0.885

CI: confidence intervals; CRT: cardiac resynchronization therapy; LV: left ventricular; LVEF: left ventricular ejection fraction; LVESV: left ventricular end-systolic volume; OR: odds ratio.

LV twist in relation to LV lead position

Considering the 71 patients with 6 months follow-up, 68 patients had the LV lead placed in a (postero-)lateral vein and 3 in an anterior vein. The 3 patients with the LV lead positioned in an anterior vein were non-responders at 6 months follow-up. Of the remaining 68 patients, the LV lead position was classified (from the right anterior oblique/postero-anterior view on fluoroscopy) as basal in 17 (25%), mid-ventricular in 34 (50%), and apical in 17 (25%) patients. At baseline, peak LV twist was not significantly different between patients with apical, mid-ventricular and basal LV lead position, (ANOVA p-value = 0.68). However, at 6 months follow-up, peak LV twist showed a significant improvement in patients with apical (from 4.3±3.1° to 8.6±3.0°, p = 0.001) and mid-ventricular (from 4.8±2.2° to 6.4±3.9°, p = 0.038) LV lead position, whereas in patients with a basal LV lead position, peak LV twist did not change significantly (5.0±3.3° vs. 4.1±3.2°, p = 0.28) (Figure 4A). Similarly, LVEF increased significantly in patients with an apical (from 26±7% to 37±7%, p <0.001) and mid-ventricular (from 26±6% to 33±8%, p <0.001) but not with a basal (26±5% vs. 28±8%, p = 0.30) LV lead position (Figure 4B). Figure 5 shows an example of responder with the LV lead placed in an apical position of a postero-lateral vein and significant improvement in peak LV twist and LVEF after CRT (both immediately after CRT implantation and at 6 months follow-up).

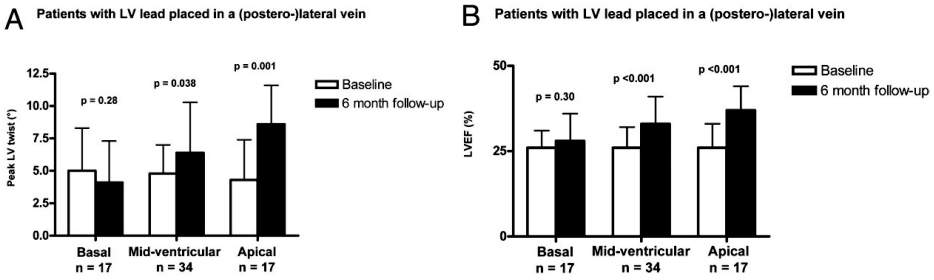


Figure 4 (LV twist and LVEF in relation to LV lead position). Panel A. Peak LV twist at baseline and 6 months follow-up in patients with basal, mid-ventricular and apical LV lead position. Significant improvement was observed in patients with an apical or mid-ventricular LV lead position but not in patients with basal LV lead position. Panel B. LVEF at baseline and 6 months follow-up in patients with basal, mid-ventricular and apical LV lead position. Significant improvement was observed in patients with an apical or mid-ventricular LV lead position but not in patients with basal LV lead position.
LV: left ventricular; LVEF: left ventricular ejection fraction

DISCUSSION

The current study evaluated the effects of CRT on LV twist and provides new insights on the relationship between LV rotational mechanics, CRT response and LV lead position. The main findings can be summarized as follows: 1) LV twist was significantly reduced in HF patients;

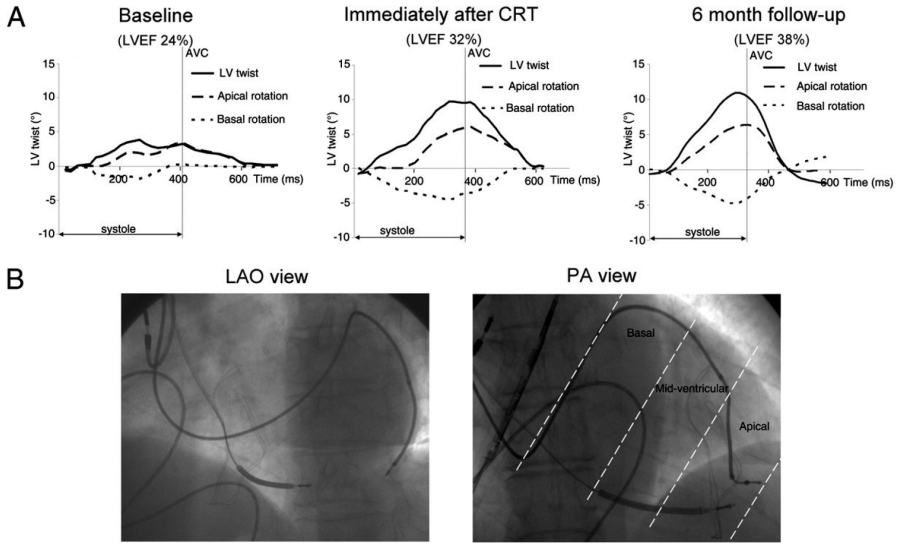


Figure 5. Example of a CRT responder with LV lead in an apical position. Panel A. Peak LV twist improved from 3.9º at baseline to 9.7º immediately after CRT implantation. Peak LV twist further improved at 6 months follow-up (peak LV twist 10.9º). AVC: aortic valve closure. Panel B. Biplane fluoroscopy: the left anterior oblique (LAO) view shows the LV lead in a posterolateral cardiac vein; in the postero-anterior (PA) view the distance between the coronary sinus/mitral plane and the cardiac apex was divided (dotted lines) in 3 parts (basal, mid-ventricular and apical).

2) LV twist improved in responders and worsened in non-responders to CRT; 3) the strongest predictor of LV reverse remodeling at 6 months follow-up was Δ peak LV twist (immediate change in LV twist after CRT); 4) an LV lead placed in a (postero-)lateral vein with apical or mid-ventricular position was associated with the greatest improvement of LV twist after CRT and with the highest response rate to CRT.

Relationship between LV twist and LV function

Several techniques have been applied for the assessment and quantification of LV twist. For this purpose, tagged cardiac magnetic resonance imaging and sonomicrometry are considered the gold standard, but the most recent speckle-tracking echocardiographic technique, used in the present study, demonstrated a good agreement with these imaging modalities [20, 21]. Previous studies, using both tagged cardiac magnetic resonance imaging and speckle-tracking analysis, suggested an important relation between LV twist and LVEF [4, 9]. Similarly, in the current study the relation between LV twist and LV systolic function was good ($r = 0.53$, $p < 0.001$), illustrating the potential role of LV twist as comprehensive index of LV systolic function. Furthermore, the results of the present study highlight that the relation between LV

systolic function and LV twist was stronger in non-ischemic patients as compared to ischemic patients. A possible reason may be the presence of regional myocardial damage in ischemic patients, involving specifically the apex or the base with a different effect on LV twist [23].

Finally, LV twist was modestly related to LV dyssynchrony ($r = -0.33$, $p < 0.001$), but at multivariable linear regression analysis, LV dyssynchrony was still independently related to LV twist. This finding points out that LV twist not only is a sensitive and thorough parameter of LV function, but also it may reflect the extent of LV (dys)synchrony.

Relationship between LV twist and CRT response

The effects of CRT on torsional mechanics were different in responders and non-responders. A trend towards more reduced LV twist at baseline in responders as compared to non-responders was observed. In the present study, a significant improvement of LV twist was observed in CRT responders and a significant worsening in non-responders. In contrast, a previous study of Zhang et al. did not show any significant increase of LV twist in responders to CRT [10]. The different results may be related to sample size and population characteristics.

In the multivariable model, baseline LV dyssynchrony and an immediate improvement in LV twist after CRT were the only predictors of LV reverse remodeling at 6 months follow-up. The predictive value of LV dyssynchrony has been shown already in previous studies [19, 24]. The novelty of the present study is that CRT may (partially) restore LV twist, possibly by providing a more physiologic electrical depolarization and mechanical contraction of the myofibers. Specifically, CRT partially restored LV torsional behavior in responders, by not only improving apical rotation but also basal rotation. In non-responders, the deterioration of LV twist was mainly due to worsening of the basal rotation underscoring the influence of the basal level on LV twist [25].

Relationship between LV twist and LV lead position

Previous studies showed that HF patients treated with CRT showed the best hemodynamic improvement when the LV pacing lead was positioned in (postero) lateral veins [26]. In the current study, 3 patients had the LV lead placed in an anterior vein, and none of them responded to CRT. The remaining 68 patients had the LV lead positioned in the (postero-)lateral vein. In these patients, the optimal position of LV lead inside the target vein was explored. Patients with a mid-ventricular or apical position had the largest systolic improvement, and showed a significant increase in LV twist, whereas patients with a basal LV lead position did not improve systolic function and decreased in LV twist, confirming that pacing site may influence torsional behavior of the LV [27]. Similarly, a recent study by Helm et al.[28] reported

that the optimal site of stimulation (although in a canine model of HF) was the LV free wall centered over the mid-apical part. This finding may be related to the fact that normal cardiac depolarization is directed from the apex towards the base [29], and an earlier activation of the LV basal region, altering the normal contraction pattern of the myofibers, may lead to a significant deterioration of LV twist. Another explanation for the findings may be related to the fact that the myocardial wall is thinner towards the apex [30, 31]; therefore, the epicardial LV lead in this position is closer to the Purkinje network. Consequently, pacing from this position may generate a cardiac pulse which spreads faster to the entire myocardium with a more physiological activation [32–34.]

CONCLUSIONS

LV twist is reduced in HF patients and improves in patients who respond to CRT. Particularly, the change in LV twist immediately after CRT predicts LV reverse remodeling at 6 months follow-up.

REFERENCES

1. Greenbaum RA, Ho SY, Gibson DG, Becker AE, Anderson RH. Left ventricular fibre architecture in man. *Br Heart J* 1981; 45:248-263.
2. Torrent-Guasp F, Kocica MJ, Corno AF, et al. Towards new understanding of the heart structure and function. *Eur J Cardiothorac Surg* 2005; 27:191-201.
3. Buchalter MB, Weiss JL, Rogers WJ, et al. Noninvasive quantification of left ventricular rotational deformation in normal humans using magnetic resonance imaging myocardial tagging. *Circulation* 1990; 81:1236-1244.
4. Kanzaki H, Nakatani S, Yamada N, Urayama S, Miyatake K, Kitakaze M. Impaired systolic torsion in dilated cardiomyopathy: reversal of apical rotation at mid-systole characterized with magnetic resonance tagging method. *Basic Res Cardiol* 2006; 101:465-470.
5. Notomi Y, Martin-Miklovic MG, Oryszak SJ, et al. Enhanced ventricular untwisting during exercise: a mechanistic manifestation of elastic recoil described by Doppler tissue imaging. *Circulation* 2006; 113:2524-2533.
6. Fuchs E, Muller MF, Oswald H, Thony H, Mohacsi P, Hess OM. Cardiac rotation and relaxation in patients with chronic heart failure. *Eur J Heart Fail* 2004; 6:715-722.
7. Abraham WT, Fisher WG, Smith AL, et al. Cardiac resynchronization in chronic heart failure. *N Engl J Med* 2002; 346:1845-1853.
8. Cleland JG, Daubert JC, Erdmann E, et al. The effect of cardiac resynchronization on morbidity and mortality in heart failure. *N Engl J Med* 2005; 352:1539-1549.
9. Sade LE, Demir O, Atar I, Muderrisoglu H, Ozin B. Effect of mechanical dyssynchrony and cardiac resynchronization therapy on left ventricular rotational mechanics. *Am J Cardiol* 2008; 101:1163-1169.
10. Zhang Q, Fung JW, Yip GW, et al. Improvement of left ventricular myocardial short-axis, but not long-axis function or torsion after cardiac resynchronisation therapy: an assessment by two-dimensional speckle tracking. *Heart* 2008; 94:1464-1471.
11. Hunt SA, Abraham WT, Chin MH, et al. ACC/AHA 2005 Guideline Update for the Diagnosis and Management of Chronic Heart Failure in the Adult: a report of the American College of Cardiology/American Heart Association Task Force on Practice Guidelines (Writing Committee to Update the 2001 Guidelines for the Evaluation and Management of Heart Failure): developed in collaboration with the American College of Chest Physicians and the International Society for Heart and Lung Transplantation: endorsed by the Heart Rhythm Society. *Circulation* 2005; 112:e154-e235.
12. Rector TS, Kubo SH, Cohn JN. Validity of the Minnesota Living with Heart Failure questionnaire as a measure of therapeutic response to enalapril or placebo. *Am J Cardiol* 1993; 71:1106-1107.
13. Lipkin DP, Scriven AJ, Crake T, Poole-Wilson PA. Six minute walking test for assessing exercise capacity in chronic heart failure. *Br Med J (Clin Res Ed)* 1986; 292:653-655.
14. Lang RM, Bierig M, Devereux RB, et al. Recommendations for chamber quantification: a report from the American Society of Echocardiography's Guidelines and Standards Committee and the Chamber Quantification Writing Group, developed in conjunction with the European Association of Echocardiography, a branch of the European Society of Cardiology. *J Am Soc Echocardiogr* 2005; 18:1440-1463.
15. Chung ES, Leon AR, Tavazzi L, et al. Results of the Predictors of Response to CRT (PROSPECT) trial. *Circulation* 2008; 117:2608-2616.
16. Schuijf JD, Kaandorp TA, Lamb HJ, et al. Quantification of myocardial infarct size and transmurality by contrast-enhanced magnetic resonance imaging in men. *Am J Cardiol* 2004; 94:284-288.

17. Leitman M, Lysyansky P, Sidenko S, et al. Two-dimensional strain-a novel software for real-time quantitative echocardiographic assessment of myocardial function. *J Am Soc Echocardiogr* 2004; 17:1021-1029.
18. Reisner SA, Lysyansky P, Agmon Y, Mutlak D, Lessick J, Friedman Z. Global longitudinal strain: a novel index of left ventricular systolic function. *J Am Soc Echocardiogr* 2004; 17:630-633.
19. Suffoletto MS, Dohi K, Cannesson M, Saba S, Gorcsan J, III. Novel speckle-tracking radial strain from routine black-and-white echocardiographic images to quantify dyssynchrony and predict response to cardiac resynchronization therapy. *Circulation* 2006; 113:960-968.
20. Helle-Valle T, Crosby J, Edvardsen T, et al. New noninvasive method for assessment of left ventricular rotation: speckle tracking echocardiography. *Circulation* 2005; 112:3149-3156.
21. Notomi Y, Lysyansky P, Setser RM, et al. Measurement of ventricular torsion by two-dimensional ultrasound speckle tracking imaging. *J Am Coll Cardiol* 2005; 45:2034-2041.
22. Albertsen AE, Nielsen JC, Pedersen AK, Hansen PS, Jensen HK, Mortensen PT. Left ventricular lead performance in cardiac resynchronization therapy: impact of lead localization and complications. *Pacing Clin Electrophysiol* 2005; 28:483-488.
23. Opdahl A, Helle-Valle T, Remme EW, et al. Apical Rotation by Speckle Tracking Echocardiography: A Simplified Bedside Index of Left Ventricular Twist. J Am Soc Echocardiogr 2008;21:1121-1128
24. Delgado V, Ypenburg C, van Bommel RJ, et al. Assessment of left ventricular dyssynchrony by spekle tracking strain imaging comparison between longitudinal, circumferential, and radial strain in cardiac resynchronization therapy. *J Am Coll Cardiol* 2008; 51:1944-1952.
25. Notomi Y, Srinath G, Shiota T, et al. Maturational and adaptive modulation of left ventricular torsional biomechanics: Doppler tissue imaging observation from infancy to adulthood. *Circulation* 2006; 113:2534-2541.
26. Butter C, Auricchio A, Stellbrink C, et al. Effect of resynchronization therapy stimulation site on the systolic function of heart failure patients. *Circulation* 2001; 104:3026-3029.
27. Notomi Y, Popovic ZB, Yamada H, et al. Ventricular untwisting: a temporal link between left ventricular relaxation and suction. *Am J Physiol Heart Circ Physiol* 2008; 294:H505-H513.
28. Helm RH, Byrne M, Helm PA, et al. Three-dimensional mapping of optimal left ventricular pacing site for cardiac resynchronization. *Circulation* 2007;115:953-961.
29. Segupta PP, Khandheria BK, Korinek J, et al. Apex-to-base dispersion in regional timing of left ventricular shortening and lengthening. *J Am Coll Cardiol* 2006;47:163-172.
30. Bogaert J, Rademakers FE. Regional nonuniformity of normal adult human left ventricle. *Am J Physiol Heart Circ Physiol* 2001;280:H610-H620.
31. Sengupta PP, Korinek J, Belohlavek M, et al. Left ventricular structure and function: basic science for cardiac imaging. *J Am Coll Cardiol* 2006; 48:1988-2001.
32. Peschar M, de Swart H, Michels KJ, Reneman RS, Prinzen FW. Left ventricular septal and apex pacing for optimal pump function in canine hearts. *J Am Coll Cardiol* 2003; 41:1218-1226.
33. Vanagt WY, Prinzen FW, Delhaas T. Reversal of pacing-induced heart failure by left ventricular apical pacing. *N Engl J Med* 2007; 357:2637-2638.
34. Vanagt WY, Prinzen FW, Delhaas T. Physiology of cardiac pacing in children: the importance of the ventricular pacing site. *Pacing Clin Electrophysiol* 2008; 31 Suppl 1:S24-S27.

CHAPTER 23

Cardiac resynchronization therapy as a therapeutic option in patients with moderate-severe functional mitral regurgitation and high operative risk

R J van Bommel, **N Ajmone Marsan**, V Delgado, C JW Borleffs, E PM van Rijnsoever, M J Schalij, and J J Bax

Circulation 2011;124:912-19.

ABSTRACT

Objectives: Functional mitral regurgitation (MR) is a common finding in heart failure (HF) patients with dilated cardiomyopathy, and has important prognostic implications. However, the increased operative risk of these patients may result in low referral or high denial rate for mitral valve surgery. Cardiac resynchronization therapy (CRT) showed to have a favorable effect on MR. Aims of this study were to: 1) evaluate CRT as a therapeutic option in HF patients with functional MR and high operative risk; and 2) investigate the effect of MR improvement after CRT on prognosis.

Methods: A total of 98 consecutive patients with moderate-severe functional MR and high operative risk underwent CRT according to current guidelines. Echocardiography was performed at baseline and 6-month follow-up; severity of MR was graded according to a multi-parametric approach. Significant improvement of MR was defined as a reduction ≥1 grade. All cause-mortality was assessed during follow-up (median 32 [6.0-116] months).

Results: Thirteen (13%) patients died before 6 months follow-up. In the remaining 85 patients, significant reduction in MR was observed in all evaluated parameters. In particular, 42 (49%) patients improved ≥1 grade of MR and were considered MR improvers. Survival was superior in MR improvers as compared to MR non-improvers, log rank p <0.001. MR improvement was an independent prognostic factor for survival (HR 0.35, C.I. 0.13-0.94, p = 0.043).

Conclusions: CRT is a potential therapeutic option in HF patients with moderate-severe functional MR and high risk for surgery. Improvement in MR results in superior survival after CRT.

INTRODUCTION

Functional mitral regurgitation (MR) is a common finding in heart failure patients with ischemic or non-ischemic dilated cardiomyopathy [1, 2]. More importantly, the presence of MR has important prognostic implications in these patients [1, 3]. The initial strategy of treating MR is optimization of medical therapy (afterload reduction and treatment of fluid load). However, in many patients significant functional MR persists and surgery may be the final option to reduce the extent of MR. The main surgical technique for treatment of functional MR is restrictive annuloplasty, with or without additional surgical left ventricular (LV) remodeling. In many of the patients however, the increased operative mortality risk may result in either a low referral, or high denial rate for mitral valve surgery. A recent study by Bach et al reported a non-referral or denial rate for surgery as high as 84% in patients with moderate-to-severe or severe functional MR [4]. Moreover, it is currently unclear whether mitral valve surgery improves prognosis in this specific group of patients [5]. As a result, indications for mitral valve surgery in heart failure patients with functional MR are not well defined by any (currently available) guideline [6].

Conversely, cardiac resynchronization therapy (CRT) showed to have a favorable effect on functional MR. There are several studies that demonstrated a reduction in extent of functional MR after CRT [7–12]. Most of these studies however, were performed in patients with only mild-moderate MR and therefore less is known about the effects of CRT in patients with moderate-severe functional MR. Furthermore, these studies were limited to changes at mid-term (6 months) follow-up and therefore no data exist with regard to the potential beneficial effects of reduction in MR on long-term prognosis. Consequently, the aims of this study were: 1) to evaluate the role of CRT as an alternative therapeutic option in heart failure patients with moderate-severe functional MR and high operative risk; and 2) to investigate the effect of reduction in severity of MR after CRT on long-term prognosis.

METHODS

Patient population and data collection

A total of 98 consecutive patients with moderate-severe functional MR and high operative risk were included. These patients are part of an ongoing registry and were referred for CRT according to the current guidelines [13]. Patient data were prospectively collected in the departmental Cardiology Information System (EPD-Vision®, Leiden University Medical Center, Leiden, the Netherlands).

Etiology of heart failure was considered ischemic in the presence of significant coronary artery disease (≥50% stenosis in 1 or more of the major coronary arteries) and/or a history of myocardial infarction or prior revascularization. The protocol was as follows: in all patients clinical status was assessed before implantation and at 6 months follow-up. Extensive echocardiography was performed at baseline and repeated 6 months after CRT to: 1) quantify LV volumes and function; and 2) evaluate the severity of MR. After the 6 months follow-up, patients were scheduled for regular visits to the outpatient clinic.

Clinical evaluation

In all patients, evaluation of heart failure symptoms according to the New York Heart Association (NYHA) classification was performed. Assessment of quality of life was performed using the Minnesota Living with Heart Failure Questionnaire (high scores indicating poor quality of life) [14] and when possible, exercise capacity was measured using the 6-minute walk test [15]. In addition, operative risk was assessed by means of the logistic Euroscore [16]. Estimated glomerular filtration rate (eGFR) was calculated using the standard formula by Cockcroft and Gault and expressed in ml/min/1.73m^2 [17]. Finally, outcome data were collected by chart review, device interrogation and telephone contact. Primary end point during long-term follow-up was death from any cause.

Echocardiography

All patients underwent echocardiography in the left lateral decubitus position before and 6 months after CRT implantation. Imaging was performed using a commercially available echocardiographic system (VIVID 7, General Electric Vingmed Ultrasound, Milwaukee, USA). Images were obtained using a 3.5 MHz transducer, at a depth of 16 cm in the parasternal and apical (2-, 3- and 4-chamber) views. All images were recorded digitally in cine-loop format and analyzed offline with commercial software (EchoPac 108.1.5, General Electric Vingmed Ultrasound, Milwaukee, USA).

LV volumes and function analysis

LV end-diastolic (LVEDV) and LV end-systolic (LVESV) volumes were determined from the conventional apical 2- and 4-chamber views and LV ejection fraction (LVEF) was calculated using the biplane Simpson's technique [18]. Volumetric response to CRT was defined as a reduction ≥15% in LVESV at 6 months follow-up [19].

Assessment of MR severity

According to the current guidelines [20, 21], the severity of MR was assessed using a multi-parametric approach, which combined the following measurements: 1) vena contracta width (VCW), measured as the narrowest portion of the MR color Doppler jet in a zoomed optimized parasternal long-axis view or in the apical 4-chamber view; 2) the ratio of the jet area to the left atrium (LA) area measured by planimetry in the 4-chamber view; 3) the effective regurgitant orifice area (EROA) calculated with the proximal isovelocity surface area (PISA) method. The color Doppler images were acquired using a Nyquist limit of 30-60 cm/sec, and a color gain that just eliminates random color speckle from non-moving regions. Severity of MR was defined using a multi-parametric approach, according to current guidelines [21], and graded on a four-point scale: mild = 1+, moderate = 2+, moderate-severe = 3+ and severe = 4+. Improvement in MR was defined as a reduction ≥1 grade, 6 months after CRT. In addition, as a measure of MV deformation, valvular tenting area was measured from the parasternal long-axis view at mid-systole as the area enclosed between the annular plane and mitral leaflets. LA volumes were measured form the 2- and 4-chamber views using the biplane Simpson's technique. Finally, estimated systolic pulmonary artery pressure (SPAP) was derived from the right ventricular to right atrial pressure gradient or tricuspid regurgitant jet gradient and calculated with the modified Bernoulli equation [22].

Statistical analysis

Continuous data are presented as mean±SD, and dichotomous data are presented as numbers and percentages. Comparison of data at baseline and 6 months follow-up was performed with the paired-samples t test. Comparison of data between patient groups was performed using the independent-samples t test for continuous data. Fisher's exact tests or χ^2 tests were used as appropriate to compare dichotomous data. Analysis of variance for repeated measurements, including interaction between group and time, was applied for comparison of data between patient groups at baseline and 6 months follow-up. The (event-free) survival of patients was evaluated with the Kaplan-Meier method and the log rank test. The effect of improvement in MR on (event-free) survival, adjusted for other variables, was investigated using the Cox proportional hazards model. Variables that showed a statistically significant effect in the univariate analyses were entered in the multivariate Cox proportional hazards model. The proportional hazards assumption was checked for continuous variables by visual inspection of scaled Schoenfeld residuals and for categorical variables by visual inspection of log-log plots. All analyses were performed with SPSS for Windows, version 16.0 (SPSS, Chicago, IL). All statistical tests were two-sided. A p-value <0.05 was considered statistically significant.

RESULTS

Patient characteristics

Baseline characteristics of the patient population are presented in Table 1. The majority of patients were male (74%) and the underlying cause of heart failure was ischemic cardiomyopathy in 62 (63%) patients. All patients had moderate-severe MR (63% grade 3+ and 37% grade 4+) with a central jet secondary to significant LV dilatation and dysfunction. Furthermore, all patients were characterized by a high operative risk (logistic Euroscore 26±13%, mean eGFR 51±22 ml/min/1.73m^2, diabetes in 19% of cases). Optimal medical therapy was administered in all patients, if tolerated. Implantation of a CRT device was successful in all patients and no procedure-related complications were observed. All devices were programmed to simultaneous biventricular pacing during the first 6 months of follow-up. Before the 6

Table 1: Patient characteristics (n = 98)

Age (years)	71±7
Male gender (n)	72 (74%)
Etiology of heart failure	
Ischemic	62 (63%)
Non-ischemic	36 (37%)
QRS duration (ms)	166±29
eGFR (ml/min/1.73m2)	51±22
Diabetes (n, %)	18 (18%)
Logistic Euroscore (%)	26±13
NYHA class	3.2±0.4
6 MWT (m)	270±111
QoL score	38±19
LVEDV (ml)	262±88
LVESV (ml)	206±80
LVEF (%)	23±7
Medication (n)	
Anticoagulants	93 (95%)
Diuretics	86 (88%)
ACE-inhibitors	86 (88%)
B-blockers	57 (58%)
Spironolactone	49 (50%)

6 MWT = 6-minute walk test; ACE = angiotensin-converting enzyme; eGFR = estimated glomerular filtration rate; LVEDV = left ventricular end-diastolic volume; LVEF = left ventricular ejection fraction; LVESV = left ventricular end-systolic volume; NYHA = New York Heart Association; QoL = quality of life

months follow-up, 13 patients died (10 patients died due to heart failure, 2 patients died due to severe infection and 1 patient died because of a malignancy). Therefore, further analysis (baseline versus follow-up) was performed in the remaining 85 patients. Of note, patients that died before the 6 months follow-up had a higher logistic Euroscore (34±15 vs. 24±12), lower eGFR (40±15 ml/min/1.73m^2 vs. 53±23 ml/min/1.73m^2) and were in higher NYHA class (3.4±0.5 vs. 3.1±0.3) at baseline as compared to patients that survived the first 6 months of follow-up.

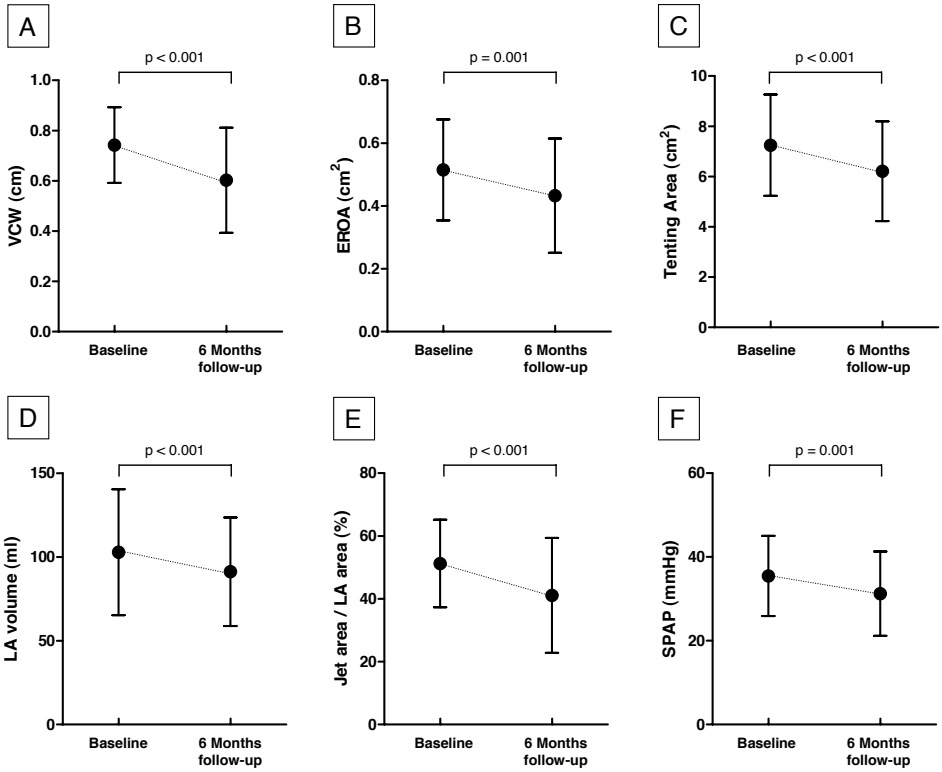


Figure 1: Changes in severity of MR at 6 months follow-up. Improvement in severity of MR at 6 months follow-up was observed in all evaluated parameters. Error bars represent standard deviation. EROA = effective regurgitant orifice area; LA = left atrium; SPAP = systolic pulmonary artery pressure; VCW = vena contracta width.

Clinical and LV functional changes after 6 months CRT

At 6 months follow-up, mean NYHA class improved from 3.1±0.3 to 2.1±0.7 (p <0.001). In addition, quality of life score decreased from 38±18 to 24±17 (p <0.001), while distance covered in the 6-minute walk test increased from 283±109 m to 368±120 m (p <0.001). Significant LV reverse remodeling was observed at 6 months follow-up, as evidenced by a decrease in LVEDV from 261±88 ml at baseline to 233±81 ml at follow-up and a decrease in LVESV from 205±81 ml to 166±72 ml (both p <0.001). Furthermore, an increase in LVEF from 23±7% at baseline to 30±9% at follow-up was noted (p <0.001). Volumetric response to CRT (reduction ≥15% in LVESV at 6 months follow-up) was observed in 54 (55%) patients.

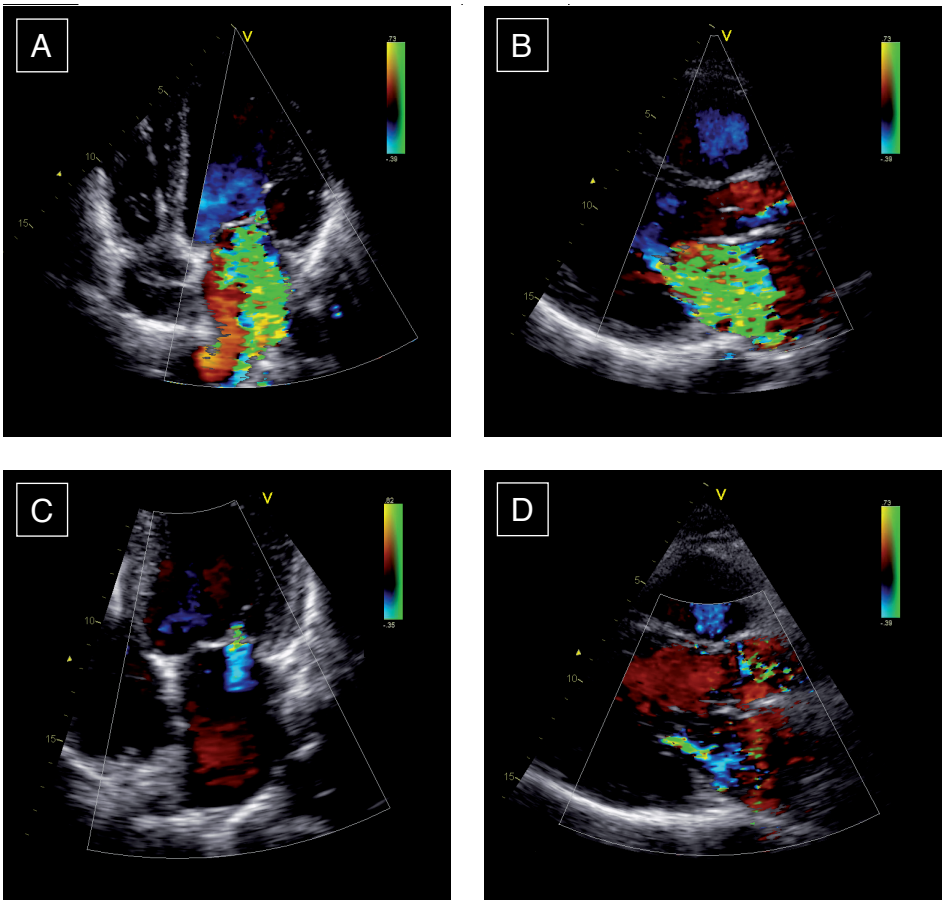


Figure 2: Example of a patient with a significant improvement in MR at 6 months follow-up. At baseline, the MR jet area exceeded 80% of the left atrium area and the effective regurgitant orifice area (EROA) was 0.61 cm^2 (Panels A [4-chamber view] and B [parasternal long-axis view]). At 6 months follow-up, the jet area decreased to 10% of the left atrium area and the EROA was 0.19 cm^2 (Panels C [4-chamber view] and D [parasternal long-axis view]).

Changes in MR severity after 6 months CRT

Severity of MR improved significantly according to all evaluated parameters (Figure 1). The VCW decreased from 0.74±0.15 cm at baseline to 0.59±0.21 cm at follow-up (p <0.001), whereas the EROA decreased from 0.51±0.16 cm^2 to 0.43±0.18 cm^2 (p = 0.001). Tenting area decreased from 7.2±2.0 cm^2 at baseline to 6.2±2.0 cm^2 at follow-up (p <0.001), and the LA volume decreased from 103±38 ml to 91±32 ml (p <0.001). Finally, the regurgitant jet area ratio decreased from 51±14% at baseline to 41±18% at follow-up (p <0.001) and mean SPAP decreased from 35±10 mmHg to 31±10 mmHg (p = 0.001). An example of significant improvement in severity of MR is displayed in Figure 2.

MR improvers versus MR non-improvers after CRT

At 6 months follow-up, MR improvement (reduction ≥1 grade of MR as previously described) was noted in 42 (49%) patients. These patients were therefore considered MR improvers. Baseline clinical characteristics were comparable between MR improvers and MR non-improvers. However, ischemic etiology of heart failure was more frequently observed among MR non-improvers (Table 2). In addition, MR improvers had slightly less symptomatic heart failure (according to the NYHA functional class).

Comparison of clinical and echocardiographic data between MR improvers and non-improvers, both at baseline and 6 months follow-up, is displayed in Table 3. At 6 months follow-

Table 2: Clinical characteristics of MR improvers and non-improvers

Variable	MR improvers (n = 42)	MR non-improvers (n = 43)	p-value
Age (years)	70±8	70±7	0.914
Men/Women	28/14	34/9	0.229
Etiology of heart failure			
Ischemic	20 (48%)	32 (74%)	0.015
Non-ischemic	22 (52%)	11 (26%)	
QRS duration (ms)	165±33	165±28	0.942
eGFR (ml/min/1.73m2)	55±23	51±23	0.432
Diabetes (n)	5 (12%)	10 (23%)	0.255
Medication (n)			
Anticoagulants	40 (95%)	41 (95%)	0.981
Diuretics	38 (90%)	39 (91%)	0.972
ACE-inhibitors	35 (83%)	38 (88%)	0.505
B-blockers	25 (60%)	25 (58%)	0.897
Spironolactone	20 (48%)	24 (56%)	0.450

6 MWT = 6-minute walk test; ACE = angiotensin-converting enzyme; eGFR = estimated glomerular filtration rate; LVEDV = left ventricular end-diastolic volume; LVEF = left ventricular ejection fraction; LVESV = left ventricular end-systolic volume; NYHA = New York Heart Association; QoL = quality of life

Table 3: Changes in clinical and echocardiographic characteristics of MR improvers and non-improvers at 6 months follow-up

Variable	MR improvers (n = 42)		MR non-improvers (n = 43)		p-value between groups	p-value interaction group and time
	Baseline	Follow-up	Baseline	Follow-up		
NYHA class	3.0±0.2	1.9±0.7‡	3.2±0.4	2.3±0.6‡	0.005	0.117
6 MWT (m)	299±113	407±121*	266±105	329±106‡	0.022	0.061
QoL score	35±17	19±16*	42±18	28±17*	0.019	0.783
LVEDV (ml)	255±84	214±78‡	267±93	252±81*	0.174	0.004
LVESV (ml)	201±80	146±69‡	208±83	187±70†	0.151	<0.001
LVEF (%)	23±7	33±10‡	23±6	27±7†	0.039	<0.001
VCW (cm)	0.73±0.14	0.44±0.16†	0.74±0.17	0.73±0.13	<0.001	<0.001
EROA (cm2)	0.51±0.16	0.31±0.12*	0.52±0.16	0.54±0.16	0.002	<0.001
TA (cm2)	7.1±2.1	5.5±1.7‡	7.4±1.9	7.1±2.0*	0.033	<0.001
LA volume (ml)	102±43	78±27‡	104±32	104±32	0.050	<0.001
Jet area / LA area (%)	51±14	29±15*	52±14	53±13	<0.001	<0.001
SPAP (mmHg)	34±10	25±6*	37±9	38±9	<0.001	<0.001
MR grade	3.3±0.5	1.8±0.6*	3.3±0.5	3.4±0.6	<0.001	<0.001

6 MWT = 6-minute walk test; EROA = effective regurgitant orifice area; LA = left atrium; LVEDV = left ventricular end-diastolic volume; LVEF = left ventricular ejection fraction; LVESV = left ventricular end-diastolic volume; MR = mitral regurgitation; NYHA = New York Heart Association; QoL = quality of life; SPAP = systolic pulmonary artery pressure; TA = tenting area; VCW = vena contracta width

* p <0.05, baseline vs. follow-up, † p = 0.001, baseline vs. follow-up, ‡ p <0.001, baseline vs. follow-up.

up, both MR improvers and MR non-improvers had an improvement in clinical characteristics. However, these improvements were more outspoken in MR improvers. All baseline echocardiographic parameters were comparable between MR improvers and non-improvers. At 6 months follow-up, reductions in LV volumes and an increase in LVEF were observed in both groups. Of note, 39 (93%) MR improvers also had significant LV volumetric response, versus only 15 (35%) patients in the MR non-improvers group (p <0.001). By definition, MR improvers had a significant decrease in MR grade from 3.3±0.5 to 1.8±0.6, and this was evidenced by significant improvement in all evaluated parameters. Conversely, MR non-improvers showed (by definition) no improvement in MR grade from 3.3±0.5 to 3.4±0.6.

Improvement in MR and long-term prognosis after CRT

To evaluate whether improvement in MR has prognostic importance after CRT, MR improvement was investigated in relation to all-cause mortality during long-term follow-up (median 32 [6.0-116] months). During this follow-up period, 34 (40%) patients died. Survival was superior in MR improvers as compared to MR non-improvers, log rank p <0.001 (Figure 3).

Respective 1- and 2-year survival rates were 97% and 92% in MR improvers as compared with 88% and 67% in MR non-improvers (log rank p = 0.117 for comparison at 1 year follow-up and log rank p = 0.013 at 2 years follow-up). Additionally, MR improvement was tested as an

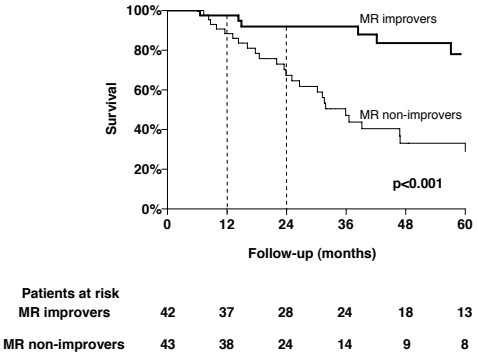


Figure 3: Kaplan-Meier survival curves for time to all-cause mortality in MR improvers versus MR non-improvers. During long-term follow-up, survival was superior in MR improvers as compared to MR non-improvers, log rank p <0.001. Respective 1- and 2-year survival rates were 97% and 92% in MR improvers as compared with 88% and 67% in MR non-improvers.

independent predictor for all-cause mortality using a multivariate Cox proportional hazards model. In univariate analysis, MR improvement reached a crude hazard ratio (HR) of 0.21 (95% Confidence Interval 0.09-0.49, p <0.001). After correction for other significant variables in the univariate analysis, MR improvement remained a strong independent predictor of survival after CRT, with a corrected HR of 0.35 (95% Confidence Interval 0.13-0.94, p = 0.043, Table 4).

Table 4: Uni- and multivariate Cox proportional hazards models for time to all-cause mortality

	Univariate		Multivariate	
	HR (95%-C.I.)	p-value	HR (95%-C.I.)	p-value
Age (years)	1.01 (0.97-1.05)	0.539		
Male gender	1.10 (0.57-2.12)	0.784		
Ischemic etiology	1.56 (0.85-2.89)	0.154		
NYHA class IV vs. III	2.42 (1.23-4.78)	0.011	1.01 (0.40-2.55)	0.981
Diabetes	1.63 (0.83-3.22)	0.156		
QRS duration (ms)	1.00 (0.99-1.01)	0.947		
eGFR (ml/min/1.73m2)	0.98 (0.97-0.99)	0.002	0.98 (0.97-1.00)	0.025
MR improvement	0.21 (0.09-0.49)	<0.001	0.35 (0.13-0.94)	0.043
LVESV response	0.25 (0.12-0.50)	<0.001	0.42 (0.18-0.97)	0.042

C.I. = confidence interval; eGFR = estimated glomerular filtration rate; HR = hazard ratio; LVESV = left ventricular end-systolic volume; MR = mitral regurgitation; NYHA = New York Heart Association

DISCUSSION

The findings of the present study can be summarized as follows: (1) CRT reduces severity of MR at 6 months follow-up in heart failure patients with moderate-severe functional MR and at high risk for MV surgery; and (2) improvement in MR results in superior survival during long-term follow-up.

Functional MR in heart failure

In heart failure patients with impaired LV systolic function, MR is a frequent finding. It is estimated that nearly half of these patients have some degree of MR, and in around 30% of these cases, extent of MR can be graded as moderate or severe [1,3,23]. In most patients, a structurally normal mitral valve is present, but the regurgitation is secondary to changes in LV geometry caused by LV remodeling (dilatation). This specific type of MR is referred to as "functional MR" [6,23]. There have been several studies which evaluated the effect of mitral valve surgery in patients with heart failure and functional MR [24–26]. Wu et al studied 682 patients with significant MR and LV systolic dysfunction [24]. Out of these 682 patients, 419 were considered candidates for surgical correction. Surprisingly, only 126 of these patients (30%) eventually underwent mitral valve repair. Mentioned reasons for non-referral or denial for surgery included cardiogenic shock, renal failure, significant valvular lesion other than MR and the fact that patients felt to be too weak to undergo surgery after evaluation by cardiac surgeon or cardiologist. Other reasons included the coexistence of conditions that increased the risk of cardiac surgery. During long-term follow-up, 112 patients (38%) who were not referred or denied for surgery died, versus 61 (48%) of those who had undergone MV surgery (p = NS). It was therefore concluded that there was no significant survival benefit in the surgical group. The finding that 70% of patients were either not referred or denied for mitral valve surgery was confirmed by another recent study from the same group [4].

Effects of CRT on functional MR

Contrasting the abovementioned results on surgery for functional MR, previous studies on the effects of CRT have not only demonstrated improved survival [27], but also a significant reduction in extent of functional MR after CRT [7–12]. Most of the studies on changes in MR after CRT were single-center studies with limited numbers of patients. Nonetheless, results among these studies are consistent and several explanations for improvement in MR, including the acute effect of resynchronization and improvement of LV contraction (inducing synchronized mechanical activation of papillary muscle insertion sites) [8,10], and the more delayed effect of favorable changes in MV geometry (LV reverse remodeling) [10,11] have been proposed. Moreover, in the CARE-HF trial, which randomized 813 patients to receive either biventricular pacing in addition to optimized medical therapy, or optimized medical therapy alone, there was a significantly greater reduction in MR (measured by the regurgitant jet area ratio) in patients that received CRT as compared to patients on optimized medical therapy alone, 3 moths after CRT (difference in means 5,1%, p <0.001) [27]. Finally, pooled data from several major studies including 357 patients implanted with a CRT device, with a follow-up of at least 6 months, showed a reduction in functional MR (measured by the regurgitant jet area) of

30–40% after CRT [28]. The abovementioned results clearly demonstrate the beneficial effects of CRT on (functional) MR.

Several contributing factors to non-response to CRT, such as inappropriate LV lead positioning and, in patients with ischemic cardiomyopathy, the extent and location of scar tissue, have been previously reported [29–32]. These factors might also have a significant effect on the changes in MR after CRT. Positioning the LV pacing lead at the optimal site (latest activated myocardial segment) may improve MR during CRT by any of the 2 mechanisms described above (synchronized mechanical activation of papillary muscle insertion sites and LV reverse remodeling during follow-up). Conversely, the presence of significant scar tissue may limit the extent of LV reverse remodeling after CRT and therefore also prevent the improvement in MR. In addition, positioning the LV lead at the level of a non-viable myocardial segment may significantly hamper the beneficial effect of CRT on LV remodeling and MR. Specific studies are needed to further explore the relationship between these different factors and the improvement of MR after CRT.

Improvement in MR versus long-term follow-up

In the current study, eGFR, LVESV response and MR improvement were all independently associated with improved long-term outcome (survival) after CRT. Previously, several studies have shown that a (significant) reduction in LVESV at 6 months follow-up resulted in superior long-term survival after CRT [33, 34]. Yu et al reported that patients with a reduction in LVESV ≥10% after CRT had significantly better survival as compared to patients with LVESV reduction <10%, while a more recent study by Ypenburg et al even related the extent of LV reverse remodeling to long-term prognosis after CRT. These observations are confirmed by the current findings, where patients with a volumetric response after CRT (defined as a reduction ≥15% in LVESV at 6 months follow-up) had significantly better long-term prognosis. A novel finding in the current study is that in addition to this significant LV reverse remodeling, a reduction of ≥1 grade of MR, 6 months after CRT (MR improvement), also resulted in superior survival during long-term follow-up (log rank p <0.001). Specifically, the 1- and 2-year survival rates were 97% and 92% in MR improvers as compared with 88% and 67% in MR non-improvers. More importantly, this beneficial survival effect of MR improvement was independent of other characteristics, including LVESV response at 6 months follow-up. This is the first study to establish a relation between improvement in MR at 6 months follow-up and superior survival during long-term follow-up after CRT. Possible explanations for this improved survival can be the (further) decrease in afterload induced by the reduction in MR or the interplay between reduction in MR and LV reverse remodeling. However, the survival benefit of MR improvement was independent of LVESV response at 6 months follow-up.

CONCLUSIONS

The observations in the present study indicate that CRT improves severity of MR at 6 months follow-up in heart failure patients with moderate-severe functional MR, who are at high risk for MV surgery. Applying CRT in this specific group may yield a new therapeutic option for MR. More importantly, patients with a reduction ≥1 grade of MR (MR improvers) had superior survival during long-term follow-up. This implicates a sustained survival benefit of CRT for heart failure patients with moderate-severe functional MR.

REFERENCES

1. Trichon BH, Felker GM, Shaw LK, Cabell CH, O'Connor CM. Relation of frequency and severity of mitral regurgitation to survival among patients with left ventricular systolic dysfunction and heart failure. *Am J Cardiol* 2003;91:538-643.
2. Robbins JD, Maniar PB, Cotts W, Parker MA, Bonow RO, Gheorghiade M. Prevalence and severity of mitral regurgitation in chronic systolic heart failure. *Am J Cardiol* 2003;91:360-362.
3. Koelling TM, Aaronson KD, Cody RJ, Bach DS, Armstrong WF. Prognostic significance of mitral regurgitation and tricuspid regurgitation in patients with left ventricular systolic dysfunction. *Am Heart J* 2002;144:524-529.
4. Bach DS, Awais M, Gurm HS, Kohnstamm S. Failure of guideline adherence for intervention in patients with severe mitral regurgitation. *J Am Coll Cardiol* 2009;54:860-865.
5. Calafiore AM, Iaco AL, Tash A, Abukudair W, Di Mauro M. Mitral valve surgery for functional mitral regurgitation in patients with chronic heart failure--update of the results. *Thorac Cardiovasc Surg* 2010;58:131-135.
6. Vahanian A, Baumgartner H, Bax J et al. Guidelines on the management of valvular heart disease: The Task Force on the Management of Valvular Heart Disease of the European Society of Cardiology. *Eur Heart J* 2007;28:230-268.
7. Breithardt OA, Sinha AM, Schwammenthal E et al. Acute effects of cardiac resynchronization therapy on functional mitral regurgitation in advanced systolic heart failure. *J Am Coll Cardiol* 2003;41:765-770.
8. Kanzaki H, Bazaz R, Schwartzman D, Dohi K, Sade LE, Gorcsan J, III. A mechanism for immediate reduction in mitral regurgitation after cardiac resynchronization therapy: insights from mechanical activation strain mapping. *J Am Coll Cardiol* 2004;44:1619-1625.
9. Lancellotti P, Melon P, Sakalihasan N et al. Effect of cardiac resynchronization therapy on functional mitral regurgitation in heart failure. *Am J Cardiol* 2004;94:1462-1465.
10. Ypenburg C, Lancellotti P, Tops LF et al. Mechanism of improvement in mitral regurgitation after cardiac resynchronization therapy. *Eur Heart J* 2008;29:757-765.
11. Solis J, McCarty D, Levine RA et al. Mechanism of decrease in mitral regurgitation after cardiac resynchronization therapy: optimization of the force-balance relationship. *Circ Cardiovasc Imaging* 2009;2:444-450.
12. Sitges M, Vidal B, Delgado V et al. Long-term effect of cardiac resynchronization therapy on functional mitral valve regurgitation. *Am J Cardiol* 2009;104:383-388.
13. Strickberger SA, Conti J, Daoud EG, Havranek E, Mehra MR, Pina IL, Young J. Patient selection for cardiac resynchronization therapy: from the Council on Clinical Cardiology Subcommittee on Electrocardiography and Arrhythmias and the Quality of Care and Outcomes Research Interdisciplinary Working Group, in collaboration with the Heart Rhythm Society. *Circulation* 2005;111:2146-2150.
14. Rector TS, Kubo SH, Cohn JN. Validity of the Minnesota Living with Heart Failure questionnaire as a measure of therapeutic response to enalapril or placebo. *Am J Cardiol* 1993;71:1106-1107.
15. Guyatt GH, Sullivan MJ, Thompson PJ et al. The 6-minute walk: a new measure of exercise capacity in patients with chronic heart failure. Can Med Assoc J 1985;132:919-23.
16. Roques F, Michel P, Goldstone AR, Nashef SA. The logistic EuroSCORE. *Eur Heart J* 2003;24:881-882.
17. Cockcroft DW, Gault MH. Prediction of creatinine clearance from serum creatinine. *Nephron* 1976;16:31-41.

18. Schiller NB, Shah PM, Crawford M et al. Recommendations for quantitation of the left ventricle by two-dimensional echocardiography. American Society of Echocardiography Committee on Standards, Subcommittee on Quantitation of Two-Dimensional Echocardiograms. *J Am Soc Echocardiogr* 1989;2:358-367.
19. Bleeker GB, Bax JJ, Fung JW et al. Clinical versus echocardiographic parameters to assess response to cardiac resynchronization therapy. *Am J Cardiol* 2006;97:260-263.
20. Zoghbi WA, Enriquez-Sarano M, Foster E et al. Recommendations for evaluation of the severity of native valvular regurgitation with two-dimensional and Doppler echocardiography. *J Am Soc Echocardiogr* 2003;16:777-802.
21. Bonow RO, Carabello BA, Chatterjee K et al. 2008 focused update incorporated into the ACC/AHA 2006 guidelines for the management of patients with valvular heart disease: a report of the American College of Cardiology/American Heart Association Task Force on Practice Guidelines (Writing Committee to revise the 1998 guidelines for the management of patients with valvular heart disease). Endorsed by the Society of Cardiovascular Anesthesiologists, Society for Cardiovascular Angiography and Interventions, and Society of Thoracic Surgeons. *J Am Coll Cardiol* 2008;52:e1-142.
22. Yock PG, Popp RL. Noninvasive estimation of right ventricular systolic pressure by Doppler ultrasound in patients with tricuspid regurgitation. *Circulation* 1984;70:657-662.
23. Faber L, Lamp B. Mitral valve regurgitation and left ventricular systolic dysfunction: corrective surgery or cardiac resynchronization therapy? *Herzschrittmacherther Elektrophysiol* 2008;19 Suppl 1:52-59.
24. Wu AH, Aaronson KD, Bolling SF, Pagani FD, Welch K, Koelling TM. Impact of mitral valve annuloplasty on mortality risk in patients with mitral regurgitation and left ventricular systolic dysfunction. *J Am Coll Cardiol* 2005;45:381-387.
25. Bach DS, Bolling SF. Early improvement in congestive heart failure after correction of secondary mitral regurgitation in end-stage cardiomyopathy. *Am Heart J* 1995;129:1165-1170.
26. Bolling SF, Pagani FD, Deeb GM, Bach DS. Intermediate-term outcome of mitral reconstruction in cardiomyopathy. J Thorac Cardiovasc Surg 1998;115:381-386.
27. Cleland JG, Daubert JC, Erdmann E et al. The effect of cardiac resynchronization on morbidity and mortality in heart failure. *N Engl J Med* 2005;352:1539-1549.
28. Vinereanu D. Mitral regurgitation and cardiac resynchronization therapy. *Echocardiography* 2008;25:1155-1166.
29. Ypenburg C, van Bommel RJ, Delgado V et al. Optimal left ventricular lead position predicts reverse remodeling and survival after cardiac resynchronization therapy. *J Am Coll Cardiol* 2008;52:1402-1409.
30. Ypenburg C, Schalij MJ, Bleeker GB et al. Impact of viability and scar tissue on response to cardiac resynchronization therapy in ischaemic heart failure patients. *Eur Heart J* 2007;28:33-41.
31. Hummel JP, Lindner JR, Belcik JT et al. Extent of myocardial viability predicts response to biventricular pacing in ischemic cardiomyopathy. *Heart Rhythm* 2005;2:1211-1217.
32. van Bommel RJ, Schalij MJ, Bax JJ. Should the left ventricular pacing lead be positioned at the site of latest mechanical activation in cardiac resynchronization therapy? *J Cardiovasc Electrophysiol* 2009;20:536-538.
33. Ypenburg C, van Bommel RJ, Borleffs CJ et al. Long-term prognosis after cardiac resynchronization therapy is related to the extent of left ventricular reverse remodeling at midterm follow-up. *J Am Coll Cardiol* 2009;53:483-490.

34. Yu CM, Bleeker GB, Fung JW et al. Left ventricular reverse remodeling but not clinical improvement predicts long-term survival after cardiac resynchronization therapy. *Circulation* 2005;112:1580-1586.

CHAPTER 24

Effect of cardiac resynchronization therapy on cerebral blood flow

R J van Bommel, **N Ajmone Marsan**, H Koppen, V Delgado, C JW Borleffs, C Ypenburg, M Bertini, M J Schalij, and J J Bax

Am J Cardiol 2010;106:73-7.

ABSTRACT

Objectives: Decreased cerebral blood flow is frequently observed in patients with heart failure and this may be the result of impaired cardiac systolic function. Cardiac resynchronization therapy (CRT) improves cardiac function and heart failure symptoms in selected patients. The effects of CRT on cerebral blood flow have not been evaluated before.

Methods: In this study, left ventricular (LV) systolic function and cerebral blood flow were assessed in 35 heart failure patients, before and 6 months after CRT. Additionally, 15 heart failure patients, not being candidates for CRT were included as a control group. Peak-systolic velocity (PSV), end-diastolic velocity (EDV), mean velocity and pulsatility index (PI = [PSV-EDV] / mean velocity) were obtained with the use of transcranial Doppler (TCD) from the right middle cerebral artery from the temporal window in all subjects. Response to CRT was defined as a reduction in LV end-systolic volume (LVESV) ≥15%.

Results: At 6 months follow-up, PSV significantly increased from 83±20 cm/s to 100±20 cm/s (p=0.001), EDV increased from 29±7 cm/s to 37±8 cm/s (p <0.001) and mean velocity increased from 47±10 cm/s to 58±11 cm/s (p <0.001), only in responders to CRT. Conversely, no significant changes in cerebral blood flow were observed in non-responders and controls.

Conclusions: CRT induces an increase in cerebral blood flow in heart failure patients. This increase in cerebral blood flow is related to the improvement in LV systolic function.

INTRODUCTION

Transcranial Doppler (TCD) has been validated as a reliable non-invasive technique to measure cerebral blood flow and is widely used [1–4]. In the current study, cerebral blood flow was measured with TCD in heart failure patients before CRT implantation and at 6 months follow-up. The aim of the study was to evaluate whether cerebral blood flow is altered after CRT, and whether changes in cerebral blood flow are related to improvement in cardiac systolic function after CRT.

METHODS

Thirty-five patients scheduled for cardiac resynchronization therapy (CRT) were evaluated in this study. The study was approved by the local ethics committee and written informed consent was obtained in all patients. The selection criteria for CRT included advanced symptoms of heart failure (New York Heart Association [NYHA] functional class III or IV), left ventricular ejection fraction (LVEF) <35%, sinus rhythm and a wide QRS complex (>120 ms) [5]. Patients with recent myocardial infarction (<3 months), decompensated heart failure, history of ischemic stroke/transient ischemic attack or known carotid stenosis were not included. Etiology of heart failure was considered ischemic in the presence of significant coronary artery disease (>50% stenosis in 1 or more of the major epicardial coronary arteries) and/or a history of myocardial infarction or prior revascularization.

Before CRT device implantation, clinical status including NYHA class, 6-minute walking distance and Minnesota Living with Heart Failure Questionnaire (MLHFQ] score was assessed. Cognitive function was specifically evaluated with the psychometric sub-score of the MLHFQ (MLHFQ-PS). This psychometric properties sub-score has recently been validated against the more extensive Medical Outcomes Study 36-Item Short Form Health Survey (SF-36) [6, 7].

In addition, left ventricular (LV) volumes and LVEF were measured using real-time three-dimensional echocardiography (RT3DE). Cerebral blood flow was evaluated with the use of TCD. At 6 months follow-up, the abovementioned measurements were repeated to assess the effect of CRT on cerebral blood flow, cognitive function and LV performance. Patients with a reduction ≥15% of LV end-systolic volume (LVESV), reflecting improvement in LV systolic function, were considered responders to CRT [8, 9].

Finally, 15 heart failure patients matched for age, gender, NYHA class and LV function, not being candidates for CRT according to current guidelines (QRS duration <120 ms), were included as a control group. These patients underwent the same clinical, echocardiographic and transcranial Doppler assessment as the CRT recipients. All patients were on stable heart failure medication and medical therapy was unchanged during the study.

Complete echocardiographic methods have been described previously [10]. In brief, patients were imaged in the left lateral decubitus position with a commercially available system (iE33, Philips Medical Systems, N.A., Bothell, Washington, USA) equipped with a X3, fully sampled matrix transducer. RT3DE data sets were stored digitally and quantitative analysis of the 3D dataset was performed off-line using a semi-automated contour tracing algorithm (Q-Lab, version 6.0, Philips Medical Systems) over a complete heart cycle.

LV systolic performance was quantified by measuring the LV outflow-tract velocity-time integral (LVOT VTI) using pulsed-wave Doppler, during end-expiratory apnea.

Transcranial Doppler images were acquired after the patient was in supine position for a minimum of 10 minutes, with the same system used for the echocardiographic examinations (iE33, Philips Medical Systems, N.A., Bothell, Washington, USA), equipped with a broadband pure wave S5-1 transducer. All TCD measurements were taken from the right middle cerebral artery from the temporal window. Blood flow velocities were measured by placing a sample volume of 2.5 mm in the bloodstream at a depth (range 40 – 65 mm) giving the highest values. The software (HighQ) automatically calculated peak-systolic velocity (PSV), end-diastolic velocity (EDV), mean velocity and pulsatility index (PI = [PSV-EDV] / mean velocity) using automatic trace of the Doppler spectrum. For each patient, blood flow velocities were obtained from a minimum of 10 cardiac cycles.

Table 1: Baseline characteristics of the study population (n = 46).

Variable	Patients (n = 32)	Controls (n = 14)	p-value
Men/Women	25/7	11/3	0.648
Age (years)	68±10	66±10	0.583
Etiology of heart failure			
Ischemic	16 (50%)	10 (71%)	0.153
Non-ischemic	16 (50%)	4 (29%)	
QRS duration (ms)	152±25	110±8	<0.001
Systolic blood pressure (mmHg)	123±15	121±12	0.696
Diastolic blood pressure (mmHg)	71±10	73±7	0.349
NYHA class	3.0±0	2.9±0.3	0.132
Medication			
ACE-inhibitors/AII-blockers	30 (94%)	13 (93%)	1.000
B-blockers	24 (75%)	13 (93%)	0.240
Diuretics	29 (91%)	10 (71%)	0.176
Spironolactone	20 (63%)	6 (43%)	0.333
Echocardiography			
Heart rate	70±17	68±13	0.558
LV end-diastolic volume (ml)	189±68	158±32	0.272
LV end-systolic volume (ml)	137±55	109±24	0.073
LV ejection fraction (%)	29±6	32±4	0.101
LV outflow-tract VTI (cm)	13±4	14±3	0.510

ACE: angiotensin converting enzyme, LV: left ventricular, NYHA: New York Heart Association, VTI: velocity time integral

Continuous data are presented as mean±SD, and dichotomous data are presented as numbers and percentages. Comparison of continuous data between 2 groups was performed using the Mann-Whitney U-test. For comparison between more than 2 groups, the Kruskal-Wallis test with manual Bonferroni post-hoc testing was performed. Fisher's exact tests or χ^2 tests were used to compare dichotomous data. Comparison of continuous data within patient groups (at baseline and 6 months follow-up) was performed with the Wilcoxon test. Additionally, linear regression analysis was performed to evaluate the relation between reduction in LVESV and increase in mean TCD velocity. All analyses were performed with SPSS for Windows, version 16.0 (SPSS, Chicago, IL). A p-value <0.05 was considered statistically significant.

Table 2: Clinical and echocardiographic characteristics of responders and non-responders (n = 32).

Variable	Responders (n = 16)	Non-responders (n = 16)	p-value
Men/Women	12/4	13/3	1.000
Age (years)	67±10	69±10	0.317
Etiology of heart failure			
Ischemic	12 (75%)	4 (25%)	0.012
Non-ischemic	4 (24%)	12 (75%)	
QRS duration (ms)	159±25	145±24	0.105
NYHA class	3.0±0	3.0±0	1.000
MLHFQ			
baseline	31±12	35±20	0.755
follow-up	16±12*	32±24	0.088
MLHFQ-PS			
baseline	6.8±4.4	7.4±6.2	0.909
follow-up	3.6±3.3*	6.1±6.3	0.413
Echocardiography			
LV end-diastolic volume (ml)			
baseline	188±67	190±70	0.836
follow-up	186±74	180±59	0.880
LV end-systolic volume (ml)			
baseline	148±65	126±43	0.429
follow-up	114±55‡	127±46	0.214
LV ejection fraction (%)			
baseline	28±8	30±4	0.557
follow-up	40±8‡	30±4	<0.001
LV outflow-tract VTI (cm)			
baseline	12±3	14±4	0.187
follow-up	14±4†	14±4	0.598

MLHFQ: Minnesota Living with Heart Failure Questionnaire, MLHFQ-PS: Minnesota Living with Heart Failure Questionnaire - Psychometric Subscore. Rest of abbreviations as in Table 2.

* p <0.05, baseline vs. follow-up, † p = 0.001, baseline vs. follow-up, ‡ p <0.0001, baseline vs. follow-up.

RESULTS

Adequate visualization of the middle cerebral artery was not feasible in 3 patients in the CRT group and in 1 control patient. These patients were excluded from further analysis and therefore the final study population consisted of 32 CRT recipients and 14 control patients. Baseline characteristics of the study population are summarized in Table 1. By definition, CRT patients and controls were comparable in terms of age, gender, NYHA class and LV function. Control patients had a significantly shorter QRS duration (110±8 ms vs. 152±25 ms, p <0.001). No differences in baseline TCD measurements (depth, number of samples, PSV, EDV, mean velocity and PI) were observed between CRT patients and controls.

At 6 months follow-up, mean NYHA class improved in the CRT group from 3.0±0 to 2.3±0.7 (p <0.001). In addition, MLHFQ score decreased from 32±16 to 24±20 (p = 0.010) and MLHFQ-SP decreased from 7.1±5.3 to 4.8±5.1 (p = 0.031), while 6-minute walking distance increased

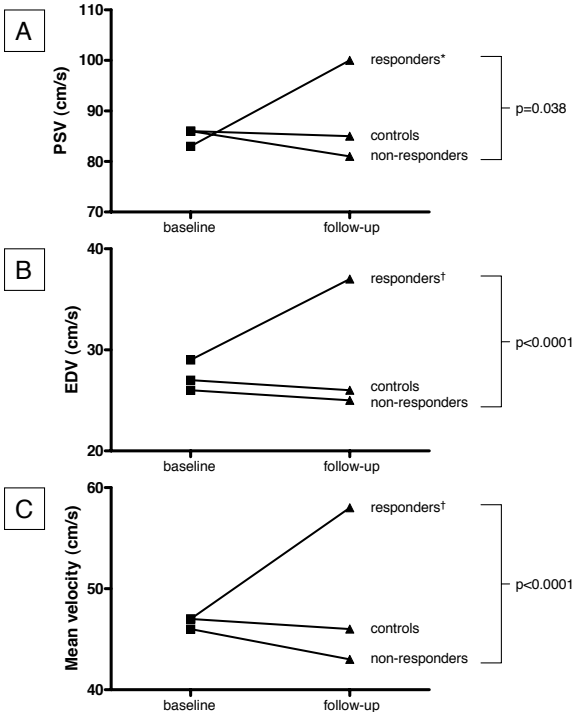


Figure 1: Changes from baseline to follow-up in cerebral blood flow; responders, non-responders and controls. A significant increase in peak systolic velocity (PSV, panel A), end diastolic velocity (EDV, panel B) and mean velocity (panel C) was observed in responders, while no changes were observed in both non-responders and control patients. Provided p-values are from the Kruskal-Wallis test for comparison of follow-up data between the 3 groups.

* p = 0.027, responders vs. non-responders

† p <0.01, responders vs. non-responders and controls

from 333±89 m to 374±114 m (p = 0.024). Furthermore, a significant LV reverse remodeling was observed with a decrease in LVESV from 137±55 ml to 120±50 ml (p = 0.001) and an improvement in LVEF from 29±6% to 35±8% (p <0.0001). Finally, there was a significant increase in LVOT-VTI from 13±4 cm to 14±4 cm (p = 0.027).

In contrast, control patients did not show any change in echocardiographic parameters (LVESV from 109±24 ml to 111±25 ml [p = 0.314], LVEF from 32±4% to 32±3% [p = 0.810] and LVOT-VTI from 14±3 cm to 15±2 cm [p = 0.180]).

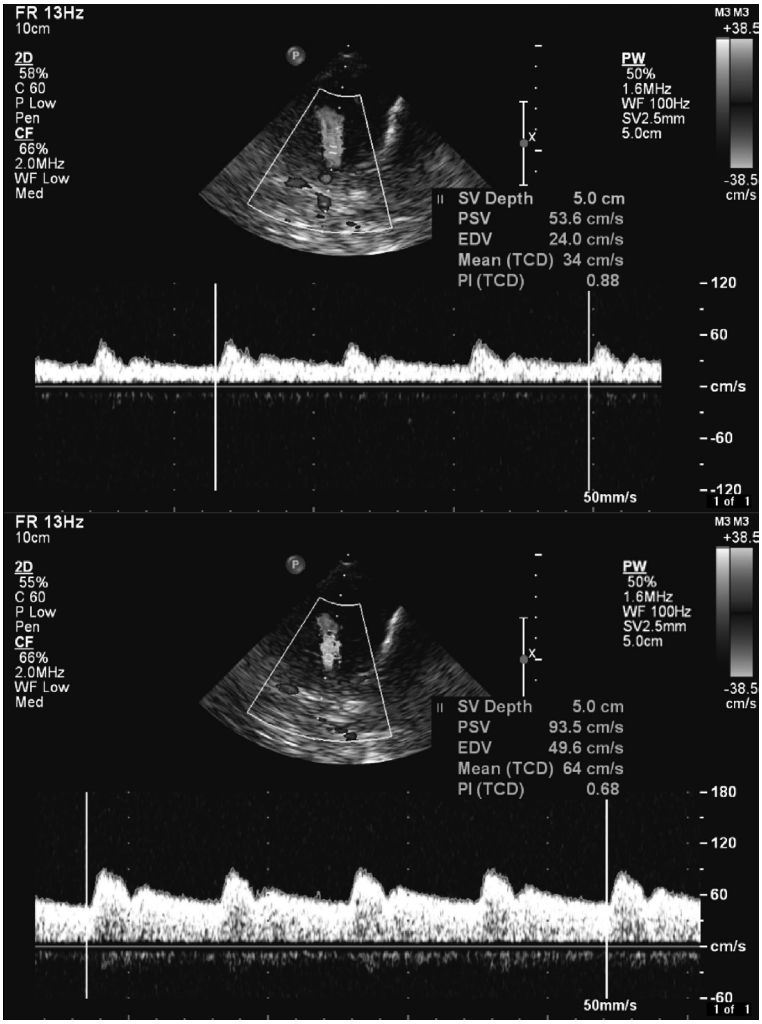


Figure 2: Example of improvement in cerebral blood flow after 6 months CRT.
(Upper panel) Before CRT, velocities are low and a dicrotic waveform can be seen. (Lower panel) After 6 moths CRT, the dicrotic waveform is still present, but velocities have increased significantly, indicating increase in cerebral blood flow.
EDV: end-diastolic velocity, PI: pulsatility index, PSV: peak-systolic velocity. SV: sample volume, TCD: transcranial Doppler.

At 6 months follow-up, 16 patients (50%) demonstrated response to CRT. There were no differences in baseline clinical characteristics between responders and non-responders, except for non ischemic etiology of heart failure, which was more frequently observed in responders. Baseline echocardiographic characteristics were comparable between the 2 groups (Table 2). Only responders showed a significant decrease in both the MLHFQ (from 31±12 to 16±12, p = 0.005) and the MLHFQ-PS (from 6.8±4.4 to 3.6±3.3, p = 0.043) reflecting an improvement in quality of life and cognitive functions.

At follow-up, responders demonstrated not only a significant reduction in LVESV (by definition) when compared to non-responders, but also a significant increase in LVEF and LVOT VTI, indicating improvement in cardiac performance (Table 2).

Insonation depth and number of samples acquired for TCD assessment were comparable between baseline and follow-up in responders, non-responders and controls. At follow-up, peak-systolic velocity significantly increased in responders from 83±20 cm/s to 100±20 cm/s (p = 0.001). Similarly, EDV increased from 29±7 cm/s to 37±8 cm/s and mean velocity increased from 47±10 cm/s to 58±11 cm/s (both p <0.001, Figure 1). The mean value of PI showed no significant change from baseline to follow-up.

Conversely, in non-responders and controls, no significant changes in any of the TCD velocities were observed (Figure 1). An example of a CRT patient that demonstrated a marked improvement in cerebral blood flow is shown in Figure 2. Linear regression analysis revealed a strong correlation (r = 0.78, p <0.001) between reduction in LVESV and increase in mean TCD velocity, demonstrating that improvement in cardiac function resulted in a significant increase in cerebral blood flow (Figure 3).

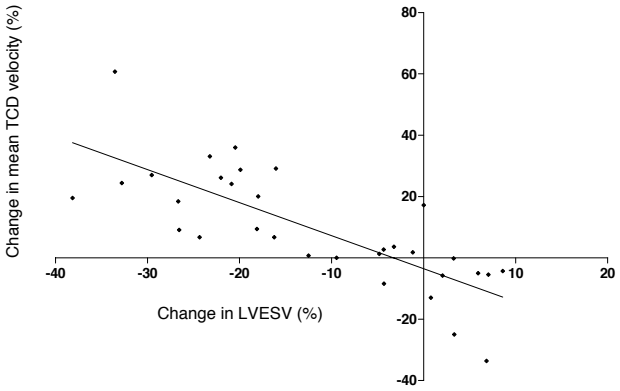


Figure 3: Relation between change in LVESV and chance in mean TCD velocity (y = -3.3 – 1.1x, n = 32, r = 0.78, p <0.0001). LVESV: left ventricular end-systolic volume, TCD: transcranial Doppler.

DISCUSSION

The findings of the present study can be summarized as follows: 1) cardiac resynchronization therapy improves cerebral blood flow in patients with heart failure; and 2) this improvement in cerebral blood flow is related to the improvement in LV systolic function following CRT.

Cerebral blood flow is decreased in symptomatic heart failure patients and this may contribute to the impaired cognitive performance frequently observed in these patients [11–13]. Choi et al reported significantly lower values for cerebral blood flow in 52 patients with heart failure secondary to idiopathic dilated cardiomyopathy, in comparison to 10 healthy controls [13]. Additionally, Vogels and co-workers noted reduced cerebral blood flow in 43 heart failure patients in comparison to 33 patients with a history of ischemic cardiac disease without symptoms of heart failure and an LVEF >55%, and 22 healthy controls [12]. Cardiac resynchronization therapy improves heart failure symptoms, quality of life, LV systolic function, and prognosis in patients with moderate or severe heart failure [14–16]. More recent studies have also linked the improvement in LV systolic function to systemic improvements [17, 18]. The first study to show an association between CRT and improvement in cognitive function was reported by Conti and co-workers [19]. The authors found significant improvements in quantitative neurocognitive measures of attention and information processing at 3 months follow-up in 10 heart failure patients treated with CRT (Digit Span increased from 50±5 to 57±7, $p = 0.04$ and Symbol Digit from 39±9 to 49±15, $p = 0.04$). Although, the precise mechanism underlying this improvement is not clear, it could be related to increase in cerebral blood flow as result of the increased cardiac systolic function.

An increase in cerebral blood flow has been previously reported in patients undergoing heart transplantation [2, 20]. Gruhn et al studied 12 healthy controls and 12 patients with severe heart failure (NYHA class III-IV) of whom 5 underwent cardiac transplantation [20]. In the patients who underwent transplantation, cerebral blood flow normalized to the level of the controls at 1 month follow-up. Similar findings were described by Massaro and co-workers in a series of 14 patients who underwent cardiac transplantation [2]. The currently observed improvement of 23.4% in mean cerebral blood flow is a significant improvement, which may translate into a substantial clinical benefit in these patients [21]. The MLHFQ and the MLHFQ-PS scores reduced significantly only in patients that showed response to CRT, probably related to the significant increase in cerebral blood flow observed in these patients. The last observation further strengthens the assumption that in patients with heart failure, increase in cerebral blood flow is the key mechanism in improvement in cognitive function.

A limitation of this study is the single-centre, non randomized, observational design. To counterbalance the absence of randomization, a control group with similar baseline characteristics, but without an indication for CRT (since these control patients did not have a wide QRS complex) was included. Still, a multi-centre, randomized trial should be performed to confirm the current findings. Second, the study sample was relatively small, and finally, no

other neurological tests were performed besides the MLHFQ-PS. Therefore, a direct relation between improvement in cerebral blood flow and improvement in cognitive function could not be shown.

REFERENCES

1. Bishop CC, Powell S, Rutt D, Browse NL. Transcranial Doppler measurement of middle cerebral artery blood flow velocity: a validation study. *Stroke* 1986;17:913-915.
2. Massaro AR, Dutra AP, Almeida DR, Diniz RV, Malheiros SM. Transcranial Doppler assessment of cerebral blood flow: effect of cardiac transplantation. *Neurology* 2006;66:124-126.
3. Brass LM. Reversed intracranial blood flow in patients with an intra-aortic balloon pump. *Stroke* 1990;21:484-487.
4. Lindegaard KF, Lundar T, Wiberg J, Sjoberg D, Aaslid R, Nornes H. Variations in middle cerebral artery blood flow investigated with noninvasive transcranial blood velocity measurements. *Stroke* 1987;18:1025-1030.
5. Strickberger SA, Conti J, Daoud EG et al. Patient selection for cardiac resynchronization therapy: from the Council on Clinical Cardiology Subcommittee on Electrocardiography and Arrhythmias and the Quality of Care and Outcomes Research Interdisciplinary Working Group, in collaboration with the Heart Rhythm Society. *Circulation* 2005;111:2146-2150.
6. Supino PG, Borer JS, Franciosa JA et al. Acceptability and psychometric properties of the Minnesota Living With Heart Failure Questionnaire among patients undergoing heart valve surgery: validation and comparison with SF-36. *J Card Fail* 2009;15:267-277.
7. McHorney CA, Ware JE, Jr., Raczek AE. The MOS 36-Item Short-Form Health Survey (SF-36): II. Psychometric and clinical tests of validity in measuring physical and mental health constructs. *Med Care* 1993;31:247-263.
8. Bleeker GB, Bax JJ, Fung JW et al. Clinical versus echocardiographic parameters to assess response to cardiac resynchronization therapy. *Am J Cardiol* 2006;97:260-263.
9. Chung ES, Leon AR, Tavazzi L et al. Results of the Predictors of Response to CRT (PROSPECT) trial. *Circulation* 2008;117:2608-2616.
10. Marsan NA, Bleeker GB, Ypenburg C et al. Real-time three-dimensional echocardiography as a novel approach to assess left ventricular and left atrium reverse remodeling and to predict response to cardiac resynchronization therapy. *Heart Rhythm* 2008;5:1257-1264.
11. Roman GC. Brain hypoperfusion: a critical factor in vascular dementia. *Neurol Res* 2004;26:454-458.
12. Vogels RL, Oosterman JM, Laman DM et al. Transcranial Doppler blood flow assessment in patients with mild heart failure: correlates with neuroimaging and cognitive performance. *Congest Heart Fail* 2008;14:61-65.
13. Choi BR, Kim JS, Yang YJ et al. Factors associated with decreased cerebral blood flow in congestive heart failure secondary to idiopathic dilated cardiomyopathy. *Am J Cardiol* 2006;97:1365-1369.
14. Abraham WT, Fisher WG, Smith AL et al. Cardiac resynchronization in chronic heart failure. *N Engl J Med* 2002;346:1845-1853.
15. Bristow MR, Saxon LA, Boehmer J et al. Cardiac-resynchronization therapy with or without an implantable defibrillator in advanced chronic heart failure. *N Engl J Med* 2004;350:2140-2150.
16. Cleland JG, Daubert JC, Erdmann E et al. The effect of cardiac resynchronization on morbidity and mortality in heart failure. *N Engl J Med* 2005;352:1539-1549.
17. Fung JW, Szeto CC, Chan JY et al. Prognostic value of renal function in patients with cardiac resynchronization therapy. *Int J Cardiol* 2007;122:10-16.
18. Boerrigter G, Costello-Boerrigter LC, Abraham WT et al. Cardiac resynchronization therapy improves renal function in human heart failure with reduced glomerular filtration rate. *J Card Fail* 2008;14:539-546.

19. Conti JB, Sears SF. Cardiac resynchronization therapy: can we make our heart failure patients smarter? *Trans Am Clin Climatol Assoc* 2007;118:153-164.
20. Gruhn N, Larsen FS, Boesgaard S et al. Cerebral blood flow in patients with chronic heart failure before and after heart transplantation. *Stroke* 2001;32:2530-2533.
21. Zuccala G, Onder G, Marzetti E et al. Use of angiotensin-converting enzyme inhibitors and variations in cognitive performance among patients with heart failure. *Eur Heart J* 2005;26:226-233.

CHAPTER 25

Cardiac resynchronization therapy in patients with ischemic versus non-ischemic heart failure: Differential effect of optimizing interventricular pacing interval

N Ajmone Marsan, G B Bleeker, R J van Bommel, C JW Borleffs, M Bertini, E R Holman, E E van der Wall, M J Schalij, and J J Bax

Am Heart J 2009;158:769-76.

ABSTRACT

Objectives: Whether sequential biventricular pacing provides substantial benefits over conventional simultaneous stimulation remains unclear, particularly regarding the differences between ischemic and non-ischemic patients. The purpose of this study was to evaluate the acute effect of inter-ventricular pacing interval (V-V) optimization on left ventricular (LV) systolic performance and dyssynchrony in ischemic versus non-ischemic patients.

Methods: 69 consecutive patients underwent cardiac resynchronization therapy. Within 3 days after implantation, V-V was optimized by measuring (every 20ms interval) LV systolic performance (LV outflow-tract velocity-time-integral, LVOT-VTI) and LV dyssynchrony (using tissue Doppler imaging). Optimal pacing configuration was the one achieving maximal increase in LVOT-VTI.

Results: Optimized sequential pacing provided a significant improvement in LVOT-VTI compared to simultaneous stimulation (from 138±42 mm to 163±38 mm, $p < 0.001$) and was associated with a significant reduction in LV dyssynchrony (from 33±31 ms to 19±24 ms, $p < 0.001$). The increase in LVOT-VTI and LV ejection fraction after implantation was greater in non-ischemic as compared to ischemic patients ($p < 0.001$). However, V-V optimization yielded a larger improvement in LV systolic performance in ischemic patients ($p = 0.03$). Consequently, the 2 groups showed comparable response after V-V optimization. A significant correlation was observed between LV scar tissue and optimal V-V interval ($r = 0.58$, $p < 0.001$), with a larger extent of scar related to a larger level of LV pre-activation, probably reflecting slow intra-LV conduction.

Conclusions: Optimized sequential biventricular pacing further increased LV systolic performance as compared to simultaneous stimulation, particularly in ischemic patients where the presence of a large scar was correlated with a larger LV pre-activation.

INTRODUCTION

Cardiac resynchronization therapy (CRT) is currently considered an important breakthrough in the treatment of selected patients with drug-refractory heart failure and has rapidly evolved from the experimental stage into an established treatment modality [1].

In the first generations of CRT devices both left ventricular (LV) and right ventricular (RV) pacing leads were activated simultaneously in order to resynchronize LV contraction. A novel feature on the more recent generations of CRT devices allows separate (sequential) timing of activation of the LV and RV pacing leads through a programmable inter-ventricular (V-V) pacing interval. Since this option is available, several studies have focused on the possibility of further enhancing the beneficial effects of CRT through optimization of the V-V pacing interval. Preliminary data have demonstrated that optimized sequential CRT, rather than simultaneous CRT, is able to further improve LV systolic performance, as measured by LV stroke volume or dP/dt [2–9]. In contrast, other studies demonstrated no or only limited additional clinical or echocardiographic benefits of V-V optimization compared with "standard" simultaneous CRT [10,11]. Moreover, the effect of V-V optimization on LV dyssynchrony has not been extensively studied and no data are available on the potential advantage of sequential CRT in patients with ischemic heart failure (who may demonstrate a less favorable response to CRT in absence of V-V optimization[12]) as compared to patients with non-ischemic heart failure. Accordingly, the purpose of this study was to evaluate the acute effects of varying degrees of RV or LV pre-activation on both LV hemodynamic profile and LV dyssynchrony. In addition, the beneficial effects of V-V optimization were compared between patients with ischemic and non-ischemic heart failure.

METHODS

Patient population

Sixty-nine consecutive heart failure patients, scheduled for implantation of a biventricular pacemaker, were included in this study. Patients were selected for CRT based on the following characteristics: LV ejection fraction (LVEF) ≤35%, QRS duration >120 ms and NYHA functional class III or IV, despite optimal medical treatment. Etiology was considered ischemic in the presence of significant coronary artery disease (>50% stenosis in ≥1 major epicardial coronary artery) on coronary angiography and/or history of myocardial infarction or previous revascularization. Patients with a recent myocardial infarction (<3 months) or decompensated heart failure were excluded.

Device implantation

The LV pacing lead was inserted transvenously via the subclavian route. First, a coronary sinus venogram was obtained using a balloon catheter. Next, the LV pacing lead (Easytrak 4512-80, Guidant Corp., or Attain-SD 4189, Medtronic Inc) was inserted through the coronary sinus, using an 8Fr-guiding catheter, and positioned in the lateral or postero-lateral vein. The right atrial and ventricular leads were positioned conventionally. The 3 leads were connected to a biventricular pacing device and, when an indication for an internal defibrillator existed, a combined device was implanted (Contak CD or Renewal, Guidant Corp., or Insync III-CD or Marquis, Medtronic Inc). These devices have two separate channels for RV and LV pacing with a programmable V-V interval. In all patients the implantation of the CRT device was successful without major complications.

Study protocol

Before CRT, echocardiography was performed to evaluate LV dimensions and systolic function, whereas the extent of LV mechanical dyssynchrony was derived from tissue Doppler imaging (TDI). Within 3 days after implantation pacemaker settings were optimized. The atrio-ventricular interval was adjusted to maximize mitral inflow duration, as assessed with pulsed-wave Doppler echocardiography using the "iterative" method [13]. Next, V-V interval was modified by advancing LV or RV pacing by 20 ms intervals. For each patient seven different V-V intervals were examined: simultaneous biventricular pacing (= 0 ms), LV pre-activation (LV60 = 60 ms, LV40 = 40 ms and LV20 = 20 ms) and RV pre-activation (RV60 = 60 ms, RV40 = 40 ms and RV20 = 20 ms). For each combination, LV systolic function and the extent of LV dyssynchrony were assessed. Each recording period was preceded by a stabilization period of 3-5 minutes.

Echocardiography

Image acquisition

Patients were imaged in the left lateral decubitus position using a commercially available system (Vingmed Vivid Seven, General Electric Healthcare, Horten, Norway). Images were obtained using a 3.5-Mhz transducer, at a depth of 16 cm in the apical views. For the TDI images, the sector width was adjusted to obtain a frame rate of at least 100 frames/second; pulse repetition frequencies were between 500 Hz and 1 kHz, resulting in aliasing velocities

between 16 and 32 cm/s. To minimize variability between examinations, all echocardiographic recordings were performed by the same operator. During the pulsed-wave Doppler acquisitions, an effort was made to maintain the same position of the sample throughout the investigation. All images were recorded digitally in cine-loop format and analyzed offline with commercial software Echopac 6.1 (General Electric-Vingmed). Off-line analysis was performed by a different observer and was blinded to the pacing mode. Each parameter was measured and averaged over three consecutive beats during sinus rhythm.

Analysis of LV systolic function and LV dyssynchrony

LV end-systolic and end-diastolic volumes were determined from the conventional apical 2- and 4-chamber views and LV ejection fraction (EF) was calculated using the biplane Simpson's technique. During V-V optimization, LV systolic function and the extent of LV dyssynchrony were assessed for each interval. As previously described [6,9], the acute changes in LV systolic performance were quantified by measuring the LV outflow-tract velocity-time integral (LVOT VTI), using pulsed-wave Doppler during end-expiratory apnea. After the optimization of the pacemaker, patients were maintained in the individually optimized sequential biventricular pacing configuration that was defined as the setting with the highest LVOT VTI and LV volumes and EF were recalculated. An absolute increase in LVEF ≥5% was considered as a significant positive response to CRT [14].

To quantify the extent of LV dyssynchrony, the maximum delay in peak velocity between the earliest and the latest activated segments within the basal segments of septum, inferior, anterior and lateral wall was calculated [15]. From previous observations, a delay ≥65 ms was considered to represent significant LV dyssynchrony [15]. Inter-observer agreement and intra-observer agreement for assessment of LV dyssynchrony were 90% and 96% respectively [16].

Statistical analysis

Continuous data are presented as mean±SD; dichotomous data are presented as numbers and percentage. Student *t* test and χ^2 test were used for appropriate comparisons. Sequential data measurements, in the total population and in the groups of patients with and without ischemic cardiomyopathy, were analyzed by repeated measures analysis of variance (ANOVA) followed by post hoc Scheffe's correction for multiple tests. A two-way ANOVA analysis was performed for comparison of time trends between patients with and without ischemic cardiomyopathy. Simultaneous biventricular pacing was considered as the reference pacing configuration to compare all sequential configurations and to assess the correlation between the change in LVOT VTI and LV dyssynchrony. Pearson's correlation coefficient was used to

quantify correlations between quantitative variables. Agreement for the optimal V-V interval between LVOT VTI and LV dyssynchrony was assessed using weighted κ statistics. A p-value <0.05 was considered to be statistically significant. A statistical software program SPSS 12.0 (SPSS Inc, Chicago, Il, USA) was used for statistical analysis.

RESULTS

Pre-implantation data

Sixty-nine patients were included (58 men; mean age 66±10 years). Baseline patient characteristics are summarized in Table 1. Most patients were in NYHA class III (88%), and 41 (59%) patients had ischemic heart failure. Echocardiography revealed severe LV dilatation and dysfunction (mean LV end-diastolic volume 251±74 ml, mean LVEF 22.9±7.8%). The mean extent of LV dyssynchrony was 75±24 ms.

Table 1. Baseline patient characteristics (n = 69)

Age, years	**66±10**
Gender, M/F	58/11
NYHA class, n (%)	
III	61 (88)
IV	8 (12)
QRS duration, ms	163±32
Rhythm, n (%)	
Sinus rhythm	57 (83)
Atrial fibrillation	12 (17)
Etiology, n (%)	
Ischemic	41 (59)
Idiopathic	28 (41)
LVEF, %	22.9±7.8
LVEDV, ml	251±74
LVESV, ml	196±73
LVOT VTI, mm	118±36
LV dyssynchrony, ms	75±24

LVEDV = left ventricular end-diastolic volume; LVEF = left ventricular ejection fraction; LVESV = left ventricular end-systolic volume; LVOT VTI = left ventricular out-flow tract velocity-time integral.

Simultaneous and sequential CRT

After CRT implantation, simultaneous CRT (V-V interval = 0 ms) resulted in a significant improvement of the cardiac output: LVOT VTI increased from 118±36 mm at baseline to 138±42

mm (p <0.001) after CRT; LVEF improved from 22.9±7.8% to 28.7±5.6% (p <0.001). A total of 34 (49%) patients showed a significant increase (≥5%) in LVEF. In addition, compared with baseline, simultaneous CRT significantly reduced LV dyssynchrony from 75±24 ms to 33±31 ms (p <0.001).

The LV systolic performance was further improved by optimizing the V-V interval, with the LVOT VTI increasing from 138±42 mm during simultaneous CRT to 163±38 mm (p <0.001) during sequential CRT and LVEF improving from 28.7±5.6% to 34.3±6.9% (p <0.001). In addition, LV dyssynchrony decreased from 33±31 ms to 19±24 ms (p <0.001). The percentage of significant response to CRT increased from 49% to 74% (51 patients).

In 18 patients (26%) the highest LVOT VTI was achieved during simultaneous CRT. In the remaining 51 patients (74%), LV pre-activation was the optimal setting in 38 patients (55%), with LV60 in 11 patients (16%), LV40 in 11 patients (16%) and LV20 in 16 patients (23%). For 13 patients (19%) RV pre-activation was the optimal setting, with RV60 in 1 patient (2%) and RV20 in 12 patients (17%); no patient had an optimal cardiac output at RV40 (Figure 1).

The concordance between V-V intervals yielding the highest LVOT VTI and the lowest LV dyssynchrony was excellent (weighted kappa = 0.88, p <0.001) (Figure 2 and Table 2). In addition, the absolute changes in LV dyssynchrony, showed a significant correlation (r = 0.58; p <0.001) with the absolute changes in LVOT VTI. Figure 3 shows an example of a patient with an optimal V-V interval of LV60 and how changes in LV dyssynchrony and LVOT VTI were clearly correlated.

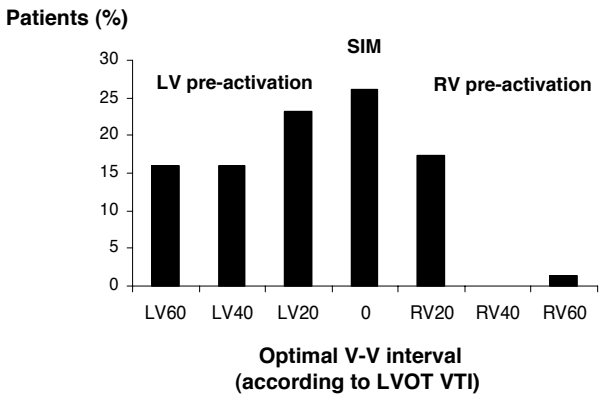


Figure 1. Distribution of optimal V-V interval configuration resulting in highest left ventricular cardiac output (LVOT VTI). LV = left ventricle; RV = right ventricle; SIM = simultaneous.

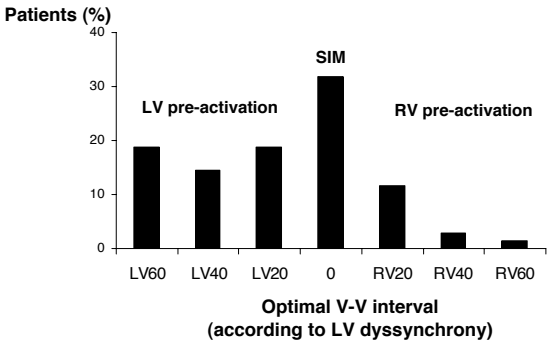


Figure 2. Distribution of optimal V-V interval configuration resulting in least left ventricular dyssynchrony. LV = left ventricle; RV = right ventricle; SIM = simultaneous.

Table 2: Kappa statistic for LVOT VTI-optimized V-V interval vs. LV dyssynchrony-optimized V-V interval.

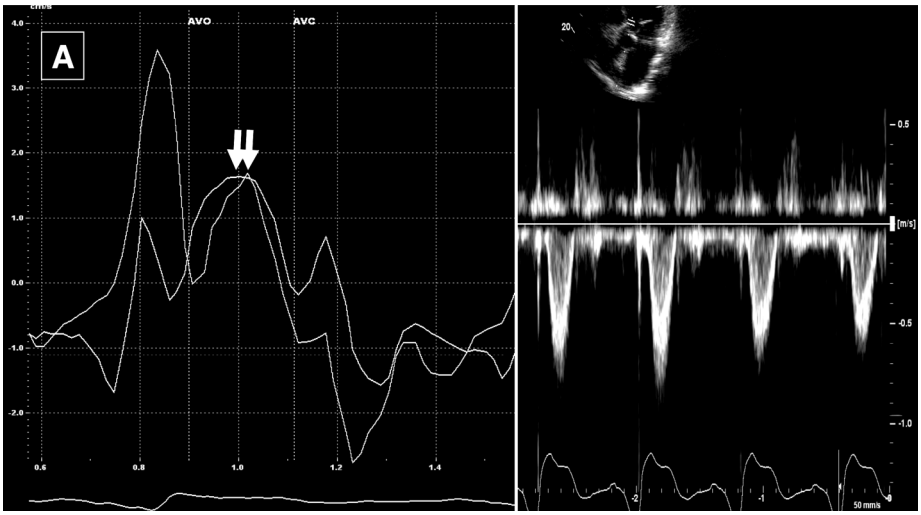
LVOT VTI LV dyssynchrony	LV60	LV40	LV20	0	RV20	RV40	RV60	Total
LV60	9	0	1	1	2	0	0	13
LV40	0	11	0	0	0	0	0	11
LV20	1	0	11	1	0	0	0	13
0	1	0	2	15	2	0	0	20
RV20	0	0	2	0	7	0	0	9
RV40	0	0	0	1	1	0	0	2
RV60	0	0	0	0	0	0	1	1
Total	11	11	16	18	12	0	1	69

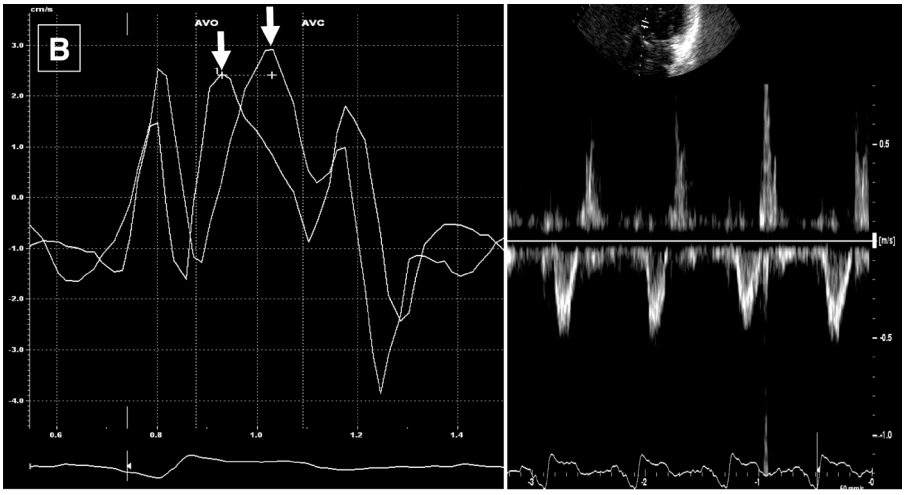
Weighted Kappa = 0.88, p <0.001; LVOT VTI = left ventricular out-flow tract velocity-time integral

V-V interval optimization in ischemic versus non-ischemic cardiomyopathy

After implantation, simultaneous CRT (V-V interval = 0 ms) resulted in a significant improvement of LVOT VTI and LVEF (p <0.01) both in ischemic and non-ischemic patients (Table 3). However, this improvement (change from baseline to simultaneous CRT) was larger in non-ischemic patients (with a relative increase in LVOT VTI of 29±30 mm and in LVEF of 8.1±6.2%) as compared to ischemic patients (with a relative increase in LVOT VTI of 14±14 mm and in LVEF of 3.4±5.5%, p <0.001 versus non-ischemic patients). Consequently, among non-ischemic patients, 19 (68%) patients showed an increase ≥5% in LVEF, while among ischemic patients, only 14 (34%) patients had a significant response to CRT.

In turn, V-V optimization yielded a larger improvement of LVOT VTI and LVEF (change from simultaneous CRT to optimized sequential stimulation) in ischemic patients (Table 3); a relative increase in LVOT VTI of 34±25 mm in ischemic patients versus a relative increase of 16±15 mm in non-ischemic patients (p = 0.03 ischemic versus non-ischemic patients); a relative increase in LVEF of 7.6±6.1% versus 4.4±5.9% in ischemic patients (p = 0.02 ischemic versus





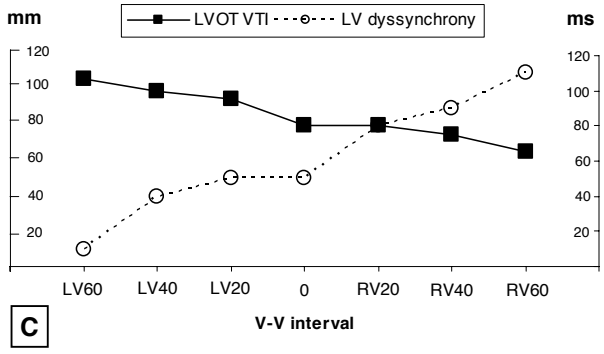


Figure 3. An example of patient with optimal V-V interval of LV60. A: LV dyssynchrony and LV out-flow-tract velocity-time integral (LVOT VTI) at V-V interval of LV60. B: LV dyssynchrony and LVOT VTI during simultaneous CRT. C: changes of LV dyssynchrony and LVOT VTI during V-V interval optimization.

Table 3. Left ventricular out-flow tract velocity-time integral (LVOT VTI) and left ventricular ejection fraction (LVEF) at baseline, during simultaneous and optimized sequential CRT, in ischemic and non-ischemic patients.

	Ischemic patients n = 41	Non-ischemic patients n = 28	p-value (ischemic vs. non-ischemic)
LVOT VTI (mm)			
Baseline	116±34	120±39	NS
Simultaneous CRT	129±41*	149±41*	<0.001
Optimized sequential CRT	163±37*	165±41*	NS
LVEF (%)			
Baseline	23.2±8.2	22.4±6.8	NS
Simultaneous CRT	26.7±5.3*	30.3±5.1*	<0.001
Optimized sequential CRT	34.1±6.6*	34.5±6.9*	NS

*: p <0.01 (two-way ANOVA)

non-ischemic patients). Consequently, the percentage of ischemic patients that showed a significant improvement in LVEF (≥5%) increased from 34% to 71% (29 patients), while in non-ischemic patients this percentage increased from 68% to 78% (22 patients). Importantly, after V-V optimization the percentage of CRT responders was similar between ischemic and non-ischemic patients.

V-V pacing interval versus the extent of scar tissue

In 24 patients (58%) with ischemic heart failure, a nuclear perfusion study was obtained during the clinical course, using single-photon emission computed tomography (SPECT, triple head camera system, GCA 9300/HG, Toshiba Corp.) and technetium-99m tetrofosmin. To quantify the extension of the scar tissue, tracer uptake was analyzed quantitatively using a standard 17-segment model and categorized on a 4-point scale: 0, tracer activity > 75% (normal, viable); 1, tracer activity = 50%-75% (minimal scar); 2, tracer activity = 25%-50% (moderate scar); 3, tracer activity <25% (extensive scar) [17]. Summation of the segmental scores yielded the total scar score, with the higher scores indicating more scar tissue (reflecting the extent of damage per patient).

Extensive regions of scar tissue were present, as indicated by a total scar score of 16.3±6.0 per patient. A significant correlation (r = 0.89; p <0.001) was observed between the SPECT total scar score and the optimal V-V interval. Figure 4 indicated that a higher scar score (representing more scar tissue), is associated with a higher level of pre-activation of the LV (patients with an optimal V-V interval of LV60 had a mean scar score of 22±3, whereas patients with an optimal V-V interval of LV20 had a mean scar score of 13±3).

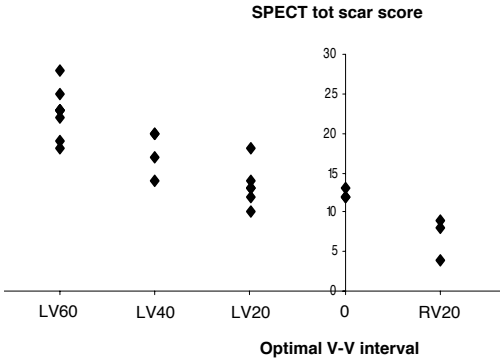


Figure 4. Correlation between the SPECT total scar score and the optimal V-V interval. $r = 0.89$, $p < 0.001$, $y = -0.19x + 10.68$

DISCUSSION

The findings of the current study can be summarized as follows: 1) Optimized sequential CRT provides a significant improvement in LV hemodynamic performance compared to conventional simultaneous stimulation. This hemodynamic improvement was associated with a significant reduction of LV dyssynchrony; 2) the increase in LVOT VTI and LVEF after implantation (simultaneous CRT) was significantly greater in non-ischemic as compared to ischemic heart failure patients. However, V-V interval optimization yielded to a larger improvement of LVOT VTI and LVEF in patients with ischemic heart failure and resulted in a comparable percentage of CRT responders in ischemic and non-ischemic heart failure patients; 3) a direct relation was observed between the extent of scar tissue and the optimal V-V interval, with a larger extent of scar tissue related to a higher level of LV pre-activation.

Simultaneous versus sequential CRT

CRT is now considered an important therapeutic option in the treatment of patients with end-stage heart failure[1], but still up to 30% of patients do not have a favorable response to CRT [18]. Since the new pacemakers allow a separate activation of the ventricular leads, several studies have investigated whether the tailored programming of V-V interval could decrease the percentage of non-responders or convert non-responders to partial or complete responders. In fact, a recent multi-center study showed that almost 50% of patients who did not exhibit a positive response to CRT had inadequate device settings (temporary VVI back-up setting) [19] and that improved LV filling and systolic function could be achieved

by optimizing the pacemaker settings. In addition, V-V optimization may also further increase the hemodynamic benefit of CRT in patients with a positive response to CRT.

Preliminary data from small single-center studies, demonstrated that optimized sequential CRT, rather than simultaneous CRT, can further improve different short-term outcomes of LV systolic performance, such as stroke volume, dP/dt, LV filling time, myocardial performance index etc [2–8]. Only few data are available on the effect of V-V optimization on LV dyssynchrony. Three trials further investigated whether there is a significant difference between optimized sequential CRT and simultaneous CRT in long-term outcome [9–11]. The InSync III study [9] showed in 397 patients that stroke volume at short-term follow-up and exercise capacity at long-term follow-up could be improved by echocardiographic optimization of the V-V interval. The DECREASE-HF trial [10] evaluated 306 patients and did not reveal a significant difference between sequential and simultaneous CRT in the improvement of LV size and function after 6 months of CRT. However, the V-V interval was programmed on the basis of intrinsic interventricular conduction measured from intracardiac electrocardiograms at the time of the implantation and was not individually optimized according to the hemodynamic response. The RHYTHM II ICD study [11] evaluated in 121 patients the improvement in clinical end-points, such as NYHA class and 6-minute walking distance, after echocardiographic optimization of the V-V interval with standard simultaneous CRT. No additional benefit was demonstrated, but the potential favorable effect on LV remodeling and function was not evaluated. These inhomogeneous results may be explained by different factors: 1) different parameters have been used to optimize the V-V interval, which included intrinsic conduction from the intracardiac electrocardiogram, invasive and non-invasive dP/dt, stroke volume, LV filling time, LV dyssynchrony and other echocardiographic parameters. No large studies have pointed out the superiority of one method of V-V optimization over another; 2) different end-points (clinical improvement versus echocardiographic improvement) have been used to evaluate the effects of V-V optimization, 3) it is possible that V-V interval optimization has a clear advantage over simultaneous CRT only in specific subgroups of patients such as those with a slow inter- and intra-ventricular conduction (e.g. after myocardial infarction with extensive scar formation).

V-V interval optimization in ischemic and non-ischemic cardiomyopathy

Recent data have suggested a slower and more attenuated response to CRT in patients with ischemic cardiomyopathy as compared to non-ischemic cardiomyopathy, probably related to repetitive episodes of ischemia or to the presence of scar tissue [12]. Initial single-center studies suggested that the amount and distribution of myocardial scar may be important determinants of response to CRT, limiting LV reverse remodeling and improvement of systolic function [20,21]. However, in these patients the best mechanical efficiency may be achieved us-

ing different pacemaker settings (and in particular the inter-ventricular activation) that might compensate for the conduction abnormalities due to the presence of ischemic and/or scar tissue.

In the current study, immediately after implantation (simultaneous pacing) a significantly better response to CRT was observed in non-ischemic patients (68% of patients with an increase ≥5% in LVEF as compared to 34% of ischemic patients). However, additional V-V optimization in patients with ischemic heart failure increased the percentage of patients with significant response to CRT from 34% to 71%. These results may be explained by the fact that the extent of myocardial scar tissue has an influence on the optimal V-V interval setting. In the current study, the presence of large areas of scar tissue was indeed related to a larger level of LV pre-activation, probably as a compensation for slow intra-ventricular conduction caused by scar tissue within the left ventricle. These findings are in line with data reported by van Gelder et al[7] showing that the mean V-V interval was significantly longer and more often with LV pre-excitation in patients with ischemic cardiomyopathy.

Study limitations

The patient cohort in the current study is relatively small, and larger populations are needed to confirm these results, particularly regarding the differences between ischemic and non-ischemic patients. In addition, the benefit of V-V interval optimization was observed acutely after CRT implantation, but the long-term effect of V-V optimization on clinical and echocardiographic outcome was not evaluated. In particular, the acute benefit of V-V optimization on LV systolic performance was assessed using LVOT VTI and LVEF; these measures were not supported by an invasive measurement but, although with a certain beat-to-beat variability, they have been previously demonstrated to be reliable and reproducible. Furthermore, in the study protocol atrio-ventricular delay optimization was not repeated after V-V delay optimization since there is no consensus so far on its potential usefulness.

CONCLUSIONS

Optimized sequential CRT provides a significant improvement of LV hemodynamic performance as compared to conventional simultaneous CRT, which is associated with a further reduction in LV dyssynchrony. Particularly in patients with ischemic heart failure, V-V interval optimization increased the response rate from 39% to 73% acutely after CRT and a larger extent of scar tissue was related to a larger level of LV pre-activation.

REFERENCES

1. Freemantle N, Tharmanathan P, Calvert MJ et al. Cardiac resynchronization for patients with heart failure due to left ventricular systolic dysfunction – a systematic review and meta-analysis. *Eur Heart J* 2006; 8:433-440.
2. Perego GB, Chianca R, Facchini M et al. Simultaneous vs. sequential biventricular pacing in dilated cardiomyopathy: an acute hemodynamic study. *Eur J Heart Fail* 2003;5:305-313.
3. Bordachar P, Lafitte S, Reuter S et al. Echocardiographic parameters of ventricular dyssynchrony validation in patients with heart failure using sequential biventricular pacing. *J Am Coll Cardiol* 2004;44:2157-2165.
4. Sogaard P, Egeblad H, Pedersen AK et al. Sequential versus simultaneous biventricular resynchronization for severe heart failure: evaluation by tissue Doppler imaging. *Circulation* 2002;106:2078-2084.
5. Porciani MC, Dondina C, Macioce R et al. Echocardiographic examination of atrioventricular and interventricular delay optimization in cardiac resynchronization therapy. Am J Cardiol 2005;95:1108-10.
6. Vanderheyden M, De Backer T, Rivero-Ayerza M et al. Tailored echocardiographic interventricular delay programming further optimizes left ventricular performance after cardiac resynchronization therapy. *Heart Rhythm* 2005;2:1066-1072.
7. van Gelder BM, Bracke FA, Meijer A et al. Effect of optimizing the VV interval on left ventricular contractility in cardiac resynchronization therapy. *Am J Cardiol* 2004;93:1500-1503.
8. Vidal B, Sitges M, Marigliano A eta l. Optimizing the programation of cardiac resynchronization therapy devices in patients with heart failure and left bundle branch block. *Am J Cardiol* 2007;100:1002-1006.
9. Leon AR, Abraham WT, Brozena S et al; InSync III Clinical Study Investigators. Cardiac resynchronization with sequential biventricular pacing for the treatment of moderate-to-severe heart failure. *J Am Coll Cardiol* 2005;46:2298-2304.
10. Rao RK, Kumar UN, Schafer J et al. Reduced ventricular volumes and improved systolic function with cardiac resynchronization therapy: a randomized trial comparing simultaneous biventricular pacing, sequential biventricular pacing, and left ventricular pacing. *Circulation* 2007;115:2136-2144.
11. Boriani G, Muller CP, Seidl KH et al; Resynchronization for the HemodYnamic Treatment for Heart Failure Management II Investigators. Randomized comparison of simultaneous biventricular stimulation versus optimized interventricular delay in cardiac resynchronization therapy. The Resynchronization for the HemodYnamic Treatment for Heart Failure Management II implantable cardioverter defibrillator (RHYTHM II ICD) study. *Am Heart J* 2006;151:1050-1058.
12. Sutton MG, Plappert T, Hilpisch KE et al . Sustained reverse left ventricular structural remodeling with cardiac resynchronization at one year is a function of etiology: quantitative Doppler echocardiographic evidence from the Multicenter InSync Randomized Clinical Evaluation (MIRACLE). *Circulation* 2006;113:266-272.
13. Kedia N, Ng K, Apperson-Hansen C et al. Usefulness of atrioventricular delay optimization using Doppler assessment of mitral inflow in patients undergoing cardiac resynchronization therapy. *Am J Cardiol* 2006;98:780-785.
14. Bleeker GB, Bax JJ, Fung JW et al. Clinical versus echocardiographic parameters to assess response to cardiac resynchronization therapy. *Am J Cardiol* 2006;97:260-263.

15. Bax JJ, Bleeker GB, Marwick TH et al. Left ventricular dyssynchrony predicts response and prognosis after cardiac resynchronization therapy. *J Am Coll Cardiol* 2004; 44:1834–1840.
16. Bleeker GB, Schalij MJ, Molhoek SG et al. Relationship between QRS duration and left ventricular dyssynchrony in patients with end-stage heart failure. *J Cardiovasc Electrophysiol* 2004;15: 544–49
17. Ypenburg C, Schalij MJ, Bleeker GB et al. Impact of viability and scar tissue on response to cardiac resynchronization therapy in ischaemic heart failure patients. *Eur Heart J* 2007;28:33-41.
18. Bax JJ, Abraham T, Barold SS et al. Cardiac resynchronization therapy: Part 1 issues before device implantation. *J Am Coll Cardiol* 2005;46:2153-2167.
19. Mullens W, Grimm RA, Verga T, et al. Insights from a cardiac resynchronization optimization clinic as part of a heart failure disease management program. *J Am Coll Cardiol* 2009;53:765-773.
20. Bleeker GB, Kaandorp TA, Lamb HJ et al. Effect of posterolateral scar tissue on clinical and echocardiographic improvement after cardiac resynchronization therapy. *Circulation* 2006;113:969-976.
21. White JA, Yee R, Yuan X et al. Delayed enhancement magnetic resonance imaging predicts response to cardiac resynchronization therapy in patients with intraventricular dyssynchrony. *J Am Coll Cardiol* 2006;48:1953-1960.

CHAPTER 26

Comparison of time course of response to cardiac resynchronization therapy in patients with ischemic versus nonischemic cardiomyopathy

N Ajmone Marsan, G B Bleeker, R J van Bommel, C Ypenburg, V Delgado, C JW Borleffs, E R Holman, E E van der Wall, M J Schalij, and J J Bax

Am J Cardiol 2009;103:690-4.

ABSTRACT

Objectives: Time course of the effects of cardiac resynchronization therapy (CRT) on left ventricular (LV) systolic function and reverse remodeling is still unknown and was the subject of this study. In particular, whether the acute benefit of CRT translates in late response was explored. Furthermore, the time course of response was compared between ischemic and non-ischemic patients.

Methods: A total of 222 consecutive heart failure patients (135 ischemic) scheduled for CRT, were included. Standard echocardiography was performed before, immediately after CRT and at 6 months follow-up (6MFU) to measure LV end-systolic (ESV) and end-diastolic (EDV) volume, and ejection fraction (EF).

Results: Immediately after CRT, a significant improvement in LVEF (from 25±8% to 31±9%, $p < 0.001$) and LVESV (from 163±68ml to 149±63ml, $p < 0.001$) was observed, followed by an additional improvement at 6MFU (to 34±9% and 132±62ml respectively, both $p < 0.001$). Significant reduction in LVEDV was observed only at 6MFU (from 217±73ml to 194±72ml, $p < 0.001$). An acute reduction in LVESV of 6% could predict response to CRT at 6MFU (defined as a reduction ≥15% in LVESV) with a sensitivity and specificity of 79% and 75%. Time course of response to CRT was similar in ischemic and non-ischemic patients, but reduction in LVESV and LVEDV was significantly greater in non-ischemic patients ($p < 0.001$).

Conclusions: The beneficial effect of CRT on LV systolic function occurs immediately after CRT, with additional improvement at 6MFU. The acute reduction in LVESV can predict response to CRT at 6MFU. Non-ischemic patients show a significantly greater LV reverse remodeling compared to ischemic patients.

INTRODUCTION

The precise time course of improvement in left ventricular (LV) function and reduction in LV volumes after cardiac resynchronization therapy (CRT) is currently unknown and was subject of the current study. For this purpose, 230 patients underwent sequential echocardiography before, 1 day and 6 months after CRT implantation. Moreover, the current study explored whether it could be possible that an acute improvement in systolic function predicts reverse remodeling at late follow-up. Finally, the time course of improvement in systolic function and reverse remodeling may be different between patients with ischemic and non-ischemic cardiomyopathy and this was also evaluated in the current study.

METHODS

A total of 230 consecutive heart failure patients, scheduled for implantation of a CRT device, were included. Traditional selection criteria for CRT were applied [1], including: New York Heart Association (NYHA) functional class III or IV, despite optimal medical therapy; LV ejection fraction (EF) ≤35% and QRS duration ≥120 ms. Patients with a recent myocardial infarction (<3 months) or decompensated heart failure were excluded. Clinical status, including assessment of NYHA class, Minnesota quality-of-life score and 6-minute walk test, was assessed before pacemaker implantation and at 6-months follow-up. QRS duration was measured at baseline, immediately after CRT and at 6 months follow-up from the surface ECG using the widest QRS complex from the leads II, V1 and V6. Moreover, 2D echocardiography was performed before and immediately after pacemaker implantation and repeated at 6 months follow-up to evaluate LV volumes and LVEF.

Patients were imaged in the left lateral decubitus position using a commercially available system (Vingmed Vivid Seven, General Electric Healthcare, Horten, Norway). Images were obtained using a 3.5-MHz transducer, at a depth of 16 cm in the standard apical views. All images were recorded digitally in cine-loop format and analyzed offline with commercial software Echopac 7.0.0 (GE Healthcare). LV end-systolic volume (ESV) and LV end-diastolic volume (EDV) were determined from the conventional apical 2- and 4-chamber views and LVEF was calculated using the biplane Simpson's technique [2]. Inter- and intra-observer agreement for assessment of LV function and volumes were 90% and 96% respectively [3].

Echocardiographic response was defined as an improvement ≥15% in LVESV [4]. Response was determined acutely after CRT implantation and at 6 months follow-up.

The LV pacing lead was inserted transvenously via the subclavian route. First, a coronary sinus venogram was obtained using a balloon catheter. Next, the LV pacing lead was inserted through the coronary sinus, using an 8Fr-guiding catheter, and positioned as far as possible in the venous system, preferably in the (postero-) lateral vein. The right atrial and ventricular

leads were positioned conventionally. When an indication for an internal defibrillator existed, a combined device was implanted (Contak CD or Renewal, Guidant Corp.; Insync III-CD or Marquis, Medtronic Inc.). In all patients the implantation was successful without major complications. Two types of LV leads were used (Easytrak 4512-80, Guidant Corp., or Attain-SD 4194, Medtronic Inc.). For each patient, the AV interval was adjusted to maximize mitral inflow duration with pulsed-wave Doppler echocardiography [5].

Continuous data are presented as mean±standard deviation; dichotomous data are presented as numbers and percentage. Comparison of data was performed using the paired or unpaired Student *t* test or χ^2 test when appropriate. For the LVESV and LVEDV, that were not normally distributed, a log-transformation has been performed. Sequential data measurements, in the total population and in the groups of patients with and without ischemic cardiomyopathy, were analyzed by repeated measures analysis of variance (ANOVA). A two-way ANOVA analysis was performed for comparison of time trends between patients with and without ischemic cardiomyopathy. To determine the relationship between immediate changes in LVESV after CRT and response to CRT at late follow-up (defined as a reduction ≥15% in LVESV), multivariable logistic regression analysis was applied including patient's clinical and echocardiographic characteristics at baseline (odds ratios with their corresponding 95% confidence intervals [CI] are reported). Receiver operating characteristic (ROC) curve analysis was also applied to obtain a cut-off value for the acute percentage change in LVESV (acute delta LVESV) that can be used in clinical practice to predict echocardiographic response to CRT at late follow-up. The 'optimal' threshold was defined as the value for which the sum of sensitivity and specificity to distinguish between echocardiographic responders/non-responders was maximized. Statistical significance was set a two tailed p-value <0.05. A statistical software program SPSS 12.0 (SPSS Inc, Chicago, Il, USA) was used for statistical analysis.

RESULTS

A total of 8 (3.5%) patients died before the 6-month follow-up was completed. Baseline characteristics of the remaining 222 patients (180 men, mean age 66±10 years) are summarized in Table 1. Most patients (94%) were in NYHA class III. Echocardiographic evaluation revealed LV dilatation with depressed LVEF.

A significant improvement in clinical status was observed at 6 months follow-up. In particular, NYHA class improved significantly from 3.1±0.3 to 1.9±0.7 (p <0.01). A total of 71% of patients exhibited a reduction in NYHA class of 1 score or more. Furthermore, the Minnesota quality-of-life score improved from 33±19 to 24±19 (p <0.01) and the 6-minute walking distance increased from 324±106 m to 392±108 m (p <0.01). QRS duration at baseline was

Table 1. Baseline characteristics of the study population (n = 222).

Age (years)	66±10
Male/Female	180/42
NYHA class	
III	208 (94%)
IV	14 (6%)
6-minutes walk test (m)	328±107
Quality of life score	31±19
QRS duration (ms)	153±26
Rhythm	
Sinus rhythm	211 (95%)
Atrial fibrillation	11 (5%)
Etiology	
Ischemic	135 (61%)
Non-ischemic	87 (39%)
Left ventricular ejection fraction (%)	25±8
Left ventricular end-diastolic volume (ml)	217±77
Left ventricular end-systolic volume (ml)	163±68
Medication	
ACE inhibitors	194 (87%)
ß-blockers	173 (78%)
Diuretics and/or spironolactone	214 (96%)
Amiodarone	47 (21%)

153±26 ms and decreased to 136±26 ms ($p < 0.01$) immediately after CRT implantation, which remained unchanged at 6 months follow-up (136±28 ms).

Acutely after CRT implantation, a significant reduction in LVESV was observed (from 163±68 ml to 149±63 ml, $p < 0.001$), with a significant improvement in LVEF (from 25±8% to 31±9%, $p < 0.001$). LVEDV remained unchanged (217±77 ml at baseline vs. 216±76 ml after CRT implantation, p = NS).

At 6 months follow-up, a further reduction in LVESV to 132±62 ml ($p < 0.001$ vs. baseline and immediate follow-up) was noted, with an additional improvement in LVEF to 34±9% ($p < 0.001$ vs. baseline and immediate follow-up). LVEDV also showed a significant reduction to 194±72 ml ($p < 0.001$ vs. baseline and immediate follow-up) at 6 months follow-up.

When a reduction in LV end-systolic volume ≥15% was used to define response to CRT, 40% of patients exhibited an immediate response to CRT, with an additional 23% of patients showing response at 6 months follow-up, resulting in a total of 63% echocardiographic responders to CRT.

Table 2 shows the results of the multivariable logistic regression analysis applied to identify whether the acute changes in LVESV after CRT and the baseline clinical and echocardiographic variables were related to response to CRT at late follow-up. After correction for the covariates, the only variables that remained significantly correlated with late response to CRT were the etiology of cardiomyopathy (OR = 0.28, 95%CI 0.13-0.63, p = 0.002) and the acute percentage

Table 2. Multivariable logistic regression analysis: estimates of correlation between the baseline clinical and echocardiographic characteristics (including the acute changes in left ventricular end-systolic volume) and response to cardiac resynchronization therapy, defined as a reduction ≥15% of left ventricular end-systolic volume at 6 month follow-up.

	Odds ratio (95% CI)	p-value
Age	0.99 (0.95-1.03)	0.74
Male gender	1.28 (0.48-3.41)	0.62
6-minute walk test	1.00 (0.99-1.00)	0.95
QRS duration	0.98 (0.97-1.01)	0.075
Ischemic etiology	0.28 (0.13-0.63)	0.002
Left ventricular ejection fraction	0.99 (0.94-1.04)	0.75
Left ventricular end-diastolic volume	0.99 (0.99-1.00)	0.56
Acute delta left ventricular end-systolic volume	1.21 (1.14-1.26)	<0.001

change in LVESV (acute delta LVESV, OR = 1.21, 95%CI 1.14-1.26, p <0.001). Furthermore, ROC curve analysis revealed that a cut-off value of 6% for acute delta LVESV yielded a sensitivity of 79% with a specificity of 75% to predict echocardiographic response to CRT (area under the curve = 0.85, p <0.001) (Figure 1).

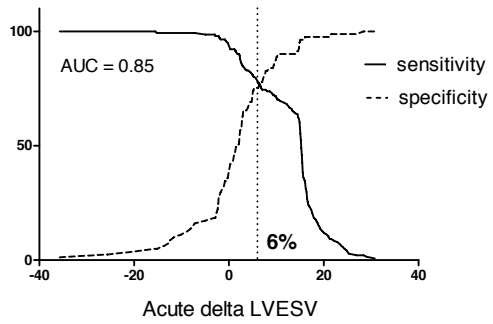


Figure 1. Optimal cut-off value of the percentage change in left ventricular end-systolic volume immediately after CRT (acute delta LVESV = [(LVESVat baseline – LVESVacutely after CRT)/LVESVat baseline] x 100) to predict echocardiographic response to CRT at late follow-up, determined by ROC curve analysis. AUC = area under the curve.

Of the 222 patients included, 135 (61%) patients had ischemic cardiomyopathy and 87 (39%) had non-ischemic cardiomyopathy. No significant differences in the baseline characteristics were noted between the 2 groups (Table 3). The immediate changes after CRT in LV volumes and LVEF in patients with ischemic cardiomyopathy are shown in Figure 2 (panels A to C). Immediately after CRT implantation, a significant reduction in LVESV (from 163±65 ml to 150±61 ml, p <0.001) and an improvement in LVEF (from 25±8% to 31±9%, p <0.001) were observed. LVEDV remained unchanged (217±74 ml vs. 217±73 ml, p = NS).

At 6 months follow-up, a further reduction in LVESV to 139±59 ml (p <0.001 vs. baseline and immediate follow-up) was detected (Figure 2, panel A). Similarly, a further improvement

Table 3. Baseline characteristics of patients with ischemic cardiomyopathy and non-ischemic cardiomyopathy.

Variable	Ischemic (n = 135)	Non-ischemic (n = 87)
Age (years)	65±10	67±17
Male/Female	57/3	28/7
QRS duration (ms)	143±28	153±33
NYHA class III/IV (n)	62/3	34/1
Left ventricular ejection fraction (%)	25±8	25±8
Left ventricular end-diastolic volume (ml)	217±74	217±82
Left ventricular end-systolic volume (ml)	163±65	163±74

in LVEF to 33±10% (p <0.001 vs. baseline and immediate follow-up) was noted (Figure 2, panel B). In addition, a reduction in LVEDV to 202±68 ml was observed (p <0.001 vs. baseline and immediate follow-up) (see Figure 2, panel C).

In 32% of patients with ischemic cardiomyopathy, an acute reduction in LVESV ≥15% was noted; at 6 months follow-up, an additional 22% showed a significant reduction in LVESV, resulting in a total of 54% echocardiographic responders to CRT out of 135 patients with ischemic cardiomyopathy.

The immediate changes after CRT in LV volumes and LVEF in patients with non-ischemic cardiomyopathy are displayed in Figure 2 (panels A to C). Immediately after CRT implantation, a significant improvement in LVESV (from 163±74 ml to 146±68 ml, p <0.001) and LVEF (from 25±8% to 32±8%, p <0.001) were observed. LVEDV remained unchanged (217±82 ml vs. 215±81 ml, p = NS).

At 6 months follow-up, a further reduction in LVESV to 122±64 ml (p <0.001 vs. baseline and immediate follow-up) was detected (Figure 2, panel A). Similarly, a further improvement in LVEF to 35±8% (p <0.001 vs. baseline and immediate follow-up) was noted (Figure 2, panel B). In addition, a reduction in LVEDV to 184±78 ml was observed (p <0.001 vs. baseline and immediate follow-up) (Figure 2, panel C).

In 53% of patients with non-ischemic cardiomyopathy an acute reduction in LVESV ≥15% was noted (p <0.05 vs. 32% of acute responders with ischemic cardiomyopathy); at 6 months follow-up, an additional 25% of patients showed a significant reduction in LVESV, resulting in a total of 78% echocardiographic responders to CRT out of 87 patients with non-ischemic cardiomyopathy (p <0.05 vs. 54% of late responders with ischemic cardiomyopathy).

A significant difference in time course after CRT implantation between ischemic and non-ischemic patients was observed for LVESV and LVEDV (Figure 2): the improvement over time of these parameters was more outspoken in patients with non-ischemic cardiomyopathy, particularly at late follow-up (two-way ANOVA p <0.001). No significant difference was found for the changes over time of LVEF between the 2 groups (Figure 2).

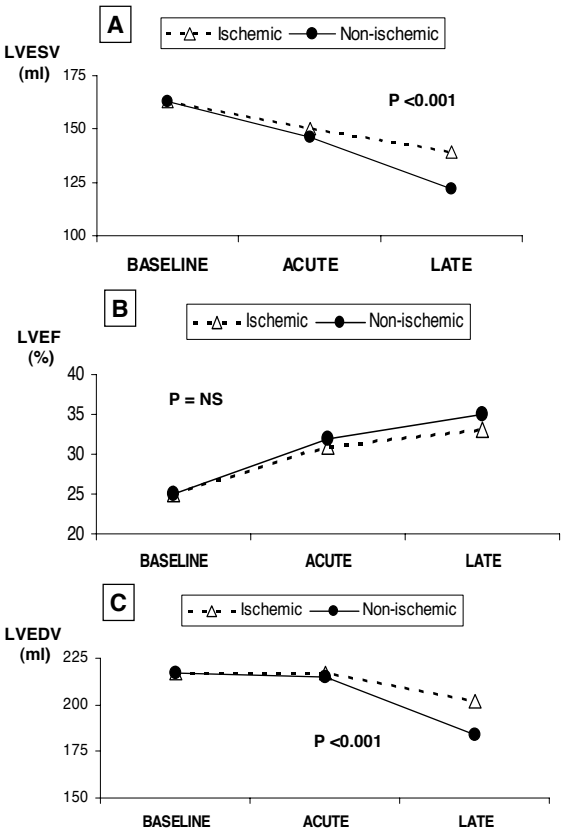


Figure 2. Comparison of the time course of changes in left ventricular (LV) volumes and function after CRT in patients with ischemic and non-ischemic cardiomyopathy.

Panel A. Both in patients with ischemic and non-ischemic cardiomyopathy, LV end-systolic volume (ESV) improved immediately after CRT (ACUTE) and at 6 months follow-up (LATE). The reduction in LVESV was significantly larger in patients with non-ischemic cardiomyopathy.

Panel B. Both in patients with ischemic and non-ischemic cardiomyopathy, LV ejection fraction (EF) improved significantly immediately after implantation and at 6 months follow-up; the LVEF at 6 months follow-up was not significantly different between patients with ischemic and non-ischemic cardiomyopathy.

Panel C. Both in patients with ischemic and non-ischemic cardiomyopathy, LV end-diastolic volume (LVEDV) did not change acutely after CRT, but revealed a significant reduction at 6 months follow-up, which was significantly larger in patients with non-ischemic cardiomyopathy.

DISCUSSION

Thus far, most of the studies addressed the effects of CRT on LV systolic function and LV reverse remodeling at mid- or long-term follow-up [6]. Both an absolute increase >5% in LVEF and a reduction ≥15% in LVESV have been used to define a favorable response to CRT [4,6,7]. Few studies focused on the acute effects of CRT [8–13]. Breithardt et al [8] demonstrated a significant increase in dP/dt_{max} immediately after CRT, while Dohi and coworkers [9] defined acute response to CRT as an increase ≥15% in LV stroke volume. Other studies applied a definition

of acute response as a reduction ≥15% in LVESV [12,13], but did not include information on long-term follow-up.

Accordingly, the precise time course of response to CRT is currently unknown. It is unclear whether improvement of LV systolic function after CRT implantation is a gradual process or whether this improvement occurs immediately and then remains unchanged, or whether some patients may not respond acutely, but do respond at later stage.

The current study evaluated the precise time course of response to CRT, systematically looking at parameters of LV systolic function (LVEF, LVESV) and LV remodeling (LVEDV, LVESV). Acutely after implantation, a significant increase in LVEF and a decrease in LVESV were observed, followed by an additional improvement in these parameters at 6 months follow-up. Of note, significant reduction in LVEDV only occurred at late follow-up. The acute improvement after CRT implantation probably indicates a pure effect of CRT on cardiac systolic performance, reflected in the changes in LVEF and LVESV (but not in LVEDV). Conversely, late improvement is the result of significant LV reverse remodeling (with a reduction in both LVEDV and LVESV) with a further improvement in LV systolic function. Indeed, the beneficial effect of CRT on LV remodeling (with changes in cardiac structure and geometry) needs more time to occur.

In clinical practice, it is important to identify whether a patient responds to CRT or not, particularly in terms of LV systolic function. In fact, an improvement in LV systolic function is most likely the base for a clinical improvement and it has been demonstrated to be the best predictor of improved survival after CRT [14]. Furthermore, the possibility to predict a significant improvement in LV systolic function (i.e. response to CRT) at long-term follow-up through the evaluation of the acute effects of CRT may be of great interest, with important implications for patient management. In the current study, the acute percentage change in LVESV was found to be an independent predictor of response to CRT at long-term follow-up, defined as a reduction ≥15% in LVESV. In particular, a reduction of 6% in LVESV immediately after implantation could predict response to CRT at late follow-up with a sensitivity of 79% and specificity of 75%.

The difference in response to CRT between patients with ischemic and non-ischemic cardiomyopathy has been a matter of debate. Additional analyses from the MUSTIC and MIRACLE [15,16] trials revealed that at mid- and long-term follow-up after CRT, the improvement in LV systolic function and LV reverse remodeling are significantly greater in patients with non-ischemic cardiomyopathy as compared to patients with ischemic cardiomyopathy.

In the present study, the time course of response to CRT was evaluated in patients with ischemic and non-ischemic cardiomyopathy. Both groups showed a similar trend over time with an immediate improvement in LVESV and LVEF, followed by an additional improvement at late follow-up, and a reduction of LVEDV only at late follow-up. However, the reduction in LVESV and LVEDV was significantly greater in patients with non-ischemic cardiomyopathy as compared to patients with ischemic cardiomyopathy, particularly at late follow-up. This

finding is probably related to the presence of more myocardial scar tissue in patients with ischemic cardiomyopathy that may limit the extent of LV reverse remodeling [17–19].

According to the abovementioned definition of response to CRT, patients with non-ischemic cardiomyopathy also showed a significantly higher percentage of responders both at acute (53% vs. 32%) and late (78% vs. 54%) follow-up. Furthermore, etiology of cardiomyopathy was found to be an independent predictor of response to CRT at long-term follow-up at the multivariable logistic regression analysis.

In the current study, the acute and late effects of CRT on LV diastolic function and on right ventricular remodeling and function were not analyzed. Furthermore, the results on LV volumes and function need to be confirmed in larger multi-center studies and eventually in comparison with a control group.

REFERENCES

1. Hunt SA, Abraham WT, Chin MH et al. ACC/AHA 2005 Guideline Update for the Diagnosis and Management of Chronic Heart Failure in the Adult: a report of the American College of Cardiology/American Heart Association Task Force on Practice Guidelines (Writing Committee to Update the 2001 Guidelines for the Evaluation and Management of Heart Failure): developed in collaboration with the American College of Chest Physicians and the International Society for Heart and Lung Transplantation: endorsed by the Heart Rhythm Society. *Circulation.* 2005;112:e154-e235.
2. Lang RM, Bierig M, Devereux RB et al. Recommendations for chamber quantification. *Eur J Echocardiogr.* 2006;7:79-108.
3. Bleeker GB, Schalij MJ, Molhoek SG et al. Relationship between QRS duration and left ventricular dyssynchrony in patients with end-stage heart failure. *J Cardiovasc Electrophysiol.* 2004;15:544-549.
4. Yu CM, Abraham WT, Bax J et al. Predictors of response to cardiac resynchronization therapy (PROSPECT)--study design. *Am Heart J.* 2005;149:600-605.
5. Kedia N, Ng K, pperson-Hansen C et al. Usefulness of atrioventricular delay optimization using Doppler assessment of mitral inflow in patients undergoing cardiac resynchronization therapy. *Am J Cardiol.* 2006;98:780-785.
6. Bax JJ, Abraham T, Barold SS et al. Cardiac resynchronization therapy: Part 1--issues before device implantation. *J Am Coll Cardiol.* 2005;46:2153-2167.
7. Bleeker GB, Bax JJ, Fung JW et al. Clinical versus echocardiographic parameters to assess response to cardiac resynchronization therapy. *Am J Cardiol.* 2006;97:260-263.
8. Breithardt OA, Stellbrink C, Kramer AP et al. Echocardiographic quantification of left ventricular asynchrony predicts an acute hemodynamic benefit of cardiac resynchronization therapy. *J Am Coll Cardiol.* 2002;40:536-545.
9. Dohi K, Suffoletto MS, Schwartzman D, Ganz L, Pinsky MR, Gorcsan J, III. Utility of echocardiographic radial strain imaging to quantify left ventricular dyssynchrony and predict acute response to cardiac resynchronization therapy. *Am J Cardiol.* 2005;96:112-116.
10. Gorcsan J, III, Kanzaki H, Bazaz R, Dohi K, Schwartzman D. Usefulness of echocardiographic tissue synchronization imaging to predict acute response to cardiac resynchronization therapy. *Am J Cardiol.* 2004;93:1178-1181.
11. Kass DA, Chen CH, Curry C et al. Improved left ventricular mechanics from acute VDD pacing in patients with dilated cardiomyopathy and ventricular conduction delay. *Circulation.* 1999;99:1567-1573.
12. Marsan NA, Bleeker GB, Ypenburg C et al. Real-time three-dimensional echocardiography permits quantification of left ventricular mechanical dyssynchrony and predicts acute response to cardiac resynchronization therapy. *J Cardiovasc Electrophysiol.* 2008;19:392-399.
13. Veire van de N, Bleeker GB, Ypenburg C et al. Usefulness of triplane tissue Doppler imaging to predict acute response to cardiac resynchronization therapy. *Am J Cardiol.* 2007;100:476-482.
14. Yu CM, Bleeker GB, Fung JW et al. Left ventricular reverse remodeling but not clinical improvement predicts long-term survival after cardiac resynchronization therapy. *Circulation.* 2005;112:1580-1586.
15. Duncan A, Wait D, Gibson D, Daubert JC. Left ventricular remodelling and haemodynamic effects of multisite biventricular pacing in patients with left ventricular systolic dysfunction and activation disturbances in sinus rhythm: sub-study of the MUSTIC (Multisite Stimulationin Cardiomyopathies) trial. *Eur Heart J.* 2003;24:430-441.

16. Sutton MG, Plappert T, Hilpisch KE, Abraham WT, Hayes DL, Chinchoy E. Sustained reverse left ventricular structural remodeling with cardiac resynchronization at one year is a function of etiology: quantitative Doppler echocardiographic evidence from the Multicenter InSync Randomized Clinical Evaluation (MIRACLE). *Circulation.* 2006;113:266-272.
17. Chalil S, Foley PW, Muyhaldeen SA et al. Late gadolinium enhancement-cardiovascular magnetic resonance as a predictor of response to cardiac resynchronization therapy in patients with ischaemic cardiomyopathy. *Europace.* 2007;9:1031-1037.
18. White JA, Yee R, Yuan X et al. Delayed enhancement magnetic resonance imaging predicts response to cardiac resynchronization therapy in patients with intraventricular dyssynchrony. *J Am Coll Cardiol.* 2006;48:1953-1960.
19. Ypenburg C, Roes SD, Bleeker GB et al. Effect of total scar burden on contrast-enhanced magnetic resonance imaging on response to cardiac resynchronization therapy. *Am J Cardiol.* 2007;99:657-660.

Summary and Conclusions

SUMMARY AND CONCLUSIONS

The general introduction of the thesis outlines the current and future role of advanced cardiac imaging modalities, such as RT3DE, myocardial deformation imaging, contrast-enhanced echocardiography and CMR, in the diagnostic process and for clinical decision-making. The main applications are described in heart failure patients referred for CRT, in patients with acute myocardial infarction and in patients with functional mitral regurgitation.

Part I

The first part of the thesis evaluates the incremental value of RT3DE over conventional echocardiography for the quantification of cardiac chambers size and function. **Part IA** focuses on the use of this technique for the assessment of LV volumes and EF and for the quantification of LV dyssynchrony. In heart failure patients, acquisition and analysis of RT3DE dataset is shown to be feasible and reproducible even in patients with severely dilated LV, and provides quantitative information on both LV volumes and LV dyssynchrony in one single analysis. This is of great importance particularly in patients candidate for CRT, in whom accurate and reliable assessment of changes in LV size and function is crucial for the evaluation of therapy success (mainly as LV reverse remodeling). In addition, direct echocardiographic assessment of LV dyssynchrony might improve CRT patient selection over traditional selection criteria, based on which approximately 30% of patients do no show favorable response after implantation. Using RT3DE, LV dyssynchrony measurement is based on the analysis of regional volumetric changes over time and quantified as the standard deviation of the time to minimum systolic volume of 16 standard LV segments (expressed as percentage of the cardiac cycle - systolic dyssynchrony index, SDI). This LV dyssynchrony index was shown to be a good predictor of echocardiographic response to CRT, with high sensitivity and specificity (see Chapter 3 but also Chapter 9, Part IB). Main advantages of this approach are also represented by a good reproducibility, due to the semi-automated analysis, and by the possibility of simultaneous evaluation of all myocardial segments with a rapid identification of the area of latest activation. The measure of SDI was also found to correlate well with LV dyssynchrony measured by gated myocardial perfusion single photon emission computed tomography (GMPS) with phase analysis (Chapter 4), which is also a 3D nuclear imaging technique previously validated for assessment of LV dyssynchrony.

For a better interpretation and application of different indices of LV dyssynchrony, normal reference values for the measurements obtained by RT3DE (but also TDI and CMR) are provided in Chapter 5. It appears that for all LV segments, longitudinal peak systolic velocity and strain rate are early systolic events, while peak systolic longitudinal displacement and strain occur in late systole, or in 20-30% of segments, during isovolumic relaxation time (similarly

to minimum systolic volume and maximum myocardial thickness). These measures therefore reflect different cardiac mechanical events and can be combined to provide more robust information on LV dyssynchrony.

A 3D dataset can also be displayed in a tri-plane modality, with simultaneous visualization of the 3 apical views. This approach can therefore also be used for the calculation of LV volumes and EF (with more accurate measures as compared to the bi-plane method) and for the assessment of LV dyssynchrony. Tri-plane TDI can in fact measure LV dyssynchrony as the standard deviation of time to peak myocardial systolic velocity in 12 LV segments (Ts-SD-12), which demonstrated a good correlation with GMPS (Chapter 6) and to predict LV reverse remodeling 6 months after CRT with good sensitivity and specificity (Chapter 7). This approach also showed to be able to rapidly identify the area of latest activation, which is of importance for the evaluation of the effect of CRT in the presence of a match with the LV pacing lead position (assessed by multi detector computer tomography, Chapter 8).

In **Part IB**, RT3DE is proposed as a novel, reliable technique for the assessment of left atrial size and function, providing unique information about phasic changes of left atrium volumes during the cardiac cycle. In patients undergoing CRT, RT3DE showed significant left atrium reverse remodeling after implantation, together with an improvement in left atrium total emptying fraction, conduit and reservoir function (Chapter 9). In patients undergoing radiofrequency catheter ablation for atrial fibrillation, RT3DE demonstrated that 3 months after the procedure, a significant reduction in left atrium volumes and a clear improvement in left atrium active contraction and reservoir function occurred only in patients without recurrences of atrial fibrillation (Chapter 10).

Part II

In this part of the thesis, a large group of patients was studied with contrast-enhanced echocardiography within 48 hours after admission for acute myocardial infarction and percutaneous coronary intervention. Since safety data on the use of this technique in acutely and critically ill patients is lacking, we reported that major adverse events were not observed, whereas minor events occurred in 4% of patients (Chapter 11). However, larger patient cohorts are needed to confirm these findings.

In addition, RT3DE acquisitions were performed with and without contrast, demonstrating that the administration of contrast agents in these patients is of incremental value, improving endocardial border visualization and reproducibility of LV function assessment (Chapter 12).

Finally, this technique also allows for the evaluation of myocardial perfusion and therefore of myocardial infarction extension, which is a fundamental parameter to take into account in the evaluation of cardiac mechanics at short- and long-term follow-up after myocardial infarction. In fact, LV function immediately after infarction was demonstrated to be inde-

pendently associated with infarct size, but also with LV dyssynchrony and LV twist (with a reduction of both basal and apical rotations). In particular, impairment of LV twist early after acute myocardial infarction was significantly and independently related to the occurrence of LV remodeling at 6-month follow-up, representing a sensitive global parameter of LV systolic performance after infarction.

Part III

In this part of the thesis, novel applications of CMR are evaluated in patients with heart failure and in patients with functional mitral regurgitation. In **Part IIIA,** different approaches for the measure of LV dyssynchrony using CMR are proposed. Velocity-encoded CMR, commonly used to perform flow measurements, can be applied for myocardial velocity analysis, similar to TDI. A strong correlation was found between TDI and velocity-encoded CMR for the assessment of myocardial peak systolic and diastolic velocities and their respective timings, with a small bias between the 2 techniques. Importantly, a strong agreement between the 2 techniques was also observed when patients were categorized according to the severity of LV dyssynchrony and LV diastolic function (using the E/E' ratio) (Chapter 15).

Another potential approach to quantify LV dyssynchrony is applied in patients referred for CRT using a standard cine-set of short-axis slices (therefore without specific acquisitions), in which endocardial and epicardial contours are identified and the changes in myocardial radial thickness over time (= myocardial deformation) are evaluated. The standard deviation of 16 segments time-to-maximum wall thickness (SDt-16) showed to be an important predictor of significant LV reverse remodeling after CRT, together with the extension of myocardial infarction. This is therefore the first study to evaluate the relative merits of these 2 important parameters (both measured by CMR) to improve CRT patient selection (Chapter 16).

CMR represents a unique approach for a comprehensive evaluation of heart failure patients, including quantification of cardiac chamber size and function and the assessment of LV dyssynchrony and myocardial viability (as demonstrated also in comparison with ^{99}mTc-tetrofosmin and ^{18}F-fluorodeoxyglucose single photon emission computed tomography, Chapter 17). It is therefore considered the reference technique for patients with LV aneurysm referred for surgical ventricular reconstruction, since accurate measures of LV shape, size, and global and regional function, together with the assessment of myocardial scar and mitral regurgitation severity are necessary to give the correct indication and plan the surgical procedure. RT3DE showed to be a potential accurate alternative imaging modality for this evaluation (Chapter 18).

In **Part IIIB**, 3D 3-directional velocity encoded CMR is applied in 64 patients with functional mitral regurgitation in a head-to-head comparison with RT3DE. A strong correlation was observed between RT3DE and CMR for the measurement of mitral regurgitant volume, with no

significant bias between these 2 techniques; conversely, 2D echocardiography significantly underestimated regurgitant volume as compared to CMR. These results are related to the fact that conventional echocardiography measures the effective regurgitant orifice area (EROA) based on the assumption of a circular shape. However, in patients with functional mitral regurgitation, the orifice is typically elongated along the semilunar-shaped leaflet coaptation line, leading to a significant underestimation when measured from the 4-chamber or parasternal long-axis views.

Part IV

Novel physiopathological aspects in CRT patients are studied in the last part of the thesis using advanced echocardiographic imaging modalities. The effect of CRT on LV rotational mechanics was evaluated in 80 heart failure patients (Chapter 22). A substantial improvement in LV twist was observed immediately after implantation only in patients who showed significant LV reverse remodeling at long-term follow-up, and therefore it strongly predicted favourable response to CRT. In addition, LV twist significantly improved in patients with an apical and midventricular, but not with a basal LV lead position. These results suggest that CRT may (partially) restore LV twist, possibly by providing a more physiological electrical depolarization (directed from the apex toward the base) and mechanical contraction of the myofibers.

CRT might also be considered as a potential therapeutic option in patients with heart failure and severe functional mitral regurgitation, who are not referred or denied for surgery due to their high operative risk. We were able to demonstrate in fact that when these patients are referred to CRT, a significant improvement of mitral regurgitation can be observed in approximately 50% of the cases, and that the improvement in mitral regurgitation resulted in superior long-term survival after CRT (Chapter 23).

Cerebral blood flow is decreased in symptomatic patients with heart failure, and it might contribute to the impaired cognitive performance frequently observed in these patients. We studied the effect of CRT on cerebral blood flow using transcranial Doppler in 35 patients before and 6 months after implantation, and in a control group of 15 heart failure patients who were not referred for CRT. A significant increase in cerebral blood flow was observed after CRT and it was strongly correlated with the improvement in LV function (Chapter 24).

Whether sequential biventricular pacing provides substantial benefits over conventional simultaneous stimulation was also explored in this part of the thesis, including ischemic and non-ischemic heart failure patients referred to CRT. Optimized sequential pacing provided a significant improvement in LV systolic performance and a significant reduction in LV dyssynchrony as compared to simultaneous stimulation. Although the absolute increase in LV EF after implantation was greater in non-ischemic as compared to ischemic patients,

inter-ventricular (V-V) interval optimization yielded a larger improvement in LV systolic performance in ischemic patients. In particular, a significant correlation between LV scar tissue and optimal V-V interval was observed, with a larger extent of scar related to a larger level of LV pre-activation, probably reflecting a compensation for a slow intra-LV conduction caused by scar tissue (Chapter 25).

In the last Chapter of the thesis, the time course of the effect of CRT on LV systolic function and reverse remodeling was evaluated in ischemic and non-ischemic heart failure patients. The beneficial effect of CRT on LV systolic function was observed immediately after CRT, but with additional improvement at 6-month follow-up. In particular, an acute decrease in LV end-systolic volume could predict echocardiographic response to CRT at 6-month follow-up with good sensitivity and specificity. Time course of response to CRT was similar between the 2 groups, but LV reverse remodeling was greater in non-ischemic as compared to ischemic patients, in whom it was probably limited by the presence of significant scar tissue.

CONCLUSIONS

Advanced cardiac imaging modalities play a crucial role in the diagnostic process and clinical management of patients with different cardiac diseases, including heart failure, valvular heart disease, myocardial infarction and atrial fibrillation. RT3DE has made an important transition from a research tool to a clinically applicable imaging technique and has been demonstrated to provide important advantages over conventional 2D echocardiography, such as a more accurate quantification of cardiac chamber size and function and the possibility of unlimited image plane orientations for better understanding of valvular heart diseases. Therefore, it is likely that RT3DE will become a routine part of most echocardiographic examinations.

Contrast-enhanced echocardiography should be performed in every patient with suboptimal acoustic window, especially with RT3DE. Importantly, in patients underwent primary percutaneous coronary intervention, perfusion analysis can provide an accurate estimate of myocardial infarction size, which is crucial information for the patient management, together with more sophisticated assessment of LV mechanics. Myocardial deformation imaging has witnessed an enormous development in the last years and is now considered an accurate tool for a more sensitive assessment of LV regional and global function and for a more detailed assessment of LV mechanics and dyssynchrony.

CMR represents the reference imaging modality for the quantification of LV volumes and function and for the identification of myocardial scar/fibrosis. It should be therefore considered for a comprehensive evaluation of heart failure patients, including more novel and sophisticated assessments of transvalvular flow and LV dyssynchrony.

Advanced cardiac imaging modalities can be applied in heart failure patients referred for CRT to explore novel physiopathological aspects, such as the effect on LV rotation mechanics, on functional mitral regurgitation and cerebral blood flow.

Samenvatting en Conclusies

SAMENVATTING EN CONCLUSIES

In de introductie van dit proefschrift wordt een overzicht gegeven van de huidige en toekomstige rol van geavanceerde beeldvormende technieken, in het bijzonder RT3DE, strain analyse, contrast echocardiografie en cardiale MRI, zowel voor diagnostiek als klinische besluitvorming. De voornaamste toepassingen worden beschreven bij patiënten met hartfalen die zijn verwezen voor CRT, patiënten met een acuut myocard infarct en patiënten met functionele mitralis insufficiëntie.

Deel I

In het eerste deel van dit proefschrift wordt de toegevoegde waarde van RT3DE boven conventionele echocardiografie voor de bepaling van de grootte en functie van de verschillende hartkamers geëvalueerd.

Deel IA richt zich voornamelijk op het gebruik van deze techniek voor de beoordeling van LV volumes en EF en voor het kwantificeren van LV dissynchronie. In patiënten met hartfalen is de acquisitie en analyse van een RT3DE dataset uitvoerbaar en reproduceerbaar, zelfs in patiënten met een zeer gedilateerde LV. Deze RT3DE dataset geeft kwantitatieve informatie over zowel LV volumes als LV dissynchronie in één enkele analyse. Dit is in het bijzonder van belang voor patiënten die in aanmerking komen voor CRT, aangezien hier een accurate en betrouwbare bepaling van veranderingen in LV grootte en functie van cruciaal belang is om het effect van de therapie te evalueren. Verder zou echocardiografische bepaling van LV dissynchronie de selectie van patiënten voor CRT kunnen verbeteren boven de huidige selectie criteria, aangezien onder deze criteria ongeveer 30% van de patiënten geen goede response heeft na implantatie. Met RT3DE wordt de mate van LV dissynchronie gebaseerd op de analyse van lokale volumeveranderingen in de tijd, gekwantificeerd als de standaarddeviatie van de tijd tot kleinste systolische volume van 16 standaard LV segmenten en uitgedrukt als een percentage van de hartcyclus (systolische dissynchronie index, SDI). Deze index blijkt een goede voorspeller van echocardiografische response op CRT, met een hoge sensitiviteit en specificiteit (zie ook Hoofdstuk 9, Deel 1B). De grootste voordelen van deze methode zijn verder de hoge reproduceerbaarheid als gevolg van de semigeautomatiseerde analyse, en de mogelijkheid tot gelijktijdige beoordeling van alle segmenten met een eenvoudige identificatie van het laatst geactiveerde segment. De mate van SDI bleek ook goed te correleren met LV dissynchronie gemeten met een andere gevalideerde 3D techniek voor het bepalen van LV dissynchronie: "gated myocardial perfusion single photon emission computed tomography" (GMPS) met fase analyse (Hoofdstuk 4). Voor een betere interpretatie van deze indexen van LV dissynchronie worden normaalwaarden verstrekt voor de verschillende metingen met RT3DE, maar ook met TDI and cardiale MRI. Het blijkt dat voor alle LV segmenten,

longitudinale piek systolische snelheid en strain rate vroeg in de systole plaatsvinden, daar waar piek systolische longitudinale verplaatsing en strain laat in de systole geschieden, of (bij 20-30% van alle segmenten) gedurende de isovolumetrische relaxatie tijd, zoals ook het minimaal systolische volume and maximale myocard dikte. Deze metingen reflecteren daarom verschillende cardiale mechanische gebeurtenissen en kunnen gecombineerd worden om een gedetailleerder beeld van LV dissynchronie te verkrijgen.

Een 3D dataset kan ook worden weergegeven in een tri-plane vorm, waarbij er gelijktijdig informatie verkregen wordt vanuit de 3 apicale vensters. Daarom kan deze aanpak worden gebruikt voor het berekenen van LV volumes en EF (met meer nauwkeurigheid vergeleken met de bi-plane methode) en voor het bepalen van LV dissynchronie. Met tri-plane TDI kan zelfs LV dissynchronie berekend worden als de standaarddeviatie van de tijd tot piek systolische snelheid van 12 LV segmenten (Ts-SD-12). Dit liet eerder een goede correlatie zien met GMPS (Hoofdstuk 6) and bleek tevens een voorspeller van gunstige verkleining in LV volumes na 6 maanden CRT, met goede sensitiviteit en specificiteit (Hoofdstuk 7). Met deze techniek kan ook snel het laatst geactiveerde segment worden geïdentificeerd, wat van belang is voor het evalueren van het effect van CRT in geval van een corresponderende positie van de LV pacemakerdraad (zoals vastgesteld met multi detector computer tomografie, Hoofdstuk 8).

In **Deel IB** wordt RT3DE besproken als een nieuwe, betrouwbare techniek voor de beoordeling van linker atrium grootte en functie. RT3DE geeft belangrijke informatie over veranderingen in linker atrium volumes gedurende de hartcyclus.

In patiënten behandeld met CRT demonstreerde RT3DE significante gunstige verkleining van het linker atrium na implantatie, evenals een verbetering in linker atrium ledigingfractie en reservoir functie. In patiënten die radiofrequente katheter ablatie hebben ondergaan voor boezemfibrilleren werd met RT3DE gedemonstreerd dat er alleen een significatie reductie in linker atrium volumes en een duidelijke verbetering in linker atrium contractie en reservoir functie optrad in patiënten vrij van episodes van boezemfibrilleren na de procedure.

Deel II

In dit deel van het proefschrift werd een grote groep patiënten bestudeerd door middel van contrast echocardiografie binnen 48 uur na opname met een acuut myocard infarct waarvoor percutane coronair interventie. Aangezien getallen over de veiligheid van deze techniek bij kritiek zieke patiënten ontbreken hebben we gerapporteerd dat grote complicaties zich niet hebben voorgedaan en kleine complicaties optraden in slechts 4% van alle patiënten. Studies in grotere patiëntengroepen moeten deze resultaten echter bevestigen. De RT3DE acquisities werden verricht met, en zonder contrast, waarmee gedemonstreerd werd dat de toevoeging van contrast in deze patiënten van toegevoegde waarde is doordat de endocardiale begrenzing beter gevisualiseerd kan worden en leidt tot een hogere reproduceerbaar-

heid van LV functie bepaling. Tenslotte kan met deze techniek ook cardiale perfusie worden geëvalueerd en daarmee de uitgebreidheid van infarcering, wat een belangrijke parameter is voor het beloop van cardiale functie op korte en lange termijn na een myocard infarct. Linker kamer functie direct na een infarct bleek niet alleen onafhankelijk geassocieerd met infarct grootte, maar ook met LV dissynchronie en LV twist (met een reductie van zowel basale als apicale rotatie. Voornamelijk afname van LV twist direct na een myocard infarct was significant en onafhankelijk geassocieerd met het optreden van ongunstige LV vergroting na 6 maanden. Dit betekent dat het een gevoelige globale parameter is van LV systolische functie na infarcering.

Deel III

In dit deel van het proefschrift worden nieuwe toepassingen van cardiale MRI in patiënten met hartfalen en functionele mitralis insufficiëntie geëvalueerd.

In **Deel IIIA** worden verschillende manieren besproken om LV dissynchronie met cardiale MRI te bepalen. Snelheid gecodeerde cardiale MRI, gewoonlijk gebruikt om bloedstroom metingen mee te verrichten, kan ook worden gebruikt om de snelheden van het bewegende myocard mee te analyseren, vergelijkbaar met TDI. Er werd een sterke correlatie gevonden tussen TDI en snelheid gecodeerde cardiale MRI voor de bepaling van cardiale piek systolische en diastolische snelheden met corresponderende timings, met een kleine bias tussen de 2 technieken. Er werd bovendien ook een sterke overeenkomst gevonden tussen de 2 technieken wanneer patiënten werden gecategoriseerd naar ernst van LV dissynchronie en LV diastolische functie (met gebruik van de E/E' ratio). Een andere mogelijke methode om LV dissynchronie te bepalen wordt toegepast in patiënten die zijn verwezen voor CRT. Deze techniek gebruikt standaard korte as opnames waarbij endocardiale en epicardiale contouren wordt geïdentificeerd en de verandering van myocard dikte in de tijd (strain) wordt geëvalueerd. De standaarddeviatie van de tijd tot maximale wanddikte van 16 segmenten (SDt-16) bleek een belangrijke voorspeller van gunstige verkleining in LV volumes na CRT, evenals de uitgebreidheid van een eerder myocard infarct. Dit is de eerste studie die de waarde van deze 2 belangrijke parameters (beide gemeten met cardiale MRI) heeft aangetoond in de verbetering van patiënt selectie voor CRT.

Cardiale MRI is een unieke manier om patiënten met hartfalen te evalueren. Het combineert de kwantificering van de hartkamer grootte en functie met de bepaling van LV dissynchronie en cardiale viability (zoals ook gedemonstreerd in vergelijking met ^{99}mTc-tetrofosmin and ^{18}F-fluorodeoxyglucose SPECT, Hoofdstuk 17). Daarom is het tevens de aangewezen techniek voor de evaluatie van patiënten met een LV aneurysma die in aanmerking komen voor chirurgische reconstructie, aangezien nauwkeurige metingen van LV grootte, vorm, en globale en regionale functie, samen met de bepaling van cardiaal littekenweefsel en ernst van eventuele

mitralis insufficiëntie, noodzakelijk zijn om de juiste indicatie te stellen en de procedure te plannen. RT3DE blijkt een mogelijk nauwkeurige alternatieve beeldvormende methode voor deze analyse (Hoofdstuk 18).

In **Deel IIIB** werd 3D 3 richtingen snelheid gecodeerde cardiale MRI direct vergeleken met RT3DE in 64 patiënten met functionele mitralis insufficiëntie. Er werd een sterke overeenkomst gevonden tussen RT3DE en cardiale MRI voor de bepaling van het mitralis insufficiënte volume, zonder significatie bias tussen deze 2 technieken. 2D echocardiografie onderschatte echter het mitralis insufficiënte volume in vergelijking met cardiale MRI. Dit wordt mede veroorzaakt door het feit dat conventionele echocardiografie de "effective regurgitant orifice area" (EROA) baseert op de aanname dat het een perfecte cirkelvorm is. In patiënten met functionele mitralis insufficiëntie is het echter vaker geelongeerd langs de halvemaanvormige coaptatie lijn. Dit resulteert in een onderschatting wanneer dit gemeten wordt vanuit een 4-kamer venster of een parasternaal lange as.

Deel IV

In het laatste deel van dit proefschrift worden nieuwe pathosfysiologische aspecten in CRT patiënten bestudeerd met behulp van geavanceerde echocardiografische technieken. Het effect van CRT op LV rotatie werd geëvalueerd in 80 patiënten met hartfalen. Er werd direct na implantatie een substantiële verbetering in LV twist geobserveerd, echter alleen in patiënten met een gunstige verkleining in LV volumes na 6 maanden CRT. Daarom lijkt het een zeer goede voorspeller van response op CRT. Verder verbeterde LV twist in patiënten met een apicaal en midventriculair geplaatste LV draad, maar niet in patiënten met een basaal geplaatste LV draad. Deze resultaten suggereren dat CRT LV twist (gedeeltelijk) kan herstellen, mogelijk doordat er een meer fysiologische elektrische depolarisatie (van de apex richting basaal) en mechanische contractie van het myocard wordt bewerkstelligd. CRT kan ook als mogelijke therapie gezien worden in patiënten met hartfalen en ernstige mitralis insufficiëntie, die niet in aanmerking komen, of worden afgewezen voor chirurgische correctie vanwege het zeer hoge operatierisico. We konden laten zien dat als deze patiënten worden verwezen voor CRT, er een significante verbetering in de ernst van de mitralis insufficiëntie wordt geobserveerd in ca. 50% van alle gevallen. Deze verbetering na CRT leidt tot een betere overleving.

Cerebrale doorbloeding is verminderd in patiënten met symptomatisch hartfalen, en dit kan mogelijk bijdragen tot (frequent geobserveerde) verminderde cognitieve vermogens. We bestudeerden het effect van CRT op cerebrale doorbloeding met behulp van transcraniele Doppler in 35 patiënten voor, en 6 maanden na implantatie, en vergeleken dit met 15 patiënten met hartfalen die niet in aanmerking kwamen voor CRT. Er werd een significante verbetering in cerebrale doorbloeding gevonden na CRT en dit was sterk gecorreleerd aan de verbetering in LV functie. Of sequentieel biventriculair pacen betere resultaten kan bereiken

dat simultaan biventriculair pacen werd ook verkend in dit deel van het proefschrift, in patiënten verwezen voor CRT met zowel ischemisch als niet-ischemisch hartfalen. Geoptimaliseerde sequentieel biventriculair pacen gaf een significante verbetering in LV systolische functie en een significante reductie in LV dissynchronie in vergelijking met simultaan biventriculair pacen. Hoewel de absolute verbetering in LVEF na implantatie groter was in patiënten met niet-ischemisch hartfalen, leidde inter-ventriculaire (V-V) interval optimalisatie tot een grotere relatieve verbetering in LV systolische functie in patiënten met ischemisch hartfalen. Er werd een significantie relatie gevonden tussen LV litteken weefsel en een optimaal V-V interval, waar een grotere hoeveelheid litteken weefsel gerelateerd was aan meer LV pre-activatie. Dit reflecteert waarschijnlijk een compensatie voor de langzamer verlopende intra-LV geleiding veroorzaakt door het litteken weefsel.

In het laatste Hoofdstuk van het proefschrift werd het effect van CRT op systolische functie en gunstige verkleining in LV volumes in patiënten met ischemisch en niet-ischemisch hartfalen in de tijd geëvalueerd. Er werd een directe verbetering gezien in LV systolische functie na CRT, maar met een aanvullende verbetering na 6 maanden. Met name een acute afname in LV eind-systolisch volume bleek voorspellend voor echocardiografische response na 6 maanden, met een goede sensitiviteit en specificiteit. Het tijdsbeloop van verbetering in LV systolische functie was gelijk voor beide groepen, maar de gunstige verkleining in LV volumes was meer uitgesproken in niet-ischemische patiënten dan in ischemische patiënten, in wie significante hoeveelheden litteken weefsel waarschijnlijk verdere verbetering belemmerde.

CONCLUSIES

Geavanceerde beeldvormende technieken spelen een cruciale rol in de diagnostiek en klinische besluitvorming van patiënten met verschillende cardiale ziekten, waaronder hartfalen, acuut myocard infarct en boezemfibrilleren.

RT3DE heeft een belangrijke overgang gemaakt van onderzoeksinstrument tot een klinisch toepasbare techniek en heeft bewezen voordelen boven conventionele 2D echocardiografie. Dit zijn onder andere een meer accurate kwantificering van de grootte en functie van de verschillende hartkamers en de mogelijkheid van oneindig veel oriëntaties voor een beter begrip van klepafwijkingen. Het is daarom aannemelijk dat RT3DE een routine onderdeel zal worden van veel echocardiografische onderzoeken.

Contrast echocardiografie zou toegepast moeten worden in elke patiënt met een suboptimaal akoestisch venster, zeker met RT3DE. In patiënten die een primaire percutane coronair interventie hebben ondergaan kan perfusie analyse een accurate inschatting maken van infarct grootte, wat samen met een meer complexe evaluatie van LV functie cruciale informatie verschaft voor patiënt management.

Strain analyse heeft een enorme ontwikkeling doorgemaakt de laatste jaren en wordt nu gezien als een bruikbaar instrument voor een gevoeligere bepaling van LV regionale en globale functie en voor een meer gedetailleerde evaluatie van LV functie in LV dissynchronie.

Cardiale MRI is de gouden standaard voor de bepaling van LV volumes en voor de identificatie van litteken weefsel en fibrose. Het moet daarom gezien worden als een zeer compleet instrument voor de evaluatie van patiënten met hartfalen, waarbij er complexe bepalingen van bloedstroming door de kleppen en LV dissynchronie mogelijk zijn.

Geavanceerde beeldvormende technieken kunnen worden toegepast bij patiënten met hartfalen die zijn verwezen voor CRT voor de evaluatie van nieuwe pathosfysiologische aspecten, waaronder het effect op LV twist, functionele mitralis insufficiëntie en cerebrale doorbloeding.

List of publications

LIST OF PUBLICATIONS

1. Ghio S, Perlini S, Palladini G, **Marsan NA**, Faggiano G, Vezzoli M, Klersy C, Campana C, Merlini G, Tavazzi L. Importance of the echocardiographic evaluation of right ventricular function in patients with AL amyloidosis. *Eur J Heart Fail* 2007;9:808-13.
2. van de Veire NR, Bleeker GB, Ypenburg C, De Sutter J, **Marsan NA**, Holman ER, van der Wall EE, Schalij MJ, Bax JJ. Usefulness of triplane tissue Doppler imaging to predict acute response to cardiac resynchronization therapy. *Am J Cardiol* 2007;100:476-82.
3. **Marsan NA**, Henneman MM, Chen J, Ypenburg C, Dibbets P, Ghio S, Bleeker GB, Stokkel MP, van der Wall EE, Tavazzi L, Garcia EV, Bax JJ. Left ventricular dyssynchrony assessed by two three-dimensional imaging modalities: phase analysis of gated myocardial perfusion SPECT and triplane tissue Doppler imaging. *Eur J Nucl Med Mol Imaging* 2008;35:166-73.
4. van de Veire NR, Yu CM, **Marsan NA**, Bleeker GB, Ypenburg C, De Sutter J, Zhang Q, Fung JW, Chan JY, Holman ER, van der Wall EE, Schalij MJ, Bax JJ. Triplane tissue Doppler imaging: a novel three-dimensional imaging modality that predicts reverse left ventricular remodelling after cardiac resynchronisation therapy. *Heart* 2008;94:e9.
5. Henneman MM, van der Wall EE, Ypenburg C, Bleeker GB, van de Veire NR, **Marsan NA**, Chen J, Garcia EV, Westenberg JJ, Schalij MJ, Bax JJ. Nuclear imaging in cardiac resynchronization therapy. *J Nucl Med* 2007;48:2001-10.
6. **Marsan NA**, Bleeker GB, Ypenburg C, Ghio S, van de Veire NR, Holman ER, van der Wall EE, Tavazzi L, Schalij MJ, Bax JJ. Real-time three-dimensional echocardiography permits quantification of left ventricular mechanical dyssynchrony and predicts acute response to cardiac resynchronization therapy. *J Cardiovasc Electrophysiol* 2008;19:392-9.
7. van Ramshorst J, Atsma DE, Beeres SL, Mollema SA, **Marsan NA**, Holman ER, van der Wall EE, Schalij MJ, Bax JJ. Effect of intramyocardial bone marrow cell injection on left ventricular dyssynchrony and global strain. *Heart* 2009;95:119-24.
8. **Marsan NA**, Henneman MM, Chen J, Ypenburg C, Dibbets P, Ghio S, Bleeker GB, Stokkel MP, van der Wall EE, Tavazzi L, Garcia EV, Bax JJ. Real-time three-dimensional echocardiography as a novel approach to quantify left ventricular dyssynchrony: a comparison study with phase analysis of gated myocardial perfusion single photon emission computed tomography. *J Am Soc Echocardiogr* 2008;21:801-7.
9. van de Veire NR, **Marsan NA**, Schuijf JD, Bleeker GB, Wijffels MC, van Erven L, Holman ER, De Sutter J, van der Wall EE, Schalij MJ, Bax JJ. Noninvasive imaging of cardiac venous anatomy with 64-slice multi-slice computed tomography and noninvasive assessment of left ventricular dyssynchrony by 3-dimensional tissue synchronization imaging in patients with heart failure scheduled for cardiac resynchronization therapy. *Am J Cardiol* 2008;101:1023-9.
10. Delgado V, Ypenburg C, van Bommel RJ, Tops LF, Mollema SA, **Marsan NA**, Bleeker GB, Schalij MJ, Bax JJ. Assessment of left ventricular dyssynchrony by speckle tracking strain imaging comparison between longitudinal, circumferential, and radial strain in cardiac resynchronization therapy. *J Am Coll Cardiol* 2008;51:1944-52.
11. Doughty RN, Gamble GD, Poppe KK, Somaratne JB, Whalley GA, Doughty RN, Klein AL, Poppe KK, Gamble GD, Dini FL, Møller JE, Quintana M, Yu CM, Whalley GA, Dini FL, Doughty RN, Gamble GD, Klein AL, Møller JE, Quintana M, Whalley GA, Yu CM, Bruch C, Feola M, Ghio S, Giannuzzi P, Hansen A, Ortiz J, Pinamonti B, Prior DL, Rossi A, Tabet JY, Temporelli PL, Yamamoto T, Prior DL, Monaco CG, Silva CE, Ferreira LD, Gil MA, Nanda NC, Monaco CA, Sanderson JE, Yu CM, Cohen-Solal A, Dahan M, Ennezat PV, Geyer C, Guiti C, Logeart D, Tabet JY, Breithardt G, Bruch C, Eckardt

L, Gotzmann M, Grude M, Rothenburger M, Scheld HH, Stypmann J, Wenzelburger F, Wichter T, Haass M, Hansen A, Krueger C, Kuebler W, Kuecherer H, Unnebrink K, Zimmermann R, Zugck C, Bosimini E, Corrà U, Galli M, Giannuzzi P, Giordano A, Imparato A, Scapellato F, Silva P, Temporelli PL, **Marsan NA**, Campana C, Gavazzi A, Ghio S, Klersy C, Laudisa ML, Recusani F, Sebastiani R, Tavazzi L, Baldini U, Boni A, Barsotti L, Cortigiani L, Dini FL, Micheli G, Nuti R, Rossi A, Cicoira M, Bonapace S, Camerini F, Di Lenarda A, Gregori D, Pinamonti B, Sinagra G, Zecchin M, Aspromonte N, Feola M, Giovinazzo P, Milani L, Valle R, Ishimoto T, Ito S, Oki T, Tabata T, Tanaka H, Wakatsuki T, Yamada H, Yamamoto T, Doughty RN, Gamble GD, Walsh HJ, Sharpe N, Whalley GA, Wright SP, Fogarty A, Frampton CM, Klein AL, Lauer MS, Martin M, Morehead AJ, Nash PJ, Pereira JJ, Prior DL, Starling RC, Tang W, Thomas JD, Troughton R, Young JB, Doughty RN, Gamble GD, MacMahon S, Sharpe DN, Whalley GA. Independence of restrictive filling pattern and LV ejection fraction with mortality in heart failure: an individual patient meta-analysis. *Eur J Heart Fail* 2008;10:786-92.

12. Nucifora G, **Marsan NA**, Siebelink HM, van Werkhoven JM, Schuijf JD, Schalij MJ, Poldermans D, Holman ER, Bax JJ. Safety of contrast-enhanced echocardiography within 24 h after acute myocardial infarction. *Eur J Echocardiogr* 2008;9:816-8.
13. Schwartz PJ, De Ferrari GM, Sanzo A, Landolina M, Rordorf R, Raineri C, Campana C, Revera M, **Marsan NA**, Tavazzi L, Odero A. Long term vagal stimulation in patients with advanced heart failure: first experience in man. *Eur J Heart Fail* 2008;10:884-91.
14. Ypenburg C, van Bommel RJ, **Marsan NA**, Delgado V, Bleeker GB, van der Wall EE, Schalij MJ, Bax JJ. Effects of interruption of long-term cardiac resynchronization therapy on left ventricular function and dyssynchrony. *Am J Cardiol* 2008;102:718-21.
15. **Marsan NA**, Bleeker GB, Ypenburg C, van Bommel RJ, Ghio S, van de Veire NR, Delgado V, Holman ER, van der Wall EE, Schalij MJ, Bax JJ. Real-time three-dimensional echocardiography as a novel approach to assess left ventricular and left atrium reverse remodeling and to predict response to cardiac resynchronization therapy. *Heart Rhythm* 2008;5:1257-64.
16. **Marsan NA**, Tops LF, Holman ER, van de Veire NR, Zeppenfeld K, Boersma E, van der Wall EE, Schalij MJ, Bax JJ. Comparison of left atrial volumes and function by real-time three-dimensional echocardiography in patients having catheter ablation for atrial fibrillation with persistence of sinus rhythm versus recurrent atrial fibrillation three months later. *Am J Cardiol* 2008;102:847-53.
17. Westenberg JJ, Roes SD, **Marsan NA**, Binnendijk NM, Doornbos J, Bax JJ, Reiber JH, de Roos A, van der Geest RJ. Mitral valve and tricuspid valve blood flow: accurate quantification with 3D velocity-encoded MR imaging with retrospective valve tracking. *Radiology* 2008;249:792-800.
18. Ypenburg C, Westenberg JJ, Bleeker GB, van de Veire NR, **Marsan NA**, Henneman MM, van der Wall EE, Schalij MJ, Abraham TP, Barold SS, Bax JJ. Noninvasive imaging in cardiac resynchronization therapy--part 1: selection of patients. *Pacing Clin Electrophysiol* 2008;31:1475-99.
19. **Marsan NA**, Breithardt OA, Delgado V, Bertini M, Tops LF. Predicting response to CRT. The value of two- and three-dimensional echocardiography. *Europace* 2008;10 Suppl 3:iii73-iii79.
20. **Marsan NA**, Westenberg JJ, Tops LF, Ypenburg C, Holman ER, Reiber JH, de Roos A, van der Wall EE, Schalij MJ, Roelandt JR, Bax JJ. Comparison between tissue Doppler imaging and velocity-encoded magnetic resonance imaging for measurement of myocardial velocities, assessment of left ventricular dyssynchrony, and estimation of left ventricular filling pressures in patients with ischemic cardiomyopathy. *Am J Cardiol* 2008;102:1366-72.
21. Roes SD, Kaandorp TA, **Marsan NA**, Westenberg JJ, Dibbets-Schneider P, Stokkel MP, Lamb HJ, van der Wall EE, de Roos A, Bax JJ. Agreement and disagreement between contrast-enhanced magnetic resonance imaging and nuclear imaging for assessment of myocardial viability. *Eur J Nucl Med Mol Imaging* 2009;36:594-601.

22. Ypenburg C, Van D, V, Westenberg JJ, Bleeker GB, **Marsan NA**, Henneman MM, van der Wall EE, Schalij MJ, Abraham TP, Barold SS, Bax JJ. Noninvasive imaging in cardiac resynchronization therapy--Part 2: Follow-up and optimization of settings. *Pacing Clin Electrophysiol* 2008;31:1628-39.
23. **Marsan NA**, Bleeker GB, van Bommel RJ, Ypenburg C, Delgado V, Borleffs CJ, Holman ER, van der Wall EE, Schalij MJ, Bax JJ. Comparison of time course of response to cardiac resynchronization therapy in patients with ischemic versus nonischemic cardiomyopathy. *Am J Cardiol* 2009;103:690-4.
24. **Marsan NA**, Arai AE, van Rossum AC, Zamorano JL, Bax JJ. Imaging highlights from the European Association of Echocardiography and the Society of Cardiovascular Magnetic Resonance. *JACC Cardiovasc Imaging* 2008;1:380-9.
25. Nucifora G, Schuijf JD, van Werkhoven JM, Jukema JW, **Marsan NA**, Holman ER, van der Wall EE, Bax JJ. Usefulness of echocardiographic assessment of cardiac and ascending aorta calcific deposits to predict coronary artery calcium and presence and severity of obstructive coronary artery disease. *Am J Cardiol* 2009;103:1045-50.
26. Nucifora G, **Marsan NA**, Holman ER, Siebelink HM, van Werkhoven JM, Scholte AJ, van der Wall EE, Schalij MJ, Bax JJ. Real-time 3-dimensional echocardiography early after acute myocardial infarction: incremental value of echo-contrast for assessment of left ventricular function. *Am Heart J* 2009;157:882-8.
27. Bertini M, Nucifora G, **Marsan NA**, Delgado V, van Bommel RJ, Boriani G, Biffi M, Holman ER, van der Wall EE, Schalij MJ, Bax JJ. Left ventricular rotational mechanics in acute myocardial infarction and in chronic (ischemic and nonischemic) heart failure patients. *Am J Cardiol* 2009;103:1506-12.
28. **Marsan NA**, Westenberg JJ, Ypenburg C, van Bommel RJ, Roes S, Delgado V, Tops LF, van der Geest RJ, Boersma E, de Roos A, Schalij MJ, Bax JJ. Magnetic resonance imaging and response to cardiac resynchronization therapy: relative merits of left ventricular dyssynchrony and scar tissue. *Eur Heart J* 2009;30:2360-7.
29. **Marsan NA**, Tops LF, Westenberg JJ, Delgado V, de Roos A, van der Wall EE, Schalij MJ, Bax JJ. Usefulness of multimodality imaging for detecting differences in temporal occurrence of left ventricular systolic mechanical events in healthy young adults. *Am J Cardiol* 2009;104:440-6.
30. Scuteri L, Rordorf R, **Marsan NA**, Landolina M, Magrini G, Klersy C, Frattini F, Petracci B, Vicentini A, Campana C, Tavazzi L, Ghio S. Relevance of echocardiographic evaluation of right ventricular function in patients undergoing cardiac resynchronization therapy. *Pacing Clin Electrophysiol* 2009;32:1040-9.
31. Roes SD, Hammer S, van der Geest RJ, **Marsan NA**, Bax JJ, Lamb HJ, Reiber JH, de Roos A, Westenberg JJ. Flow assessment through four heart valves simultaneously using 3-dimensional 3-directional velocity-encoded magnetic resonance imaging with retrospective valve tracking in healthy volunteers and patients with valvular regurgitation. *Invest Radiol* 2009;44:669-75.
32. Delgado V, Tops LF, van Bommel RJ, van der Kley F, **Marsan NA**, Klautz RJ, Versteegh MI, Holman ER, Schalij MJ, Bax JJ. Strain analysis in patients with severe aortic stenosis and preserved left ventricular ejection fraction undergoing surgical valve replacement. *Eur Heart J* 2009;30:3037-47.
33. Ng AC, Delgado V, Bertini M, Nucifora G, Shanks M, **Marsan NA**, Holman ER, van de Veire NR, Leung DY, Bax JJ. Advanced applications of 3-dimensional echocardiography. *Minerva Cardioangiol* 2009;57:415-41.
34. Bertini M, **Marsan NA**, Delgado V, van Bommel RJ, Nucifora G, Borleffs CJ, Boriani G, Biffi M, Holman ER, van der Wall EE, Schalij MJ, Bax JJ. Effects of cardiac resynchronization therapy on left ventricular twist. *J Am Coll Cardiol* 2009;54:1317-25.

35. Rossi A, Temporelli PL, Quintana M, Dini FL, Ghio S, Hillis GS, Klein AL, **Marsan NA**, Prior DL, Yu CM, Poppe KK, Doughty RN, Whalley GA. Independent relationship of left atrial size and mortality in patients with heart failure: an individual patient meta-analysis of longitudinal data (MeRGE Heart Failure). *Eur J Heart Fail* 2009;11:929-36.
36. Delgado V, Tops LF, Trines SA, Zeppenfeld K, **Marsan NA**, Bertini M, Holman ER, Schalij MJ, Bax JJ. Acute effects of right ventricular apical pacing on left ventricular synchrony and mechanics. *Circ Arrhythm Electrophysiol* 2009;2:135-45.
37. Tops LF, Den Uijl DW, Delgado V, **Marsan NA**, Zeppenfeld K, Holman ER, van der Wall EE, Schalij MJ, Bax JJ. Long-term improvement in left ventricular strain after successful catheter ablation for atrial fibrillation in patients with preserved left ventricular systolic function. *Circ Arrhythm Electrophysiol* 2009;2:249-57.
38. Roes SD, Borleffs CJ, van der Geest RJ, Westenberg JJ, **Marsan NA**, Kaandorp TA, Reiber JH, Zeppenfeld K, Lamb HJ, de Roos A, Schalij MJ, Bax JJ. Infarct tissue heterogeneity assessed with contrast-enhanced MRI predicts spontaneous ventricular arrhythmia in patients with ischemic cardiomyopathy and implantable cardioverter-defibrillator. *Circ Cardiovasc Imaging* 2009;2:183-90.
39. **Marsan NA**, Bleeker GB, van Bommel RJ, Borleffs CJ, Bertini M, Holman ER, van der Wall EE, Schalij MJ, Bax JJ. Cardiac resynchronization therapy in patients with ischemic versus non-ischemic heart failure: Differential effect of optimizing interventricular pacing interval. *Am Heart J* 2009;158:769-76.
40. **Marsan NA**, Tops LF, Nihoyannopoulos P, Holman ER, Bax JJ. Real-time three dimensional echocardiography: current and future clinical applications. *Heart* 2009;95:1881-90.
41. **Marsan NA**, Westenberg JJ, Ypenburg C, Delgado V, van Bommel RJ, Roes SD, Nucifora G, van der Geest RJ, de Roos A, Reiber JC, Schalij MJ, Bax JJ. Quantification of functional mitral regurgitation by real-time 3D echocardiography: comparison with 3D velocity-encoded cardiac magnetic resonance. *JACC Cardiovasc Imaging* 2009;2:1245-52.
42. Bertini M, Sengupta PP, Nucifora G, Delgado V, Ng AC, **Marsan NA**, Shanks M, van Bommel RJ, Schalij MJ, Narula J, Bax JJ. Role of left ventricular twist mechanics in the assessment of cardiac dyssynchrony in heart failure. *JACC Cardiovasc Imaging* 2009;2:1425-35.
43. Nucifora G, Bertini M, **Marsan NA**, Delgado V, Scholte AJ, Ng AC, van Werkhoven JM, Siebelink HM, Holman ER, Schalij MJ, van der Wall EE, Bax JJ. Impact of left ventricular dyssynchrony early on left ventricular function after first acute myocardial infarction. *Am J Cardiol* 2010;105:306-11.
44. Tamborini G, **Marsan NA**, Gripari P, Maffessanti F, Brusoni D, Muratori M, Caiani EG, Fiorentini C, Pepi M. Reference values for right ventricular volumes and ejection fraction with real-time three-dimensional echocardiography: evaluation in a large series of normal subjects. *J Am Soc Echocardiogr* 2010;23:109-15.
45. van Bommel RJ, Ypenburg C, Borleffs CJ, Delgado V, **Marsan NA**, Bertini M, Holman ER, Schalij MJ, Bax JJ. Value of tissue Doppler echocardiography in predicting response to cardiac resynchronization therapy in patients with heart failure. *Am J Cardiol* 2010;105:1153-8.
46. Nucifora G, **Marsan NA**, Bertini M, Delgado V, Siebelink HM, van Werkhoven JM, Scholte AJ, Schalij MJ, van der Wall EE, Holman ER, Bax JJ. Reduced left ventricular torsion early after myocardial infarction is related to left ventricular remodeling. *Circ Cardiovasc Imaging* 2010;3:433-42.
47. Delgado V, Mooyaart EA, Ng AC, Auger D, Bertini M, van Bommel RJ, Yiu KH, Ewe SH, Witkowski TG, **Marsan NA**, Schuijf JD, van der Wall EE, Schalij MJ, Bax JJ. Echocardiography and non-invasive imaging in cardiac resynchronization therapy. *Minerva Cardioangiol* 2010;58:313-32.

48. **Marsan NA**, Bax JJ. Non-invasive imaging in percutaneous mitral valve procedures. *EuroIntervention* 2010;6 Suppl G:G28-G37.
49. van Bommel RJ, **Marsan NA**, Koppen H, Delgado V, Borleffs CJ, Ypenburg C, Bertini M, Schalij MJ, Bax JJ. Effect of cardiac resynchronization therapy on cerebral blood flow. *Am J Cardiol* 2010;106:73-7.
50. **Marsan NA**, Bax JJ. Changes in functional mitral regurgitation after cardiac resynchronization therapy. *Eur Heart J* 2010;31:2323-5.
51. van Bommel RJ, Borleffs CJ, Ypenburg C, **Marsan NA**, Delgado V, Bertini M, van der Wall EE, Schalij MJ, Bax JJ. Morbidity and mortality in heart failure patients treated with cardiac resynchronization therapy: influence of pre-implantation characteristics on long-term outcome. *Eur Heart J* 2010;31:2783-90.
52. Bertini M, Delgado V, Nucifora G, **Marsan NA**, Ng AC, Shanks M, van Bommel RJ, Borleffs CJ, Ewe SH, Boriani G, Biffi M, Schalij MJ, Bax JJ. Effect of cardiac resynchronization therapy on subendo- and subepicardial left ventricular twist mechanics and relation to favorable outcome. *Am J Cardiol* 2010;106:682-7.
53. Shanks M, Siebelink HM, Delgado V, van de Veire NR, Ng AC, Sieders A, Schuijf JD, Lamb HJ, **Marsan NA**, Westenberg JJ, Kroft LJ, de Roos A, Bax JJ. Quantitative assessment of mitral regurgitation: comparison between three-dimensional transesophageal echocardiography and magnetic resonance imaging. *Circ Cardiovasc Imaging* 2010;3:694-700.
54. van Bommel RJ, Tanaka H, Delgado V, Bertini M, Borleffs CJ, **Marsan NA**, Holzmeister J, Ruschitzka F, Schalij MJ, Bax JJ, Gorcsan J, III. Association of intraventricular mechanical dyssynchrony with response to cardiac resynchronization therapy in heart failure patients with a narrow QRS complex. *Eur Heart J* 2010;31:3054-62.
55. van Bommel RJ, van Rijnsoever EP, Borleffs CJ, Delgado V, **Marsan NA**, Bertini M, Schalij MJ, Bax JJ. Effect of cardiac resynchronization therapy in patients with New York Heart Association functional class IV heart failure. *Am J Cardiol* 2010;106:1146-51.
56. Auger D, van Bommel RJ, Bertini M, Delgado V, Ng AC, Ewe SH, Shanks M, **Marsan NA**, Mooyaart EA, Witkowski T, Poldermans D, Schalij MJ, Bax JJ. Prevalence and characteristics of patients with clinical improvement but not significant left ventricular reverse remodeling after cardiac resynchronization therapy. *Am Heart J* 2010;160:737-43.
57. Bertini M, Delgado V, Nucifora G, **Marsan NA**, Ng AC, Shanks M, Antoni ML, van de Veire NR, van Bommel RJ, Rapezzi C, Schalij MJ, Bax JJ. Left ventricular rotational mechanics in patients with coronary artery disease: differences in subendocardial and subepicardial layers. *Heart* 2010;96:1737-43.
58. **Marsan NA**, Bax JJ. Cardiomyopathies: Myocardial fibrosis assessed by CMR to predict events in HCM. *Nat Rev Cardiol* 2010;7:604-6.
59. Delgado V, Ewe SH, Ng AC, van der Kley F, **Marsan NA**, Schuijf JD, Schalij MJ, Bax JJ. Multimodality imaging in transcatheter aortic valve implantation: key steps to assess procedural feasibility. *EuroIntervention* 2010;6:643-52.
60. Nucifora G, Delgado V, Bertini M, **Marsan NA**, van de Veire NR, Ng AC, Siebelink HM, Schalij MJ, Holman ER, Sengupta PP, Bax JJ. Left ventricular muscle and fluid mechanics in acute myocardial infarction. *Am J Cardiol* 2010;106:1404-9.
61. Ewe SH, **Marsan NA**, Pepi M, Delgado V, Tamborini G, Muratori M, Ng AC, van der Kley F, de Weger A, Schalij MJ, Fusari M, Biglioli P, Bax JJ. Impact of left ventricular systolic function on clinical and echocardiographic outcomes following transcatheter aortic valve implantation for severe aortic stenosis. *Am Heart J* 2010;160:1113-20.

62. **Marsan NA**, Westenberg JJ, Roes SD, van Bommel RJ, Delgado V, van der Geest RJ, de Roos A, Klautz RJ, Reiber JC, Bax JJ. Three-dimensional echocardiography for the preoperative assessment of patients with left ventricular aneurysm. *Ann Thorac Surg* 2011;91:113-21.
63. Delgado V, van Bommel RJ, Bertini M, Borleffs CJ, **Marsan NA**, Ng AC, Nucifora G, van de Veire NR, Ypenburg C, Boersma E, Holman ER, Schalij MJ, Bax JJ. Relative merits of left ventricular dyssynchrony, left ventricular lead position, and myocardial scar to predict long-term survival of ischemic heart failure patients undergoing cardiac resynchronization therapy. *Circulation* 2011;123:70-8.
64. van Bommel RJ, **Marsan NA**, Delgado V, van Rijnsoever EP, Schalij MJ, Bax JJ, Wellens HJ. Value of the surface electrocardiogram in detecting right ventricular dilatation in the presence of left bundle branch block. *Am J Cardiol* 2011;107:736-40.
65. Tops LF, Delgado V, Bertini M, **Marsan NA**, Den Uijl DW, Trines SA, Zeppenfeld K, Holman ER, Schalij MJ, Bax JJ. Left atrial strain predicts reverse remodeling after catheter ablation for atrial fibrillation. *J Am Coll Cardiol* 2011;57:324-31.
66. Witkowski TG, Ten Brinke EA, Delgado V, Ng AC, Bertini M, **Marsan NA**, Ewe SH, Auger D, Yiu KH, Braun J, Klein P, Steendijk P, Versteegh MI, Klautz RJ, Bax JJ. Surgical ventricular restoration for patients with ischemic heart failure: determinants of two-year survival. *Ann Thorac Surg* 2011;91:491-8.
67. van Bommel RJ, Mollema SA, Borleffs CJ, Bertini M, Ypenburg C, **Marsan NA**, Delgado V, van der Wall EE, Schalij MJ, Bax JJ. Impaired renal function is associated with echocardiographic nonresponse and poor prognosis after cardiac resynchronization therapy. *J Am Coll Cardiol* 2011;57:549-55.
68. Brandts A, Bertini M, van Dijk EJ, Delgado V, **Marsan NA**, van der Geest RJ, Siebelink HM, de Roos A, Bax JJ, Westenberg JJ. Left ventricular diastolic function assessment from three-dimensional three-directional velocity-encoded MRI with retrospective valve tracking. *J Magn Reson Imaging* 2011;33:312-9.
69. **Marsan NA**, Maffessanti F, Tamborini G, Gripari P, Caiani E, Fusini L, Muratori M, Zanobini M, Alamanni F, Pepi M. Left atrial reverse remodeling and functional improvement after mitral valve repair in degenerative mitral regurgitation: a real-time 3-dimensional echocardiography study. *Am Heart J* 2011;161:314-21.
70. Maffessanti F, **Marsan NA**, Tamborini G, Sugeng L, Caiani EG, Gripari P, Alamanni F, Jeevanandam V, Lang RM, Pepi M. Quantitative analysis of mitral valve apparatus in mitral valve prolapse before and after annuloplasty: a three-dimensional intraoperative transesophageal study. *J Am Soc Echocardiogr* 2011;24:405-13.
71. Shanks M, Delgado V, Ng AC, Auger D, Mooyaart EA, Bertini M, **Marsan NA**, van Bommel RJ, Holman ER, Poldermans D, Schalij MJ, Bax JJ. Clinical and echocardiographic predictors of nonresponse to cardiac resynchronization therapy. *Am Heart J* 2011;161:552-7.
72. Abdulrahman RM, Delgado V, Hoftijzer HC, Ng AC, Ewe SH, **Marsan NA**, Holman ER, Hovens GC, Corssmit EP, Romijn JA, Bax JJ, Smit JW. Both exogenous subclinical hyperthyroidism and short-term overt hypothyroidism affect myocardial strain in patients with differentiated thyroid carcinoma. *Thyroid* 2011;21:471-6.
73. Ewe SH, Delgado V, Ng AC, Antoni ML, van der Kley F, **Marsan NA**, de Weger A, Tavilla G, Holman ER, Schalij MJ, Bax JJ. Outcomes After Transcatheter Aortic Valve Implantation: Transfemoral Versus Transapical Approach. *Ann Thorac Surg* 2011.

74. Mooyaart EA, **Marsan NA**, van Bommel RJ, Thijssen J, Borleffs CJ, Delgado V, van der Wall EE, Schalij MJ, Bax JJ. Comparison of long-term survival of men versus women with heart failure treated with cardiac resynchronization therapy. *Am J Cardiol* 2011;108:63-8.
75. Antoni ML, Ten Brinke EA, Atary JZ, **Marsan NA**, Holman ER, Schalij MJ, Bax JJ, Delgado V. Left atrial strain is related to adverse events in patients after acute myocardial infarction treated with primary percutaneous coronary intervention. *Heart* 2011;97:1332-7.
76. van Bommel RJ, Ypenburg C, Mollema SA, Borleffs CJ, Delgado V, Bertini M, **Marsan NA**, van der Wall EE, Schalij MJ, Bax JJ. Site of latest activation in patients eligible for cardiac resynchronization therapy: patterns of dyssynchrony among different QRS configurations and impact of heart failure etiology. *Am Heart J* 2011;161:1060-6.
77. Auger D, Bertini M, **Marsan NA**, Hoke U, Ewe SH, Thijssen J, Witkowski TG, Yiu KH, Ng AC, van der Wall EE, Schalij MJ, Bax JJ, Delgado V. Prediction of response to cardiac resynchronization therapy combining two different three-dimensional analyses of left ventricular dyssynchrony. *Am J Cardiol* 2011;108:711-7.
78. van Bommel RJ, **Marsan NA**, Delgado V, Borleffs CJ, van Rijnsoever EP, Schalij MJ, Bax JJ. Cardiac resynchronization therapy as a therapeutic option in patients with moderate-severe functional mitral regurgitation and high operative risk. *Circulation* 2011;124:912-9.
79. Antoni ML, Ten Brinke EA, **Marsan NA**, Atary JZ, Holman ER, van der Wall EE, Schalij MJ, Bax JJ, Delgado V. Comprehensive assessment of changes in left atrial volumes and function after ST-segment elevation acute myocardial infarction: role of two-dimensional speckle tracking strain imaging. *J Am Soc Echocardiogr* 2011.
80. Ten Brinke EA, Witkowski TG, Delgado V, Klein P, Klok M, **Marsan NA**, Klautz RJ, van der Wall EE, Bax JJ, van der Laarse A, Steendijk P. Myocardial collagen turnover after surgical ventricular restoration in heart failure patients. *Eur J Heart Fail* 2011.
81. Shanks M, Antoni ML, Hoke U, Bertini M, Ng AC, Auger D, **Marsan NA**, van Erven L, Holman ER, Schalij MJ, Bax JJ, Delgado V. The effect of cardiac resynchronization therapy on left ventricular diastolic function assessed with speckle-tracking echocardiography. *Eur J Heart Fail* 2011.
82. Ewe SH, Ng AC, Schuijf JD, van der Kley F, Colli A, Palmen M, de Weger A, **Marsan NA**, Holman ER, de Roos A, Schalij MJ, Bax JJ, Delgado V. Location and severity of aortic valve calcium and implications for aortic regurgitation after transcatheter aortic valve implantation. *Am J Cardiol* 2011.
83. Hemodynamic and clinical impact of prosthesis-patient mismatch following transcatheter aortic valve implantation. Ewe SH, Muratori M, Delgado V, Pepi M, Tamborini G, Fusini L, Klautz RJ, Gripari P, Bax JJ, Fusari M, Schalij MJ, **Marsan NA**. *J Am Coll Cardiol* 2011.

BOOK CHAPTER

Structural and valvular heart disease: Non invasive imaging. *Percutaneous interventional cardiovascular medicine, The PCR-EAPCI textbook*. PCR Publishing, 5 Rue Saint Pantaléon, BP 61508 – 31015, Toulouse cedex 6, France.

Acknowledgments

ACKNOWLEDGMENTS

This thesis would have not been possible without the help and support of all the friends and colleagues I had the opportunity to meet and work with in the past years at the Department of Cardiology of the Leiden University Medical Center.

First of all, I would like to thank all the Dutch and foreign research fellows I worked with, for their cooperation and friendship. Dear Victoria, thank you in particular for the nice discussions we always have, for your sincere advices and support, and for your friendship.

I express also my gratitude to the secretaries of the Department of Cardiology, with special thank to Talitha and Cora, for their kind help. I would like to thank all the staff members, and in particular Eduard, Hans-Marc and Arthur, for their support. My thanks go also to all the echocardiography technicians and the secretaries from the Department of Cardiac Function: I enjoy very much working with you all.

Sincere thanks also to the Department of Radiology (in particular to Jos), Thoracic surgery, Rheumatology, Pulmonology and Endocrinology for their productive cooperation. I express my gratitude also to all the doctors from the IRCCS San Matteo of Pavia (in particular to Dr. S. Ghio), Centro Cardiologico Monzino of Milan (in particular to Dr. M. Pepi and Dr. G. Tamborini) and Centro Diagnostico Italiano of Milan (in particular to Dr. R. Bigi and Prof. C. Fiorentini) with whom I had the pleasure to work and from whom I learned a lot.

Dear Louisa and Patricia, thanks for being my paranymphs. With you it was, it is and it will always be great fun.

To all my dear friends, thank you for the wonderful time we had together. Dear Federica, Silvia and Chiara, thank for our "quartet" adventures in the Netherlands and for your friendship although we are now spread all over the world. Thank also to all my Dutch class mates, who were with me in the difficult journey of learning Dutch. Dear Cristina and all Pavia's friends, thanks for being there in the most important moments. Dear Cecilia, thanks for your long life friendship and for your support in the difficult moments.

Rutger, you are the one that I want to thank most for this thesis, but I also have to thank this thesis for the opportunity of meeting you. In you I finally found what I always wanted and since that moment, my life with you is a great and fun adventure.

I would like to thank also Rutger's family and friends for the warm welcome since the first day in the Netherlands. Particular thank goes to Olga for her constant support and understanding.

Last but not least, I would like to express all my gratitude to my big "great" family: thank to my Grandma, my special aunts and my crazy cousins. Part of the family are also Claudio and Daniela, Massimo and Patrizia, and all the other friends from the University of Siena.

Special thanks to my father, who although could not witness this moment and many other happy events of my life, is always next to me.

Dear mum, thanks for your unconditional love, for showing me always the positive side of everything, for supporting my crazy ideas and for your guidance in the most important decisions. To you in particular I dedicate this thesis.

Curriculum Vitae

CURRICULUM VITAE

The author of this thesis was born in Rome (Italy), the 12th of November 1976. After graduating from the Liceo Classico Virgilio (Rome) in 1995, she studied Medicine at the University of Pavia where she obtained her medical degree, cum laude, in 2001. During this period, she completed a fellowship in experimental Immunology in Cambridge (UK). After a 4 year residency in Cardiology at the University of Pavia, she graduated cum laude as a Cardiologist in 2005. She spent the following year as a cardiologist at the Cardiology Department of IRCCS San Matteo, Pavia and as a principal investigator of the international trial for vagal stimulation in heart failure patient: CARDIOFIT™ for Heart Failure Clinical Study Protocol. In autumn 2006, she moved to Leiden to start her PhD fellowship at the Department of Cardiology, Leiden University Medical Center (supervisors Prof. Dr. J.J. Bax and Prof. Dr. M.J. Schalij). This research fellowship focused on novel imaging techniques such as 3D echocardiography, speckle tracking analysis, cardiac magnetic resonance imaging (MRI) and multi-slice computed tomography (MSCT), and was supported by a research grant of the European Society of Cardiology. The results of this fellowship are presented in this thesis. From October 2008 to October 2009 she worked as a cardiologist involved in the echolab and in the report of cardiac MRI and MSCT at the Centro Cardiologico Monzino (Dr. M. Pepi) and Centro Diagnostico Italiano (Dr. R. Bigi), Milan, Italy. In November 2009, she returned to Leiden to work as a senior researcher and later she joined the Department of Cardiology as a staff member. She is an active reviewer for Circulation, Circulation Imaging, Journal of American College of Cardiology, JACC Cardiovascular imaging, American Journal of Cardiology, Heart, Journal of the American Society of Echocardiography, European Journal of Echocardiography and for the abstracts of the annual ESC congress. She is married to Rutger J. van Bommel.